The background of the image is a dark, abstract space filled with glowing, wavy lines in various colors including blue, green, yellow, and white. These lines are densely packed and appear to represent data flow or energy pathways. Interspersed among the lines are numerous small, glowing orange and yellow dots, which likely represent nodes or specific data points within a complex network.

The Future of Energy Storage

An Interdisciplinary MIT Study

The Future of Energy Storage

AN INTERDISCIPLINARY MIT STUDY

Other reports in the MIT *Future of* series:

The Future of Nuclear Power (2003)

The Future of Geothermal Energy (2006)

The Future of Coal (2007)

Update to the Future of Nuclear Power (2009)

The Future of Natural Gas (2011)

The Future of the Nuclear Fuel Cycle (2011)

The Future of the Electric Grid (2011)

The Future of Solar Energy (2015)

The Future of Nuclear Energy in a Carbon-Constrained World (2018)



Copyright © 2022 Massachusetts Institute of Technology.

All rights reserved.

Incorporated in the cover art is a 3D concept illustration of battery cells, a form of electrochemical energy storage. © Getty Images

ISBN (978-0-578-29263-2)

Second version, published June 3, 2022.

Study participants

Study chair

Robert Armstrong

Chevron Professor, Department of Chemical Engineering, MIT
Director, MIT Energy Initiative

Study co-chair

Yet-Ming Chiang

Kyocera Professor, Department of Materials Science and Engineering, MIT

Executive director

Howard Gruenspecht

Senior Energy Economist, MIT Energy Initiative

Study group

Fikile Brushett

Cecil and Ida Green Associate Professor, Department of Chemical Engineering, MIT

John Deutch

Institute Professor, Department of Chemistry, MIT

Seiji Engelkemier

PhD Student, Department of Mechanical Engineering, MIT

Emre Gençer

Research Scientist, MIT Energy Initiative

Robert Jaffe

Morningstar Professor of Science, Department of Physics, MIT

Paul Joskow

Elizabeth and James Killian Professor of Economics and Management, Department of Economics, MIT

Dharik Mallapragada

Research Scientist, MIT Energy Initiative

Elsa Olivetti

Esther and Harold E. Edgerton Associate Professor,
Department of Materials Science and Engineering, MIT
Co-Director, MIT Climate and Sustainability Consortium

Richard Schmalensee

Professor of Economics, Emeritus, Department of Economics, MIT
Dean and Howard W. Johnson Professor of Management, Emeritus, Sloan School of Management, MIT

Robert Stoner

Deputy Director for Science and Technology,
MIT Energy Initiative

Chi-Jen Yang

Former Visiting Researcher, MIT Energy Initiative

Contributing authors

Bjorn Brandtzaeg

Former Visiting Fellow, Sloan School of Management, MIT

Patrick Brown

Former Research Scientist, MIT Energy Initiative

Kevin Huang

Research Scientist, Department of Materials Science and Engineering, MIT

Johannes Pfeifenberger

Visiting Scholar, MIT Center for Energy and Environmental Policy Research

Research advisors

Francis O'Sullivan

Senior Lecturer, Sloan School of Management, MIT

Yang Shao-Horn

JR East Professor of Engineering, Department of Mechanical Engineering, MIT

Students and research assistants

Meia Alsup

MEng, Department of Electrical Engineering
and Computer Science ('20), MIT

Andres Badel

SM, Department of Materials Science
and Engineering ('22), MIT

Marc Barbar

PhD, Department of Electrical Engineering
and Computer Science ('22), MIT

Weiran Gao

PhD Candidate, Department of Chemical
Engineering, MIT

Drake Hernandez

SM, Technology and Policy ('21), MIT

Cristian Junge

MSc, Engineering and Management ('22), MIT

Thaneer Malai Narayanan

PhD, Department of Mechanical
Engineering ('21), MIT

Kara Rodby

PhD, Department of Chemical Engineering ('22), MIT

Cathy Wang

SM, Technology and Policy ('21), MIT

Advisory Committee

Linda Stuntz – Chair

Partner, Stuntz, Davis & Staffier, P.C.

Norman Bay

Partner, Willkie Farr & Gallagher LLP

Terry Boston

Strategic Partner, Acelerex

Mark Brownstein

Senior Vice President, Energy, Environmental Defense Fund

Judy Chang

Undersecretary of Energy, Massachusetts Office of Energy and Environmental Affairs

Manlio Coviello

President, Terna Plus

George Crabtree

Director, Joint Center for Energy Storage Research (JCESR), Argonne National Laboratory

Philip Deutch

Founder and CEO, NGP Energy Technology Partners III

Julien Dumoulin-Smith

Managing Director and Head of U.S. Power, Utilities, and Alternative Energy Research, Bank of America Securities

Elizabeth E. Endler

Senior Principal Science Expert (Electrification, Integration, and Storage) and Principal Technology Advisor – Electric Power, Shell International Exploration & Production

Andy Karsner

Co-Founder, Elemental Labs

Arun Majumdar

Jay Precourt Provostial Chair Professor, Stanford University

Lucio Monari

Former Director, Infrastructure, Europe and Central Asia, World Bank

Pedro J. Pizarro

President and CEO, Edison International

John Podesta

Founder and Chair, Board of Directors, Center for American Progress

Praveer Sinha

CEO and Managing Director, Tata Power Co., Ltd.

Fredrick Støa

Investment Manager, Equinor Ventures, Equinor ASA

Ellen Williams

Distinguished University Professor, University of Maryland

While the members of the advisory committee provided invaluable perspective and advice to the study group, individual members may have different views on one or more matters addressed in the report. They are not asked to individually or collectively endorse the report findings and recommendations.



Table of contents

| | |
|--|-----|
| Foreword and acknowledgments | ix |
| Executive summary | xi |
| Chapter 1 – Introduction and overview | 1 |
| Chapter 2 – Electrochemical energy storage | 15 |
| Chapter 3 – Mechanical energy storage | 67 |
| Chapter 4 – Thermal energy storage | 113 |
| Chapter 5 – Chemical energy storage | 147 |
| Chapter 6 – Modeling storage in high VRE systems | 171 |
| Chapter 7 – Considerations for emerging markets and developing economies | 233 |
| Chapter 8 – Governance of decarbonized power systems with storage | 271 |
| Chapter 9 – Innovation and the future of energy storage | 291 |
| Appendices | |
| Appendix A – Cost and performance calculations for electrochemical energy storage technologies | 301 |
| Appendix B – Cost and performance calculations for thermal energy storage technologies | 319 |
| Appendix C – Details of the modeling analysis for high-VRE systems with energy storage in three U.S. regions | 327 |
| Appendix D – Details of the modeling analysis for developing country markets | 349 |

| | |
|----------------------------|-----|
| Acronyms and abbreviations | 367 |
| List of figures | 369 |
| List of tables | 373 |
| Glossary | 376 |

Foreword and acknowledgments

The Future of Energy Storage study is the ninth in the MIT Energy Initiative's *Future of* series, which aims to shed light on a range of complex and vital issues involving energy and the environment. Previous studies have focused on the role of technologies such as nuclear power, solar energy, natural gas, geothermal, and coal (with capture and sequestration of carbon dioxide emissions), as well as systems such as the U.S. electric power grid. Central to all these studies is understanding the role these particular technologies can play in both decarbonizing global energy systems and meeting future energy needs. Energy storage will play an important role in achieving both goals by complementing variable renewable energy (VRE) sources such as solar and wind, which are central in the decarbonization of the power sector.

The study will prove beneficial for a wide array of global stakeholders in government, industry, and academia as they develop the emerging energy storage industry and consider changes in planning, oversight, and regulation of the electricity industry that will be needed to enable greatly increased reliance on VRE generation together with storage. The report is the culmination of more than three years of research into electricity energy storage technologies—including opportunities for the development of low-cost, long-duration storage; system modeling studies to assess the types and roles of storage in future, deeply-decarbonized, high-VRE grids in both U.S. regions and emerging market, developing economy countries; and implications for electricity system planning and regulation.

The study was guided by a distinguished external Advisory Committee whose members dedicated a significant amount of their time to participate in multiple meetings; to comment on our preliminary analysis, findings, and recommendations; and to make available experts from their own organizations to answer questions and contribute to the content of the report. We would especially like to acknowledge the wise and able leadership of the Committee's Chair, Linda Stuntz. The study is certainly better as a result of this thoughtful, expert input. However, the study is the responsibility of the MIT study group; the Advisory Committee members do not necessarily endorse all of its findings and recommendations, either individually or collectively.

The Future of Energy Storage study gratefully acknowledges our sponsors: Core funding was provided by The Alfred P. Sloan Foundation and The Heising-Simons Foundation. Additional support was provided by MIT Energy Initiative members Shell and Equinor. As with the Advisory Committee, the sponsors are not responsible for and do not necessarily endorse the findings and recommendations. That responsibility lies solely with the MIT study group.

This study was initiated and performed within the MIT Energy Initiative. Alexandra Goodwin, Senior Administrative Assistant at MITEI, provided support to both the study team and the Advisory Committee. Special thanks are due to the MITEI events team, specifically to Carolyn Sinnes, Administrative Assistant; Debi Kedian, Events Manager; and

Kelly Hoarty, Events Planning Manager, for their skill and dedication. Thanks also to MITEI communications team members Jennifer Schlick, Digital Project Manager; Kelley Travers, Communications Specialist; Turner Jackson, Communications Assistant; and Tom Melville,

Communications Director. Additional thanks to Martha Broad, MITEI Executive Director, for her vital role in bringing the study to fruition. Finally, we thank Marika Tatsutani for editing the report with great skill and dedication.

Executive summary

This interdisciplinary MIT study examines the important role of energy storage in future decarbonized electricity systems that will be central to the fight against climate change. Deep decarbonization of electricity generation together with electrification of many end-use activities is necessary to limit climate change and its damages. Wind and solar generation—which have no operating carbon dioxide emissions, have experienced major cost reductions, and are being deployed at scale globally—are likely to provide a large share of future total generation. Unlike traditional generators, the output from these variable renewable energy (VRE) resources depends on weather conditions, which sometimes change rapidly; thus, VRE generators cannot be dispatched to follow variations in electricity demand. Electricity storage, the focus of this report, can play a critical role in balancing electricity supply and demand and can provide other services needed to keep decarbonized electricity systems reliable and cost-effective. As we discuss in this report, energy storage encompasses a spectrum of technologies that are differentiated in their material requirements and their value in low-carbon electricity systems. As electricity grids evolve to include large-scale deployment of storage technologies, policies must be adjusted to avoid excess and inequitable burdens on consumers, to encourage electrification for economy-wide decarbonization, and to enable robust economic growth, particularly in emerging market developing economy countries. Social justice and equity must be included in system design. The time horizon for this study is 2050, consistent with previous *Future of* studies in this series, though we are also interested in technologies that can be deployed at scale in the nearer timeframe of 2030.

Energy storage enables cost-effective deep decarbonization of electric power systems that rely heavily on wind and solar generation without sacrificing system reliability.

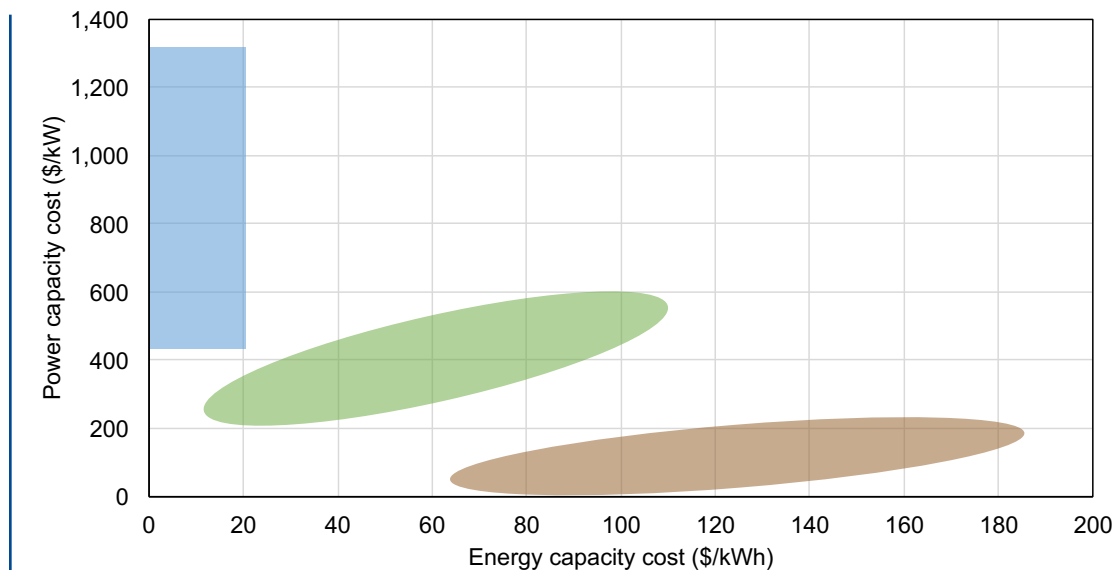
Assuming favorable cost reduction trends for VRE technologies continue, the modeling analysis conducted for this study identifies cost-effective pathways for decarbonizing electricity systems—reducing emissions by 97%–99% relative to 2005 levels in the United States, for example—while maintaining grid reliability. Efficient decarbonization will require substantial investments in multiple energy storage technologies, as well as in transmission, clean generation, and demand flexibility. If “negative emissions” technologies—that is, technologies for removing carbon dioxide from the atmosphere—become available, they can provide emissions offsets that enable small amounts of natural gas generation to be part of a cost-effective net-zero electricity system.

Energy storage basics

Four basic types of energy storage (electrochemical, chemical, thermal, and mechanical) are currently available at various levels of technological readiness. All perform the core function of making electric energy generated during times when VRE output is abundant and wholesale prices are relatively low available at times when VRE output is scarce and wholesale prices are relatively high. This flexibility provides a range of benefits to power systems.

An energy storage facility can be characterized by its maximum instantaneous *power*, measured in megawatts (MW); its *energy* storage capacity, measured in megawatt-hours (MWh); and its *round-trip efficiency* (RTE), measured as the fraction of energy used for charging storage

Figure ES.1: Three groups of storage technologies based on power- and energy-capacity costs



The blue region, with high power and low energy capacity costs, includes thermal, chemical (e.g., hydrogen), metal-air battery, and pumped hydro storage technologies. Lithium-ion batteries fall in the brown area, with low power, but high energy-capacity costs; flow batteries fall in the intermediate, green region. In addition to the two parameters displayed in this figure, other cost and performance attributes, e.g., charge and discharge efficiencies, are also important when comparing storage technologies within and across each class. The full set of characteristics used in system modeling are discussed in Chapter 6.

that is returned upon discharge. The ratio of energy storage capacity to maximum power yields a facility's storage *duration*, measured in hours—this is the length of time over which the facility can deliver maximum power when starting from a full charge. Most currently deployed battery storage facilities have storage durations of four hours or less; most existing pumped storage hydro (PSH) facilities have durations of eight to twelve hours or more. Storage technologies also differ in energy density, which is the maximum amount of energy that can be stored per unit volume. Battery technologies with high energy density are particularly well-suited for use in electric vehicles (EVs) and mobile electronics; technologies with lower energy density can nonetheless be used for storage in electricity system applications where the efficient use of space is generally less important. Energy storage technologies also differ in other attributes,

including the extent of facility-specific scale economies (geographical footprint, modularity) and the extent to which their performance degrades with use.

The technologies considered in this report fall into three main groups based on their power and energy capacity costs (Figure ES.1). Generally, technologies with low energy-capacity costs and high power-capacity costs (the blue area in the figure) are most suitable for longer duration storage applications (up to multiple days) and less frequent charge-discharge cycles; these include thermal, chemical, metal-air battery, and pumped hydro storage options. Technologies in the brown area, including lithium-ion batteries, are better suited to shorter duration applications (a few hours) and more frequent cycling. Technologies with intermediate capabilities, including flow batteries, are in the green area.

Electricity system storage technologies

The study examines electricity-to-electricity storage technologies in four categories: electrochemical, thermal, chemical, and mechanical. We do not catalog, let alone evaluate, all options within each of these categories; rather, we focus on examples of storage technologies in each category and seek to highlight issues that apply across a broad set of technologies within these categories. Some of the technologies we consider, such as lithium-ion batteries, pumped storage hydro, and some thermal storage options, are proven and available for commercial deployment. Others would require further research, development, and demonstration, and may not be commercially available at scale until the 2030s or 2040s. Table ES.1 summarizes our assessment of the availability of various storage technologies and storage-supporting technologies and practices in the near term (by 2030). All the technologies we consider in this report could be commercially available by 2050.

Successful innovation for energy and many other manufacturing-related technologies typically passes through five stages: idea creation → R&D → engineering at pilot scale → technology demonstration → deployment. Table ES.1 indicates the current stage of innovation for various storage technologies. The private sector has provided significant venture capital for storage technologies generally, and for lithium-ion batteries used in vehicles in particular. As discussed in this study, EV battery development has significantly improved prospects for short-duration electricity system storage. So far, long-duration storage technologies have not experienced similar help from other market drivers. While the value of long-duration storage (>12 hours) is low when VRE penetration is low, long-duration storage technologies clearly become more valuable as decarbonization requirements become more stringent and reliance on VRE generation grows. This is especially true if grid operators

are precluded from using natural-gas-fueled generation, with or without carbon capture and storage, to provide balancing capacity during extended supply troughs for VRE generation or during unusually high levels of demand due to extended extreme weather events. The value that long-duration storage could provide in a highly decarbonized electricity system argues for increased federal support of various kinds of long-duration storage options, depending on the stage of innovation different technologies have reached.

The current policy focus on relatively near-term decarbonization goals pushes both public and private attention toward downstream technology demonstration and deployment involving relatively mature technologies. The U.S. Department of Energy (DOE) can play a helpful role in this area, but its involvement should reflect two important lessons learned from past demonstration and deployment efforts. First, Congress should enable more joint technology demonstration projects with industry, unfettered by the Federal Acquisition Regulation and other rules that constrain technology development and demonstration on commercial terms. The purpose of public investment in technology demonstration and early deployment activity is to disseminate knowledge, which is inconsistent with policies such as requiring cost sharing in exchange for intellectual property rights.

Second, efforts to accelerate the deployment of any commercial technology should rely on incentives and mechanisms that reward success but do not interfere in project management. The Biden administration has proposed tax credits for a wide range of storage technologies, in addition to tax credits for transmission and various clean generation technologies, including wind and solar. In contrast to electricity generation technologies, where performance-based payments such as production tax credits can be directly linked to output measures,

Table ES.1: Summary of findings on the current innovation status of selected energy storage technologies

| Technology | Current innovation status | Chapter |
|---|---------------------------|----------|
| Electrochemical storage | | 2 |
| Li-ion batteries | (2) (4) (5) | 2 |
| Flow batteries (aqueous inorganic) | (2) (4) (5) | 2 |
| Flow batteries (aqueous organic) | (1) (2) (3) | 2 |
| NaS batteries | (4) (5) | 2 |
| Metal-air batteries | (2) (3) | 2 |
| Critical materials supply (metals and rare earths) | (1) (2) (3) | 2 |
| Battery re-cycling | (1) (2) (3) (4) | 2 |
| Battery second use | (1) (2) | 2 |
| Advanced power electronics | (2) (3) (4) | |
| Pumped hydro storage | (4) (5) | 3 |
| Thermal storage | (2) (3) (4) | 4 |
| Hydrogen | | 5 |
| Production, transport, storage | (1) (2) (4) | 5 |
| H ₂ generation—photoelectric, very high temperature gas reformation, advanced electrolysis | (2) | 5 |

- (1) Idea creation, study, and analysis—public and private sponsors
- (2) R&D—university, national laboratory, and private sector performers
- (3) Pilot scale engineering
- (4) Demonstration & testing
- (5) Deployment—depends upon progress and market conditions.

Further discussion is found in the chapters listed in the right column.

performance-based support for non-generation energy technologies such as storage must be based on preset development and operational testing measures.

Electrochemical storage

Electrochemical storage systems, which include well-known types of batteries as well as new battery variants discussed in this study, generally have higher energy density than mechanical and thermal storage systems, but lower energy density than chemical systems. Round-trip efficiency for battery storage ranges widely, from as much as 95% for lithium-ion (Li-ion) chemistries to as little as 40% for metal-air chemistries. A compact footprint and independence from hydrological and geological resources make batteries a versatile and highly scalable technology that can be sized for a range

of applications, from power plants down to residential uses. Our study yields several key takeaways.

Lithium-ion batteries possess high energy density, high power density, and high roundtrip efficiency, facilitating their near-ubiquitous use in electric vehicles and their widespread use in short-duration (typically 4 hours or less) electricity system storage applications. The dominant role of Li-ion batteries in the rapidly growing EV market has attracted significant investment from the private sector and is supporting rapid expansion of battery manufacturing capacity in the United States (currently most of this investment is coming from foreign firms). Cost and limits on the availability of key materials currently used in battery manufacture have set a floor on

Li-ion battery costs and may constrain future deployment, inspiring a shift toward chemistries that use more earth-abundant elements. Other advances being vigorously pursued for Li-ion battery components will also support cost and performance improvements. With these trends, Li-ion batteries will continue to be a leading technology for EVs and for short-duration storage, but their storage capacity costs are unlikely to fall low enough to enable widespread adoption for long-duration (> 12 hours) electricity system applications.

To enable economical long-duration energy storage (> 12 hours), the DOE should support research, development, and demonstration to advance alternative electrochemical storage technologies that rely on earth-abundant materials. Cost, lifetime, and manufacturing scale requirements for long-duration energy storage favor the exploration of novel electrochemical technologies, such as redox-flow and metal-air batteries that use inexpensive charge-storage materials and battery designs that are better suited for long-duration applications. While several novel electrochemical technologies have shown promise, remaining knowledge gaps with respect to key scientific, engineering, and manufacturing challenges suggest high value for concerted government support. Innovation in these technologies is being actively pursued in other countries, notably China.

Thermal energy storage

Thermal energy storage (TES) has attributes suitable for long-duration storage including the ability to store heat effectively in low-cost materials. This report discusses several generic TES strategies that reflect varying degrees of technology readiness.

One possible near-term TES approach focuses on reducing the cost of converting heat to electric power, the main component of overall

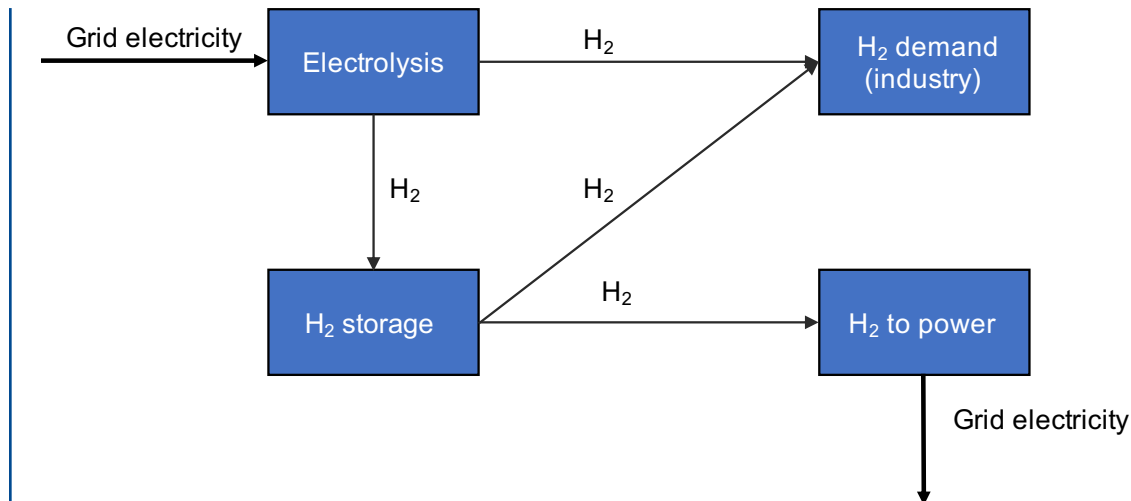
TES system cost, by reusing steam turbines at existing power plants and adding thermal storage and new steam generators in place of existing fossil-fuel boilers. This retrofit can be done today using commercially available technologies, and it may be attractive to plant owners and local communities as a way to use assets that would otherwise be abandoned as electricity systems decarbonize.

Chemical energy storage: Hydrogen

Hydrogen is widely considered a leading chemical energy storage medium because it can be directly produced from electricity in a single step and consumed either as a fuel to produce power or as a feedstock or heat source for other industrial processes. We focus on hydrogen in this chemical storage section.

Hydrogen's role as a form of energy storage for the electricity sector will likely depend on the extent to which hydrogen is used in the overall economy, which in turn will be driven by the future costs of hydrogen production, transportation, and storage, and by the pace of innovation in hydrogen end-use applications. Hydrogen is currently produced, transported, and sold as a feedstock for numerous industrial processes. Today, the dominant technology for hydrogen production relies on fossil fuels and produces carbon emissions. The ability to produce low-carbon hydrogen by splitting water (also known as electrolysis) using low-carbon grid electricity can support decarbonization in end-use sectors such as industry and transportation, as well as in the power sector. Figure ES.2 shows how hydrogen produced via electrolysis can serve as a low-carbon fuel for industry as well as for electricity generation during periods when VRE generation is low. Use of electrolyzers as a dispatchable load for the power system could also reduce the costs of power system decarbonization by increasing capacity utilization of VRE resources.

Figure ES.2: Illustration of cross-sector (power-industry) coupling of hydrogen



Coupling leads to cost reductions through increased utilization of variable renewable energy assets and operation of electrolyzers as dispatchable loads.

We support the effort that the DOE is leading to create a national strategy that addresses hydrogen production, transportation, and storage. In particular, the ability of existing natural gas transmission pipelines to carry hydrogen without suffering embrittlement, either at reduced pressures or if hydrogen is blended with natural gas or other compounds, remains an open question that deserves government-supported study by the DOE and the U.S. Department of Transportation. An important step in this direction is the call in recent legislation for the creation of at least four hydrogen hubs.

Mechanical storage

Electrical energy can be converted into various forms of mechanical energy such as gravitational potential energy and kinetic energy; electrical energy can also be used to compress a gas such as air. Some of these forms of mechanical energy are suitable for large-scale and long-duration energy storage. As a category, mechanical energy storage includes a wide variety of technologies. A common feature

of all these technologies, however, is that their energy density is much lower than the energy density of chemical or electrochemical storage technologies. Consequently, mechanical energy storage systems tend to have large footprints and require geologically favorable locations—thus, they are not well suited for use in small-scale facilities.

Pumped storage hydropower (PSH) stores energy in the potential energy of water pumped uphill. PSH is a mature, widely deployed technology that accounts for well over 90% of the functional grid-scale energy storage capacity that currently exists, both globally and in the United States. Yet, PSH deployment has significantly slowed in the United States and in many other countries since the 1990s (the notable exception is China). This trend reflects, among other factors, the reduced value of intraday energy arbitrage as a result of the increased use of flexible gas-fired generation. In addition, PSH projects have high initial costs and inflexible sizing and siting requirements; historically, these projects have also experienced long construction periods and major cost overruns.

While not strictly an electricity-to-electricity storage technology, existing conventional hydropower systems with storage reservoirs could play a larger role in balancing supply and demand in electricity systems that rely heavily on VRE generation. Where there is significant potential to play this role, system planners should consider options for increasing the amount of water that is held behind dams for use in balancing electricity systems.

Compressed air energy storage (CAES) systems store pressurized air in underground cavities or above-ground tanks; some CAES systems also store the heat that is generated when the air is compressed. This technology has been widely discussed as a potential grid-scale energy storage option, but it faces significant hurdles to deployment at scale. Although cost estimates for CAES are subject to multiple uncertainties, estimates of energy cost for this technology are generally higher than estimates for other energy storage technologies that are expected to be available in the future.

Co-locating energy storage systems with existing power plants that are being retired could reduce storage costs by enabling the reuse of existing grid interconnections and, in some cases, other power plant components. Using existing interconnections would save time as well as cost. In addition, as noted above, existing turbines can be reused in thermal storage systems that repower existing turbines using zero-emissions heat or fuel. The DOE should investigate the cost and system impacts of thermal storage technologies and other options that offer promise for reusing existing assets, as well as the social acceptance of such reuse strategies by neighboring communities, and should sponsor demonstration projects where appropriate.

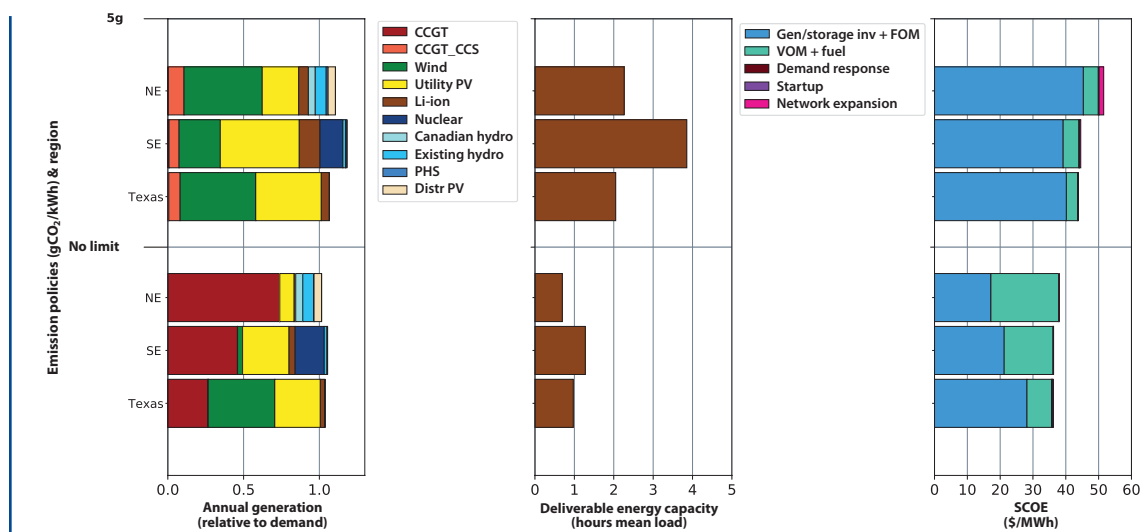
Efficient high-VRE electricity systems with storage: Modeling results and implications for governance and policy

This section examines potential roles for storage in a developed country context and in an emerging market developing economy country context. These two country contexts are illustrated by results for three different regions in the U.S. and for India, respectively.

Modeling results for a developed country: Three U.S. regions

Our modeling for the U.S. power sector focused on three regions: the Northeast (New York and New England), the Southeast, and Texas for largely “greenfield” systems in 2050. These regions differ significantly in their electricity demand profiles, wind and solar resources, and availability of hydropower and existing nuclear resources. These differences affect both the least-cost generation mix in the absence of emissions constraints and the cost of achieving different degrees of decarbonization. Figure ES.3 shows modeled projections for annual generation, deliverable energy capacity, and system cost of electricity for each region in 2050 under two policy scenarios: no carbon constraint and emissions constrained to 5 grams of carbon dioxide per kilowatt-hour (gCO_2/kWh). If 2050 electricity demand remains the same as the 2018 level, then reducing the average carbon intensity of the U.S. power sector to 5 gCO_2/kWh would lower 2050 emissions by 99.2% relative to 2005. On the other hand, if electricity use grows such that demand in 2050 is greater than in 2018, as projected in the electricity demand scenario used to model energy storage impacts for this study (Mai et al. 2018), a U.S. sector-wide average carbon intensity of 5 gCO_2/kWh would deliver a 98.7% reduction in power sector emissions relative to 2005. The illustrative results in Figure ES.3 are from scenarios that assume only Li-ion battery and pumped hydro storage

Figure ES.3: Annual generation relative to demand



Annual generation relative to demand, deliverable energy capacity from storage (measured in hours of discharge at mean load), and system average cost of electricity (SCOE) in the Northeast (NE), Southeast (SE), and Texas in 2050. Modeling results are shown for a scenario with no limit on emissions (bottom half of each chart) and for a policy scenario with an emissions intensity limit of 5 gCO₂/kWh (top half of each chart) (note that the policy scenario assumes decarbonization to a level that reduces U.S. power sector emissions by approximately 99% relative to 2005). SCOE includes total annualized investment; fixed O&M; operational costs of generation, storage, and transmission; and any non-served energy penalty. Emissions intensity under the “No Limit” policy case for each region is as follows: NE: 253 gCO₂/kWh, SE: 158 gCO₂/kWh, Texas: 92 gCO₂/kWh. For the Northeast region, “Wind” represents the sum of onshore and offshore generation. In this illustration, Li-ion batteries are the sole new technology deployed for energy storage purposes in the power sector. The full report discusses modeling results for a wide range of storage technologies, of which Li-ion batteries are only one example. PHS = Pumped Hydro Storage. VOM = Variable O&M cost.

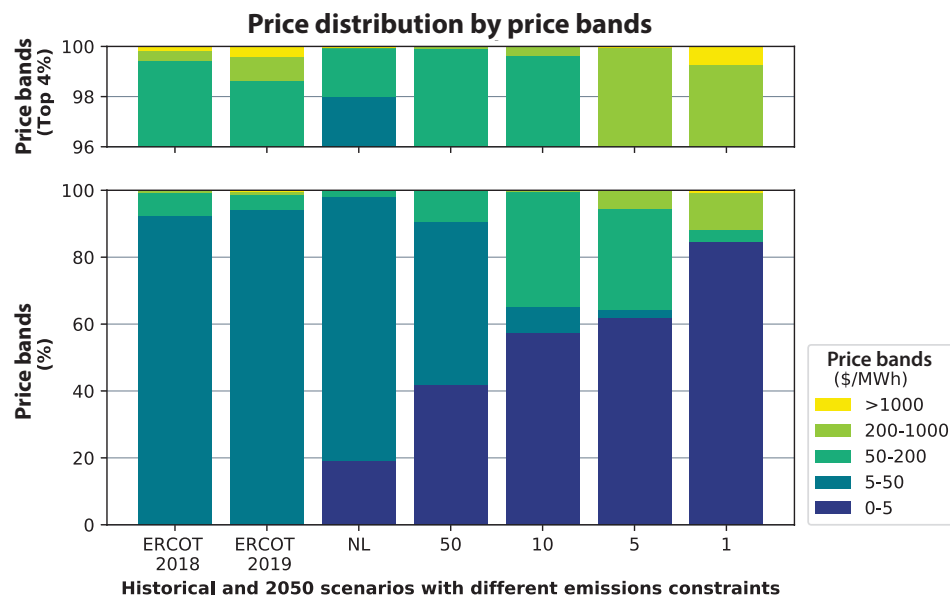
are available; our modeling of U.S. regions (discussed in Chapter 6) examines a wide range of other storage technologies.

The ability of storage technologies to substitute for, or complement, essentially all other elements of a power system (including generation, transmission, and demand response), coupled with uncertain climate change impacts on electricity demand and supply, means that more sophisticated analytical tools are needed to plan, operate, and regulate the power systems of the future and to ensure that these systems are reliable and efficient. Important focus areas include system stability and dispatch (including enabling the participation and compensation of distrib-

uted storage and generation (PV) assets in system dispatch and wholesale markets), resource adequacy, and retail rate design. The development of new analytical tools must be accompanied by additional support for complementary staffing and upskilling programs at regulatory agencies. This effort should be led by the DOE in cooperation with independent system operators and regional transmission organizations (ISOs/RTOs).

The distribution of hourly wholesale prices or marginal value of energy will change in deeply decarbonized bulk power systems, with many more hours of zero or very low prices and more hours of high prices compared to today’s wholesale markets.

Figure ES.4: Hourly marginal wholesale price of energy for Texas



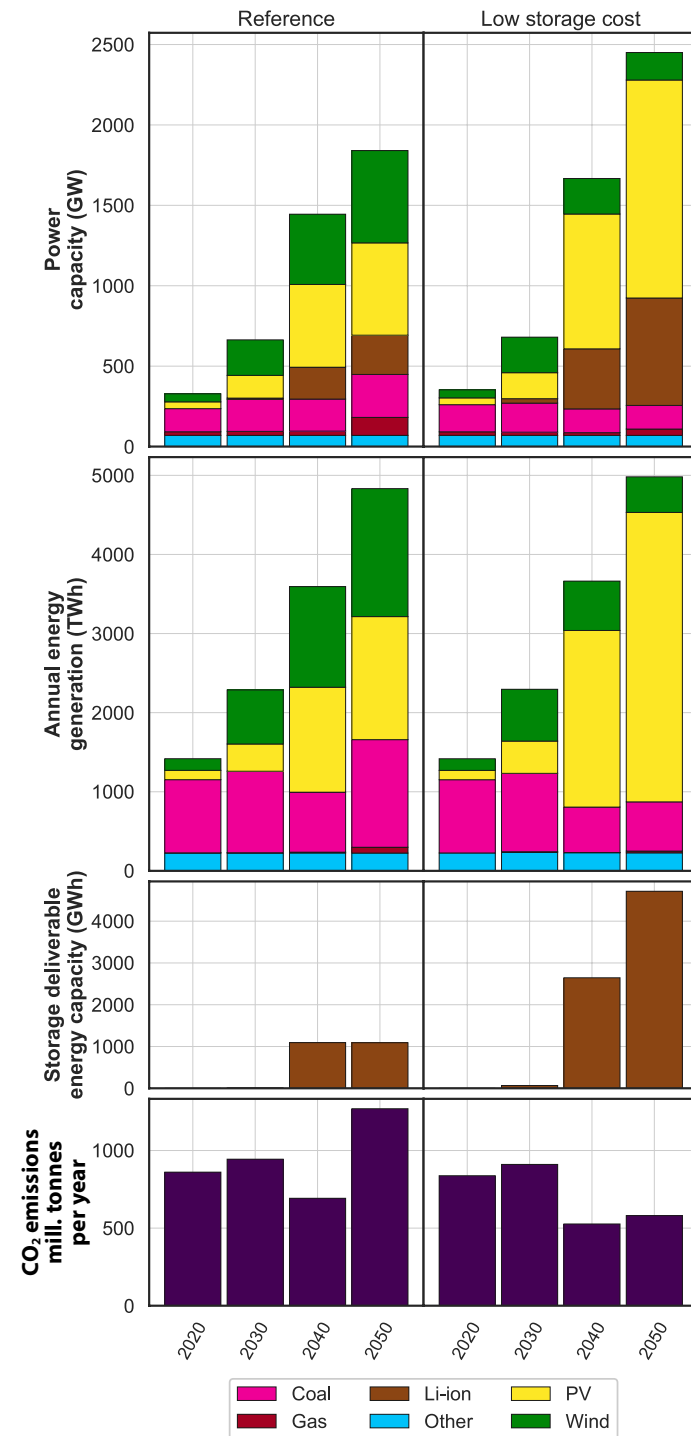
Hourly marginal wholesale price of energy for Texas under various emissions scenarios ranging from no limit (NL, 3rd bar from left) to 1 gCO₂/kWh (right-most bar). The price bands are based on the known marginal cost of various generation technologies; we zoom in on the top 4% of the price bands to show the price distributions at that extreme. Historical price distributions in ERCOT are shown for reference. For the purposes of this figure, we assume Li-ion battery storage only. The effect of including other storage technologies on these results is discussed in Section 6.3.4.

This is because VRE-dominant bulk power systems with storage will have relatively high fixed (capital) costs and relatively low marginal operating costs compared to today's bulk power systems, which largely rely on thermal generators. Figure ES.4 compares the distribution of historical hourly wholesale electricity prices for 2018 and 2019 in the ERCOT system, which covers nearly all of the state of Texas, with 2050 scenarios. Bars represent the distributions of prices for the no-limit and carbon-constrained Texas modeling cases. Increased reliance on VRE generation, with zero marginal cost, greatly increases the percentage of hours when prices, represented by marginal system costs in our modeling, are under \$5 per MWh. This effect increases as the carbon constraint becomes more stringent (i.e., allowable emissions are ratcheted down). During the highest-price hours, shown at the top of the bars and in the

exploded section of the figure, modeled prices are significantly above those in the present ERCOT market.

The combination of relatively high capital costs and many more hours when prices are very low will create financing challenges for both VRE generation and storage, particularly since regulators will likely continue to cap (as they do at present) extremely high prices that could otherwise support cost recovery. Future patterns of wholesale electricity prices and the goal of decarbonizing other sectors through electrification with decarbonized electricity also reinforces the benefit of adopting retail pricing and retail load management options that reward all consumers for shifting electricity uses away from times when high wholesale prices indicate scarcity to times when low wholesale prices signal abundance.

Figure ES.5: Impact of Li-ion storage cost projections on cost-optimal bulk power system evolution in India



Installed capacity (1st row), annual energy generation (2nd row), storage energy capacity (3rd row), and annual CO₂ emissions (4th row). Results in the left column are for a reference case, which uses a mean estimate for future Li-ion battery capital costs. The right column assumes a low-cost trajectory for future Li-ion battery capital costs.

Transmission expansion, which allows for increased VRE deployment in locations with higher-quality VRE resources and improves VRE integration by balancing resource intermittency across connected areas and smoothing the effects of geographical differences in VRE supply and demand, is also important for cost-effective decarbonization. The current likelihood that cost-effective transmission projects to bring generation from areas with high-quality VRE resources to major load centers will face extended delays or possible rejection suggests the need for statutory and regulatory changes to reduce barriers to transmission expansion. A shortfall in new transmission capacity may lead to a larger role for storage as well as higher costs in future decarbonized electricity systems.

Modeling results for an emerging market, developing economy country: India

Coal-dependent emerging market and developing economy countries that lack access to abundant low-cost gas or gas infrastructure, such as India, represent a very large and important future market for electricity-system applications of energy storage technologies. Modeling for this study suggests that energy storage will be deployed predominantly at the transmission level, with important additional applications within urban distribution networks. Overall economic growth and, notably, the rapid adoption of air conditioning will be the chief drivers of energy storage deployment. Assuming continued technology cost declines, we find that VRE generation and storage compete favorably with new coal from a cost standpoint in India over the medium and long term, but existing coal plants linger absent carbon pricing, as shown on the left panel of Figure ES.5.

Modeling results for a scenario that assumes the availability of low-cost storage and VRE generation technology in India are shown in the right panel of Figure ES.5. These results point to significant reductions in both system cost¹ and modeled carbon dioxide emissions from India's electricity system relative to baseline projections (captured in the left panel). Reductions in system cost and CO₂ emissions occur whether or not there are caps or taxes on carbon emissions. This result highlights the global environmental benefit of lower costs for electricity storage.

Additional study

Several storage-related topics beyond those addressed in this study deserve attention.

These include: (1) manufacturing and supply chain trends, and their impacts in terms of the availability and cost of energy storage technologies and U.S. competitiveness; (2) the relationship between the stability of an economic and regulatory policy framework for economy-wide decarbonization and the time required to achieve a net-zero-carbon electricity sector; (3) the establishment of expectations for recycling and reuse for end of life batteries; (4) identification of environmental, health, and safety aspects of specific electricity storage systems; and (5) the practically available scope for load flexibility and demand response to reduce grid storage needs and associated costs.

References

- Mai, T., P. Jadun, J. Logan, C. McMillan, M. Muratori, D. Steinberg, L. Vimmerstedt, R. Jones, B. Haley, B. Nelson. (2018). *Electrification Futures Study: Scenarios of Electric Technology Adoption and Power Consumption for the United States*. Golden, CO: National Renewable Energy Laboratory.

¹ The resulting average system costs of electricity in 2040 and 2050 are reduced by 22% and 39%, respectively.



Chapter 1 – Introduction and overview

1.1 Motivation and focus

This study is the latest in a series of *Future of* studies produced by the MIT Energy Initiative that aims to provide useful references for decision makers and balanced, fact-based recommendations to improve public policy, particularly in the United States. Earlier studies in this series have considered the futures of nuclear power, coal (with capture and sequestration of carbon dioxide emissions), natural gas, the electric grid, and solar energy—all major features in today’s energy landscape. These studies have in common a focus on the role that a specific technology (or infrastructure, in the case of the electric grid) might play in an economically efficient, carbon-constrained world and a focus on what needs to be done to facilitate these contributions. The time horizon for these studies has been 2050 (and beyond); this study likewise uses a 2050 horizon, though we are also interested in technologies that can be deployed at scale in the nearer timeframe of 2030.

1.1.1 Motivation

This study considers the future of energy storage within the electric power system. Electric energy storage is certainly not new. The initial application of pumped hydroelectricity storage occurred in the late 19th century in Europe, and in 2020 pumped storage hydro still accounted for around 99% of total grid-scale electricity storage capacity in the United States and globally.¹ Global recognition of the need to mitigate damages from climate change by dramatically reducing economy-wide emissions of greenhouse gases, most importantly carbon dioxide (CO₂), is the root cause of increased interest and investment in energy storage.

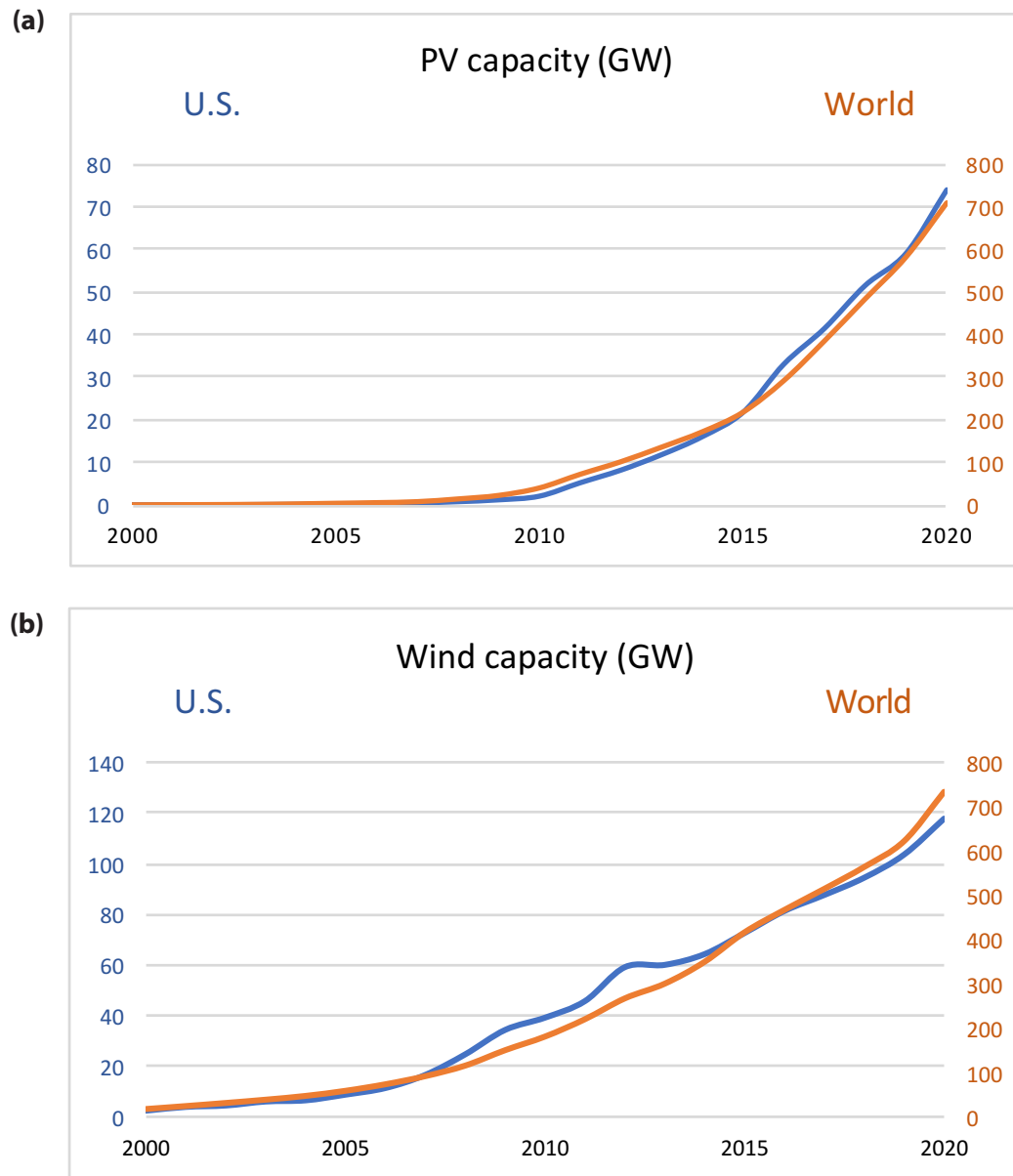
A variety of state, regional, national, and international targets and timetables for climate-change mitigation call for achieving net-zero CO₂ emissions or zero CO₂ emissions; timelines range from 2035 to 2050 and beyond. Net-zero emissions allows for the possibility of offsetting small amounts of emissions in future energy systems via negative emissions technologies (National Academies of Sciences, Engineering, and Medicine 2019), which remove CO₂ from the atmosphere and store it, whereas zero emissions targets do not allow for such offsets.

Achieving very low economy-wide CO₂ emissions will require all sectors to achieve significant reductions. Most studies conclude that the path to very low economy-wide emissions involves decarbonizing the power sector and substituting decarbonized electricity for fossil fuels as much as possible in transportation, industry, and buildings. The main focus of this study is the role that energy storage can play in decarbonizing the power sector in a cost-effective manner.

The most significant current and foreseeable change in the electricity sector is the rapid substitution of variable renewable energy (VRE)—i.e., wind and solar energy—for fossil fuels in electricity generation. Figure 1.1 illustrates historical growth rates for wind and solar generating capacity in the United States and globally. Rapid growth of these technologies has been accompanied by cost reductions, as shown in Figure 1.2 for the United States. Similar cost trends have been observed globally. Both capacity expansion and cost reductions for VRE resources are generally expected to continue.

¹ Measured in terms of power capacity (megawatts) rather than energy capacity (megawatt-hours), pumped hydro accounted for roughly 87% and 90% of U.S. and global storage, respectively, in 2020.

Figure 1.1 U.S. and global installed capacity of (a) solar and (b) wind generation

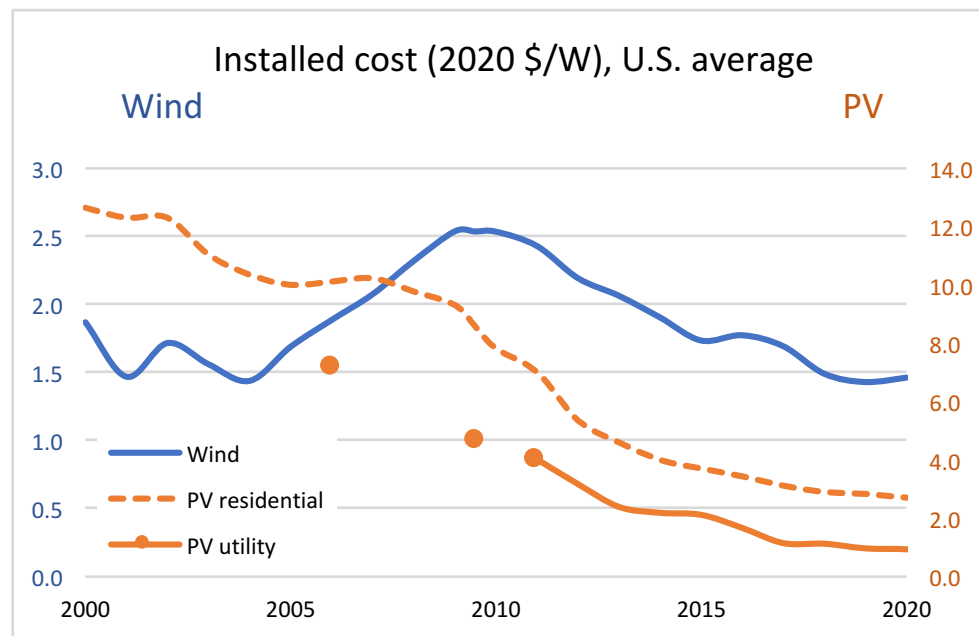


Source: BP (2021).

Increased penetration of VRE generation makes storage more attractive because VRE generation is intermittent: Its output is variable over time and imperfectly predictable. One approach to coping with intermittency is to use storage to perform energy arbitrage—that is, to move electric energy availability from times when it is abundant (lower price) to times when it

is scarce (higher price). At the same time as the penetration of VRE generation has grown, the cost of lithium-ion (Li-ion) batteries has declined rapidly, as shown in Figure 1.3. This cost reduction is due primarily to increasing electrification of light-duty vehicles in the transportation sector and the use of Li-ion batteries in mobile consumer electronics.

Figure 1.2 Installed cost of solar and wind generation in the United States as a function of time



Wind data: U.S. Department of Energy (2021); solar data: Feldman et al. (2012); Ramasamy et al. (2021). Utility PV data are for fixed tilt installations. The solid line for PV represents available yearly data; the discrete points capture data not available on a yearly basis.

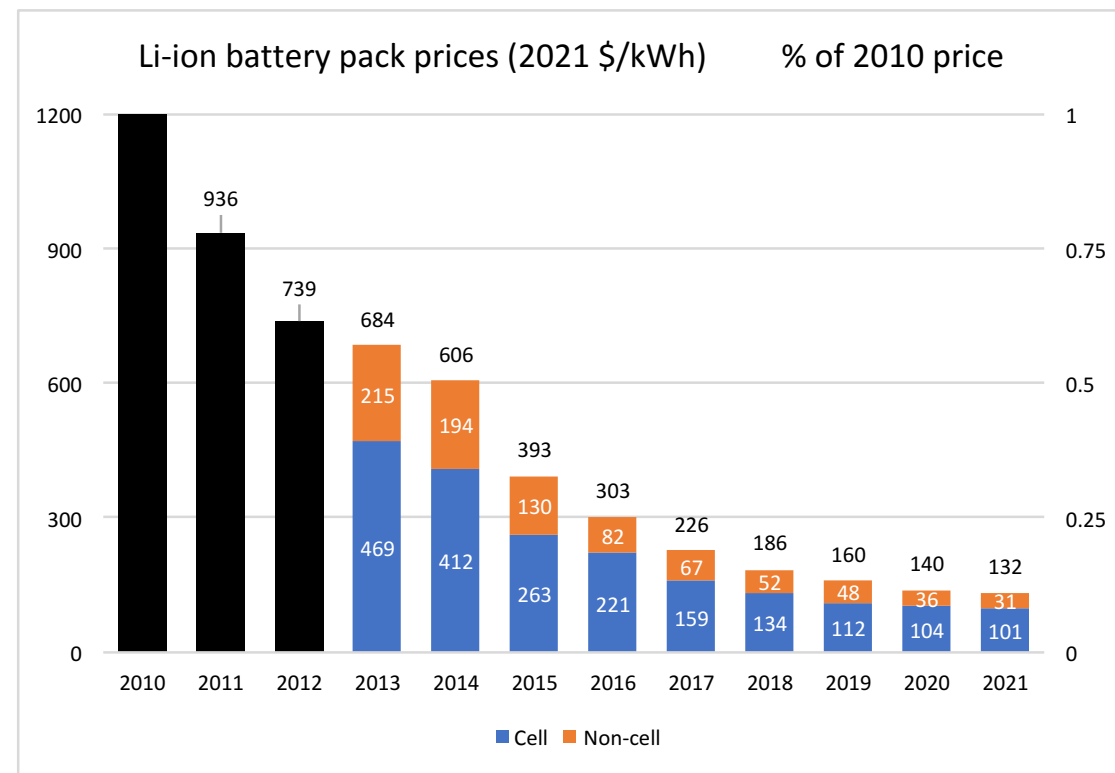
Demand for these batteries for storage in the electricity sector has been quite small relative to demand in these other two areas (Figure 1.4), but deployment of Li-ion batteries in the electricity sector has become more attractive and has increased rapidly in the last several years.

Recent years have also seen advances in a range of storage technologies, including new chemistries for lithium-ion batteries that aim to improve performance and reduce dependence on elements with constrained supply chains. In addition, new approaches to thermal storage for electricity and chemical storage (for example, via the production and storage of hydrogen that can be used to generate electricity), suggest that these may be useful additions to the suite of technologies for electricity system storage. This study finds that a wide range of storage technologies, at different stages of technological

readiness, show promise as economical means of coping with VRE intermittency.

As Chapter 6 discusses in detail, deployment of storage is only one tool to cope with VRE intermittency efficiently. For example, it may be optimal to build sufficient VRE capacity to meet more than 100% of demand on average. As a consequence of such “overbuilding,” VRE generation could meet most demand even when VRE resources are low (for example, during the wintertime for solar), but at other times VRE generation would substantially exceed demand and would need to be curtailed. Transmission expansion can also alleviate some variability in VRE resources by averaging VRE generation over larger geographical regions. Advances in clean, dispatchable generation, such as geothermal or biomass, may obviate the need for at least some storage. In addition, increasing the ability of businesses and

Figure 1.3 Global Li-ion battery prices for 2010–2021



Source: Bloomberg New Energy Finance (2021).

households to shift electricity demand from times when energy is scarce (and prices are high) to other times, or to curtail electricity use entirely in periods of energy scarcity, will facilitate VRE integration. Finally, advances in negative emissions technologies may provide economical offsets to facilitate reaching net-zero emissions while allowing some fossil fuel generation to firm up VREs. Natural gas generation with less than 100% complete carbon capture and sequestration (CCS) is a prime example of a technology that would benefit from economical offsets.

1.1.2 Focus of the study

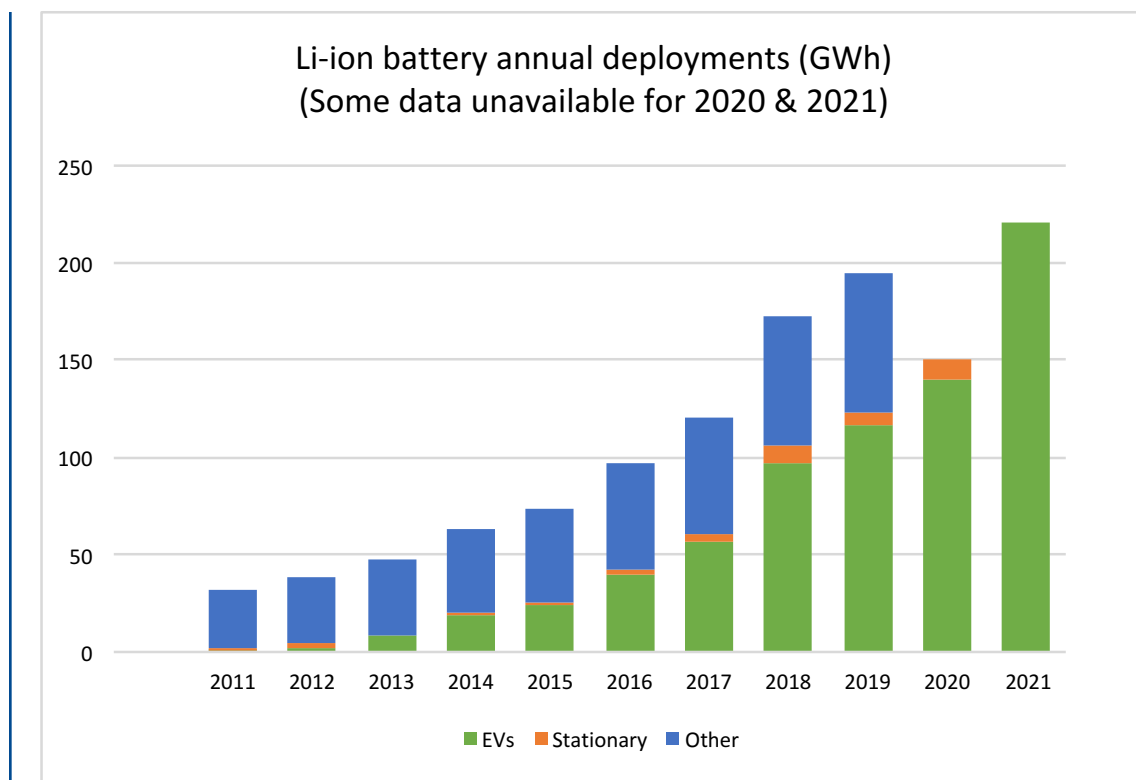
In this study, we limit our focus to future opportunities for storage within the electricity sector. That is, we include only storage that takes in electrical energy, stores that energy in a

variety of forms, and then returns the stored energy to the electricity system as electricity. Examples of technologies we discuss in detail are lithium-ion batteries, redox flow batteries, metal-air batteries, pumped hydroelectric storage, heat pumps, and hydrogen storage.

As noted above, the cost declines that lithium-ion batteries have enjoyed are largely due to their development and use outside the electricity system, particularly in electric vehicles (EVs). This study looks at potential benefits from similar cross-sector couplings for two other storage technologies: thermal energy storage and hydrogen storage.

Although we study the use of heat as a mechanism for storing electricity, heat is used widely beyond electricity generation. In the industrial sector, high-temperature heat is important for

Figure 1.4 Global deployment of Li-ion batteries over the period 2011–2021 for electric vehicles and energy storage in the electricity sector



Sources: U.S. Department of Energy (2020); Kane (2021b); Kane (2021a); Wehling and Abraham (2021). For 2021, EV data were not available for the full year; the number shown is obtained by applying the percent increase that occurred during the first half of the year to the second half of the year.

core processes such as iron and steel manufacturing, cement making, and chemical and refining operations. In the buildings sector, heat is needed for space temperature conditioning and hot water. Storing the heat that is produced for thermal power generation—or by transforming electricity into heat—can be very cost-effective in cross-sectoral applications, allowing more efficient use of thermal generation resources such as nuclear, fuel, geothermal, and VRE (via resistance heating) by buffering the heat source from end use (in multiple sectors). This decoupling idea leads naturally to the thermal storage retrofit strategies for thermal power plants examined in Chapter 4. There is certainly a much broader scope for thermal storage beyond the boundaries of this study.

Hydrogen production and use also illustrates the potential importance of cross-sector interactions. A challenge for hydrogen in electricity applications is that, for the foreseeable future, the cost-efficient volume of hydrogen storage for the electricity sector is too small to drive significant reductions in the cost of producing hydrogen by using VRE-generated electricity to split water. In addition, hydrogen does not currently benefit from significant demand in other sectors in the same way that demand from transportation applications has benefitted Li-ion batteries. We therefore investigate whether the industrial sector, which might benefit from the availability of inexpensive hydrogen to replace natural gas as a high-temperature heat source, might play that role.

This study is aimed primarily at the U.S. electricity system. In our modeling work, we address geographic variations within the United States that might affect storage deployment in future power systems. This diversity derives from regional variations in VRE and other resources; from public attitudes towards different generation options, land use, and siting for transmission; from the nature of the demand for electricity; and from different regional policies and approaches to decarbonization. Lessons learned from regional studies in the U.S. context can be useful in informing possible roles for electricity storage in future energy systems in other parts of the world. We look specifically at opportunities in the Indian context, which differs from the U.S. situation in a number of important ways, particularly in the lack of a significant domestic supply of natural gas and in very rapid growth in electricity demand.

A number of storage-related topics beyond those addressed in this study deserve attention in other work: (1) manufacturing and supply chain trends, and their impacts on the availability and cost of storage and U.S. competitiveness; (2) the relationship between the stability of an economic and regulatory policy framework for economy-wide decarbonization and the time and cost required to achieve a net-zero-carbon electricity sector; (3) the need to establish expectations for end-of-life recycling and/or reuse for batteries; (4) identification of environmental, health, and safety aspects of specific electricity storage systems; and (5) the practically available scope for load flexibility and demand response to reduce grid storage needs and associated costs.

1.2 Roles for storage in electricity systems

Energy storage services can broadly be classified in four categories: energy arbitrage, ancillary services, transmission and distribution infrastructure services, and customer energy

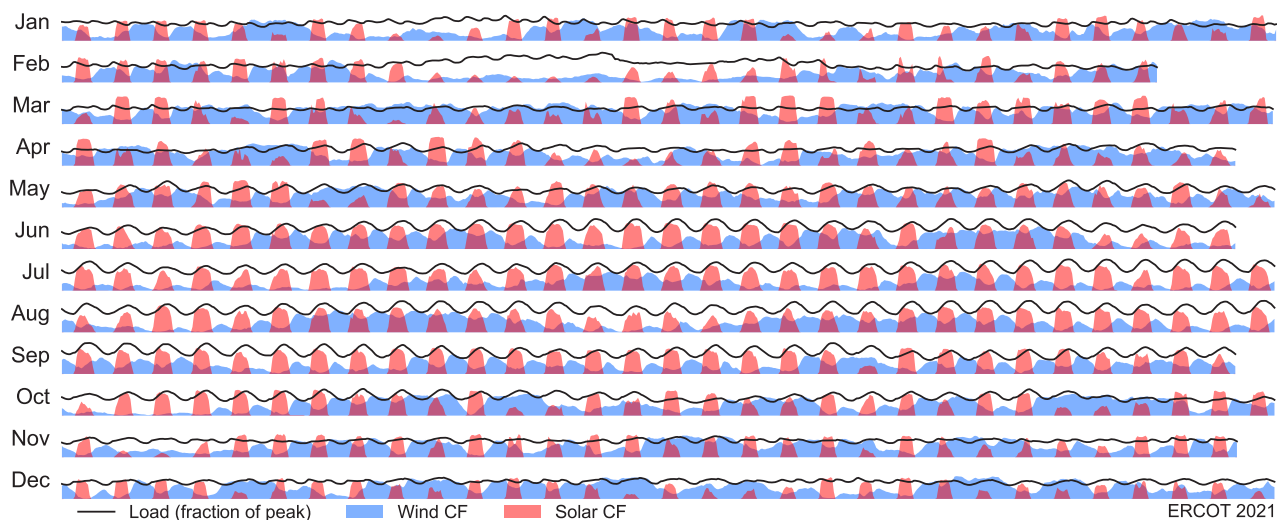
management services. This section provides definitions and examples of services that can be provided by storage (definitions are adapted from the International Energy Agency's *Technology Roadmap: Energy Storage* (2014)). In practical usage, a single energy storage technology or several storage technologies may support multiple services.

Energy arbitrage—defined as moving electrical energy from low-value to high-value periods—is the principal role for energy storage in the electricity system today and is likely to be its principal role going forward. Integration of intermittent VRE generation drives this opportunity, which will grow as VRE penetration increases. Figure 1.5 shows daily and seasonal variations in solar and wind resources and load for all of 2021 in ERCOT, the electricity system that covers most of Texas. Sometimes wind availability complements the solar resource from day to night (and vice versa), but there are extended periods, say the latter part of June into the beginning of July 2021, with minimal wind generation. This results in a significant potential gain from intraday shifting, today most often over a time span of 4 hours or less, as well as shifting across multiple days, over timespans of, say, greater than 12 hours. We examine multiple storage technologies to understand which ones will be suited for these short- and long-duration roles in future energy systems.

Energy storage assets that provide **ancillary services** to the bulk power system deliver power for short durations but require faster response times (from less than a second to minutes). These ancillary services include the following:

Frequency regulation is the use of storage to dampen fluctuations caused by momentary differences between power generation and load demand. This is often performed automatically on a minute-to-minute, or shorter, basis. In VRE-dominant systems, this function

Figure 1.5 Daily variability of wind and solar resources in Texas



Daily variability of wind (blue) and solar (red) resources in Texas relative to load (black line) in 2021.
Days of the month are in the columns and months of the year are in rows. CF = Capacity factor.
Source: Electric Reliability Council of Texas (2021).

replaces the inertia provided by spinning turbines in thermal generators.

Load following, similar to frequency regulation, is a continuous electricity balancing mechanism that manages system fluctuations. However, in this case, the time frame of the intervention is longer, ranging from 15 minutes to 24 hours.

Voltage support refers to the maintenance of voltage levels in the transmission and distribution system.

Black start capability refers to a power station's ability to restart without relying on the transmission network in the event of a wide-area power system collapse.

Supplemental reserves can supply extra power to the grid (historically from extra generating capacity) with a response time of less than 10 minutes (and sometimes meeting other requirements). These reserves can be used

to maintain system frequency stability during unforeseen load swings or emergency conditions (U.S. Department of Energy 2011).

Transmission and distribution (T&D)

infrastructure services help defer the need for capital-intensive T&D upgrades or investments to relieve temporary congestion or potential substation overloads in the T&D network.

These services, which work by injecting energy into the grid between the bottleneck and load during peak periods, turn out to be particularly important in the Indian context discussed in Chapter 7.

Customer energy management services

including enhanced reliability and reduction of peak loads, may be provided by relatively small storage systems located on customer premises. When managed by aggregators, these systems can also provide energy services at the bulk power level.

1.3 Key attributes, cost dimensions, technology classes, and environmental, health, and safety considerations for storage technologies

Electrical storage technologies considered in this study have a range of characteristics with respect to technological readiness, cost and performance, modularity, abundance and cost of component materials, energy storage density per unit of volume or weight, and environmental, health, and safety (EHS) impacts. Among these attributes (and others) we focus on cost characteristics, because cost will be a dominant factor in deployment at scale in the electricity system. Factors like energy density or efficiency at small scale matter much less in this sector than in EV or consumer electronics applications, for example. We expect that all the storage technologies included in our modeling could be ready for commercial deployment by 2050.

1.3.1 Cost dimensions and technology classes

It is useful to review the standard cost analysis of electric generation facilities as background for the more complex analysis of energy storage systems. The capacity of generating facilities is typically described by their maximum instantaneous power capacity, which is measured in megawatts (MW). To a first approximation, the cost of a generation plant has two components: the annualized capital cost per MW of capacity (including any annual costs that do not vary with generation) and the operating cost per megawatt-hour (MWh) of electric energy produced (including fuel, if any, plus any other annual costs that vary with generation).

Some analysts summarize technology-specific generation costs by using a quantity called the levelized cost of energy or LCOE.² Computing the LCOE for a particular thermal generation technology requires making assumptions about fuel cost and annual output profile for a typical facility. The LCOE can then be calculated as the average revenue per MWh produced that just covers a typical facility's capital and operating cost. It should be apparent that the LCOE cannot sensibly be used to compare the attractiveness of investments in thermal plants with very different output profiles: a nuclear plant that is run all the time to provide baseload power and a gas-fired plant that is used only to meet peak demand, for instance. For the same reason and because the value of VRE output depends on when the output occurs, using LCOE to compare VRE generators and thermal generators makes even less sense (Joskow 2011). We do not use LCOE in this study.

Describing storage facility costs is considerably more complex than describing generating facility costs. (Table 6.3 summarizes the storage cost assumptions used in modeling for this study.) Storage capacity has at least two and possibly three dimensions of capacity that can generally be independently varied. Like generating plants, one element of a storage facility's capacity is the maximum instantaneous power, measured again in megawatts (MW), that it can supply to the grid—in other words, its *discharge* power capacity. For some technologies, the maximum instantaneous power that a facility can take from the grid—also called its *charge* power capacity—can be different from its discharge power capacity. In addition, every storage facility can be characterized by its

² See U.S. Energy Information Administration (2021) for a general discussion of LCOE and LCOS. We share the EIA's conclusion that "LCOE and LCOS do not capture all of the factors that contribute to actual investment decisions, making direct comparisons of LCOE and LCOS across technologies problematic and misleading as a method to assess the economic competitiveness of various generation alternatives."

energy storage capacity, measured in megawatt-hours (MWh). The ratio of a facility's energy storage capacity to its maximum discharge power capacity is its *duration*, measured in hours: This is the length of time the facility can provide maximum power starting from a full charge. Most existing battery storage facilities currently have durations of four hours or less; most existing pumped storage hydro (PSH) facilities have durations of twelve hours or more.³

A facility's round-trip *efficiency* (RTE), defined as the fraction of energy used for charging storage that is available for discharge, is generally determined by the technology employed and does not vary with power or energy capacity. (It is sometimes useful to distinguish between a facility's *charge* (or *up*) power efficiency, the fraction of energy taken from the grid that ends up as useful charge, and its *discharge* (or *down*) power efficiency, the fraction of useful charge that can be discharged to the grid. The product of these two parameters is round-trip efficiency.) Finally, energy stored using some technologies is gradually lost over time. The rate at which this occurs is called the *self-discharge rate*.

Some analysts have summarized the costs of various storage technologies by computing a quantity called the leveled cost of storage (LCOS). To compute this quantity for a particular technology requires specifying the storage duration for a typical facility and making assumptions about charge/discharge cycles over time and the cost of the power used to charge the facility.⁴ To compute annual facility cost, operation and maintenance costs must be added to the annualized cost of capacity; these O&M costs may depend on

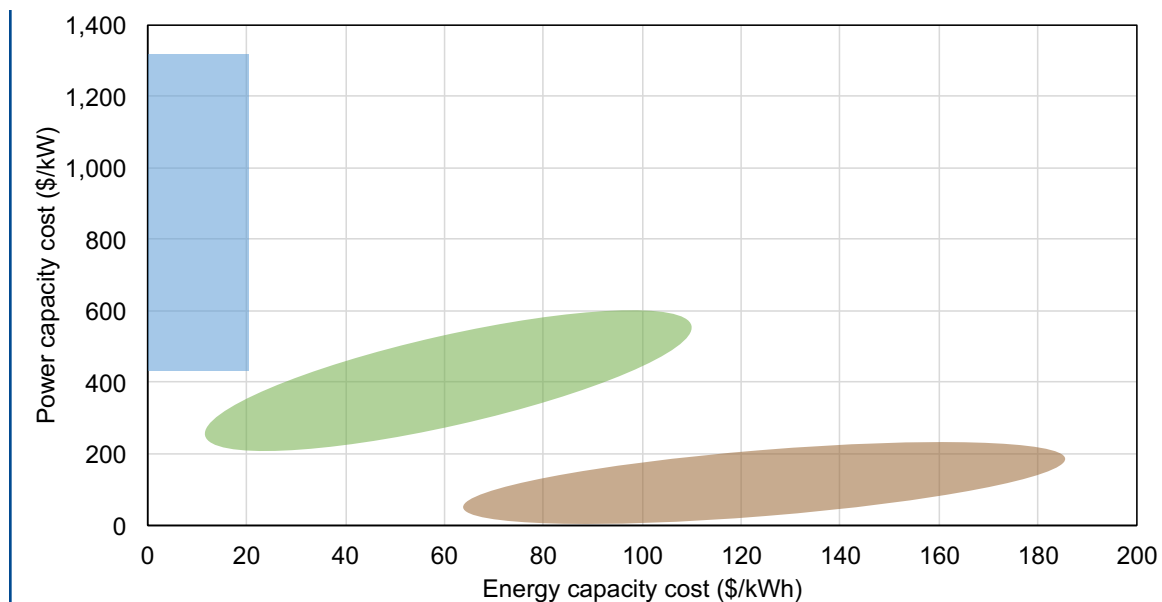
assumed usage and (for batteries) the cost of degradation implied by assumed usage. As in the case of LCOE, LCOS can then be computed as the average revenue per MWh discharged that just covers the facility's assumed capital and operating cost. The estimated LCOS for any particular technology will thus depend on how the typical facility is assumed to be used, so that storage technologies likely to play different roles, like generation technologies that play different roles, cannot be usefully compared. Moreover, LCOS computations rest heavily on assumptions about the cost of charging that are essentially arbitrary. We do not use LCOS in this study. Instead, in the modeling exercises described in Chapter 6, we use mathematical programming to determine optimal capacities and operations of available generation and storage technologies given assumptions about costs, regional wind and solar resources and other regional resources, the demand for electricity over time, and constraints on CO₂ emissions.

The technologies considered in this report fall into three main groups based on their per-unit discharge power and energy capacity costs (Figure 1.6). Generally, technologies with low energy-capacity costs and high power-capacity costs (the blue area in the figure) are most suitable for longer-duration storage applications (up to multiple days) and less frequent charge/discharge cycles; these include thermal and chemical forms of storage, metal-air batteries, and pumped storage hydro options. Technologies in the brown area, including lithium-ion batteries, are better suited to shorter-duration applications (a few hours) and more frequent cycling. Technologies with intermediate capabilities, including flow batteries, are in the green area. As we discuss in Chapter 6, however,

³ The unusually long duration of PSH facilities explains the fact that, although PSH accounted for around 99% of energy storage capacity (MWh) in the United States and globally in 2020, it accounted for only 87% of power capacity (MW) in the United States and 90% globally.

⁴ Lazard (2021) provides a particularly clear example of LCOS calculations.

Figure 1.6 Three groups of storage technologies based on power- and energy-capacity costs



The blue region, with high power and low energy capacity costs, includes thermal, chemical (e.g., hydrogen), metal-air battery, and pumped storage hydro technologies. Lithium-ion batteries fall in the brown area, with low power, but high energy-capacity costs; flow batteries fall in the intermediate, green region.

the efficient use of any particular storage technology generally involves a mix of storage cycles of different durations.

1.3.2 Environmental, health, and safety considerations

U.S. firms generally pay attention to environmental, health, and safety (EHS) concerns in investment and operations decisions and in innovation efforts. An unanticipated EHS issue can create lengthy project delays, significant cost increases, and loss of public support. There are several notable examples of such issues in the history of the energy industry in the United States: the Three Mile Island nuclear accident, particulate emissions from coal-fired electric power plants and diesel trucks, and air and water quality impacts from hydraulic fracturing techniques employed in unconventional oil and natural gas production. EHS concerns figured

prominently in the 2003 Future of Nuclear Power study and the 2007 Future of Coal study. The MIT Energy Initiative strives to include EHS aspects on a par with technical and economic aspects in its work on energy and climate subjects and related research projects.

Several EHS issues arose in the course of this Future of Energy Storage study. The diversity of the storage technologies we considered and the disparate roles those technologies might play in a decarbonized electricity system precluded the construction of a single handbook of EHS procedures and best practices. Similarly, this diversity makes the creation of an industry-wide electricity storage institute similar to the Institute of Nuclear Operations (INPO) problematic. EHS management for an energy storage facility must be tailored to the specific technology, scale, application, and physical location of the facility, resulting in

distinct approaches on a largely case-by-case basis. However, it can be expected that different technology classes will have characteristic EHS concerns that may have an impact on siting challenges, inform operating constraints, and require the introduction of auxiliary systems to safely manage storage facilities. Rather than list these concerns here, we integrate this information in the technology chapters.

Several examples of storage-related EHS issues deserve mention here, however. Perhaps the most significant and far-reaching involve the mining of metal ores such as cobalt, nickel, and vanadium, which must be expanded substantially to enable electrochemical storage technologies to play a meaningful role in future energy systems. Currently, the extraction and beneficiation of these ores is concentrated in developing nations in Africa and Latin America that may lack adequate regulatory resources and enforcement mechanisms to effectively manage EHS concerns. The lack of regulatory capacity in these countries heightens EHS concerns and deserves greater attention. Other technologies raise other potentially important EHS concerns: Examples include flammability hazards associated with lithium-ion batteries, risks from hydrogen-induced embrittlement of conventional pipelines and the impacts of hydrogen leakage, as well as the ecological and geological impacts of pumped hydroelectric storage. Although this study does not address these or other storage-technology-related EHS issues in depth, it is important to make readers aware of the importance of these EHS topics.

It should also be mentioned that EHS concerns are increasingly being raised in the context of a broader focus on environmental, social, and governance (ESG) matters that encompasses the community and income distribution impacts of climate change itself, and of climate-related policies. At present, ESG impacts from energy storage innovation, manufacturing, and

deployment are nuanced and depend on project, technology, and location specifics that challenge a broad assessment. Thus, the recommendation in Chapter 6 of this study to invest public resources in improving modeling and simulation tools includes tools that would enable a better understanding of environmental and economic outcomes from alternative approaches to decarbonized electricity systems with energy storage.

1.4 Report structure

The remainder of this report is comprised of three major sections: storage technologies, system modeling, and implications for policy and innovation. The storage technologies section follows this chapter and is divided into four chapters, each focused on one of the four technology areas of importance to the electricity sector: electrochemical storage, mechanical storage, thermal storage, and chemical storage. Each chapter develops high-, medium-, and low-cost estimates for promising technologies in these four categories, which are used for analyzing future electricity systems (described below).

Chapter 2, which deals with **electrochemical energy storage**, focuses on three types of battery storage technologies involving different chemistries and formats: lithium-ion batteries, redox flow batteries, and metal-air batteries. Brief consideration is also given to other battery technologies that have been deployed for stationary energy storage in the past. A major section of this chapter deals with materials costs and availability, since these considerations may have a significant bearing on the future scalability and adoption of electrochemical technologies. Materials criticality, supply chains, diversity of sourcing, and considerations for recycling are all part of this discussion.

Chapter 3 examines **mechanical energy storage** technologies and consists of two distinct sections. The first deals with pumped hydro-power storage, which still dominates energy storage globally (International Energy Agency 2019). The second section of the chapter deals with compressed air energy storage (CAES). Since compressing air generates a great deal of heat, CAES systems can be distinguished by whether this heat is discarded or saved for re-expanding the compressed air. Only the latter is a true energy storage technology and is the main focus of the latter half of Chapter 3.

Chapter 4 discusses a variety of **thermal energy storage** options. A general challenge for these technologies is the low efficiency of converting heat back to electricity. One option for mitigating this low conversion efficiency involves taking advantage of opportunities for retrofitting existing thermal power plants. The chapter also examines options like heat pumps that may be available in a mid-term (2030) timeframe. Finally, very high temperature options, which promise much more efficient discharge from heat to electricity, are examined for a 2050 horizon. Chapter 4 also looks at the potential for using very low-cost materials for thermal storage, which can lead to attractive costs for long-duration storage.

Finally, Chapter 5 looks at options for **chemical energy storage**. Because of the large amount of energy stored in chemical bonds, chemical energy storage has advantageous energy density, which can be useful when space is limited and/or for very-long-duration storage applications. In addition, the chemical stability of these bonds provides very low self-discharge rates, again making chemicals attractive for long-duration storage. Hydrogen is used as an example for chemical energy storage in this chapter, because hydrogen can be directly produced from electricity in a single step (by using electric current to split water molecules) and consumed either as a fuel to produce power or as a feedstock or heat source for other sectors.

The second section of the report uses cost estimates and information about other technology attributes from the four technology chapters in combination with capacity expansion models to analyze future power systems in two distinct contexts: developed countries (Chapter 6) and emerging market and developing economy (EMDE) countries (Chapter 7). To explore the characteristics of future decarbonized systems in a developed country context we study three U.S. regions: the Northeast, Southeast, and Texas; in addition, we present results at a national level, although with less detail. India is used as an example of power system evolution in an emerging market, developing economy country. In these country- and region-specific studies, we consider a number of different constraints on power sector carbon emissions, ranging from no limit at all down to 5 grams of carbon dioxide per kilowatt-hour (gCO_2/kWh). To provide a sense of the stringency of this lower limit on emissions, holding the U.S. electricity system to an average emissions intensity of 5 gCO_2/kWh in 2018 would have reduced power-sector emissions (relative to actual 2005 emissions) by 99.2%. The India case study is interesting not only because the policies India is likely to enact will be different, but because electricity demand in India and other EMDE countries will likely grow much faster than in developed nations. At the same time, India does not have a significant source of domestic natural gas. This means that new energy storage options in India will not have to compete against natural gas as vigorously as they would in the U.S. context.

This study concludes with a section that examines the implications of our technology and modeling findings for regulatory and policy decisions. Chapter 8 looks at the governance of decarbonized power systems with storage and considers how alternative organizational, regulatory, and policy arrangements can enable storage to play different roles in these systems at the lowest possible total cost, with appropriate attention to equity considerations.

The chapter also discusses arrangements that are important to avoid, because they undermine the efficient deployment and utilization of storage on the grid and because they would make it more difficult to replace fossil fuels by decarbonized electricity in other sectors. We focus primarily on the United States, though the general issues we discuss are relevant in other developed regions. The final chapter, Chapter 9, examines the role of technology innovation in ensuring that energy storage can play a significant role in future electric power systems. It discusses the nature and pace of innovation needed in order for energy storage to have a positive impact on future electricity systems with large amounts of variable renewable energy resources. In addition, Chapter 9 points to specific U.S. programs for advancing innovation, discusses who should lead them, and considers how these programs can be conducted so as to avoid previous mistakes.

Finally, this report includes several appendices that provide additional detailed material, reference data, and calculation results that can be helpful to some readers.

References

- Bloomberg New Energy Finance. 2021. "Battery Pack Prices Fall to an Average of \$132/kWh, But Rising Commodity Prices Start to Bite." *Bloomberg New Energy Finance*. November 30. https://about.bnef.com/blog/battery-pack-prices-fall-to-an-average-of-132-kwh-but-rising-commodity-prices-start-to-bite/#_ftn1.
- BP. 2021. "Statistical Review of World Energy." *BP*. <https://www.bp.com/en/global/corporate/energy-economics/statistical-review-of-world-energy.html>.
- Electric Reliability Council of Texas. n.d. "Generation." *ERCOT*. <https://www.ercot.com/gridinfo/generation>.
- Feldman, David, Galen Barbose, Robert Margolis, Ryan Wiser, Naïm Darghouth, and Alan Goodrich. 2012. "Photovoltaic (PV) Pricing Trends: Historical, Recent, and Near-Term Projections." *U.S. Department of Energy SunShot Program*. November. <https://www.nrel.gov/docs/fy13osti/56776.pdf>.
- International Energy Agency. 2014. "Technology Roadmap - Energy Storage." *International Energy Agency*. <https://www.iea.org/reports/technology-roadmap-energy-storage>.
- . 2019. "Will pumped storage hydropower expand more quickly than stationary battery storage? Analysis from Renewables 2018." *International Energy Agency*. March 4. <https://www.iea.org/articles/will-pumped-storage-hydropower-expand-more-quickly-than-stationary-battery-storage>.
- Joskow, Paul L. 2011. "Comparing the Costs of Intermittent and Dispatchable Generation Technologies." *American Economic Review* 101(3): 238–241. 10.1257/aer.101.3.238.
- Kane, Mark. 2021a. "Global Passenger xEV Battery Market Stats: H1 2021." *Inside EVs*. September 26. <https://insideevs.com/news/535967/global-xev-battery-market-h12021/>.
- . 2021b. "SNE Research: Global xEV Battery Market - 142.8 GWh In 2020." *Inside EVs*. February 18. <https://insideevs.com/news/488274/sne-research-global-xev-battery-market-2020>.
- Lazard. 2021. "Lazard's Levelized Cost of Storage, Version 7.0." *Lazard*. <https://www.lazard.com/media/451882/lazards-levelized-cost-of-storage-version-70-vf.pdf>.
- National Academies of Sciences, Engineering, and Medicine. 2019. *Negative Emissions Technologies and Reliable Sequestration: A Research Agenda*. Washington, DC: The National Academies Press. <https://doi.org/10.17226/25259>.
- Ramasamy, Vinges, David Feldman, Jal Desai, and Robert Margolis. 2021. "U.S. Solar Photovoltaic System and Energy Storage Cost Benchmarks: Q1 2021." *National Renewable Energy Laboratory*. November. <https://www.nrel.gov/docs/fy22osti/80694.pdf>.
- U.S. Department of Energy. 2011. "Electric Market and Utility Operation Terminology." *U.S. Department of Energy Solar Energy Technologies Program*. <https://www.nrel.gov/docs/fy11osti/50169.pdf>.
- . 2020. "Energy Storage Grand Challenge: Energy Storage Market Report." *U.S. Department of Energy Energy Storage Grand Challenge*. https://www.energy.gov/sites/prod/files/2020/12/f81/Energy%20Storage%20Market%20Report%202020_0.pdf.
- . 2021. "Land-Based Wind Market Report: 2021 Edition." *U.S. Department of Energy Office of Energy Efficiency and Renewable Energy*. https://emp.lbl.gov/sites/default/files/land-based_wind_market_report_2021_edition_final.pdf.
- U.S. Energy Information Administration. 2021. "Levelized Costs of New Generation Resources in the Annual Energy Outlook 2021." *U.S. EIA*. February. https://www.eia.gov/outlooks/archive/aoe21/pdf/electricity_generation.pdf.
- Wehling, Mark, and Allen Tom Abraham. 2021. "Global Energy Storage Outlook." *Bloomberg New Energy Finance*. August 11. https://content.macquarie.com/macquarie-capital/asia/2021/events/group-call/ess-day/2021-08-11-%20BloombergNEF%20Energy%20Storage_Macquarie%20Securities.pdf.

Chapter 2 – Electrochemical energy storage

2.1 Introduction

Electrochemical energy storage devices, commonly called batteries, interconvert chemical and electrical energy through reduction and oxidation (redox) reactions. These reactions occur on two different electrodes (positive and negative) that are electrically connected through an external circuit and physically separated by an ionically conducting medium (i.e., an electrolyte). While so-called “primary” batteries, which are discharged once and then disposed of or recycled, are of interest for many applications, the battery technologies that are relevant for grid storage and emphasized in this study are, almost without exception, rechargeable or “secondary” batteries in which the redox processes are electrically reversible.

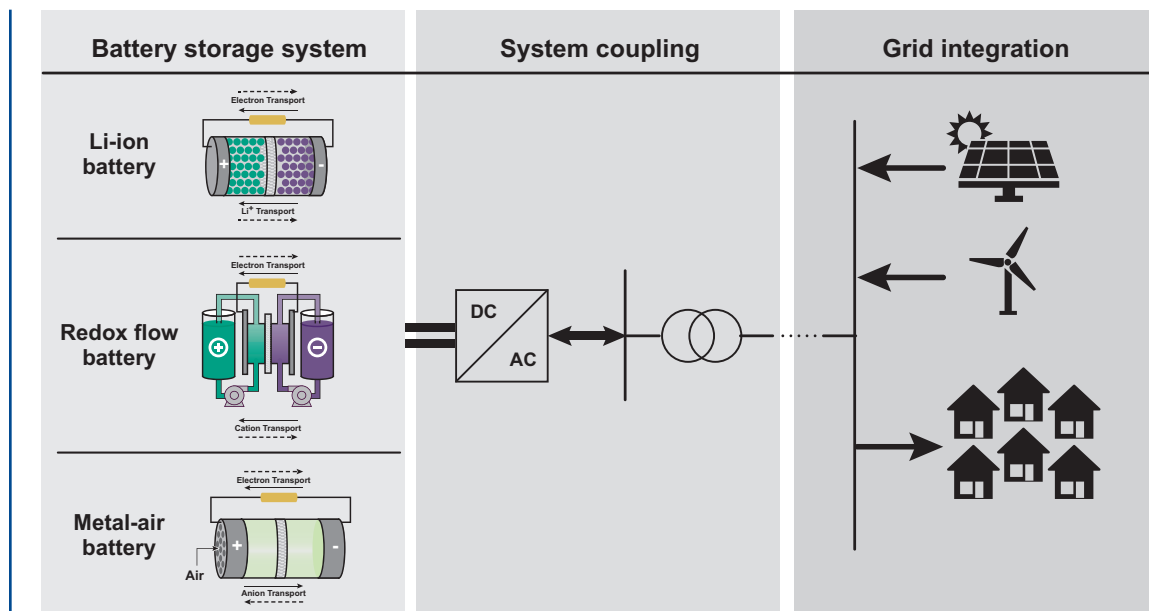
Since Alessandro Volta first conceived the idea of a battery in 1800, electrochemical energy storage has enjoyed a rich history of research, development, demonstration, and commercialization resulting in a number of battery technologies that now play important roles in modern society. A notable example is the lead-acid battery, which is widely used for engine start and onboard power in internal combustion automobiles and for back-up power in homes and industry. Another is the lithium-ion battery, which underpinned the portable electronics revolution and for which the 2019 Nobel Prize in Chemistry was awarded to John B. Goodenough, M. Stanley Whittingham, and Akira Yoshino. While electrochemistry can play a role in numerous technologies across the broader energy system, here we limit our focus to electrochemical

technologies that complete the loop of receiving, storing, and delivering electricity. We do not attempt to be encyclopedic in our coverage of batteries, rather, we limit our analysis and modeling to battery chemistries that have either reached a technology readiness level (TRL) of 6 or higher¹ in grid-scale electricity storage, or demonstrated, at an early stage, particularly promising attributes for future deployment. These batteries primarily fall into three categories: lithium-ion (Li-ion) batteries, redox flow batteries (RFBs), and metal-air batteries, as illustrated in Figure 2.1.

The chapter is organized as follows: Section 2.2 discusses, in general terms, the technical and cost performance metrics used to compare different battery technologies for grid-scale energy storage. Subsequent sections detail the current status and outlook for individual battery technologies. Specifically, Sections 2.3–2.6 cover Li-ion batteries, RFBs, metal-air batteries, and other closed-system batteries (i.e., lead-acid and high-temperature batteries). For Li-ion, redox flow, and metal-air batteries, we summarize technical performance parameters and estimate likely cost ranges in 2050—these estimates are used as inputs to the modeling analyses described in Chapters 6 and 7. The following part of the chapter, Section 2.7, discusses the materials availability issues that may arise at projected levels of electrochemical energy storage deployment over the next 10 to 30 years (i.e., by 2030 and 2050), with an emphasis on the materials or elements that are central to state-of-the-art Li-ion and RFB chemistries. The last section, Section 2.8, summarizes key takeaways from the chapter.

¹ Technology Readiness Levels (TRL) are a type of measurement system used to assess the maturity level of a particular technology (TRL 1 is the lowest and TRL 9 is the highest). TRL 6 is defined by the U.S. Department of Energy as one in which “engineering-scale models or prototypes are tested in a relevant environment.” Source: Technology Readiness Assessment Guide (U.S. Department of Energy 2011).

Figure 2.1 Categories of electrochemical storage technologies



Categories of electrochemical storage technologies, lithium-ion (Li-ion) batteries, redox flow batteries, and metal-air batteries, and their role in an integrated electricity system. Dashed and solid arrows show the directions of electron and cation transport during charging and discharging, respectively. Depending on the application, additional components not shown in the figure (e.g., thermal and battery management systems, etc.) may also be needed to ensure the proper and safe operation of the storage system.

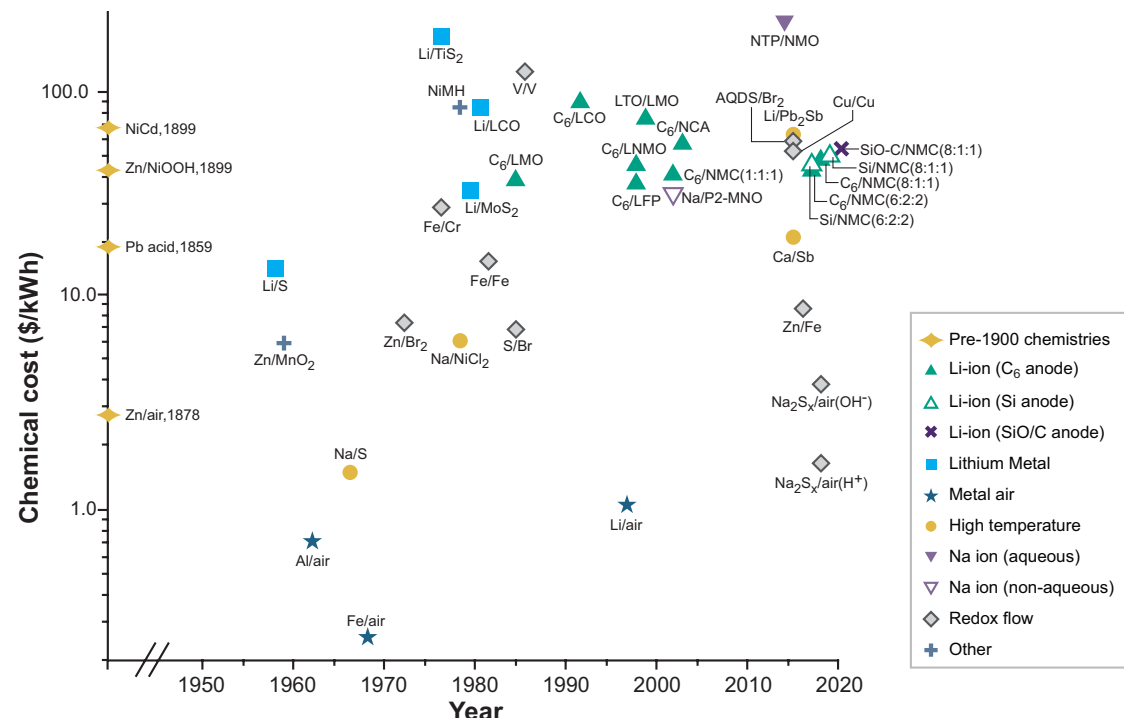
2.2 Electrochemical systems for grid-scale energy storage

Electrochemical energy storage systems generally have higher energy densities than mechanical (Chapter 3) or thermal (Chapter 4) storage systems and can achieve a wide range of roundtrip energy efficiencies (the ratio of energy output to energy input), from as high as 95% for certain Li-ion battery chemistries to as low as 40% for certain metal-air battery chemistries. Because of their compact footprint and independence from geographical and geological resources, batteries are a versatile technology that can be readily deployed at a variety of scales, from centralized large-scale facilities down to the level of distributed residential users, and face fewer siting constraints. Whereas energy-dense batteries are favored for mobile applications, which emphasize compact cell formats and high-capacity chemistries, battery cost and service lifetime

are of greater importance in stationary applications. This means a broader range of battery chemistries and system configurations can be considered for grid-scale energy storage.

The elements and compounds that comprise the positive and negative electrodes in which chemical energy is stored or extracted are a large component of the battery's cost. On this basis, the chemical cost of stored energy, in dollars per kilowatt-hour (\$/kWh), varies by more than two orders of magnitude among known battery types, from less than \$1/kWh for the most earth-abundant elements, to more than \$30/kWh for some high-specific-energy Li-ion chemistries, to more than \$100/kWh for vanadium RFBs (Figure 2.2). It should be noted, however, that these costs are not purely a function of the materials cost, but also the battery's energy density and efficiency. Further, the installed cost of a battery system comprises more than its chemical costs because it includes

Figure 2.2 The chemical cost of stored energy for battery electrochemistries



The chemical cost of stored energy for battery electrochemistries, shown against the year in which the system first appeared in the public domain. Technologies pre-1900 are shown against the left axis. Chemical cost is calculated as the cost of the negative electrode material, positive electrode material, and electrolyte, divided by the stored energy. Abbreviations: LMO = lithium manganese oxide, LCO = lithium cobalt oxide, LFP = lithium iron phosphate, LNMO = lithium nickel manganese oxide, LTO = lithium titanium oxide, NMC = lithium nickel manganese cobalt oxide, NCA = lithium nickel cobalt aluminum oxide, P2-MN = P2-type sodium manganese nickel oxide, NTP = sodium titanium phosphate, NMO = nickel manganese oxide, NiCd = nickel–cadmium, NiMH = nickel metal hydride, AQDS = 9,10-anthraquinone-2,7-disulfonic acid (adapted from (Li et al. 2017); see Appendix A for details).

costs for the supporting materials needed to produce a battery cell, pack, or electrochemical stack (depending on the system architecture); the cost of mechanical and power electronics components; the cost of manufacturing; and the cost of installation and interconnection, among other costs. Thus, the chemical cost of stored energy represents a floor on the cost of any battery. These costs can dominate overall cost, as is the case for today's high-specific-energy Li-ion batteries. The recognition that chemical costs may fall more slowly than other costs as battery technologies mature warrants a two-stage learning curve model for battery cost projections (Hsieh et al. 2019). However, recent

developments in grid-scale storage favor low-cost, widely available chemical components (e.g., iron, manganese, zinc, and sulfur) that shift more of the cost burden to other system components. For the lowest cost chemistries, the cost structure for battery storage systems is not unlike that for pumped hydroelectric or compressed air storage systems, in which the cost of the energy storage medium (water or air) is a small to negligible percentage of total system cost. Battery chemistries that utilize earth-abundant elements can also benefit from a diverse and secure supply chain that may enable rapid scaling of systems for grid applications.

Every battery chemistry comprises a trade-off in attributes such as energy density, safety, durability, and cost, and system architectures are generally optimized for a specific chemistry-application fit. Historically, rechargeable battery development has been driven by mobile applications, which favor high-capacity chemistries and compact system designs. In emerging stationary applications, by contrast, system cost and lifetime are prioritized—in some cases, at the expense of energy density or roundtrip efficiency. Notably, Li-ion batteries are constrained to specific architectures that tend to yield lower power costs but higher energy costs (Table 2.1). This has made Li-ion batteries most competitive, on a capital cost basis, for short-duration storage applications (less than four hours of storage). Projected cost declines may make Li-ion batteries competitive for storage durations up to about eight hours. Emerging alternatives, such as RFBs and metal-air batteries, allow a broader range of chemistries to be used, including high-abundance and low-cost active species (e.g., iron, zinc, oxygen) that make capital costs for these batteries attractive for longer storage durations (over eight hours). Furthermore, flow and metal-air battery architectures can be designed to allow for periodic maintenance of some system components, which reduces the levelized cost of storage over long service life. However, the relative immaturity of these battery technologies, including limited engineering experience, uncertainty in manufacturing costs and methods, and the lack of a fully developed supply chain, presents barriers to deployment and increases perceived risks from practical, operational, and financial points of view. Conversely, demand for longer duration applications is still emerging, challenging the development of technologies that are primarily competitive in these spaces.

As part of this study, we estimate figures of merit for performance and cost for Li-ion batteries, RFBs, and metal-air batteries for the

present day (2020) and the future (2050). Our estimates of future cost include a low, medium, and high value. These cost estimates are then used in the grid modeling analyses discussed in Chapter 6. Numerous studies have examined historic, current, and projected future costs for Li-ion batteries. We use numbers from the National Renewable Energy Laboratory (NREL) Annual Technology Baseline (ATB) of 2020, a widely cited source that is in good agreement with many other published reports. For current (2020) costs, the NREL ATB uses a bottom-up cost model that contains detailed cost information for components of the battery storage system (Feldman et al. 2021), including Li-ion battery pack, inverter, and the balance of system needed for installation. For future (2050) Li-ion battery costs, the NREL ATB makes projections based on a literature review of 19 sources published in 2018 or 2019 (Cole and Frazier 2020). We use the lower-bound, median, and higher-bound projections from this literature review as the low-, mid-, and high-cost assumptions in our modeling analysis, respectively. A techno-economic assessment for the less-developed technologies we consider (i.e., RFBs and metal-air batteries) is challenged by limited sources of information for component and system costs as well as a lack of established field-wide standards in engineering design and manufacturing. To mitigate these information gaps, we surveyed the published literature and engaged industry experts. Our estimated values are in general agreement with those in other published reports around the time of writing (February 2022) and rely on inputs, assumptions, and calculations that are based on peer-reviewed work. Nevertheless, these values should be considered early-stage estimates that may be refined in the future as commercialization expands and specific chemistries develop. Details on our cost calculations for RFBs, metal-air batteries, and balance-of-plant subsystems can be found in Appendix A.

Table 2.1 Estimated and projected capital costs, operating costs, efficiencies, and self-discharge rates

| Tech | | Discharging capital cost (\$/kW) | Storage capital cost (\$/kWh) | FOM (\$/kW-year) | FOM (\$/kWh-year) | Efficiency-charge (%) | Efficiency-discharge (%) | Self-discharge rate (%/month) |
|------------------|-------------|----------------------------------|-------------------------------|------------------|-------------------|-----------------------|--------------------------|-------------------------------|
| Li-ion | 2020 | 257 | 277 | 1.4 | 6.8 | 92% | 92% | 1.5 |
| Li-ion | 2050 Low | 32 | 70.9 | 0.3 | 1.4 | 92% | 92% | 1.5 |
| Li-ion | 2050 Mid | 110 | 125.8 | 0.8 | 2.2 | 92% | 92% | 1.5 |
| Li-ion | 2050 High | 154 | 177.0 | 1.4 | 3.2 | 92% | 92% | 1.5 |
| RFB | 2020 | 583–650 | 171 | 4.1 | 0.0 | 92% | 88% | 0.0 |
| RFB | 2050 Low | 297 | 15.5 | 4.1 | 0.0 | 92% | 88% | 0.0 |
| RFB | 2050 Mid | 396 | 48.0 | 4.1 | 0.0 | 92% | 88% | 0.0 |
| RFB | 2050 High | 530 | 102.2 | 4.1 | 0.0 | 92% | 88% | 0.0 |
| Metal-air | 2020 | 1,068–1,135 | 3.7 | 26.7–28.4 | 0.1 | 72% | 60% | 7.3 |
| Metal-air | 2050 Low | 595 | 0.1 | 14.9 | 0.0 | 70% | 59% | 1.5 |
| Metal-air | 2050 Mid | 643 | 2.4 | 16.1 | 0.1 | 73% | 63% | 1.5 |
| Metal-air | 2050 High | 950 | 3.6 | 23.7 | 0.1 | 72% | 60% | 1.5 |

Estimated and projected capital costs, operating costs, efficiencies, and self-discharge rates for lithium-ion (Li-ion) batteries, redox flow batteries (RFBs), and metal-air batteries in 2020 and 2050, respectively. For each technology, a range of possible 2050 costs (low, mid, and high) is given. All operations and maintenance (O&M) costs are treated as fixed operations and maintenance (FOM) costs and reflect routine component servicing and replacement due to degradation. For Li-ion and metal-air batteries, FOM costs are assumed to equal 2.5% of capital cost per year, while for RFBs the FOM cost assumes replacement of membranes and electrodes every decade.

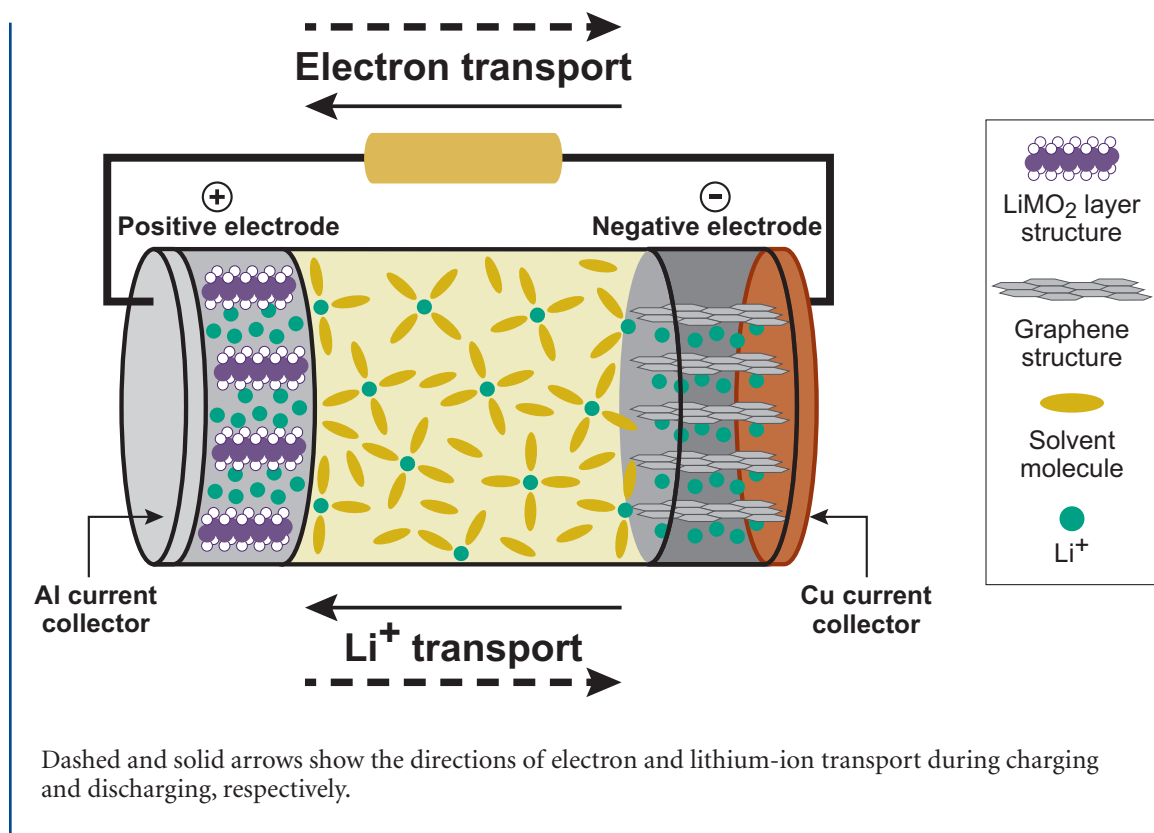
2.3 Lithium-ion batteries

2.3.1 Technology overview

Lithium-ion (Li-ion) batteries are a family of rechargeable batteries that utilize solid compounds at both the negative and positive electrodes as hosts for reversible lithium-ion storage. During discharge, lithium ions migrate internally from the negative electrode to intercalate into the positive electrode through a liquid electrolyte, while electrons simultaneously move in the same direction through an external circuit, powering the device to which the battery is connected. During charge, the process is reversed, with lithium ions migrating from the positive to the negative electrode, and electrons flowing through the external circuit, under voltage supplied by an external power

source. The Li-ion battery is a relatively mature technology that has benefited from more than three decades of commercial development. Thanks to several factors—including the low atomic mass of lithium; the development of positive and negative electrodes that are capable of reversibly storing lithium ions at high mass and volume concentrations and with large differences in electrode potential (cell voltage); and the development of high conductivity electrolytes, supporting components, cell designs, and manufacturing methods—Li-ion batteries today offer energy and power densities that are superior to most other battery types. State-of-the-art Li-ion battery cells have a nominal voltage of 3.6–4.0 volts (V), a specific energy (or gravimetric energy density) between 100 and 250 watt-hours per kilogram (Wh/kg), and an energy density between 300 and 650

Figure 2.3 Schematic of a Li-ion battery cell



watt-hours per liter (Wh/L) (Li et al. 2018; Zubi et al. 2018). They have high roundtrip energy efficiency (85%–95%, depending on the rate of charge and discharge), low maintenance requirements, adequate cycle life for many applications (up to several thousand full charge/discharge cycles), and a low self-discharge rate. These merits have made Li-ion batteries the incumbent technology for a wide range of applications, from portable electronics and power tools to electric vehicles (EVs) and stationary energy storage systems.

A Li-ion cell contains several key components within its external housing (Figure 2.3): a positive electrode, a negative electrode, aluminum and copper foil current collectors to which the positive and negative electrodes are respectively adhered, a liquid electrolyte, and a porous

separator to electrically isolate the two electrodes from one another. The positive electrode (commonly referred to as the cathode, although this terminology is technically correct only during the discharge step) is typically a lithium transition-metal oxide such as lithium cobalt oxide (LCO), lithium manganese oxide (LMO), lithium nickel-manganese-cobalt oxide (NCM or NMC), or lithium iron phosphate (LFP). The electrode also contains electrochemically inactive materials that improve electrical and structural characteristics, typically conductive carbon powders and a polymeric binder. The mixture of active and inactive materials is coated on an aluminum foil current collector, which, in turn, is connected to the external electrical terminals of the cell. The negative electrode (or anode during discharge) is typically a graphite-based material, with

higher-specific-energy Li-ion battery cells now incorporating silicon in varying amounts. These active materials are also mixed with conductivity enhancers and binders and subsequently coated on a copper current collector. To a large extent, the choice of compounds for positive and negative electrodes defines battery performance and favored applications of different types of Li-ion battery cells. The liquid electrolyte enables the movement of lithium ions between the two electrodes during charge and discharge; it consists of a lithium salt (e.g., lithium hexafluorophosphate, LiPF_6) dissolved in an organic solvent, which is most commonly composed of a blend of alkyl and cyclic carbonates (e.g., ethylene carbonate, propylene carbonate, ethyl methyl carbonate, etc.). Various chemical additives in the electrolyte are used to improve the performance, lifetime, and safety of the cell. The liquid electrolyte can also be infused into a polymer, forming a gel electrolyte; Li-ion batteries that use this type of electrolyte are typically called lithium-polymer (or Li-poly) batteries (Dahn and Ehrlich 2010). In addition to gel electrolytes, fully solid polymer electrolytes have been used—albeit in batteries produced at relatively low volumes; today, inorganic compounds (ceramics) are being widely studied as possible successors to liquid electrolytes (Doughty 2010). Solid-state batteries using either organic or inorganic electrolytes have potential advantages in safety and energy density compared to liquid electrolyte systems, but lag in commercial maturity.

Li-ion cells are manufactured in a wide range of sizes and in two basic forms: cylinders and rectangular prisms. Cylindrical cells are typically contained in a metal can, while prismatic cells may be contained in a metal can or in a sealed bag made from a multilayered polymer sheet, forming a so-called pouch cell. Individual

Li-ion cells, for which the nominal cell voltage is determined by the specific combination of positive and negative electrode materials, can be directly used in small-scale applications such as cell phones. To deliver the increased capacity and operating voltage required for larger-scale applications, multiple cells are interconnected in various series and parallel configurations to form battery modules and packs. Applications that require a large number of interconnected Li-ion cells, such as EVs and grid-scale energy storage systems, also require several additional subsystems to ensure proper and safe operation. These subsystems include thermal management systems that help maintain a proper cell temperature range and battery management systems (BMSs) that electronically monitor and control the operating state of the cells and battery pack. For grid storage applications, additional electronics in the form of inverters and transformers are used to connect the storage systems to each other and to the grid; in addition, supervisory controls are used to monitor the entire system and provide an interface between the BMS and the grid (Figure 2.1) (Hesse et al. 2017; Lawder et al. 2014).

2.3.2 Li-ion battery chemistries

Positive electrodes

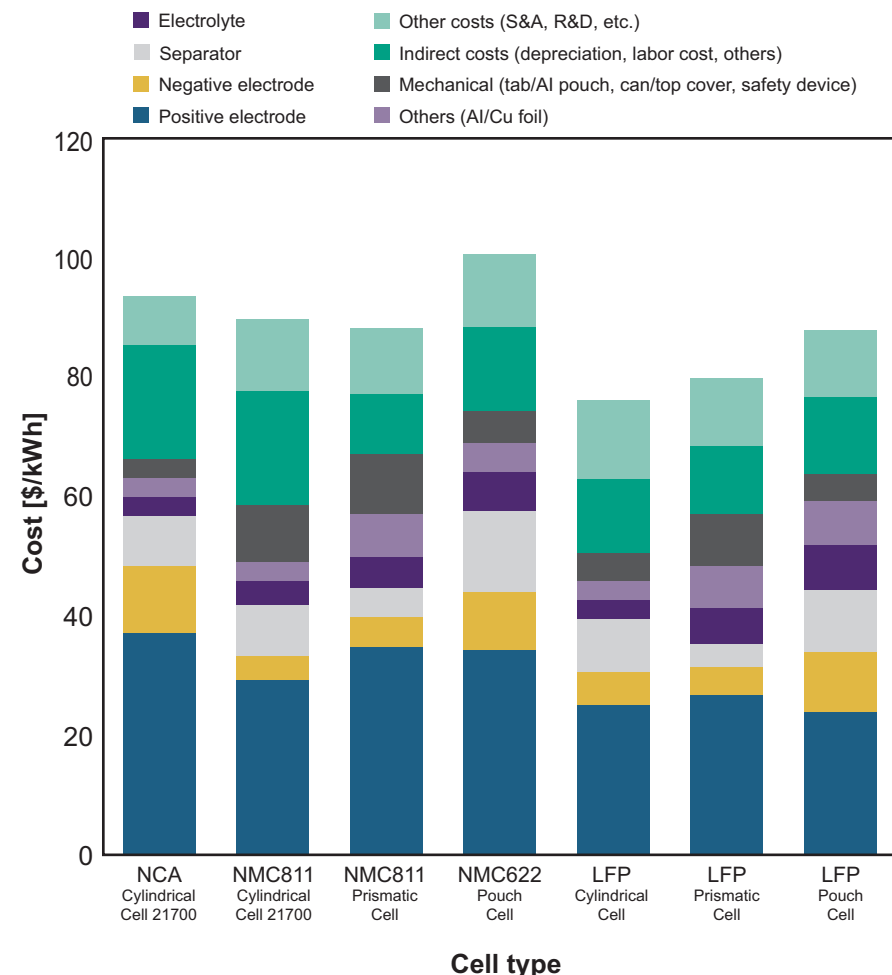
A variety of positive electrode compounds are used in Li-ion batteries depending on the desired combination of energy density, power density, lifetime, safety, and cost. Table 2.2 shows today's most common positive electrode families and their corresponding applications. The positive electrode active material is generally the most expensive single component in the cell, representing 30%–50% of the total material cost, as shown in Figure 2.4, which breaks down material costs for Li-ion cells of several types.

Table 2.2 Classes of positive electrode materials

| Tech | Consumer electronics | Power tools | Light duty vehicles | Cars | Commercial vehicles | Buses | Grid/energy storage systems |
|------------|----------------------|-------------|---------------------|------|---------------------|-------|-----------------------------|
| LFP | Y | Y | Y | Y | Y | Y | Y |
| NCA | Y | N | Y | Y | N | N | Y |
| LMO | Y | Y | Y | Y | N | N | Y |
| LCO | Y | N | N | N | N | N | N |
| NMC | Y | Y | Y | Y | Y | Y | Y |

Classes of positive electrode materials for Li-ion batteries and the applications in which they are preferred (Frost and Sullivan 2020). LFP = the exemplar compound LiFePO_4 , NCA = $\text{Li}(\text{Ni},\text{Co},\text{Al})\text{O}_2$, LMO = LiMn_2O_4 , LCO = LiCoO_2 , and NMC = $\text{Li}(\text{Ni},\text{Mn Co})\text{O}_2$ (the nomenclature “NCM” is also used). Here, Y and N stand for “applicable” and “not applicable.”

Figure 2.4 Cost breakdown



Cost breakdown for various types of Li-ion cells (SNE Research 2020). NCA = lithium nickel cobalt aluminum oxide, NMC = lithium nickel manganese cobalt oxide, LFP = lithium iron phosphate.

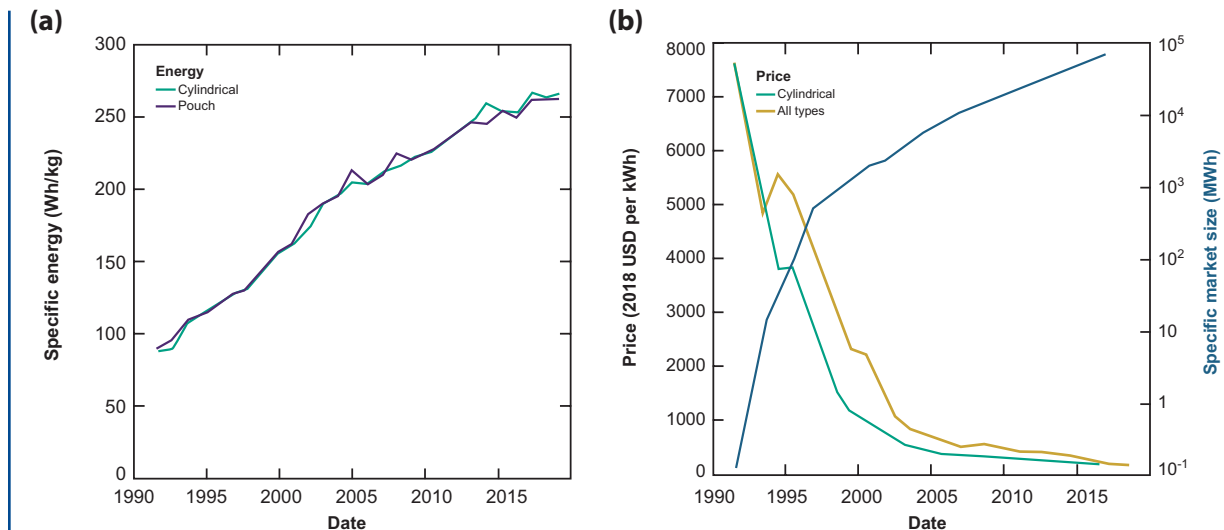
The first commercially successful Li-ion batteries, launched by Sony Corporation of Japan in 1991, used lithium cobalt oxide (LCO) as the positive electrode material. When paired with a graphite negative electrode, these batteries produced a cell voltage of about 3.8 V, considerably exceeding the voltage of aqueous chemistries and necessitating the use of non-aqueous electrolytes. The main drawbacks of LCO are its relative instability against thermal abuse (thermal runaway is initiated at temperatures as low as 150°C) (Zubi et al. 2018), its relatively short life (500–1,000 cycles), and the high cost of cobalt. While LCO-based Li-ion batteries continue to be widely used in portable electronic devices due to their attractive specific energy, this type of battery is unlikely to see use in grid storage applications given the existence of subsequently developed Li-ion alternatives.

Several structural analogs to LCO positive electrodes have been commercialized that partly or completely substitute nickel, manganese, and aluminum for cobalt. These analogs are motivated by the desire to achieve lower cost, greater resource availability, and/or improved safety, while retaining high specific energy. Lithium nickel cobalt aluminum oxide (NCA)-based cells have been developed with comparable specific energy to LCO-based cells (200–250 Wh/kg, for cells designed for a life of 1,000–2,000 cycles) while using lower-cost metals (typically 85% nickel and 15% aluminum) (Li et al. 2018; Armand et al. 2020); NCA has been the primary Li-ion positive electrode chemistry used in Tesla EVs. Lithium nickel-manganese-cobalt-oxide (NMC) is a family of positive electrodes in which the relative amounts of the three transition metals vary from a ratio of 1:1:1 to a ratio of 8:1:1 in standard formulations (the relative proportions are indicated by the nomenclature, such as “NMC-111” and “NMC-811”). Higher nickel content provides higher voltage and specific energy, but at the expense of poorer thermal stability and cycle life. Nonetheless, by

fine-tuning material composition, synthesis methods, and electrolyte composition, NMC-622 and NMC-811 chemistries have been successfully commercialized for EV applications. Thus, the development pathway for this family of positive electrodes has led from a starting point of 100% cobalt in LCO to only 10% cobalt in NMC-811, and NMC positive electrodes with even lower cobalt content are imminent. While multiple advances helped increase the specific energy of commercial Li-ion cells from an upper bound of about 100 Wh/kg in 1991 to approximately 260 Wh/kg today (Figure 2.5a), the systematic development of the LCO-NCA-NMC class of positive electrodes has played an especially important role.

Two classes of Li-ion positive electrodes have the potential to achieve even lower cost per stored energy than high-nickel NMCs: lithium manganese oxide (LMO) and lithium iron phosphate (LFP). However, both have lower specific energy than the NMC family of positive electrodes. Lithium manganese oxide was the first of the two to reach commercial production, around 1996 (Ding et al. 2019). Compared to LCO positive electrodes, LMO positive electrodes (when used with graphite negative electrodes) have a similar operating voltage of about 3.9 V, but their lower practical specific capacities (Armand et al. 2020) result in a lower specific energy at the cell level of 100–140 Wh/kg (Zubi et al. 2018). For grid applications, the main limitation of LMO positive electrodes is that they are subject to a mode of chemical degradation related to the dissolution of manganese and its migration to the negative electrode. This type of degradation, which is exacerbated at temperatures above about 50°C (Manthiram 2020), limits the life of LMO positive electrodes to 1,000–1,500 cycles (Zubi et al. 2018). However, LMO batteries have been used in power tools, electric bicycles, and medical devices; in addition, LMO has been blended with NMC positive electrodes to

Figure 2.5 Historical increases and decreases



Historical increase in specific energy (a) and decrease in price with increased market size (b) of Li-ion battery cells (Ziegler and Trancik 2021).

improve power density and reduce cost. There are several possible avenues to mitigate the elevated temperature dissolution issue (e.g., positive electrode particle coatings, electrolyte composition design, ion-blocking membranes), which, if successful, could make LMO-containing Li-ion batteries an attractive low-cost option for grid storage.

LFP was first commercialized in the early 2000s. Among commercial positive electrodes, it is the most chemically stable, it does not contain resource-limited elements, and it is capable of lasting several tens of thousands of cycles. LFP-graphite cells using nanoscale powders are among the highest power density Li-ion cells available. LFP has the lowest cell voltage of commercialized Li-ion chemistries—about 3.5 V when used with a graphite negative electrode—which contributes to its stability. This feature, along with a moderate specific capacity, results in a cell-level specific energy of 90–140 Wh/kg (Zubi et al. 2018). The lower specific energy has limited the use of LFP positive electrode in some applications—

for example, EVs with long driving range—but the combination of power, safety, lifetime, and cost they offer has led to use in a broad range of small and large commercial applications ranging from power tools to residential and grid-scale energy storage applications. LFP positive electrodes are also increasingly used in batteries for passenger EVs where maximizing driving range is not a priority. They represent perhaps the most attractive low-cost Li-ion positive electrode option available today for stationary storage systems.

Negative electrodes

The original development of the Li-ion battery was enabled by carbon-based negative electrodes and graphitic carbon continues to be the most widely used anode material today. However, two alternative negative electrodes have made inroads into commercial products. Lithium titanate spinel is a metal oxide negative electrode that provides high power and exceptionally good cycle life but at the expense of a smaller cell voltage (of about 2.5 V when used

with typical Li-ion positive electrodes) and a concomitant reduction in energy density. The cost of chemicals per unit stored energy is high for Li-ion batteries using this type of negative electrode (Figure 2.2); as a result, it is limited to applications that require high power and high cycling frequency. A second alternative to carbon is silicon-based negative electrodes, which are attractive for high energy density applications given that the specific capacity of silicon, at greater than 3,000 milliamperere-hours per gram (mAh/g), is nearly ten times that of graphite (372 mAh/g). In practice, the capacity of silicon anodes must be constrained to lower values to obtain adequate cycle life for most applications. Currently, silicon (commonly in the form of micro or nano particles) is added to graphite-based negative electrodes in small amounts to achieve a combined specific capacity of 400–500 mAh/g. A current trajectory of development is toward negative electrodes with higher silicon concentrations for use in high-energy-density Li-ion battery applications such as EVs. Over time, silicon-based negative electrodes may find use in Li-ion batteries for grid storage.

2.3.3 Growth of the Li-ion industry

Applications of Li-ion batteries were mainly concentrated in portable electronic devices from the inception of this technology in 1991 through the mid-2000s (BCC Research 2016; Sanders 2016). Thereafter, applications in power tools and motor vehicles took hold, such that Li-ion has become the dominant battery architecture across each of those markets today. As of 2016, electronic devices accounted for about 35% of the Li-ion battery market, cars and buses accounted for 50% (mostly in China), and industrial and energy storage systems (e.g., grid storage, uninterruptible power supplies) accounted for 5%; the remainder of the market (10%) was for other uses such as medical devices, power tools, and e-bikes (Sanders 2016). Since 2016, growth has been primarily driven by the hybrid and

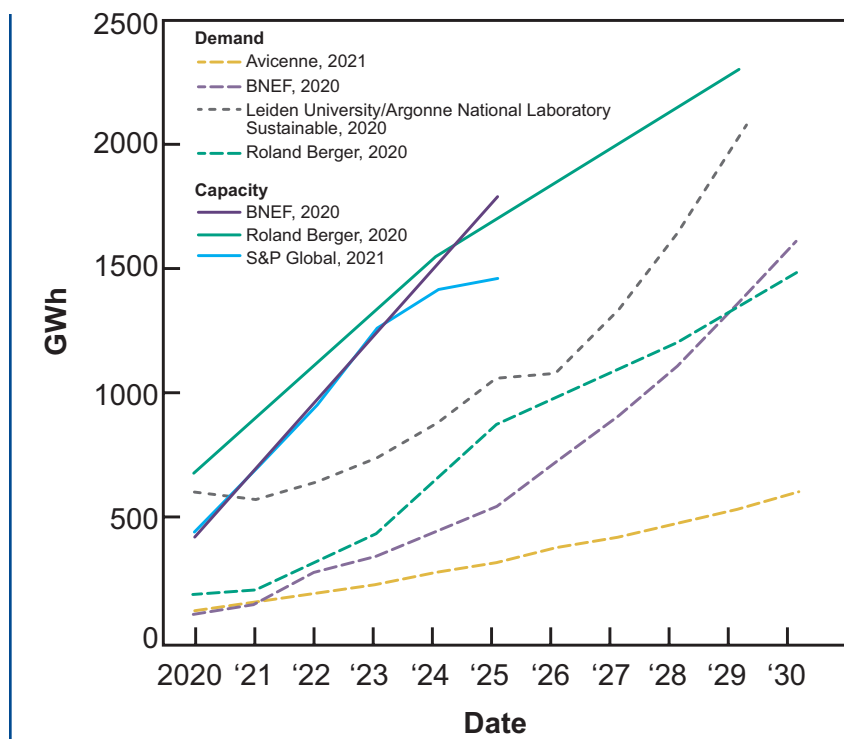
all-electric vehicle markets, electric buses, and industrial applications (Pillot 2019). Since 1995, the size of the Li-ion market, as measured by total storage capacity, has grown by a factor of about one thousand (Figure 2.5b), reaching approximately 100 gigawatt-hours (GWh) of annual production (globally) in 2019.

Concurrently, prices for Li-ion batteries have dropped 97% since 1991 (Figure 2.5b). Between 2010 and 2019, Li-ion prices fell by about 85% (BloombergNEF 2019). Despite declining prices, total market size in dollar terms increased from about \$9 billion in 2008 (BCC Research 2016) to \$37 billion in 2019; the market is projected to reach \$129 billion by 2027 (Choudhary and Prasad 2020). Multiple projections signal enormous growth in Li-ion manufacturing capacity between now and 2030, driven mainly by growth in the EV market. From about 500 GWh worldwide today, the upper bound of projected manufacturing capacity in 2030 is about 2,500 GWh worldwide, as summarized in Figure 2.6.

2.3.4 Drivers for continued cost reductions and deployment in grid storage

The rapid projected expansion in Li-ion manufacturing capacity will likely allow costs to continue down the “learning curve.” In addition, several directions for future development hold promise for further reducing cost and making Li-ion technology more suitable for grid applications. One is the implementation of lower-cost Li-ion chemistries, specifically using LFP but also potentially LMO positive electrodes. Other possibilities include the development of lower-cost cell manufacturing methods, such as methods for producing electrodes that do not require conventional solvent-based coating and drying operations (24M Technologies, Inc.) (Irvine and Rinaldo) and cell or pack designs that make more efficient use of materials and simplify manufacturing. Projected costs for EV Li-ion packs provide a useful benchmark for the likely cost

Figure 2.6 Projected growth in Li-ion battery manufacturing capacity and demand worldwide from 2020 to 2030



of future grid storage systems, since the additional costs associated with grid storage installations are well-understood. The Vehicle Technologies Office of the U.S. Department of Energy (DOE) has set near-term (2028) targets for Li-ion cell cost at \$60/kWh (Granholm 2021) and pack cost at \$80/kWh (U.S. Department of Energy). BloombergNEF has projected average Li-ion battery pack prices below \$100/kWh and \$58/kWh by 2024 and 2030, respectively (McKerracher et al. 2021). Tesla has projected that a suite of technical advances will reduce pack costs from about \$125/kWh in 2020 to about \$55/kWh by 2025 (Irvine and Rinaldo).

One trend in Li-ion battery development that will benefit grid storage applications is longer life, in terms of both cycle life and calendar life. For Li-ion batteries, cycle life is typically defined as the number of complete charge/

discharge cycles the battery can perform before it degrades to 80% of its initial storage capacity. However, cycle life does depend on the details of the duty cycle (i.e., application in which it is utilized); for example, high current rates and deep discharge cycles degrade batteries more quickly than low current rates and shallow cycling. Calendar life reflects the aging of the battery, which occurs whether or not the battery is being cycled; aging of this type is accelerated if the battery is held at high states of charge and at elevated temperatures. Typically, cycle life is the more important factor in applications that require frequent cycling, as is the case for many consumer electronics and EVs, or in short-duration grid applications such as frequency regulation. The Li-ion battery cells commercially available today are designed for a typical life of about 500 cycles for portable electronics and about 2,000 cycles for EVs. For stationary storage applications,

cost-effectiveness can be evaluated using the cost of delivered electricity over service life (often referred to as the levelized cost)—namely the discounted total cost of the system (capital cost plus operations and maintenance costs) divided by the discounted total energy (kWh) delivered. Battery life of 5,000 cycles or more (at room temperature) has been demonstrated for commercial cells with degradation-resistant chemistries such as LFP. However, even for high-energy-density NMC chemistries, advances in electrolyte chemistry and active material design, such as the use of single-crystalline cathode powders (Harlow et al. 2019), are enabling Li-ion cycle life in the range of 5,000 full charge/discharge cycles. Given the high sensitivity of Li-ion battery life to temperature, advances in thermal management systems for EVs (Zichen and Changging 2021; Tete, Gupta and Joshi 2021; Wu et al. 2019) will likely also transfer to stationary storage applications and benefit service life.

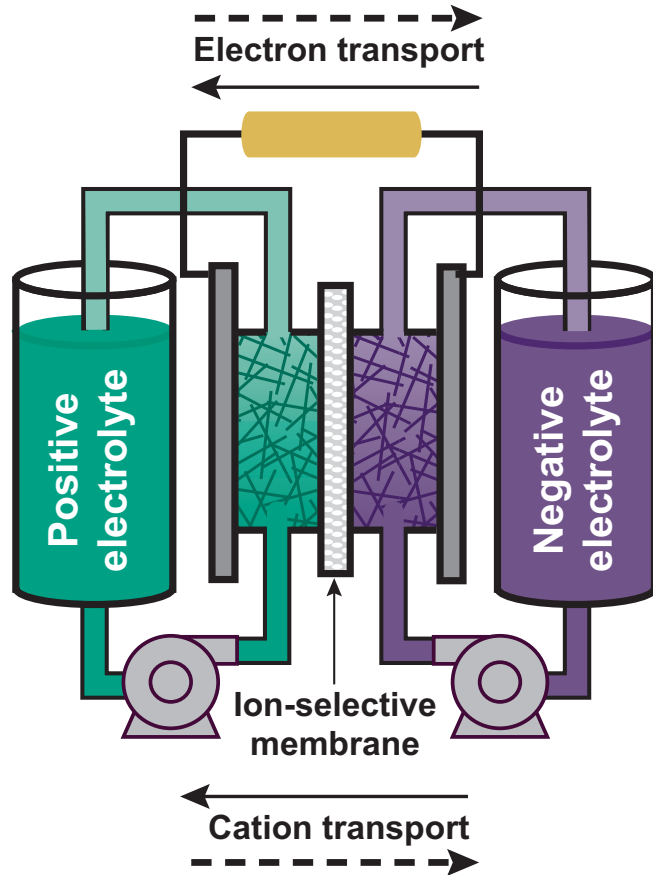
Li-ion batteries that have reached the end of their service life may be recycled or repurposed for less demanding applications. Batteries that have lost 20% of their storage capacity and cannot meet automotive specifications, for example, may still be suitable for grid storage. The techno-economic issues that determine whether recycling or repurposing is preferable are complex and beyond the scope of this study. However, as discussed in Section 2.7, recycling and repurposing EV batteries is unlikely to have a major impact on materials availability constraints until 2040, given the expected lifetime of EV batteries; beyond 2040, recycling and repurposing could play a significant role, but the cost-benefit trade-offs remain to be fully understood.

2.4 Redox flow batteries

Redox flow batteries (RFBs) are rechargeable electrochemical devices in which charge-storage species are dissolved in liquid electrolytes, stored in inexpensive tanks, and circulated through a power-converting reactor where they are oxidized and reduced to alternately charge and discharge the battery (Figure 2.7) (Weber et al. 2011). Within the reactor, two electrolytes—often called the “positive electrolyte” and “negative electrolyte” based on their respective electrode potentials—are separated by a species-selective membrane and undergo reduction and oxidation on the surfaces of porous electrodes. Ions traverse the membrane to balance charge between the two electrolytes, thereby maintaining electroneutrality, while ideally blocking the charge-storage species. As with other energy storage systems, RFBs require balance-of-plant subsystems to support operation, including fluidic, thermal, and state-of-charge management systems, the exact specifications of which are determined by the battery chemistry (Darling et al. 2014; Skyllas-Kazacos and Kazacos 2011).

Several unique features of the RFB architecture are advantageous for stationary energy storage. First, the physical separation of power and energy components means that the sizes of the reactor and the electrolyte-filled tanks can be varied independently, making it possible to tailor systems to particular installation requirements and, potentially, to selectively upgrade existing installations to address changing demands. This feature also means that the characteristic storage duration (time = energy/power) can be varied over a wider range than in most other battery designs. With increasing storage duration, system costs transition from being power-component-dominated (e.g., electrodes, membranes, other cell/reactor components) to energy-component-dominated (e.g., electrolytes, tanks). Ultimately, system

Figure 2.7 Schematic diagram of an RFB



Dashed and solid arrows show the directions of electron and cation transport during charging and discharging respectively. For some RFB chemistries, anions are exchanged between the electrolytes during operation. In those cases, the direction of the anion transport is opposite that of the cation transport.

costs asymptotically approach the cost of the electrolytes in the tanks. By comparison, power and energy components in static batteries are contained within the device and cannot be easily nor independently modified. In RFBs, the physical separation between system components also enables targeted maintenance of subsystems, which reduces costs for servicing and improves operational safety since the oxidized and reduced species are not in close proximity (Whitehead et al. 2017). The use of soluble charge-storage species in RFBs enables a long service life (in some cases, greater than 20 years), as redox reactions occurring at the

electrode-electrolyte interface are free of several material degradation processes that reduce the lifetime of intercalation-based batteries such as Li-ion. While electrolyte decay can still occur in RFBs, the modularity mentioned previously enables more facile remediation and replacement at regular intervals. Finally, manufacturing costs for RFB systems can be significantly lower than manufacturing costs for Li-ion batteries since there is less need for precision assembly machinery, low-moisture facilities, and/or factory lines dedicated to particular electrode chemistries or electrolyte formulations.

A characteristic limitation of RFBs is lower energy density, typically by an order of magnitude compared to Li-ion batteries, due to the lower concentrations of redox-active species that can be stored in a solution compared to a solid and due to less compact component packaging at a system level. In addition, state-of-the art RFBs use aqueous electrolytes rather than nonaqueous electrolytes, which leads to lower cell voltages due to the narrower window of electrochemical stability for water as compared to nonaqueous solvents. Current systems utilize polymeric membranes that have low ohmic resistance (high ionic conductivity) but imperfect species selectivity. As a result, charge storage species can exchange between the positive and negative electrolytes at appreciable rates (termed “crossover”), which reduces battery performance and lifetime (Perry, Saraidaridis and Darling 2020). To address some of these issues, hybrid flow battery systems have been developed that replace one or both solution-phase electrodes with deposition/dissolution electrodes (e.g., metal stripping and plating). Such approaches increase battery energy density but sacrifice design flexibility as the sizing of the power and energy components is no longer fully decoupled, and the need for uniform deposition of a solid without dendrite formation typically limits operating current densities.

2.4.1 Status of RFBs

Early chemistries

The RFB architecture is inherently flexible to the choice of chemistry, and many redox couples have been considered over the past half-century. We limit our discussion to systems that have advanced to the stage of significant demonstration and commercialization. The advent of RFB technology in the 1970s and 1980s began with the development of an iron-chromium (Fe-Cr) system by the U.S. National Aeronautics and Space Administration (NASA) as a potential energy storage solution

for deep-space missions (Hu et al. 2019). This chemistry ultimately proved to be unsatisfactory for the purposes originally envisioned by NASA, due to its low energy density and a sluggish chromium reaction that requires elevated temperatures ($> 50^{\circ}\text{C}$) to improve reaction rates to acceptable levels. Furthermore, the low electrode potential at which the chromium redox reaction occurs results in hydrogen gas evolution during charging, reducing battery performance by directing energy toward a side reaction, which in this instance can also create a flammability hazard (Ghan, Hagedorn and Ling 1983; Ghan, Hagedorn and Johnson 1985). While the Fe-Cr chemistry has not seen significant or sustained commercial deployment, its reactants have reasonably low costs, and other advances in RFB technology over the intervening 30 years could likely be applied to improve its performance. Indeed, the Fe-Cr chemistry is being revisited in some academic and commercial efforts (Zeng et al. 2016; Wang et al. 2020; Wei and Li 2020).

Almost concurrent with the development of the Fe-Cr chemistry by NASA, Exxon was developing the zinc-bromine (Zn-Br) chemistry. Zn-Br is a hybrid chemistry (Rajarathnam and Vassallo 2016) in which zinc is reversibly plated and stripped as solid metal at the negative electrode, while molecular bromine is reacted in solution at the positive electrode. The Zn-Br redox chemistry has a relatively high cell voltage for aqueous systems (about 1.7 V), but faces issues common to hybrid systems—in particular, the operating potential and current density on battery charge must be carefully managed to mitigate both hydrogen evolution (which is further catalyzed by the plated zinc) and zinc metal dendrite formation, which can puncture the separator and short-circuit the cell (Sun et al. 2016). In general, this leads to lower power densities and reduced operational flexibility as compared to many solution-phase RFBs. Other challenges associated with the bromine electrolyte are the added expense of

complexing agents needed to reduce bromine volatility and enhance aqueous solubility, and safety concerns related to bromine toxicity (Biswas et al. 2017; Narayan et al. 2019). While research, development, and commercialization efforts involving Zn-Br (and Fe-Cr) chemistries continue as these technologies hold promise, the majority of RFB commercialization efforts over the last decade have centered around the vanadium redox flow battery (VRFB).

Vanadium redox flow batteries

Pioneered by Professor Maria Skyllas-Kazacos at the University of New South Wales (Australia) in the 1980s, VRFB technology is the most commercially advanced flow battery chemistry today (Skyllas-Kazacos, Rychick and Robins 1988). This battery employs acidic electrolytes (e.g., sulfuric acid at ≥ 2 molar concentration), maintains an open-circuit voltage of about 1.4 V, and operates with vanadium concentrations of up to 2 molar, resulting in a relatively high energy density for a fully dissolved aqueous chemistry (Kazacos, Cheng and Skyllas-Kazacos 1990). Rapid redox reactions in VRFBs, corresponding to high current densities (≥ 200 milliamperes per square centimeter (mA/cm^2)), are facilitated by the use of porous, carbonaceous electrode materials with high surface areas and, often, electrocatalytic surface functionalization. However, accessible rates of charging are limited by oxidation of the carbon electrodes at high potentials (i.e., cell voltages ≥ 1.7 V) (Nibel et al. 2017). VRFBs—like many aqueous chemistries that utilize an acidic electrolyte—are susceptible to hydrogen gas evolution, but optimization of cell/reactor design and operating conditions has largely mitigated this issue (Roznyatovskaya et al. 2016). VRFB systems generally use a cation exchange membrane (CEM) between the electrodes to allow proton exchange between the two electrolytes while minimizing crossover of the vanadium species and preventing electrical shorting between the electrodes (Prifti et al. 2012). The most

commonly used CEMs are based on NafionTM, a perfluorosulfonic acid (PFSA) polymer discovered in the late 1960s by DuPont.

A key advantage of the VRFB is its “symmetric” chemistry, in which both the positive and negative electrolyte are based on the same parent compound, vanadyl sulfate. This symmetry is facilitated by vanadium’s somewhat unusual ability to adopt four oxidation states, all of which are stable and accessible within the electrochemical stability window of aqueous acidic electrolytes on carbon electrodes. Changes in oxidation state between V^{2+} and V^{3+} occur in the negative half-cell and between V^{4+} (VO^{2+}) and V^{5+} (VO_2^{+}) in the positive half-cell. Accordingly, crossover of vanadium cations between the two electrolytes does not lead to irrecoverable capacity losses. Rather, these losses are recoverable via electrolyte rebalancing (Skyllas-Kazacos and Kazacos 2011), which is inexpensive, given the modularity and relative ease of maintenance inherent to RFBs, allowing the electrolyte to be used indefinitely if non-crossover related losses (e.g., side reactions, component degradation, material loss due to leaks, etc.) can be effectively managed. While other symmetric chemistries are known, the VRFB is the canonical example.

Deployment

Around the time of this writing, more than 30 MW (100 MWh) of total flow battery capacity has been deployed globally, and installations totaling another 240 MW (960 MWh) have been contracted, announced, or are under construction (U.S. Department of Energy 2020). The vast majority of these RFB installations, particularly the newer ones, use the VRFB chemistry. Still, RFBs account for less than 1.5% of energy storage systems under development—a low rate of deployment that has been mainly attributed to cost factors (U.S. Department of Energy 2020). RFBs in general, and VRFBs in particular, have relatively high upfront capital costs today (approximately

\$170/kWh in energy costs and approximately \$600/kW in power costs for greenfield installations, see Table 2.1). As most of the demand for storage is still for 4-hour or shorter durations, the large power costs combined with expensive vanadium electrolytes challenge the ability of RFBs to compete with Li-ion batteries that continue to decline in cost. While VRFBs can compete with Li-ion batteries at storage durations beyond 6 hours, they still fall short of the DOE’s grid storage cost target (U.S. Department of Energy 2013; Advanced Research Projects Agency-Energy 2016) due to the high price of vanadium itself (Brushett et al. 2020; Rodby et al. 2020). Vanadium prices have been volatile for the past 40 years, and particularly so in more recent years, peaking in late 2018 at nearly ten times the price at the start of 2016 (Vanadium Price 2021). A more detailed discussion of vanadium resource issues appears in Section 2.7. Adding to the challenge of high and fluctuating vanadium cost is the cost of certain other components used in VRFBs, such as Nafion™ membranes, that can account for 20% or more of the total system cost. Nonetheless, there are cost-reduction pathways that show promise for facilitating broader deployment of RFBs; they are discussed in the next section (Section 2.4.2) (Minke and Turek 2015).

Upfront cost has not been the only impediment to broader RFB deployment—other perceived risks have also slowed development and dampened demand. The longer-duration applications in which RFBs become competitive (Table 2.1) are only recently being recognized. In the field, there are few RFB systems that have been deployed for more than five years, which creates a further barrier to financing RFB projects on a large scale. In comparison, Li-ion batteries have benefitted from three decades of deployment at increasing scales, from portable electronics to electric vehicles to grid energy storage, which

has served to build confidence in the technology. Meanwhile, the less-developed supply chain for RFBs also results in higher component costs. In short, RFBs have yet to benefit from the learning curve and economies of scale that propelled dramatic cost reductions in Li-ion battery technology over the past decade. As discussed in Chapter 6, however, deeper decarbonization of the electricity system is expected to rapidly increase demand for multi-hour to multi-day energy storage, for which RFBs may be best suited. A stronger government role in de-risking RFBs—especially in the form of support for large-scale demonstrations—may be important to realize the potential of this technology.

2.4.2 Technology improvement and cost reduction pathways for RFBs

Electrolyte leasing

An emerging market approach that takes advantage of the replaceable nature of electrolytes in an RFB installation and which could reduce the financial risk of RFBs is electrolyte leasing. The general concept is that the customer receives a reduction in upfront system costs that is approximately equal to the cost of the electrolyte, in exchange for annual payments, thereby shifting some of the capital expense to operating expense. Although logistical details of such arrangements are limited, reducing the upfront investment hurdle for the buyer may have the desired effect of reducing investment risk. This approach is most appealing for expensive electrolytes and has been implemented for VRFBs (Rodby et al. 2020; Skyllas-Kazacos 2019), but could be applied to other chemistries provided the materials are of high enough value to warrant such an arrangement and can retain value over the duration of the RFB project (in other words, there is minimal electrolyte decomposition).

Alternative chemistries

Given the economic challenges of the vanadium chemistry, numerous alternative chemistries are being actively researched with an increasing focus on utilizing earth-abundant, low-cost redox species. Given the multiplicity of interconnected requirements for RFB electrolytes (e.g., redox potential, solubility, stability, cost), none of these alternatives has demonstrated the same market readiness as the VRFB, but two classes of low-cost chemistries are of particular interest.

Abundant inorganic elements, such as iron, sulfur, manganese, or iodine, dissolved in suitable aqueous electrolytes, continue to be of interest. Many of these materials are generated either as products or by-products of commodity-scale industrial processes, which offers the benefits of scale and production infrastructure. Further, the use of waste materials may offer another revenue stream to chemical manufacturers and align with process sustainability goals. These approaches are presently challenged by several factors: the need to upgrade materials to electrochemical grade, the technical attributes of the chemistries, and the cost of other system components. High-purity electrolytes are needed to prevent side reactions within RFBs, particularly hydrogen generation on the negative electrode, which can be catalyzed by the deposition of metal impurities on the electrode. If an electrolyte requires purification prior to use, this can offset any cost-savings associated with switching to a less expensive active material. In addition, technical attributes of these materials do not always compare favorably with vanadium, which can lead to systems with lower-cost electrolyte chemistries but more expensive reactors, balance-of-plant systems, and long-term maintenance needs. Of particular note is the challenge of crossover in RFBs with different species on either side of the semi-permeable membrane. In contrast to a symmetric VRFB, the fact that many of these new materials are suitable for only one side of

the battery means a dissimilar material must be used on the other side (e.g., Fe-Cr). Over time, the different species will leak through the membrane, resulting in a loss of battery capacity and efficiency that cannot be easily recovered. Historically, one approach to mitigating this issue has been to premix the electrolyte such that both species exist on either side of the membrane, thereby reducing the driving force for crossover. This approach is often called a “spectator strategy” since, in each electrolyte, one species is active in charge storage and the other is a bystander. However, the spectator strategy comes with trade-offs, including reduced energy density and increased electrolyte cost. In addition, not all charge-storage materials are suitable for this approach, as they may drive side reactions within the opposing electrolyte. Thus, there is a continued need to identify inexpensive membranes with improved selectivity to enable new chemistries.

Redox-active organic molecules and coordination complexes (metal ions chelated by organic ligands) composed of earth-abundant elements represent another promising class of chemistries for RFBs. Over the past decade, many organic and organometallic molecular families have been proposed and pursued including quinones, viologens, nitroxide radicals, azaromatics, and transition-metal-centered coordination complexes, among others. A key feature of these compounds is the ability to tune physicochemical and electrochemical properties through molecular functionalization. For example, substituent groups can be appended to charge-storage materials to increase stability and solubility, shift electrode potential in the positive or negative direction, or prevent crossover through membranes (e.g., size- or charge-exclusion) (Doris et al. 2017). Moreover, redox-active organic molecules offer several secondary benefits including compatibility across a wide pH range, rapid redox kinetics, and multielectron transfer capabilities. In some cases, the relevant synthetic precursors of the final charge-storage compound are

intermediates in, or products of, large-scale industrial processes and require one- or two-step modifications for use in RFBs, potentially enabling cost-competitive manufacturing at low volumes (Dieterich et al. 2018; Gregory, Perry and Albertus 2021). Still, the current materials portfolio is challenged by molecular stability and uncertain manufacturing costs (Brushett, Aziz and Rodby 2020; Gregory, Perry and Albertus 2021). Despite improvements enabled by molecular engineering (Jin et al. 2020; Wu et al. 2020), electrolyte formulations, and operational strategies (Goulet et al. 2020), the decay rates for organic materials within RFBs are too high for long-duration use, and the array of decomposition products generated can compromise battery performance in a number of ways (Kwabi, Ji and Aziz 2020). Electrolyte management strategies including periodic replacement or rejuvenation have yet to be identified but, in combination with suitably inexpensive and stable charge-storage materials, such strategies may offer a pathway toward extended use (Rodby, Perry and Brushett 2021). Uncertainty in synthesis costs stems from the range of molecules under consideration, their compatibility with current manufacturing routes and infrastructure, the reliance on production scale, and the technical requirements for cost-effective battery operation (e.g., allowable chemical costs, purity) (Gregory, Perry and Albertus 2021).

Nevertheless, the breadth and diversity of the organic design space continues to offer opportunities for the discovery and development of new charge-storage materials enabled by advances at the frontiers of high-performance computation, molecular modeling, and automated synthesis (Dave et al. 2020; Sanchez-Lengeling and Aspuru-Guzik 2018; Trahey et al. 2020). Finally, transitioning from aqueous electrolytes to nonaqueous electrolytes can enable wider electrochemical stability windows, allowing for higher cell voltages. This can also enable the use of a broader range of redox-active organic and organometallic compounds,

many of which are incompatible with aqueous electrolytes due to low solubility, chemical reactivity, or redox potentials outside the stability window.

Taken together, new pathways to low-cost RFBs may be available, but the subfield is nascent and archetypal systems have yet to emerge (Darling et al. 2014). Still, we can consider a theoretical low-cost and high-abundance aqueous RFB chemistry to estimate future (i.e., 2050) costs. With continued technical advances to these alternative chemistries, we estimate RFB costs may drop to approximately \$50/kWh in energy costs and approximately \$400/kW in power costs (for greenfield installations) (see Table 2.1).

Reactor and architecture improvements

Beyond lowering chemical costs (Figure 2.2), RFB cost reductions can be achieved through improvements in other system components. Of the numerous components in an RFB system (Ke et al. 2018), we highlight two: the membrane and the electrodes. These components, within the electrochemical stack (reactor), play a significant role in performance and cost.

The membrane that separates the positive and negative electrolytes within the reactor has a considerable impact on the technical and economic performance of RFBs (Darling, Gallagher and Brushett 2016). While specific requirements are chemistry-dependent, typical sets of properties to be balanced are conductivity, selectivity, stability, and material cost (Choi et al. 2018; Oldenburg, Schmidt and Gubler 2017). For many RFB chemistries, preventing crossover is critical to maintaining performance over the system's operational lifetime. Most current RFB chemistries employ ion-selective membranes, which separate molecules based on their charge, but there is emerging interest in size-selective membranes, which separate molecules by their solvated diameter. This approach is particularly attractive with

engineered charge-storage species (e.g., redox-active organics), which tend to be larger than the charge-balancing ions in the electrolyte solutions (Milshtein et al. 2017). An alternate approach, described earlier in this chapter, is the use of capacity-management strategies that offset imperfect membranes by periodically rebalancing the two electrolytes (e.g., through volume exchanges between tanks). The approach is effective for RFBs with the same electrolyte composition on either side of the battery, including VRFBs, which use vanadium's four different oxidation states, and Fe-Cr batteries, which use the spectator strategy described earlier in this section.

The porous electrodes used in RFBs facilitate a variety of performance-defining phenomena, including dispersion of electrolytes across the reaction volume, access to the heterogeneous reaction sites for charge and discharge reactions, and passage of current into and out of the reactor (Forner-Cuenca and Brushett 2019). Accordingly, the surface chemistry and microstructure of the electrodes play an important role in observed electrochemical and fluid dynamic performance. Most commercial porous electrodes consist of micrometric carbon fibers that are consolidated into paper, felt, or cloth, each with a different microstructure and, consequently, divergent physical properties (e.g., flexibility, porosity). As this manufacturing approach typically leads to low surface area with undesirable composition, electrode materials are typically pretreated before they are used in RFBs to increase the area where reactions can occur and to functionalize the surface to promote redox reactions. Continued advances in the development of porous electrodes, including tailoring materials for specific redox chemistries and system designs, may enable improvements in power density without sacrificing efficiency.

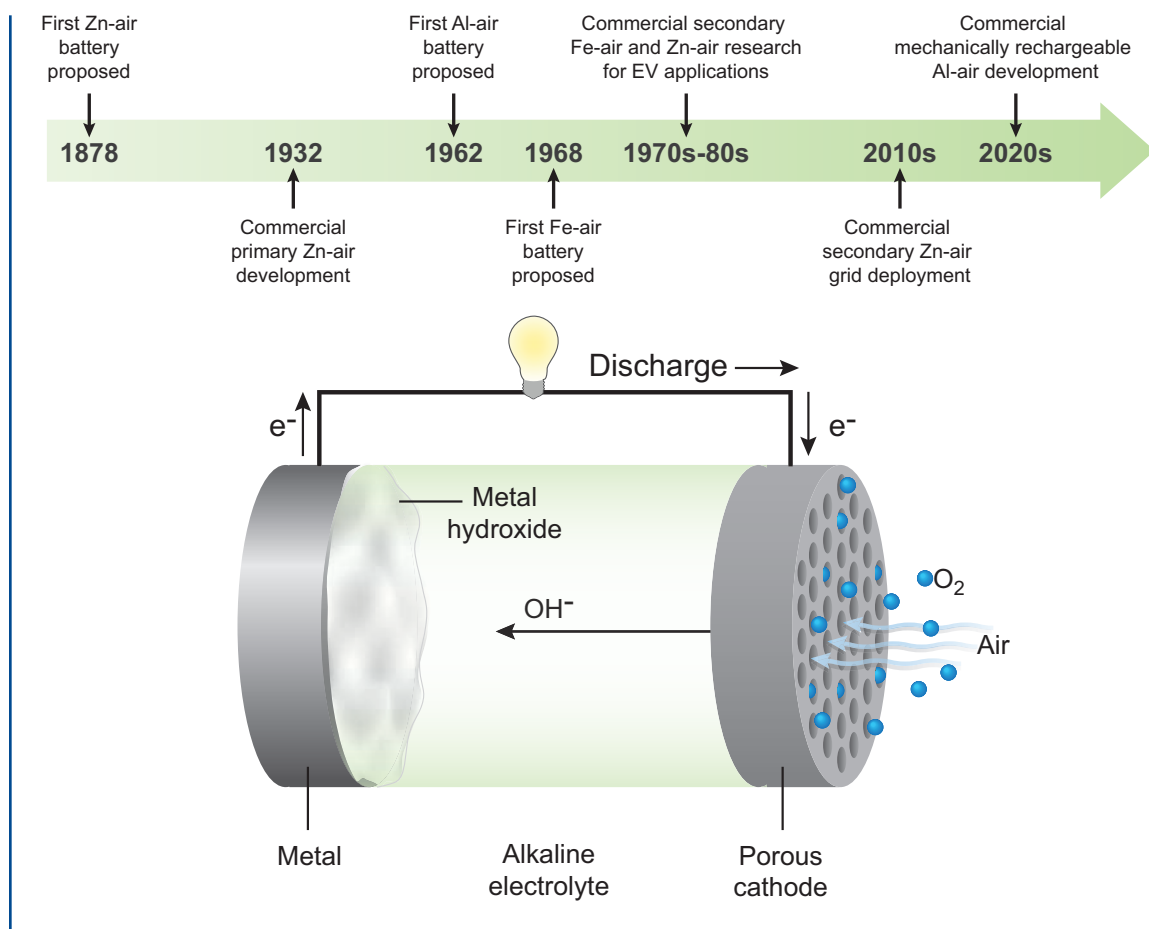
Finally, there is growing interest in energy-dense RFB configurations that incorporate solid-state storage materials without sacrificing the favorable attributes of the system

architecture (Soloveichik 2015). In one embodiment, solid materials are suspended in an electrolyte and the resulting slurry is pumped through the reactor. Here, the electronically conductive solid materials serve as flowable electrodes storing charge either through intercalation reactions (e.g., Li-ion battery materials) or through electrodeposition reactions (e.g., metal deposition on carbon particles) (Duduta et al. 2011; Petek et al. 2015). In a second embodiment, solid charge-storage materials are packed into the electrolyte tanks and the soluble redox species serve as mediators, shuttling the charge between the reactor to the tank; this approach is often termed “redox-targeting” or “redox-mediation” (Gentil, Reynard and Girault 2020; Zhang et al. 2021). While potentially promising, these systems have complex electrochemical and rheological behavior and the impact of this behavior on scalability and cost-effective operation remains unknown.

2.4.3 Summary

RFBs are an attractive energy storage solution for longer-duration applications (>6 hours) due to their unique system architecture, which decouples the energy and power components and allows for low-cost capacity scaling. The technology platform can incorporate a wide array of chemistries, among which the most developed at present is the VRFB, which is unique for its ability to perform indefinitely with inexpensive operational maintenance. While the modeling undertaken for this study (Chapter 6) shows a promising role for RFBs in grid applications as decarbonization proceeds, deployment to date has been low due to high upfront costs and perceived financial risk. Alongside technical developments such as the advent of new redox chemistries that use low-cost and abundant elements and the improvement of reactor performance through the use of better membranes and electrodes, RFB deployment may also be accelerated through new financial models such as electrolyte leasing.

Figure 2.8 History of metal-air battery development and schematic design of a typical metal-air battery cell



Given the relative absence of applications outside of grid energy storage, successful demonstrations and pilot projects are important for de-risking RFBs and encouraging commercial deployments. Here, government can play an important role (Goldstein 2021) by supporting demonstration projects at various stages of development (e.g., through the DOE's Office of Electricity or ARPA-E's SCALEUP program) up to commercial pilots for relatively mature technologies.

2.5 Metal-air batteries

Metal-air batteries deliver electrical energy upon discharge through the spontaneous (energetically “downhill”) oxidation of the metal (Figure 2.8). The metal serves as the negative electrode (the anode, during discharge) and is paired with a positive electrode (the “air cathode,” during discharge), which does not store any electrical charge itself, but which takes oxygen from the air and produces hydroxyl ions in the electrolyte during discharge—an electrochemical reduction process. Electrons flow from the metal negative electrode to the positive electrode through an external circuit, providing electric power. In rechargeable metal-air batteries, this metal-oxidation reaction can

be reversed through the application of voltage and current to store inputs of electrical energy. Although virtually any metal that spontaneously oxidizes can serve as the basis for a metal-air battery, relatively few metals have all the attributes desired for an electrically rechargeable battery. Historically, metal-air batteries have primarily been used as disposable low-power batteries in small consumer devices, the most common example being zinc-air batteries for hearing aids. Although research on rechargeable metal-air batteries has been ongoing for several decades, commercial products have only recently reached the marketplace, in the form of rechargeable zinc-air batteries (Fehrenbacher 2016).

Two main categories of metal-air batteries have received the most attention to date. They are distinguished by the type of electrolyte they use, which is either aqueous (typically alkaline) or non-aqueous (typically based on an ether or alkyl carbonate organic solvent). The choice of electrolyte reflects its stability against parasitic reactions under the operating voltage of the cell: zinc-air, iron-air, and aluminum-air batteries can use aqueous alkaline electrolytes, whereas lithium-air and sodium-air batteries have higher cell voltages that are attractive for higher energy and power densities but require non-aqueous electrolytes. Metal-air batteries of both types have high theoretical specific energy (defined as the amount of energy that can be stored upon oxidizing the entire mass of metal). The theoretical specific energies of lithium-air batteries and zinc-air batteries is about 50 times and 5 times the demonstrated specific energy of commercial Li-ion batteries, respectively (Wang and Xu 2019). However, it has been challenging to attain these high specific energies in practice; commercial primary (disposable) zinc-air batteries reach only about 35% of their theoretical energy density (Li and Lu 2017). Losses arise from various operating inefficiencies leading to incomplete oxidation of the metal, and

energy density is further diluted by supporting materials and structures that add considerable mass and volume. Promising attributes of aqueous metal-air batteries also include safety and cost: They are safer than Li-ion batteries, largely because the aqueous electrolyte is not flammable, and they have one of the lowest chemical costs of stored energy for rechargeable batteries (Figure 2.2). These beneficial properties are offset by lower power and roundtrip efficiency, due to high electrical polarization at the air electrode, passivation of the metal electrode, and/or parasitic reactions such as hydrogen evolution at the negative electrode. Open-circuit voltages for metal-air batteries are lower than for Li-ion batteries—2.9 V for lithium-air, 1.65 V for zinc-air, and 1.28 V for iron-air—and cycle life is typically shorter due to degradation of one or both electrodes. Lower cell voltage means that more cells are needed in series to reach a high system voltage when compared to Li-ion batteries. The use of an air electrode can result in more complex cell or system designs to provide for gas management.

Metal-air batteries using an alkaline aqueous electrolyte are currently most attractive for stationary electrical storage applications, largely due to their safety and cost benefits. The cost of non-aqueous metal-air chemistries tends to be higher than that for aqueous chemistries, primarily because of metal and electrolyte costs. For example, lithium metal is more than an order of magnitude more expensive by mass than zinc or iron: In 2019, spot market prices for lithium ranged from \$80 to \$120 per kilogram (kg) (U.S. Geological Survey 2020); in contrast, commodity prices for zinc have been in the range of \$2–\$3/kg since 2004 (Markets Insider), and prices for iron are in the range of \$0.1–\$0.2/kg (Markets Insider). After accounting for cell voltage, specific capacity, and electrolyte costs, the chemical cost of storage for these three metal-air chemistries is approximately \$40/kWh, \$6/kWh, and \$0.6/kWh, respectively (Figure 2.2). Through low chemical

costs, aqueous alkaline metal-air batteries have the potential to achieve system costs for energy storage below \$10/kWh. For long-duration electrical storage, in particular, these low energy costs represent a favorable trade-off against the higher power costs and lower roundtrip efficiencies of this battery technology.

In contrast to Li-ion and redox flow batteries, for which numerous combinations of positive and negative active materials are of potential interest, only a few metals have the combination of cost (Figure 2.2) and other attributes to facilitate metal-air batteries for practical use in grid-scale energy storage. Of these, zinc-air batteries are the most technologically mature, and have been developed as both primary and secondary batteries. In the 1970s and 1980s, there was brief interest in iron-air batteries for electric vehicle applications; this chemistry is now attracting renewed interest for grid-scale storage. (McKerracher et al. 2015; Gold 2021) Aluminum-air batteries also have low chemical cost, but their recharging performance is poor; for this reason, they have mostly been commercialized as primary (single-use) batteries to date, although aluminum-air systems may be considered “mechanically rechargeable” via anode reprocessing (Bharadwaj 2021).

Compared to Li-ion batteries, commercial uses of zinc-air secondary batteries are recent and limited in scale due to the trade-offs mentioned previously. Multiple efforts to deploy commercial systems for stationary storage applications have been documented, including reports of tens of megawatt-hours of storage being fielded in small-scale systems across 3,000 installations (Hanley 2018). The New York Power Authority announced a commercial partnership to install a 100-kW/1-MWh zinc-air system, as part of a bid to install 3 GW of energy storage in the state of New York by 2030 (New York Power Authority 2020). Some of these efforts project manufacturing costs for zinc-air systems below \$100/kWh (Hanley 2018), which may be competitive with future Li-ion costs.

System-level costs below \$20/kWh have been projected for iron-air battery storage (McKerracher et al. 2021).

The remainder of this section discusses key technology considerations at the component level that impact the performance of metal-air batteries, with an aim toward understanding technical barriers and potential paths forward for successfully developing these technologies. Other low-cost chemistries that are not metal-based but are considered “air-breathing” are briefly discussed.

2.5.1 Electrochemistry of metal-air batteries

All metal-air batteries have in common a metal negative electrode that is oxidized on discharge and reduced back to the metal on charge, and an air positive electrode at which oxygen is absorbed from the gas phase on discharge and evolved as gas on charge. In some designs, the two functions of the air cathode are split between two different electrodes with one taking in oxygen gas and the other evolving oxygen gas. The metal anode undergoes reversible oxidation to form metal ions dissolved in the liquid electrolyte, or may form an insoluble solid metal oxide or metal hydroxide reaction product at the surface of the metal negative electrode. In addition to the metal negative electrode and air positive electrode, major components of a metal-air battery include a separator and a liquid electrolyte. The separator prevents the two electrodes from coming into physical contact and may serve other functions such as preventing the cross-over of dissolved species or formation of metal dendrites that may cause internal electrical short circuits.

The electrolyte is usually the same for both the negative and positive electrode chambers and can cross the separator freely. Aqueous metal-air batteries typically use an alkaline electrolyte for high ionic conductivity and compatibility

with low-cost, air negative electrode materials. In zinc-air systems, alkaline electrolytes are also favored due to their high solubility for the zinc reaction products, which prevents passivation of the zinc surface that otherwise inhibits continued reaction of zinc (Mainar et al. 2018). The most commonly used aqueous electrolytes are based on a potassium hydroxide (KOH) solution with a molar concentration (M) of 6 or higher, plus various performance-enhancing additives.

The metal-air battery architecture is unique among battery designs in that one electrode, the air positive electrode, must be exposed to ambient atmosphere in order to allow for an influx of air or oxygen on discharge and the evolution of oxygen on charge. The metal negative electrode is typically sealed, although there are designs that employ a circulating electrolyte to distribute dissolved metal ions or to reduce metal dendrite formation (Fu, Cano, et al. 2017).

Metal negative electrodes: Status and challenges

Metal electrodes typically benefit in utilization (extent to which they are reversibly oxidized) and rechargeability if the oxidation product has some solubility in the liquid electrolyte. Taking zinc as an example, in highly alkaline electrolytes the zinc redox reaction forms zincate ion ($Zn(OH)_4^{2-}$), which is soluble. This is initially beneficial since it allows zinc oxidation to continue. However, once the concentration of zincate reaches its solubility limit in the electrolyte, the zincate precipitates as zinc oxide (ZnO). This “side reaction” reduces cell performance, since the zinc oxide typically precipitates as a passivating layer at the electrode surface that limits the utilization of the zinc negative electrode and increases electrical resistance unless it is removed or redissolved into the solution as zincate (Fu, Cano, et al. 2017). An irreversible loss of negative electrode capacity occurs if zinc oxide precipitates elsewhere in

the cell and is not redissolved. Zinc oxide precipitation can also take place at the positive electrode surface, where it has the added detriment of inhibiting the oxygen redox reaction (Wang and Xu 2019). Crossover of zincate ions from the anode to the cathode can be reduced by using membranes designed to block zincate while allowing hydroxide ions to pass freely (Gu et al. 2017), but such membranes add to the cost of the system (Fu, Cano, et al. 2017).

A second type of detrimental reaction that must be managed for efficient cycling of zinc electrodes is dendrite formation. During the charging step, zincate ions are reduced back to zinc metal at the electrode surface, a process that occurs preferentially at protrusions of the metal electrode where the electric field is highest. This self-propagating process can result in the formation of needle-like metal dendrites that can grow through the separator and cause battery failure via short circuits, or cause capacity loss if the dendrites fracture from the anode and become electrically inaccessible during subsequent discharge (Zhao et al. 2019). Separators with high mechanical strength can mitigate dendrite penetration, but this must be balanced against the simultaneous need for high conductivity and zincate crossover suppression (Fu, Cano, et al. 2017). It is also possible for dense zinc negative electrode morphologies to form during cycling, which reduce accessed capacity and lifetime by decreasing the electrochemically active surface area that is available during cycling (Fu et al. 2017; Mainar et al. 2018). These anode morphology challenges do not occur in all aqueous metal-air systems. Notably, the iron-air couple shows no signs of dendrite formation in alkaline electrolytes (McKerracher et al. 2015)—behavior that is related to the low solubility of iron hydroxide, which forms as a solid hydroxide surface film rather than dissolving and plating from solution (Weinrich et al. 2019).

Another common deleterious side reaction at the anode in aqueous metal-air systems is the evolution of hydrogen during charging, which is thermodynamically favored over the metal hydroxide reduction reaction for aqueous zinc, aluminum, and iron-air systems. Hydrogen evolution consumes current that would otherwise go towards metal hydroxide reduction, lowering the efficiency during charging. The reaction of the metal with water forming metal hydroxide and releasing hydrogen is another side reaction that results in self discharge of the battery. These effects lead to a state-of-charge imbalance between the half cells in a metal-air battery, reducing the accessible capacity. The side reactions also consume electrolyte, decreasing the shelf life of the battery unless supplemental water is added or the evolved hydrogen is catalytically combined with oxygen within the cell to re-form water.

The above-described failure mechanisms can be mitigated to some extent by changing the architecture of the electrode material or cell, modifying the composition of the metal electrode or electrolyte, or developing a suitable separator. The most common modifications to electrode architecture attempt to increase utilization and reaction rate by increasing the accessible surface area of the electrode, typically through the use of alternative materials such as a 3D metal sponge or powder-based electrode (Fu et al. 2017; Gu et al. 2017). Some modifications of this type have little impact on anode cost (Hopkins et al. 2020). However, high-surface-area electrodes also have greater area for the hydrogen evolution and self-discharge reactions, can lose electrical contact more easily, and are less mechanically robust. At the cell level, a widely used architectural modification is to incorporate electrolyte flow through the negative electrode chamber. Forced convection can be designed to knock weakly bound oxides off the metal surface to reduce resistance from passivation layers, break off dendrites, or reduce zincate concentration gradients that

amplify morphology changes (Fu et al. 2017; Zhao et al. 2019). However, methods to address decay and extend cycle life increase the cost and complexity of the system.

Electrode and electrolyte additives perform some combination of limiting metal-ion dissolution, regulating the surface structure to mitigate dendrite formation, and stabilizing the metal electrode against side reactions. Alloying a metal electrode with other metals, such as lead, nickel, or indium, can suppress hydrogen evolution. Coatings on the electrode surface can do the same while also suppressing zincate dissolution. Solid additives in the electrode and dissolved additives in the electrolyte have been widely studied as strategies to mitigate the various shortcomings of metal negative electrodes (Zhao et al. 2019; Li and Dai 2014).

The separator can play a key role in suppressing undesirable crossover of ions (such as zincate) between the two electrode chambers, but it must be selective enough to permit the transport of working ions. Improved ion selectivity can reduce metal crossover-related capacity losses and detrimental metal oxide deposition on the air electrode. However, these improvements must avoid compromising chemical and mechanical stability, ionic conductivity, and separator cost. Separator design challenges are usually greater for metal negative electrodes that have a high solubility of the oxidized species.

Air positive electrodes: Status and challenges

The positive electrode assembly serves as the electroactive interface between the liquid electrolyte and the gas phase. It must be designed to strike an appropriate balance between hydrophilicity and hydrophobicity, provide electronic conductivity, support oxygen electrocatalysts, and allow oxygen gas to diffuse to the catalytic reaction sites. Zinc-air battery positive electrodes contain a carbon-based gas

diffusion layer (GDL) that has been adapted from decades of work on fuel-cell oxygen electrodes (Wang and Xu 2019). However, whereas fuel-cell electrodes are only required to take in oxygen (the oxygen reduction reaction, ORR), a rechargeable air electrode must also evolve oxygen (the oxygen evolution reaction, OER). ORR requires high porosity and some hydrophobicity so that there is an adequate density of three-phase sites where the electrolyte, gas phase, and electrocatalyst meet, and to facilitate oxygen transport to those sites (Gu et al. 2017; Fu, Liang, et al. 2019). OER requires hydrophilicity, so that the liquid phase from which oxygen is evolving can wet the catalytic sites, as well as stability at the high oxidation potentials of this reaction. The ORR and OER functions may be combined in a single “bifunctional” air electrode or split between separate electrodes (Li and Dai 2014).

Development of metal-air battery positive electrodes has mainly focused on materials stability issues at high oxidizing potentials (especially the stability of carbon scaffolds and substitutes) and the development of efficient, low-cost, bifunctional electrocatalysts (Fu, Cano, et al. 2017; Gu et al. 2017; Wei et al. 2020). Positive electrode structural degradation is accelerated at high operating potentials and high current densities. Carbonate and bicarbonate ions that form when carbon dioxide is absorbed from the air by the alkaline electrolyte can affect air electrode activity. Metal-air batteries designed for long-duration storage are typically less demanding of air electrodes since current densities can be lower and the total number of charge-discharge cycles experienced over the lifetime of the battery are fewer than in short-duration applications.

Other air-breathing chemistries

Two other variants of the metal-air battery may have potential for grid-scale storage. One is the “mechanically rechargeable” primary battery, in

which the oxidized metal anode or the entire cell is physically replaced after the cell is discharged. Spent anode material can then be recycled back to its metallic form (Fu, Liang, et al. 2019) and the cost of reprocessing becomes part of the cost structure for the system.

Aluminum-air batteries are one candidate for this approach as they have high energy density and low cost, but poor electrical reversibility. A second variant is exemplified by the air-breathing aqueous sulfur flow battery (Li et al. 2017), in which there is no direct reaction between the redox-active materials, sulfur and oxygen. Instead, the alkali ions traverse a membrane that separates an air positive electrode from a negative electrode comprising dissolved polysulfide species. A change in the sodium-ion concentration of the electrolytes used in the air or sulfur electrodes causes the uptake or release of oxygen, concurrent with a change in the sulfur charge state. Chemical costs for this variant can be as low as \$1/kWh (Figure 2.2) and, in a flow battery configuration, it offers the capability for independent scaling of power and energy, which favors long-duration storage. The main drawback of air-breathing aqueous sulfur flow batteries is the challenging requirement for an ion-selective membrane that can separate positive and negative electrolytes of low and high pH, respectively.

2.5.2 Commercialization status

The potential for very low materials costs, high energy density, relatively simple cell designs, and inherent safety make aqueous metal-air batteries one of the more promising electrochemical technologies for grid-scale energy storage. In comparison to Li-ion batteries, current iterations of metal-air batteries have lower roundtrip energy efficiency, higher power cost, and lower cycle life. This combination of attributes makes metal-air batteries well-suited for energy storage durations greater than about 12 hours, where the ratio of stored energy to discharge power is high. Moreover, the metallic

negative electrodes that allow for low chemical cost (e.g., zinc, iron, and aluminum) are commodity metals that are already produced in high volumes for other industries. These characteristics suggest that, once developed, metal-air batteries could scale in production volume much more quickly than has been the case for Li-ion batteries. However, the commercialization of rechargeable metal-air batteries is still at an early stage, and learning curves for technological performance and cost reduction have yet to be established.

Nonetheless, it is possible to develop bottom-up cost projections for metal-air battery storage based on the performance metrics and costs associated with specific designs, which we have done as part of our modeling analysis for this study (Appendix A). Our projected power costs for metal-air batteries are relatively high (\$590–\$950/kW, compared to \$30–\$150/kW for Li-ion batteries and \$290–\$530/kW for RFBs), but projected energy costs are extremely low (\$0.1–\$4.0/kWh), suggesting potentially important roles for this technology in long-duration storage applications. For greenfield metal-air systems (i.e., those installed at new sites), we expect the total cost of ownership (defined as the total cost of installing and maintaining the system for its expected lifetime) to be below \$100/kWh for storage durations greater than 12 hours. Brownfield systems (using existing facilities) are further cost advantaged, with projected power cost reductions of as much as \$150/kW.

2.6 Other batteries of relevance to stationary storage

2.6.1 Lead-acid batteries

The lead-acid (Pb-acid) battery was the first rechargeable battery invented (Figure 2.2). Despite strong competition from a wide range

of newer technologies, as of 2018, Pb-acid batteries still comprised 48% (\$37.5 billion) of total battery sales worldwide (Pillot 2019). Vehicle applications account for about 75% of current Pb-acid deployment (by energy capacity) (Pillot 2019). This technology is also used in stationary applications, but mostly for behind-the-meter applications, which comprised about 4.5% of the total electrochemical energy storage capacity deployed worldwide in 2017 (International Renewable Energy Agency 2018). In the United States, only 1% of total deployed electrochemical energy storage—most of which was added between 2003 and 2018—is comprised of Pb-acid batteries (U.S. Energy Information Administration 2021). Pb-acid batteries made up 27% of the total electrochemical storage capacity deployed in China in 2018 (China Energy Storage Alliance 2019), but this share fell to 14% in 2019 (China Energy Storage Alliance 2020), mainly due to strong growth in Li-ion battery deployment.

Pb-acid batteries are a highly mature technology with well-understood advantages and disadvantages. Both the positive and negative electrodes are lead-based, and an aqueous sulfuric acid electrolyte ($\text{pH} < 2$) provides a source of sulfate ions to the cell reaction. In the discharged state both electrodes comprise lead sulfate (PbSO_4), while in the charged state the positive electrode is oxidized to lead oxide (PbO_2) and the negative electrode is reduced to lead metal (Pb). Pb-acid batteries have a lower specific energy (30–40 Wh/kg) (Dell and Rand 2001) than Li-ion batteries (150–200 Wh/kg), but this metric is less important for stationary storage than for mobile applications. Roundtrip efficiency is reasonably high at 79%–86% (Mongird et al. 2020). Chemical cost is lower than for Li-ion batteries (Figure 2.2) and manufacturing is simpler. The installed cost of a 4-hour Pb-acid battery is estimated to be

\$260–\$290 per kWh, very close to that for Li-ion (\$275–\$290/kWh).² Pb-acid batteries also have a mature supply chain and high recycling rate (> 99% in the United States and Europe) (May, Davidson and Monahov 2018). Since they use an aqueous electrolyte, they are arguably safer than Li-ion batteries.

The main reason grid deployment of Pb-acid batteries is currently being surpassed by that of Li-ion batteries in most locations is their short cycle life. The cyclic phase changes incurred at the electrodes during battery operation lead to progressive material loss (Lopes and Stamenkovic 2020), which—combined with parasitic reactions such as water electrolysis, acid stratification, and impermeable sulfate buildup on the electrodes—contributes to shortened cycle life (May, Davidson and Monahov 2018). Over more than a century of development, some of these issues have been resolved through improved electrode formulations, cell designs, and manufacturing methods (Consortium for Battery Innovation 2019; Dell and Rand 2001). Nonetheless, when cycled at 80% depth of discharge, Pb-acid batteries have a shorter cycle life of around 600–1,000 cycles compared to 1,000–3,000 cycles for Li-ion batteries cycled to the same depth of discharge (Mongird et al. 2020; U.S. Agency for International Development 2021). This results in higher cost of delivered energy per cycle in grid applications. As previously mentioned, the cycle life of Li-ion batteries only continues to increase. Moreover, the installed-cost gap between the two is expected to shrink in coming years, largely because Li-ion costs continue to decline whereas Pb-acid costs have long since plateaued. Developing countries may provide an exception to this trend—in these settings, costs for Pb-acid batteries can be as

much as a factor of two less than for Li-ion batteries (U.S. Agency for International Development 2021), and Pb-acid batteries can be expected to continue to play a major role in stationary storage until at least 2030.

2.6.2 High-temperature batteries

We classify high-temperature batteries as those in which a molten metal is used for at least one of the electrodes. Here, we discuss three examples: the sodium-sulfur (Na-S) battery, the sodium-nickel chloride (Na-NiCl₂) battery, and the liquid-metal battery. Although the Na-S battery was originally developed by the Ford Motor Company in the 1960s for EV applications (Energy Storage Association), today, interest in all three chemistries is primarily motivated by potential grid storage applications. Na-S batteries use molten sodium as the negative electrode, molten sulfur as the positive electrode, and a solid sodium-ion conductor, typically beta-alumina (β -alumina), as the solid electrolyte. Na-S batteries are usually operated at temperatures between 300°C and 350°C, a range in which both electrodes are molten and the ionic conductivity of the solid electrolyte is elevated (Hueso, Armand and Rojo 2013). A typical cell design uses a large number of close-ended β -alumina tubes to contain the molten sodium metal, while the molten sulfur electrode surrounds these tubes.

In the Na-NiCl₂ battery, termed the ZEBRA battery because it originated with the Zeolite Battery Research Africa Project in South Africa in the 1970s, the molten sulfur electrode is replaced by a solid NiCl₂ electrode. Both Na-S and Na-NiCl₂ batteries (Hueso, Armand and Rojo 2013) have very good cycle life of 3,000–5,000 cycles at 80% depth of discharge and have

² A 12V Pb-acid battery pack with storage racks is estimated to cost \$150–\$180 per kWh (Mongird et al. 2020). (Assuming the balance-of-plant (BOP) and engineering, procurement, and commissioning (EPC) costs are similar for both technologies (\$111 per kWh for 4 hour discharge assuming a brownfield installation, calculated following the methodology in Appendix A), the installed cost for Pb-acid batteries is in the range of \$261– \$291 per kWh, nearly the same as for Li-ion batteries (\$275–\$290 per kWh).

been considered for front-of-meter grid storage applications. As of early 2020, NGK of Japan, the primary commercial developer of Na-S technology, had deployed about 560 MW/4 GWh of Na-S battery capacity worldwide (Spoerke et al. 2020). (Grid deployment of Na-NiCl₂ batteries is negligible by comparison.) While both battery technologies were historically significant, cost is their main competitive challenge today: Current installed costs are in the range of \$600–\$700 per kWh, with the potential to decline further to \$500/kWh (Spoerke et al. 2020). By comparison, installed costs for Li-ion systems are in the range of \$275–\$290 per kWh today.

The liquid-metal battery (Kim et al. 2013) is a high-temperature battery that differs from the Na-S and Na-NiCl₂ batteries in that it also has a liquid electrolyte, selected to be immiscible with the metal electrodes. In addition, the three phases are selected to have differences in density that result in self-segregation with the liquid electrolyte layer residing between the two metal electrodes. The cathode, anode, and electrolyte are sealed in a metal container to form a high-temperature electrochemical cell. While a number of metal combinations have been described for this technology—examples include lithium-antimony-lead (Li-Sb-Pb), magnesium-antimony (Mg-Sb), calcium-bismuth (Ca-Bi), and calcium-antimony (Ca-Sb) (Kim et al. 2013)—current development efforts appear to be focused on the Ca-Sb couple and with an operating temperature of 500°C, at which calcium is liquid and pure antimony is solid (Ambri). At current metal prices, the chemical cost for Ca-Sb is about \$20 per kWh, about a factor of two below the mid-range of Li-ion chemical costs (Figure 2.2). (Note that this takes into account a decrease in the price of antimony by about a factor of two between 2012 and 2020 (Antimony Prices).) This nascent technology appears to be nearing the demonstration stage; claimed advantages are a lower cost of manufacturing compared to Li-ion, cycle life in the tens of thousands of

cycles (resulting in favorable leveled cost of delivered electricity), calendar life exceeding 20 years, and stable operation over a wide range of ambient temperatures (assuming that the high internal battery temperature is maintained)(Ambri). A potential risk of the Ca-Sb chemistry is the supply risk for antimony, a metal which has consistently appeared on listings of critical elements and is sourced primarily from outside the United States. Applying the materials availability analysis described in the next section of this chapter (Section 2.7) to antimony indicates that supply constraints are even more restrictive than those for vanadium.

2.7 Materials availability issues for electrochemical storage

Like many advanced energy technologies, electrochemical energy storage is materials intensive. Batteries require specific chemical elements for which functional substitutes are sometimes not readily available. In many cases, these elements are used in direct proportion to the energy storage capacity of the technology. For example, every kilowatt-hour of Li-ion battery storage requires a certain amount of lithium.

To achieve near-decarbonization of the U.S. economy by 2050, battery deployment for both grid-scale storage and electric vehicle applications will have to scale rapidly to very high levels. Similar efforts overseas will further add to global demand. These trends can be expected to increase society's dependence on certain critical chemical elements, making it necessary to evaluate their availability and understand their complex and sometimes underdeveloped supply chains. For example, grid-scale energy storage in the United States, which is the subject of this report, is unlikely to dominate future demand for Li-ion batteries, but grid-scale storage might nevertheless suffer from any fluctuations or interruptions in materials supply that might be driven by larger Li-ion

battery consumers. In this section, we explore how materials availability and supply chains could affect the scalability of electrochemical storage technologies over the time horizon of this report.

Criticality is an emergent system property that derives from the confluence of supply risk (limited availability of key elements) along multiple time horizons and vulnerability (impact of a possible supply disruption, which may affect the behavior of an organization or a geopolitical entity). An element may be intrinsically rare in the Earth's crust, poorly concentrated by natural processes, or primarily produced in one or a small number of countries, which increases the risk that supply could be affected by market manipulation or political instability. In some locations, extraction and production may entail unacceptable environmental or social costs. The availability of elements that are produced primarily as byproducts may be limited by the economics of the primary product with which they are associated. Technical expertise in extraction, processing, and other supply technologies tends to follow the resources, leaving the United States at a further disadvantage when an element is primarily produced overseas. The existence of effective substitutes for a given material can reduce its criticality for a particular technology, as can the potential for functional recycling. In general, criticality is determined not by whether the supply of a material might run out, but rather by whether perceived (or actual) supply risk, based on a set of factors, is deemed too high and affects the deployment of a storage technology at scale.

Ideally, risk could be quantified by measuring the sensitivity of technology adoption to material price increases or price volatility. Given the huge uncertainties involved in relating materials availability to price, we make no attempt to predict prices for different battery elements. Instead, we focus on

materials-related risk by studying constraints on availability and by exploring the impact of disruptions to the supply of elements that we believe to be critical to the electrochemical technologies identified earlier in this chapter. Previous work has found that materials costs may set practical lower bounds on the costs for electrochemical technologies (Hsieh et al. 2019). Technology costs, in turn, may set a limit on the ability of any given storage option to scale in the near term. So, understanding the materials risks that can influence technology cost is critical.

We begin in Section 2.7.1 by identifying potential critical elements for the electrochemical energy storage technologies discussed in this chapter. Section 2.7.2 goes on to describe basic metrics and criteria related to materials supply, considers these metrics in the context of deployment at scale, and applies them to the critical elements identified in Section 2.7.1. Section 2.7.3 comments on the potential role of recycling within the time horizon of this report (that is, from the present to 2050), and Section 2.7.4 describes material supply concerns for the most critical elements we identified.

2.7.1 Critical elements for electrochemical energy storage

For the electrochemical energy storage systems of interest in this report, the elements of concern lie in the components that scale with energy capacity: positive electrodes, negative electrodes, and electrolytes. We do not consider materials required for casings, interconnections, and power conversion electronics. In general, when we refer to a "material" we mean specifically a chemical element. In some cases, however, elements must be available in a particular form to be usable in batteries. For example, nickel pig iron and ferronickel, which account for more than 50% of nickel production, are not currently suitable for use in the positive electrodes of a Li-ion battery. Thus, these forms

of nickel must be considered independently in a detailed analysis of nickel availability for battery-grade applications. The list of materials employed in the battery technologies we have considered includes aluminum, cobalt, graphite (carbon), iron, lead, lithium, manganese, nickel, phosphorus, sodium, sulfur, vanadium, and zinc. Several metrics can provide initial insight into availability constraints for these materials. We first consider global *resources*³ of a given element. For some elements, global resources are large and broadly distributed such that there is little concern about meeting world demand, including for battery deployment at the scale envisioned in this report, well into the future. Aluminum, graphite, iron, lead, manganese, phosphorus, sodium, sulfur, and zinc fall into this category (U.S. Geological Survey 2020). By contrast, cobalt, lithium, nickel, and vanadium are potentially critical elements for electrochemical energy storage from a global resource standpoint. The size of the global resource base alone, moreover, is not sufficient to guarantee adequate supply of a given element. How much of that element might be economically extracted and how much is consumed (or produced) must also be considered—and both can change over time. The “static depletion index” is the ratio of *reserves*⁴ to annual production. Generally, the stability of this number is an indication that, historically, newly extractable reserves have developed in response to changes in production. An index that is decreasing or increasing over time, however, indicates the potential for market volatility. Figure 2.9 plots the static depletion index for several key elements over time (in five-year increments) relative to the fraction of supply from the top-producing country. It shows that the depletion index for elements related to steel

(i.e., manganese, nickel), zinc, and lead has been relatively stable over the last twenty years (Figure 2.9a), whereas both the static depletion index and the supply concentration for lithium, cobalt, and vanadium have been more volatile (Figure 2.9b). In particular, cobalt production has become more geographically concentrated and cobalt’s static depletion index has declined over time.

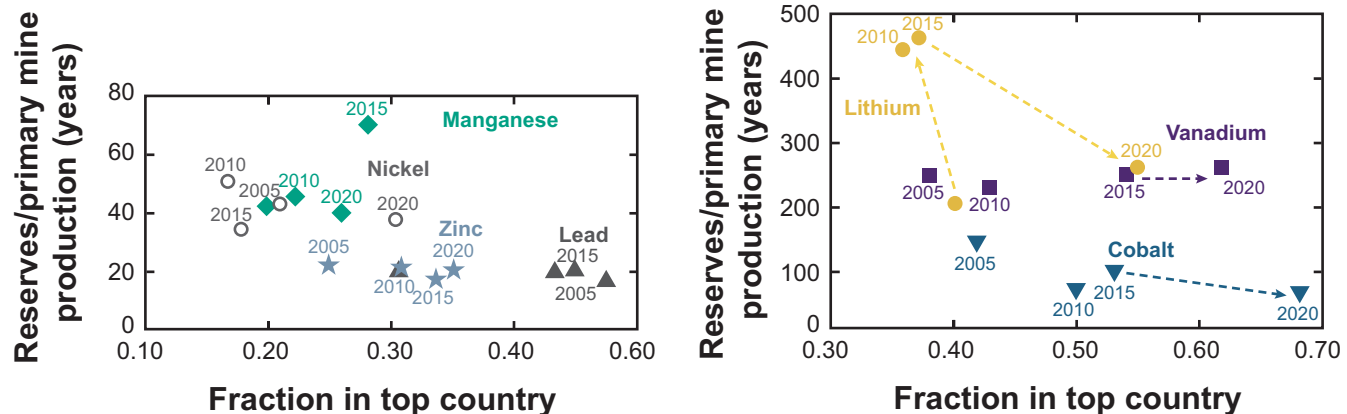
Table 2.3 provides more detailed information on current levels of production and estimates of reserve and resource size (U.S. Geological Survey 2020), as well as reserves-to-production and resources-to-production ratios. These ratios are significantly larger for lithium and vanadium than for cobalt and nickel, suggesting that the supplies of the former two elements may be less constrained than supplies of the latter two. Evidence from historic examples and modeling suggests that prices can increase significantly as production shifts from demonstrated economic reserves to speculative resources that are presently marginally economic or uneconomic to extract.

Another relevant metric for assessing materials availability risk is geopolitical supply concentration. For the set of elements we consider, we estimate geopolitical supply concentration using the Herfindahl–Hirschman Index (HHI). The HHI is large when production is dominated by one or a small number of countries; it is small when production is widely distributed. We calculate production for each element by country using data from the U.S. Geological Survey’s Mineral Commodity Summaries (2020). The U.S. Department of Justice and the U.S. Federal Trade Commission have designated materials “not concentrated” when their HHI is

³ A resource is defined by the U.S. Geological Survey (USGS) as “A concentration of naturally occurring material in or on the Earth’s crust in such form and amount that economic extraction of a commodity from the concentration is currently or potentially feasible.”

⁴ Reserves, again as defined by the USGS, are that part of an identified resource that “could be economically extracted or produced at the time of determination.” Reserves are smaller than resources for a given element.

Figure 2.9 Static metrics of resource use



Static metrics of resource use for Ni, Mn, Zn, and Pb (left) and Li, V, and Co (right), including fraction in top-producing country versus static depletion over time (arrow indicates increasing time) (Olivetti et al. 2017).

less than 1,500, which is true for aluminum, iron, manganese, sulfur, and zinc; “moderately concentrated” for an HHI between 1,500 and 2,500, which is true for nickel; and “highly concentrated” for an HHI above 2,500, which is true for cobalt, lithium, and vanadium. Of the latter three, cobalt has the highest HHI, at more than 5,300 in 2020.

Another relevant metric is whether a material is mined as a primary product or as a byproduct, meaning that it is mined and produced in the process of extracting another material. A material may also be considered a coproduct in the sense that the revenue it generates is similar to that of other materials it is produced with. One potential implication of being a byproduct material is that a price increase can have little effect on supply because supply is governed by the market dynamics for the carrier metal. Also, the data surrounding byproduct reserves and resources may be less indicative, as there may be less incentive to develop a full inventory of the element. Among the elements of interest for this study, lithium and nickel are primarily mined as principal products, whereas cobalt and vanadium may be mined as byproducts

in connection with another carrier metal, although the degree of byproduct fraction will vary by deposit.

Based on this preliminary assessment, we further investigated several materials based on their relevance to this study. We included lithium, cobalt, and nickel because of their relevance to Li-ion batteries, the most widely installed electrochemical storage technology. We also included vanadium since it is the chemical basis for the most widely deployed RFB. We assess these materials in the context of potential demand given the “material intensity” (defined below) of different battery chemistries. Finally, we comment on phosphorus, even though global phosphorus resources are vast, in light of current interest in lithium iron phosphate (LFP) batteries.

2.7.2 Linking supply to demand for screened metals

Material intensity by technology

Material intensity—which for batteries may be expressed as the mass of a substance required to store a given amount of energy (in units of

Table 2.3 World annual production, world reserves, and resources of lithium, cobalt, nickel, and vanadium in 2020⁴

| | Lithium | Cobalt | Nickel | Vanadium |
|--|----------------------|-----------------------|--------------------------------|----------------------|
| World annual production | 8.2×10^7 | 1.4×10^8 | 2.5×10^9 | 8.6×10^7 |
| World resources (kg) | 2.1×10^{10} | 7.1×10^9 | 9.4×10^{10} | 2.2×10^{10} |
| World reserves (kg) | 8.6×10^{10} | $2.5 \times 10^{10*}$ | $3.0 \times 10^{11}**,\dagger$ | 6.3×10^{10} |
| Reserves to production ratio (y) | 256 | 51 | 38 | 256 |
| Resources to production ratio (y) | 1,049 | 179 | 120 | 733 |

*Excluding sea floor nodules, which are estimated to contain 1.2×10^{11} kg.

**Excluding resources in sea floor crusts and nodules.

†World resources of nickel increased by a factor of two between 2019 and 2020, when the ore quality threshold was decreased from 1% to 0.5%.⁴

kg/kWh)—is a basic measure of the material requirements of any technology. Material intensity changes as technologies mature, a factor that must be accounted for in our analysis.

In the case of Li-ion batteries, the negative electrode is typically graphite and the electrolyte is typically an organic liquid containing a lithium salt. We focus on the positive electrode, which typically consists of layered oxides in the LiMO_2 family (where M represents transition metals and other metals). As in earlier sections of this chapter, we focus on nickel-manganese-cobalt oxide (NMC) battery chemistry, which contains a combination of cobalt, nickel, aluminum, and manganese. The ratios of nickel, manganese, and cobalt in a Li-ion positive electrode are denoted by writing “NMC-xyz,” where the numbers given for “xyz” represent the relative molar fractions of nickel, manganese, and cobalt, respectively. NMC-111 is in widespread use at present, NMC-622 has made an appearance in recent years, and NMC-811 appears in roadmaps for Li-ion battery development. To accommodate evolution in these ratios, Table 2.4 provides estimates of material intensity for the three constrained elements (lithium, cobalt, and nickel) for all three of these NMC formulations (Olivetti et al. 2017).

In contrast to Li-ion closed batteries, the material intensity of vanadium in vanadium RFBs—which currently stands at about 3.40 kg/kWh—is expected to be relatively stable over time. We explore the implications of these material intensities for the deployment of prominent battery types later in this section.

Connecting production to deployment

As discussed in Chapter 6, the total energy storage capacity that may need to be deployed to fully decarbonize the U.S. electricity sector might approach 100 terawatt-hours (TWh) by 2050. What fraction of this capacity will be provided by electrochemical storage is uncertain in light of likely competition among different storage technologies and other factors, such as the challenge of matching renewables supply to demand, the success of efforts to expand transmission networks, and variations in the cost of storage. Significant additional demand for electrochemical grid-based storage is expected to come from overseas and—to an even greater extent—from battery use in EVs. In all, we conclude that a figure on the order of 100 TWh is reasonable as a target estimate for the total electrochemical energy storage capacity required worldwide by 2050.

Table 2.4 Material intensities

| NMC | Li [kg/kWh] | Co [kg/kWh] | Ni [kg/kWh] |
|-------|-------------|-------------|-------------|
| [111] | 0.139 | 0.394 | 0.392 |
| [622] | 0.126 | 0.214 | 0.641 |
| [811] | 0.111 | 0.094 | 0.750 |

Material intensities [kg/kWh] for Li, Co, and Ni for Li-ion batteries with three choices for an NMC negative electrode (Olivetti et al. 2017).

Table 2.5 Years of current production for 100 TWh of Li-ion batteries

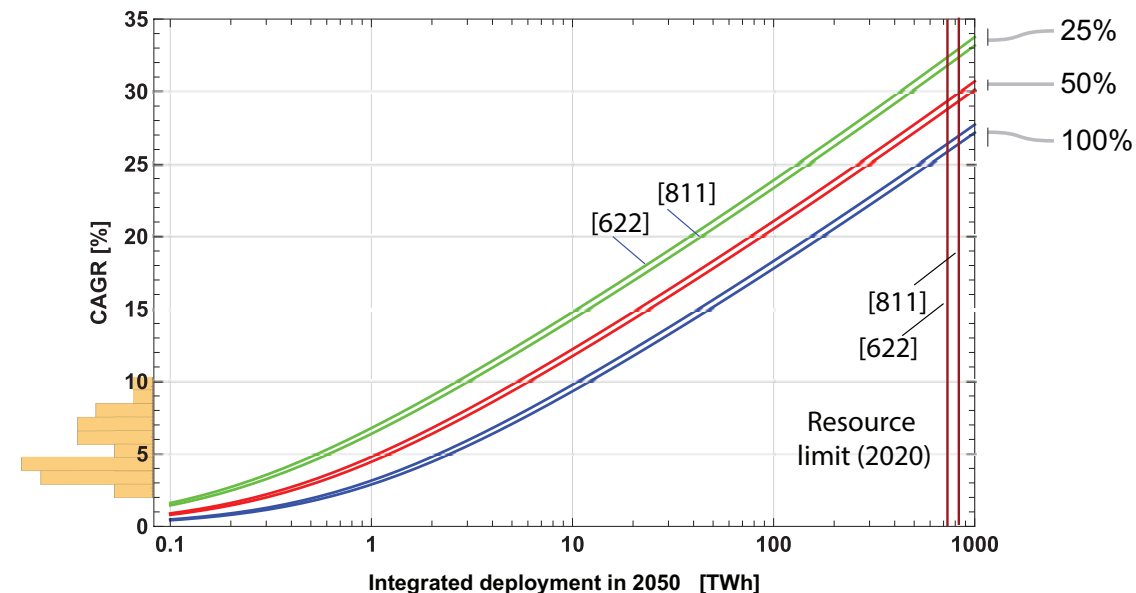
| Composition | Li [y/(100 TWh)] | Co [y/(100 TWh)] | Ni [y/(100 TWh)] |
|-------------|------------------|------------------|------------------|
| [111] | 167 | 281 | 15.7 |
| [622] | 152 | 153 | 25.6 |
| [811] | 133 | 67 | 30.0 |

Our question is whether sufficient quantities of lithium, cobalt, and nickel, or vanadium (for use in vanadium RFBs) can be obtained to create and deploy electrochemical storage at the TWh scale. One traditional approach to answering this question is to compute how many years, at current rates of production, would be needed to create a supply of an element sufficient for the manufacture of enough batteries to store, for example, 100 TWh. This quantity is easily calculated from the material intensity data in Table 2.4 and the production data in Table 2.3. Results, assuming Li-ion batteries with different NMC composition ratios, are given in Table 2.5. It is important to note, however, that this approach fails to allow for the possibility that present production of a material may be small relative to the size of the resource because of lack of demand rather than other factors, and that future production could therefore ramp up considerably in response to increased demand.

Another more flexible and dynamic approach for assessing material supply constraints is to calculate the compound annual growth rate (CAGR) of production needed to meet demand for different battery elements assuming a given energy capacity target for 2050. Figures 2.10–2.13

show CAGR plots (Kavlak et al. 2015) for lithium, cobalt, nickel, and vanadium to reach specified targets for integrated deployment by 2050. Production is assumed to begin at the 2020 level (U.S. Geological Survey 2020) and grow by a constant CAGR year-over-year. The effects of variable battery composition (for Li-ion batteries) and competition with other applications are simply displayed on these graphs. In Figure 2.10, for example, bands of different colors are used to show how required CAGR varies with different assumptions about the fraction of new production devoted to battery production (assumed constant at, for example, 25%, 50%, and 100%). The width of the colored bands for Li-ion component elements shows how required production growth depends on different choices for NMC composition, with nickel, manganese, and cobalt ratios assumed to range from 6:2:2 to 8:1:1. The vertical bars on the graphs give the energy capacity limits imposed by the total estimated global resource (based on 2020 estimates), assuming 100% of the element is dedicated to battery production. Finally, the histogram on the left-axis of the graph gives the number of 20-year periods between 1970 and 2020 during which the average CAGR for the element in question corresponded to the value

Figure 2.10 Lithium CAGR for Li-NMC deployment through 2050



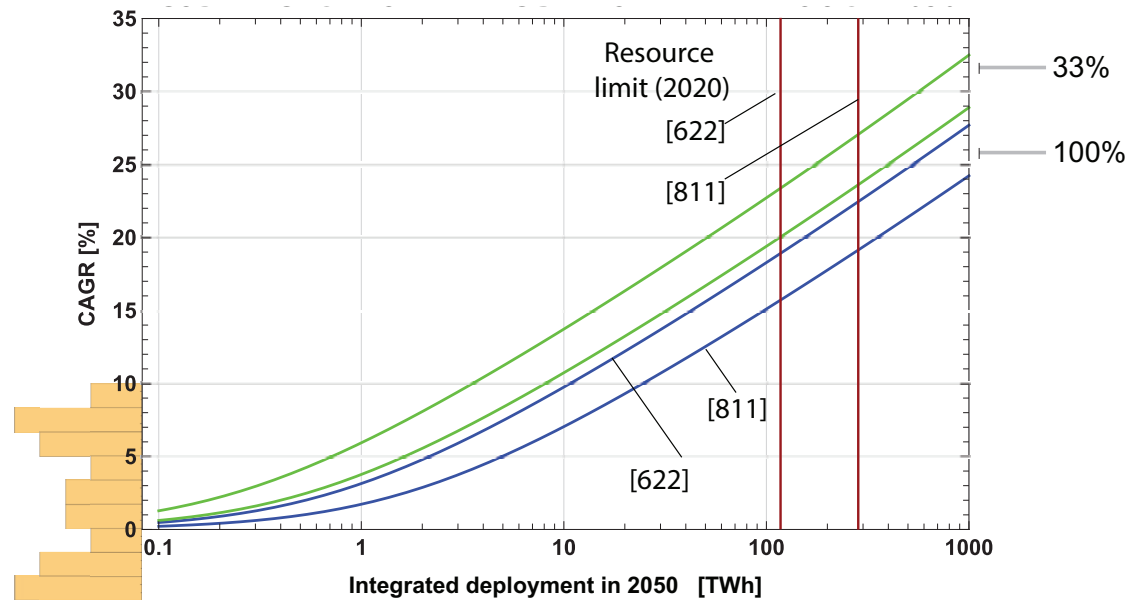
Compound annual growth rate (CAGR) of lithium production required for a specified integrated deployment of Li-ion NMC batteries by the year 2050. NMC ratios from 622 to 811 are indicated by the colored bands which correspond to different fractions of new lithium production dedicated to battery deployment. Historical values of CAGRs for 20-year averaged lithium production over the period 1970–2020 are displayed in the histogram on the left.

on the vertical axis. A closer study of these figures reveals how dramatically (and perhaps unrealistically) the production of lithium, cobalt, nickel, and vanadium would have to grow to support the deployment of electrochemical energy storage capacity on a scale of, for example, 100 TWh by 2050.

Of the elements included here, lithium (Figure 2.10) has perhaps the most optimistic supply outlook for battery deployment on the order of 10–100 TWh. Lithium production is already primarily directed toward batteries (71% of lithium production in 2020) (U.S. Geological Survey 2020); production has grown rapidly in recent years, and estimates of the global resource have increased dramatically, from 33 million metric tons (Mt) in 2010 to 86 Mt in 2020. All of these developments favor rapid expansion of future lithium production.

The situation for cobalt is illustrated in Figure 2.11. If NMC-622 were the dominant Li-ion battery chemistry, the resource limit just exceeds that necessary to support 100 TWh of deployment. If all new mined cobalt were used in batteries, production would need to increase at a CAGR of just above 10%, well above the historical average, to meet demand associated with 100 TWh of deployment by 2050. In contrast to lithium, however, almost half the cobalt consumed in the United States goes to high-performance alloys, an application that may not be easily displaced by battery demand. Cobalt production has grown moderately in recent years (from 88,000 metric tons in 2010 to 140,000 metric tons in 2020) as has the estimated global resource (from 15 Mt in 2010 to 25 Mt in 2020, excluding sea-floor deposits). But cobalt production is highly concentrated in the Congo (70% of world cobalt production in 2020) and is mostly produced as a byproduct or coproduct with copper or nickel production.

Figure 2.11 Cobalt CAGR for Li-NMC deployment through 2050



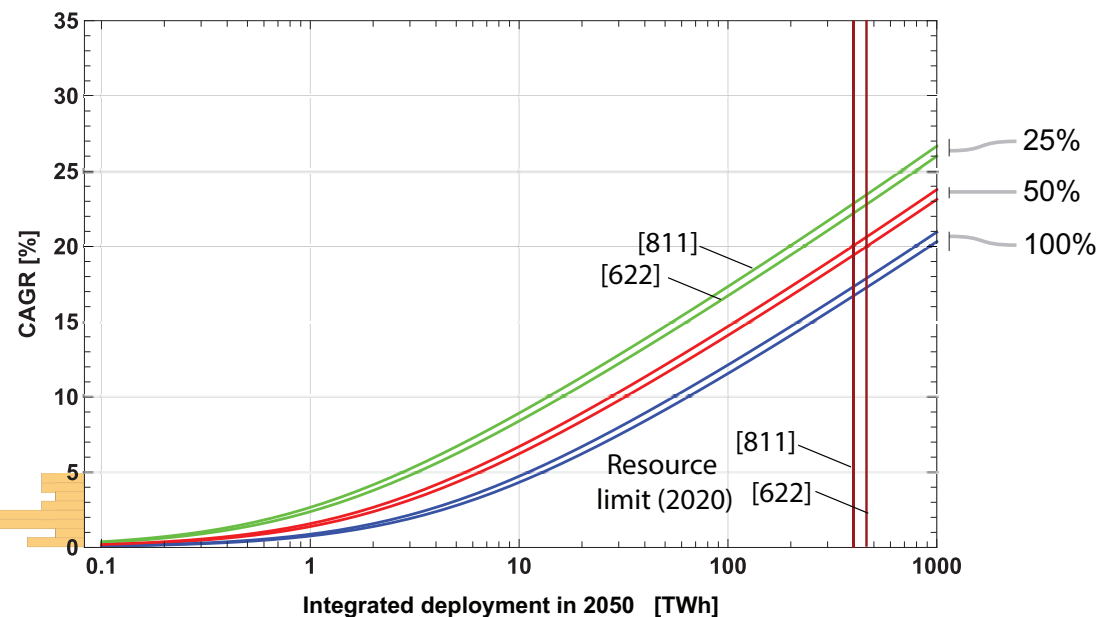
Compound annual growth rate (CAGR) of cobalt production required for a specified integrated deployment of Li-ion NMC batteries by the year 2050.

For these reasons, we regard cobalt as an element of concern for Li–NMC battery deployment.

For nickel, Figure 2.12 points to a CAGR of production between 3.9% (for Li-ion batteries with NMC-622 composition) and 4.4% (for Li-ion batteries with NMC-811 composition), sustained over 30 years (that is, from 2020 to 2050), if 100% of increased nickel production is devoted to battery production. If, instead, 50% or 25% of newly produced nickel goes to Li-ion batteries, the required CAGR jumps to 6.2%–6.7% for NMC-622 or 6.7%–8.8% for NMC-811. The left-hand histogram displays historical data on 20-year average CAGRs for nickel production; it shows a historic maximum CAGR of 5%. Thus, for example, if 25% of nickel production were devoted to Li-ion batteries with NMC-811 composition, the required CAGR of 9.5% would exceed the highest 20-year CAGR observed over the past 50 years by about a factor of two—a daunting prospect.

Primary uses of nickel at present are for the production of stainless steel and other high-performance steel alloys (about 85% of domestic production), making it unlikely that a large fraction of nickel production could rapidly be turned to battery deployment. Nickel production has shown the lowest and least variable CAGRs over the past 50 years (Figure 2.12). World nickel resources were stable at about 130 Mt in ores exceeding 1% nickel content between 2010 and 2019. The global resource inventory jumped to 300 Mt in 2020—largely because current estimates include ores down to 0.5% nickel content, based on the fact that economic extraction of nickel from lower quality ores is now considered potentially feasible (U.S. Geological Survey 2020). Nickel is widely distributed across the world, suggesting relatively small risk of political supply disruptions. Given the trend in Li-NMC chemistry toward higher nickel content and the relative inflexibility of nickel production, we regard nickel as an element of concern for Li-NMC battery deployment. Capital investment and

Figure 2.12 Nickel CAGR for Li-NMC deployment through 2050



Compound annual growth rate (CAGR) of nickel production required for a specified integrated deployment of Li-ion NMC batteries by the year 2050.

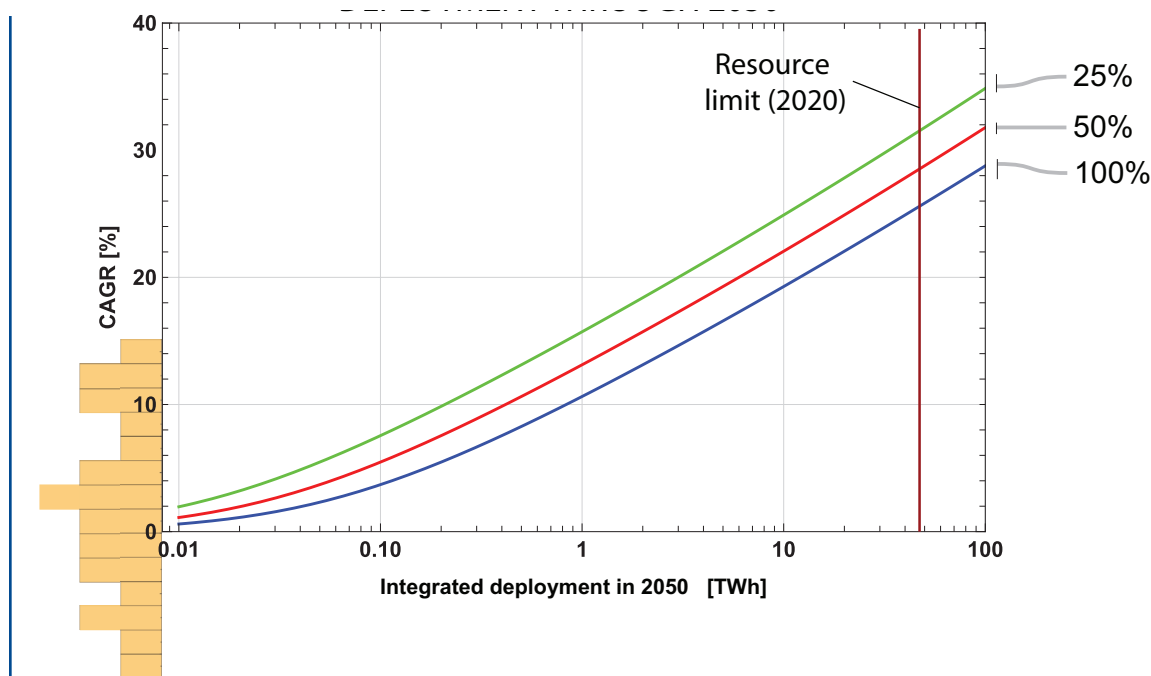
infrastructure needs associated with nickel production will have to be addressed to support rapid deployment.

Target values for the deployment of vanadium redox flow batteries (VRFBs) by 2050, as shown in Figure 2.13, are in the 1–10 TWh range—lower than the deployment targets for Li-ion batteries. Niobium may substitute for current uses of vanadium in steel alloys, which would allow the fraction of vanadium production dedicated to VRFBs to expand. Estimates of the global vanadium resource have held steady at about 63 Mt for the past decade although production has fluctuated over the past 50 years, showing a larger range of historic CAGRs (Figure 2.13) than for the other elements considered here. Because vanadium is almost always produced as a byproduct (or coproduct), vanadium production may be subject to the economic constraints mentioned earlier. Also, quoted vanadium resources may underestimate available supplies (U.S. Geological Survey 2020). Although resource limits would seem

to preclude VRFB deployment above the tens of TWh of storage capacity, resources and observed CAGRs would seem to put deployment on the scale of 1–10 TWh within range. Given the dispersed nature of vanadium production and the fact that vanadium is currently produced as a byproduct, we regard it as an element of concern for VRFB deployment.

Criticality frameworks quantify materials availability along three dimensions: supply risk in both the medium and long term, environmental implications, and vulnerability to supply restriction (Nassar et al. 2020). Political and social risks associated with a particular producing region are captured within supply risk, which includes factors such as geopolitical stability as well as social and regulatory indices. Worldwide governance indicators cataloged by the World Bank include six dimensions of governance including accountability, absence of violence, government effectiveness, regulatory quality, rule of law, and control of corruption (Fu et al. 2020). In 2019, 72% of the world's

Figure 2.13 Vanadium CAGR for VFB deployment through 2050



Compound annual growth rate (CAGR) of vanadium production required for a specified integrated deployment of VRFBs by the year 2050. See Figure 2.10 and the text for further description.

cobalt came from the Democratic Republic of the Congo, which ranks in the bottom 10th percentile globally across all these governance dimensions. By comparison, Indonesia—which accounted for 33% of nickel extraction in 2019—ranks between the 40th and 60th percentile.

As a contrast to lithium, cobalt, nickel, and vanadium, we also performed a CAGR analysis for iron, sulfur, and zinc—the three key elements in emerging electrochemical storage technologies that are perceived as utilizing less resource-constrained materials. These technologies include LFP-based Li-ion, iron-air, zinc-air, lithium-sulfur, high-temperature sodium-sulfur, and sulfur-air flow batteries. Materials intensity for iron is six-fold lower in LFP Li-ion batteries compared to iron-air batteries—680 kilotons (kT)⁵ per TWh vs. 4,000 kT per TWh,

respectively—but in either case, current levels of iron production globally are already so high that the CAGR of production required to reach 100 TWh of deployed storage by 2050 is less than 1%. Materials intensity for sodium likewise varies with technology (from 280 kT/TWh for lithium-sulfur batteries to 900 kT/TWh for high-temperature sodium-sulfur batteries to 3,200 kT/TWh for sulfur-air flow batteries), but the corresponding CAGR remains within 1%–2%. Zinc, on the other hand, is only slightly less constrained than nickel: If 100% of new zinc production went to zinc-air batteries, the CAGR to reach 100 TWh of deployed capacity by 2050 is about 10%.

Remaining sections in this chapter examine the implications of recycling for critical materials availability, offer further details on the three

⁵ A kiloton is equal to 1,000 metric tons or 0.001 Mt.

most critical elements we identified (i.e., cobalt, nickel, and vanadium), and briefly describe supply issues for phosphorous since there has been discussion in the open literature on the availability of this element for some time (Penuelas et al. 2020).

2.7.3 Potential impacts of battery recycling

To what extent recycling and reuse could ameliorate material demands and potential supply constraints for large-scale battery deployment over the next several decades is a significant unknown. Based on material flow modeling, recycling of grid-scale storage batteries is unlikely to significantly alleviate demand for critical materials in the context of exponentially growing demand for grid-scale storage, simply because the grid-scale storage batteries that will be reaching the end of their useful service life within a mid-century timeframe will represent only a small fraction of new deployment. Likewise, since it takes time for EV batteries to retire, recycling and repurposing EV batteries for grid applications is unlikely to have a major impact on materials availability constraints for grid-scale Li-ion battery deployment until 2040, even in a scenario of high EV growth. Battery recycling could become more important in the second half of this century, after deployment levels off, but that timeframe is largely outside the analysis window for this report.

Beginning about 2040, a different re-use pathway could significantly reduce critical material risks for grid-scale battery deployment. Batteries that reach the end of their service life in EVs could, in principle, be refitted for use in grid-scale applications that can accommodate lower efficiency and perhaps lower reliability than is acceptable in EV applications. Because battery deployment in EVs is expected to greatly exceed deployment for grid applications, reusing EV batteries could supply a significant fraction of demand for new grid-scale deployment.

The cost-benefit trade-offs of recycling and repurposing are still unclear due to the many challenges involved in analyzing these trade-offs. Developing strategies for battery recovery is itself challenging, whether the end objective is reuse, repurposing, or recycling. Challenges for battery recovery stem from a lack of information (particularly with respect to assessing and managing batteries in various “states of health”) and from the need for standardization to safely and effectively move batteries through a recovery system such that responsibility and liability issues are explicit and consistently handled (Dunn et al. 2021). For example, costs to transport batteries, particularly batteries that contain lithium, are high because of associated safety hazards. Emerging technology developments may allow for more effective monitoring of a battery pack’s state of health early in the chain of custody to determine whether the pack should be reused or repurposed. Other policy-related discussions involve extended producer responsibility for the cost of collecting and shipping batteries to a repurposer or recycler. Batteries for EVs vary significantly and there is uncertainty about how they will evolve in the future, including with respect to battery chemistry, form factor, cell configuration within the pack, and pack-joining processes—all of which affect the suitability of EV batteries for grid storage applications. Without greater standardization within the battery manufacturing supply chain, the hurdles to cost-effective recovery are substantial (Harper et al. 2019).

Thus, the technology requirements and economics of functional reuse compared to other forms of recycling should be studied in anticipation that significant streams of end-of-life EV batteries will need to be managed in the post-2040 timeframe. The limited state of existing U.S. markets for battery recycling and repurposing underscores the need for clear analysis. Currently, many retired batteries are shipped to regions that have more developed markets for battery recycling and for repurposing batteries to be used in grid services.

2.7.4 Details regarding materials of concern

This section provides additional details concerning supply risks for cobalt, nickel, and vanadium—the three materials of concern identified in previous sections—and offers some observations about phosphorus. Even in elemental form, the United States relies on imports for a significant fraction of its supply of these elements: 76% for cobalt, 50% for nickel, and 96% for vanadium (U.S. Geological Survey 2020). Supply risk for the U.S. manufacturing sector is a function of the likelihood of foreign supply disruptions, the ability to withstand such disruptions, and manufacturers' dependency on foreign supplies (Nassar et al. 2020). Of the three critical elements we identified, supply risks are greatest for cobalt, followed by vanadium and nickel.

Cobalt

The world's primary supplies of cobalt are heavily geographically concentrated, both for cobalt mining and for cobalt refining. Approximately 70% of all cobalt is mined in the Democratic Republic of the Congo. Cobalt processing is also heavily concentrated, with a similar percentage of processing (70%) located in China (Nassar et al. 2020). With expected increases in demand, this geographic concentration in cobalt mining and processing creates supply risks in the short term. Another challenge, from a revenue perspective, is the nature of cobalt extraction. Cobalt is mined as a byproduct of nickel and copper extraction, meaning that higher prices for cobalt do not necessarily drive increases in supply. According to some estimates, global demand for cobalt will exceed current refining capacity by more than 300% by 2030 (Fu et al. 2020).

The materials analysis conducted for this study suggests that while the supply of mined cobalt is likely to remain stable in the short term and may even operate at a surplus, significant challenges would arise in downstream capacity

for extraction and refining if demand for battery storage approaches 100 TWh over the next three decades (i.e., by 2050) with reliance on cobalt-dominated chemistries. The expectation is that future sources of cobalt will become more diversified geographically, and cobalt will be more often mined as a byproduct of nickel over the next decade. To meet future demand, however, sustained investments will be needed to develop supplies of refined cobalt and methods for secondary recovery.

Nickel

Nickel sulfate is currently the only economic production route that yields a grade of nickel appropriate for use in batteries. Instead, current nickel production has been dominated by the expanded use of nickel pig iron for stainless steel or ferronickel, and there have been fewer ore discoveries that would lead to further sulfide smelting. For the integrated sulfide producers, smelting sulfide concentrates to produce matte requires investments in new sulfide discoveries (which themselves have a long trajectory). There is potential for hydro-metallurgical recovery of nickel from laterite ores or as an add-on to sulfates, but the economics are challenging. If increased demand leads to higher prices for cobalt, then revenue streams from cobalt and cobalt byproducts could offset the operational costs of a mine. Potential also exists for disruptive alternatives to obtaining battery-grade nickel from nickel pig iron sources, similar to the changes that were seen in manganese production around the Pidgeon process several decades ago (Pidgeon and Alexander 1944).

Vanadium

The abundance of vanadium in the Earth's crust is generally high, and current production is much less than known resources (U.S. Geological Survey 2020). Based on a materials intensity of 3.40 kg/kWh (for VRFBs), reserves also outweigh potential supply requirements.

However, the challenge is that vanadium is dispersed and present in many different forms. In addition, a great number of industrial and combustion wastes have vanadium content, including fly ash and slag. Vanadium recycling has not yet been economical and vanadium is produced as a byproduct for only a few purposes (dominated by ferrovanadium) and by only a few countries, including China, South Africa, and Russia (Moskalyk and Alfantazi 2003). Thus, considerable effort would be needed to scale up the technologies and infrastructure required to produce more vanadium. Significant efforts have been devoted to vanadium recovery and refining; in addition, the quality and purity of vanadium needed for electrochemical storage applications does not differ significantly from metallurgical-grade vanadium (Fan, Yang and Zhu 2017). Once demand and interest is high enough, we believe physical resource availability and technical processes could allow for scaled access to vanadium (Park et al. 2018). The current volume of production is low, and therefore the CAGR needed to support large-scale deployment would be challenging.

Phosphorus

While we did not perform a detailed materials analysis for phosphorus, this element warrants further comment in light of its potential application in LFP chemistries. Global phosphate reserves are not going to be depleted (Koppelaar and Weikart 2013). Based on an assumed materials intensity of 0.38 kg/kWh in LFP batteries, one year of world phosphorus production could support 50 TWh of LFP battery capacity. At present, the dominant use of phosphorus is for fertilizer and this use will remain dominant even with significant deployment of LFP storage. However, there is concern around the regional availability of phosphorus for fertilizer manufacture, which could lead to food security concerns, particularly in high-population countries (such as India and Brazil) that depend on a few phosphorous-rich

producing countries (Cooper et al. 2011). Supply is reasonably concentrated and may become more so over time (Yuan et al. 2018); currently, 85% of reserves are in five countries: Morocco, China, Algeria, Syria, and South Africa (Morocco has the largest reserves). There are also significant environmental concerns associated with the potential release of phosphorous into the environment, which can lead to immediate eutrophication from land applications, longer-term releases from pooled accumulations, and changes in the nitrogen-phosphorous-carbon balance leading to perturbations in the biogeochemical cycling of these elements (Penuelas et al. 2020).

2.7.5 Insights from the materials analysis

At the higher rates of deployment considered in this study, the required increase in production of critical battery elements such as cobalt, nickel, lithium, and vanadium equals or exceeds maximum historical rates of growth. This implies the expansion of extraction, beneficiation, and refinement facilities beyond current infrastructure. It also implies additional supply chain shifts. For example, more cobalt is expected to come from nickel resources in the next decade. For lithium, other routes such as direct extraction will likely become cost competitive.

Recycling will not significantly ameliorate material constraints in the context of an exponentially growing deployment trajectory. Beginning about 2040, however, a strategy for managing EV batteries at the end of their service life in vehicles through recycling or repurposing quickly becomes imperative. While the cost-benefit trade-offs of recycling and repurposing are still quite unclear due to the complexities involved, it is important to begin addressing these questions now. In particular, the United States must determine if it wishes to nurture a competitive domestic industry in battery manufacturing, recycling, and/or repurposing.

Finally, rapid scale-up to the high levels of energy storage deployment considered in this study will require more effective management of resource extraction for battery technologies, including more effective efforts to address the environmental and social impacts of mining and beneficiation.

2.8 Conclusion and key takeaways

This chapter considers closed-loop, electricity-to-electricity electrochemical energy storage technologies that are currently at Technology Readiness Level (TRL) 6 or higher. We assessed technical strengths and weaknesses, cost and performance metrics, and future development opportunities for different classes of rechargeable batteries that have significant potential for grid energy storage. We also considered materials resource constraints that might affect the cost and availability of elements that underpin many of these technologies. Though important, we did not consider in detail possible innovations in supply chain, manufacturing, and battery recycling or end-of-life disposal. The remainder of this section summarizes key takeaways from this chapter for electrochemical storage technologies in general, for the four specific categories of batteries we considered (i.e., lithium-ion, redox flow, metal-air, and other closed architecture batteries) and for material availability.

Electrochemical storage technologies

- Compared to thermal or mechanical energy storage technologies, electrochemical technologies have high energy densities that are surpassed only by chemical energy storage. Battery systems typically provide more power for a given area (e.g., megawatts per acre), face fewer siting restrictions, are simpler in design, and can reach equivalent economies of scale at smaller scales (kilowatts to megawatts).

- Due to a favorable combination of energy density, power density, and efficiency, Li-ion batteries are well-suited to shorter-duration grid storage applications. However, other battery chemistries (e.g., RFBs or metal-air batteries) have inherently lower materials costs and allow for more flexible scaling of energy vs. power, which makes them increasingly attractive for emerging long-duration applications.
- The manufacturing model for Li-ion batteries is mature and is now evolving at a slower rate than over the past two decades. Manufacturing approaches for less mature battery chemistries (e.g., RFBs or metal-air batteries) are less well established but have the potential to achieve significantly lower costs.
- The development of Li-ion batteries has benefited and will continue to benefit from the widespread application of this technology in electric vehicles and mobile devices, as well as in stationary energy storage. Applications for other battery (and non-battery) storage technologies considered in this study have been less diverse, which may contribute to slower technology learning curves.
- Rapid deployment of batteries in the United States and abroad, primarily in electric vehicles and secondarily for grid-scale energy storage, will require increased production of certain critical battery elements at rates that far exceed historical averages. Constraints on scaling the production of these critical elements already exist and will likely persist, which will have implications for technology development pathways.

- For any of the battery technologies considered in this study, there are large cost differentials between greenfield and brownfield installations for front-of-meter energy storage. We expect brownfield deployment to have persistent cost advantages.

Lithium-ion batteries

- Li-ion batteries excel in energy density, power density, and roundtrip efficiency. Among the electrochemical technologies currently deployable at scale, Li-ion batteries afford the highest energy and power output per footprint.
- Portable electronics and electric vehicle applications have historically driven Li-ion battery growth and deployment. However, these applications require smaller systems and have lower lifetime requirements and higher cost tolerance than grid-scale energy storage. Still, as an incumbent technology, Li-ion has been deployed more widely than any other battery technology in grid storage applications over the last decade (although total installed battery capacity in the power sector remains less than 1% that of installed pumped hydroelectric storage).
- Although the cost of battery components (including, most significantly, the cost of the active electrode materials) sets a floor for Li-ion costs, Li-ion batteries continue to evolve toward chemistries that require lower concentrations of resource-constrained elements, such as cobalt and nickel, or avoid using these elements altogether. Moreover, the fact that grid storage applications are less sensitive to energy density unlocks chemistries that use more earth-abundant elements, such as manganese, iron, phosphorus, silicon, and sulfur. Thus, the cost floor

for Li-ion batteries is expected to continue to decline for all applications, with lithium becoming the limiting component in terms of cost and supply.

- The cycle life and calendar life of Li-ion batteries is improving but is currently too low to deliver acceptable returns on investment for certain grid applications. The technology remains challenged in applications with longer, less frequent, and less predictable discharge durations.

Redox flow batteries

- RFBs, which decouple power and energy, offer advantages in terms of scaling to larger systems and longer storage durations. While a wide range of chemistries are possible in this format, vanadium RFBs represent the state-of-the-art due to their comparatively high energy density, low maintenance costs, and long operational lifetime. Vanadium RFBs account for most of the flow batteries installed to date, but the deployment scale is challenged by the cost of vanadium. In a scenario with high technology adoption, the role for this type of RFB may ultimately be limited by the cost and availability of vanadium.
- Many next-generation chemistries beyond vanadium, particularly those utilizing active species made from low-cost and high-abundance precursors, are currently being explored in the RFB field. Such systems are likely crucial to enable significant reductions to the system cost and thus facilitate the broader-scale deployment of RFBs. However, to date, no archetypal systems (i.e., those that can meet cost and performance metrics while being practically operable for 20+ years) have been identified.

- In general, RFBs remain a nascent technology. Strengthening the innovation pipeline to accelerate the progression from discovery science to supply chain and manufacturing development to demonstration, while also leveraging technology advances and lessons learned from adjacent fields (e.g., polymer electrolyte fuel cells, Li-ion batteries), may enable rapid improvements in performance and concomitant reductions in cost.

Metal-air batteries

- Metal-air batteries for grid-scale energy storage are based on earth-abundant metals such as zinc, iron, and aluminum, and use aqueous electrolytes. As a result, materials costs and associated system-level energy costs are low. However, metal-air batteries typically have higher power cost and lower roundtrip efficiency than Li-ion batteries and RFBs. These attributes make metal-air batteries attractive for applications that involve long discharge periods and infrequent use.
- Pathways to improved performance and lower cost for metal-air batteries include advances in air electrode performance and cost, and the ability to use lower-cost metal electrodes. Among these systems, zinc-air batteries are the most developed, while iron-air batteries are attracting new interest. As with most battery technologies, the durability of metal-air batteries in utility-scale applications has not yet been demonstrated.

Other batteries

- Two other types of batteries have reached TRLs greater than 6 in grid storage applications: lead-acid and high-temperature sodium-sulfur batteries. Both have been largely displaced by Li-ion batteries. Lead-acid batteries have a similar installed cost to Li-ion batteries, but have a shorter cycle and calendar life than Li-ion batteries. Lead-acid batteries do offer the benefit of a well-established recycling infrastructure. The primary improvement that would make lead-acid batteries more competitive would be to increase cycle life over a greater depth of discharge. The main challenge facing high temperature sodium-sulfur batteries is their higher cost in comparison to Li-ion batteries as well as most other battery chemistries under consideration for grid scale storage.

Materials availability

- At the deployment rates anticipated for grid storage and, where relevant, electric vehicles, the production of critical battery elements such as cobalt, nickel, lithium, and vanadium would have to increase at a rate that equals or exceeds historical rates of growth. Materials availability for batteries that are used to provide grid energy storage will be influenced by electric vehicle demand for those batteries that are competitive in both applications. This implies that current infrastructure for extraction, beneficiation, and refinement will have to be expanded, as well as shifts in supply chains. For example, more cobalt is expected to come from nickel ores in the next decade. For lithium, other extraction routes such as membrane-based systems may become cost competitive.

- Recycling of batteries used for grid storage will not significantly ease materials supply constraints for any exponentially growing deployment trajectory. After the next decade, however, end-of-life management strategies for electric vehicle batteries that include recycling will quickly become necessary—not only to maintain and redeploy storage technologies, but also to meet continued growth in demand as the extraction of component materials from primary sources begins to plateau. Cascaded or repurposed use of electric vehicle batteries in grid storage applications may ameliorate materials demands.
- Vanadium resources will need to be developed to enable the deployment of vanadium RFBs on a scale comparable to Li-ion batteries in grid applications. Supply concerns around the future large-scale use of this technology stem from the fact that vanadium is currently mined primarily as a byproduct from dispersed waste sources.

References

- 24M Technologies, Inc. n.d. "Press Release." Accessed 06 15, 2021. <https://24-m.com/pressrelease>.
- Advanced Research Projects Agency-Energy. 2016. "ARPA-E: The First Seven Years." https://arpa-e.energy.gov/sites/default/files/documents/files/Volume_1_ARPA-E_ImpactSheetCompilation_FINAL.pdf.
- n.d. Ambri. Accessed October 3, 2021. <https://ambri.com>.
- n.d. "Antimony Prices." *US Antimony*. Accessed March 1, 2022. <https://www.usantimony.com/antimony-prices>.
- Armand, M, P Axmann, D Bresser, M Copley, K Edström, C Ekberg, D Guyomard, et al. 2020. "Lithium-Ion Batteries – Current State of the Art and Anticipated Developments." *Journal of Power Sources* 479. <https://doi.org/10.1016/j.jpowsour.2020.228708>.
- BCC Research. 2016. "Lithium Batteries: Markets and Materials." January. <https://www.bccresearch.com/market-research/fuel-cell-and-battery-technologies/FCB028B.html>.
- Bharadwaj, S. 2021. "An electric vehicle battery that doesn't need electricity for charging." *The Times of India*. April 6. <https://timesofindia.indiatimes.com/auto/news/an-ev-battery-that-doesnt-need-electricity-for-charging/articleshow/81902959.cms>.
- Biswas, S, A Senju, R Mohr, T Hodson, N Karthikeyan, K Knehr, A G Hsieh, X Yang, B E Koel, and D A Steingart. 2017. "Minimal architecture zinc–bromine battery for low cost electrochemical energy storage." *Energy and Environmental Science* 10, 114-120.
- BloombergNEF. 2019. "Battery Pack Prices Fall As Market Ramps Up With Market Average At \$156/KWh In 2019." December 3. <https://about.bnef.com/blog/battery-pack-prices-fall-as-market-ramps-up-with-market-average-at-156-kwh-in-2019>.
- Brushett, F R, M J Aziz, and K E Rodby. 2020. "On Lifetime and Cost of Redox-Active Organics for Aqueous Flow Batteries." *ACS Energy Letters* 5, 879-884.
- China Energy Storage Alliance. 2019. "2019 CNESA White Papers."
- China Energy Storage Alliance. 2020. "2020 CNESA White Papers."
- Choi, S, T Kim, S Jo, J Y Lee, S Cha, and Y T Hong. 2018. "Hydrocarbon membranes with high selectivity and enhanced stability for vanadium redox flow battery applications: Comparative study with sulfonated poly(ether sulfone)s and sulfonated poly(thioether ether sulfone)s." *Electrochimica Acta* 259, 427-439.
- Choudhary, Ayushi, and Eswara Prasad. 2020. "Lithium-ion Battery Market Size and Share | Industry Analysis by 2027." *Allied Market Research*. April. Accessed December 1, 2020. <https://www.alliedmarketresearch.com/lithium-ion-battery-market>.
- Cole, W, and A W Frazier. 2020. "Cost Projections for Utility-Scale Battery Storage: 2020 Update." *Renewable Energy* 21.
- Consortium for Battery Innovation. 2019. "An Innovation Roadmap for Advanced Lead Batteries: Technical Specifications and Performance Improvements."
- Cooper, J, R Lombardi, D Boardman, and C Carliell-Marquet. 2011. "The future distribution and production of global phosphate rock reserves." *Resources, Conservation, and Recycling* 57, 78-86.
- Dahn, J, and G M Ehrlich. 2010. "Chapter 26: Lithium-Ion Batteries." In *Linden's Handbook of Batteries*, 1-26, 79. McGraw-Hill Professional.
- Darling, R M, K G Gallagher, J A Kowalski, H Seungbum, and F R Brushett. 2014. "Pathways to low-cost electrochemical energy storage: a comparison of aqueous and nonaqueous flow batteries." *Energy and Environmental Science* 3459-3477.
- Darling, R, K Gallagher, and F R Brushett. 2016. "Transport Property Requirements for Flow Battery Separators." *Journal of the Electrochemical Society* 163 (1), A5029.
- Dave, A, J Mitchell, K Kandasamy, H Wang, S Burke, B Paria, B Póczos, J Whitacre, and V Viswanathan. 2020. "Autonomous Discovery of Battery Electrolytes with Robotic Experimentation and Machine Learning." *Cell Reports Physical Science* 1 (12), 100264.
- Dell, R, and D Rand. 2001. "Lead-acid Batteries." In *Understanding Batteries*, 100-125. Royal Society of Chemistry.
- Dieterich, V, J D Milshtein, J L Barton, T J Carney, and R M Darling. 2018. "Estimating the cost of organic battery active materials : a case study on anthraquinone disulfonic acid Estimating the cost of organic battery active materials : a case study on anthraquinone disulfonic acid." *Translational Materials Research* 5, 034001.

- Ding, Y, Z P Cano, A Yu, J Lu, and Z Chen. 2019. "Automotive Li-Ion Batteries: Current Status and Future Perspectives." *Electrochemical Energy Reviews* 2 (1), 1-28. <https://doi.org/10.1007/s41918-018-0022-z>.
- Doris, S E, A L Ward, A Baskin, P D Frischmann, N Gavvalapalli, E Chénard, C S Sevov, D Prendergast, J S Moore, and B A Helms. 2017. "Macromolecular Design Strategies for Preventing Active-Material Crossover in Non-Aqueous All-Organic Redox-Flow Batteries." *Angewandte Chemie* 129 (6), 1617-1621.
- Doughty, D H. 2010. "Chapter 27: Rechargeable Lithium Metal Batteries (Ambient Temperature)." In *Linden's Handbook of Batteries*, 1-28. McGraw-Hill.
- Duduta, M, V C Wood, P Limthongkul, V E Bruini, W C Carter, and Y-M Chiang. 2011. "Semi-solid lithium rechargeable flow battery." *Advanced Energy Materials* 1 (4), 511-516.
- Dunn, J, M Slattery, A Kendall, H Ambrose, and S Shen. 2021. "Circularity of Lithium-Ion Battery Materials in Electric Vehicles." *Environmental Science and Technology* 55(8): 5189-5198.
- Energy Storage Association. n.d. "Sodium Sulfur (NAS) Batteries." <https://energystorage.org/why-energy-storage/technologies/sodium-sulfur-nas-batteries>.
- Fan, C L, H T Yang, and Q S Zhu. 2017. "Preparation and electrochemical properties of high purity mixed-acid electrolytes for high energy density vanadium redox flow battery." *International Journal of Electrochemical Science* 12, 7728-7738.
- Fehrenbacher, Katie. 2016. "A Battery Made From Metal and Air Is Electrifying the Developing World." *Fortune*. May 23. <https://fortune.com/2016/05/23/a-battery-made-from-metal-and-air-is-electrifying-the-developing-world>.
- Feldman, D, V Ramasamy, R Fu, A Ramdas, J Desai, and R Margolis. 2021. "U.S. Solar Photovoltaic System and Energy Cost Benchmark: Q1 2020." *Renewable Energy* 120.
- Ferrara, M, Y-M Chiang, and J M Deutch. 2019. "Demonstrating Near-Carbon-Free Electricity from Renewables and Storage." *Joule* 3 (11), 2585-2588.
- Forner-Cuenca, A, and F R Brushett. 2019. "Engineering porous electrodes for next-generation redox flow batteries: recent progress and opportunities." *Current Opinions on Electrochemistry* 18, 113-122.
- Frost and Sullivan. 2020. "Global Li-ion Battery Materials Market, Forecast to 2026." 29-31.
- Fu, J, Ruilin Liang, G Liu, A Yu, Z Bai, L Yang, and Z Chen. 2019. "Recent Progress in Electrically Rechargeable Zinc–Air Batteries." *Advanced Materials* 31, 1805230.
- Fu, J, Z P Cano, M G Park, A Yu, M Fowler, and Z Chen. 2017. "Electrically Rechargeable Zinc–Air Batteries: Progress, Challenges, and Perspectives." *Advanced Materials* 29, 1604685.
- Fu, X, D N Beatty, G G Gaustad, G Ceder, R Roth, R E Kirchain, M Bustamante, C Babbitt, and E A Olivetti. 2020. "Perspectives on cobalt supply through 2030 in the face of changing demand." *Environmental Science Technology* 2985-2993.
- Gentil, S, D Reynard, and H H Girault. 2020. "Aqueous organic and redox-mediated redox flow batteries: a review." *Current Opinions on Electrochemistry* 21, 7-13.
- Ghan, R F, N H Hagedorn, and J A Johnson. 1985. "Cycling Performance of the Iron- Chromium Redox Energy Storage System Conservation and Renewable Energy." NASA TM-87034.
- Ghan, R, N Hagedorn, and J Ling. 1983. "Single Cell Performance Studies on the Fe / Cr Redox Energy Storage System Using Mixed Reactant Solutions at Elevated Temperature Conservation and Renewable Energy Division of Energy Storage Systems." *Proc. Eighteenth Intersoc. Energy Convers. Eng. Conf.* Orlando, Florida. Vol. 4 1647-1652.
- Gold, Russel. 2021. "Startup Claims Breakthrough in Long-Duration Batteries." *The Wall Street Journal*. July 22. <https://www.wsj.com/articles/startup-claims-breakthrough-in-long-duration-batteries-11626946330>.
- Goldstein, Anna. 2021. "Federal Policy to Accelerate Innovation in Long-Duration Energy Storage : The Case for Flow Batteries." *Information Technology and Innovation Foundation*.
- Goulet, M, L Tong, D A Pollack, D P Tabor, S A Odom, A Aspuru-Guzik, E E Kwan, R G Gordon, and M J Aziz. 2020. "Extending the Lifetime of Organic Flow Batteries via Redox State Management." *Journal of the American Chemical Society* 141, 20, 8014-8019.
- Granholm, J M. 2021. "National Blueprint for Lithium Batteries 2021-2030." June. https://www.energy.gov/sites/default/files/2021-06/FCAB%20National%20Blueprint%20Lithium%20Batteries%200621_0.pdf.
- Gregory, T D, M L Perry, and P Albertus. 2021. "Cost and price projections of synthetic active materials for redox flow batteries." *Journal of Power Sources* 499, 229965.

- Gu, P, M Zheng, Q Zhao, X Xiao, H Xue, and H Pang. 2017. "Rechargeable zinc–air batteries: a promising way to green energy." *Journal of Materials Chemistry A* 5, 7651-7666.
- Hanley, Steve. 2018. "NantEnergy Says Zinc-Air Battery Ideal for Grid Storage." *CleanTechnica*. September 28. <https://cleantechnica.com/2018/09/28/nantenergy-says-zinc-air-battery-ideal-for-grid-storage>.
- Harlow, J E, X Ma, J Li, E Logan, Y Liu, N Zhang, L Ma, et al. 2019. "A Wide Range of Testing Results on an Excellent Lithium-Ion Cell Chemistry to Be Used as Benchmarks for New Battery Technologies." *Journal of the Electrochemical Society* 166 (13). <https://doi.org/10.1149/2.0981913jes>.
- Harper, G, R Sommerville, E Kendrik, L Driscoll, P Slater, R Stolkin, A Walton, et al. 2019. "Recycling lithium-ion batteries from electric vehicles." *Nature* 575, 75-86.
- Hesse, H C, M Schimpe, D Kucevic, and A Jossen. 2017. "Lithium-Ion Battery Storage for the Grid—A Review of Stationary Battery Storage System Design Tailored for Applications in Modern Power Grids." *Energies* 10 (12), 2107. <https://doi.org/10.3390/en10122107>.
- Hopkins, B J, C N Chervin, M B Sassin, J W Long, D R Rolison, and J F Parker. 2020. "Low-cost green synthesis of zinc sponge for rechargeable, sustainable batteries." *Sustainable Energy and Fuels* 4, 3363-3369.
- Hsieh, I-Y L, M S Pan, Y-M Chiang, and W H Green. 2019. "Learning Only Buys You so Much: Practical Limits on Battery Price Reduction." *Applied Energy* 239, 218-224. <https://doi.org/10.1016/j.apenergy.2019.01.138>.
- Hu, B, C DeBruler, M Hu, W Wu, and L T Liu. 2019. "Redox-Active Inorganic Materials for Redox Flow Batteries." In *Encyclopedia of Inorganic and Bioinorganic Chemistry*, 211-236. Wiley.
- Hueso, K.B., Armand, M., and Rojo, T. (2013). High temperature sodium batteries: status, challenges and future trends. *Energy Environ. Sci.* 6, 734–749
- International Renewable Energy Agency. 2018. "Electricity Storage and Renewables: Costs and Markets to 2030."
- Irvine, Mark, and Mats Rinaldo. n.d. "Tesla's Battery Day and the Energy Transition." DNV. Accessed June 16, 2021. <https://www.dnv.com/feature/tesla-battery-day-energy-transition.html>.
- Jin, S, E M Fell, L Vina-Lopez, Y Jing, P W Michalak, R G Gordon, and M J Aziz. 2020. "Near Neutral pH Redox Flow Battery with Low Permeability and Long-Lifetime Phosphonated Viologen Active Species." *Advanced Energy Materials* 2000100, 1-10.
- Kavlak, G, J McNerney, R L Jaffe, and J E Trancik. 2015. "Metal production requirements for rapid photovoltaics deployment." *Energy and Environmental Science* 8, 1651-1659.
- Kazacos, M, M Cheng, and M Skyllas-Kazacos. 1990. "Vanadium redox cell electrolyte optimization studies." *Journal of Applied Electrochemistry* 463-467.
- Ke, X, J M Prahl, J I Alexander, J S Wainright, A Zawodzinski, and R F Savinell. 2018. "Rechargeable redox flow batteries: flow fields, stacks and design considerations." *Chemical Society Reviews* 47, 8721-8743.
- Kim, H, Dane Boysen, J M Newhouse, B L Spatocco, B Chung, P J Burke, D J Bradwell, et al. 2013. "Liquid Metal Batteries: Past, Present and Future." *Chemical Reviews* 113, 2075-2099.
- Koppelaar, R, and H P Weikart. 2013. "Assessing phosphate rock depletion and phosphorus recycling options." *Global Environmental Change* 23, 1454, 1466.
- Kwabi, D, Y Ji, and M J Aziz. 2020. "Electrolyte Lifetime in Aqueous Organic Redox Flow Batteries: A Critical Review." *Chemical Reviews* 120, 14, 6467-6489.
- Lawder, M T, B Suthar, P W C Northrop, S De, C M Hoff, O Leitermann, M L Crow, S Santhanagopalan, and V R Subramanian. 2014. "Battery Energy Storage System (BESS) and Battery Management System (BMS) for Grid-Scale Applications." *Proceedings of the IEEE* 102 (6), 1014-1030. <https://doi.org/10.1109/JPROC.2014.2317451>.
- Li, M, J Lu, Z Chen, and K Amine. 2018. "30 Years of Lithium-Ion Batteries." *Advanced Materials* 30 (33). <https://doi.org/10.1002/adma.201800561>.
- Li, Y, and H Dai. 2014. "Recent advances in zinc–air batteries." *Chem. Soc. Rev* 43, 5257-5275.
- Li, Y, and J Lu. 2017. "Metal–Air Batteries: Will They Be the Future Electrochemical Energy Storage Device of Choice?" *ACS Energy Letters* 2, 1370-1377.
- Li, Z, M S Pan, L Su, P-C Tsai, A Badel, J Valle, S Eiler, K Xiang, F Brushett, and Y-M Chiang. 2017. "Air-Breathing Aqueous Sulfur Flow Battery for Ultralow-Cost Long-Duration Electrical Storage." *Joule* 306-327.

- Lopes, P P, and V R Stamenkovic. 2020. "Past, present, and future of lead–acid batteries." *Science* 369, 923–924.
- Mainar, A R, E Iruin, L C Colmenares, A Kvasha, I Meazza, M Bengoechea, O Leonet, I Boyano, Z Zhang, and J A Blazquez. 2018. "An overview of progress in electrolytes for secondary zinc-air batteries and other storage systems based on zinc." *Journal of Energy Storage* 15, 304–328.
- Manthiram, A. 2020. "A Reflection on Lithium-Ion Battery Cathode Chemistry." *Nature Communications* 11 (1), 1550. <https://doi.org/10.1038/s41467-020-15355-0>.
- Markets Insider. n.d. "Commodity Prices | Commodity Market." <https://markets.businessinsider.com/commodities>.
- May, G J, A Davidson, and B Monahov. 2018. "Lead batteries for utility energy storage: A review." *Journal of Energy Storage* 15, 145–157.
- McKerracher, Colin, A O'Donovan, N Albanese, N Soulopoulos, D Doherty, M Boers, R Fisher, et al. 2021. "Electric Vehicle Outlook 2021." *Bloomberg NEF*. <https://about.bnef.com/electric-vehicle-outlook/>.
- McKerracher, R D, C Ponce de Leon, R G Wills, A A Shah, and F C Walsh. 2015. "A Review of the Iron–Air Secondary Battery for Energy Storage." *ChemPlusChem* 80, 323–335.
- Milshtein, J D, R M Darling, J Drake, M L Perry, and F R Brushett. 2017. "The Critical Role of Supporting Electrolyte Selection on Flow Battery Cost." *Journal of the Electrochemical Society* 164 (14), A3883.
- Minke, C, and T Turek. 2015. "Economics of vanadium redox flow battery membranes." *Journal of Power Sources* 286, 247–257.
- Mongird, K, V Viswanathan, J Alam, C Vartanian, V Sprenkle, and R Baxter. 2020. "2020 Grid Energy Storage Technology Cost and Performance Assessment." *Pacific Northwest National Laboratory* 117.
- Moskalyk, R R, and A M Alfantazi. 2003. "Processing of vanadium: a review." *Miner. Eng.* 16, 793–805.
- Narayan, S R, A Nirmalchandar, A Murali, B Yang, L Hoober-Burkhardt, S Krishnamoorthy, and G K Surya Prakash. 2019. "Next-generation aqueous flow battery chemistries." *Current Opinion in Electrochemistry* 18, 72–80.
- Nassar, Nedal T, J Brainard, A Gulley, R Manley, G Matos, G Lederer, L R Bird, et al. 2020. "Evaluating the mineral commodity supply risk of the US manufacturing sector." *Science Advances* eaay8647.
- New York Power Authority. 2020. "NYPA Announces New Energy Storage Demonstration Project Supporting Further Integration of Renewable Power Sources Into the Grid." January 17. <https://www.nypa.gov/news/press-releases/2020/20200117-zinc>.
- Nibel, O, S M Taylor, A Patru, E Fabbri, L Gubler, and T J Schmidt. 2017. "Performance of Different Carbon Electrode Materials: Insights into Stability and Degradation under Real Vanadium Redox Flow Battery Operating Conditions." *Journal of the Electrochemistry Society* 164, A1608–A1615.
- Oldenburg, F, T J Schmidt, and L Gubler. 2017. "Tackling capacity fading in vanadium flow batteries with amphoteric membranes." *Journal of Power Sources* 368, 68–72.
- Olivetti, E A, G Ceder, G G Gaustad, and X Fu. 2017. "Lithium-Ion Battery Supply Chain Considerations: Analysis of Potential Bottlenecks in Critical Metals." *Joule* 1.
- Park, J H, J J Park, H J Lee, B S Min, and J H Yang. 2018. "Influence of metal impurities or additives in the electrolyte of a vanadium redox flow battery." *Journal of the Electrochemical Society* 165, A1263.
- Penuelas, J, I A Janssens, P Ciais, M Obersteiner, and J Sardans. 2020. "Anthropogenic global shifts in biospheric N and P concentrations and ratios and their impacts on biodiversity, ecosystem productivity, food security, and human health." *Global Change Biology* 26, 1962–1985.
- Perry, M L, J D Saraidaridis, and R M Darling. 2020. "Crossover Mitigation Strategies for Redox-Flow Batteries." *Current Opinion in Electrochemistry* 21, 311–318.
- Petek, T J, N C Hoyt, R F Savinell, and J S Wainright. 2015. "Slurry electrodes for iron plating in an all-iron flow battery." *Journal of Power Sources* 294, 620–626.
- Pidgeon, L M, and W A Alexander. 1944. "Thermal production of magnesium-Pilot plant studies on the retort ferrosilicon process." *Trans. AIME* 159, 315–352.
- Pillot, C. 2019. "The Rechargeable Battery Market and Main Trends 2011–2020." *Power Tools*.
- Prifti, H, A Parasuraman, S Winardi, T M Lim, and M Skyllas-Kazacos. 2012. "Membranes for redox flow battery applications." *Membranes* Vol. 2, 275–306.
- Rajarathnam, G P, and A M Vassallo. 2016. *The Zinc/Bromine Flow Battery: Materials Challenges and Practical Solutions for Technology Advancement*. Springer.

- Rodby, K E, M L Perry, and F R Brushett. 2021. "Assessing capacity loss remediation methods for asymmetric redox flow battery chemistries using levelized cost of storage." *Journal of Power Sources* 506, 203005.
- Rodby, K E, T J Carney, Y A Gandomi, J L Barton, R M Darling, and F R Brushett. 2020. "Assessing the levelized cost of vanadium redox flow batteries with capacity fade and rebalancing." *Journal of Power Sources* 460, 227958.
- Roznyatovskaya, N, T Herr, M Küttlinger, M Fühl, J Noack, K Pinkwart, and J Tübke. 2016. "Detection of capacity imbalance in vanadium electrolyte and its electrochemical regeneration for all-vanadium redox-flow batteries." *Journal of Power Sources* 302, 79-83.
- Sanchez-Lengeling, B, and A Aspuru-Guzik. 2018. "Inverse molecular design using machine learning: Generative models for matter engineering." *Science* 361 (6400), 360-365.
- Sanders, M. 2016. "Lithium-Ion Battery Raw Material Supply and Demand 2016-2025." *Advanced Automotive Battery Conference*. <http://www.avicenne.com/pdf/Lithium-Ion%20Battery%20Raw%20Material%20Supply%20and%20Demand%202016-2025%20C.%20Pillot%20-%20M.%20Sanders%20Presentation%20at%20AABC-US%20San%20Francisco%20June%202017.pdf>.
- Syllas-Kazacos, M, and M Kazacos. 2011. "State of charge monitoring methods for vanadium redox flow battery control." *Journal of Power Sources* 196, 8822-8827.
- Syllas-Kazacos, Maria, M Rychick, and R Robins. 1988. All-vanadium redox flow battery. United States of America Patent US4786567A.
- Syllas-Kazacos, M. 2019. "Performance Improvements and Cost Considerations of the Vanadium Redox Flow Battery." *ECS Trans* 89, 29-45.
- SNE Research. 2020. "LIB Cell, Module, Pack Cost Analysis and Forecast (~2030)." http://www.sneresearch.com/_new/eng/sub/sub1/sub1_01_view.php?mode=show&id=1005&sub_cat=.
- Soloveichik, G L. 2015. "Flow Batteries: Current Status and Trends." *Chemical Reviews* 115, 11533-11558.
- Spoerke, E D, M M Gross, L J Small, and S J Percival. 2020. "Chapter 4: Sodium-Based Battery Technologies." In *U.S. DOE Energy Storage Handbook*.
- Sun, H, J Ho, H Won, C Jin, and J Hoon. 2016. "Critical rate of electrolyte circulation for preventing zinc dendrite formation in a zinc e bromine redox flow battery." *Journal of Power Sources* 325, 446-452.
- Tete, P R, M M Gupta, and S S Joshi. 2021. "Developments in Battery Thermal Management Systems for Electric Vehicles: A Technical Review." *Journal of Energy Storage* 35, 102255. <https://doi.org/10.1016/j.est.2021.102255>.
- Trahey, L, F R Brushett, N P Balsara, and G W Crabtree. 2020. "Energy storage emerging: A perspective from the Joint Center for Energy Storage Research." *Proceedings of the National Academy of Sciences of the United States of America* 117 (23), 12550-12557.
- U.S. Agency for International Development. 2021. Power Africa Nigeria Power Sector Program Quarterly Report. Retrieved from https://pdf.usaid.gov/pdf_docs/PA00XJS2.pdf
- U.S. Agency for International Development. 2021. "Power Africa - Nigeria Power Sector Program: Battery Storage Report."
- U.S. Department of Energy. n.d. "Batteries, Charging, and Electric Vehicles ." Accessed June 15, 2021. <https://www.energy.gov/eere/vehicles/batteries-charging-and-electric-vehicles>.
- . 2020. "DOE OE Global Energy Storage Database." <https://www.sandia.gov/ess-ssl/global-energy-storage-database-home>.
- . 2013. "Grid Energy Storage." https://www.energy.gov/sites/prod/files/2014/09/f18/Grid_Energy_Storage_December_2013.pdf.
- U.S. Energy Information Administration. 2021. "Battery Storage in the United States: An Update on Market Trends."
- U.S. Geological Survey. 2020. "Mineral Commodity Summaries 2020." <https://pubs.usgs.gov/periodicals/mcs2020/mcs2020.pdf>.
2021. "Vanadium Price." <https://www.vanadiumprice.com>.
- Wang, H-F, and Q Xu. 2019. "Materials Design for Rechargeable Metal-Air Batteries." *Matter* 1, 565-595.
- Wang, S, Z Xu, X Wu, H Zhao, J Zhao, J Liu, C Yan, and X Fan. 2020. "Analyses and optimization of electrolyte concentration on the electrochemical performance of iron-chromium flow battery." *Applied Energy* 271, 115252.

- Weber, A, M Mench, J P Meyers, P N Ross, J T Gostick, and Q Liu. 2011. "Redox Flow Batteries: A Review." *Journal of Applied Electrochemistry* 41, 1137-1164.
- Wei, K, and L Li. 2020. Fe-Cr redox flow battery systems including a balance arrangement and methods of manufacture and operation. United States of America Patent US10777836B1. 2020.
- Wei, L, E H Ang, Y Yang, Y Qin, Y Zhang, M Ye, Q Liu, and C C Li. 2020. "Recent advances of transition metal based bifunctional electrocatalysts for rechargeable zinc-air batteries." *Journal of Power Sources* 477, 228696.
- Weinrich, H, Y E Durmus, H Tempel, H Kunzl, and R-A Eichel. 2019. "Silicon and Iron as Resource-Efficient Anode Materials for Ambient-Temperature Metal-Air Batteries: A Review." *Materials* 12, 2134.
- Whitehead, A H, T J Rabbow, M Trampert, and P Pokorny. 2017. "Critical safety features of the vanadium redox flow battery." *Journal of Power Sources* 351, 1-7.
- Wu, M, Y Jing, A A Wong, E M Fell, S Jin, Z Tang, R G Gordon, and M J Aziz. 2020. "Extremely Stable Anthraquinone Negolytes Synthesized from Common Precursors." *Chem* 6 (6), 1-11.
- Wu, W, S Wang, K Chen, S Hong, and Y Lai. 2019. "A Critical Review of Battery Thermal Performance and Liquid Based Battery Thermal Management." *Energy Conversion and Management* 182, 262-281. <https://doi.org/10.1016/j.enconman.2018.12.051>.
- Yuan, Z, S Jiang, H Sheng, X Liu, H Hua, X Liu, and Y Zhang. 2018. "Human perturbation of the global phosphorus cycle: changes and consequences." *Environmental Science and Technology* 52, 2438-2450.
- Zeng, Y K, X L Zhou, L An, L Wei, and T S Zhao. 2016. "A high-performance flow-field structured iron-chromium redox flow battery." *Journal of Power Sources* 324, 738-744.
- Zhang, F, M Gao, S Huang, H Zhang, X Wang, L Liu, M Han, and Q Wang. 2021. "Redox Targeting of Energy Materials for Energy Storage and Conversion." *Advanced Materials* 33, 2104562.
- Zhao, Z, X Fan, J Ding, W Hu, C Zhong, and J Lu. 2019. "Challenges in Zinc Electrodes for Alkaline Zinc–Air Batteries: Obstacles to Commercialization." *ACS Energy Letters* 2259-2270.
- Zichen, W, and D A Changging. 2021. "A Comprehensive Review on Thermal Management Systems for Power Lithium-Ion Batteries." *Renewable and Sustainable Energy Reviews* 139. <https://doi.org/10.1016/j.rser.2020.110685>.
- Ziegler, M S, and J E Trancik. 2021. "Re-examining rates of lithium-ion battery technology improvement and cost decline." *Energy & Environmental Science* 14 (4), 1635-1651. <https://doi.org/10.1039/D0EE02681F>.
- Zubi, G, R Dufo-López, M Carvalho, and G Pasaoglu. 2018. "The Lithium-Ion Battery: State of the Art and Future Perspectives." *Renewable and Sustainable Energy Reviews* 89, 292-308. <https://doi.org/10.1016/j.rser.2018.03.002>.



Chapter 3 – Mechanical energy storage

3.1 Introduction

Electrical energy can be converted, for purposes of storage, into various forms of mechanical energy such as gravitational potential energy or kinetic energy; it can also be used to compress a gas. Some of these mechanical forms of energy storage are suitable for applications that demand large-scale, long-duration storage. As a category, mechanical energy storage includes a variety of technologies that do not resemble each other in the way that batteries, even when they are based on different chemistries, do. In fact, the principal technologies discussed in this chapter, pumped storage hydropower (PSH) and compressed air energy storage (CAES), have little in common from a technology or implementation standpoint. PSH and CAES do, however, have an important attribute in common: The energy density of these forms of storage is much lower than the energy density of chemical and electrochemical storage. Consequently, the two main mechanical energy storage options have large footprints, must be sited in geologically favorable locations, and do not lend themselves to modularity.

PSH works by storing the potential energy of water pumped uphill. It is a mature and widely deployed technology that in 2020 accounted for over 98% of U.S. grid-scale energy storage capacity and 87% of U.S. storage power capacity. Yet, PSH deployment has slowed significantly in the United States and in many other countries (China is a notable exception) since the 1990s. This slowdown reflects, among other factors, the reduced value of intra-day energy arbitrage as a result of the increased use of flexible gas-fired generation and the difficulty of financing PSH projects in restructured electricity markets. Recent analyses and licensing experience in the U.S. context, however, show significant potential for siting new,

environmentally acceptable PSH capacity.

Realizing this potential depends on the value of long-duration storage in deeply decarbonized electricity systems, the competitiveness of PSH relative to other long-duration storage options, and the ability to finance PSH projects.

CAES works by compressing air and storing the heat that is generated when air is compressed. CAES has been widely discussed as a potential grid-scale energy storage solution for decades, but the technology has seen no large-scale deployment in the last 30 years (two related projects were commissioned in 1978 and 1991). At present, significant hurdles exist to new CAES deployment at scale.

Although our focus here is on PSH and CAES, this chapter briefly discusses other mechanical energy storage technologies, such as gravity energy storage of solids, underground pressurized fluid storage, and liquid air energy storage. Kinetic energy storage systems, such as systems that use flywheels, have energy capacities too small to be of interest for supporting grids that rely heavily on variable renewable energy and are not discussed here.

3.2 Hydropower storage

3.2.1 An overview of hydropower storage

A pumped storage hydropower (PSH) station consists of two water reservoirs at different elevations. Energy is stored by pumping water from the lower reservoir to the upper one, typically during off-peak hours when demand for electricity is low. Power is then generated during on-peak hours by releasing water from the higher reservoir through a hydraulic turbine and into the lower reservoir. Roundtrip efficiencies range from 65% to 80% for existing PSH facilities. Common efficiency estimates for

new projects are around 75% (MWH 2009), but the roundtrip efficiency of some projects may be up to 82% (U.S. Department of Energy 2021).

PSH is by far the dominant electricity storage technology in the United States and globally in terms of both installed power and energy capacity. The power capacities of individual PSH stations typically range from hundreds of megawatts (MW) to several gigawatts (GW). Typical energy capacities are in the range of several gigawatt-hours (GWh). At the end of 2018, the installed base of operational PSH capacity totaled 166 GW globally, more than 50 GW of additional PSH capacity were under construction (with expected completion by 2030), and many more projects were planned (International Hydropower Association 2019). Data on the energy capacity of PSH stations are incomplete, but reservoirs at those stations for which data are available typically hold enough water, when full, to allow for 8–12 hours of discharge at rated power. Some PSH reservoir systems are large enough to allow for several days, or, in rare cases, a week or more of discharge at full power. Assuming an average storage capacity of 10 hours for stations about which more specific information is not available, we estimate that PSH energy capacity at current facilities totals about 8,000 GWh globally.

Conventional hydropower with reservoir storage differs from PSH and the other storage technologies that are the focus of this study in that it does not offer a direct electricity-to-electricity storage pathway. Nonetheless, conventional hydropower can be an important source of zero-carbon dispatchable electricity to complement intermittent wind and solar resources in decarbonized electricity systems. For example, systems that release stored water to generate power can reduce their baseline releases to accommodate wind and solar generation when these resources are producing at high levels. While this scenario does not involve pumping water to a higher reservoir (as in a PSH system), the integration of

hydropower generation with newly added wind and solar generation leaves more water in reservoir storage to support increased hydro generation during periods when wind and solar generation are low. Investments in existing hydropower systems and in related transmission assets could further increase the ability of these systems to complement wind and solar generation—indeed, this approach could be widely applied in both developed and emerging market developing economies with significant hydropower assets (Box 3.1).

3.2.2 Diverging regional growth trajectories for pumped storage hydro

PSH facilities were first deployed in Europe starting in the 1890s. Until 1970, more than half of global PSH capacity was located in Europe. Starting in the 1970s, significant PSH facilities were built in the United States and Japan. New PSH capacity additions were often associated with the buildup of large coal and nuclear plants that had high capital costs but low fuel costs relative to other types of generators. PSH enabled these plants to run at or near full capacity around the clock because excess power produced during the night, when electricity demand was low, could be used to pump water for power generation during high-demand portions of the day. Until 2000, Japan, the United States, and Europe together accounted for over 80% of global PSH capacity (Figure 3.1). Starting in the early 2000s, China quickly became the leading builder of PSH, with more new projects than the rest of the world combined. China currently has the largest base of installed PSH capacity worldwide, having surpassed the United States in 2015 and Japan in 2017. Although more than 40 countries have PSH stations, the top 20 countries account for 91% of global capacity. Outside of China, new PSH projects are highly concentrated in Western Europe, although Japan, South Korea, and India are also adding some capacity. Few PSH projects have been undertaken in smaller and less developed countries.

Box 3.1 Repurposing conventional hydropower as an option to balance variable renewable energy (VRE) generation

Existing hydropower is a very large resource in terms of both power capacity and energy storage potential. Global hydropower capacity totaled 1,132 GW in 2019, including 78 GW in the United States, with hydropower accounting for 16% of global generation and 7% of U.S. generation that year. Currently, some countries rely on hydro for more than half of their electricity supply (International Hydropower Association 2019; IEA 2020). Conventional hydropower includes systems with storage reservoirs, the predominant type in the United States, as well as “run-of-the river” systems that do not store water (Johnson et al. 2021).

Even without pumping capability, reservoir storage capacity on hydropower systems mitigates weather-related risks, notably the risk that precipitation patterns deviate from seasonal norms, potentially for months or even years, affecting water inflows on which hydropower systems depend. Climate change could lead to changes in seasonal water inflow norms for existing hydropower systems that either increase or reduce average storage or storage variability. The energy potential stored in a conventional hydropower reservoir depends on the volume of water stored and the height difference between the water surface and the turbine generator (called the “head”). Some hydropower projects have reservoir storage capacities that dwarf the capacity of PSH systems. The Canadian province of Quebec, for example, reports reservoir storage capacity of 176,000 GWh—roughly equal to a full year of electricity production and use (the province relies on hydropower for nearly all its electricity needs) (Hydro Quebec 2019). Quebec’s reservoir storage capacity alone is roughly 840 times the combined total energy storage capacity of all PSH systems in the United States, and roughly 170,000 times the amount of grid-connected battery energy storage capacity in the United States as of 2019. Norway, with average hydropower production of 130,000 GWh in recent years, has storage reservoir capacity of 85,000 GWh (Graabak et al. 2017).

Conventional hydropower projects often serve purposes other than electricity generation, including flood control, water supply for irrigation and other critical needs, and recreational uses. These uses, as well as restrictions on daily, monthly, and seasonal flows to protect endangered species and ecosystems, can constrain opportunities to optimize the operation of conventional hydropower to balance electricity systems that rely heavily on intermittent resources. Even where flexibility is limited, however, the immense power and energy storage capacities of existing hydro systems with large storage reservoirs may enable these systems to generate at lower levels during periods of high wind and solar availability and at higher levels during periods of low wind and solar availability, thereby providing a form of storage for renewable generation even without pumping capability.

The integration of existing hydro with new wind and solar capacity can provide significant cost savings for clean energy systems. While past electricity trade between Quebec and the northeastern United States (New England and New York) centered on one-way flows of hydropower to the south, researchers have recently considered how a low-carbon electricity system spanning New England and Quebec might benefit from increased two-way trading between Quebec’s hydro resources and expanded wind and solar generation resources in New England (Dimanchev, Hodge and Parsons 2020). In simulations of a future cost-optimal low-carbon power system for the combined region, transmission assets are used to send power from New England to Quebec in hours of excess wind and solar generation, saving water in hydro reservoirs that can then generate power for export to New England in hours when wind and solar generation is scarce. Shifting dispatchable hydropower generation to hours when marginal supply costs to the combined region

continued

Box 3.1 Repurposing conventional hydropower as an option to balance variable renewable energy (VRE) generation

continued

are highest benefits both Quebec and New England. In a 2050 scenario that does not add new hydropower generation or increase transmission capacity linking Quebec and New England, two-way trading is estimated to reduce power system costs by 5%–6%, depending on the level of decarbonization imposed on the system. In another scenario that adds 4 GW of transmission capacity, the increased utilization of existing hydro reservoirs as a balancing resource reduces the estimated cost of a zero-emission power system across New England and Quebec by 17%–28%. Another recent study of the Quebec–New England region that examines opportunities to reduce the cost of low-carbon systems over different timescales also finds significant savings (Williams et al. 2018). Similar opportunities for synergistic trade utilizing the storage capacity of Canadian hydro reservoirs exist between the United States and the Canadian provinces of Manitoba and British Columbia.

Beyond operational changes or transmission enhancements, other opportunities to boost the storage potential of existing hydro projects have also been considered. One idea is to add turbines to existing hydro projects to increase their peak generating capacity (Jacobson et al. 2015), although it is important to recognize the high cost of additional power capacity (Clack et al. 2017). The applicability of any of these strategies to an existing project can be limited if efforts to increase energy storage capacity conflict with the non-electricity-related services provided by the project or give rise to environmental concerns associated with changing flow patterns or maximum flow rates. In some cases,

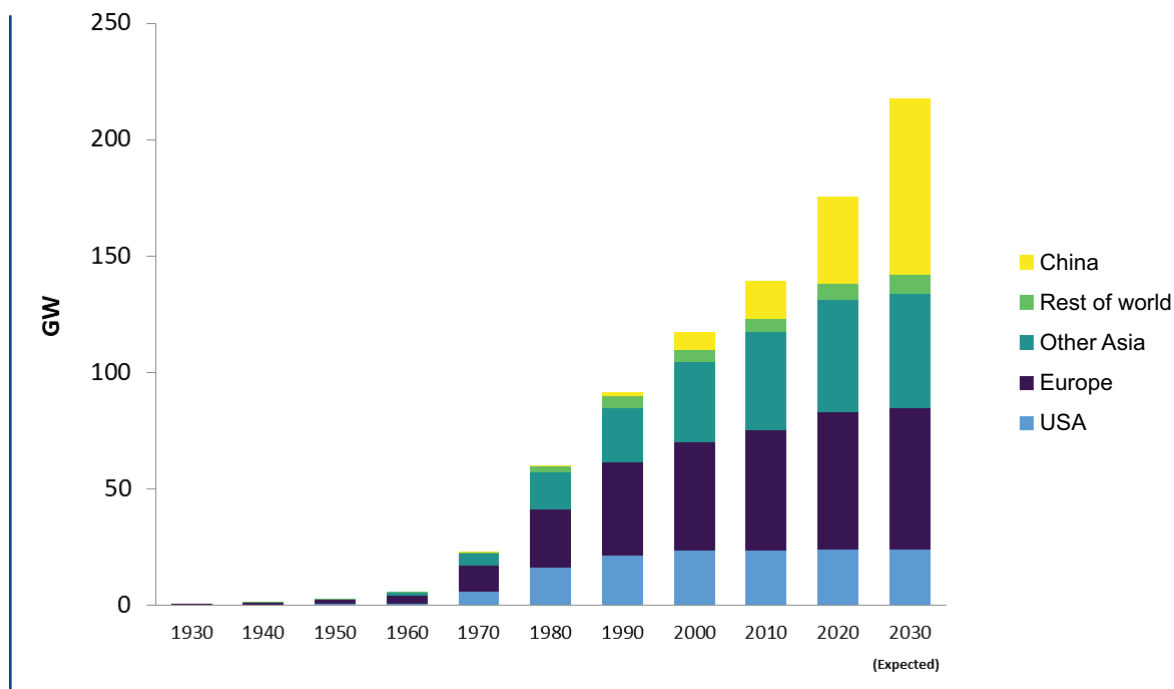
elements of an existing conventional hydro project could be used to add PSH storage at lower cost than building a new, standalone PSH project. Where technically and environmentally feasible, these strategies must be evaluated in the context of alternative options for balancing clean generation systems, including the option to deploy other types of storage technologies that may become significantly more cost-competitive in coming decades.

In sum, existing hydropower facilities, particularly those that have large storage reservoirs, offer significant potential to help balance electricity systems that rely heavily on intermittent wind and solar generation. Differences across these facilities, in terms of the purposes they serve and any environmental constraints that apply, suggest that their potential to provide operational flexibility to balance electricity systems must be considered on a case-by-case basis.

Operators of existing hydro projects should therefore review the operational capabilities of their facilities and work with stakeholders and regulators to determine whether opportunities exist to create and/or provide additional flexibility for system balancing purposes without adversely affecting other project purposes or the environment.

At the same time, developed and developing countries should actively explore the potential to add VRE and other low- or zero-carbon generation to maximize the value of their reservoir storage hydropower capacity in the context of efforts to achieve deep grid decarbonization.

Figure 3.1 Growth of pumped storage capacity by region



3.2.3 Physical characteristics of PSH technology

Several PSH designs have been successfully implemented around the world. Existing systems are distinguished by two primary design features: pure vs. hybrid (or mixed) and closed-loop vs. open-loop.

- Pure vs. hybrid: A pure PSH design generates electricity only from previously stored energy, with no natural water inflow to the upper reservoir. A hybrid PSH design uses both natural flows of water to the upper storage reservoir and pumped water to generate power.
- Closed vs. open loop: In closed-loop PSH facilities, the reservoir (or reservoirs) is located away from natural surface water features and surface water or groundwater withdrawals are made solely for purposes of the initial fill or for periodic recharging as needed to operate the facility (Federal Energy

Regulatory Commission 2019). Open-loop PSH facilities utilize at least one natural body of surface water.

Hybrid PSH facilities are always open loop. Closed-loop PSH facilities are always pure, but pure PSH designs may be either closed loop or open loop. Open-loop facilities come in many different variants. One type of hybrid design involves damming a river at two places to form an upper and a lower reservoir. Because the water in the upper reservoir comes from both the river and the pump-back operation, this design serves as both a conventional hydro-power generator and an energy storage facility.

In another open-loop configuration, an upper reservoir is constructed by using either a ring embankment on a hilltop or dams to enclose a dry valley. This is the design used at the Lewiston PSH facility near Niagara Falls and the Luddington PSH facility above Lake Michigan. Both are examples of pure, open-loop designs because the upper reservoir is

filled exclusively with pumped water even though the lower reservoir is continuously connected to a natural flowing water feature.

Because PSH involves large civil engineering projects and utilizes large volumes of water, these facilities inevitably come with significant environmental impacts, including impacts on land and aquatic ecosystems and impacts on landscapes and scenic values. In general, open-loop systems tend to have more significant environmental impacts than closed-loop systems. PSH designs that require the damming of natural rivers typically have more severe impacts on aquatic ecosystems than other designs. The operation of an open-loop PSH system that utilizes one or more river dams can change flow patterns, water levels, turbidity, and temperature and cause adverse effects on flora and fauna in the connected water body or riparian zone (Evans, Carpenter and Farr 2018).

Awareness of the environmental impacts of dams began growing in the 1970s. By the 1990s, almost all large dam projects in the United States ceased and the environmental movement shifted its focus to dam removal (Stevenson 2017). Since then, the attention of PSH developers has shifted to off-river, closed-loop projects. Even these types of projects, however, have been difficult to develop in the United States.

Finally, there are PSH concepts that seek to avoid reliance on freshwater resources or reduce the need for the siting and development of new above-ground reservoirs. Seawater can be used for PSH but this approach entails special design considerations, including the need to use corrosion-resistant hydraulic machinery and to take measures aimed at preventing soil contamination around the upper reservoir. Only one plant of this type has been constructed to date.

The use of underground caverns and abandoned mines as the lower reservoirs in PSH systems has been proposed and promoted for decades (Tam, Blomquist and Kartsounes 1979). In theory, such systems could avoid adverse environmental impacts. In recent years, several underground projects have been proposed in the United States, including projects in Pennsylvania that use abandoned mines as part of a PSH system. The Federal Energy Regulatory Commission has ruled that these projects do not require federal licenses, but the developers have not been able to secure financing.

3.2.4 Trends in PSH utilization

Trends in the utilization of existing PSH plants reflect the changing value of energy storage. Analysis conducted for this report shows that PSH utilization has increased since 2000 in Austria, China, Germany, Portugal, South Korea, and Switzerland. By contrast, PSH utilization declined over the same period in Greece, Ireland, Italy, Japan, Spain, and the United States.

Comparing experience across countries, decreasing utilization of PSH generally correlates with increasing use of low-cost natural gas, which tends to reduce wholesale power prices while adding flexibility and load-following capability to the generation mix. To date, the growth of variable renewable energy (VRE) resources has not necessarily increased PSH utilization except in systems with little or no flexible natural gas generation. This natural-gas-driven decline in PSH utilization appears to be attributable to two factors: (1) a reduced gap between peak and off-peak electricity prices (and resulting lower energy market arbitrage values) associated with low natural gas prices, and (2) the high flexibility of modern natural gas generating plants compared to the often still limited flexibility of older existing PSH plants.

Regarding the first factor, increased reliance on natural gas in the U.S. generation mix, which accelerated with the rapid growth of low-cost gas production from domestic shale resources since the mid-2000s, has reduced intra-day energy price arbitrage opportunities in many U.S. regions. When both off-peak and on-peak prices are set by natural gas plants, or by a combination of coal and natural gas plants with very similar fuel costs, the economic value of pumped hydro storage is relatively low.

This may change with increasing reliance on VRE generation, which will result in market prices that are more frequently near zero (or even negative) when the marginal unit of generation comes from a VRE resource that has zero fuel costs. To what extent older PSH plants, which may be considerably less flexible than modern natural gas plants, will be able to take advantage of VRE-related market opportunities is unclear, however.¹ One recent study (Ruiz et al. 2018) points out that existing PSH plants are not fully optimized for today's wholesale markets, which offer distinct opportunities to sell into day-ahead and real-time energy markets, and to provide various ancillary services. The study finds that fully optimizing existing PSH plants to take advantage of organized wholesale markets could more than triple the market revenues these plants currently generate.

Meanwhile, additional challenges stand in the way of developing new PSH plants. Historically, state-regulated, vertically integrated utilities or public entities played a dominant role in PSH development (Barbour, Wilson, et al. 2016). But global deployment of PSH capacity slowed in the 1990s, coinciding with the deregulation of

electricity markets in many developed countries. Numerous projects were cancelled in the United States throughout the 1990s and 2000s. A review of developers' statements with regard to these cancellations clearly shows that market uncertainty was the main issue (Yang and Jackson 2011). While concerns about environmental impact and siting did play a significant role in some cancellations, the extended hiatus in PSH investment is not, for the most part, attributable to the scarcity of suitable PSH sites or to environmental challenges.

Other long-term trends have reduced demand for energy storage in many electricity systems (Guittet, Capezzali and Guadard 2016). First, the operational flexibility of many coal-fired plants and of some nuclear power plants improved over time such that these generators could better follow load. Second, gas turbines emerged as an increasingly popular, low-cost, and highly flexible option for generating electricity, including under peak load conditions when ramping needs are high. Despite widespread anticipation that increased use of renewable energy would boost demand for energy storage, the observed trend in many countries, as already noted, has been one of declining utilization of existing PSH capacity.

The combination of declining PSH utilization, historically low wholesale market prices, significant long-term market and energy policy uncertainties, high and uncertain capital costs, siting and permitting challenges, and long development lead times has made it very challenging to develop and finance new PSH plants. However, attractive PSH development opportunities exist at some brownfield locations where it is possible to reduce costs, permitting

¹ For example, older PSH plants (many still without variable-speed pumps and generators) may have operational limitations in terms of their ramp rates, the number of times they can be cycled each year, and the range within which output can be regulated when the plant is generating (e.g., a narrow range between minimum and maximum output) or pumping (e.g., only "on" and "off").

challenges, and development timelines by utilizing existing infrastructure, such as the reservoirs of existing hydro power plants or substation and transmission equipment at recently retired coal plants. Several brownfield PSH projects have been proposed in the United States.

3.2.5 Strengths and limitations of pumped storage hydro

Among currently deployed electricity system storage technologies, PSH facilities generally have the lowest energy storage capacity cost. However, given their large scale, high costs of power capacity, and long development timelines, construction costs for new PSH projects are typically in the range of hundreds of million to billions of dollars. This can present financing challenges and it means that public entities, such as government- and state-owned corporations, often play an important role in financing PSH projects.

A shift away from vertically integrated utilities in the electricity sector has increased the difficulty of financing new PSH projects. Equity financing is rarely a practical option for a private project developer because it entails large upfront capital requirements. Commercial financing also poses significant challenges, particularly when the owner is unable to secure a long-term buyer willing to make fixed payments in exchange for services provided by the project. Buyers' reluctance to commit to long-term contracts for PSH services may reflect their concern that the value of those services at any point in the future will depend on both the overall demand for energy storage services and the cost of competing storage (and non-storage) technologies that can provide comparable services at that time.

On the other hand, restructuring can also provide PSH operators with access to

wholesale markets where they may sell energy, capacity, and ancillary services at non-regulated rates to buyers from a much larger geographic region. For example, with increased access to regional wholesale markets the Taum Sauk PSH station in Missouri operated about 300 days per year, compared to about 100 days per year before access was increased (Rogers and Watkins 2008).

PSH stations have very long service lifetimes. In fact, dams are among the most durable man-made structures on Earth. Reliable empirical data on the useful lives of PSH reservoirs are lacking because very few such reservoirs have been retired. It is reasonable to assume that the reservoirs of PSH stations can remain operational for 100 years or more, provided they are properly maintained.

The electromechanical components of PSH facilities are not as durable as the reservoirs. Typical design life for motor-generators ranges from 40 to 60 years, although actual useful life may be significantly longer (Nie et al. 2017; Ma 2017). At the end of its service life, the most vulnerable parts of the motor-generator rotor (typically the magnet yoke and pole) inevitably suffer from metal fatigue, potentially compromising safety and reliability. However, rotors and other electromechanical equipment with shorter design lifetimes than reservoirs and other PSH civil works can be, and routinely are, refurbished or replaced at a cost that represents a very small percentage of the total value of the PSH station. Taking account of such practices, the actual operational lifespan of a PSH facility depends on the durability of the facility's civil works, which in many cases extends beyond 100 years.

The economics of PSH projects in the United States are often analyzed over a period that is limited to 30 years. Using discount rates based on commercial financing costs, the net present

value of operations beyond the first 30 years is small (even if a terminal value to reflect longer service life is considered). Projects in China, by contrast, are typically analyzed over periods ranging from 20 to 50 years (Zhang and Jiang 2012), with longer periods applied to larger projects with long payback times and vice versa. In sum, financing terms and choice of discount rate determine the relevant period for economic analysis, but that period does not typically reflect the expected useful life of a PSH facility. In today's interest-rate environment, both policy makers and investors may want to reconsider what choice of discount rate is reasonable.

Limited experience with the sale of existing PSH facilities after decades of use illustrates their long-lived value. The case studies in Box 3.2 show that after decades of operation several PSH stations were sold at prices that were above their inflation-adjusted construction cost. Thus, published studies that assume the asset value of a PSH facility is zero after only a few decades of operation likely overestimate the cost of services provided by these facilities. Few other energy storage technologies, if any, have demonstrated capital appreciation potential that can significantly offset or exceed their inflation-adjusted acquisition cost.

In sum, PSH investment presents a financial conundrum. On the one hand, existing PSH facilities will very likely remain available as a low-cost solution for bulk energy storage for many years. On the other hand, it is extremely difficult to finance new PSH plants due to the combination of challenges noted previously (i.e., long development times, large size, high and uncertain capital costs, and market and policy uncertainties). These challenges are in sharp contrast to the advantages of some other storage technologies, such as batteries, which offer modularity, much shorter development times (e.g., a year compared to a decade), and lower capital costs for shorter-duration

applications—all factors that greatly reduce development and financing risks.

3.2.6 Recent PSH costs and prospects for cost reduction

Figures 3.2 and 3.3 show construction costs for PSH projects on a per-kW and per-kWh basis for major countries and regions since 1995. The overall trends appear stable, except for a few outliers. Costs vary significantly from project to project and from country to country. Construction costs for most projects fall in the range of \$600–\$2,500 per kW and \$30–\$300 per kWh. China appears to have the best record of managing PSH costs, with project costs that are both highly consistent and all near the low end of the distribution.

Operation and maintenance (O&M) costs for PSH facilities are very low, with fixed O&M cost at about \$16/kW-year and variable O&M cost at about 0.00025 cents/kWh (Pacific Northwest National Laboratory 2019).

Civil works (e.g., dams, reservoirs, penstock tunnels, powerhouse caverns) and land acquisition typically account for 60%–70% of total construction cost for new PSH stations (Breeze 2018). Constructing civil works is labor intensive. The cost of labor varies greatly from country to country and tends to increase over time. Several dam projects in China have demonstrated experimental unmanned construction trucks and roller-compactors enabled by artificial intelligence (Zhong et al. 2019; Chen et al. 2019; Zhang et al. 2019). Beyond reducing labor costs, unmanned vehicles may improve efficiency and construction quality by reducing human errors. However, this technology is still at an early stage of development, and it is too early to tell whether unmanned equipment will eventually reduce labor and civil construction costs. Overall, most PSH-related civil engineering innovations appear more

Box 3.2 Case studies on pumped storage hydropower asset resale values

Northfield Mountain (1,168 MW) (USA)

Original construction cost for this facility in 1972 was \$136 million, equal to \$522 million in inflation-adjusted terms in 2006 when the Northfield Mountain PSH station was sold by Northeast Utilities to Energy Capital Partners. The sale was part of a \$1.34-billion package deal totaling 1,442 MW, including the 1,168-MW PSH station, 12 conventional hydro stations, a coal-fired power plant, and a combustion turbine peaking generator. Prorating the total sale price by the capacity of each of these assets, the Northfield Mountain PSH station was worth roughly \$1.09 billion in 2006.

Based on this figure, the asset value of Northfield Mountain PSH station in 2006 was 108% higher than its inflation-adjusted construction cost after 34 years of operation.

Bear Swamp (600 MW) (USA)

New England Power Company built this facility in 1974 at a cost of \$120 million, equal to \$406 million in inflation-adjusted terms in 2005 when the facility was sold to Brascan Power and Emera Inc. of Toronto (50%-50% joint venture) for \$92 million.

Dinorwig (1,728 MW) (UK)

The original construction cost for this facility in 1984 was £425 million, equal, in inflation-adjusted terms, to £774 million in 1995 and £912 million in 2004. National Grid Transco sold the station to Edison International (USA) in 1995 for £570 million.

Edison resold the Dinorwig station in 2004 as part of a £1.27-billion deal that also included the 360-MW Ffestiniog station. Prorating the total sale price by the capacity of these two assets, the value of Dinorwig in 2004 was about £1.05 billion.

Based on these figures, the resale value of the station after 11 years of operation was 26% lower than its inflation-adjusted cost. However, its resale value after 20 years was 15% higher than its inflation-adjusted cost.

Ffestiniog (360 MW) (UK)

Original construction cost for this facility in 1963 was £13.5 million, equal to £185 million in inflation-adjusted terms in 2004 when the station was sold as part of the £1.27-billion package deal (with the 1,728-MW Dinorwig station) discussed above. Prorated by capacity, the value of Ffestiniog as part of this package deal was £220 million.

Thus, the resale value of the station in 2004, after 41 years of operation, was 19% higher than its inflation-adjusted construction cost.

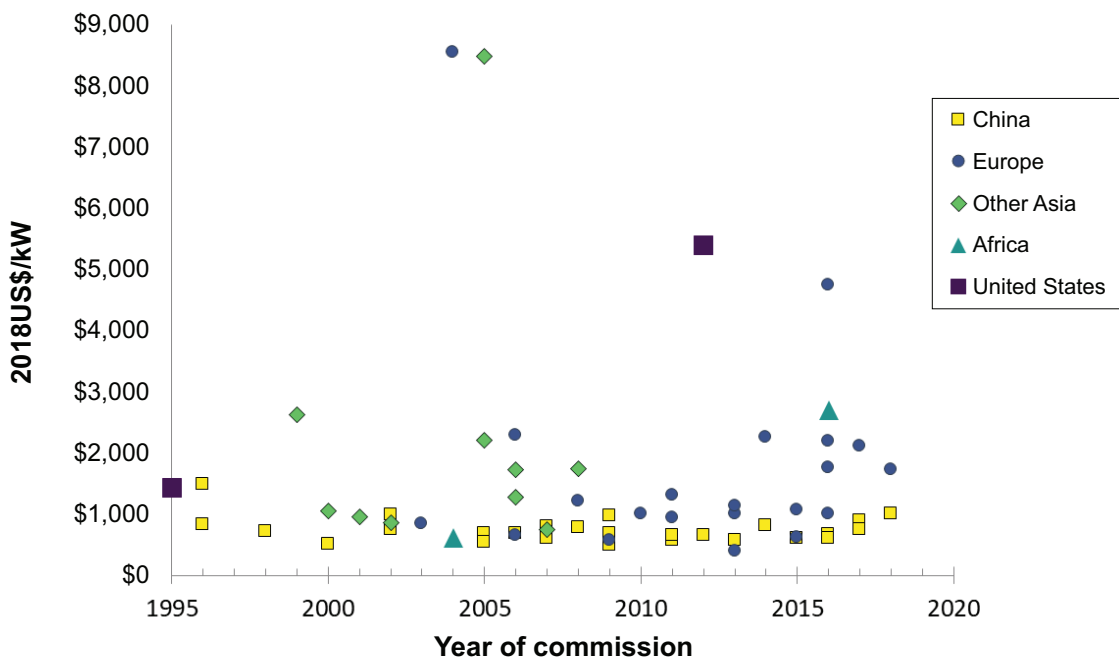
Taum Sauk (450 MW) (USA)

Original construction cost for the Taum Sauk station in 1963 was \$47 million, equal to \$140 million in inflation adjusted terms in 2010, when the upper reservoir had to be rebuilt because of a dam failure. The rebuild, which was completed in 2010, cost \$490 million. Based on the owner's willingness to make this repair, the value of the station to the owner at that point in time must have far exceeded its original construction cost.

focused on shortening construction time and improving quality rather than lowering cost. Construction costs for civil works are highly site-specific. Some locations, for example, offer existing basins or valleys that can reduce the required size of embankments for reservoirs. At some sites, abandoned quarries, mines, or

caverns can be utilized as lower reservoirs for very low cost. In principle, developers can be expected to develop the lowest-cost sites before they consider less favorable locations. This means that costs for future PSH projects are likely to increase over time.

Figure 3.2 Capital cost per kW



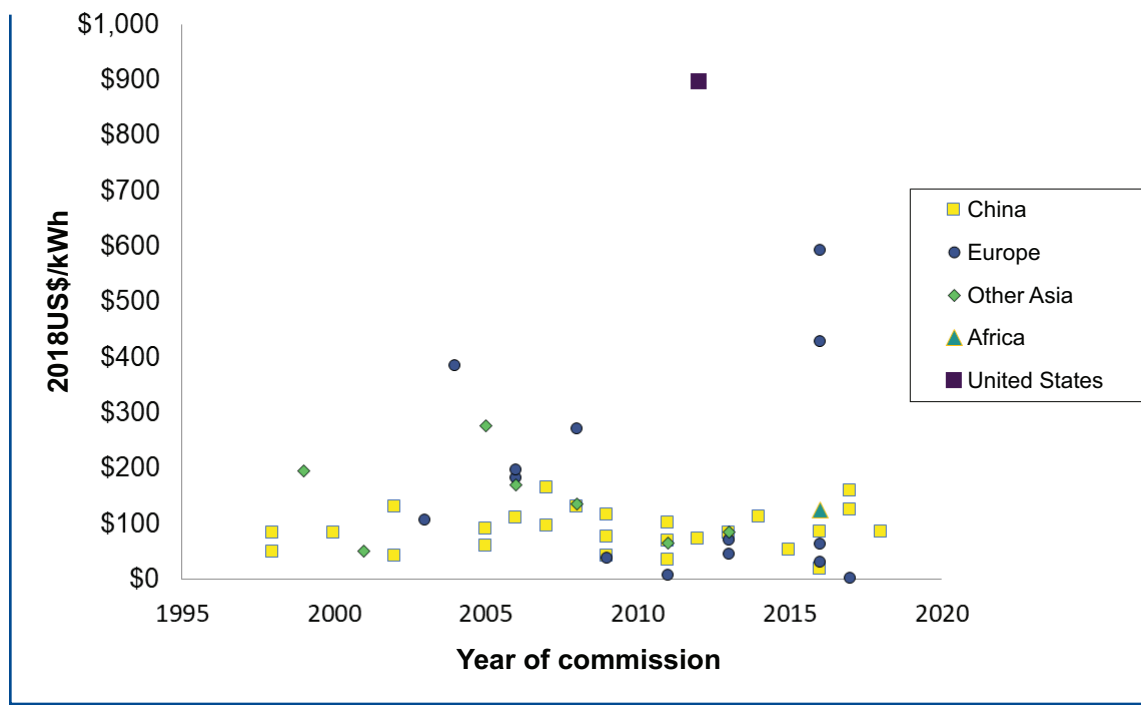
Pump-turbine technology has been through several major revolutions. Before the 1950s, PSH stations were typically equipped with separate pumps and generators (Baxter 2006). The advent of reversible pump-generators reduced the number of required penstock tunnels and the need for other equipment while also reducing the required size of the powerhouse cavern. Starting in the 1990s, Japan pioneered the use of variable-speed pump-turbines, which improved the efficiency and flexibility of PSH operations. Many PSH stations in Europe have been converted to variable-speed systems since the 2000s (Yang 2016). In short, the reliability and efficiency of electromechanical equipment for PSH facilities have improved over time (Pacific Northwest National Laboratory 2019), but the cost of these facilities has not dropped. Further improvements in reliability and efficiency may be expected in the future, but significant cost reduction seems unlikely.

3.2.7 PSH potential

The water heads of existing PSH stations range from 15 to 1,400 meters. The most attractive water heads are in the range of 300 to 600 meters (China Renewable Energy Engineering Institute 2018). Lower water heads lead to lower roundtrip efficiency, while very high water heads lead to very high water pressure, which presents challenges in the design of hydraulic machinery.

Although topography is an important criterion, it is not as limiting as often believed. Several formal assessments indicate that potential sites for PSH are plentiful (Australian National University 2019; Hall and Lee 2014; Dames and Moore 1981). The Australian National University (ANU) publishes a Global Pumped Hydro Atlas that identifies over 600,000 sites worldwide with suitable topography for PSH development. Identified storage potential at these sites is 23,000 terawatt-hours (TWh) globally, including roughly 1,457 TWh in the

Figure 3.3 Capital cost per kWh



United States. Importantly, however, the ANU assessment does not consider water availability, which can be a serious issue for open-loop PSH systems (it is a lesser consideration for closed-loop systems), nor does ANU consider proximity to transmission lines or load centers. Also, many topographically feasible sites may raise environmental concerns or could be expected to face public opposition for a variety of reasons related to social or aesthetic impact. Nonetheless, PSH development at even a very small fraction of identified sites could provide large amounts of storage capacity.

Siting, licensing, and permitting processes vary from country to country as does the influence of local communities. In the United States, siting and licensing costs typically account for less than one percent of total project costs. The length of time required for siting and licensing varies greatly from project to project. Siting closed-loop PSH projects is relatively simple and may be completed in a few years. From this perspective, the main hurdle to additional PSH

development is not the availability of sites but market challenges and financing barriers, including the need to secure regulatory commitments or long-term contracts to support project financing.

Experience supports the conclusion that the business case for PSH is difficult, at least in the United States. Risks related to the potential for significant construction cost overruns only contribute to this difficulty and are likely more important than siting and licensing hurdles in explaining the dearth of current PSH development activity.

3.2.8 PSH siting and licensing activities in the United States

In the United States, the Federal Energy Regulatory Commission (FERC) has primary responsibility for permitting hydropower plants, including PSH facilities. A “preliminary permit” grants the permittee first priority in applying for a license for a proposed project. The

permittee conducts investigations, surveys, and environmental impact assessments; holds public hearings and consultations with stakeholders; and makes plans for the project. After siting activities have been completed, the permittee may apply for an “original license” authorizing project construction and operation for a period of up to 50 years. Most siting activities occur between the approval of the preliminary permit and the original license.

An original license requires the licensee to commence project construction within two years of the license issuance date and to complete construction within five years of license issuance. FERC may allow a one-time extension of the construction deadline by two additional years. A recent law, the America’s Water Infrastructure Act of 2018, allows FERC to grant extensions of as much as eight years. In 2019, FERC established an expedited licensing process for facilities at existing non-power-generating dams and closed-loop PSH projects. The expedited process requires FERC to issue a final licensing decision within two years after the license application.

A hydropower project falls under FERC’s mandatory jurisdiction if it is located on navigable waters, occupies federal lands, or uses water or hydropower from a federal dam, or affects the interests of interstate or foreign commerce (for example, if power from the project is sold on the interstate grid). Thus, most hydropower projects are subject to FERC jurisdiction. Even in a case where a PSH project does not require a FERC license, the project developer may find it preferable to obtain one because a FERC license preempts state and local laws.

3.2.9 Recent history and present status of PSH projects in the United States

Table 3.1 summarizes PSH projects that have successfully completed the siting and licensing process since 1990. The Iowa Hill project, which was first proposed in 2004, is a good example of the challenges that currently confront PSH development in the United States. After 10 years of siting activities, FERC approved a construction license for this project in 2014. A year later, the Sacramento Municipal Utilities District (SMUD) re-evaluated its energy storage needs and decided that the Iowa Hill project was too big. The original cost estimate of about \$800 million had subsequently been revised to \$1.45 billion. Having concluded that an upfront capital expenditure of this size would severely constrain its finances and crowd out other future capital investments, SMUD cancelled the project in 2016. Although the siting and permitting processes for the Iowa Hill project were lengthy and challenging, they had been completed and a license had been issued before the project was cancelled. Since the 1990s, in fact, the reasons for terminating PSH projects have mostly involved demand uncertainties and financial risks, rather than siting and licensing problems. This still seems to be the case for most, if not all, new PSH projects in the United States.

After Iowa Hill, FERC issued licenses for three more proposed PSH projects (Eagle Mountain, Gordon Butte, and Swan Lake). Table 3.2 shows that the time required to complete the siting process for these projects is not atypical compared to siting timelines for other large construction projects and is, in fact, shorter than the typical PSH permitting time in China, which is about 10 years. However, none of these projects has been successfully financed, largely due to the inability of project developers to secure offtake agreements for PSH services. Some developers are still trying. In addition,

Table 3.1 PSH projects licensed in the United States since 1990

| Project name | State | License issued | License terminated | Cause of termination/delay |
|-----------------------|------------|----------------|--------------------|----------------------------|
| Mt Hope | New Jersey | 1992 | 2006 | Market uncertainty |
| River Mountain | Arkansas | 1994 | 2003 | Market uncertainty |
| Summit | Ohio | 1991 | 2001 | Market uncertainty |
| Blue Diamond | Nevada | 1997 | 2005 | Market uncertainty |
| Iowa Hill | California | 2014 | 2016 | Financial risk |
| Eagle Mountain | California | 2014 | | No offtaker |
| Gordon Butte | Montana | 2016 | | No offtaker |
| Swan Lake | Oregon | 2019 | | No offtaker |

Table 3.2 Siting time for recently licensed PSH projects in the United States

| Project name | Preliminary permit issued | License issued | Years spent on siting |
|-----------------------|---------------------------|----------------|-----------------------|
| Eagle Mountain | 2005 | 2014 | 9 |
| Gordon Butte | 2013 | 2016 | 3 |
| Swan Lake | 2012 | 2019 | 7 |

FERC ruled that several other proposed projects did not require a FERC license. However, none of these proposed projects was able to secure financing and proceed to construction.

The only new PSH project built after 1995 in the United States is the Olivenhain-Hodge station, which was completed in 2012. It is small (40 MW) and, as a conduit project, did not require a FERC license. Though quite expensive (at \$5,931 per kW and \$898 per kWh), the Olivenhain-Hodge station was able to secure financing because construction of the reservoirs could be justified as providing emergency water storage for San Diego. The value of energy storage services alone, in other words, would not have justified the cost of the project—rather it was the region's severe water scarcity that made this project financially viable. Similar multi-value opportunities may exist at other sites where PSH facilities could provide benefits in addition to energy storage—similar to the way many large existing

hydropower plants provide flood control and irrigation services in addition to electricity generation.

Since 2010, developers have sought preliminary FERC permits for more than 160 PSH projects. The large number of proposed projects is a further indication that feasible topographies for PSH are not scarce. It is important to note that applying for a preliminary permit is merely the beginning of the siting process. At that point, the developer has concluded that the site is likely technically feasible, but no determination has been made about the likelihood of successful development. Until investors are convinced about the long-term prospects for PSH demand, the chance of any of these sites being utilized is minimal.

According to the U.S. Department of Energy's U.S. Hydropower Market report (U.S. Department of Energy 2021), only 1.3 GW of PSH capacity was added over the period 2010–2019,

mainly through upgrades to existing stations. Improvements in electromechanical equipment can increase power capacity and efficiency at existing facilities, but energy storage capacity will generally remain the same. Because most PSH facilities in the United States were built between 1960 and 1990, further upgrades to existing stations are likely in the future.

3.2.10 Recent history and present status of PSH projects in Europe

PSH capacity in Europe expanded dramatically starting in the 1960s, mainly to facilitate the growth of nuclear power production. Funding for PSH projects came primarily from integrated state-owned utilities that valued the flexibility PSH provides to balance grid supply and demand.

Power-sector deregulation in Europe combined with a sharp slowdown in nuclear capacity additions to curtail the growth of PSH starting in the 1990s. But Europe still has the largest base of installed PSH capacity in the world, accounting for 30% of the global total. Seven countries—Austria, France, Germany, Italy, Spain, Switzerland, and the United Kingdom—account for more than 80% of Europe's installed PSH capacity. As part of a drive to decarbonize the power sector, many European countries have begun significantly expanding wind and solar PV generation. Increased reliance on these intermittent generators has increased demand for flexible resources to balance the power system. This flexibility has been provided by already built PSHs and conventional hydro resources, but also, importantly, by combined cycle gas turbines (CCGTs). There has been only limited expansion of PSH capacity in Europe in recent years, principally because of the difficulty of financing new PSH projects in light of their uncertain revenue prospects. The PSH projects that have gone ahead have typically been balance sheet financed by large European utilities. Many

newly completed PSH plants in Europe are reporting severe financial losses. Lack of profitability and financial uncertainty have caused many new projects to be put on hold.

The European Union has embraced the goal of reaching net-zero greenhouse gases by 2050. This implies a diminishing role for CCGTs—which in turn means that alternative options for flexible generation or energy storage will be needed to maintain system flexibility in many European countries' power systems. The European Commission recognizes that expanding PSH could help address challenges for E.U. power systems as they transition to increasing reliance on variable renewable generation. Although a recent E.U. report addressing the role of storage in both the 2030 and 2050 time frames identifies significant potential for new PSH projects over both horizons, the optimal scenarios presented in the report do not suggest significant additions of new PSH capacity as part of a net-zero electricity system (European Commission 2020).

3.2.11 Recent history and present status of PSH projects in China

Mass deployment of PSH in China started around 2005 and continues to this day. In 2002, after the electricity industry was restructured and two state grid corporations had been established (Yang 2017), Chinese policy makers officially categorized PSH as a part of the transmission system and gave responsibility for PSH construction and operation to the state grid corporations (Yang 2016). Although the role of PSH in grid balancing is commonly understood, China is unique in allowing PSH projects to recover their costs through transmission tariffs.

China, which added 24 GW of PSH capacity between 2005 and 2020, surpassed Japan as the country with the world's largest installed base of PSH capacity in 2018. At the end of 2019,

34 PSH projects with combined capacity of 45 GW were under construction in China—this is five times more than current levels of PSH construction across the rest of the world. Chinese policy makers appear to have increasingly ambitious plans for PSH deployment. The government's 13th Five-Year Plan (2016–2020) set a 2020 target for installed PSH capacity of 40 GW; this target was later increased to 60 GW (it was not met). A news report in 2019 indicated that the government's 2030 and 2050 targets for PSH deployment are 150 GW and 300 GW, respectively (Gu 2019).

Aggressive PSH development in China may be driven by features of China's generation mix that increase the value of energy storage—notably the very small share of generation that comes from natural gas. Nevertheless, and despite having more installed PSH capacity than any other country in the world, PSH still accounts for less than 2% of China's total electric power capacity. Proportionate to the size of its power sector, in fact, China's deployment of PSH to date still lags that of Japan, Europe, and the United States. Meanwhile, shortages of flexible dispatchable capacity in the country are so severe that Chinese power companies have been conducting flexibility enhancement programs that utilize coal-fired power stations as peaking units. Although it is inexpensive to retrofit underutilized coal plants for this purpose, the environmental impacts are high. PSH is a cleaner choice and can also be relevant to a future generation mix in which variable renewable energy sources and nuclear energy play a growing role.

China has many institutional characteristics that favor PSH development. The two state grid corporations are capable of financing dozens of PSH projects simultaneously. The national planning system offers the long-term certainty the power industry needs to finance such projects. Treating PSH stations as transmission facilities also ensures cost recovery.

A unitary government and national planning system allow Chinese policy makers to implement very long-term plans. PSH projects are sited as part of national programs. In 2014, the China Renewable Energy Engineering Institute recommended 59 PSH sites with a combined capacity of 77 GW, and 7 optional sites. In 2017, the National Energy Administration announced 238 sites for seawater PSH projects. Conducting technical, economic, and environmental assessments of prospective PSH sites typically takes about 10 years in China. The siting process for PSH projects is also considerably more difficult and time-consuming than for most other types of energy infrastructure. Ultra-high-voltage transmission lines, for example, have often been sited in China in a matter of months. Lengthy siting processes, however, have not been a barrier to massive Chinese investment in PSH, likely because the government makes very long-term plans and started these processes early with a nationally coordinated siting program.

In the past two decades, the State Grid Corporation of China (SGCC) and China Southern Grid have become the largest developers of PSH projects in the world. Their ability to develop many projects in parallel offers several advantages in terms of standardization and accumulation of experience. The SGCC has standardized designs and construction management protocols throughout the supply chain of PSH planning, construction, and operation, which are reported in a series of published books. Standardization has led to better cost control. Massive PSH buildup has allowed the grid corporations to establish workforces that are experienced in PSH construction. Outside China, large PSH projects frequently suffer cost overruns and delays, in part because PSH stations and equipment are designed, built, and manufactured in a tailor-made manner. In China, by contrast, such projects are usually finished on time and on

budget. Indeed, highly predictable PSH costs are unique to China and have not been observed in the rest of the world.

The Chinese government has been slowly and gradually reforming the country's electricity sector to make it more market oriented. After some vacillation in recent years, which has produced a number of sudden, hard-to-understand changes in policy, the National Development and Reform Commission (NDRC) announced a new policy on PSH pricing on May 7, 2021. According to the policy, a "capacity rate" for PSH will be included in transmission tariffs, while revenues from energy arbitrage will be determined competitively. The capacity rate will be set at a level that guarantees capital cost recovery. China's 14th Five-Year Plan (2021–2025) reaffirmed the government's continued commitment to PSH buildout and set a target of 62 GW for operational PSH capacity by 2025. This is less ambitious than previously reported targets.

3.2.12 Business models and ownership structures for PSH projects

PSH projects require large upfront investments, but the value they generate is spread over many decades. Financing these projects therefore requires a stable regulatory and financial environment. Competitive electricity markets, by definition, are more dynamic and therefore provide less long-term certainty. As a result, participants in competitive markets are generally unwilling to sign long-term contracts, which in turn makes it difficult for project developers to secure financing. Competition also drives down wholesale power prices, which creates additional challenges for technologies with large upfront capital requirements.

Furthermore, in a competitive market, the supply/value chain of electricity is

disaggregated with different revenue streams for energy, capacity (resource adequacy), balancing services, transmission, and distribution. Although PSH energy storage can provide value at many points along the supply/value chain, it is often not clear how future markets will be organized, how the demand/supply balance in each segment will affect competitive prices, and whether institutional arrangements will enable storage owners to capture all value streams. Where electricity markets are still evolving, the risk of making a large, long-term commitment to a technology such as PSH is inevitably very high (Hester and Harrison 2019).

Table 3.3 shows new PSH capacity commissioned during the 1999–2019 period broken down by owner type. State-owned entities, vertically integrated utilities, governments, and local authorities initiated all the projects undertaken during this period. China's global dominance in building PSH projects is based on a state-owned monopoly. A few other countries with relatively rapid growth of PSH capacities, like Spain and Portugal, also have state-owned utilities.

While no merchant developer has succeeded in building a major PSH facility, independent developers in the United States are actively seeking to advance new PSH projects. These developers generally handle the siting and licensing processes, then attempt to contract with offtakers for PSH services to secure revenue streams that can be used as a basis for financing project construction. Alternatively, a developer may sell a fully sited and licensed project to a utility or to another entity that can finance, build, and possibly operate it. Despite these efforts, a viable and replicable business model for PSH project development in competitive electricity markets has not yet been demonstrated.

Table 3.3 Developer/owner of new PSH projects 2000–2019

| Owner type | Capacity (MW) |
|---------------------------------------|---------------|
| Government | 2,307 |
| Local authority | 1,251 |
| State-owned energy company | 1,917 |
| State-owned grid company | 25,994 |
| State-owned hydropower company | 3,608 |
| State-owned company (other) | 900 |
| Vertically integrated utility | 17,335 |

Source: Authors' calculations based on information provided on websites of PSH plants added globally between 2000 and 2019.

3.2.13 Prospects for overcoming barriers to new PSH development in the United States

The modeling analysis discussed in Chapter 6 of this report suggests that the value of long-duration storage to the electricity system will not support significant deployment of new long-duration storage systems until very high levels of decarbonization are required. Moreover, while PSH dominates the long-duration storage capacity that exists today, its future attractiveness vis-à-vis other storage options, including electrochemical, chemical, and thermal options, is uncertain as costs for these alternatives decline.

PSH projects take a long time to develop, face significant construction cost uncertainty, and have useful lives that greatly exceed typical project finance horizons. Innovative business and financing models are likely needed to overcome these barriers and enable further PSH development.

Offtake agreements, spanning a decade or more, for arbitrage, capacity, and ancillary services provided by PSH facilities could improve prospects for commercial financing. Given the extremely long service life of such facilities, it may be worth exploring new ways to involve investors who are seeking very long-lived income streams.

Vertically integrated utilities played a major role in developing existing PSH projects. While this type of utility structure is no longer ubiquitous, those vertically integrated utilities that remain might add new PSH in the future if they (and their regulators) see enough value to warrant such investments. An additional challenge is that PSH projects are economically efficient only at a large scale (at least hundreds of MW). Thus, even among vertically integrated utilities, few would likely have the financial capability to build one or more large projects. Smaller PSH projects are prohibitively expensive.

Federal entities, including the U.S. Army Corps of Engineers, Bureau of Reclamation, and Tennessee Valley Authority, played pivotal roles in developing hydropower and PSH resources before the 1990s. These entities still own numerous "brownfield" candidate sites (i.e., conventional hydropower dams) that may be retrofitted as PSH facilities. However, federal investment in PSH is unlikely to be justified unless and until the utilization of existing PSH assets begins to increase again and the long-term outlook for value generated by new PSH capacity becomes more certain.

3.2.14 Summary findings and recommendations related to pumped storage hydro

The widely held view that siting is the main barrier to PSH deployment in the United States is a misperception. Technically feasible sites are numerous and many siting/licensing processes for new plants have been completed in the past 20 years. Nearly all of these projects were cancelled, however, because of uncertainty about future demand and financial risks. A viable business model for new PSH in competitive electricity markets has not yet been demonstrated.

Lack of current demand and uncertain prospects for future demand are the main barriers to new PSH projects. So long as natural gas remains an available option for grid balancing, long-duration energy storage in general, and PSH in particular, is unlikely to be competitive. For many existing PSH facilities in the United States and other countries, the trend has been toward declining utilization.

Massive PSH investment in China is enabled by unique institutional and regulatory conditions. It will be difficult, if not impossible, to replicate the Chinese experience elsewhere. It is also unlikely that the United States can replicate China's ability to achieve low and predictable costs through economies of scale and standardization. PSH costs in the United States will probably remain high and cost overruns should be expected.

Recommendations that could advance PSH without introducing distortions fall into two categories: (1) technology-neutral actions that reduce uncertainty regarding the future role of storage and (2) actions specifically addressing PSH issues. Starting with the first category, establishing plausible timetables for power sector decarbonization at the national and subnational levels would provide greater

long-term certainty about demand for grid-scale energy storage, and thus greater confidence in future revenue streams from PSH and other storage investments. Also, utility regulators and grid operators should develop technology-neutral competitive mechanisms that enable load-serving entities, transmission systems, and system operators to enter into offtake agreements for services from PSH and other storage projects.

Turning to PSH-specific actions, the federal government should consider further steps to extend the life of PSH licenses so that developers can maintain a roster of "shovel-ready" projects as decarbonization efforts progress. The federal government could also privatize federally owned PSH stations to incentivize efficient utilization. Auctioning these stations would provide useful information on the resale value of PSH assets, which could help facilitate the financing of new projects. Finally, the electric power industry and financial institutions should continue efforts to develop new business models and financing strategies for PSH projects.

A further discussion of findings, key takeaways, and recommendations for pumped storage hydro is provided at the end of this chapter, together with conclusions for other mechanical storage that are considered in the next section of this chapter.

3.3 Compressed air energy storage

3.3.1 An overview of compressed air energy storage

Compressed air energy storage (CAES) is a mechanical energy storage technology that uses electricity to compress air; the compressed air is then stored and re-expanded at a later time to generate electricity. The compression of the air generates a considerable amount of thermal energy. CAES systems can be categorized by how this thermal energy is handled and where the compressed air is stored.

Box 3.3 Other gravitational energy storage systems

In addition to PSH, other methods of using gravitational potential energy as an energy storage mechanism have been proposed. While none have been deployed, some gravitational energy storage (GES) concepts are actively being developed. Such systems can be characterized as either wet or dry depending on whether water is used as a working fluid (our focus here is on dry systems). One form of wet GES, called geomechanical pumped storage, involves storing fluids that are pressurized by the weight of overlying rock.

Dry gravity storage systems are conceptually simple: Electric motors lift a mass to increase its potential energy. This energy can then be recovered when the mass is lowered. Vertical systems use pulleys to raise and lower masses in a shaft or stack masses atop one another. Inclined “railway” systems raise and lower masses over a gradient.

The energy density of GES systems is similar to that of PSH systems, with adjustments for the relative density of the matter being lifted compared to water (ρ/ρ_{water}). For a given energy capacity and vertical displacement, GES systems are also similar to PSH facilities in size and

footprint. Unlike PSH systems, however, GES systems typically require complex machinery and engineered materials, with the result that their energy capacity costs are generally higher. Like PSH, GES is suitable for long-duration energy storage; given short response times and “black start” capability, such systems could also provide energy services and perhaps facilitate load shifting. Finally, GES systems can be modular, which can help avoid the large upfront capital costs that have handicapped PSH deployment in the United States and elsewhere. Although GES is unlikely to play a significant role in grid storage applications over the mid-century timeframe that is the focus of this study, some deployment of this technology may occur before 2050.

A multi-crane project, based in Switzerland and sponsored by a company called Energy Vault, is the most developed example of vertical GES technology (Energy Vault 2022). (For a description of another vertical dry GES system that raises and lowers masses in an underground shaft, see (Gravitricity 2022; reNews 2020).) In the Energy Vault project, electricity is used to

continued

Figure 3.4 A model of the Energy Vault technology



The left-most image shows the system in its fully charged state; the images to the right show various stages of discharge. (Source: Energy Vault)

Box 3.3 Other gravitational energy storage systems

power a multiheaded crane that stacks masses onto a taller, narrower primary tower; at times of high demand, electricity is generated by transferring masses from the primary tower to build a shorter, wider secondary tower (see Figure 3.4). According to one source, a full-scale 35-MWh demonstration plant is under construction in northern Italy (Kelly-Detwiler 2019). The plant will feature a primary tower that is 150 meters tall and uses about 6,000 35-metric-ton masses. Proponents claim that the technology has a roundtrip efficiency between 80% and 90%, an output power of 4–8 MW, and a cost of approximately \$7–\$8 million (Shieber 2018) with a discharge time of between 4 and 8 hours. These figures do not distinguish between energy and power capacity costs, but if we ignore the cost of the presumably inexpensive hoisted masses, they imply a power capacity cost of roughly \$875/kW.

Inclined GES systems can store energy on large scales (>1 GWh), but they have considerably larger land footprints than vertical systems or even PSH systems because the grades involved are on the order of 6%–7% (as compared to a vertical drop). Advanced rail energy storage (ARES) is an emerging concept that uses railway technology (Advanced Rail Energy Storage North America 2022). An ARES project with 50 MW capacity for ancillary services is now under construction in Pahrump, Nevada (Advanced Rail Energy Storage North America 2022). This project employs 210 cars weighing a total of 75,000 metric tons running on 10 tracks over about 8.9 kilometers with an elevation

continued

differential of 600 meters (6.7% grade), for a maximum energy capacity of 125 MWh and a discharge time of 2.5 hours at 50 MW. The Pahrump project is estimated to have a power cost of \$1,200/kW, comparable to PSH systems. A larger-scale installation with a power rating of 670 MW and an energy capacity of 5.3 GWh is proposed.

Another mechanical storage concept, called geomechanical pumped storage (GPS), employs electric energy to pump water from surface ponds to underground geological reservoirs where the water can be held in high-pressure storage “lenses” for long periods of time (Quidnet Energy 2022). When stored energy is needed, the water is released to drive hydroelectric turbines at the surface, returning electricity to the grid. In contrast to PSH, the turbines in a GPS facility are sited at the upper reservoir. This storage concept makes use of existing technologies and supply chains including hydroelectric turbines and drilling machinery. The surface footprint of GPS systems is less than that of PSH or GES systems and the technology offers greater siting flexibility than compressed air energy storage since suitable geological formations are more abundant (Burdick 2020). While these claims have not been verified, advocates quote a power capacity of 1–10 MW per well with a discharge storage of 10 hours or greater. Advocates also claim that capital costs for GPS systems could be less than 50% of PSH capital costs at \$10 per marginal kWh of energy storage capacity (Zhou 2020).

In diabatic CAES (D-CAES) systems, the heat of compression is expelled irreversibly to the environment and restored by gas combustion upon expansion. In adiabatic CAES (A-CAES) systems, the heat of compression is captured, stored separately from the compressed air, and returned during expansion.

CAES systems can also be distinguished based on whether they store compressed air above or below ground. In aboveground systems, the compressed air is stored in pressurized vessels made of materials such as steel or concrete. In underground systems, the compressed air is stored in existing geologic formations or in mined cavities.

In its simplest configuration, an A-CAES system consists of an air compressor, a storage chamber that holds the pressurized air, a thermal energy storage facility, and a turbine. In a D-CAES system, the thermal storage facility is replaced by a fuel combustion system.

A-CAES is a true energy storage technology; the efficiency of these systems is measured by dividing their electrical energy output by the electrical energy input. Ideally, an A-CAES system could function at a thermodynamic efficiency of 100%. Studies of A-CAES systems have estimated efficiencies on the order of 55%–65% based on simulations (Hartmann et al. 2012; Barbour, Pottie and Eames 2021). The energy density of the aboveground thermal storage of A-CAES is comparable to that of thermal energy storage (without compressed air), making the aboveground footprint of an A-CAES facility similar to that of a thermal energy storage facility (see Section 3.3.5). Based on the values that have been reported for A-CAES systems regarding low energy cost, moderate efficiency, and low self-discharge rate—and assuming that these values can be achieved in practice—A-CAES technology could be suitable for long-duration storage.

D-CAES systems are not emission-free if they are fueled by natural gas, as is typically proposed. Thus D-CAES does not qualify as an energy storage technology (by our definition), rather these types of systems provide a mechanism for using cheap electricity to enhance the power generation efficiency and lower the CO₂ emissions of a gas turbine. For this reason, we do not discuss D-CAES in detail in this report, though we do note, in a later section of this chapter (Section 3.3.7), that such systems may still merit investigation as an option for reducing emissions from otherwise stranded gas turbine generators or as the basis for an improved stand-alone gas turbine that uses carbon capture. In both cases, however, the volume of compressed air stored by the

D-CAES system would limit the duration of any performance improvements achieved by adding D-CAES.

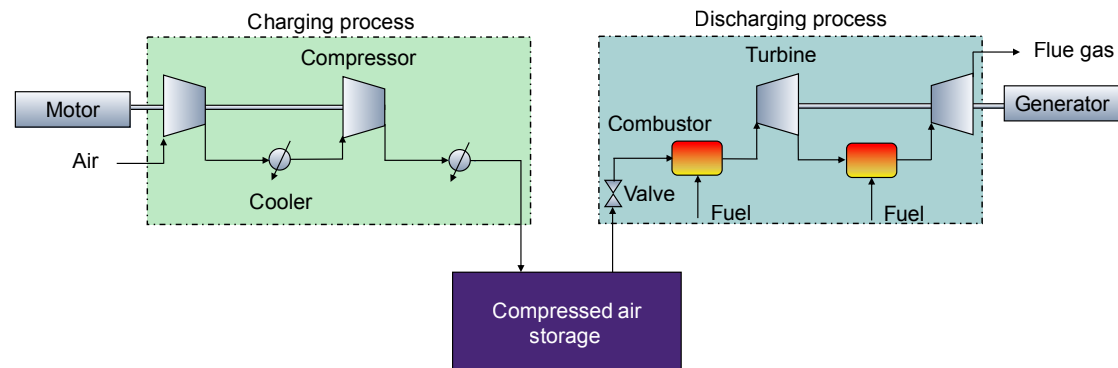
3.3.2 CAES development efforts to date

Storing energy by compressing air is an old idea that has been used in industrial settings since the 19th century. In industrial settings, compressed air was stored aboveground and was used to operate pneumatic equipment. Compressed air was first proposed as a grid-scale energy storage option in the 1940s (Gay 1948). It drew increased attention in the 1960s, prompted by interest in finding ways to store power from inflexible generators, such as large nuclear and coal-fired power plants, during periods of low demand (Budt et al. 2016; Donadei and Schneider 2016). D-CAES systems were the first options to be studied and two facilities of this type were commissioned: one in 1978 at Huntorf, Germany, and one in 1991 at McIntosh, Alabama.

The Huntorf plant, based on the flowsheet shown in Figure 3.5, has power and energy capacities of 321 MW and 640 MWh, respectively, and a discharge time of two hours. This plant stores compressed air in caverns with volume 310,000 cubic meters (m³) excavated in a salt dome and operates between minimum and maximum pressures of approximately 45 and 70 atmospheres (atm) respectively.

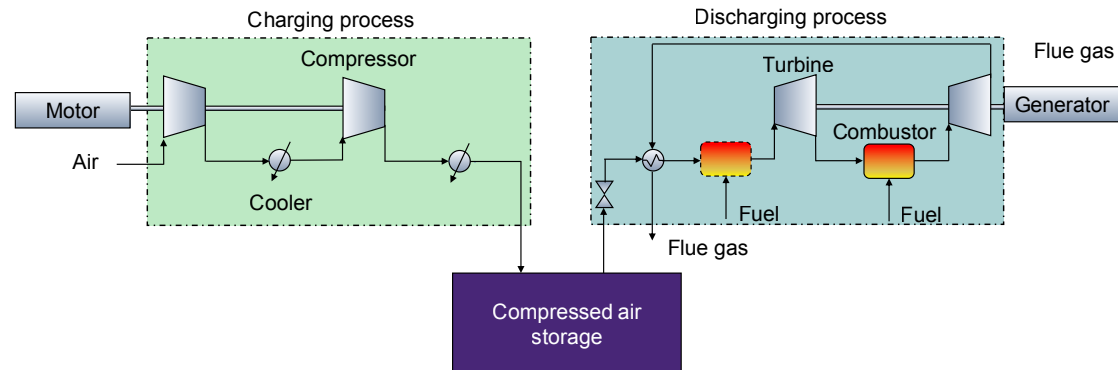
The McIntosh facility is based on a more advanced design (Figure 3.6); it has a power capacity of 110 MW, which is smaller than Huntorf, but a higher energy capacity of 2.86 GWh and a maximum discharge time of 26 hours. The compressed air is stored in a 270,000-m³ salt cavern and the system operates between approximately the same maximum and minimum pressures as the Huntorf plant. In both plants, natural gas combustion contributes significantly to energy capacity. At McIntosh, for example, for every unit of

Figure 3.5 Flowsheet of a conventional diabatic CAES system with two combustors



This figure describes the D-CAES plant at Huntorf, Germany.

Figure 3.6 Flowsheet of a diabatic CAES system with a recuperator



This figure describes the D-CAES plant at McIntosh, Alabama.

electrical energy taken from the grid, about 1.05 units of energy from natural gas are required to deliver 0.6 units of electricity back to the grid during discharge.

Though many D-CAES projects were proposed over the last three decades, all were subsequently abandoned; as a result, no D-CAES plants have been constructed since 1991.² In the United States, recently abandoned proposals include major projects sited in an abandoned

limestone mine in Norton, Ohio and another sited in sandstone aquifers near Des Moines, Iowa. Apex-CAES is pursuing development of a 324-MW, 16-GWh D-CAES facility near Bethel, Texas, but has not yet reached a final investment decision.

Some of the reasons for this lack of deployment activity are common to other storage technologies, including lower than expected deployment of nuclear power, increased adoption of

² For a brief historical overview, see Budt et al. (2016) and Donadei and Schneider (2016).

combined cycle power plants, and, more recently, lower natural gas prices. Other challenges are unique to grid-scale CAES including the need for large, typically geological, air-storage chambers with capacities on the order of tens of thousands to millions of cubic meters and the need to efficiently capture, store, and later return the large amounts of thermal energy that are generated when air is compressed.

At present, there are no active, grid-scale A-CAES facilities, though small-scale A-CAES facilities have been built. As with D-CAES, many projects have been proposed and then discontinued. This was the case for two highly visible recent initiatives: the Adele Advanced Adiabatic CAES project in Europe, which was proposed in 2012, and the Lightsail Energy project in the United States, which was launched in 2008. Both were cancelled within the past few years. On a more positive note, Hydrostor, a Canadian company, successfully commissioned a 1.75-MW (discharge), 15-MWh commercial A-CAES facility in Goderich, Canada in 2019 (Hydrostor). Hydrostor has also announced plans for a 500-MW project in Kern County, California, which, if completed, would represent the first grid-scale deployment of A-CAES. Hydrostor excavates caverns in hard rock to store the compressed air, which is maintained under constant pressure by means of a surface water reservoir. In addition, ALACAES, a Swiss company, successfully tested a 600-kW, 1-MWh A-CAES pilot plant using a mountain cavern in 2016 (ALACES). At least two A-CAES test facilities are currently operational in China. The larger of the two uses aboveground storage and has a capacity of 10 MW and 40 MWh (Tong, Cheng, and Tong 2021). Other A-CAES and liquid air energy storage facilities for testing and commercial uses are reported to be under construction in China (Tong, Cheng, and Tong 2021).

The only geological formations used for large-scale CAES storage to date have been salt domes, but bedded salt, hard rock caverns, and saline aquifers have also been studied for compressed air storage. Design constraints include the ability to maintain pressures on the order of 100 atm for hours to days and sufficient internal permeability to allow rapid discharge of the compressed air.³

Besides diabatic and adiabatic CAES, there is a third form of compressed air energy storage known as “isothermal CAES.” In this method, heat is continuously removed from the air as it is compressed (versus after each compression stage), so that the air temperature remains constant. The process is reversed for expansion. Isothermal compression and expansion processes are in principle more efficient than diabatic or adiabatic CAES, but it is difficult to achieve efficient and cost-effective isothermal processes in practice. Isothermal CAES has been the subject of some research and commercial development efforts, but no large-scale system of this type has yet been built (St. John 2015). This is in part because isothermal CAES does not address the key barriers to CAES deployment.

3.3.3 Outlook

Despite the fact that no grid-scale CAES facility has been deployed recently, the technology continues to attract interest. This is partly because CAES, in contrast to some other long-duration energy storage concepts, does not face fundamental technical challenges aside from identifying suitable underground sites for storing compressed air. Nonetheless, given the lack of progress, the future for CAES is unclear. Remaining sections of this chapter discuss mechanical and thermal requirements, cost estimates, and promising areas for technology improvement that could be relevant in

³ For further discussion, see Section 3.3.6.

determining whether CAES has a role to play in achieving a decarbonized electrical grid by 2050.

3.3.4 Basic principles of adiabatic CAES

When air is compressed adiabatically — meaning that the air is insulated from the environment during the compression process— it heats up. Thus, for example, if air initially at room temperature and pressure were compressed to 75 atm (a typical pressure for a CAES system), and if all the heat of compression were retained in the air, its temperature would reach approximately 750°C. This air has the capacity to do work because it is both hot and under pressure.

Storing hot, compressed air is impractical, however. One issue is that hot air occupies much more volume than the same mass of air at room temperature, increasing the cost of storage. Air at 750°C, for example, occupies about 3.4 times the volume of the same amount of air at the same pressure at room temperature. Furthermore, insulating a large volume of hot, pressurized air is difficult and expensive. For these reasons, a CAES system must remove the heat of compression so that the compressed air is left at a temperature close to that of the ambient environment. In an A-CAES system, a heat exchanger transfers this thermal energy to a thermal energy storage (TES) system.

In fact, all the work used to compress the air ends up as thermal energy. This stored heat together with the compressed air contribute to the useful work that can be recovered from storage. The capacity to do useful work is known as *exergy* in engineering thermodynamics. Technically, the exergy of a system equals the maximum useful work that can be extracted by

bringing the system into equilibrium with its environment. Exergy, also known as *available work*, is a very useful concept for the study of CAES.⁴

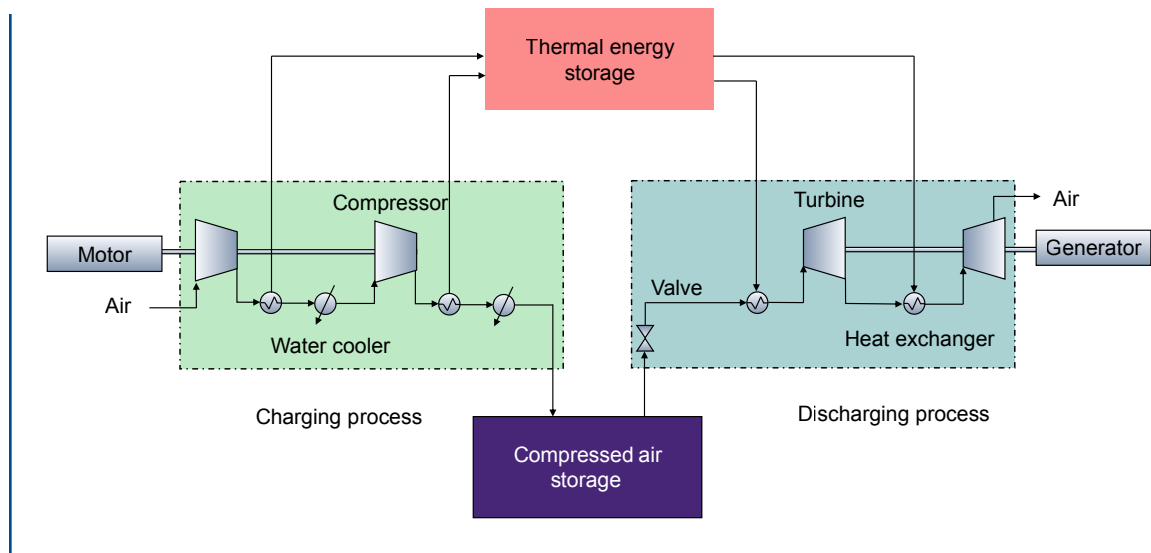
Storing the heat of compression requires an extensive TES system, comparable in size and complexity to a stand-alone TES system of the same capacity. In A-CAES systems, both the compressed air and the stored thermal energy contain exergy in different proportions depending on the pressure of the compressed air and the temperature of the TES system.

Figure 3.7 shows a schematic flowsheet for an A-CAES facility with two compression and two expansion stages. After each compression stage the air is cooled back down to near-ambient temperature by sending its thermal energy to thermal storage.

The thermodynamic constraints on a CAES system are illustrated in simplified form in Figure 3.8. Figure 3.8a shows the amount of available work or exergy stored in the compressed air (the blue area under the curve) and in the TES system (the red area under the curve), along with the temperature of the TES medium, assuming single-stage compression, for different compression ratios (r). Figure 3.8b shows the same information for a two-stage compression system, assuming that each stage compresses the air by a factor of the square root of the compression ratio r . These figures illustrate an ideal system with no losses. In a real system, inefficiencies would reduce the work available from both sources. For a single-stage system, roughly half the exergy is stored in the TES system; less exergy goes to TES in the case of a two-stage system. Both exergy

⁴ Exergy and energy should not be confused. Unlike energy, which is always conserved, inefficient processes diminish the useful work that can be obtained from the exergy of a system—these inefficiencies can be viewed as “destroying” exergy. Passing compressed air through a throttle, for example, lowers its pressure without doing any useful work and, in that sense, destroys exergy.

Figure 3.7 Flowsheet of a conventional adiabatic CAES system with two compression and two expansion stages



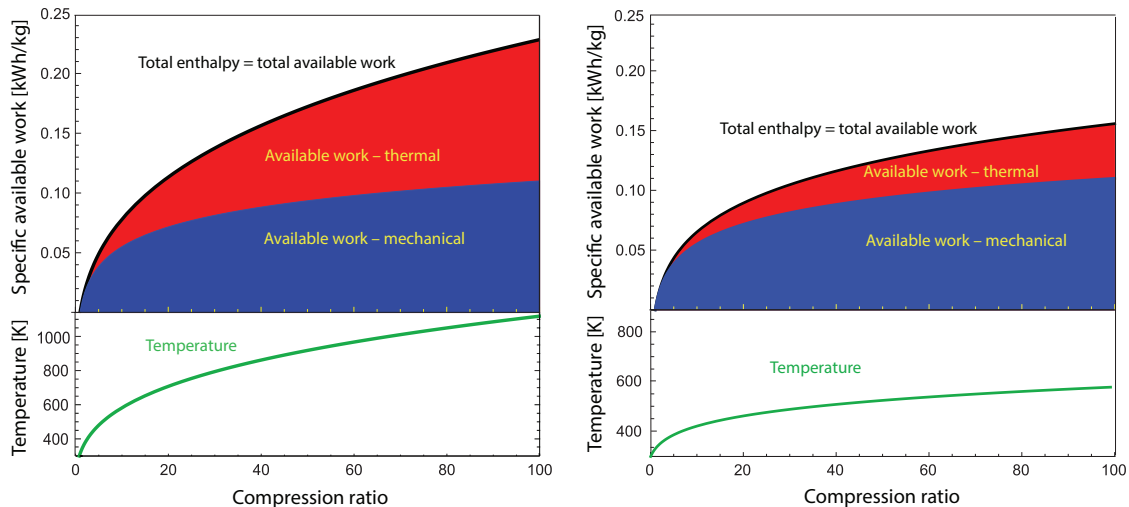
and energy are conserved in a lossless system, so in both cases shown in Figure 3.8, the work available from the compressed air and from the TES sum to the total amount of stored energy (the black curve), which in turn is equal to the electrical energy put into the A-CAES system.

In an ideal A-CAES system, the thermal energy of the air (shown in red) is extracted upon compression and then returned to the stored air upon expansion. The energy capacity of the TES system must be approximately the same, independent of the number of compression stages. This is because all the input energy is stored in the TES system, independent of the number of compression stages. Nevertheless, the work that can be extracted from the stored thermal energy decreases with the number of compression stages. This is because the greater the number of compression stages, the lower the temperature of the TES system, and thermodynamics dictates that a smaller fraction of this thermal energy can be extracted as useful work as the temperature of storage declines. Offsetting these losses, additional compression stages reduce demands on the compressors and allow for lower temperature in the TES system.

Many practical considerations require modifications to the mechanical and thermal energy dynamics of an A-CAES system. Most of these trade-offs depend on the details of the system such as choice of operating temperatures and pressures, choice of heat transfer and storage systems, and so on. Two important operational issues are quite general and deserve mention here.

First, expansion turbines are designed to operate at a fixed input pressure, whereas the pressure of air stored in a fixed volume drops continuously as the air is released. To accommodate turbine constraints, it is therefore necessary to throttle the air down to a fixed pressure as it exits storage. Throttling destroys exergy, so the throttling process reduces work output and therefore the efficiency of the overall CAES system. Second, the release of air must be stopped before the air pressure falls below the turbine's specified minimum input pressure. This leaves a significant amount of exergy unclaimed in the residual pressurized air. Both these effects reduce the energy capacity and efficiency of the CAES system and have prompted interest in constant pressure or

Figure 3.8 Mechanical and thermal exergy of compressed air



Mechanical (blue) and thermal (red) exergy ([kWh/kg]) of compressed air as a function of compression ratio for single-stage (left) and double-stage (right) compression. The sum of the two is the total stored specific enthalpy, shown in black. The temperature of the compressed air is shown in green.

isobaric CAES designs (as opposed to constant volume designs). Isobaric CAES is discussed further in the next section.⁵

3.3.5 Mechanical and thermal storage requirements

Grid-scale deployment of CAES depends on the availability of suitable, large-scale, underground air storage. The locations of such sites might not overlap with the preferred locations for energy storage. Furthermore, air storage might need to compete at some sites against the storage of other gases such as carbon dioxide and hydrogen.

Thermal storage requirements for a given plant configuration depend on the design of the compression and expansion processes. In a system with single-stage compression, about half the electrical energy is converted to

mechanical exergy, the other half is converted to thermal exergy as described in the previous section. As the number of compression stages increases, the temperature of the TES system decreases, but the total thermal energy in storage is always equal to the input electrical energy. In isothermal CAES systems, thermal energy is removed continuously from the air as it is compressed and expelled to the environment at the ambient temperature.

Air storage and geological siting

CAES with aboveground air storage

Given the need to store large volumes of air at high pressure, aboveground storage options such as tanks or pipelines are expensive for long-duration storage. Further, locating many pressurized tanks in close proximity introduces safety risks. One potentially feasible option for

⁵ Excellent reviews detailing the thermodynamics of CAES systems are available in the literature. See, for example, Budt et al. (2016), and Garvey and Pimm (2016).

longer-duration, aboveground storage is liquid air energy storage, which is discussed separately in Section 3.3.7.

For shorter-duration applications, CAES would compete with electrochemical storage technologies, such as lithium-ion and flow batteries, and other grid-balancing strategies, such as demand management. A new-build CAES plant would have power costs about two to three times higher than lithium-ion batteries, which currently represent the leading short-duration storage technology (Table 6.3 summarizes costs). If CAES power costs can be reduced to comparable levels, potentially by repurposing gas turbines as discussed later in this chapter, energy costs for CAES would need to be lower than for batteries (battery energy costs are about \$250/kWh_e). According to the literature on pressure vessels and aboveground D-CAES, air storage costs in the range of \$50–\$200 per kWh_e are achievable, although costs in this range have not yet been demonstrated in practice (Cárdenas et al. 2019; Thompson 2016). Additional costs are incurred for thermal storage.

Even if aboveground CAES systems can achieve power and energy costs that are competitive with other grid-balancing options, other considerations such as efficiency, siting flexibility, response time, and modularity would favor electrochemical storage technologies or demand management. In regard to siting flexibility, Figure 3.9 illustrates the typical range of energy densities for CAES systems (Budt et al. 2016; He, Dooner, et al. 2021); energy densities for pumped storage hydropower and lithium-ion batteries are shown for comparison. As an example, a 4-hour, 100-MW CAES system with an energy density of 10 kWh_e/m³ would require air storage capacity of approximately 40,000 m³, about equivalent to the

volume of 16 Olympic-sized swimming pools.⁶ An equivalent lithium-ion storage system would occupy 30 to 65 times less space.

For these reasons, CAES with aboveground air storage is generally not favorable for short- or long-duration storage. Aboveground liquid air storage, discussed later in this chapter (Section 3.3.7) may be an exception.

CAES with underground air storage

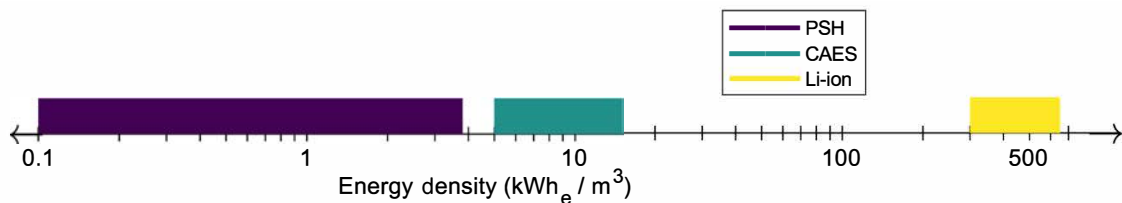
For underground storage, the commonly studied geological options are domal or bedded salt caverns, aquifers, depleted oil and gas wells, and hard rock mines. Figure 3.10 illustrates each option.

Domal and bedded salt storage caverns are created using solution mining. This process starts with drilling a hole into the salt formation, then pumping water underground to dissolve the salt. The saturated brine is removed for waste disposal. The shape of the dome is controlled with a layer of oil to prevent dissolution of the cavern ceiling. Solution mining is a well-developed process that is used to create caverns for storing natural gas and waste. In the United States, suitable salt formations are concentrated around the Gulf Coast, the eastern half of the Great Lakes region, and in pockets of the Great Plains.

Aquifers and depleted oil and gas wells are generally used “as found,” compared to other air storage options that involve mining operations. During first time setup at aquifers, air is injected to adjust the water level (Medeiros et al. 2018). For oil and gas wells, setup may involve flushing out residual hydrocarbon liquids and gases. Otherwise, residual hydrocarbons that are not removed before the well is used for CAES could mix into the stored air

⁶ The volume of air storage is much greater than the volume of thermal storage. Therefore, air volume is the main factor in the energy density of CAES.

Figure 3.9 Typical ranges of energy density



Typical ranges of energy density, on a logarithmic scale, for pumped storage hydropower systems with heads of approximately 50 to 1,400 meters, CAES, and Li-ion batteries.

and be released when the air is extracted, contributing to greenhouse gas emissions.

Hard rock caverns left behind from mining operations can be suitable for air storage. In some cases, mine sections may have to be sealed off to prevent leakage. This type of geology is attractive for compressed air storage, but suitable sites are limited. New caverns can be created using standard mining methods, although the cost may be prohibitively high unless there is value in the mined material.

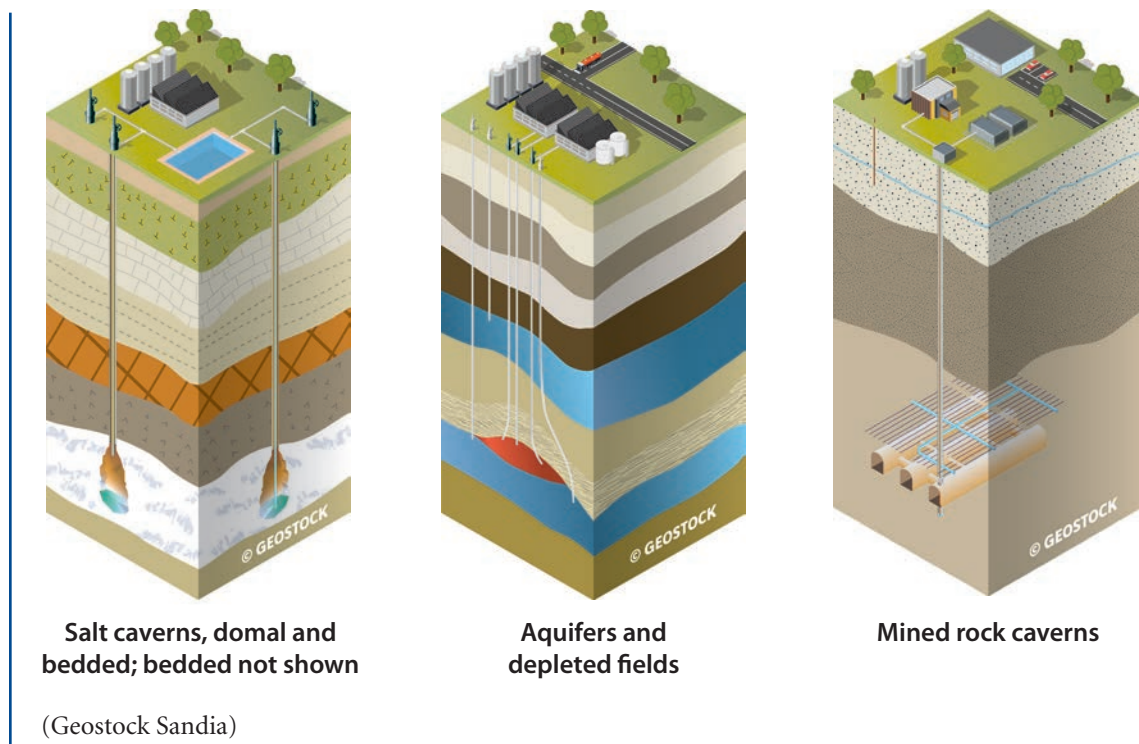
Note that salt and hard rock caverns can be sized to hold the volume of compressed air needed to deliver a specified energy capacity (via solution or rock mining). On the other hand, the maximum volume of aquifers and depleted oil and gas wells is fixed by geology. If the desired energy capacity exceeds the available volume, adjacent formations must be identified and developed.

Several metrics are used to compare underground formations. The first one is the capital cost to evaluate and develop a site. This amount includes the cost to drill rock samples and test wells, apply for permits, conduct seismic testing, and test injections, among other steps. Most of the cost relates to energy capacity although some costs, such as the drilling of injection/extraction wells, relates to the rate of

air flow and thus to the system's power capacity. Other metrics are the minimum and maximum pressures of the stored air. A minimum pressure is needed to maintain the structural integrity of the underground formation and to match the minimum turbine input pressure. The gas that maintains this pressure is called cushion gas, which is injected but never extracted. The minimum pressure is set either by considerations of structural integrity or by the designed inlet pressure of the first expander, whichever is greater. Maximum pressure is set by the physical properties of the underground formation.

Other metrics are porosity and permeability. Porosity is a measure of the empty space in a material. Permeability is a measure of how easily a fluid can flow through a material. A material can be porous without being permeable. Aquifers and depleted wells are filled with rocks of various shapes and sizes, leaving room for air in the voids between them and in the accessible pores of the rocks themselves. Low porosity means less volume for air. Low permeability means higher pressure losses when injecting or withdrawing air. The air-flow rate (and thus power) can be reduced to minimize pressure losses or additional injection/extraction wells can be added. Salt formations and hard rock caverns are almost entirely empty, so losses are lower when injecting or extracting air.

Figure 3.10 Illustrations of underground formations to store compressed air



Another consideration for injection and extraction rates is the structural integrity of the underground formation used to hold the air. This affects cycling frequency and thus can restrict the operational profile of a CAES plant.

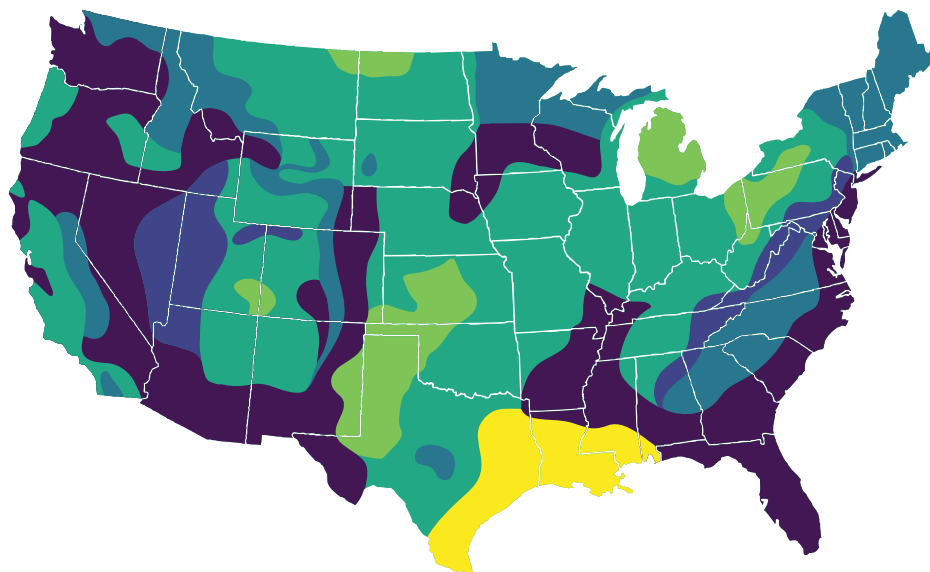
The self-discharge rate of the storage site, which is air leakage through the surrounding earth, is also important. Often, the permeability of the overlying rock is distinct from the permeability of the geologic layer where the compressed air resides. For salt formations and hard rock caverns, leakage rates can be quite low. For other underground air storage options, leakage rates are site dependent. In any case, the primary factor in a plant's self-discharge rate will likely be the thermal storage.

The literature suggests that much of the United States has favorable geology for CAES, as seen in Figure 3.11 (Barnes and Levine 2011). The literature also finds favorable geology in other countries (Aghahosseini and Breyer 2018; King

et al. 2021). Regional analyses are often done at the macro scale, however, whereas technical and economic feasibility must be assessed at specific locations.

The most favorable type of storage for compressed air is a salt cavern because salt caverns entail lower development risks, minimize internal pressure losses, and are compatible with frequent cycling. However, CAES will have to compete with other current and future uses for salt caverns: such caverns are used today to store natural gas and waste and could be used in the future to store hydrogen and possibly captured carbon dioxide. Hydrogen, in particular, presents storage challenges because it is a small molecule that can diffuse easily through many materials and can be chemically and biologically reactive. Salt caverns have so far been the preferred choice for underground hydrogen storage, since other forms of storage are more susceptible to leakage and salt has low reactivity with hydrogen (Zivar, Kumar and

Figure 3.11 Regions of the United States favorable for CAES



- Salt domes — most favorable for solution cavities
- Salt beds — favorable for solution or mined cavities
- Sedimentary — favorable for mined cavities and injection in porous rocks
- Granitic, plutonic — favorable for cavities in hard rock
- Sedimentary — injection in porous rocks limited to favorable structure
- Volcanic and sedimentary — not favorable

This map commissioned for underground petroleum storage, shows regions of the United States that are favorable for CAES (Barnes and Levine 2011).

Forozesh 2020). CAES has approximately ten times lower energy density than chemical energy storage, and chemical energy storage is not limited to electricity generation since hydrogen and other molecules can be used as feedstocks for chemical processes (Ozarslan 2012). Thus, if the supply of salt caverns available for storage applications is geologically limited, chemical energy (i.e., hydrogen) storage would be the higher-value and therefore preferred choice rather than CAES.

Porous geological media, which include aquifers and depleted wells, have also been used to store natural gas, but these facilities are cycled seasonally rather than daily or weekly as might be expected for CAES. Low cycling frequency

for natural gas storage is economical because of the high energy density of chemical bonds. For CAES systems, which rely on mechanical exergy, more frequent cycling may be possible, depending on site conditions. Hydraulic fracturing for CAES might be used to improve permeability, but very little research has been published in this area.

An attempt was made between 2009 and 2016 to develop an abandoned natural gas reservoir for a D-CAES project, but the effort did not proceed beyond the request-for-proposals stage because the project proved economically uncompetitive with alternative storage bids. While A-CAES could mitigate some of the technical issues that made this project

uncompetitive, removing residual methane from the reservoir without significant emissions would have been a remaining challenge.

A recent paper by Guo et al. provides a good review of CAES with aquifers (2021). It discusses relevant analytical studies and summarizes results from an aquifer-based plant in Iowa that was proposed in 2003 and from field testing of an aquifer in Illinois during the early 1980s. Guo et al. conclude that a main challenge is the geological heterogeneity of aquifers and the need for better modeling and characterization methods to accurately assess a given aquifer's suitability for CAES. Under the right conditions, a porous medium could have cost and performance characteristics that could make it viable for underground air storage.

Unless information is available from prior studies, site-specific data must be collected for any underground storage option to determine feasibility. This requires hundreds of thousands to millions of dollars in upfront investment depending on the analyses required (Holst et al. 2012; Medeiros et al. 2018). While there is no guarantee of feasibility for any of the underground storage options, there will be greater uncertainty about the suitability of porous media storage sites.

Overall, the most favorable options for compressed air storage are salt caverns and abandoned hard rock mines. Both are in demand for competing uses, such as for chemical energy storage, and both are limited in supply. For porous media, suitability depends on site-specific conditions and on ensuring that resulting energy capacity costs and effects on efficiency are acceptable. Historically, some attempts to develop CAES projects in the United States have underestimated siting challenges. Looking ahead, more research on the challenge of identifying suitable

underground storage sites would be needed to assess whether CAES could have a meaningful role in grid-scale energy storage.

Thermal energy storage capacity requirements

As described in Section 3.3.4, A-CAES systems require that the thermal energy generated in compression be stored and later restored during expansion of the compressed air. Given the high pressures and temperatures involved, using a pressurized vessel for thermal storage is impractical. As a result, heat exchange is necessary—potentially using an intermediate heat transfer fluid between the air and thermal storage. Temperatures of 300°C–400°C are typical of proposed A-CAES systems. These temperatures are lower than those encountered in the systems covered in Chapter 4 on thermal energy storage. Still, the overall design process is the same, with flexibility to make different choices about thermal storage material, insulation, containment, heat exchanger, etc. The key difference is that lower temperatures allow for the use of cheaper materials—for storage and throughout the system—so that thermal energy storage costs (\$/kWh_{th}) can be lower.

Although there is some latent heat associated with water condensation due to ambient humidity, air intercooling is predominantly the removal of sensible heat from air.⁷ While thermal storage using latent heat or combined sensible and latent heat is possible, it is likely most cost-effective to use sensible heat storage to recover as much thermal energy as possible from compressed air. A maximum temperature of 400°C is comparable to the temperatures found in parabolic trough designs for concentrated solar power stations that use thermal oil. Although thermal oil may be a suitable heat transfer fluid, it would not be the cheapest option for energy storage. Other options are thermoclines or solid storage using materials

⁷ Chapter 4 provides additional information on sensible and latent heat.

Box 3.4 Isochoric or isobaric compressed air storage

In isochoric storage, the volume of compressed air stays constant while the pressure changes.

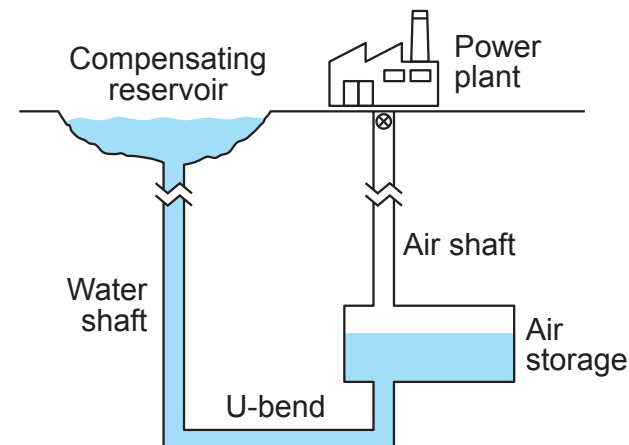
The McIntosh and Huntorf plants both use isochoric storage in salt caverns.

Isobaric storage systems use a fluid, such as water, to maintain the compressed air at a constant pressure. This fluid can be stored in a pool on the surface so that the hydrostatic pressure equals the pressure of the compressed air in the underground formation. On discharge, the fluid replaces the volume previously occupied by air, so a cushion gas is not required, although the minimum storage pressure is still constrained by the turbine's required input pressure. Because isobaric storage designs can maintain constant high pressure, they reduce the need for throttling. Thus, isobaric storage systems can achieve exergy densities two to three times greater than isochoric storage

systems (Garvey and Pimm 2016; He, Luo, et al. 2017).

While isobaric storage can provide higher energy densities, the choice of pressure-compensating fluid has practical constraints. In a salt formation, salt would dissolve in the water, creating a saturated brine that would be corrosive to pipes and power equipment. Protective coatings could mitigate corrosion at additional cost. Another method of mitigation could be to use a thin layer of oil to reduce evaporation of brine into the compressed air (Giramonti and Smith 1983). Alternatively, fluids other than water could be used but they would have to be cheap and non-toxic since they would be needed in large quantities. For these reasons, isobaric storage is often suggested for proposed projects that use hard rock caverns.

Figure 3.12 Surface reservoir provides pressure to enable air extraction at constant pressure



(Giramonti and Smith 1983)

such as recycled concrete or scrap metal. Solid storage systems could use indirect or direct contact heat exchange with the heat transfer fluid, subject to the compatibility of the two materials.

3.3.6 Cost estimates

Since no large-scale A-CAES systems have been built, cost estimates must be developed from reports and the academic literature. Many of these sources, however, provide estimates for D-CAES systems or do not specify whether the system is diabatic or adiabatic. A further issue is that among available papers and reports, several rely on the same few sources. As a result, older cost estimates have propagated to the more recent literature, often without clear justification. This introduces uncertainties as to the true versus reported costs of CAES.

Nonetheless, estimates for high, middle, and low costs can be developed and compared against reported numbers. For example, cost information for gas turbines and thermal energy storage systems can be used to estimate reference costs for CAES power and energy capacity, respectively. Because the aboveground power components of a CAES system, such as compressors, expanders, and heat exchangers, are technologically mature, their costs for a given plant design can be estimated by engineering firms. Costs for low- and medium-temperature thermal storage can be estimated with some accuracy using data from concentrated solar power applications. Costs for higher-temperature storage (above 600°C) are more uncertain; some estimates are available in Chapter 4. Most of the remaining uncertainty around CAES costs comes from uncertainty about the cost of air storage.

For purposes of this report, we identified five sources that together provide a total of six cost estimates for A-CAES systems (Guerra et al. 2020; Huang et al. 2017; NYSERDA 2009;

Gallo et al. 2016; International Energy Agency 2015). Gallo et al. (2016) provide high- and low-cost cases; we include both in this analysis. Another study, by Guerra et al. (2020) presents minimum, baseline, and maximum costs—in that case we included in our analysis only the baseline estimates because the underlying paper is focused on modeling the system effects of long-duration storage technologies and does not focus on CAES in particular.

Costs were adjusted for inflation from the year specified to 2020 using the consumer price index. If the year was not specified, the date of publication was used. In addition, some sources assumed roundtrip efficiencies higher than what is likely to be achievable in practice (e.g., 75% vs. 55%–65%) and did not disaggregate roundtrip efficiency into charge and discharge efficiencies (Yu, Engelkemier and Gençer 2022). Based on our calculations, charge and discharge efficiencies have similar values. Therefore, as a simple approximation, the square root of the reported round trip efficiency was used to approximate charge and discharge efficiencies. To normalize our cost estimates, we multiplied the quoted energy cost by the ratio of approximated discharge efficiency to the discharge efficiency from our simulations. Where reported efficiencies are higher than our estimates, this approach increases energy cost. Similarly, we multiplied power costs by the ratio of reported roundtrip efficiency to roundtrip efficiency from our simulations (59%) (Yu, Engelkemier and Gençer 2022). After adjusting for inflation and efficiency, we then averaged the six estimates to arrive at a single estimate for power and energy costs in 2020.

Most references report power costs as a single value, but the charge and discharge power components can be sized independently. Therefore, it was necessary to attribute some fraction of “total” power cost to charging and the remainder to discharging. For an ideal

A-CAES system, the charging and discharging systems would be symmetric, so a 50/50 split would be expected. Of our five sources, two disaggregated power costs. One assumed a 40/60 split for charging and discharging; the other assumed a 55/45 split. In an actual system, the charging side is at a higher temperature and pressure, so charging power cost should be slightly higher. In this report, we disaggregate power costs using a 55/45 split.

We use our estimates of 2020 cost to project costs for 2050 by applying cost-reduction assumptions from references that provide cost estimates for the near-present and 2050. The fact that no A-CAES plant has been built creates additional uncertainty here. Based on our review of the literature, we assume that power costs could decline by 0%, 8%, and 24% from 2020 to 2050 in the high-, medium-, and low-cost scenarios, respectively. For context, the 2020 Annual Technology Baseline (ATB) published by the U.S. National Renewable Energy Laboratory projects that capital costs for gas turbines will decline by 14% between 2020 and 2050. Although the ATB does not explain the basis for these assumptions, design and manufacturing improvements to turbo-machinery and other gas turbine components would generally be applicable to CAES as well. We likewise use values from the literature as the basis for our assumption that energy costs could decline by 0%, 11%, and 50% between 2020 and 2050 for high-, medium-, and low-cost scenarios, respectively. Our low-energy-cost scenario reflects the potential for improvements in siting and developing air storage facilities, along with cost declines in thermal storage. Table 3.4 summarizes our estimates for 2020 and 2050 cost and efficiency values.

Given limited cost data, we do not estimate fixed and variable O&M costs for the charge, discharge, and energy components of an A-CAES system. This is one reason that we excluded A-CAES from the capacity expansion

modeling analysis discussed in Chapter 6 of this report. However, A-CAES costs can be compared to those of other modeled storage options to infer the technology's potential role. On the axes of capital cost of power versus energy (Figure 6.7), A-CAES could function as a long-duration storage option if it can achieve similarly low energy costs. Otherwise, A-CAES will not be competitive for long- or short-duration storage.

3.3.7 Potential for CAES technology improvement

This section briefly describes a few technology concepts that could be used to improve CAES performance or cost. This discussion focuses primarily on concepts that could be relevant in situations where suitable underground storage sites can be identified. Only liquid air energy storage meaningfully addresses the problems with aboveground air storage. We begin by discussing two concepts that could be applied to both adiabatic and diabatic CAES systems (i.e., bypass turbines and reuse of gas turbines); we then discuss liquid air storage before going on to other concepts that would be specific to either adiabatic or diabatic systems.

Bypass turbines

The requirement to throttle air down to the input pressure of the first turbine during discharge, as shown in Figure 3.7, significantly reduces the discharge efficiency of a CAES system. This efficiency loss can be reduced with a variable pressure throttle. During discharge, the throttle regulates the air to two pressure levels in sequence, and both turbines can be maintained at constant operating conditions. At the beginning of the discharging process, the compressed air is throttled to match the high-pressure turbine inlet; it then passes through both turbines in series. When the cavern pressure falls below the pressure required at the first turbine inlet, the

Table 3.4 Cost assumptions for A-CAES in 2020 and 2050

| Variable | Units | 2020 | 2050 | | |
|------------------------|------------------------|-----------|------|-------|-----|
| | | Reference | High | Mid | Low |
| Charging power cost | \$/kW _e | 452 | 452 | 418 | 344 |
| Discharging power cost | \$/kW _e | 617 | 617 | 570 | 469 |
| Energy storage cost | \$/kWh _{CAES} | 42 | 42 | 38 | 21 |
| Efficiency, charge | | | | 74% | |
| Efficiency, discharge | | | | 79.5% | |

The energy storage cost includes compressed air and thermal storage costs. It can be converted to electrical energy cost (in units of \$/kWh_e) by dividing by the discharge efficiency.

compressed air bypasses the first turbine and is throttled to match the second turbine's inlet pressure. Reducing exergy losses through the throttling valve enhances the discharge efficiency of the system.

Reuse of gas turbines

One cost-cutting approach that has been proposed involves reusing stranded gas turbines to reduce the cost of CAES charge and discharge power (Nakhamkin 2010). To complete the CAES system, however, other components are still needed to perform functions such as heat exchange, thermal storage, and air storage.

Significant modifications are required to reuse existing gas turbines. These units contain integrated compressor and turbine stages. Some of the motive power generated during expansion drives the compression stage while the remaining motive power is used to generate electricity. This mode of operation requires compression and expansion to occur at the same time. For CAES operation, however, the compression (charge) and expansion (discharge) steps must be decoupled. One approach to deal with this design difference is to decouple the compressor and expander by adding a clutch mechanism to the gas turbine unit. Another approach is to use one half of the gas turbine by removing blades from the compressor and adding a bypass to use just the

expansion section, and vice versa. With this modification, two gas turbines are needed to create a compressor and expander pair.

An additional consideration is that gas turbines are designed to operate with specific pressure ratios and within a maximum pressure limit, so they could only be reused for the low-pressure compression and expansion stages. An additional challenge with this retrofit approach is that the location of existing turbines may not coincide with sites where underground air storage is available. Alternatively, there would be costs to relocating gas turbines. Given these issues, repurposing retired gas turbines seems unlikely to be an attractive option.

Liquid air energy storage

A liquid air energy storage (LAES) system charges by compressing air to high pressure, similar to an A-CAES system, but the air is then cooled before its pressure is reduced to near-ambient levels. The pressure reduction can cool air to temperatures around -196°C where some of the air becomes liquid. (Air is a mixture of gases; its dominant component is nitrogen, which liquefies at -195.8°C .) The air that does not become liquid remains as a cold gas at ambient pressure; this air goes through a heat exchanger to cool the high-pressure, ambient-temperature gas. To generate electricity, the liquid air can be pumped to high pressure,

heated back to a gas, and then run through one or more turbines, using a simple Brayton cycle or a derivative. Other methods have been proposed that use a Rankine cycle. In either approach, the heat from compression is stored so that it can be used during discharge, as with A-CAES. The ability to recover cold thermal energy during discharge and use that energy for the next charging cycle is unique to LAES.

Charge and discharge power capacity for LAES systems can be sized independently, as in CAES. Unlike CAES, however, LAES offers siting flexibility since all components are above ground. Liquid air has an estimated energy density around 95 kWh/m³, which is about 10–20 times the energy density of CAES. This greatly reduces the challenges associated with aboveground storage (Guizzi et al. 2015). Energy storage capacity for LAES systems scales with the size of their cryogenic tanks and hot and cold thermal stores. Gas liquefaction, using either the Hampson-Linde cycle, the Claude cycle, or another cycle, is a mature process that is already in use for industrial gas supply, natural gas liquefaction, and other applications. Compared to other liquefaction processes, the novelty in a LAES system lies in recycling the hot and cold thermal energy, which is key to increasing roundtrip efficiencies of approximately 50%–60% (Borri et al. 2021). In non-LAES gas liquefaction plants, heat recovery from compression and expansion is not possible because the gas is typically exported. Integration with waste heat from a nearby source can further improve the efficiency of LAES systems.

For LAES, technological maturity is not the primary concern, although gas liquefaction facilities do require advanced industrial capabilities and skilled labor. The key questions center on cost and efficiency. Given limited development to date, reliable cost estimates

are not currently available. Small-scale plants (300 kW/2.5 MWh and 5 MW/15 MWh) have been built, and plans for larger facilities have been announced (Borri et al. 2021).

Adiabatic CAES with resistively heated thermal storage

For a typical adiabatic system, the temperature of thermal storage depends on the pressure ratio of the compressors and on the decision to employ intercooling (or not). Resistive heating can be used to increase the temperature of thermal storage. Higher temperatures increase discharge efficiency and energy capacity for a given volume of stored air. Additionally, higher temperatures increase design flexibility with respect to the compression stages.

Since resistive heating introduces additional energy beyond the energy used for compression, systems that have this feature are no longer adiabatic, by definition. They still qualify as a form of electricity storage because only electricity enters and leaves the plant. In the literature, these systems are described as “combined heat and compressed air energy storage” or “hybrid thermal-CAES” (Houssainy, Janbozorgi and Kavehpour 2018).

A thermal storage system can be designed to meet the maximum allowable temperature for each expansion stage. For the high-pressure turbine, maximum temperature is constrained by material limits. For the final expansion stage, allowable turbine inlet temperatures can be as high as those for open Brayton turbines, which are around 1,400°C, although materials in the heat exchanger could enforce a lower limit. With resistive heating, the thermal storage component for a CAES plant could resemble the thermal energy storage systems described in Chapter 4.

Diabatic CAES for grid decarbonization

Although D-CAES is not a focus of this chapter, there may be a role for the technology when looking at the bigger challenge of decarbonizing the overall power system. As the modeling analysis discussed in Chapter 6 of this report shows, dispatchable generation resources such as gas turbines with carbon capture and sequestration (at an approximately 90% carbon capture rate) are deployed even in highly carbon constrained scenarios. D-CAES systems paired with carbon capture and sequestration (CCS) can be viewed as analogous to gas turbines with CCS. The difference is that D-CAES systems can use low-carbon electricity to compress air ahead of time, increasing fuel efficiency during discharge. When the stored air is depleted, a D-CAES plant can switch modes to operate the compressor and expansion train simultaneously, like a gas turbine (McCafferty 1980). Alternatively, hydrogen can be used instead of natural gas to eliminate the need for on-site CCS. For more technical detail and an example of a D-CAES system suited for CCS, see Zeynalian et al. (2020).

3.3.8 Summary findings and recommendations related to compressed air energy storage

Despite decades-long interest in adiabatic CAES and experience from two operational D-CAES plants, this energy storage technology has not found recent success. Aboveground CAES has been the subject of some research, but we believe that it is impractical. CAES with underground air storage does not present major technical challenges with respect to its aboveground components—rather the challenge is finding and developing suitable underground sites to store compressed air.

Caverns in salt domes, bedded salt, and hard rock are attractive options for underground air storage. However, chemical energy (e.g., hydrogen) storage is a competing use for these

geological features that may be more economical given its higher energy density. Studies indicate that porous media, such as aquifers and depleted oil and gas wells, are usable for CAES, but these options have not been demonstrated yet.

A-CAES is generally suited for long-duration storage, where low energy cost is a key metric. Key cost drivers for these systems are the siting process, the development of air storage facilities, and thermal storage equipment. Although cost estimates for CAES are subject to multiple uncertainties, estimates of energy cost for this technology are generally higher than estimates for other energy storage technologies that are expected to be available in the future. Power costs for CAES are not expected to decline significantly.

Potential opportunities to increase efficiency and lower power costs include incorporating a bypass turbine, reusing existing gas turbines, and applying resistive heating to the thermal storage component. However, none of these options addresses the critical issue of developing adequate underground air storage. Liquid air storage does solve the air storage problem, so it may offer a promising path forward. Given the early stage of development of liquid air systems, however, more data on performance and cost are needed to assess whether liquid air could be a competitive storage technology.

Ultimately, deployment of A-CAES with underground storage seems viable, and in some regions with favorable geological resources it may play a non-trivial role in the future. However, geological constraints and limited cost reduction potential would appear to make CAES less competitive over time as other long-duration storage technologies mature. Unless liquid air energy storage proves a major exception, we believe CAES is unlikely to play a significant role in grid-scale storage—in the United States or globally.

3.4 Conclusion and key takeaways

This chapter focuses on the two most widely discussed forms of mechanical energy storage: pumped storage hydropower (PSH) and compressed air energy storage (CAES). These forms of storage have little in common from a technology or implementation standpoint, but they do share the common attribute of low energy density relative to other technologies such as chemical and electrochemical storage. Consequently, PSH and CAES facilities have large footprints, must be sited in geologically favorable locations, and do not lend themselves to modularity.

Pumped storage hydropower

- Pumped storage hydropower is by far the dominant electricity storage technology in the United States and globally in terms of both installed power and energy capacity.
- Utilization of PSH has been declining; in several countries, including the United States, an increased reliance on low-cost, flexible natural gas generation has reduced intraday electricity price arbitrage opportunities.
- Expanded deployment of PSH still faces formidable hurdles due to a current lack of demand for its services and uncertain prospects for future demand, though this could change with increasing reliance on VRE generation. Recent, massive PSH investment in China is enabled by unique institutional and regulatory conditions that will be difficult, if not impossible, to replicate elsewhere.
- Fully optimizing existing PSH plants to take advantage of organized wholesale markets could more than triple the market revenues these plants currently generate.

In addition, few other energy storage technologies, if any, have demonstrated capital appreciation potential that can significantly offset or exceed their inflation-adjusted acquisition cost.

- Nonetheless, a viable business model for new PSH in competitive electricity markets has not yet been demonstrated. Resulting uncertainty and financial risk—not siting—thus remain the main barriers to PSH deployment in the United States.
- Establishing plausible timetables for power sector decarbonization and developing competitive mechanisms that would support offtake agreements for services from PSH and other storage projects would help address these barriers.
- Meanwhile, the U.S. government should consider further steps to extend the life of PSH licenses and privatize federally owned PSH stations to incentivize efficient utilization. At the same time, the electric power industry and financial institutions should continue efforts to develop new business models and financing strategies for PSH projects.

Compressed air energy storage

- Using compressed air for grid-scale energy storage is an old idea, but only two projects to demonstrate this concept have been built (both are diabatic systems, meaning that the heat of compression is expelled irreversibly to the environment and restored by gas combustion upon expansion). Other CAES projects (including adiabatic systems in which the heat of compression is captured, stored separately from the compressed air, and returned during expansion) have been proposed but none have been built.

- CAES systems can also be distinguished based on whether they store compressed air above or below ground. Because of inherent problems with aboveground air storage, grid-scale deployment of CAES depends on the availability of suitable, large-scale, underground air storage.
- Even if aboveground CAES systems can achieve power and energy costs that are competitive with other grid-balancing options, other considerations such as efficiency, siting flexibility, response time, and modularity would favor electrochemical storage technologies or demand management. For these reasons, CAES with aboveground air storage is generally not favorable for short- or long-duration storage.
- Only liquid air energy storage meaningfully addresses the problems with aboveground air storage.
- Regional analyses of potential underground air storage sites are often done at the macro scale, but technical and economic feasibility must be assessed at specific locations.
- If the supply of salt caverns available for storage applications is geologically limited, chemical energy (i.e., hydrogen) storage would be the higher-value and therefore preferred choice rather than CAES.
- More research on the challenge of identifying suitable underground air storage sites would be needed to assess whether CAES could have a meaningful role in grid-scale energy storage.
- A-CAES could function as a long-duration storage option if it can achieve energy costs comparable to other long-duration options.
- Ultimately, adiabatic CAES with underground air storage seems viable, and in some regions with favorable geological resources it may play a non-trivial role in the future. However, geological constraints and limited cost reduction potential seem likely to make CAES less competitive over time as other long-duration storage technologies mature. Unless liquid air energy storage proves a major exception, CAES is unlikely to play a significant role in grid-scale energy storage, in the United States or globally.

References

- Abu-Khashaba, Mohamed I., and Adam A El-Ashaai. 2014. "Investigating the possibility of constructing low cost roller compacted concrete dam." *Alexandria Engineering Journal* 53 (1): 131-142. <https://doi.org/10.1016/j.aej.2013.11.009>.
- Aghahosseini, Arman, and Christian Breyer. 2018. "Assessment of Geological Resource Potential for Compressed Air Energy Storage in Global Electricity Supply." *Energy Conversion and Management* 169 (August): 161–73. <https://doi.org/10.1016/j.enconman.2018.05.058>.
- ALACES. n.d. ALACES. Accessed June 27, 2021. <https://alacaes.com>.
- Advanced Rail Energy Storage North America. n.d. "ARES Nevada 50 MW Regulation Energy Management Storage System." *ARES North America*. Accessed February 1, 2022. https://s3.amazonaws.com/siteninja/multitenant/assets/21126/files/original/ARES_Nevada_Technical_Specification_Sheet.pdf.
- . 2022. *ARES North America*. <https://aresnorthamerica.com/>.
- Australian National University. 2019. *Global Pumped Hydro Atlas*.
- Barbour, Edward, Daniel L Pottie, and Philip Eames. 2021. "Why Is Adiabatic Compressed Air Energy Storage yet to Become a Viable Energy Storage Option?" *IScience* 24 (5): 102440. <https://doi.org/10.1016/j.isci.2021.102440>.
- Barbour, Edward, I A Grant Wilson, Jonathan Radcliffe, Yulong Ding, and Yongilang Li. 2016. "A review of pumped hydro energy storage development in significant international electricity markets." *Renewable and Sustainable Energy Reviews* 61: 421-432. <https://doi.org/10.1016/j.rser.2016.04.019>.
- Barnes, Frank S, and Jonah G Levine. 2011. *Large Energy Storage Systems Handbook*. Boca Raton: CRC Press. <https://doi.org/10.1201/b10778>.
- Baxter, Richard. 2006. *Energy Storage: A Nontechnical Guide*. Pennwell Corporation.
- Borri, Emiliano, Alessio Tafone, Alessandro Romagnoli, and Gabriele Comodi. 2021. "A Review on Liquid Air Energy Storage: History, State of the Art and Recent Developments." *Renewable and Sustainable Energy Reviews* 137 (March): 110572. <https://doi.org/10.1016/j.rser.2020.110572>.
- Breeze, Paul. 2018. "Chapter 10 — The Cost of Electricity from Hydropower Plants." In *Hydropower 1st Edition*, by Paul Breeze. Academic Press.
- Budt, Marcus, Daniel Wolf, Roland Span, and Jinyue Yan. 2016. "A Review on Compressed Air Energy Storage: Basic Principles, Past Milestones and Recent Developments." *Applied Energy* 170 (May): 250–68. <https://doi.org/10.1016/j.apenergy.2016.02.108>.
- Burdick, Guy. 2020. "Quidnet Leverages Drilling Tech to Provide Pumped Hydro Type Storage at Half the Price." *Utility Dive*. July. <https://www.utilitydive.com/news/quidnet-leverages-drilling-tech-to-provide-pumped-hydro-type-storage-at-hal/580839>.
- Cárdenas, Bruno, Adam Hoskin, James Rouse, and Seamus D Garvey. 2019. "Wire-Wound Pressure Vessels for Small Scale CAES." *Journal of Energy Storage* 26 (December): 100909. <https://doi.org/10.1016/j.est.2019.100909>.
- Chen, Zuyu, Zhao Yufei, Zou Bin, Jiang Long, and Zhao Huimin. 2019. "Study and application of unmanned driving technology or filling and rolling construction of earth-rockfill dam." *Water Resources and Hydropower Engineering (Chinese)* 50(8): 1-7.
- China Renewable Energy Engineering Institute. 2018. "The Technology and Development of Pumped Storage Power Stations." *China Water and Power Press*.
- Clack, Christopher T M, Staffan A Qvist, Jay Apt, and Jay F Whitacre. 2017. "Evaluation of a proposal for reliable low-cost grid power with 100% wind, water, and solar." *Proceedings of the National Academy of Sciences* 114 (26): 6722-672. <https://doi.org/10.1073/pnas.1610381114>.
- Dames and Moore. 1981. "An Assessment of Hydroelectric Pumped Storage." *U.S. Army Engineer Institute for Water Resources*. November.
- de Oliveira e Silva, Guilherme, and Patrick Hendrick. 2016. "Pumped hydro energy storage in buildings." *Applied Energy* 179: 1242-1250. <https://doi.org/10.1016/j.apenergy.2016.07.046>.
- Dimanchev, Emil, Joshua Hodge, and John Parsons. 2020. "Two-Way Trade in Green Electrons: Deep Decarbonization of the Northeastern U.S. and The Role of Canadian Hydropower." *MIT Center for Energy and Environmental Policy Research*. February 12. <https://dspace.mit.edu/handle/1721.1/130577>.
- Donadei, Sabine, and Gregor-Sönke Schneider. 2016. "Chapter 6 - Compressed Air Energy Storage in Underground Formations." In *Storing Energy*, 113-133. Elsevier. <https://doi.org/10.1016/B978-0-12-803440-8.00006-3>.
- Energy Vault. 2022. "Energy Vault - Enabling a Renewable World™." *Energy Vault*. www.energyvault.com.

- European Commission. 2020. "Study on energy storage – Contribution to the security of the electricity supply in Europe. Final Report." *Directorate-General for Energy, Internal Energy Market*. <https://op.europa.eu/en/publication-detail/-/publication/a6eba083-932e-11ea-aac4-01aa75ed71a1>.
- Evans, David J, Gideon Carpenter, and Gareth Farr. 2018. "Mechanical Systems for Energy Storage – Scale and Environmental Issues. Pumped Hydroelectric and Compressed Air Energy Storage." In *Energy Storage Options and Their Environmental Impact*, by R E Hester and R M Harrison, 42–114. London, UK: Royal Society of Chemistry.
- Federal Energy Regulatory Commission. 2019. "Guidance for Applicants Seeking Licenses or Preliminary Permits for Closed-Loop Pumped Storage Projects at Abandoned Mine Site." *Federal Energy Regulatory Commission*.
- Gallo, A B, Simões-Moreira, H K M Costa, M M Santos, and E Moutinho dos Santos. 2016. "Energy Storage in the Energy Transition Context: A Technology Review." *Renewable and Sustainable Energy Reviews* 65 (November): 800–822. <https://doi.org/10.1016/j.rser.2016.07.028>.
- Gao et al. G-Q. 2016. "Prediction of Fatigue Life for Pumped Storage Unit Runner." *Journal of Zhejiang University of Water Resource and Electric Power* 28(2): 17–21.
- Garvey, Seamus D, and Andrew Pimm. 2016. "Chapter 5 - Compressed Air Energy Storage." In *Storing Energy*, by Trevor M Letcher, 87–111. Elsevier. <https://doi.org/10.1016/B978-0-12-803440-8.00005-1>.
- Gay, Frazer W. 1948. Means for storing fluids for power generation. United States Patent US2433896A. April 16.
- Geostock Sandia. n.d. *Our Expertise*. <https://www.entrepose.com/en/geostock-sandia/expertise/>.
- Giramonti, A J, and E B Smith. 1983. "Analytical Simulation of the Champagne Effect in CAES Power Plants." *Journal of Energy* 7 (6): 570–74. <https://doi.org/10.2514/3.62700>.
- Graabak, Ingebord, Stefan Jaehnert, Magnus Korpas, and Birger Mo. 2017. "Norway as a Battery for the Future European Power System: Impacts on the Hydropower System." *Energies* 10, 2054. <https://doi.org/10.3390/en10122054>.
- Gravitricity Storage. 2022. *Home – Gravitricity Renewable Energy Storage*. <https://gravitricity.com>.
- Gu, Gubiao. 2019. (In Chinese). "Energy Storage Development in the Energy Transformation." Keynote presentation, First China Energy Storage Academic Forum and Wind and Solar Energy Storage Innovation Technology Conference, Beijing, August 7.
- Guerra, Omar J, Jiazi Zhang, Joshua Eichman, Paul Denholm, Jennifer Kurtz, and Bri-Mathias Hodge. 2020. "The Value of Seasonal Energy Storage Technologies for the Integration of Wind and Solar Power." *Energy and Environmental Science* <https://doi.org/10.1039/D0EE00771D>.
- Guittet, Mélanie, Massimiliano Capezzali, and Ludovic Guadard. 2016. "Study of the drivers and asset management of pumped-storage power plants historical and geographical perspective." *Energy* 111: 560–579. <https://doi.org/10.1016/j.energy.2016.04.052>.
- Guizzi, Giuseppe Leo, Michele Manno, Ludovica Maria Tolomei, and Ruggero Maria Vitali. 2015. "Thermodynamic Analysis of a Liquid Air Energy Storage System." *Energy* 93 (December): 1639–47. <https://doi.org/10.1016/j.energy.2015.10.030>.
- Guo, Chaobin, Cai Li, Keni Zhang, Zuansi Cai, Tianran Ma, Federico Maggi, Yixiang Gan, Abbas El-Zein, Zhejun Pan, and Lumig Shen. 2021. "The Promise and Challenges of Utility-Scale Compressed Air Energy Storage in Aquifers." *Applied Energy* 286 (March): 116513. <https://doi.org/10.1016/j.apenergy.2021.116513>.
- Hall, Douglas, and Randy Lee. 2014. "Assessment of Opportunities for New United States Pumped Storage Hydroelectric Plants Using Existing Water Features as Auxiliary Reservoirs." *Idaho National Laboratory*. 03 1.
- Hartmann, Niklas, O C Vöhringer, C Kruck, and L Eltrop. 2012. "Simulation and Analysis of Different Adiabatic Compressed Air Energy Storage Plant Configurations." *Applied Energy* 93 (May): 541–48. <https://doi.org/10.1016/j.apenergy.2011.12.007>.
- He, Wei, Mark Dooner, Marcus King, Dacheng Li, Songshan Guo, and Jihong Wang. 2021. "Techno-Economic Analysis of Bulk-Scale Compressed Air Energy Storage in Power System Decarbonisation." *Applied Energy* 282 (January): 116097. <https://doi.org/10.1016/j.apenergy.2020.116097>.
- He, Wei, Xing Luo, David Evans, Jonathan Busby, Seamus Garvey, Daniel Parkes, and Jihong Wang. 2017. "Energy Storage of Compressed Air in Cavern and Cavern Volume Estimation of the Large-Scale Compressed Air Energy Storage System." *Applied Energy* 208 (December): 745–57. <https://doi.org/10.1016/j.apenergy.2017.09.074>.

- Hester, R E, and R M Harrison. 2019. *Energy Storage Options and their Environmental Impact*. London, UK: London Royal Society of Chemistry.
- Holst, Kent, Georgianne Huff, Robert H Schulte, and Nicholas Critelli. 2012. "Lessons from Iowa: Development of a 270 Megawatt Compressed Air Energy Storage Project in Midwest Independent System Operator : A Study for the DOE Energy Storage Systems Program." *Sandia National Laboratories SAND2012-0388*, 1035330. <https://doi.org/10.2172/1035330>.
- Houssainy, Sammy, Mohammad Janbozorgi, and Pirouz Kavehpour. 2018. "Thermodynamic Performance and Cost Optimization of a Novel Hybrid Thermal-Compressed Air Energy Storage System Design." *Journal of Energy Storage* 18 (August): 206–17. <https://doi.org/10.1016/j.est.2018.05.004>.
- Huang, Y, H S Chen, X J Zhang, P Keatley, M J Huang, I Vorushylo, Y D Wang, and N J Hewitt. 2017. "Techno-Economic Modelling of Large Scale Compressed Air Energy Storage Systems." *Energy Procedia* 105 (May): 4034–39. <https://doi.org/10.1016/j.egypro.2017.03.851>.
- Hydro Equipment Association. 2015. "Global Technology Roadmap." *Hydro Equipment Association*.
- Hydro Quebec. 2019. *Overview of Hydro-Quebec's Energy Resources*. November. <https://www.hydroquebec.com/data/achats-electricite-quebec/pdf/electricity-supply-plan-2020-2029.pdf>.
- Hydrostor. n.d. *Hydrostor – Advanced Compressed Air Energy Storage*. Accessed June 27, 2021. <https://www.hydrostor.ca>.
- Immendoerfer, Andrea, Ingela Tietze, Heidi Hottenroth, and Tobias Viere. 2017. "Life-cycle impacts of pumped hydropower storage and battery storage." *International Journal of Energy and Environmental Engineering* 8(3): 231–245. <https://doi.org/10.1007/s40095-017-0237-5>.
- International Energy Agency. 2015. "Technology Roadmap Hydrogen and Fuel Cells." *International Energy Agency*.
- International Hydropower Association. 2019. "International Hydropower Association Pumped Storage Tracking Tool." *International Hydropower Association*.
- Iria-Martinez, Rocio, Megan Johnson, and Rui Shan. 2021. "U.S. Hydropower Market Report." *U.S. Department of Energy*.
- Jacobson, Mark Z, Mark A Delucchi, Mary A Cameron, and Bethany A Frew. 2015. "Low-cost solution to the grid reliability problem with 100% penetration of intermittent wind, water, and solar for all purposes." *Proceedings of the National Academy of Sciences of the United States of America* 112 (49) 15060–15065. <https://doi.org/10.1073/pnas.1510028112>.
- Johnson, M M, S-C Kao, N M Samu, and R Urias-Martinez. 2021. "Existing Hydropower Assets." *Oak Ridge National Laboratory*. <https://hydrosource.ornl.gov/dataset/EHA2021>.
- Kaminker, Christopher, Osamu Kawanishi, Fiona Stewart, Ben Caldecott, and Nicholas Howarth. 2013. "Institutional Investors and Green Infrastructure Investments: Selected Case Studies." *OECD*. https://www.oecd-ilibrary.org/finance-and-investment/institutional-investors-and-green-infrastructure-investments_5k3xr8k6jb0n-en.
- Kelly-Detwiler, Peter. 2019. "Energy Vault Receives \$110 Million From SoftBank For Gravity-Assisted Power Storage." *Forbes*. August. <https://www.forbes.com/sites/peterdetwiler/2019/08/14/tower-of-power-110-million-investment-primes-energy-vault-to-take-on-global-energy-storage-markets>.
- King, Marcus, Anjali Jain, Rohit Bhakar, Jyotirmay Mathur, and Jihong Wang. 2021. "Overview of Current Compressed Air Energy Storage Projects and Analysis of the Potential Underground Storage Capacity in India and the UK." *Renewable and Sustainable Energy Reviews* 139 (April): 110705. <https://doi.org/10.1016/j.rser.2021.110705>.
- Krueger, K. 2021. "4.1 Pumped Hydroelectric Storage." In *Thermal, Mechanical, and Hybrid Chemical Energy Storage Systems*, by Klaus Brun, Timothy Allison and Dennis Richard, 139–166. London: Academic Press.
- LEAPS. 2007. "Final Environmental Impact Statement Lake Elsinore Advanced Pumped Storage Project FERC Project No. 11858."
- Levy et al. 2013. "Renewable Energy REITs: A New Capital Source for Energy Funds and Developers." *Real Estate Finance Journal* 29(1): 52–64.
- Liang, Q. 2017. "Prediction of Fatigue Life for Pumped Storage Unit Runner." *Journal of Henan University of Engineering (in Chinese)* 29(4): 72–75.
- Lin, W-E. 2002. "Preliminary feasibility study of using TBM in the construction of headrace tunnel of Ta-Nan-Ao pumped storage hydro power project." *Taipower Engineering Month* (in Chinese: 台電工程月刊).

- Ma, J-F. 2017. "Life Assessment of the Magnetic Pole and Yoke High Stress Zone of a Pumped-storage Generating Unit." *Yunan Water Power* (in Chinese) 33(1): 165-168.
- Manolakos, D, G Papdakis, D Papantonis, and S Kyritsis. 2004. "A stand-alone photovoltaic power system for remote villages using pumped water energy storage." *Energy* 29(1): 57-69. <https://doi.org/10.1016/j.energy.2003.08.008>.
- McCafferty, Thomas. 1980. "Compressed Air Energy Storage: Preliminary Design and Site Development Program in an Aquifer. Final Draft, Task 1." *EPRI* <https://doi.org/10.2172/6743232>.
- Medeiros, Michael, Robert Booth, James Fairchild, Doug Imperato, Charles Stinson, Mark Ausburn, Mike Tietze, et al. 2018. "Technical Feasibility of Compressed Air Energy Storage (CAES) Utilizing a Porous Rock Reservoir." *DOE-PGE--00198-1, 1434251*. <https://doi.org/10.2172/1434251>.
- MWH. 2009. "Technical Analysis of Pumped Storage and Integration with Wind Power in the Pacific Northwest." *U.S. Army Corps of Engineers Northwest Division Hydroelectric Design Center*.
- Nakhamkin, Michael. 2010. Retrofit Of Simple Cycle Gas Turbine For Compressed Air Energy Storage Application Having Expander For Additional Power Generation. United States Patent US20100083660A1. April 8.
- Nie, Liangliang, Mengxiao Zhagn, Libei Zhu, Jian-Chao Pang, Ge Yao, Yunzian Mao, and Man Chen. 2017. "Fatigue life prediction of motor-generator rotor for pumped-storage plant." *Engineering Failure Analysis* 79: 8-24. <https://doi.org/10.1016/j.engfailanal.2017.03.013>.
- NYSERDA. 2009. "Compressed Air Energy Storage Engineering and Economic Study." 10-09.
- Ozarslan, Ahmet. 2012. "Large-Scale Hydrogen Energy Storage in Salt Caverns." *International Journal of Hydrogen Energy*, HYFUSEN 37 (19): 14265-77. <https://doi.org/10.1016/j.ijhydene.2012.07.111>.
- Pacific Northwest National Laboratory. 2019. *Energy Storage Technology and Cost Characterization Report*. Pacific Northwest National Laboratory.
- Peltier, R. 2006. "Kannagawa Hydropower Plant." *Power* 150(6): 54-58.
- Quidnet Energy. 2022. *Quidnet Energy*. <https://www.quidnetenergy.com>.
- reNews. 2020. "Work Underway on Gravitricity Storage Demo." *ReNEWS – Renewable Energy News*. August 31. <https://www.renews.biz/62778/work-begins-gravitricitys-11m-energy-storage-demonstrator>.
- Rogers, David J, and Conor M Watkins. 2008. "Overview of the Taum Sauk pumped storage power plant upper reservoir failure, Reynolds County, MO." *Sixth International Conference on Case Histories in Geotechnical Engineering*. Arlington, VA.
- Ruiz, Pablo, James Read, Johannes Pfeifenberger, Roger Lueken, and Judy Chang. 2018. "The Brattle Group Response to DOE RFI#: DE-FOA-0001886 to United States Department of Energy, Office of Energy Efficiency and Renewable Energy, Water Power Technologies Office." *The Brattle Group*. https://www.brattle.com/wp-content/uploads/2021/05/13692_tbg_response_to_doe_eere_wpto_rfi_de-foa-0001886_sent.pdf.
- Schnitter, Nicholas J. 1994. *A History of Dams: The Useful Pyramid*. Rotterdam: Aa Balkema.
- Scuero, Alberto, and Gabriella Vaschetti. 2013. "PVC geomembranes in pumped storage schemes." *WasserWirtschaft - Hydrologie, Wasserbau, Hydromechanik, Gewässer, Ökologie, Boden* 103(5): 120-123.
- Shieber, Jonathan. 2018. "The Cost of Energy Storage Has Stalled Adoption of Renewable Power. Energy Vault Has a Solution." *TechCrunch*. November. <https://social.techcrunch.com/2018/11/07/the-cost-of-energy-storage-has-stalled-adoption-of-renewable-power-energy-vault-has-a-solution>.
- St. John, Jeff. 2015. "SustainX to Merge With General Compression, Abandon Above-Ground CAES Ambitions." *Greentech Media*. March 31. <https://www.greentechmedia.com/articles/read/sustainx-to-merge-with-general-compression-abandon-above-ground-caes-ambiti>.
- Stevenson, Ian. 2017. "Viewpoint: Introducing Environmental History into Vernacular Architecture: Considerations from New England's Historic Dams." *Buildings and Landscapes: Journal of the Vernacular Architecture Forum* 22(2): 1-21.
- Succar, Samir, and Robert H Williams. 2008. "Compressed Air Energy Storage: Theory, Resources, And Applications For Wind Power." https://acee.princeton.edu/wp-content/uploads/2016/10/SuccarWilliams_PEI_CAES_2008April8.pdf.
- Tam, S W, C A Blomquist, and G T Kartsounes. 1979. "Underground Pumped Hydro Storage—An Overview." *Energy Sources* 4(4): 329-351. <https://doi.org/10.1080/00908317908908068>.
- Thompson, Amy. 2016. *DOE/EPRI Electricity Storage Handbook in Collaboration with NRECA*. 450.

- Tong, Zheming, Zhewu Cheng, and Shuguang Tong. 2021. "A review on the Development of Compressed Air Energy Storage in China: Technical and Economic Challenges to Commercialization." *Renewable and Sustainable Energy Reviews* 135 (January): 110178. <https://doi.org/10.1016/j.rser.2020.110178>.
- U.S. Department of Energy. 2021. "Hydropower Market Report."
- Weh, Markus, and Francois Bertholet. 2011. "TBM advance in the main adit to the Nant de Drance pumped storage power plant / TBM Vortrieb im Hauptzugangstunnel zum Pumpspeicherkraftwerk Nant de Drance." *Geomechanics and Tunnelling* 4(5): 584-591. <https://doi.org/10.1002/geot.201100025>.
- Williams, J H, R Jones, G Kwok, and B Haley. 2018. "Deep Decarbonization in the Northeastern United States and Expanded Coordination with Hydro-Québec. A report of the Sustainable Development Solutions Network in cooperation with Evolved Energy Research and Hydro-Québec." <https://www.evolved.energy>.
- Witt, Adam M, Hadjerioua Boualem, Martinez Rocio, and Bishop Norm. 2015. *Evaluation of the feasibility and viability of modular pumped storage hydro (m-PSH) in the United States*. Oak Ridge, TN: Oak Ridge National Laboratory.
- World Bank. 2018. "Upper Cisakan Pumped Storage Hydro-Electrical Power (1040 MW) Project (P112158)."
- Yang, Chi-Jen. 2016. "Chapter 2 - Pumped Hydroelectric Storage." In *Storing Energy*, by T. M. Letcher, 25-38. Elsevier.
- . 2017. *Energy Policy in China*. London; New York: Routledge, Taylor and Francis Group.
- Yang, Chi-Jen, and Robert B Jackson. 2011. "Opportunities and barriers to pumped-hydro energy storage in the United States." *Renewable and Sustainable Energy Reviews* 15(1): 839-844. <https://doi.org/10.1016/j.rser.2010.09.020>.
- Yu, Haoshui, Seiji Engelkemier, and Emre Gençer. 2022. "Process Improvements and Multi-Objective Optimization of Compressed Air Energy Storage (CAES) System." *Journal of Cleaner Production* 335 (February): 130081. <https://doi.org/10.1016/j.jclepro.2021.130081>.
- Zeynalian, Mirhadi, Amir Hossein Hajjalirezaei, Amir Reza Razmi, and M Torabi. 2020. "Carbon Dioxide Capture from Compressed Air Energy Storage System." *Applied Thermal Engineering* 178 (September): 115593. <https://doi.org/10.1016/j.applthermaleng.2020.115593>.
- Zhang , C, and Z Jiang. 2012. "Pumped Storage Power Station Design (In Chinese: 抽水蓄能电站设计)." *China Electric Power Press* (中国电力出版社).
- Zhang, Jianmin, and Qianzhi Zhang. 2014. "High-rise building mini-hydro pumped-storage scheme with Shanghai Jinmao Tower as a case study." *2014 IEEE PES General Meeting | Conference & Exposition*. National Harbor, Maryland: IEEE. <https://doi.org/10.1109/pesgm.2014.6939339>.
- Zhang, Qinglong, Tianyun Liu, Zhaosheng Zhang, Zehua Huangfu, Qingbin Li, and Zaizhan An. 2019. "Unmanned rolling compaction system for rockfill materials." *Automation in Construction* 100: 103-117. <https://doi.org/10.1016/j.autcon.2019.01.004>.
- Zhang, Sufang, Philip Andrews-Speed, and Pradeep Perera. 2015. "The evolving policy regime for pumped storage hydroelectricity in China: A key support for low-carbon energy." *Applied Energy* 150: 15-24. <https://doi.org/10.1016/j.apenergy.2015.03.103>.
- Zhong, D, M Shi, B Cui, and J Wang. 2019. "Research progress of the intelligent construction of dams." *Journal of Hydraulic Engineering (in Chinese)* 50(1): 38-52. <https://doi.org/10.13243/j.cnki.slxb.20181131>.
- Zhou, Joe. 2020. "Powering the Carbon-Free Electric Future." *Quidnet Energy* 9.
- Zivar, Davood, Sunil Kumar, and Jalal Forozesh. 2020. "Underground Hydrogen Storage: A Comprehensive Review." *International Journal of Hydrogen Energy* September, S0360319920331426. <https://doi.org/10.1016/j.ijhydene.2020.08.138>.



Chapter 4 – Thermal energy storage

4.1 Introduction

In 2017, about 75% of the world’s electricity supply was generated by thermal power sources—that is, by plants where a fuel is combusted to heat steam, air, or another fluid that drives a turbine (International Energy Agency 2019). As the electricity sector decarbonizes, the heat sources used for thermal power generation will transition away from fossil fuels to relatively greater reliance on sources such as geothermal energy, hydrogen fuel, solar thermal energy, biomass, nuclear fission, and possibly nuclear fusion. Some of these plants will need to respond to variations in the availability of renewable energy sources; for these types of generators, thermal energy storage (TES) can provide flexibility. Some concentrated solar power plants, which have been deployed to a significantly lesser extent than solar photovoltaics, already use TES with thermal oil or molten salt to shift generation from peak sunlight hours to match demand. Researchers have proposed TES for nuclear plants to decouple the power block from the reactor so that a plant can provide both base-load and peaking capacity (Forsberg, Brick and Haratyk 2018). In these roles, TES can improve efficiency, serve combined heat and power needs, and deliver other services. Together, these opportunities present interesting opportunities for TES technologies in the decarbonized grid of the future.

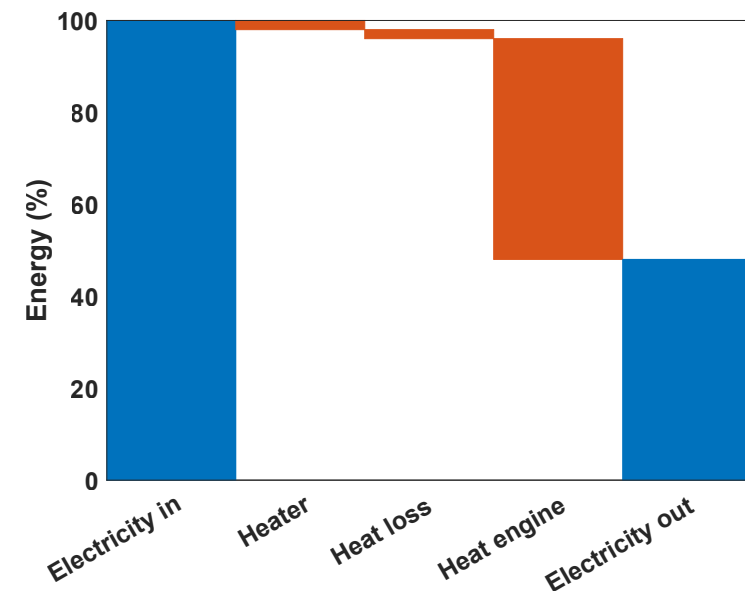
This chapter focuses on electricity-to-electricity storage, which is a significant but narrower opportunity for TES. The potential of electricity-to-electricity TES centers on the ability to use very low-cost storage materials such as crushed rock. To utilize such low-cost storage mediums, the key challenges to overcome are the low efficiency and high capital cost of converting heat to electricity.

A combination of high power and low energy costs suggests that TES will be most interesting as a long-duration storage technology. Basic geographic constraints may be a factor, primarily the ability to deliver the several thousand tons of storage material needed for a gigawatt-hour-scale facility. A TES facility would have a similar areal footprint as a thermal power plant, which typically requires tens to hundreds of hectares on relatively flat land. Water demands for cooling will depend on the system design. Economies of scale generally disfavor electricity-heat-electricity TES in small-scale applications such as behind-the-meter electricity storage.

A review of the TES systems that have been proposed by commercial developers and researchers suggests three main strategies for overcoming the key challenges of heat-to-electricity efficiency and cost of power. In all strategies, TES utilizes low-cost storage materials. In the first strategy, TES is installed at existing thermal power plants, particularly coal plants, to replace heat from fuel combustion and to reuse the existing power generation equipment, which reduces the cost of power. The second strategy considers more efficient power cycles with peak temperatures slightly above the range of thermal storage technologies used presently. The third strategy relies on even higher temperature storage to increase efficiency, and, in some embodiments, requires research and development on newer power conversion technologies. These strategies provide several pathways for TES to support a decarbonized grid.

This chapter begins with a brief description of how thermal energy storage works, followed (in Section 4.3) by an overview of TES technologies grouped by function: charge, store, and discharge. With that foundation, Section 4.4 describes systems that utilize each of the three

Figure 4.1 Energy losses in a thermal energy storage system



Energy losses (in orange) for each step of a generic TES system. The heat loss during storage will depend on how the system is operated.

strategies for overcoming TES’s key technical challenges. Section 4.5 provides cost estimates for two illustrative systems in 2050; Section 4.6 concludes.

4.2 What is thermal energy storage?

TES systems use electricity to heat up a material; the heated material is then insulated until the energy is needed, and finally the heat is converted back to electricity through a power conversion device. Figure 4.1 illustrates typical energy losses associated with each step for a generic TES system with 47% roundtrip efficiency (where “roundtrip efficiency” is defined as the fraction of electricity delivered back to the grid over the electricity drawn from the grid).

The figure shows one of the key challenges of TES: the efficiency of the heat-to-electricity

conversion step is the limiting factor for roundtrip efficiency. By contrast, the first step—converting electricity to heat—can be accomplished with minimal losses; given sufficient insulation, losses to the ambient environment during heat storage (step two) can also be limited to acceptable levels. More details are provided in Section 4.3.

4.3 Technology

The three main steps in TES are converting electricity to heat, storing heat, and converting heat back to electricity. While this basic description is true for storage technologies in their own medium, it is worth examining the different technology options at each step before discussing entire systems. Certain synergies between these options are relevant for overall system design; these synergies are discussed in Section 4.4.

Box 4.1 Thermal energy storage for non-electricity storage

Although this study focuses on energy storage using electricity as the only input and output, thermal energy storage can also be utilized in other applications.

Flexibility for thermal power plants

Thermal storage can be used to store heat from a relatively inflexible heat source, such as a large coal or nuclear plant, so that this heat can be used later to generate electricity on demand. This flexibility can help thermal power plants respond to variable renewable generation more efficiently. Steam accumulators, which store pressurized steam from a boiler or another heat source and later return steam directly to the system, represent an early form of thermal storage. They have been used in power plants and industrial facilities for decades (González-Roubaud, Pérez-Osorio and Prieto 2017). For longer-duration storage, it would be more economical to store heat in an unpressurized fashion because pressure vessels are expensive. There is interest in systems that incorporate thermal storage between a nuclear reactor and its power generation unit as a way to address ramping constraints on the reactor (Forsberg, Brick and Haratyk 2018). Similarly, thermal storage could be used to provide flexibility in the operation of combined heat and power plants. Separately, an existing commercial TES project in Australia stores heat from either combusted biogas produced by a wastewater treatment plant or from grid charging. Heat from both sources is used to generate electricity (Power Technology 2019).

Heat end use

As seen in Figure 4.1, converting heat back to electricity is the most inefficient step in TES

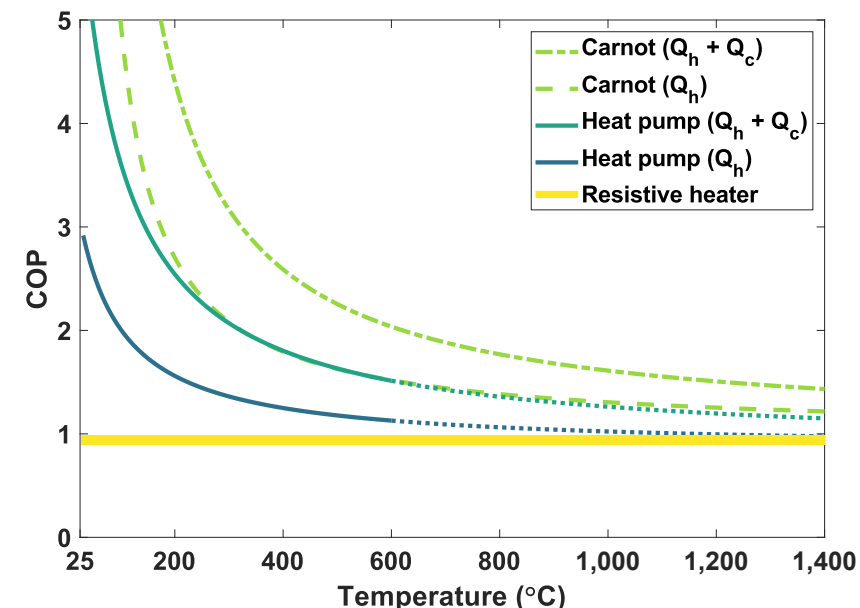
systems. Therefore, TES can be valuable in applications where heat is the desired output, enabling greater demand-side flexibility. For example, instead of using electrical energy storage to power heating or cooling equipment, thermal storage can be used with materials such as wax or ice. This is an opportunity for TES given growing demand for cooling and electrification of heating, as discussed in Chapters 6 and 7.

There are companies that are already providing TES for space cooling and refrigeration in commercial buildings such as offices, warehouses, and data centers (Greentech Media 2020; Google 2021).

In countries like France and China, tariff structures support off-peak electric heating of hot-water tanks or firebricks (for space heating) to even out load profiles for baseload generators. At Drake Landing, a planned residential community in Canada, heat from rooftop solar thermal collectors is stored seasonally in boreholes (Mesquita et al. 2017). In the winter, a district heating system circulates warm fluid to the homes, which are equipped with heat pumps.

The industrial sector is characterized by diverse processes with a range of specific requirements for temperature, heat transfer rates, and process integration, among other constraints. For example, milk pasteurization and cement clinker production have notably different requirements. Thus, the applicability of thermal storage to industrial applications will vary (Friedman, Fan and Tang 2019; Thiel and Stark 2021).

Figure 4.2 Charging coefficient of performance (COP)



Comparison of COP values for electricity-to-heat technologies. The Carnot lines show the ideal case; the upper line is applicable if sub-ambient (cold) thermal energy is utilized. The solid lines, for non-ideal cases, indicate the approximate COP within the range of operating temperatures. The dotted section continues the trend to higher temperatures. See Appendix B for further details.

4.3.1 Charging: Electricity to heat

Since the scope of this study is limited to TES systems that have only electrical energy as the input and output, we ignore other potential sources of heat although such sources can be utilized in real systems and can improve system performance. These other potential sources include waste heat, nuclear, geothermal, combustion, and solar thermal.

Technology options for charging a TES system—that is, for converting electricity to heat—include a resistive heater, inductive heater, or heat pump. Heat pumps transfer heat from a low-temperature environment to a higher-temperature one, so they are often described as refrigerators running in reverse. The figure of merit for converting electricity to heat is called the coefficient of performance (COP) to distinguish it from thermal efficiency. Thermal efficiency is how much electricity is generated

from a quantity of heat—it cannot be higher than 100% and is often much lower. COP can be greater than 100%, which means more heat is transferred than electricity is used, without violating the laws of thermodynamics. For reference, a residential heat pump has a COP around 2 to 4 depending on ambient and desired temperatures. For relatively small temperature differences, the COP can be high, but as the temperature differences increase, COP falls, as seen in Figure 4.2. The figure shows a nominal case where low-temperature heat is supplied by ambient air at 25°C. Changes in heat pump design could improve the COP slightly and adjust the ratio of high and low temperature thermal energy. Higher capital and operating costs are drawbacks of heat pumps compared to resistive and inductive heaters. Exact values are unknown since high-temperature heat pumps are not commercially available yet.

Resistive heaters can convert electricity to heat with a COP above 90%, but their COP cannot exceed 100% (Amy, Seyf, et al. 2018). Resistive heaters can be placed directly in the storage material, built into piping, or placed close to the container or pipes for indirect heating. Induction heating uses oscillating magnetic fields to generate heat within the storage material or an intermediate heat transfer fluid. Induction heating can overcome some heat transfer resistance compared to indirect resistive heating; however, inductive heating equipment is more expensive and not easily applied to all materials.

The maximum storage temperature will be a factor in choosing the heater. Current heat pump designs have practical limits around 550°C due to the properties of the materials available (at reasonable cost) for use in turbomachinery (Frate, Ferrari and Desideri 2020; Laughlin 2017). Meanwhile, inductive heaters can heat materials to 3,000°C, but ambient conditions and containment materials may set a lower limit (AZO Materials 2015; Inductotherm Corporation 2020). Resistive heaters made of metallic materials can reach 1,400°C in oxidative environments (Kanthal 2018), and heaters made of ceramics or other materials can exceed 2,000°C depending on the environment (Amy, Seyf, et al. 2018). Higher-temperature heaters tend to be more expensive.

In a power system with high shares of variable renewable generation, electricity prices are expected to be low for many hours of the year—as discussed in Chapter 6 and in the literature (Sepulveda et al. 2021). Thus, it may be advantageous (though not necessarily so) to trade off higher COP in favor of lower charging power cost. Even so, charge efficiency and cost are found to be of secondary importance compared to other parameters discussed in Chapter 6.

Lower charging efficiency means more electricity will be used for the same amount of heat stored. This has no impact on the amount of storage capacity needed to meet a target discharge profile, which is determined by discharge efficiency and the rate of self-discharge. Resistive heaters will likely be the most common type of heating element used for TES systems given their simplicity and lower cost per unit of power.

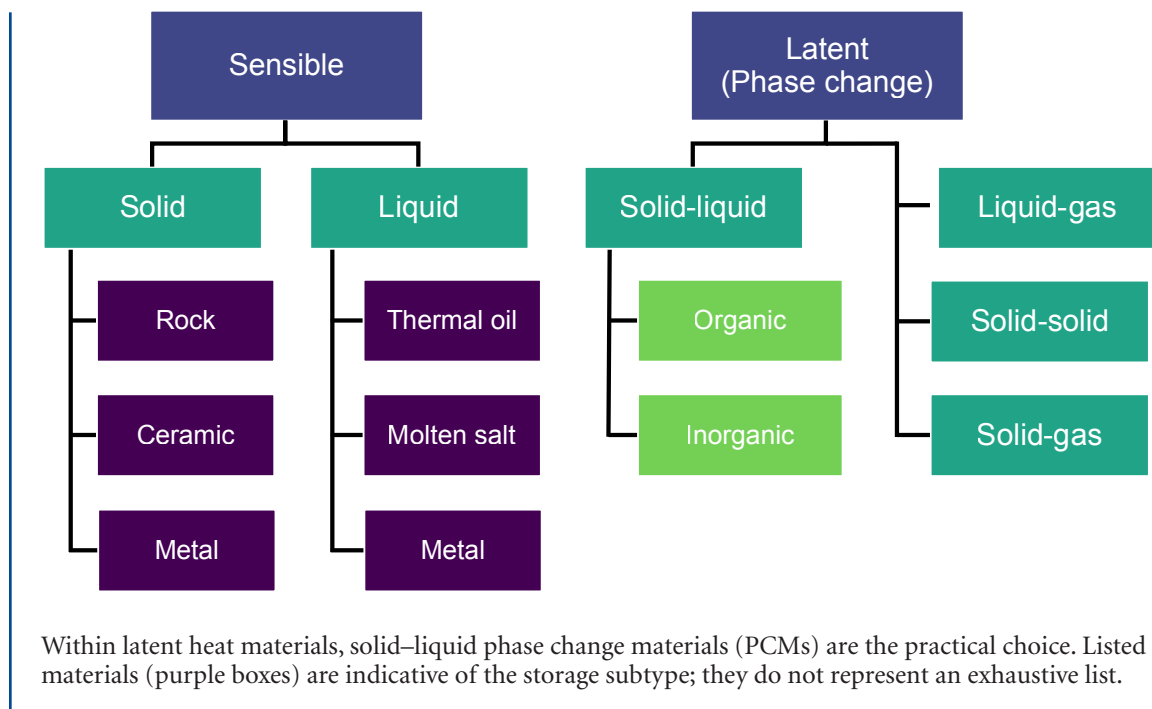
4.3.2 Heat storage

As mentioned in the introduction to this chapter, the advantage of thermal energy storage compared to most other forms of storage is the ability to use low-cost storage materials. Long-duration storage, which TES systems are suited for, should aim for a capital cost below \$20 per kilowatt-hour of electrical energy (kWh_e) (Albertus, Manser and Litzelman 2020; Ziegler et al. 2019).

To help understand the material selection process, we can separate the storage cost expressed in units of electricity (\$/ kWh_e) into the discharge efficiency penalty and the thermal storage cost (\$/ kWh_{th}). If we assume a heat-to-electricity efficiency of 50%, the storage cost should be below \$10 per kWh_{th} . Efficiency values range from approximately 40% to 60%, as discussed in the next section on discharging technologies. Regardless of the exact efficiency, this cost target significantly constrains which materials can be used. The cost of some materials would itself exceed the target, even before accounting for containment, insulation, and construction, which are costs associated with energy capacity.

As discussed in Section 4.3.3, which focuses on the discharging step in TES, higher storage temperatures can increase thermal efficiency (converting stored heat back to electricity).

Figure 4.3 Classification of thermal storage materials



Although the efficiency of this step will largely depend on the energy conversion system used, thermal inefficiencies act as a penalty on the capital cost of energy. Thus, high-temperature materials are desired because they enable higher efficiency (see discussion on Carnot efficiency in Section 4.3.3). However, costs for containment and insulation also increase with temperature. Different systems make different trade-offs between energy cost, power cost, and heat-to-electricity efficiency—one of the key design challenges for TES.

The temperature–efficiency relationship generally rules out materials that cannot go above 400°C. These materials may still be useful for applications other than power generation, such as those described in Box 4.1.

Thus, considerations of materials-based energy cost can quickly filter out incompatible choices.

Material cost per unit of thermal energy can be estimated with just a few variables. For sensible heat, the variables are cost per mass, specific heat capacity, and change in temperature.¹ For latent heat storage, the variables are cost per mass and latent heat of fusion; latent heat of fusion is the energy associated with the phase transition between solid and liquid.

Besides cost, there are several ways to categorize storage materials. The broadest distinction is between storing thermal energy as sensible heat or latent heat as shown in Figure 4.3. An object that increases in temperature as it is heated gains sensible heat, where the term “sensible” refers to the fact that the heat can be sensed through a change in temperature. By contrast, latent heat is the heat absorbed or released at a constant temperature or within a temperature range during a phase change.

¹ Trivially, cost per mass can be expressed as cost per volume and density.

A benefit of latent heat storage compared to sensible heat storage is higher specific energy (energy per mass) and energy density (energy per volume). For latent heat, these values can be an order of magnitude larger than for sensible heat. However, for grid-scale storage, the space occupied by the plant is not a primary concern. Rather, the primary concern is cost—provided that the energy storage technology can meet the requirements of the specific application. For the heat storage applications described in Box 4.1, such as residential heating, higher energy density is favorable.

Sensible heat storage

Materials for sensible heat storage can be grouped by whether they are solid versus liquid. Liquids can be moved easily, which facilitates efficient heat transfer, but there is a risk that they will solidify, which could damage the system. In concentrated solar plants, this problem is solved by using electrical heat tracing in the pipes and cold storage tank. Downsides of this approach are increased capital cost and parasitic energy losses.

Molten salt is an example of a liquid storage material that has been used to provide over 13 gigawatt-hours (GWh_e) of storage in concentrated solar power plants.² Most molten salts in use for storage today are nitrate salts with maximum service temperatures around 550°C (Laughlin 2017), but their cost exceeds the target of $\$10/\text{kWh}_\text{th}$ (Glatzmaier 2011). There have been efforts to reduce cost by increasing the temperature limit of molten salts with carbonate and chloride salts, but corrosion has been a major challenge (Liu et al. 2016). Other liquids such as molten glass and silicon have been proposed as candidate materials. Glass and silicon can reach temperatures of $1,200^\circ\text{C}$ and $2,400^\circ\text{C}$ respectively, but each introduces

new challenges (Mohan, Venkataraman and Coventry 2019; Amy, Seyf, et al. 2018; Amy, Pishahang, et al. 2021).

Traditionally, liquids have been stored in two tanks, one for the hot liquid and one for the cold. This requires that the containment volume is double the storage material volume. An alternative design is a thermocline tank, which stores the hot and cold liquid in the same tank with a means to reduce internal heat transfer losses (Black and Veatch 2010). Such means include physical barriers and stratification. The capital cost savings of eliminating one tank must outweigh the operational costs of increased heat loss from the hot section to the cold.

One area of research involves filling thermocline tanks with cheaper solids while using a liquid to transfer heat in and out of the tank. This is better understood as a form of solid storage with immersion in the heat transfer fluid than as a form of liquid storage because the majority of the heat capacity is supplied by the solids. Other forms of solid storage operate without constant immersion.

Solid storage has the potential to be less costly than liquid storage if earth-abundant materials are used. The challenge then becomes transferring heat to and from the solid. At larger storage volumes, both the heat transfer rate and amount of useful heat decrease if the process relies only on thermal conduction through the solid.

To avoid this, one option is to arrange the solid material so that fluids can flow through the interstices. Flow is easier to control for shaped materials like firebricks than for bulk materials like crushed rock (Soprani et al. 2019). The heat transfer fluid may make direct contact or flow

² Calculated from “DOE Global Energy Storage Database” (U.S. Department of Energy).

in pipes for indirect heat transfer. As with thermocline tank systems, solid storage designs need to account for internal losses due to temperature gradients during charge or discharge. Additionally, solids can break down over time due to thermal cycling. This damage can be managed with controlled heat transfer rates and material selection. Thermal cycling can also cause settling of loose solids to the bottom of the container, placing stress on the container when it cools (Flueckiger, Yang and Garmiella 2013).

Another solid storage option uses particles stored in tanks along with particle-compatible heat exchangers (Ma, Ruichong and Sawaged 2017). Unlike solids in other forms, particles can be moved around readily, which makes it possible to separate the design of the heat storage component from the design of the heat transfer process. If the solid storage component is not required to do both, the heat exchanger can be sized independently of the system's energy storage capacity to reduce total system cost. Particles can be moved by conveyors or through fluidization. Fluidization involves blowing gas under the particles and lifting them such that they move like a fluid. Fluidization has been used for decades in some combustion and chemical processes. As with liquid storage, particles can be stored in two tanks or a single tank.

Latent heat storage

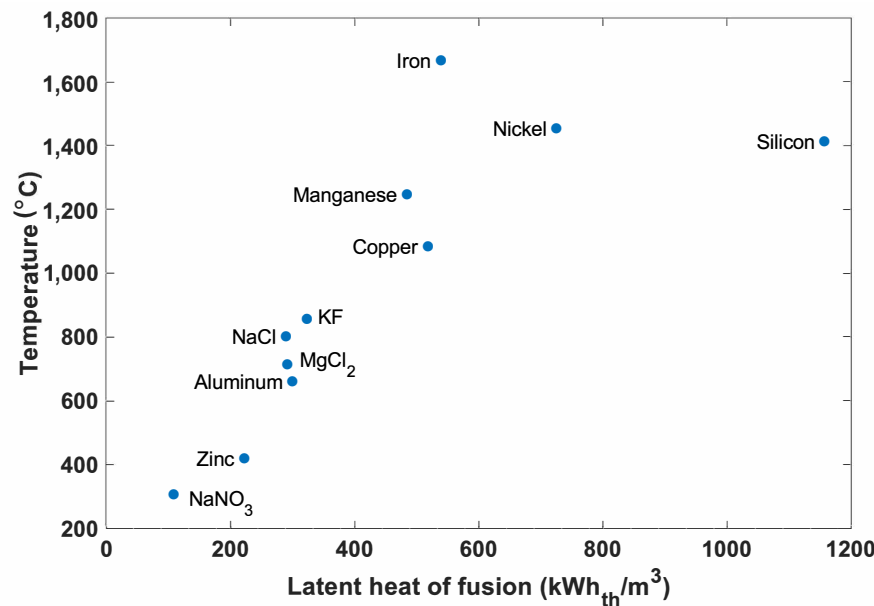
As we have already noted, latent heat storage utilizes a phase transition, hence the name “phase change materials” (PCMs). Most PCMs rely on solid–liquid transitions. Liquid–gas and solid–gas transitions are not practical because the large difference in volume creates significant engineering challenges and costs. Solid–solid transformations either occur at low temperatures or have relatively low latent heats—less than 25% of the latent heat of metal-based

PCMs undergoing solid–liquid transitions (Nishioka et al. 2010; Fallahi et al. 2017). A PCM can store additional heat as sensible heat in its liquid and solid phases.

In the simplest case, a single material such as a metal alloy undergoes phase transition to absorb or release heat. A mixture of materials can also be used to reduce cost or lower the high melting point of a cheap material such as silicon. Reducing the melting temperature is desirable for lower-temperature systems because it reduces costs associated with high-temperature tolerance. At a specific ratio of the constituent materials, a mixture is eutectic, which means that the mixture undergoes phase change at a single temperature. Non-eutectic mixtures undergo phase change over a temperature range within which solid and liquid phases co-occur. Figure 4.4 shows several options for PCMs and compares their melting temperature to energy density.

Since PCMs solidify as they release heat, they cannot flow like the liquids used for sensible heat storage. For this reason, heat transfer for PCMs presents challenges similar to those for bulk solids used in sensible heat storage. There are several potential engineering solutions. Some designs embed heat exchangers into the PCM and pump heat transfer fluids through the assembly. Filler materials with high thermal conductivity, such as metal fibers, can be added to the PCM to improve heat transfer rates (Lin et al. 2018). The PCM can be encapsulated so that a heat transfer fluid can flow over the PCM without mixing or reacting with it (Wickramaratne et al. 2018). An interesting variation on encapsulation involves the use of miscibility gap alloys, which embed a PCM inside a matrix of a different material instead of in individual capsules (Sugo, Kisi and Cuskelly 2013). The bulk encapsulation process could be cheaper than individual encapsulation. For example, aluminum can be embedded in a

Figure 4.4 Latent heat materials



Comparing potential phase change materials by their melting temperature and latent heat of fusion.

graphite matrix and copper can be embedded in an iron matrix (Reed et al. 2019; Sugo, Kisi and Cuskelly 2013).

Beyond heat transfer, other design concerns include cycle life, component segregation for multi-component materials, and undesired reactions with containment materials (Myers and Goswami 2016; Fernández et al. 2017). Another challenge in some systems is volume expansion during melting or solidification. This can introduce stresses that cause the containment vessel to fracture over time (Datas et al. 2016).

Figure 4.5 shows cost estimates for several sensible and latent heat storage options. The estimates are based only on direct material costs to provide a general comparison. Assumptions used to generate this figure can be found in Appendix B.

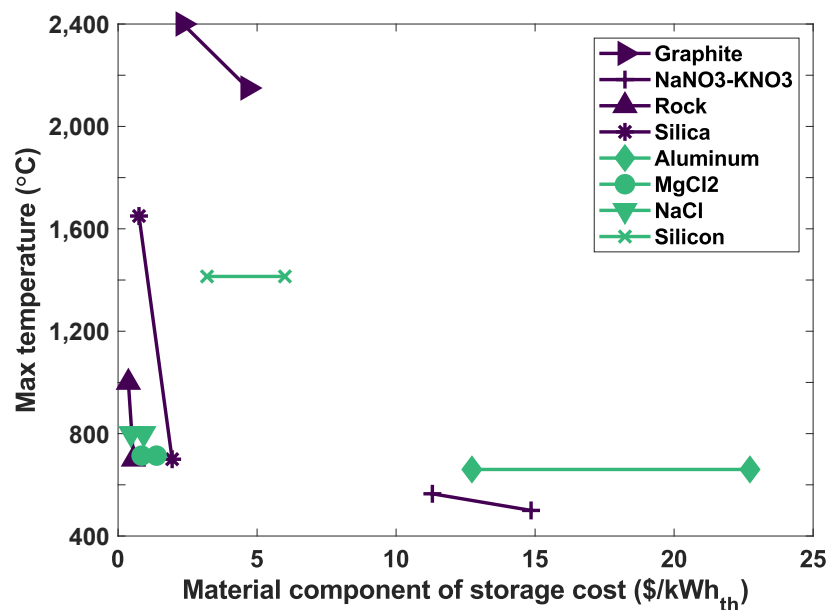
In addition to grouping materials by the heat storage mechanism they use (i.e., sensible vs. latent heat), materials can be classified by their

thermal and mechanical properties, and by other characteristics such as toxicity and reactivity with container materials. While there is flexibility in selecting storage materials, this design choice involves trade-offs that affect the rest of the system in terms of its ability to achieve low cost per unit of energy with acceptable efficiency and discharge power cost.

Containment and insulation

Containment and insulation are integral parts of the storage system. Higher temperatures can increase the probability of containment failure through mechanisms such as corrosion and creep. Reliable containment is necessary so that the system can last hundreds or thousands of cycles over a plant's lifetime. Without reliable containment, leakage of storage materials or heat transfer fluids would lead to downtime and necessitate potentially challenging repairs for some designs. Compatibility between the storage and containment materials can be system specific.

Figure 4.5 Material temperature vs. storage cost



Sensible heat materials (purple) are shown with fixed material cost and variable maximum operating temperature. Latent heat materials (green) are shown at melting temperature with a range of material costs. The figure does not show cost estimates for materials that utilize both sensible and latent heat.

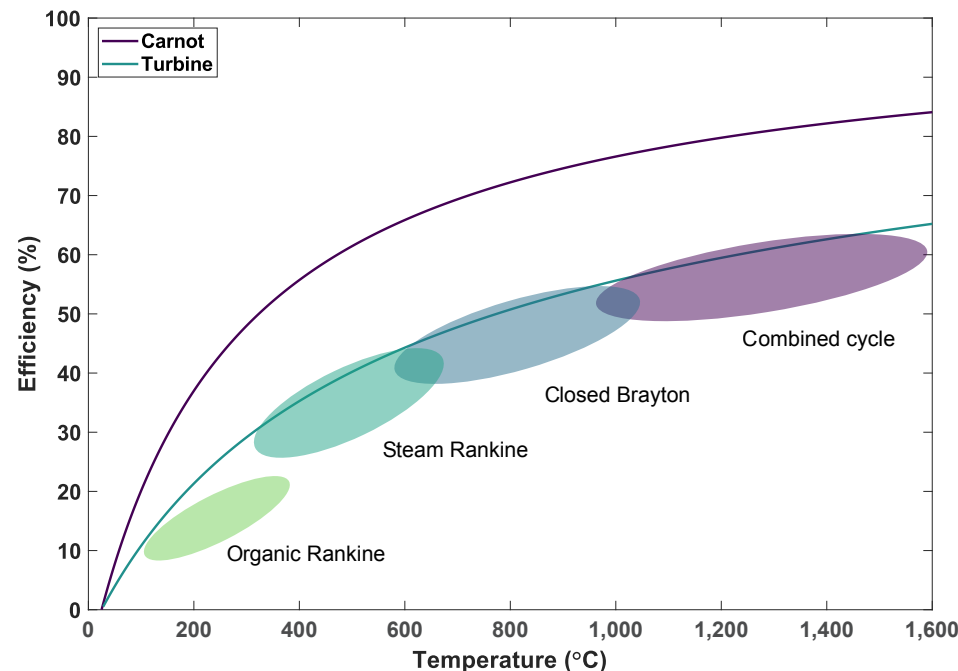
Insulation is a key factor in setting the self-discharge rate. For reference, current molten salt tanks lose roughly 1% of stored heat per day (Sioshansi et al. 2009). Although this may seem high relative to other technologies, a constant heat loss rate of 1% per day leaves about 85% of total capacity after two weeks. Besides insulation, two other important factors are the ratio of the container's surface area to its volume and the temperature of the storage material. The larger the system, the smaller its surface area relative to its thermal mass. This results in lower rates of heat leakage and makes insulation more cost-effective.

In sensible heat storage systems, heat loss reduces the amount of energy stored and the temperature of the medium. Lower temperatures reduce discharge efficiency. In latent heat storage systems, energy capacity will be lower, but the temperature will stay constant provided that the PCM has not completely solidified.

That may be beneficial for maintaining discharge efficiency, but the temperature difference to the ambient environment maintains a higher self-discharge rate. In both cases, the storage medium can be heated above the designed discharge temperature to offset predicted self-discharge losses, assuming the system can tolerate higher temperatures.

High-temperature insulation can be expensive—it is sometimes 10 or 100 times more costly than fiberglass insulation, which is typical for lower-temperature applications. Therefore, high-temperature insulation is usually limited to the hottest sections of the system. As the temperature decreases away from the inner layers, lower-cost materials such as aluminum silicate and mineral fiber can be utilized. Instead of air within the insulation, inert gases such as nitrogen and argon can be used to reduce oxidation, which can degrade insulation materials.

Figure 4.6 Approximate efficiencies of heat-to-electricity technologies plotted against Carnot efficiency



The line labeled “Turbine” is an estimate of realistic efficiency potential for technologies that involve heating up compressible fluids (Henry and Prasher 2014).

In high-temperature systems, radiative heat loss will also be a concern. One option that has been suggested involves low-emissivity coatings using metallic films (Robinson 2018). Low-pressure environments or vacuum-insulated panels have been suggested as means to improve thermal insulation by reducing convective heat transfer (Robinson 2018). While such panels are used in buildings, reliability may be a challenge for hotter structures.

As a fraction of system cost, insulation costs can be quite significant. This can make high-temperature heat storage materials less attractive despite their low costs. According to some estimates from the literature, insulation costs can account for about half of the total energy capacity cost of TES systems (Amy, Seyf, et al. 2018; Ma, Davenport and Zhang 2020). This suggests that lower-cost production methods

or cheaper insulation alternatives are areas for future research.

4.3.3 Discharging: Heat to electricity

In the heat-to-electricity conversion step, higher temperatures yield higher efficiencies as seen in Figure 4.6, although further efficiency gains become incremental at very high temperatures (beyond roughly 1,200°C).

Still, one reason to go to high temperatures is to enable higher rates of radiative heat transfer, which is crucial for some solid-state energy conversion devices. In addition to efficiency, key metrics are cost, flexibility, and technical readiness. Flexibility encompasses startup time and cost, ramp rates, minimum load, and part-load efficiency. For purposes of this study, we assume that future TES systems (2050 timeframe) will be sufficiently flexible to

Table 4.1 Comparison of heat-to-electricity conversion methods

| Power block | Current | | | Alternative | |
|----------------------------------|---------------------------|----------------------|---------------------------------------|--|--|
| | Steam turbine | Air Brayton turbine | Combined cycle | Closed Brayton | Solid-state ^[1] |
| Technology maturity | Mature | Mature | Mature | Early commercial pilots, historical experience | Lab and small scale |
| Capital cost (relative) | High | Moderate to high | High | Moderate to high | Moderate to low |
| Operating cost (relative) | High | Medium | Medium | Medium | Low |
| Maximum temperature | 600°C | 1,500°C | 1,500°C | 800°C ^[2] | >1,500°C |
| Efficiency | 30%–45% | 30%–45% | 50%–63% | 45%–55% | 15%–60% |
| Characteristics | Slow startup time (hours) | Fast response (mins) | Moderate response time (mins – hours) | Fast response time (mins) | Fastest response time (secs); lacks rotational inertia |

Alternative technologies have the potential for reduced capital and operating costs, but they have not been demonstrated yet. [1] “Solid-state” encompasses several technologies: thermoelectric, thermo-photovoltaic, and thermionic generators and electrochemical heat engines. [2] Value for supercritical CO₂; the exact value will depend on the gas and thermodynamic cycle used.

warrant excluding these considerations from the modeling analysis presented in Chapter 6. The value of flexibility depends on factors beyond the boundary of a storage plant. Table 4.1 compares currently dominant thermal power conversion technologies and alternative options that are at various stages of development.

Steam Rankine cycle

The steam Rankine cycle works by pumping and heating water, and then expanding the hot, pressurized steam over turbine blades. This turns a shaft which is connected to an electric generator. The steam is then condensed before repeating the cycle. Modifications to the basic steam Rankine cycle, such as superheat, reheat, and regeneration, are commonly used to increase efficiency. Additionally, plants can be designed to operate with subcritical,

supercritical, or ultra-supercritical steam.³ Higher pressures and temperatures require more expensive materials. Steam temperatures can be as high as 620°C and research is ongoing on systems that reach 700°C. For reference, the maximum operating temperature of nitrate molten salts currently used in concentrated solar power systems is about 550°C.

If the power plant has been shut off for a period of time, such that components have cooled down, components are heated gradually over several hours before generating power. This reduces thermal stress, which can shorten the lifetime of components. Electrical trace heaters and other measures can reduce the startup time (Flake 2016; International Renewable Energy Agency 2019). Once running, steam plants can adjust power output faster, at a rate of around 2% of nameplate capacity per minute (International Renewable Energy Agency 2019).

³ A supercritical fluid exists in a range of temperatures and pressures where it is not distinctly a gas or liquid. Supercritical fluids have useful properties such as higher density, which increases the power density of an electricity generation system.

Overall, steam Rankine cycles use mature technology and can achieve 30%–45% heat-to-electricity conversion efficiency (Beér 2007).

Open Brayton cycle

In an open Brayton cycle, a gas is drawn from the atmosphere, compressed, heated (via combustion) to temperatures that are typically in the range of 1,000°C–1,500°C, and expanded before being exhausted back to the atmosphere. Since the gas, called the working fluid, is drawn from and exhausted to the atmosphere, the only practical working fluid is air. Although various open Brayton cycle designs are possible, the most common one involves axial compressors and expanders. In this case, the power from the expander is used to rotate the compressor and generator.

The Brayton cycle or slight variations of it underlie combustion turbines that have generated power for decades. Most gas turbines today combust natural gas directly in the working fluid to provide heat, although oil and other fuels can be used.⁴ Less common are indirectly fired open Brayton turbines, which use a heat exchanger to supply heat from coal, biomass, or other fuels with high ash content that would otherwise damage the equipment. Work is ongoing to adapt turbines for non-combustion applications, driven by interest from the nuclear and concentrated solar power communities (Forsberg, McDaniel and Zohuri 2021; Brayton Energy 2011).

Open Brayton turbines have much faster start up and response times compared to steam turbines given their lower thermal inertia; some can start up in less than 10 minutes and have

ramp rates around 10% per minute (International Renewable Energy Agency 2019).

Improvements in materials and blade cooling have allowed for higher peak temperatures in combustion turbines, which increases efficiency. The limitation for TES is building a heat exchanger that can withstand high pressure and temperature to deliver desired efficiencies. Demonstrations have been limited to around 1,000°C (Zhang et al. 2018).

The exhaust from a turbine (or multiple turbines) can be hot enough to heat steam in a Rankine cycle; this configuration is called a combined cycle power plant.⁵ Compared to standalone natural gas turbines, which have efficiencies around 30%–40%, a combined cycle power plant can reach 50%–62% efficiency (Power Engineering 2018). However, start-up time and overall flexibility are worse for a combined cycle plant than for a standalone turbine due to the constraints of the steam Rankine cycle.

Alternative technologies

Several alternative technologies are not necessarily new, but their lower performance to date or their early stage of development has limited their use for broad applications in power generation. With additional research, development, and deployment, they may have the potential to become more cost-effective than or to be used with today's technologies.

Closed Brayton cycle

Although closed Brayton cycle turbines are uncommon today, they were initially preferred over open cycle gas turbines in the 1950s

⁴ “Gas turbine” here refers to the natural gas in a combustion turbine rather than to the gas that is the working fluid. Additionally, “turbine” can refer either to the entire gas turbine unit, which includes the compressor, combustor, and expander, or just to the expander. We use “turbine” to refer to the entire unit and “expander” to refer to the component.

⁵ The high- and low-temperature cycles are commonly referred to as the topping and bottoming cycles.

because the internal combustion of low-quality fuel would ruin turbines (McDonald 2012). In a closed Brayton cycle, the working fluid is reused—it is cooled down after the expander and then returned to the compressor. To increase efficiency, heat is transferred from the low-pressure expander exhaust to the high-pressure gas before external heat is supplied—this process, which is known as recuperation, reduces external heating requirements. Closed Brayton cycles allow for the use of working fluids other than air. Another advantage of these designs is that the background pressure—i.e., that of the low-pressure gas—can be increased to raise the gas density, which in turn increases the power density of the system and reduces costs.

Early designs used either air, nitrogen, or helium as the working fluid. Compared to using air, nitrogen reduces oxidation which extends the lifetime of components. Still, like open Brayton cycles, air and nitrogen require high temperatures (above 1,000°C) for high efficiency.

Helium is attractive for its favorable heat transfer characteristics and inertness for potential coupling with nuclear reactors. However, there are challenges with helium systems such as leakage and unwanted vibrations that can cause damage. Historic experience with helium turbines and further details about the challenges of this technology are described by McDonald (2012). One concern with helium is long-term supply adequacy: The current supply is expected to last around 100 years, although new discoveries would extend that estimate (Bradshaw and Hamacher 2021; Glowacki, Nuttall and Clarke 2013). Although a 100-year supply would extend beyond the 2050 timeframe of this study, most helium is co-produced with natural gas extraction, which is expected to decline, thus introducing uncertainty in current estimates. Given this concern, the benefits of helium may not outweigh its

disadvantages when compared to other working fluids.

Currently, supercritical carbon dioxide ($s\text{CO}_2$) has been the focus of much research. There is potential to achieve thermal efficiencies of 50% or greater with peak temperatures around 700°C and work is ongoing to increase the temperature (ARPA-E 2019). There has been interest in developing this cycle from the nuclear community (for high-temperature reactors) and from the concentrated solar power community (for increased efficiency). There is also interest in using $s\text{CO}_2$ in fossil fuel-based power plants, for which some designs include integrated carbon capture. The idea for a $s\text{CO}_2$ power cycle has been around since the mid-20th century; however, there have been challenges in developing materials and components that can withstand high temperature and pressure (U.S. Department of Energy 2015). There is also a version where the $s\text{CO}_2$ becomes liquid for the compression stage of the power cycle, in which case it is a $s\text{CO}_2$ Rankine cycle.

Since work on developing $s\text{CO}_2$ technology is ongoing and there are few commercially operational facilities, current estimates of cost are uncertain. In its SunShot program, the U.S. Department of Energy (DOE) has set a cost target of \$900/kW_e with 50% heat-to-electricity efficiency and air cooling at 40°C (Mehos et al. 2016). Projects that use $s\text{CO}_2$ are being built beyond the benchtop scale. One company has delivered electricity to the grid from a 50-MW_{th} combustion-based $s\text{CO}_2$ demonstration plant in Texas using a variation known as the Allam-Fetvedt cycle (Patel 2021). Another company offers an 8-MW $s\text{CO}_2$ Rankine system designed for waste heat recovery; this system has been factory tested and one unit is slated for commissioning in 2022 (Held 2014; Siemens Energy 2021). Although early applications of $s\text{CO}_2$ cycles may rely on combustion, much of the underlying knowledge and experience will be

transferrable to TES and other non-combustion applications.

Solid-state thermal energy converters

Unlike turbines, this class of devices avoids the need to simultaneously contend with large thermal fluxes and mechanical forces (Henry and Prasher 2014). This opens the door to a broader variety of materials.

Thermoelectric generator

The Seebeck effect, which underlies thermoelectric generators, has been known for over two centuries. Thermoelectric generators have found use in applications including satellites and rovers, which use heat from nuclear material. This technology is well suited for applications that have volume constraints and require long lifetimes with minimal maintenance. However, efficiency has been limited to a range of 1%–15% due to trade-offs inherent to these devices' material properties (Henry and Prasher 2014; Zhang et al. 2017). Unless efficiency can be improved significantly, thermoelectric generators are unlikely to be a primary conversion method for TES.

Thermophotovoltaics

Thermophotovoltaics (TPV) are photovoltaic cells that are designed to convert photons from a thermal emitter—instead of the sun—into electricity. The thermal emitter is usually hotter than 1,000°C and has a different wavelength distribution than the sun. Accordingly, TPV cells are designed differently than solar PV cells. Recent work has demonstrated efficiencies greater than 40% and pathways to greater than 50% efficiency (LaPotin et al. 2022; Omair et al. 2019). These pathways involve advances in multi-junction cells, spectrally selective emitters, and back-surface reflectors to increase efficiency, as well as reusable substrates for lower cost manufacturing (Amy, Seyf, et al. 2018). Given similarities to solar photovoltaics, existing research and fabrication methods can be

leveraged for faster progress. A study from 2003 estimated TPV costs at around \$3 per watt (Palfinger et al. 2003) and projected future costs around 30 cents per watt. The latter projection is supported by similar estimates from newer studies (Seyf and Henry 2016).

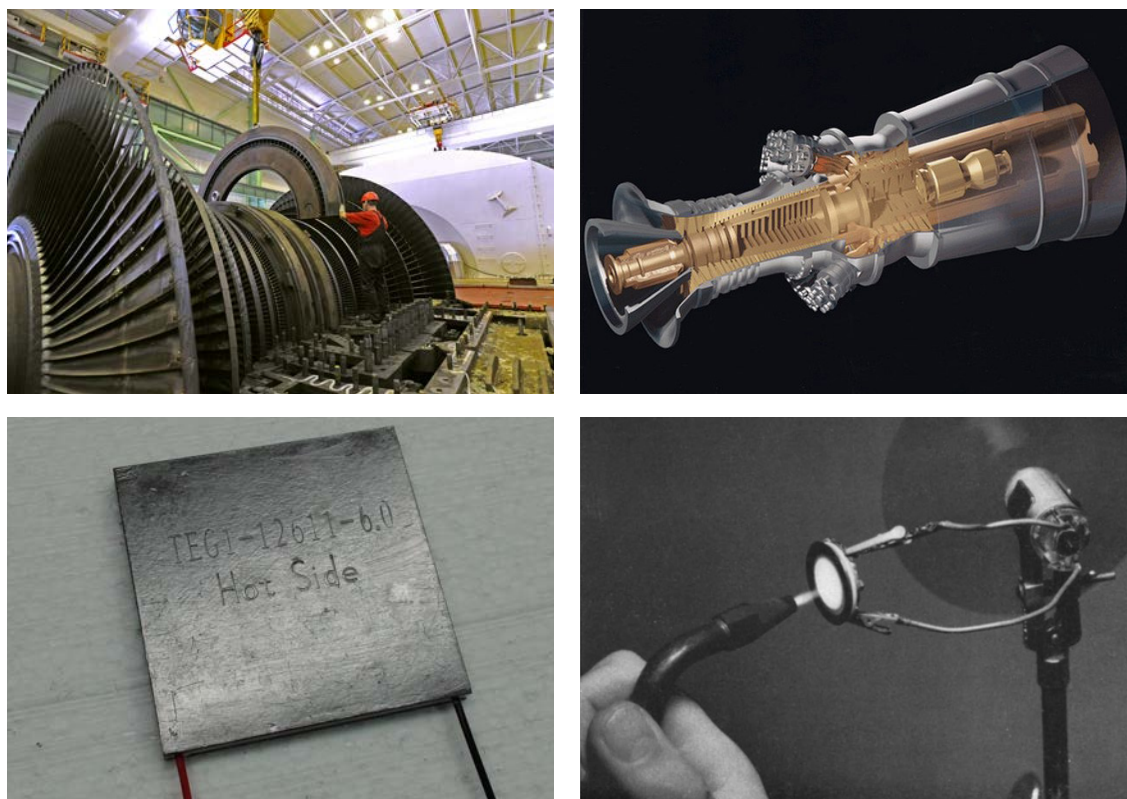
Electrochemical heat engine

Electrochemical heat engines, often called thermally regenerative electrochemical systems, use temperature-driven changes in electrochemical potential to generate electricity. Some systems cycle a battery between two temperatures; however, these designs have achieved low performance to date (Lee et al. 2014; Linford et al. 2018). Others use a heat-driven pressure gradient to pass ions through an electrolyte (Limia et al. 2017). Recently, a new class of continuous electrochemical heat engines was introduced that could enable greater efficiency by decoupling thermal and electrical conduction pathways (Poletayev et al. 2018; Henry 2018). In one version, heat is supplied to a high-temperature electrolyzer that generates hydrogen, and a lower-temperature fuel cell converts the hydrogen into electricity. The devices can be assembled in a closed loop with heat exchange between the chemical products of both devices to increase efficiency. Some electricity from the fuel cell powers the electrolyzer. With a supply of external heat to reduce the electrical demand of the electrolyzer, net electrical output is positive with efficiencies estimated around 10% (Poletayev et al. 2018). Different symmetric reactions can be used, so that devices can be designed for low- or high-temperature heat sources.

Thermionic converter

Thermionic converters have a hot cathode and a cold anode. Heat is applied to the cathode which causes electrons to be emitted; the electrons then travel—either through a vacuum gap or through a vapor—to the anode. The electron balance is restored by electrically connecting the cathode and anode, which

Figure 4.7 Images of heat-to-power technologies



Clockwise from top left: steam turbine, gas turbine, thermionic converter, thermoelectric generator.
Images: Seetenky (2007), U.S. Department of Energy (2006), Gerardtv (2010), and Chao (2016).
For scale, the gas turbine is several meters in length, and the thermoelectric generator is a few centimeters in length.

powers a load. Active research efforts during the latter half of the 20th century focused on using thermionic converters with nuclear power, particularly for space applications (Khalid et al. 2016). Renewed research on thermionics will need to address challenges around materials and fabrication before this technology can see use with TES (Go et al. 2017). Commercialization efforts, typically with fuels as the heat source, for applications such as remote or portable power and combined heat and power are ongoing (Temple 2020).

Figure 4.7 shows what a few of these heat-to-electricity technologies look like as built.

Other technologies

Several other heat-to-electricity conversion technologies are in use commercially or are the subject of active research. At present, however, these technologies seem unlikely to be competitive with the options described above as the primary conversion method in TES applications. Examples of technologies in the research phase are pyroelectrics and thermoacoustics (Pandya et al. 2019; Timmer, de Blok and van der Meer 2018).

Systems that use an organic Rankine cycle are used commercially for waste heat recovery and geothermal applications. They are designed to generate power from low-temperature heat,

Table 4.2 Three near- and long-term strategies for TES

| Strategy | Reutilization of power plant infrastructure | Increased efficiency at medium temperatures | High-temperature systems |
|--------------------------|---|---|------------------------------------|
| Readiness | Today | Low - moderate risk < 10 years | Moderate - high risk > 10 years |
| Power conversion | Steam turbine | Closed Brayton e.g., sCO ₂ | Combined cycle, solid-state |
| Storage materials | Crushed rock, molten salt | PCM e.g., metal alloys | Silicon, silica, graphite |
| Max temperature | 650°C | 850°C | 1,200°C |
| Efficiency | 30%–45% | 40%–55% | 50%–60+% |
| Response time | mins - hours | mins | sec - mins |
| Minimum load | 10%–50% | 10%–50% | ~1%–40% |

so their efficiency is relatively low: typically 10%–20% (Quoilin et al. 2013). This precludes the use of an organic Rankine cycle as the primary discharge method in a TES system, though such systems can be used in conjunction with other technologies.

Stirling engines are technologically mature and have the potential to achieve high efficiency. This makes them attractive for small scale, distributed power generation. However, the cost per unit of power remains high compared to Brayton turbines or combined cycle plants of similar thermal efficiency.

4.4 TES systems

The technologies discussed so far can be assembled in a variety of combinations to form a complete system. In weighing trade-offs, some designs balance cost, performance, and feasibility better than others. A review of academic papers and commercial efforts to develop thermal energy storage shows that systems tend to follow one of three strategies:

- 1) Reutilization of power plant infrastructure
- 2) Increased efficiency at medium temperatures
- 3) High-temperature systems

We have listed these three strategies in order of decreasing technical maturity. As noted in

Table 4.2, technologies from each strategy will mature over time, providing a role for TES from the present day to beyond 2050.

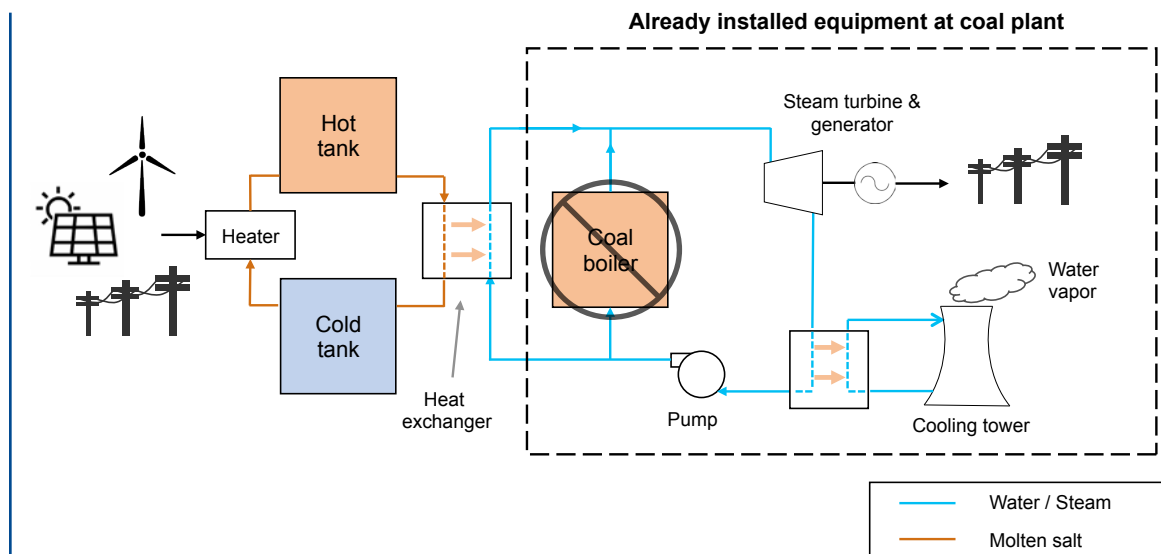
4.4.1 Reutilization of power plant infrastructure

A number of power plants, particularly coal-fired ones, are being retired before the end of their expected lifetime because they can no longer run economically or meet environmental standards. This is happening today in industrialized regions like the United States and European Union. Early retirements are also likely in countries with younger power plant fleets, such as China and India, as they try to meet decarbonization targets.

There is an opportunity to reuse these power plants for thermal energy storage. As shown in Figure 4.8, thermal storage and a heat exchanger to generate steam would replace the combustion boiler. Resistive heaters or heat pumps would draw (low-/zero-carbon) electricity from the grid to charge the system. The existing turbine, pumps, cooling tower, and other equipment would be reused to generate electricity without emissions.

At first glance, the efficiency of steam Rankine cycles seems too low to make the system economical. However, it might be possible to acquire existing plants at low cost if the

Figure 4.8 Schematic for steam turbine retrofit with TES



Simplified diagram of how a thermal storage system can reuse equipment at a steam turbine power plant. In this example, two-tank molten salt is used; cheaper, alternative storage methods are available.

alternative is early retirement. Retirement could have negative value to the plant owner due to decommissioning costs net scrap value. In addition, existing grid connections can be reused. Lastly, with peak temperatures around 600°C, a wide variety of cheap storage materials can be utilized, allowing for lower energy capital cost compared to current, two-tank molten salt storage systems. Together, these factors could allow for economical reuse of fossil fuel-powered steam turbines in regions with high shares of renewable generation.

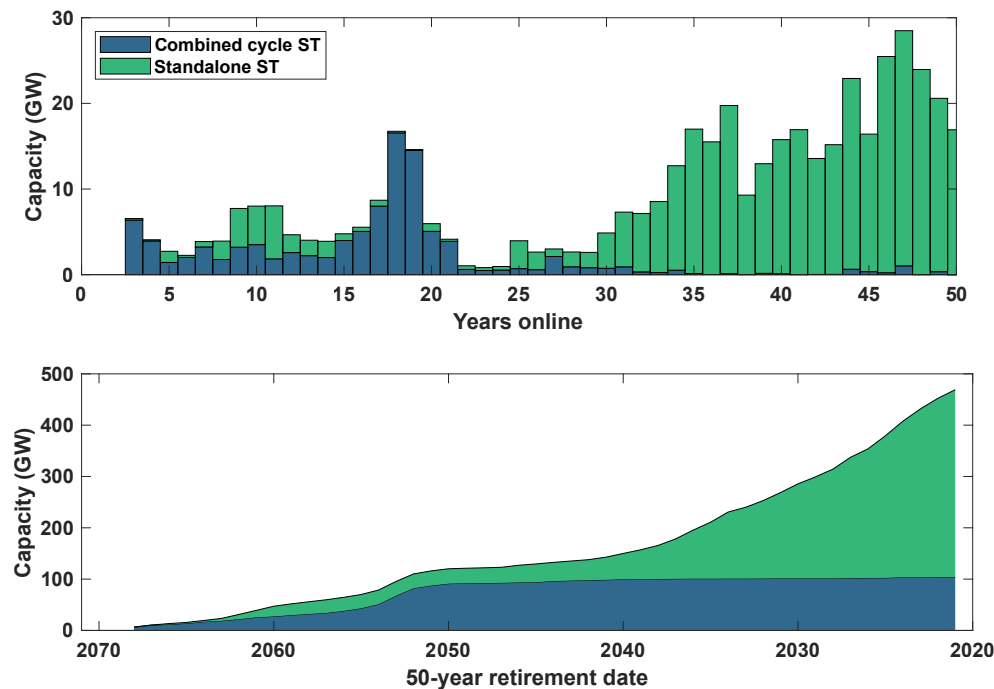
An important consideration is the remaining lifetime of the power plant being repurposed. On average, a steam turbine plant in the United States operates for 50 years (Grubert 2020). Although there is variation between plants based on equipment, operational history, and repairs, this is a useful approximation. Use of steam turbine plants for energy storage could extend or shorten the nominal 50-year lifetime through a combination of lower utilization and more cycling. The top chart in Figure 4.9 shows

the age distribution of installed steam turbine capacity in the United States that is less than 50 years old. The bottom chart shows when that capacity is expected to retire based on a 50-year assumed lifetime. The figure uses data from the U.S. Environmental Protection Agency's 2018 eGRID database and does not consider new capacity additions.

Many U.S. coal plants will reach 50 years of operating life between now and 2040, limiting their potential lifetime as energy storage plants. Steam turbines attached to combined cycle plants could remain available longer since most were built after 2000. Although more detailed analysis is required, the lifetime of these plants, after they are retrofitted with TES, could be extended with targeted repairs.

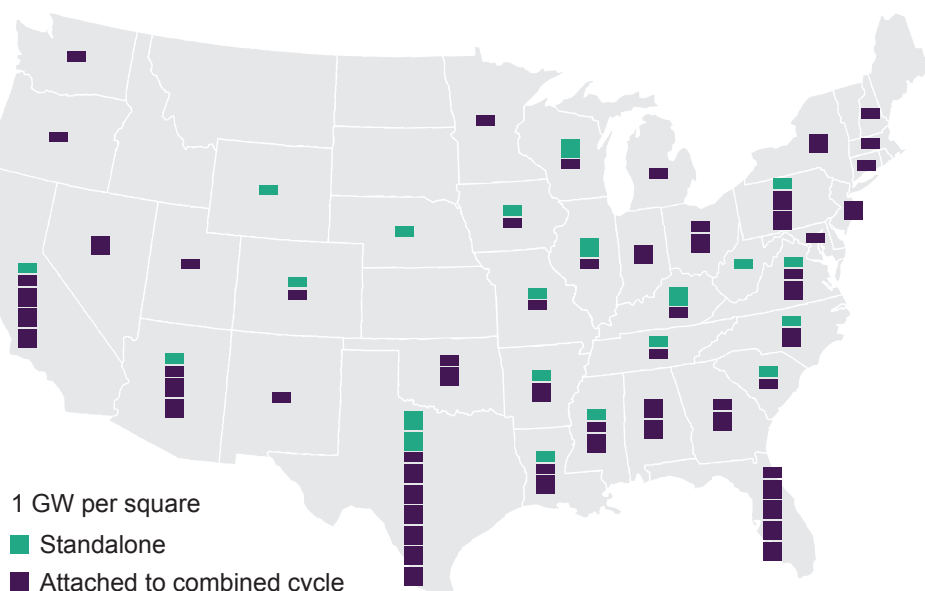
As shown in Figure 4.10, existing power plants are distributed throughout the continental United States, so this strategy is not geographically limited. The window of time to utilize U.S. coal plants is short, given that retrofitted plants

Figure 4.9 Age distribution of U.S. steam turbine capacity



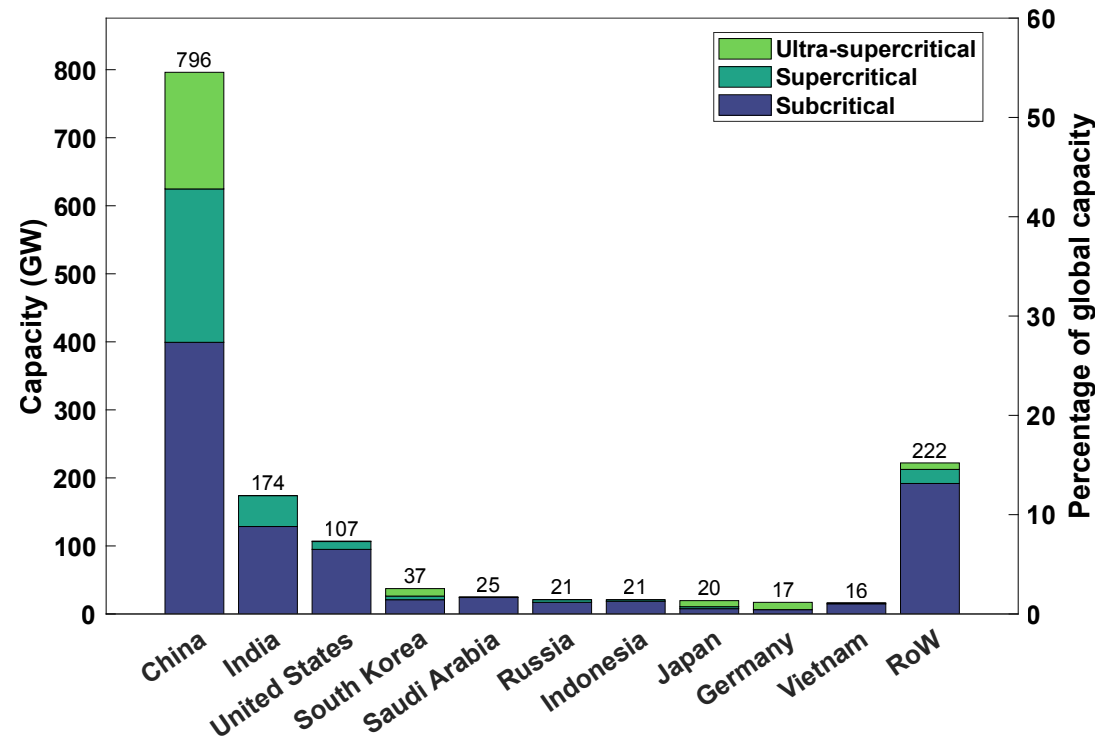
The upper graph shows the age distribution of operational steam turbine capacity in the United States, including standalone turbines (coal, gas, nuclear, solar thermal, etc.) and turbines in combined cycle power plants. The lower graph projects available capacity for future years assuming a 50-year lifetime. Data are from EPA's eGRID 2018 database, so plants brought online after 2018 are not counted.

Figure 4.10 Geographic distribution of steam turbine capacity in the United States



Capacity expected to be available in 2050, using the same data source and assumptions as Figure 4.9.

Figure 4.11 Steam turbine capacity for plants that will be 50 years old or less in 2050 for top-ten countries and the rest of the world (RoW)



The figure includes turbines that are attached to combined cycle gas plants. Calculated from S&P Global Platts database, 2016.

need to have sufficient remaining life to recover costs. Fortunately, the technologies required to implement this strategy are at a high level of technical readiness and could be deployed quickly with public and private coordination. Further, there is relevant experience to guide design from the construction of concentrated solar power plants and the repowering of coal plants as combined cycle power plants.

Internationally, there is a longer window of opportunity because coal plants have been built more recently and continue to be built, particularly in emerging market and developing economy countries. Plans to install new steam turbine capacity, mostly coal-fired, are generally being scaled back as countries reevaluate the economics and environmental impact of

coal-fired electricity (CREA 2021). Figure 4.11 shows the steam turbine capacity that will be less than 50 years old in 2050 for the ten countries with the largest installed base of currently operating plants. The figure does not account for the construction of new plants. In China and India, which currently lead the world in new capacity additions, most new and recently built plants are either supercritical or ultra-supercritical and therefore have typical efficiencies above 40% (Hart, Bassett and Johnson 2017).

Researchers and commercial developers have recognized this opportunity. Designs have been proposed that use phase-change silicon, ceramic packed beds, or rocks to store heat cheaply (Meroueh and Chen 2019; Alumina

Energy 2021; Parnell 2020; GIZ 2020). One company started operating a pilot project in Germany during 2019 that has an energy capacity of 130 MWh_{th} and discharge capacity of 30 MW. The facility uses rocks, resistive heaters, and a steam turbine (Proctor 2019). While it did not repurpose an existing power plant, that is the intent for future projects (Collins 2021).

While some steam turbine retrofit concepts use resistive heating to charge the system, whereas others envision using a heat pump, a steam turbine would still be used to generate electricity. In the United States, the DOE has funded feasibility studies of this concept (Office of Fossil Energy 2020). In Germany, work towards a pilot project is underway (Deign 2019). A heat pump for charging would improve roundtrip efficiency, and lower costs for discharge power would offset some of the increased cost for charging equipment.

Despite this potential, realistically, only some fraction of existing power plants will have sufficient efficiency and flexibility and be in an appropriate location to operate as TES plants. At this point in time, it is unclear how large that fraction is. As an example, one technical challenge will be to modify existing plants and design their thermal storage components such that the repurposed facilities can operate more flexibly than they were originally designed to for purposes of baseload power generation. Otherwise, frequent cycling will shorten plant lifetimes. Solutions can be leveraged from ongoing work to increase coal plant flexibility in response to intermittent renewable generation (International Renewable Energy Agency 2019) and through strategies such as pairing batteries with TES (St. John 2017). Batteries could provide short-duration storage to reduce cycling, and, when longer-duration storage is needed, batteries could provide time for the plant to warm up.

In the future, a strategy of reusing existing power plants may overlap with the third strategy: deploying high-temperature systems. A high-temperature topping cycle could repower a steam plant as a combined cycle plant or run in parallel to (and later replace) a natural gas combustion turbine at a combined cycle plant. Similarly, TES retrofits could function as intermediate storage options until it becomes economical to convert TES steam plants into combined cycle systems that use hydrogen or other carbon-neutral fuels. At that point, the thermal storage components could provide operational flexibility.

4.4.2 Increased efficiency at medium temperatures

Although the definition of “medium temperatures” is ambiguous in the literature, we use it here to refer to approximately 550°C–1,000°C. Heat at these temperatures can drive alternative power cycles, such as closed Brayton cycles, to achieve roundtrip efficiencies in the range of 40%–55%. These cycles can be paired with sensible heat storage materials such as rocks, or with phase change materials like aluminum alloys.

Some proposed systems use sCO₂ Brayton or Rankine cycles for power generation. These cycles can increase efficiency with heat recuperation, as shown in Figure 4.12. With recuperation, less external heat is required and the heat is supplied within a smaller temperature window near the peak cycle temperature. For this reason, latent heat storage is a more obvious match than sensible heat storage for sCO₂ and other systems with similar recuperation. The energy cost for sensible heat storage systems increases when these systems operate over a small temperature range, but sensible heat storage is still an option if the storage materials are cheap enough. For charging, resistive heaters are generally a better match since high-temperature heat pumps rely on sensible heat exchange rather than latent heat.

Figure 4.12 Diagram of recuperated, closed Brayton power cycle

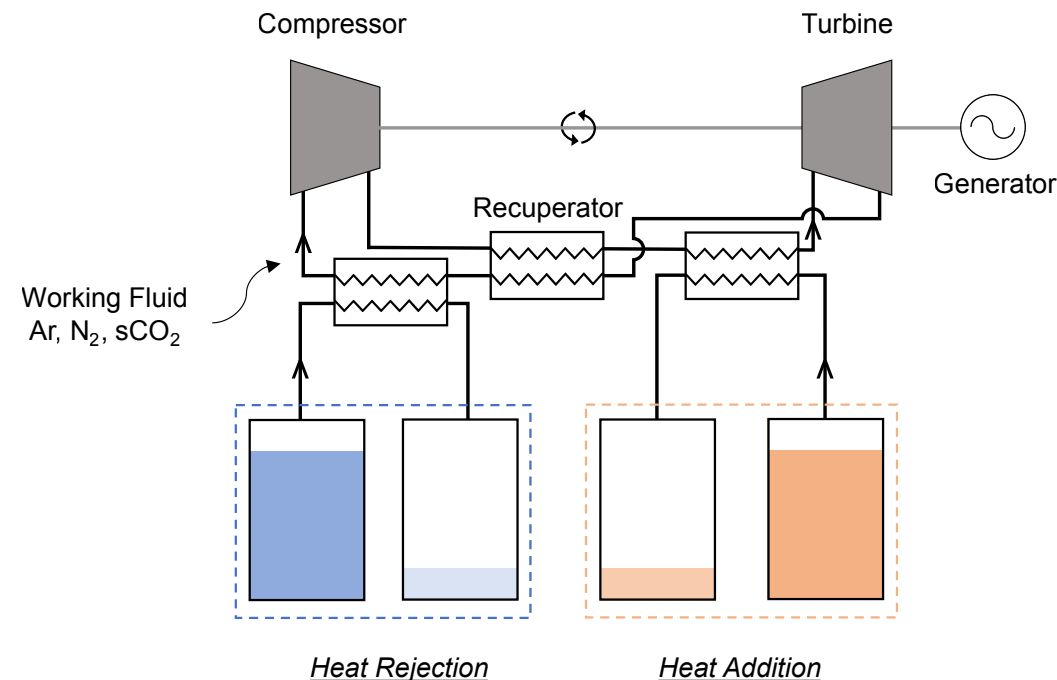


Diagram of recuperated, closed Brayton power cycle commonly used for medium-temperature TES systems (Turchi, Ma and Dyreby 2012; McTigue et al. 2019). A heat pump (not pictured) could charge the hot (dark orange) and cold (dark blue) storage tanks. Heat addition is shown with a two-tank liquid medium although other formats are possible. Heat rejection can be accomplished by air cooling instead of cold storage, which would be favorable for resistively charged systems.

Others have proposed using sCO₂ or non-supercritical fluids in a closed Brayton cycle to discharge the system, and a reverse Brayton cycle (i.e., a heat pump) to charge the system (Laughlin 2017; McTigue et al. 2019). This approach is commonly called pumped thermal energy storage or pumped heat storage. A heat pump system would be similar to the system shown in Figure 4.12 except the positions of the compressor and turbine would be switched as well as the flow direction. For non-supercritical fluids, research has concentrated on the use of inert gases such as helium, argon, and nitrogen for the working fluid. This approach increases the roundtrip efficiency by focusing on improvements to the charging efficiency, which can reduce the delivered cost of electricity. Heat recuperation can be used to increase charge and discharge efficiency. Even with recuperation,

some versions of this power cycle can have a larger temperature range for external heat, making it amenable to latent and/or sensible heat storage.

As mentioned in Section 4.3.1, low electricity prices reduce the benefit of high charging efficiency relative to capital cost for charging power. Additionally, charging efficiency does not affect the amount of storage material needed.

A heat pump can be also used to store thermal energy at sub-ambient temperatures. Cold storage increases the discharge efficiency without requiring the hot storage to be at a higher temperature. The downside to using a heat pump for charging is that it will require an additional set of turbomachinery equipment

Figure 4.13 A sample of high-temperature TES systems with different designs

| | Sensible heat | Latent heat |
|--------------------------|---------------|-------------|
| Turbomachinery | | |
| Alternative technologies | | |

Clockwise from top left: particle storage with combined cycle (National Renewable Energy Laboratory 2018), silicon PCM in container atop a heat exchanger with Brayton turbine (Taylor et al. 2020), silicon PCM with TPV (Datas et al. 2016), liquid silicon with TPV (Amy, Seyf, et al. 2018).

beyond the set used for discharging, which increases capital cost. This additional cost can be mitigated if reversible turbomachinery is developed (ARPA-E 2018).

Some versions of pumped thermal energy storage can use readily available equipment, which reduces commercialization risks. Current efforts to develop sCO₂ power systems range from projects that use lab-scale equipment at kilowatt capacities to megawatt-scale demonstration plants. Since there is more uncertainty about the power block than about the energy storage components of sCO₂ systems, the

current rate of progress indicates that utility-scale deployments are likely to be possible before 2050.

4.4.3 High-temperature systems

This third strategy uses storage at high temperatures, ranging from 1,000°C to 2,400°C, or potentially higher. Temperatures in this range enable the use of combined cycles or solid-state energy converters that can achieve similarly high efficiencies of 50%–60%. Sensible or latent heat is possible with both technologies.

Examples of each type are shown in Figure 4.13.

Turbomachinery-based designs generally limit technical risk to the heat exchanger that connects storage to the turbomachinery and to the energy-related components, for either sensible or latent heat systems. However, technological improvements with respect to attributes such as start-up time and ramp rate may be limited, particularly if a combined cycle system employs a steam Rankine bottoming cycle. By comparison, alternative energy converters, namely solid-state devices, still require R&D to achieve similar efficiencies and cost per power, but they hold potential for better all-around performance. This includes high efficiency even at small scales.

At a systems level, these designs introduce risk in both the storage and discharge components. By comparison, the retrofit strategy can use established technologies for both storage and discharge. Most of the risk of the second strategy lies within the discharge components, although the use of latent heat storage introduces risks as well.

Figure 4.13 does not provide an exhaustive sampling of high-temperature systems. The variety of available designs suggests that, given the technical uncertainties, no dominant design has emerged yet. The system shown in the top left of the figure uses particle storage with a fluidized bed heat exchanger to power a combined cycle. The system at the top right uses the latent heat of silicon with an air Brayton turbine. A version of this system has been deployed for a commercial pilot project in Australia (the same one mentioned in Box 4.1). However, that project incorporates gas heating, so it does not represent a pure storage technology (Power Technology 2019). With further development, combined cycle configurations of this system are possible to boost efficiency. The system shown at the bottom right uses phase change silicon alloys with thermionic-enhanced thermophotovoltaic cells (Datas et al. 2016). Its

modular design may prove useful to overcome scaling challenges. The system at the bottom left uses sensible heat from liquid silicon at a peak temperature of 2,400°C to power thermophotovoltaic cells.

High-temperature systems face several challenges. As one example, metallurgical-grade silicon is a common choice in high-temperature systems because it melts at a high temperature (1,414°C) and is inexpensive (Figure 5.5). Silicon expands as it freezes, however, which creates stresses in the container. Over time, these stresses can cause cracks and lead to containment failure (Jiao et al. 2019; Moriarty 2019). One solution is to alloy silicon to reduce this expansion; however, the alloy elements may be expensive even in small proportions (Jiao et al. 2019). Additionally, chemical reactions can occur between the container and the silicon or silicon alloys—for this reason, ensuring low reactivity has been a topic of research (Hoseinpur and Safarian 2020; Amy, Pishahang, et al. 2021).

One design (not pictured) uses long, horizontal graphite blocks laid in parallel to store heat around 2,000°C and generates electricity with TPV panels (Gilbert 2021). Heat is transferred radiatively to the TPV panels as they slide between the blocks. Fewer moving parts and the use of sensible heat simplify the system design. As with all bulk solid storage systems, a trade-off of this design is that, under partial discharge conditions, thermal gradients will develop within or between the blocks and cause some energy loss.

Another challenge arises from a phenomenon known as “creep,” which refers to the deformation of a material under stress even at levels of stress that are significantly below the material’s breaking strength. High temperature accelerates creep, leading to problems such as imperfect seals and changes in expected failure mode.

Table 4.3 System cost estimate

| Technology | Units | Crushed rock & sCO ₂ | | | Liquid silicon & multi-junction TPV | | |
|---------------------------------|----------------------|---------------------------------|------|------|-------------------------------------|------|------|
| Cost scenario | | High | Mid | Low | High | Mid | Low |
| Charging capital cost | \$/kW _e | 3.3 | 3.3 | 3.3 | 24 | 24 | 24 |
| Discharging capital cost | \$/kW _e | 1,226 | 736 | 494 | 880 | 498 | 362 |
| Storage capital cost | \$/kWh _{th} | 9 | 5.4 | 2.9 | 26 | 16 | 6.4 |
| | \$/kWh _e | 20 | 11 | 5.3 | 52 | 30 | 11 |
| Charge efficiency | % | 99.5 | 99.5 | 99.5 | 99.5 | 99.5 | 99.5 |
| Discharge efficiency | % | 46 | 50 | 55 | 50 | 54 | 57 |
| FOM discharge | \$/kW-yr | 3.9 | 3.9 | 3.9 | 3.6 | 2.1 | 1.5 |
| VOM | \$/kWh _e | 0 | 0 | 0 | 0 | 0 | 0 |

Key metrics for two illustrative TES systems. FOM and VOM are fixed and variable operation and maintenance costs, respectively. The storage cost in \$/kWh_e is calculated by the cost expressed as \$/kWh_{th} divided by the discharge efficiency. The crushed rock system follows the strategy of increasing efficiency at medium temperatures. The liquid silicon system uses high temperatures to increase efficiency.

In the trade-off between cost, performance, and technology readiness, the high-temperature strategy picks the first two. Achieving increased efficiency and flexibility while maintaining low storage cost requires high-temperature storage and/or new power conversion devices. On the structural side, more research is needed to understand material performance at high temperatures and to ensure reliability for the intended lifetime of the plant.

4.5 Cost estimates

Table 4.3 shows illustrative values for key metrics for two representative TES systems. The full set of metrics is given in Table 6.3. Data from published papers and reports were used directly or as parameters to develop cost estimates. Although some demonstration plants have been built, no utility-scale TES facility has been built yet. At this early stage, significant uncertainties apply when projecting costs and performance to 2050. This study makes several assumptions, for example with respect to learning rates for power conversion devices. Details of the cost estimation process are provided in Appendix B Table B.3.

Crushed rock storage with a sCO₂ power block is representative of systems that follow the strategy of increasing efficiency at medium temperatures. Liquid silicon storage with TPV cells is representative of systems that follow the high-temperature strategy. Although neither system is technologically ready today, the crushed-rock-and-sCO₂ system was chosen as the representative TES technology in the capacity expansion model because of its lower technology risk.

The estimates in Table 4.3 show that there is potential for TES to achieve a cost target of less than \$20 per kWh_e for long-duration storage technologies.

One of the differences between the two systems is the trade-off they make between storage cost and efficiency. The liquid silicon system has higher storage cost due to higher temperatures, which enable slightly higher efficiency. We expect lower discharge power costs for a futuristic TPV-based system, as compared to a turbomachinery-based system, because of TPV cells' modularity and manufacturing process (Kavlak, McNerney and Trancik 2018).

Figure 6.7 in Chapter 6 (Modeling High VRE Systems with Storage) compares the energy and power costs of TES to those of other storage technologies. TES has energy and power costs similar to those for other proposed long-duration storage technologies.

4.6 Conclusion and key takeaways

Thermal energy storage (TES) is a promising option for long-duration energy storage because heat can be stored in cheap materials. The main challenge for this class of technologies is converting heat back into electricity efficiently and cost-effectively. This chapter describes three approaches that address this challenge: repurposing existing steam turbine power plants, using alternative power cycles, and developing high-temperature materials and power conversion devices to reach higher levels of efficiency and reduce power costs. Key takeaways for each strategy and related policy recommendations are summarized below.

- The strategy of repurposing existing steam turbine power plants by replacing the fossil fuel and boiler used in those plants with thermal storage and a new steam generator can be implemented today since it relies on commercially de-risked technologies.
 - Areas for improvement include reducing the cost of energy and creating engineering plans for optimal integration and operation. Experience with concentrated solar power is translatable to subcritical steam plants—and with more work, TES can be extended to supercritical and ultra-supercritical plants. The latter two types of plants will likely remain online longer given their higher efficiencies and deployment in countries with longer decarbonization timelines.

– In the interim, adding TES to supplement combustion would reduce emissions and provide flexibility in responding to intermittent output from solar and wind generators. Once this strategy is demonstrated, governments and owners of fossil fuel power plants may find that TES offers an attractive opportunity for repurposing otherwise stranded assets.

- The second strategy uses alternative power cycles, namely closed Brayton cycles, that have higher efficiency at medium temperatures (550°C–1,000°C).
 - Although there are still technical challenges to resolve, commercial demonstrations of these power cycles are underway in non-storage applications.
 - As the demand for gas-fired open Brayton turbines declines, the gas turbine industry may find a significant opportunity in manufacturing and servicing these turbines for low- or zero-carbon thermal power plants.
 - Progress in non-storage applications will drive down power block costs, with benefits for systems that follow this strategy.
- R&D is required to advance the third strategy of utilizing high-temperature materials and power conversion devices to reach high levels of efficiency and reduce power costs. For this reason, grid-scale deployment is unlikely to be feasible in the 2030s, but could be viable before 2050.
 - A challenge for this approach is improving the lifetime performance of high-temperature materials to ensure they are reliable for the lifetime of the plant. This includes all the “auxiliary” components such as pipes, pumps, and sensors, which may need to be re-designed from their lower-temperature counterparts.

- If engineering issues can be resolved, high-temperature TES systems hold promise for low energy cost, relatively lower power cost, high efficiency, and favorable flexibility.
- Policies for advancing each of these strategies should reflect the stage of development of the different TES technologies involved.
 - The U.S. DOE has already funded studies on the integration of TES with coal plants. An analysis of national, retrofit-capable capacity combined with detailed studies of representative plants would provide a more accurate assessment of the potential for the retrofit strategy.
 - Support for first-of-a-kind projects through the U.S. DOE’s Loan Program Office, state energy innovation grants, or other programs could kickstart the industry.
 - Efforts to commercialize alternative power cycles (the second strategy) would benefit from funding for scale-up programs and support for manufacturing.
 - Efforts to develop high-temperature TES systems (the third strategy) would benefit from applied research to improve understanding and capabilities for high-temperature materials, engineering, and energy conversion systems.
- Just as experience and price reductions for rechargeable batteries have been driven by larger volume markets like personal electronics and electric vehicles, TES would benefit from earlier adoption in applications for thermal power plant flexibility and heat-only storage. Learning in these areas would increase the industry’s experience and the market’s familiarity with this type of energy storage, paving the way for grid-scale TES. Meanwhile, the technology could support emissions reductions in the buildings and industrial sectors.

References

- Albertus, Paul, Joseph S Manser, and Scott Litzelman. 2020. "Long-Duration Electricity Storage Applications, Economics, and Technologies." *Joule* 4 (1): 21-32. <https://doi.org/10.1016/j.joule.2019.11.009>.
- Alibaba. 2021a. "99.5% NaCl Pool Salt Refined Industrial Salt." https://web.archive.org/web/20210827145841/https://sgdinghao.en.alibaba.com/product/1600056895051-821750555/99_5_NaCl_Pool_Salt_Refined_Industrial_Salt.html.
- . 2021b. "MgCl₂ Price per Ton." <https://web.archive.org/web/20210827144939/https://www.alibaba.com/showroom/mgcl2-price-per-ton.html>.
- . 2021c. "Natural Black Basalt Price Ton Stones For Construction." <https://web.archive.org/web/20210827143705/https://www.alibaba.com/showroom/basalt-price-ton.html>.
- Alumina Energy. 2021. "Our Technology." *Alumnia Energy*. <https://www.aluminaenergy.com/technology>.
- Amy, Caleb, Hamid Reza Seyf, Myles A Steiner, Daniel J Friedman, and Asegun Henry. 2018. "Thermal Energy Grid Storage Using Multi-Junction Photovoltaics." *Energy and Environmental Science* 12 (1): 334-343. <https://doi.org/10.1039/C8EE02341G>.
- Amy, Caleb, Mehdi Pishahang, Colin C Kelsall, Alina LaPotin, and Asegun Henry. 2021. "High-Temperature Pumping of Silicon for Thermal Energy Grid Storage." *Energy* 233: 121105. <https://doi.org/10.1016/j.energy.2021.121105>.
- ARPA-E. 2018. "Duration Addition to ElectricitY Storage (DAYS) Overview." ARPA-E. https://arpa-e.energy.gov/sites/default/files/documents/files/DAYS_ProgramOverview_FINAL.pdf.
- ARPA-e. 2019. "HITEMMP Project Descriptions." ARPA-e. https://arpa-e.energy.gov/sites/default/files/documents/files/HITEMMP%20project%20descriptions_FINAL.pdf.
- AZo Materials. 2015. "What Is Induction Heating and How Do Induction Coils Work?" AZoM.com. January 20. <https://www.azom.com/article.aspx?ArticleID=11659>.
- Balakrishnan, Anita. 2015. "Road Salt: Winter's \$2.3 Billion Game Changer." *NBC News*. February 18. <https://www.nbcnews.com/business/economy/road-salt-winters-2-3-billion-game-changer-n308416>.
- Beér, János. 2007. "High Efficiency Electric Power Generation: The Environmental Role." *Progress in Energy and Combustion Science* 33 (2): 107-134. <https://doi.org/10.1016/j.pecs.2006.08.002>.
- Black and Veatch. 2010. "Solar Thermocline Storage Systems: Preliminary Design Study." *EPRI*.
- BP. 2021. "BP's Statistical Review of World Energy 2021." <https://www.bp.com/en/global/corporate-energy-economics/statistical-review-of-world-energy.html>.
- Bradshaw, A M, and T Hamacher. 2021. "Nuclear Fusion and the Helium Supply Problem." *Fusion Engineering and Design, Proceedings of the 27th Symposium On Fusion Technology (SOFT-27)*. Liège, Belgium. 88 (9): 2694-2697. <https://doi.org/10.1016/j.fusengdes.2013.01.059>.
- Brayton Energy. 2011. "Brayton Power Conversion System." *DOE Contract # DE-FC36-08GO18029/A000*. <https://www.osti.gov/servlets/purl/1045668>.
- Carlson, Matthew D, Bobby M Middleton, and Clifford K Ho. 2017. "Techno-Economic Comparison of Solar-Driven SC₂O Brayton Cycles Using Component Cost Models Baseline With Vendor Data and Estimates." *ASME 2017 11th International Conference on Energy Sustainability, V001T05A009*. Charlotte, North Carolina, USA: American Society of Mechanical Engineers. <https://doi.org/10.1115/ES2017-3590>.
- Chao, Julie. 2016. *Hand-built research converters and thermionic demonstration device heated with a flame to produce power*. Lawrence Berkeley National Laboratory, <https://phys.org/news/2016-03-scientists-thermionic-energy-conversion-efficient.html>.
- . 2016. "Scientists Look to Thermionic Energy Conversion for Clean and Efficient Power Generation." *Phys.org*. March 1. <https://phys.org/news/2016-03-scientists-thermionic-energy-conversion-efficient.html>.
- Collins, Leigh. 2021. "Siemens Gamesa: Utilities Are Lining up for Our €40-50/MWh Long-Duration Thermal Energy Storage." *Recharge*. February 26. <https://www.rechargenews.com/technology/siemens-gamesa-utilities-are-lining-up-for-our-40-50-mwh-long-duration-thermal-energy-storage/2-1-969626>.
- CREA. 2021. "Overseas Coal Briefing." *Center for Research on Energy and Clean Air*. <https://energyandcleanair.org/wp/wp-content/uploads/2021/06/CH-Overseas-Coal-Briefing.pdf>.
- Datas, Alejandro, Alba Ramos, Antonio Martí, Carlos del Cañizo, and Antonio Luque. 2016. "Ultra High Temperature Latent Heat Energy Storage and Thermophotovoltaic Energy Conversion." *Energy* 107: 542-549. <https://doi.org/10.1016/j.energy.2016.04.048>.

- Deign, Jason. 2019. "Germany Looks to Put Thermal Storage Into Coal Plants." *Greentech Media*. March 18. <https://www.greentechmedia.com/articles/read/germany-thermal-storage-into-coal-plants>.
- Essig, Stephanie, Christophe Allebé, Timothy Remo, John F Geisz, Myles A Steiner, Kelsey Horowitz, and Loris Barraud. 2017. "Raising the One-Sun Conversion Efficiency of III-V/Si Solar Cells to 32.8% for Two Junctions and 35.9% for Three Junctions." *Nature Energy* 2 (9): 1-9. <https://doi.org/10.1038/nenergy.2017.144>.
- Fallahi, Ali, Gert Guldentops, Mingjiang Tao, Sergio Granados-Focil, and Steven Van Dessel. 2017. "Review on Solid-Solid Phase Change Materials for Thermal Energy Storage: Molecular Structure and Thermal Properties." *Applied Thermal Engineering* 127 (December): 1427-1441. <https://doi.org/10.1016/j.applthermaleng.2017.08.161>.
- Fernández, A. Inés, Camila Barreneche, Martín Belusko, Mercé Segarra, Frank Bruno, and Luisa F Cabeza. 2017. "Considerations for the Use of Metal Alloys as Phase Change Materials for High Temperature Applications." *Solar Energy Materials and Solar Cells* 171 (November): 275-281. <https://doi.org/10.1016/j.solmat.2017.06.054>.
- Flake, Shawn. 2016. "Using Steam Turbine Warming Blankets to Reduce Startup Time and Rotor Stress." *Power Magazine*. March 1. <https://www.powermag.com/using-steam-turbine-warming-blankets-reduce-startup-time-rotor-stress>.
- Flueckiger, Scott M, Zhen Yang, and Suresh V Garmiella. 2013. "Review of Molten-Salt Thermocline Tank Modeling for Solar Thermal Energy Storage." *Heat Transfer Engineering* 34 (10): 787-800. <https://doi.org/10.1080/01457632.2012.746152>.
- Forsberg, Charles, and Ali S Aljefri. 2020. "100-Gigawatt-Hour Crushed-Rock Heat Storage for CSP and Nuclear." 8.
- Forsberg, Charles, Patrick J McDaniel, and Bahman Zohuri. 2021. "Nuclear Air-Brayton Power Cycles with Thermodynamic Topping Cycles, Assured Peaking Capacity, and Heat Storage for Variable Electricity and Heat." *Nuclear Technology* 207 (4): 543–57. <https://doi.org/10.1080/00295450.2020.1785793>.
- Forsberg, Charles, Stephen Brick, and Geoffrey Haratyk. 2018. "Coupling Heat Storage to Nuclear Reactors for Variable Electricity Output with Baseload Reactor Operation." *The Electricity Journal* 31 (3): 23–31. <https://doi.org/10.1016/j.tej.2018.03.008>.
- Frate, Guido Francesco, Lorenzo Ferrari, and Umberto Desideri. 2020. "Multi-Criteria Economic Analysis of a Pumped Thermal Electricity Storage (PTES) With Thermal Integration." *Frontiers in Energy Research* 8 (April): 53. <https://doi.org/10.3389/fenrg.2020.00053>.
- Friedman, Julio S, Zhiyuan Fan, and Ke Tang. 2019. "Low-Carbon Heat Solutions for Heavy Industry: Sources, Options, and Costs Today." *Columbia Center on Global Energy Policy*.
- Gerardtv. 2010. "Picture of a Thermoelectric Seebeck Module (w:En:Thermoelectric Generator), Apparently Manufactured by TECTEG MFR." 10 15. https://commons.wikimedia.org/wiki/File:Thermoelectric_Seebeck_power_module.jpg.
- Gerardtv. 2010. *Thermoelectric Seebeck power module*. https://commons.wikimedia.org/wiki/File:Thermoelectric_Seebeck_power_module.jpg.
- Gibson, David. 2011. "Common Road Salt Is Toxic." *The Adirondack Almanack*. January 12. <https://www.adirondackalmanack.com/2011/01/dave-gibson-common-road-salt-is-toxic-to-the-adirondacks.html>.
- Gilbert, Haley. 2021. "Antora Energy | Afwerx Energy Challenge Virtual Showcase." <https://reimagining.afwerx.com/exhibitor/antora-energy-11675>.
- GIZ. 2020. "Repurposing of Existing Coal-Fired Power Plants into Thermal Storage Plants for Renewable Power in Chile." *Deutsche Gesellschaft für Internationale Zusammenarbeit*. <https://4echile-datastore.s3.eu-central-1.amazonaws.com/wp-content/uploads/2020/09/01031505/200928-GIZ-Chile-ExecSummary-v6-English-corrected.pdf>.
- Glatzmaier, Greg. 2011. "Developing a Cost Model and Methodology to Estimate Capital Costs for Thermal Energy Storage." *National Renewable Energy Laboratory NREL/TP-5500-53066*, 1031953. <https://doi.org/10.2172/1031953>.
- Glowacki, Bartek A, William J Nuttall, and Richard H Clarke. 2013. "Beyond the Helium Conundrum." *IEEE Transactions on Applied Superconductivity* 23 (3): 0500113–0500113. <https://doi.org/10.1109/TASC.2013.2244633>.
- Go, David B, John R Haase, Jeffrey George, Jochen Manhart, Robin Wanke, Alireza Nojeh, and Robert Nemanich. 2017. "Thermionic Energy Conversion in the Twenty-First Century: Advances and Opportunities for Space and Terrestrial Applications." *Frontiers in Mechanical Engineering* 3 (November): 13. <https://doi.org/10.3389/fmech.2017.00013>.

- González-Roubaud, Edourad, David Pérez-Osorio, and Cristina Prieto. 2017. “Review of Commercial Thermal Energy Storage in Concentrated Solar Power Plants: Steam vs. Molten Salts.” *Renewable and Sustainable Energy Reviews* 80 (December): 133–48. <https://doi.org/10.1016/j.rser.2017.05.084>.
- Google. 2021. “Changhua County, Taiwan – Data Centers – Google.” *Google Data Centers*. <https://www.google.com/about/datacenters/locations/changhua-county/>.
- Greentech Media. 2020. “Storing Energy in the Freezer: Long-Duration Thermal Storage Comes of Age.” July 28. <https://www.greentechmedia.com/articles/read/storing-energy-in-the-freezer-long-duration-thermal-storage-comes-of-age>.
- Gross, Robert, Richard Hanna, Ajay Gambhir, Philip Heptonstall, and Jamie Speirs. 2018. “How Long Does Innovation and Commercialisation in the Energy Sectors Take? Historical Case Studies of the Timescale from Invention to Widespread Commercialisation in Energy Supply and End Use Technology.” *Energy Policy* 123 (December): 682–99. <https://doi.org/10.1016/j.enpol.2018.08.061>.
- Grubert, Emily. 2020. “Fossil Electricity Retirement Deadlines for a Just Transition.” 4.
- Hart, Melanie, Luke Bassett, and Blaine Johnson. 2017. “Everything You Think You Know About Coal in China Is Wrong.” *Center for American Progress*. May 15. <https://www.americanprogress.org/issues/green/reports/2017/05/15/432141/everything-think-know-coal-china-wrong>.
- Held, Timothy J. 2014. “Initial Test Results of a Megawatt-Class Supercritical CO₂ Heat Engine.” *The 4th International Symposium – Supercritical CO₂ Power Cycles*. Pittsburgh, Pennsylvania. 12.
- Henry, Asegun. 2018. “A New Take on Electrochemical Heat Engines.” *Joule* 2 (9): 1660–61. <https://doi.org/10.1016/j.joule.2018.08.007>.
- Henry, Asegun, and Ravi Prasher. 2014. “The Prospect of High Temperature Solid State Energy Conversion to Reduce the Cost of Concentrated Solar Power.” *Energy and Environmental Science* 7 (6): 1819–28. <https://doi.org/10.1039/C4EE00288A>.
- Hoseinpur, Arman, and Jafar Safarian. 2020. “Mechanisms of Graphite Crucible Degradation in Contact with Si-Al Melts at High Temperatures and Vacuum Conditions.” *Vacuum* 171 (January): 108993. <https://doi.org/10.1016/j.vacuum.2019.108993>.
- HowMuchIsIt. 2018. “How Much Does Rock Excavation Cost?” August 9. <https://www.howmuchisit.org/rock-excavation-cost>.
- Inductotherm Corporation. 2020. “FAQs: General.” *Inductotherm Corporation*. <https://www.howmuchisit.org/rock-excavation-cost>.
- International Energy Agency. 2019. “Electricity Information 2019.” *International Energy Agency*.
- International Renewable Energy Agency. 2019. “Innovation Landscape Brief: Flexibility in Conventional Power Plants.” *International Renewable Energy Agency*.
- Jiao, Jianmeng, Bettina Grorud, Caroline Sindland, Jafar Safarian, Kai Tang, Kathrine Sellevoll, and Merete Tangstad. 2019. “The Use of Eutectic Fe-Si-B Alloy as a Phase Change Material in Thermal Energy Storage Systems.” *Materials* 12 (14). <https://doi.org/10.3390/ma12142312>.
- Kanthal. 2018. “Resistance Heating Alloys and Systems for Industrial Furnaces.”
- Kavlak, Goksin, James McNerney, and Jessika E Trancik. 2018. “Evaluating the Causes of Cost Reduction in Photovoltaic Modules.” *Energy Policy* 123 (December): 700–710. <https://doi.org/10.1016/j.enpol.2018.08.015>.
- Kelsall, Colin C, Kyle Buznitsky, and Asegun Henry. 2021. “Technoeconomic Analysis of Thermal Energy Grid Storage Using Graphite and Tin.” *ArXiv:2106.07624 [Physics]* <http://arxiv.org/abs/2106.07624>.
- Khalid, Abdul, Kamarul Aizat, Thye Jien Leong, and Khairudin Mohamed. 2016. “Review on Thermionic Energy Converters.” *IEEE Transactions on Electron Devices* 63 (6): 2231–2241. <https://doi.org/10.1109/TED.2016.2519009>.
- LaPotin, Alina, Kevin L. Schulte, Myles A. Steiner, Kyle Buznitsky, Colin C. Kelsall, Daniel J. Friedman, Eric J. Tervo, et al. “Thermophotovoltaic Efficiency of 40%.” *Nature* 604, no. 7905 (April 2022): 287–91. <https://doi.org/10.1038/s41586-022-04473-y>.
- Laughlin, Robert B. 2017. “Pumped Thermal Grid Storage with Heat Exchange.” *Journal of Renewable and Sustainable Energy* 9 (4): 044103. <https://doi.org/10.1063/1.4994054>.
- Lee, Seok Woo, Yuan Yang, Hyun-Wook Lee, Hadi Ghasemi, Daniel Kraemer, Gang Chen, and Yi Cui. 2014. “An Electrochemical System for Efficiently Harvesting Low-Grade Heat Energy.” *Nature Communications* 5 (1): 1–6. <https://doi.org/10.1038/ncomms4942>.

- Limia, Alexander, Jong Min Ha, Peter Kottke, Andrey Gunawan, Andrei G Fedorov, Seung Woo Lee, and Shannon K Yee. 2017. "A Dual-Stage Sodium Thermal Electrochemical Converter (Na-TEC)." *Journal of Power Sources* 371 (December): 217–24. <https://doi.org/10.1016/j.jpowsour.2017.10.022>.
- Lin, Yaxue, Yuting Jia, Guruprasad Alva, and Guiyin Fang. 2018. "Review on Thermal Conductivity Enhancement, Thermal Properties and Applications of Phase Change Materials in Thermal Energy Storage." *Renewable and Sustainable Energy Reviews* 82 (February): 2730–42. <https://doi.org/10.1016/j.rser.2017.10.002>.
- Linford, Patrick A, Lin Xu, Botao Huang, Yang Shao-Horn, and Carl V Thompson. 2018. "Multi-Cell Thermogalvanic Systems for Harvesting Energy from Cyclic Temperature Changes." *Journal of Power Sources* 399 (September): 429–35. <https://doi.org/10.1016/j.jpowsour.2018.07.080>.
- Liu, Ming, N.H. Steven Tay, Stuart Bell, Martin Belusko, Rhys Jacob, Geoffrey Will, Wasim Saman, and Frank Bruno. 2016. "Review on Concentrating Solar Power Plants and New Developments in High Temperature Thermal Energy Storage Technologies." *Renewable and Sustainable Energy Reviews* 53 (January): 1411–32. <https://doi.org/10.1016/j.rser.2015.09.026>.
- Ma, Zhiwen, Patrick Davenport, and Ruichong Zhang. 2020. "Design Analysis of a Particle-Based Thermal Energy Storage System for Concentrating Solar Power or Grid Energy Storage." *Journal of Energy Storage* 29 (June): 101382. <https://doi.org/10.1016/j.est.2020.101382>.
- Ma, Zhiwen, Zhang Ruichong, and Fadi Sawaged. 2017. "Design of Particle-Based Thermal Energy Storage for a Concentrating Solar Power System." *ASME 2017 11th International Conference on Energy Sustainability*, V001T05A003. Charlotte, North Carolina: American Society of Mechanical Engineers. <https://doi.org/10.1115/ES2017-3099>.
- McDonald, Colin F. 2012. "Helium Turbomachinery Operating Experience from Gas Turbine Power Plants and Test Facilities." *Applied Thermal Engineering* 44 (November): 108–42. <https://doi.org/10.1016/j.applthermaleng.2012.02.041>.
- McTigue, Joshua, Pau Farres-Antunez, Kevin Ellingwood, Ty Neises, and Alexander White. 2019. "Pumped Thermal Electricity Storage with Supercritical CO₂ Cycles and Solar Heat Input: Preprint." *Renewable Energy* 14.
- Mehos, Mark, Craig Turchi, Jennie Jorgensen, and Paul Denholm. 2016. "On the Path to SunShot: Advancing Concentrating Solar Power Technology, Performance, and Dispatchability." *U.S. Department of Energy*.
- Meroueh, Laureen, and Gang Chen. 2019. "Thermal Energy Storage Radiatively Coupled to a Supercritical Rankine Cycle for Electric Grid Support." *Renewable Energy* 145 (June): 604–21. <https://doi.org/10.1016/j.renene.2019.06.036>.
- Mesquita, Lucio, Doug McClenahan, Jeff Thornton, Jarrett Carriere, and Bill Wong. 2017. "Drake Landing Solar Community: 10 Years of Operation." *Proceedings of SWC2017/SHC2017*. Abu Dhabi, United Arab Emirates: Abu Dhabi: International Solar Energy Society. 1–12. <https://doi.org/10.18086/swc.2017.06.09>.
- Mohan, Gowtham, Mahesh B Venkataraman, and Joe Coventry. 2019. "Sensible Energy Storage Options for Concentrating Solar Power Plants Operating above 600 °C." *Renewable and Sustainable Energy Reviews* 107 (June): 319–37. <https://doi.org/10.1016/j.rser.2019.01.062>.
- Moriarty, Kevin. 2019. "Technology and Commercial Review Update." *1414 Degrees* <https://1414degrees.com.au/wp-content/uploads/2020/06/Technology-Commercial-Review-Update-1.pdf>.
- Myers, Philip D, and D. Yogi Goswami. 2016. "Thermal Energy Storage Using Chloride Salts and Their Eutectics." *Applied Thermal Engineering, Special Issue: Solar Energy Research Institute for India and the United States (SERIIUS) – Concentrated Solar Power* 109 (October): 889–900. <https://doi.org/10.1016/j.applthermaleng.2016.07.046>.
- National Renewable Energy Laboratory. 2018. "News Release: NREL Awarded \$2.8M from ARPA-E to Develop Low-Cost Thermal Energy Storage." *National Renewable Energy Laboratory*. <https://www.nrel.gov/news/press/2018/nrel-awarded-28m-from-arpa-e-to-develop-low-cost-thermal-energy-storage.html>.
- Nishioka, Koki, Naoyuki Suura, Ko-ichiro Ohno, Takayuki Maeda, and Masakata Shimizu. 2010. "Development of Fe Base Phase Change Materials for High Temperature Using Solid–Solid Transformation." *ISIJ International* 50 (9): 5.
- Office of Fossil Energy. 2020. "Areas of Interest: DOE Invests Nearly \$7.6M to Develop Energy Storage Projects." December. <https://www.energy.gov/fe/articles/areas-interest-doe-invests-nearly-76m-develop-energy-storage-projects>.

- Olympios, Andreas V, Joshua D McTigue, Paul Sapin, and Christos N Markides. 2021. "Pumped-Thermal Electricity Storage Based on Brayton Cycles." In *Reference Module in Earth Systems and Environmental Sciences*, <https://doi.org/10.1016/B978-0-12-819723-3.00086-X>. Elsevier.
- Omair, Zunaid, Gregg Scranton, Luis M Pazos-Outón, T Patrick Xiao, Myles A Steiner, Vidya Ganapati, Per F Peterson, John Holzrichter, Harry Atwater, and Eli Yablonovitch. 2019. "Ultraefficient Thermophotovoltaic Power Conversion by Band-Edge Spectral Filtering." *Proceedings of the National Academy of Sciences* 116 (31): 15356–61. <https://doi.org/10.1073/pnas.1903001116>.
- Palfinger, Günther, Bernd Bitnar, Wilhelm Durisch, Jean-Claude Mayor, Detlev Grützmacher, and Jens Gobrecht. 2003. "Cost Estimate of Electricity Produced by TPV." *Semiconductor Science and Technology* 18 (5): S254–61. <https://doi.org/10.1088/0268-1242/18/5/317>.
- Pandya, Shishir, Gabriel Velarde, Lei Zhang, Joshua D Wilbur, Andrew Smith, Brendan Hanrahan, Chris Dames, and Lane W Martin. 2019. "New Approach to Waste-Heat Energy Harvesting: Pyroelectric Energy Conversion." *NPG Asia Materials* 11 (1): 1–5. <https://doi.org/10.1038/s41427-019-0125-y>.
- Parnell, John. 2020. "How Siemens Gamesa Could Give Coal Plants a Second Life." *Greentech Media*. February 20. <https://www.greentechmedia.com/articles/read/how-siemens-gamesa-could-give-coal-plants-a-second-life>.
- Patel, Sonal. 2021. "Breakthrough: NET Power's Allam Cycle Test Facility Delivers First Power to ERCOT Grid." *POWER Magazine*. November 18. <https://www.powermag.com/breakthrough-net-powers-allam-cycle-test-facility-delivers-first-power-to-ercot-grid>.
- Poletayev, Andrey D, Ian S McKay, William C Chueh, and Arun Majumdar. 2018. "Continuous Electrochemical Heat Engines." *Energy and Environmental Science* 11 (10): 2964–71. <https://doi.org/10.1039/C8EE01137K>.
- Power Engineering. 2018. "GE-Powered Plant Awarded World Record Efficiency by Guinness." *Power Engineering*. March 27. <https://www.powereng.com/2018/03/27/ge-powered-plant-awarded-world-record-efficiency-by-guinness>.
- Power Technology. 2019. "1414 Degrees Begins Operations of Biogas Energy Storage System." *Power Technology*. May 2. <https://www.power-technology.com/news/1414-degrees-energy-storage>.
- Proctor, Darrel. 2019. "Volcanic Rock Offers New Take on Energy Storage." *POWER Magazine*. August 1. <https://www.powermag.com/volcanic-rock-offers-new-take-on-energy-storage>.
- Quoilin, Sylvain, Martijn Van Den Broek, Sébastien Declaye, Pierre Dewallef, and Vincent Lemort. 2013. "Techno-Economic Survey of Organic Rankine Cycle (ORC) Systems." *Renewable and Sustainable Energy Reviews* 22 (June): 168–86. <https://doi.org/10.1016/j.rser.2013.01.028>.
- Reed, Samuel, Heber Sugo, Erich Kisi, and Peter Richardson. 2019. "Extended Thermal Cycling of Miscibility Gap Alloy High Temperature Thermal Storage Materials." *Solar Energy* 185 (June): 333–40. <https://doi.org/10.1016/j.solener.2019.04.075>.
- Robinson, Adam. 2018. "Ultra-High Temperature Thermal Energy Storage. Part 2: Engineering and Operation." *Journal of Energy Storage* 18 (August): 333–39. <https://doi.org/10.1016/j.est.2018.03.013>.
- Sargent and Lundy. 2020. "Capital Costs and Performance Characteristics for Utility Scale Power Generating Technologies." *Energy Information Agency*.
- Schmidt, O, A Hawkes, A Gambhir, and I Staffel. 2017. "The Future Cost of Electrical Energy Storage Based on Experience Rates." *Nature Energy* 2 (8): 1–8. <https://doi.org/10.1038/nenergy.2017.110>.
- Seetenky, Alexander. 2007. *Maintenance of a low pressure section of a steam turbine at the Balakovo Nuclear Power Plant*. The Centre of the Public Information Balakovo NPP, https://commons.wikimedia.org/wiki/File:BalNPP_m_st2.jpg.
- Seetenky, Alexander. n.d. "Maintenance of a Low Pressure Section of a Steam Turbine at the Balakovo Nuclear Power Plant." CPI BalNpp (The Centre of the Public Information Balakovo NPP). https://commons.wikimedia.org/wiki/File:BalNPP_m_st2.jpg.
- Sepulveda, Nestor A, Jesse D Jenkins, Aurora Edington, Dharik S Mallapragada, and Richard K Lester. 2021. "The Design Space for Long-Duration Energy Storage in Decarbonized Power Systems." *Nature Energy* <https://doi.org/10.1038/s41560-021-00796-8>.
- Seyf, Hamid Reza, and Asegun Henry. 2016. "Thermophotovoltaics: A Potential Pathway to High Efficiency Concentrated Solar Power." *Energy & Environmental Science* 9 (8): 2654–65. <https://doi.org/10.1039/C6EE0137D>.

- Siemens Energy. 2021. "Siemens Energy signs agreement to build first-of-its-kind waste heat-to-power facility in Canada." *Siemens Energy*. February 12. <https://press.siemens-energy.com/global/en/pressrelease/siemens-energy-signs-agreement-build-first-its-kind-waste-heat-power-facility-canada>.
- Sioshansi, Ramteen, Paul Denholm, Thomas Jenkin, and Jurgen Weiss. 2009. "Estimating the Value of Electricity Storage in PJM: Arbitrage and Some Welfare Effects." *Energy Economics* 31 (2): 269–77. <https://doi.org/10.1016/j.eneco.2008.10.005>.
- Soprani, Stefano, Fabrizio Marongiu, Ludvig Christensen, Ole Alm, Kenni Dinesen Petersen, Thomas Ulrich, and Kurt Engelbrecht. 2019. "Design and Testing of a Horizontal Rock Bed for High Temperature Thermal Energy Storage." *Applied Energy* 251 (October): 113345. <https://doi.org/10.1016/j.apenergy.2019.113345>.
- Specialty Grading. 2020. "Rock Excavation Cost in Prescott, AZ (2020 Prices)." *Specialty Grading*. July 16. <https://www.specialtygrading.com/rock-excavation-cost>.
- St. John, Jeff. 2017. "Inside GE and SoCal Edison's First-of-a-Kind Hybrid Peaker Plant With Batteries and Gas Turbines." *Greentech Media*. April 18. <https://www.greentechmedia.com/articles/read/inside-ge-and-socal-edisons-battery-integrated-gas-fired-peaker-plants>.
- Stack, Daniel C, Daniel Curtis, and Charles Forsberg. 2019. "Performance of Firebrick Resistance-Heated Energy Storage for Industrial Heat Applications and Round-Trip Electricity Storage." *Applied Energy* 242 (May): 782–96. <https://doi.org/10.1016/j.apenergy.2019.03.100>.
- Statista. 2019. "Global Graphite Price 2018–2019." *Statista*. June. <https://www.statista.com/statistics/1075217/graphite-price-worldwide>.
- . 2017. "Market Distribution of Photovoltaic Module Manufacturers 2017." *Statista*. www.statista.com/statistics/269812/global-market-share-of-solar-pv-module-manufacturers.
- Strefler, Jessica, Thorben Amann, Nico Bauer, Elmar Kriegler, and Jens Hartmann. 2018. "Potential and Costs of Carbon Dioxide Removal by Enhanced Weathering of Rocks." *Environmental Research Letters* 13 (3): 034010. <https://doi.org/10.1088/1748-9326/aaa9c4>.
- Sugo, Heber, Erich Kisi, and Dylan Cuskelly. 2013. "Miscibility Gap Alloys with Inverse Microstructures and High Thermal Conductivity for High Energy Density Thermal Storage Applications." *Applied Thermal Engineering* 51 (1–2): 1345–50. <https://doi.org/10.1016/j.applthermaleng.2012.11.029>.
- Systems, The Design Space for Long-Duration Energy Storage in Decarbonized Power. 2021. "The Design Space for Long-Duration Energy Storage in Decarbonized Power Systems." *Nature Energy* March. <https://doi.org/10.1038/s41560-021-00796-8>.
- Taylor, Chad, Matthew Johnson, Nathan Levinson, and Jonathan Whalley. 2020. Energy Storage and Retrieval System. United States of America Patent US20200018557A1.
- Temple, James. 2020. "Tony Pan." *MIT Technology Review*. June. <https://www.technologyreview.com/innovator/tony-pan>.
- Thiel, Gregory P, and Addison K Stark. 2021. "To Decarbonize Industry, We Must Decarbonize Heat." *Joule* 5 (3): 531–50. <https://doi.org/10.1016/j.joule.2020.12.007>.
- Timmer, Michael A G, Kees de Blok, and Theo H van der Meer. 2018. "Review on the Conversion of Thermoacoustic Power into Electricity." *The Journal of the Acoustical Society of America* 143 (2): 841–57. <https://doi.org/10.1121/1.5023395>.
- Trading Economics. 2021. "Aluminum | 1989–2021 Data | 2022–2023 Forecast | Price | Quote | Chart | Historical." <https://tradingeconomics.com/commodity/aluminum>.
- Turchi, Craig S, Zhiwen Ma, and John Dyreby. 2012. "Supercritical Carbon Dioxide Power Cycle Configurations for Use in Concentrating Solar Power Systems." *ASME Turbo Expo 2012: Turbine Technical Conference and Exposition*. Copenhagen, Denmark: American Society of Mechanical Engineers. 967–973. <https://doi.org/10.1115/GT2012-68932>.
- U.S. Department of Energy. n.d.
- . 2006. "A GE H Series Stationary Gas Turbine Used for Electrical Power Generation." <http://www.netl.doe.gov/scng/projects/end-use/at/images/at31176>. https://commons.wikimedia.org/wiki/File:GE_H_series_Gas_Turbine.jpg.
- U.S. Department of Energy. 2015. "Chapter 4: Advancing Clean Electric Power Technologies. Technology Assessments: Supercritical Carbon Dioxide Brayton Cycle." In *Quadrennial Technology Review 2015*, <https://www.energy.gov/sites/prod/files/2016/06/f32/QTR2015-4R-Supercritical-Carbon-Dioxide-Brayton%20Cycle.pdf>. Department of Energy.
- . n.d. "DOE Global Energy Storage Database." Accessed October 2020. <https://www.sandia.gov/ess/>.
- . 2006. "GE H series Gas Turbine." https://en.wikipedia.org/wiki/File:GE_H_series_Gas_Turbine.jpg.

U.S. Energy Information Agency. 2015. “State Electricity Profiles: Data for 2013.” <https://www.eia.gov/electricity/state/archive/2013>.

U.S. Geological Survey. 2021. “Mineral Commodity Summaries 2021.” <https://doi.org/10.3133/mcs2021>.

Wickramaratne, Chatura, Jaspreet S Dhau, Rajeev Kamal, Philip Myers, D Y Goswami, and E Stefanakos. 2018. “Macro-Encapsulation and Characterization of Chloride Based Inorganic Phase Change Materials for High Temperature Thermal Energy Storage Systems.” *Applied Energy* 221 (July): 587–96. <https://doi.org/10.1016/j.apenergy.2018.03.146>.

Zhang, Qihao, Jincheng Liao, Yunshan Tang, Ming Gu, Chen Ming, Pengfei Qiu, Shengqiang Bai, Xun Shi, Ctirad Uher, and Lidong Chen. 2017. “Realizing a Thermoelectric Conversion Efficiency of 12% in Bismuth Telluride/Skutterudite Segmented Modules through Full-Parameter Optimization and Energy-Loss Minimized Integration.” *Energy and Environmental Science* 10 (4): 956–63. <https://doi.org/10.1039/C7EE00447H>.

Zhang, Xiang, Hadi Keramati, Martinus Arie, Farah Singer, Ratnesh Tiwari, Amir Shooshtari, and Michael Ohadi. 2018. “Recent Developments In High Temperature Heat Exchangers: A Review.” *Frontiers in Heat and Mass Transfer* 11 (July). <https://doi.org/10.5098/hmt.11.18>.

Ziegler, Micah S, Joshua M Mueller, Gonçalo D Pereira, Juhyun Song, Marco Ferrara, Yet-Ming Chiang, and Jessika E Trancik. 2019. “Storage Requirements and Costs of Shaping Renewable Energy Toward Grid Decarbonization.” *Joule* <https://doi.org/10.1016/j.joule.2019.06.012>.

Chapter 5 – Chemical energy storage

5.1 Overview of chemical energy storage

A chemical energy storage system stores energy in chemical bonds (Schlögl 2013). While this type of energy storage can be achieved using many different chemicals, the essential features are always the same: A chemical compound is produced with electricity and stored until there is demand for the stored energy, at which point the chemical compound is converted to generate electric power. Chemical energy storage offers certain advantages over electrochemical or thermal energy storage—primarily, low cost relative to energy capacity and very low self-discharge of energy stored over extended periods of time. These attributes, and the ability to scale power and storage capacities independently, make chemical systems suitable for long-duration energy storage. Also, and in contrast to electrochemical energy storage, chemical storage offers the potential for stored chemicals to be used directly in applications beyond the electricity system: For example, stored chemicals could be used as fuels or feedstocks in transportation and industrial applications (Gençer and Agrawal 2016; Gençer, Al-musleh, et al. 2014). This multi-use potential could allow for increased capital utilization of some components of chemical storage systems, thereby improving the technology’s cost-effectiveness for long-duration energy storage in the electricity sector (this point is further explored in Section 3 of Chapter 6).

The potential to provide “chemical energy storage” is not limited to a specific molecule or group of molecules, since many molecules can be produced using electric power. Hydrogen is

widely considered a leading chemical energy storage medium because it can be directly produced from electricity in a single step and consumed either as a fuel to produce power or as a feedstock or heat source for other industrial processes. Because hydrogen is a gas at standard temperature and pressure, specialized equipment is required to store it, either as a compressed gas or cryogenic liquid. Moreover, the volumetric energy density of hydrogen (where volumetric energy density is defined as the amount of energy contained in a unit volume of an energy carrier) is roughly one-third that of natural gas at standard temperature and pressure. It is possible to liquefy hydrogen to increase its volumetric energy density, but the process of cooling hydrogen to the required temperature of -253°C (-423°F) and maintaining it at this temperature in a storage tank is very energy intensive (Hydrogen and Fuel Cell Technologies Office).¹

To achieve higher volumetric energy density, it is also possible to combine hydrogen with other molecules to produce synthetic fuels or liquid organic hydrogen carriers (LOHCs). As an example, hydrogen can be combined with carbon dioxide (CO₂) in a Fischer-Tropsch process to produce synthetic hydrocarbons which can then be used as a fuel in existing combustion-based technologies. Alternatively, hydrogen can be used as a feedstock to produce ammonia or methanol, both of which exist in liquid phase at standard temperature and pressure and have higher volumetric energy density than hydrogen at standard temperature and pressure. Ammonia and methanol can be converted back to hydrogen or used directly to produce electricity.

¹ For comparison, natural gas liquefaction requires a temperature of -162°C (-260°F).

Hydrogen provides the foundation for low-carbon production of each of the chemical energy storage compounds mentioned above and is therefore the focus of discussion throughout this chapter. A hydrogen-based chemical energy storage system encompasses hydrogen production, hydrogen transport and storage, and power production using hydrogen as a fuel input.

While hydrogen generates no carbon emissions at the point of end use regardless of how it is produced, deep decarbonization also requires a low-carbon process for producing hydrogen. One potential production pathway of particular interest for this study is electricity-driven electrolysis. Hydrogen produced via electrolysis can be compressed and stored, either in an above-ground tank or in an underground geologic storage facility. During periods when electricity is needed, hydrogen could be drawn from storage and used as a fuel to generate power from either a gas turbine or a large stationary fuel cell. Hydrogen-fueled power generation assets could act as a direct, zero-carbon substitute for existing natural-gas-fueled peaking plants to balance the grid at times of low variable renewable energy (VRE) availability. As discussed in Chapter 6, costs for geological hydrogen storage are lower than costs for electrochemical (i.e., battery) storage of electric power on an energy basis. Moreover, relatively low-cost underground storage makes it possible to store bulk supplies of hydrogen on a seasonal basis, similar to the way natural gas and petroleum are stored today. Thus, electrolytic hydrogen production at scale has the potential to serve as a massive source of long-duration, flexible load for addressing electricity system imbalances that may arise during extended periods of low VRE availability or high electricity demand from other less flexible end uses.

5.1.1 Hydrogen production

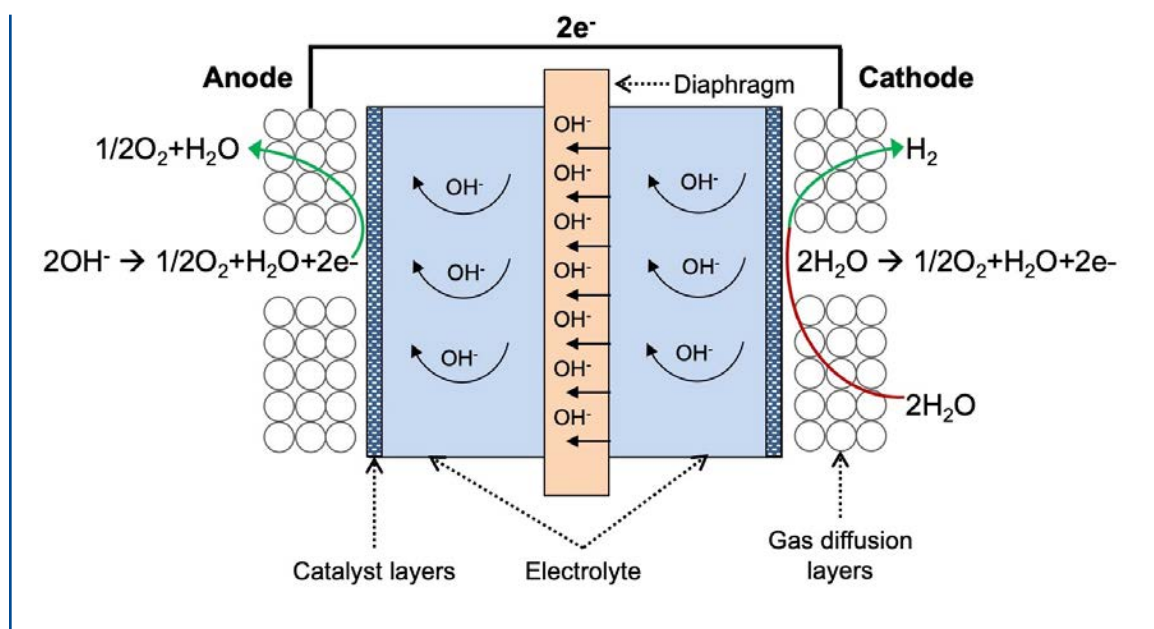
The upstream element of the chemical energy storage value chain is comprised of the hydrogen production unit.

There are many pathways for producing hydrogen—some of which are considerably more carbon-intensive than others. Historically, a process called steam methane reforming (SMR)—in which water and heat are used to reform a natural gas molecule into component parts—has accounted for the vast majority of global and U.S. hydrogen production to date. This process is quite carbon-intensive: For each kilogram of hydrogen produced, between 8 and 10 kilograms of CO₂ are produced.² Carbon capture technology can be added to mitigate up to 95% of these emissions, but that approach will not entirely eliminate emissions from SMR (Preston 2018; CE Delft 2018).

Since the main subject of this study is the role of energy storage in achieving deep decarbonization of the electricity system, we focus on hydrogen production using electrolysis, a technology that is already commercially available. In electrolysis, electricity is used to separate water into hydrogen and oxygen. Electrolyzers can operate at either low or high temperature. High-temperature systems, such as solid-oxide electrolyzers, pair steam with the hydrogen production process to increase overall efficiency. Such technologies, however, have yet to be commercialized and require an outside source of steam to operate. The potential exists to co-locate high-temperate electrolysis with other industrial processes or nuclear power production to take advantage of waste heat, but these are likely to be niche opportunities relative to low-temperature electrolysis, which does not require an exogenous heat

² Researchers have estimated that if upstream emissions from the natural gas value chain are included, CO₂ emissions from SMR increase to 10–16 kilograms per kilogram of hydrogen produced (Parkinson et al. 2019).

Figure 5.1 Representation of alkaline electrolyzer reaction



source (International Energy Agency 2019; International Renewable Energy Agency 2020). We therefore limit the discussion in this chapter to low-temperature electrolyzers—specifically, alkaline and proton exchange membrane (PEM) electrolyzers, which are the two most mature low-temperature electrolysis technologies.

Alkaline electrolyzers

Alkaline electrolyzers are the more mature of the two main low-temperature electrolysis technologies. These systems consist of an anode and cathode and use electricity to split water into its constituent molecules, hydrogen and oxygen, based on the following reaction (Keçebas, Kayfeci and Bayat 2019):

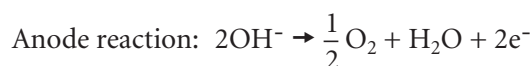


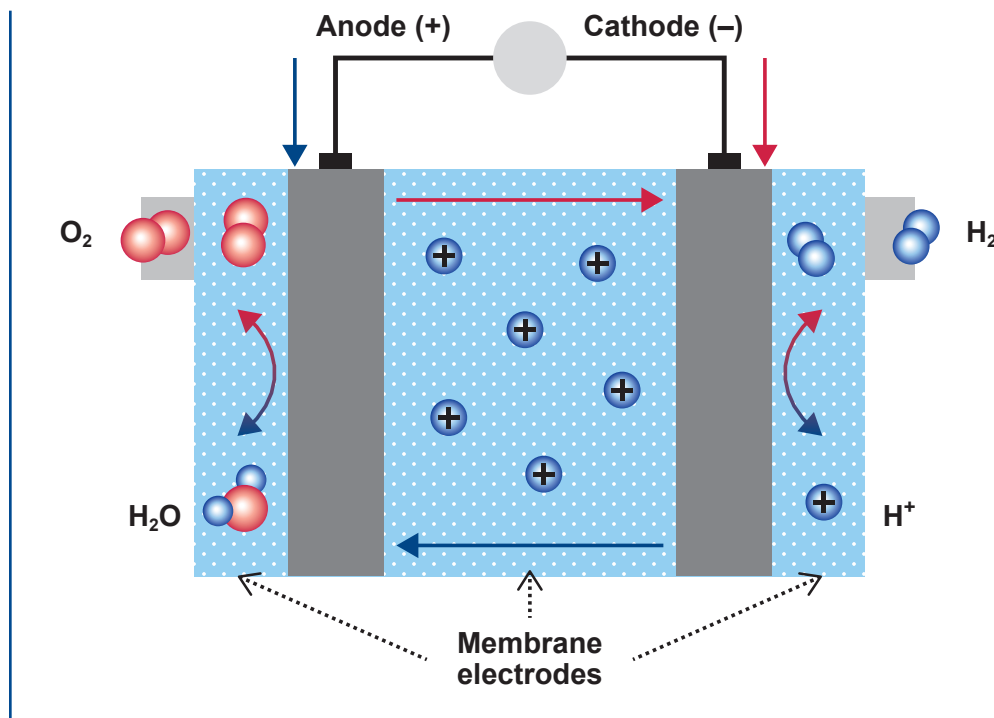
Figure 5.1 depicts the operation of an alkaline electrolyzer.

Alkaline electrolysis has been utilized for decades, but the technology has several drawbacks: first, the alkaline solution is corrosive and second, slow ramping limits flexibility to respond quickly to demand, diminishing the technology's value for electricity systems (International Energy Agency 2019).

PEM electrolyzers

Like alkaline electrolyzers, PEM electrolyzers produce hydrogen by splitting water into its constituent elements using an anode and cathode. In a PEM electrolyzer, however, the anode and cathode are separated by a polymer membrane in an alkaline solution (by contrast, only the positively charged hydrogen molecules are allowed to move from the anode to the cathode). Figure 5.2 illustrates the internal operation of a PEM electrolyzer.

Figure 5.2 Representation of PEM electrolyzer



PEM electrolysis uses fewer components and pumps and, as such, requires less maintenance. Moreover, the use of a membrane instead of an alkaline solution minimizes corrosion. This type of electrolyzer can operate at small and large scale to provide distributed or centralized hydrogen production. Relative to alkaline electrolyzers, these systems produce hydrogen at higher pressure and purity, operate at lower temperatures, and can quickly ramp up and down over a wide operating range, which can be very valuable from a grid balancing perspective. High manufacturing costs, due in part to the use of platinum and iridium catalysts, have been a key disadvantage for PEM electrolyzers (International Energy Agency 2019).

5.1.2 Hydrogen transport, distribution, and storage

The midstream section of the chemical energy storage value chain links the upstream production of hydrogen and its downstream

consumption. Not surprisingly, the economic feasibility of chemical energy storage relies on ready access to low-cost hydrogen storage technologies. The two main modes of hydrogen storage are aboveground and underground.

Aboveground hydrogen storage

At present, hydrogen is commercially stored in aboveground tanks, much like other industrial gases. These tanks can store either gaseous hydrogen in a pressurized tank or liquified hydrogen in a tank outfitted with refrigeration technology.

Given the technical maturity of aboveground storage, compressed and refrigerated tanks offer an option to store hydrogen today. Moreover, aboveground hydrogen storage affords the opportunity to store hydrogen regardless of geologic constraints, in contrast to underground storage, which we discuss next.

Figure 5.3 A pressurized hydrogen storage tank



Image courtesy of Linde plc.

Underground hydrogen storage

Underground, or geologic, storage of hydrogen is a commercially viable technology that has been deployed at scale—in fact, hydrogen is currently stored in underground salt caverns in many locations throughout the world.

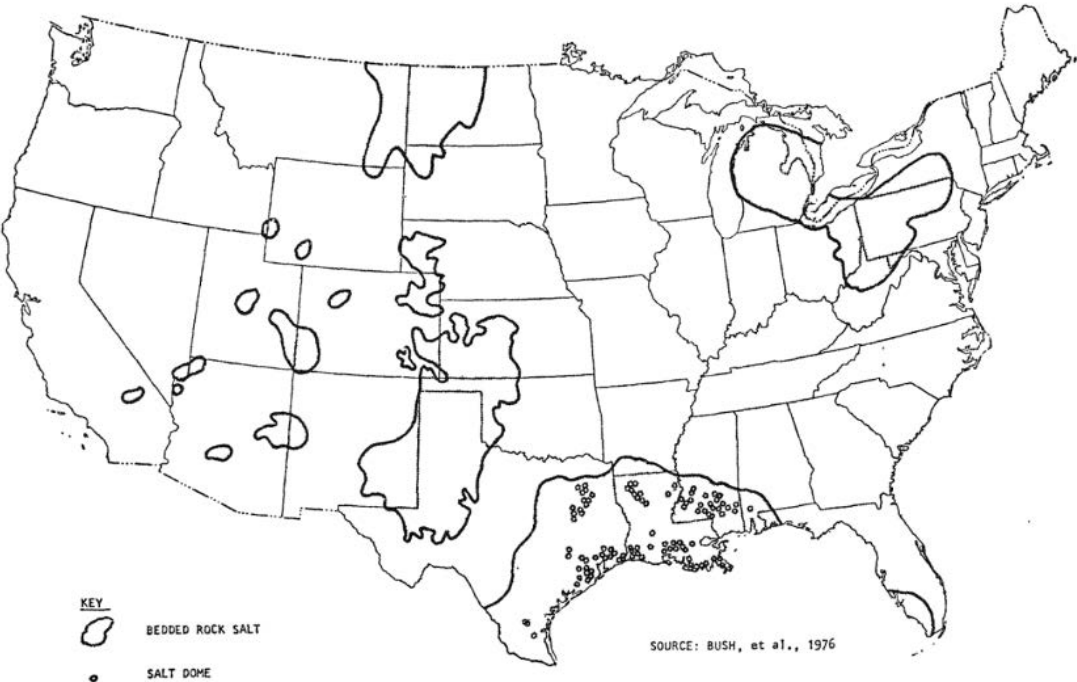
Underground storage facilities are much larger than aboveground facilities and have the capacity to store orders-of-magnitude more hydrogen, on an energy basis (Lord, Kobos and Borns 2014; International Energy Agency 2015). However, underground storage requires suitable geology and locations with salt caverns that could be mined are limited. Figure 5.4 shows salt beds and salt domes in the United States.

According to Lord, Kobos and Borns (2014), the only commercially feasible salt caverns can be mined in salt domes. However, the Advanced Clean Energy Storage (ACES) project in Utah is looking to develop a salt cavern for hydrogen storage in bedded rock salt deposits (Magnum Development 2019). These caverns are mined

through a process called leaching, in which a hole is drilled into the salt dome and fresh water is used to leach away the salt until a roughly cylindrical cavern has been mined. A stylized rendition of a salt cavern for hydrogen storage is shown in Figure 5.5.

As a point of reference, natural gas is also stored underground throughout the United States. However, these storage sites are not limited to salt domes. In 2019, only 8% of the natural gas delivered daily from underground storage facilities in the United States was being stored in salt caverns (International Energy Agency 2019). Natural gas is also stored in depleted oil and gas reservoirs, aquifers, and hard rock caverns. But because of its physical and chemical properties, hydrogen can only be stored in salt caverns. Specifically, there are issues with the reactivity of hydrogen, and the physical size of hydrogen molecules can lead to leaks in other types of geologic storage media—this is an area of active research (Lord, Kobos and Borns 2014).

Figure 5.4 Salt deposits in the United States



Source: Foh et al. (1979)

Figure 5.5 Stylized representation of underground salt cavern

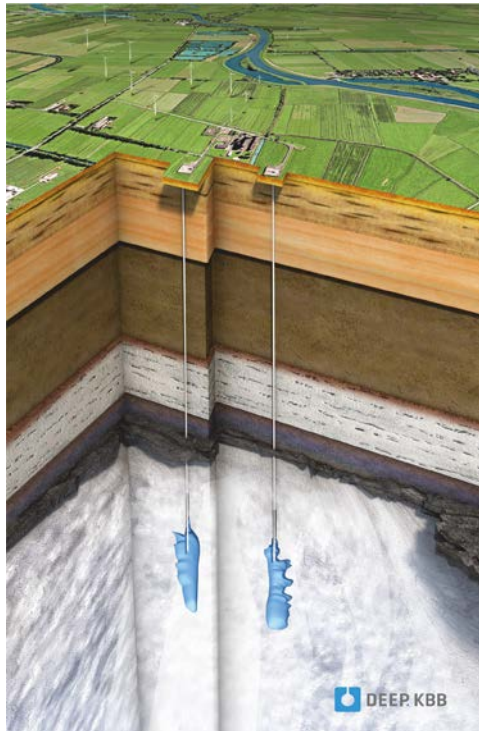


Image is copyright DEEP.KBB GmbH.

5.1.3 Hydrogen consumption

The downstream element of the chemical energy storage value chain involves the conversion of hydrogen back to power. Several technologies can be used in this step: For example, a traditional thermal power generation unit such as a gas turbine, steam turbine, or combined cycle power plant can be directly fueled by hydrogen, or hydrogen can be used in a large stationary fuel cell.

Thermal plants

Because of the physico-chemical properties of hydrogen, existing thermal power generators would need to be reengineered to utilize hydrogen as a fuel input. A key issue is that hydrogen combustion, while it does not generate CO₂, does produce emissions of nitrogen oxides (NO_x), a pollutant linked to acid rain and ground-level ozone. In fact, the higher temperature of hydrogen combustion means that NO_x emissions can be nearly double the levels typical for natural gas combustion (Ditaranto, Heggset and Berstad 2020). Historically, NO_x emissions from thermal plants have been controlled by either premixing air and fuel prior to combustion; diluting fuel with steam, water, or nitrogen; or removing exhaust gases. Given the higher flammability limits of hydrogen relative to natural gas, premixing fuel with air prior to combustion is problematic (Chiesa, Lozza and Mazzocchi 2005). Therefore, many original equipment manufacturers (OEMs) are actively researching and developing hydrogen-fired gas turbines with the appropriate levels of diluent and the exhaust gas management systems needed to keep NO_x emissions from the combustion process appropriately low (Goldmeer 2019; Mitsubishi Hitachi Power Systems 2019; Siemens Energy 2020).

Based on conversations with gas turbine OEMs, the industry view is that both new builds of hydrogen-fired thermal plants and retrofits of existing plants to use hydrogen as the central

fuel are technically and commercially feasible. Reports of retrofit projects have appeared in the trade press, along with announced plans by OEMs and their partners to retrofit existing natural gas-fired power plants for operation on blends of hydrogen and natural gas *en route* to burning 100% hydrogen fuel within the decade (Mitsubishi Hitachi Power Systems 2020; Malik 2020).

Fuel cells

The mechanics of a fuel cell are similar to those of an electrolyzer. In fact, a fuel cell can be described as an electrolyzer that simply operates in reverse. The fuel cell takes hydrogen and oxygen as fuel inputs and transforms the hydrogen into electric power and water. A stylized rendition of a fuel cell is shown in Figure 5.6.

As compared to thermal power generation units, fuel cells are a much more nascent technology. Many breakthroughs have been achieved in developing fuel cells sized for vehicular applications—that is, on the order of kilowatts of useful power output—but the development of megawatt-scale stationary fuel cells that could be used for power generation has lagged. To the extent stationary fuel cell projects have been developed in the United States, these projects have generally used natural gas inputs rather than hydrogen (Saur et al. 2016). Hydrogen is produced internally by reforming the natural gas. The produced hydrogen is then used to generate electric power.

5.1.4 Combining elements of a chemical storage system

The elements of the value chain can be combined to create a clear picture of a hydrogen-based chemical energy storage system. Figure 5.7 shows a stylized representation of such a system.

Figure 5.6 Rendition of a PEM fuel cell

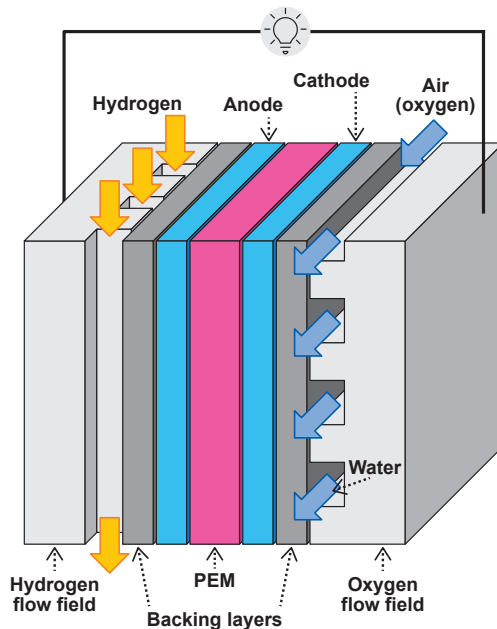
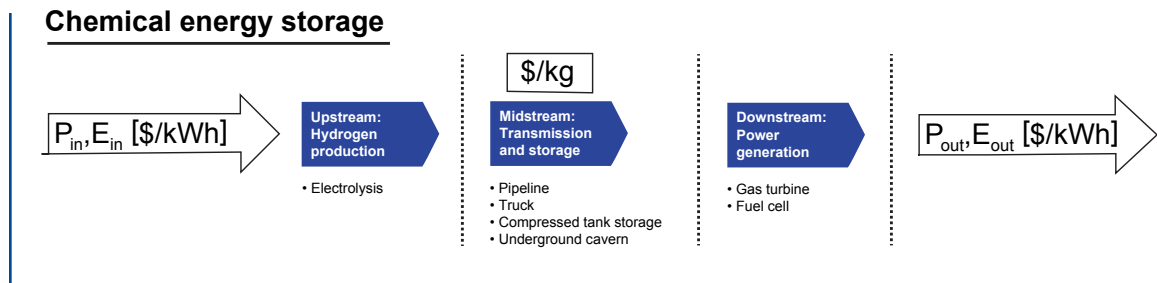


Figure 5.7 Stylized chemical energy storage system



As noted previously, the chemical energy storage pathway takes electric power, either directly from the power grid or from a dedicated generation source, produces hydrogen through the operation of an electrolyzer, transports and stores the hydrogen, and generates electric power through gas-to-power technologies when demand for power exceeds available supply.³

The total cost to store energy using this chemical storage pathway includes the cost of the electricity needed to produce the hydrogen and the cost to generate power using hydrogen as a fuel input.

5.2 Techno-economic modeling

Using the framework described in the foregoing section, we build bottom-up models to assess the techno-economics of each element of the

³ If an electrolyzer is co-located with hydrogen demand, the transportation element of the value chain may not be relevant.

Table 5.1 Assumptions for hydrogen production cost modeling

| | Value | Source |
|---------------------------------|--------|-------------------------|
| Water cost [\$/liter] | 0.0017 | Assumption ⁴ |
| Project lifetime [Years] | 20 | Assumption |
| Discount rate [%] | 10 | Assumption |

chemical energy storage value chain. The models can be combined to estimate the total cost of power produced via a hydrogen-fueled power plant where the hydrogen has been produced from grid-supplied electricity.

5.2.1 Hydrogen production costs

To model the cost of producing hydrogen from alkaline and PEM electrolyzers, we consider several exogenous variables:

- capital expenditures (“capex”)
- fixed operations and maintenance (FOM) costs
- cost of power
- cost of water
- capacity factor of the electrolyzer
- efficiency of the electrolyzer

The model uses these variables to endogenously solve for the cost of producing hydrogen.

Cost estimates for 2020

To estimate the cost of producing hydrogen in 2020 using electrolysis powered by grid-supplied electricity, we first set the assumptions shown in Table 5.1.

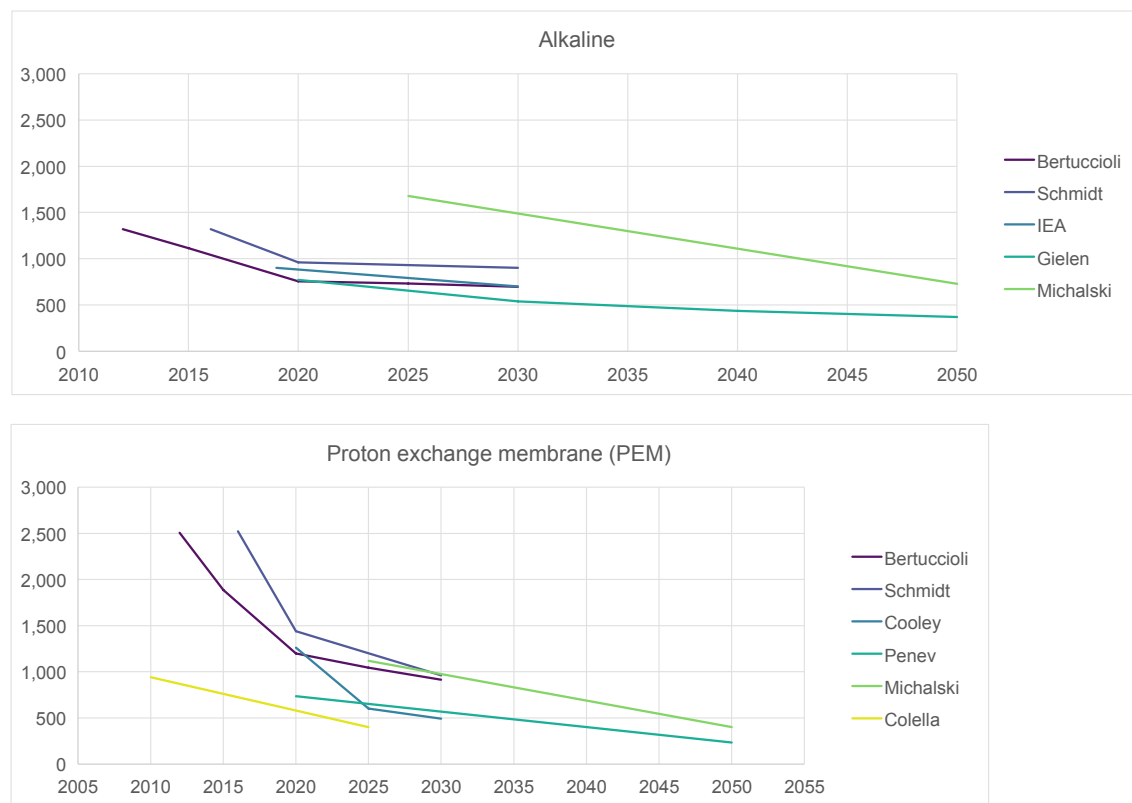
Electrolyzer capital and operating costs

Our estimates for electrolyzer capital and operating costs are based on a review of the academic literature and commercial publications. Projected reductions in capital cost for alkaline and PEM electrolysis technologies are shown in Figure 5.8.

Based on these forecasts, we estimate the capital cost for an alkaline electrolysis system in 2020 at \$850 per kilowatt (kW). Our capital cost estimate for PEM systems is \$1,240/kW. These estimates include stack cost and balance-of-plant costs at the site. To translate these capital costs into overnight installed costs, our model assumes a “soft cost” factor of 30%. This factor, which is based on the National Renewable Energy Laboratory’s (NREL’s) H2A model, considers the total cost associated with procuring land, obtaining permits, and constructing a facility (National Renewable Energy Laboratory). Including these costs, we estimate overnight capital cost at \$1,200/kW for an alkaline system and \$1,800/kW for a PEM system. Our model assumes combined annual fixed operations and maintenance (FOM) costs of \$75.20 per kilowatt-year (\$/kW-yr) for a PEM system in 2020 (Guerra et al. 2018). Applying the same proportion of FOM cost to overnight capital cost, we estimate FOM costs for an alkaline system at \$55/kW-yr. The model solves for variable costs, specifically for power and water, endogenously based on total hydrogen production.

⁴ MITEI analysis based on water rates for the city of Phoenix.

Figure 5.8 Forecast capital costs for alkaline and PEM electrolyzers



Source: Bertuccioli et al. (2014); Gielen, Taibi, and Miranda (2019); International Energy Agency (2019); Michalski et al. (2017); Schmidt et al. (2017); Colella et al. (2014); Cooley (2019); and Penev et al. (2019).

Electrolyzer technical specifications

Electrolyzers are technologically complex. To estimate hydrogen production cost for the two types of electrolyzers, we consider three main technical specifications: hydrogen flow, water consumption, and efficiency.

Hydrogen flow refers to the rate of hydrogen production. It can be described in units of hydrogen mass, volume, or energy content per unit time, or in units of power. For this study, we assume an alkaline system produces hydrogen at a rate of 60 cubic meters per hour (m^3/hr), whereas a PEM system produces hydrogen at a rate of 1,000 m^3/hr . This figure is based on technical specifications for electrolyzers that

are commercially available from the manufacturer Cummins (formerly Hydrogenics) (Hydrogenics 2018).

Electrolyzer water consumption refers to the quantity of water needed to produce a unit of hydrogen. We assume water consumption of 1.7 liters per cubic meter of hydrogen (liter/m^3) and 1.4 liters/ m^3 for alkaline and PEM systems, respectively (Hydrogenics 2018).

Electrolyzer efficiency is measured as the amount of electrical energy required to produce a unit of hydrogen. Our model assumes both types of systems have the same efficiency and require 5.2 kilowatt-hours of electricity to

Figure 5.9 Modeled cost of hydrogen produced via electrolysis in 2021

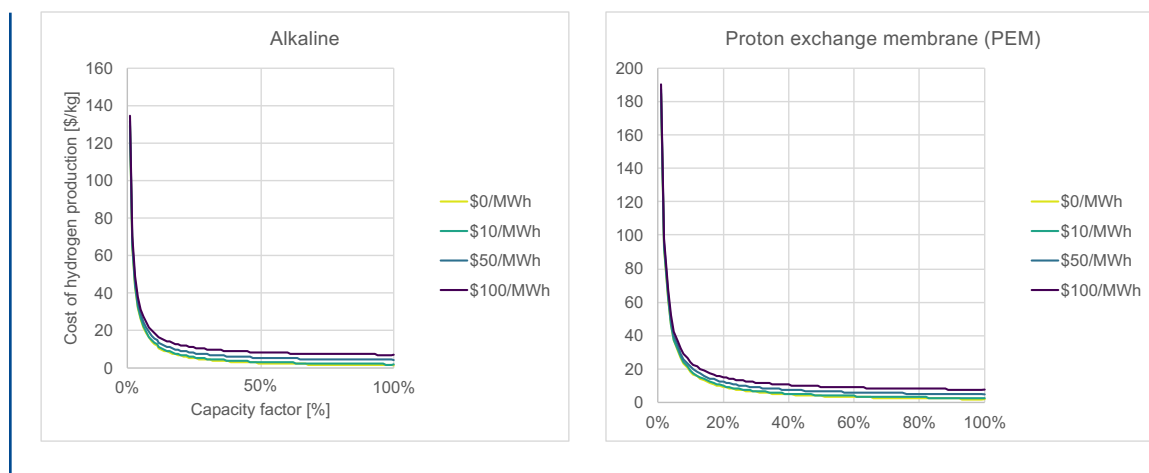


Table 5.2 Operating variables for electrolyzer technologies

| | Alkaline | PEM |
|---|----------|-------|
| Capex [\$/kW] | 1,214 | 1,771 |
| FOM [\$/kW-yr] | 55 | 75 |
| Hydrogen production rate [m ³ H ₂ /hr] | 60 | 1,000 |
| Water consumption [liter/m ³ H ₂] | 1.7 | 1.4 |
| Efficiency [kWh/m ³ H ₂] | 5.2 | 5.2 |

produce a cubic meter of hydrogen (kWh/m³). Table 5.2 summarizes our assumptions for electrolyzer costs and technical specifications.

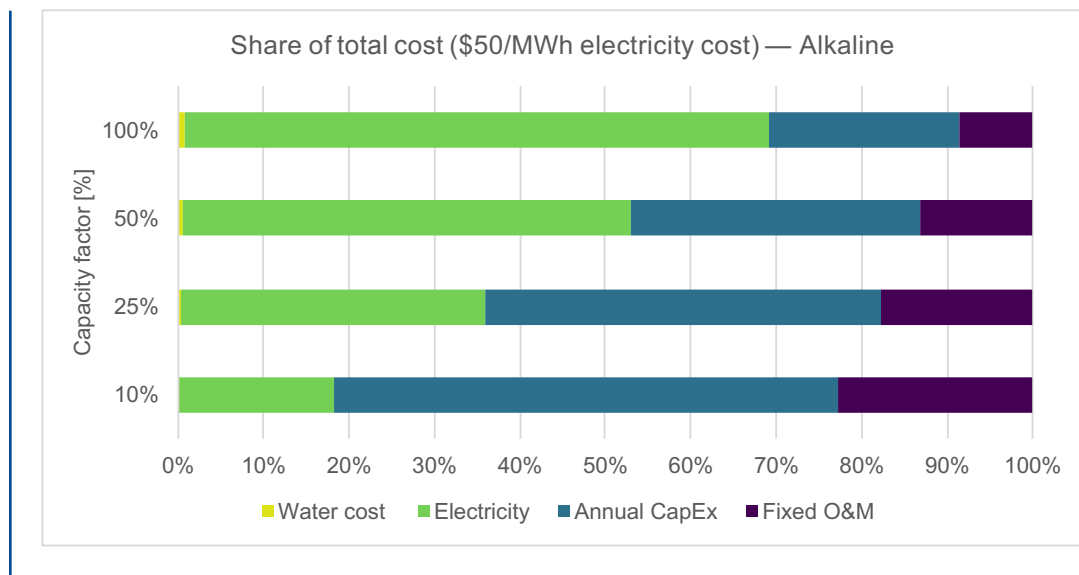
Using these assumptions, the model solves for the cost of producing hydrogen over a range of electricity costs and plant capacity factors (where capacity factor is a measure of plant utilization, typically calculated as the ratio of actual output to maximum “nameplate” output). Results are shown in Figure 5.9.

Based on our model, the lowest achievable cost to produce hydrogen via electrolysis, using current (2020) cost and technical assumptions, is \$1.32 per kilogram (kg) for an alkaline electrolyzer operating at 100% capacity factor and utilizing free or costless electricity (i.e., power costs of \$0/MWh). Although electricity prices may fall to zero during periods of high VRE availability, \$0/MWh power will not be

obtainable for every hour in the year. At a cost of \$50/MWh, which is closer to actual delivered electricity costs for many industrial customers, the lowest achievable hydrogen production cost is \$4.70/kg (U.S. Energy Information Agency 2021) for an alkaline electrolyzer.

Figure 5.10 shows a breakdown of cost elements at different electrolyzer capacity factors. Whereas capital costs are not negligible, especially at lower capacity factors, it is clear that most of the levelized cost of hydrogen production, once plant utilization reaches or exceeds 50%, is driven by the cost of electricity to power the electrolyzer. (It should be noted that Figure 5.10 compares the role of different cost drivers at different capacity factors—it does not show final production cost. In addition, the figure assumes a static electricity price of \$0.05/kWh. At lower capacity factors it might be feasible to limit plant utilization to periods

Figure 5.10 Cost breakdown by variable



when electricity prices are below \$0.05/kWh, or even close to zero—for example, when there is excess VRE availability—thereby reducing final production costs. Thus, the figure should not be read to imply that hydrogen production is necessarily uneconomic at lower electrolyzer capacity factors simply because capital costs, in that scenario, account for a relatively larger share of total cost.

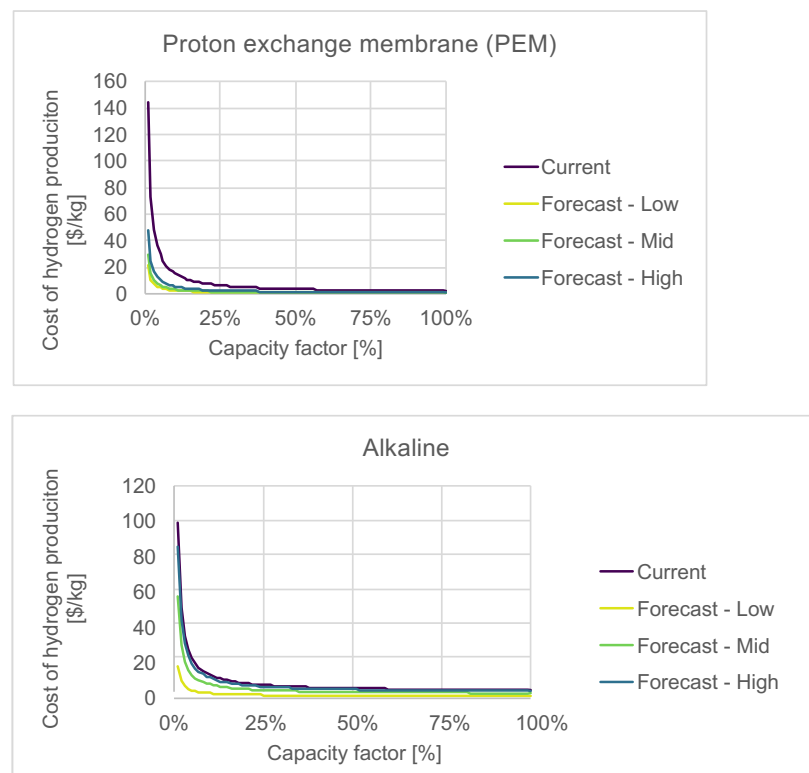
Cost forecasts for 2050

While a review of the current economics of electrolytically produced hydrogen provides useful perspective on the potential role of chemical energy storage, hydrogen is not likely to compete as an energy storage medium in the short term because current costs are too high and required support infrastructure is not available. We therefore model costs for hydrogen production out to 2050, the timeframe of interest for this study, using a range of assumptions about how various technology-specific cost factors might change over the next three decades (Table 5.3). Capital costs in Table 5.3 are estimated from Figure 5.8 for each

technology, and FOM costs are assumed to fall in proportion to modeled reductions in capital cost. While we do not assume any change in hydrogen production or water consumption rates for the two electrolyzer technologies, we do consider the effect of improvements in electrolyzer efficiency. In the high-cost case, we assume there are no efficiency gains for alkaline systems and only marginal improvements for PEM systems between 2020 and 2050. In the low-cost case, we assume aggressive efficiency improvements for each technology. Our mid-cost estimates are in between. Figure 5.11 shows modeled hydrogen production costs based on the input assumptions summarized in Table 5.3.

In our modeling, the lowest cost for hydrogen production via electrolysis in 2050 is \$0.70/kg. This is lower than the 2030 cost target set by the U.S. Department of Energy (DOE) as part of its Earthshots Initiative, which was announced in June 2021 (U.S. Department of Energy 2021). In contrast to estimates of “current” cost, our modeling shows future costs falling rapidly as electrolyzer capacity factor increases from 0%

Figure 5.11 Forecast 2050 hydrogen production costs



Source: Bertuccioli et al. (2014); Gielen, Taibi, and Miranda (2019); International Energy Agency (2019); Michalski et al. (2017); Schmidt et al. (2017); Colella et al. (2014); Cooley (2019); and Penev et al. (2019).

Table 5.3 Cost and operational assumptions by production technology (2020 and 2050)

| Technology | Case | Capex ⁵ [\$/kW] | FOM ⁶ [\$/kW-yr] | Energy [kWh/m ³] |
|------------|---------|----------------------------|-----------------------------|------------------------------|
| Alkaline | Current | 1,214 | 51 | 5.2 |
| | High | 1,041 | 44 | 5.2 |
| | Mid | 730 | 31 | 5 |
| | Low | 236 | 10 | 4.75 |
| PEM | Current | 1,771 | 75 | 5.2 |
| | High | 602 | 25 | 5 |
| | Mid | 479 | 20 | 3.94 |
| | Low | 356 | 15 | 3.8 |

⁵ Forecast capex figures are based on the sources listed in Figure 5.8. Note that the capex figure shown in Table 5.3 reflects overnight capital cost, which includes soft costs associated with facility construction, while the forecasts in Figure 5.8 reflect uninstalled costs.

⁶ The FOM figure scales with capital cost reductions. The assumed FOM is equal to 4.2% of the overnight capex (Guerra et al. 2018).

to 25% and plateauing beyond a 25% capacity factor. This rapid decline in production cost at low capacity factors reflects affordable low-carbon hydrogen production using low-cost grid electricity. Based on the results shown in Figure 5.11, capacity factors for an electrolyzer in 2020 must be very high (above 60%) before cost declines begin to slow. With this plateau occurring earlier in our cost forecasts for 2050, the power production profiles of variable renewable generators will allow for the production of low-cost, low-carbon hydrogen.

5.2.2 Hydrogen storage costs

As noted previously, hydrogen can be stored in aboveground tanks, either as a compressed gas or liquid; alternatively, it can be stored as a gas in an underground geologic storage facility. To quantify the storage element of the hydrogen value chain for the modeling analysis in Chapter 6 of this report, we estimate the capital cost associated with constructing hydrogen storage assets, the FOM costs associated with operating these assets, and the efficiency of the assets. Capital cost is measured on a cost-per-unit-stored basis; for purposes of our modeling, we use dollars per megawatt-hour of hydrogen stored (\$/MWh). One MWh of hydrogen is approximately equivalent to 30 kg of hydrogen. We use an energy unit for hydrogen storage to facilitate comparison with other energy storage technologies. We assume annual FOM costs are a proportion of capital cost. Efficiency is given as a percentage; it accounts for the energy required to compress the hydrogen prior to storage. For example, 93% efficiency means that the equivalent of 7% of the energy content in the original quantity of hydrogen produced is consumed during the process of conditioning hydrogen for storage. Table 5.4 shows 2020 and 2050 assumptions for each of the key metrics used to estimate hydrogen storage costs.

5.2.3 Costs to generate power using hydrogen

Similar to our approach for estimating the upstream costs of producing hydrogen, we build a bottom-up model to assess the cost of generating electricity using hydrogen. We consider three generation technologies: gas turbines, combined cycle gas turbines, and large stationary fuel cells.

Our model calculates total cost to produce electricity from hydrogen by solving endogenously for several exogenous variables:

- overnight capital costs
- fixed operation and maintenance (FOM) costs
- variable operation and maintenance (VOM) costs
- plant efficiency

Techno-economic assumptions

The capital cost of a hydrogen-fired thermal generator is difficult to estimate given that such generators have not been widely developed and information about the installed cost of the small number of plants that do exist is not publicly available. In discussions with OEMs, we estimate the capital cost of a 100% hydrogen-fired gas turbine at \$1,000/kW. We further assume that an additional NO_x control element is needed on the back end of the combustion turbine to address NO_x emissions—specifically, we assume that a selective catalytic reduction (SCR) asset is integrated into the system. Adding a capital cost of \$320/kW for the NO_x control system brings the total capital cost for a hydrogen-fired gas turbine to an estimated \$1,320/kW (Sargent and Lundy 2010). To estimate capital cost for a hydrogen-fired combined cycle plant, we used data from the Annual Technology Baseline (ATB) published by the U.S. National Renewable Energy

**Table 5.4 Techno-economic estimates for hydrogen storage technologies
(2020 and 2050)**

| Technology | Case | Capex [\$/MWh] | FOM [\$/MW-yr] | Efficiency [%] |
|--------------------|---------|---------------------|-------------------|-------------------|
| Aboveground | Current | 8,000 ⁷ | 80 ⁸ | 96% ⁹ |
| | High | 8,000 | 80 | 96% |
| | Mid | 7,000 | 70 | 96% |
| | Low | 6,000 | 60 | 96% |
| Geologic | Current | 1,179 ¹⁰ | 29 ¹¹ | 93% ¹² |
| | High | 1,179 | 29 | 93% |
| | Mid | 1,144 | 26 | 93% |
| | Low | 1,120 | 22 | 93% |

Laboratory (NREL) to calculate the ratio of capital costs for a natural gas-fired combined cycle unit to capital costs for a natural gas-fired gas turbine. We then applied this ratio to our capital cost estimate for a hydrogen-fired gas turbine (i.e., \$1,320/kW) to estimate the capital cost of a hydrogen-fired combined cycle plant at \$1,333/kW.

To forecast capital cost reductions, we relied on capital cost forecasts from the NREL ATB for natural gas-fired gas turbines and combined cycle plants. We assume capital costs for hydrogen-fired thermal generators will fall in line with costs for natural gas-fired thermal generators. In our high-cost case we assume

the capital cost reductions forecast in the ATB do not fully materialize, in the mid-cost case we assume cost reductions follow the ATB, and in the low-cost case we assume more aggressive cost reductions than the ATB.

Given the nascent nature of hydrogen-fired thermal power generation technologies, we assume the fixed and variable operations and maintenance (FOM and VOM) costs for these technologies are the same as for natural gas-fired thermal generation. These values are not anticipated to change over time according to the NREL ATB; accordingly, we assume no change in FOM and VOM costs for hydrogen-fired thermal generation assets.

⁷ This figure represents an average of high and low estimates for pressurized-tank hydrogen storage. The high-cost assumption is no change from current cost, the mid-cost case is set to the average of current cost and current stated low cost, and the low-cost case is equal to current low cost (International Energy Agency 2015, 32). Inflated to \$2,020 from \$2,015.

⁸ O&M costs are assumed to equal 1% of capex for current and forecast O&M (Penev et al. 2019).

⁹ Ramsden et al. assume 1.2 kWh needed to store 1 kg of hydrogen. This implies compressor efficiency of 96%. We assume that compressor efficiency does not improve for future cases (Ramsden, Kroposki and Levine 2008).

¹⁰ We assume capital cost for compression to 120 standard atmosphere (atm) is \$35/kg-H₂. This was converted to units of \$/MWh based on the lower heating value of hydrogen (120 MJ/kg). We assume future capex at 100%, 97%, and 95% of current capex for geologic hydrogen storage in our high-, mid-, and low-cost cases, respectively (Ahluwalia et al. 2019, 19).

¹¹ All operations and maintenance costs are rolled into FOM. Current FOM is 2.5% of capex for current case. Values are set at 2.5%, 2.25%, and 2% of capex for high-, mid-, and low-cost cases, respectively. FOM is calculated as a percent of capex, per Table 10 in Erichsen et al. (2019).

¹² This efficiency figure of 93% represents an average of high and low efficiencies for geologic storage facilities. We assume forecast efficiencies do not improve. See table 6 in International Energy Agency (2015).

OEMs around the world are pioneering fuel cell technology in which the internal steam methane reforming (SMR) unit is split from the system, leaving only the fuel cell, which is powered by pure hydrogen and oxygen. Given that large-scale fuel cell technology of this type is still in the nascent stages of development, it is difficult to estimate future costs. Initial capital cost estimates for PEM fuel cells are on the order of \$3,000/kW, but the Lawrence Berkeley National Lab estimates that economies of scale and increased manufacturing efficiencies through learning-by-doing could reduce PEM fuel cell capital costs to roughly \$950/kW in the future (Weidner, Ortiz Cebolla and Davies 2019; Wei 2016). Cost declines of this magnitude are comparable, in percentage terms, to estimated cost declines for electrolyzers (ITM Power 2020). Given that the materials and manufacturing processes used to construct electrolyzer and fuel cell systems are similar, it makes sense that both technologies would experience similar cost declines.

Our estimate for the efficiency of PEM fuel cells, based on key references, is 50% in 2030. This compares to current efficiencies on the order of 45%. Given the uncertainty associated with PEM fuel cell technology, we assume 2050 efficiency remains at 50% in our mid-cost case. For our low-cost case, assume a marginal improvement in efficiency to 55% (Weidner, Ortiz Cebolla and Davies 2019).

Based on the technological similarity between a PEM fuel cell and a PEM electrolyzer, we assume similar FOM costs. Specifically, we assume that all operational costs for a PEM fuel cell are captured in the annual FOM charge and that this charge is 4.2% of the installed capital cost throughout the forecast period.

Our modeling assumptions for downstream power-generation costs are summarized in Tables 5.5 and 5.6.

Estimated costs for hydrogen-based electricity generation in 2020

Using the assumptions listed in Table 5.6, we estimate the cost of produced power for different generation technologies. The results from this techno-economic analysis are shown in Figures 5.12 and 5.13.

Several observations from Figures 5.12 and 5.13 are worth highlighting. First, it is clear that the cost of producing power, regardless of generation technology, falls off sharply as plant capacity factor increases from 0 to 15%. Thereafter, further cost reductions begin to level off substantially. Second, under our assumptions, combined cycle plants yield the most cost competitive hydrogen-generated power across a range of capacity factors and hydrogen prices. Third, there is a threshold where, depending on plant capacity factor and the price of hydrogen at the plant gate, power can be produced more cheaply from a PEM fuel cell than from a gas turbine.

Cost forecasts for hydrogen-based electricity generation in 2050

Leveraging forecast cost and operational characteristics for different generation technologies (Table 5.6), we are able to estimate the cost of power produced from these technologies. The results from this modeling exercise are shown in Figures 5.14 and 5.15.

Notably, combined cycle turbines still produce the lowest-cost power of the generation technologies we modeled, across all hydrogen prices and capacity factors, in 2050. Relative to our 2020 estimates, forecast power production costs for a PEM fuel cell are closer to those for a gas turbine. This is primarily because we forecast a dramatic decline in PEM capital costs relative to gas turbine capital costs. Given that gas turbine technology is mature, we believe it is unlikely that a radically cheaper gas turbine

Table 5.5 Global assumptions used in downstream model

| | Value |
|---------------------------------|--------------|
| Project lifetime [Years] | 20 |
| Discount rate [%] | 10 |
| Plant size [MW] | 100 |
| Hydrogen cost [\$/kg] | Varies |
| Capacity factor [%] | Varies |

**Table 5.6 Techno-economic inputs for different generation technologies
(2020 and 2050)**

| Technology | Case | Capex [\$/kW] | Efficiency [%] | FOM [\$/kW-yr] | VOM [\$/MWh] |
|-----------------------------------|-------------|-------------------------|--------------------------|--------------------------|------------------------|
| Gas turbine | Current | 1,320 | 30% | 14 | 2.0 |
| | High | 1,188 | 35% | 14 | 2.0 |
| | Mid | 1,148 | 45% | 14 | 2.0 |
| | Low | 1,109 | 55% | 14 | 2.0 |
| Combined cycle | Current | 1,333 | 45% | 11 | 1.7 |
| | High | 1,200 | 60% | 11 | 1.7 |
| | Mid | 1,160 | 65% | 11 | 1.7 |
| | Low | 1,120 | 70% | 11 | 1.7 |
| PEM fuel cell¹³ | Current | 3,500 | 45% | 147 | — |
| | High | 2,500 | 45% | 105 | — |
| | Mid | 1,500 | 50% | 63 | — |
| | Low | 950 | 55% | 40 | — |

alternative will emerge. A California case study is recently published by Hernandez and Gençer (2021). Stationary PEM fuel cells, on the other hand, are at a much earlier stage of development. As noted previously, this means the technology could still benefit from substantial cost declines as expanded deployment results in enhanced manufacturing processes and generates economies of scale.

5.3 Chemical energy storage and power market dynamics

Of the three power generation technologies considered in the previous section, the combined cycle power plant yields the lowest-cost

hydrogen-based electricity for all the cases we modeled. Notably, the lowest cost achieved by this technology in a “realistic” future case with \$1/kg hydrogen and a plant capacity factor of 30% is on the order of \$120/MWh. To put this figure in perspective, Figure 5.16 shows a histogram of day-ahead hourly electricity prices for the Los Angeles area in 2019; the vertical line indicates an hourly price of \$120/MWh.

Of course, the distribution of hourly prices for the deeply decarbonized power systems of the future will almost certainly look dramatically different from the distribution of current systems. Nonetheless, the results presented in

¹³ All O&M costs (both VOM and FOM) are rolled into the FOM, which is assumed to be equal to 4.2% of the capex (similar to the assumption made for PEM electrolyzers).

Figure 5.12 Modeled 2020 cost of power produced from hydrogen-fueled power generator vs. capacity factor of plant

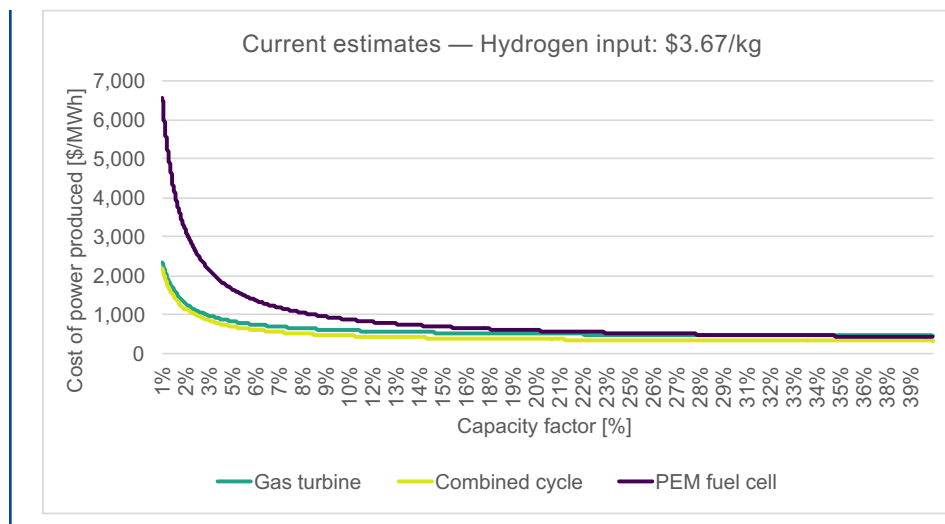
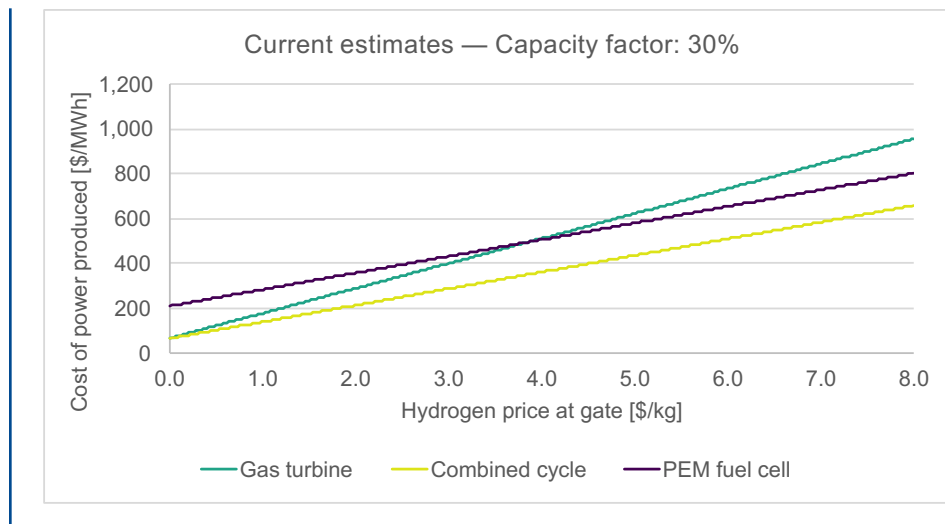


Figure 5.13 2020 modeled cost of power produced from hydrogen-fueled generator vs. hydrogen price at plant's gate



our analysis align with the view that hydrogen, used as an energy storage medium, will serve to help address imbalances in the bulk power system. A grid that is supplied primarily by VRE generators will experience imbalances between supply and demand. Short-term imbalances will be met by more cost-effective short-duration energy storage technologies such as lithium-ion batteries, but if imbalances

persist (for example, if there are weeks when the wind does not blow and the sun does not shine), power markets will reflect supply scarcity. These would be the times when hydrogen-fueled generators could be called upon to provide power. Chapter 6 explores this dynamic by integrating hydrogen as an energy storage medium in power market modeling under different decarbonization scenarios.

Figure 5.14 2050 forecast cost of power produced by technology vs. capacity factor

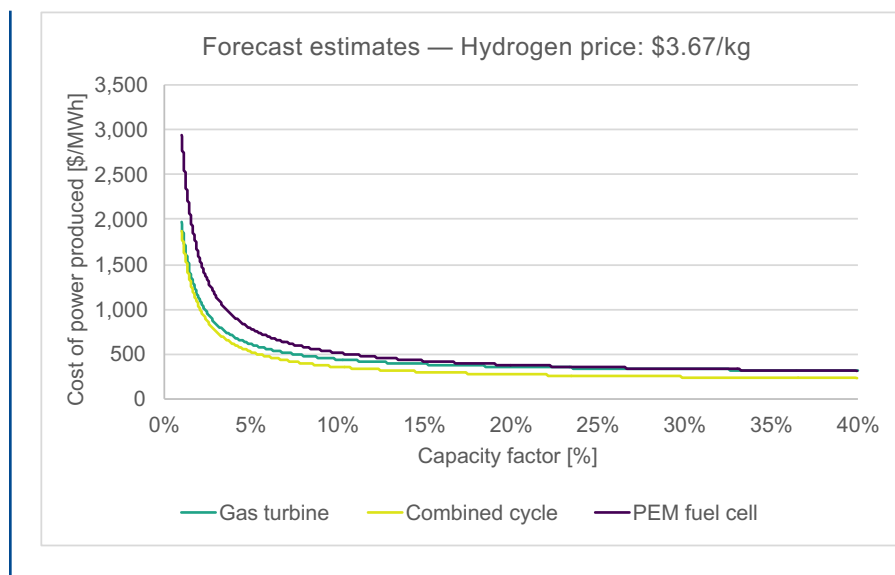
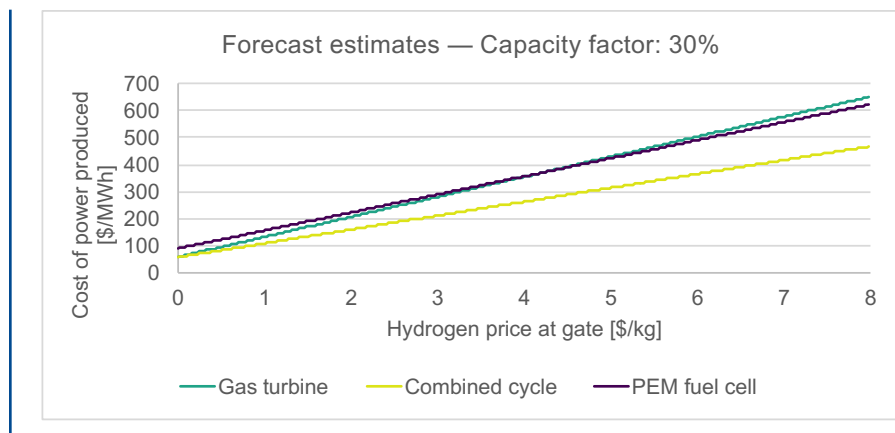


Figure 5.15 Forecast cost of power produced by technology vs. price of hydrogen at plant gate



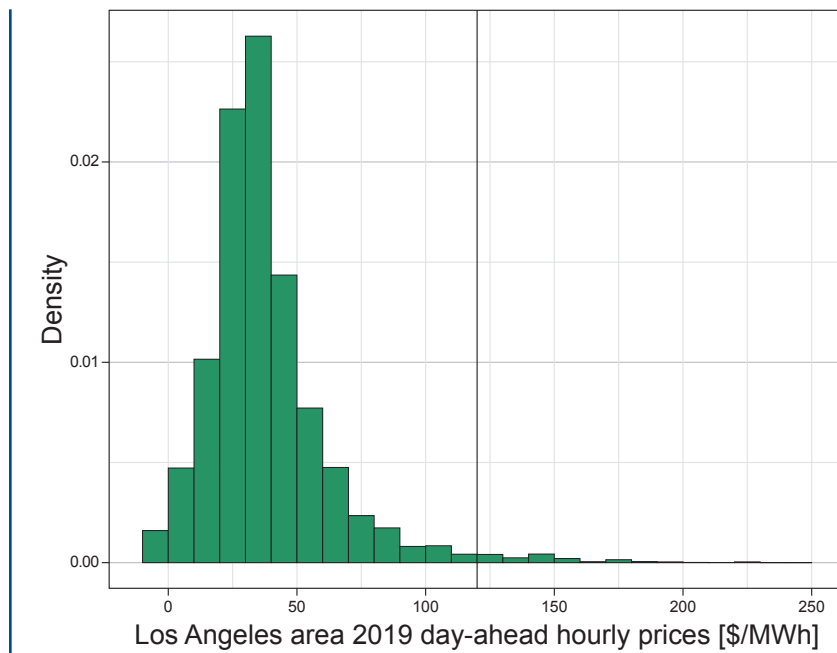
5.4 Demand for hydrogen outside the power sector

While chemical energy storage (and long-duration energy storage more generally) will be required as the power system transitions from very low to zero carbon emissions, it is likely that the electric power sector will not be the main driver of future demand for hydrogen. Rather, hydrogen is more likely to compete on

an economic basis with low-carbon substitutes in other areas of the energy sector—notably transportation, buildings, and industry.

For example, the European Fuel Cell and Hydrogen Joint Undertaking (FCH) projects that efforts to decarbonize transportation and natural gas networks will drive most of Europe's demand for hydrogen in 2050. Power sector decarbonization and renewable energy

Figure 5.16 Histogram of 2019 day-ahead hourly electricity prices in the Los Angeles area



integration, by contrast, are expected to account for only a very small share (approximately 0.5%) of hydrogen demand. Increased demand for “green” hydrogen will drive down the cost of green hydrogen production technologies, eventually making power generation via hydrogen more cost competitive. Final demand for hydrogen will vary by region, however. In the United States, the DOE estimates that demand for hydrogen could grow ten-fold, with the electric power sector accounting for roughly 15% of overall demand by 2050. While this would be a larger share of final hydrogen demand than is currently anticipated for Europe based on the FCH projections, seasonal energy storage using hydrogen as the storage medium still makes up only a fraction of total U.S. hydrogen demand in the DOE’s projections (Ruth et al. 2020).

5.5 Conclusion and key takeaways

Hydrogen and other chemical energy storage media could potentially play a significant role in a future decarbonized energy system. But while low energy capacity costs make hydrogen, and fuels derived from hydrogen, good candidates for long-duration energy storage, value streams beyond energy storage exist for these fuels. Namely, sector coupling could stimulate demand for “clean” hydrogen across the industrial and transportation sectors as countries pursue economy-wide decarbonization. In addition, the production of hydrogen to meet energy needs in other sectors could provide value as a demand-side management strategy in the power sector (for example, hydrogen production facilities could operate when the grid has to manage excess VRE generation). Moreover, key regulatory issues, such as the current lack of a regulatory framework for hydrogen infrastructure development in the United States, must be proactively addressed before hydrogen can play a major role in the energy sector more generally.

Several key takeaways emerge from our consideration of hydrogen's potential role as an energy storage medium within the power sector:

- Low capital cost, on an energy basis, and a high technological readiness level across the value chain make chemical energy media, such as hydrogen, a viable option for long-duration energy storage.
- Our analysis focuses specifically on hydrogen because the production, bulk storage, and consumption of hydrogen can occur with no CO₂ emissions.
- The production of other chemical energy storage media generally requires the production of hydrogen at some point in the process. The production of hydrogen-derived energy storage chemicals results in more inefficiencies across the value chain.
- Hydrogen is currently produced, transported, and sold to industry as a feedstock for numerous industrial processes. There is no significant consumer market.
- Commercially proven technologies exist for all aspects of the hydrogen value chain except for electricity production via hydrogen.
- Progress has been made in developing power generation technologies that use hydrogen as a fuel.
 - Many gas turbine OEMs are pushing to develop 100% hydrogen-fueled gas turbines and combined cycle units that would produce electric power via the combustion of hydrogen. This mode of power production relies on proven technologies; however, the existing technologies must be adapted

to accommodate hydrogen's higher combustion temperature, longer flame length, and subsequent NO_x emissions. Potential cost reductions associated with improvements in hydrogen-based electricity generation technologies are marginal as the technologies themselves are mature.

- Efforts are also underway to develop stationary fuel cells that would produce power via the synthesis of water from hydrogen and oxygen. This mode of power production is currently very expensive relative to more mature combustion technologies. Given the similarity of fuel cells to electrolyzers, however, the cost of fuel cells can be expected to decline precipitously.
- While low costs to store hydrogen make hydrogen an appealing energy storage medium for long-duration applications, using hydrogen as a fuel to produce power is very expensive relative to similarly positioned thermal power generation assets.
- Long-duration energy storage will likely not be the main driver of hydrogen demand in a future decarbonized energy system for the simple reason that hydrogen will be more valuable as a way to indirectly electrify otherwise difficult-to-electrify energy end uses in sectors such as transportation and industry (an example would be the use of hydrogen fuel cells in long-distance vehicles). Future demand for hydrogen will likely also be driven by needs such as industrial process heating, aviation, and maritime shipping. So long as cheap natural gas-fueled power generation assets remain on the grid, it will be difficult for power produced via hydrogen to compete in the power market.

References

- Ahluwalia, R K, D D Papdias, J-K Peng, and H S Roh. 2019. "System Level Analysis of Hydrogen Storage Options." *Argonne National Laboratory*. https://www.hydrogen.energy.gov/pdfs/review19/st001_ahluwalia_2019_o.pdf.
- Ali, Umar. 2019. "How Salt Caverns Could Transform Renewable Energy Storage for the US." *Power Technology*. https://power.nridigital.com/future_power_technology_yearbook_2019/how_salt_caverns_could_transform_renewable_energy_storage_for_the_us.
- Bertuccioli, Luca, Alvin Chan, David Hart, Franz Lehner, Ben Madden, and Eleanor Standen. 2014. "Study on development of water electrolysis in the EU." *E4tech and Element Energy Ltd*. February. [https://www.fch.europa.eu/sites/default/files/FCHJUElectrolysisStudy_FullReport%20\(ID%20199214\).pdf](https://www.fch.europa.eu/sites/default/files/FCHJUElectrolysisStudy_FullReport%20(ID%20199214).pdf).
- CE Delft. 2018. "Feasibility study into blue hydrogen – Technical, economic & sustainability analysis." Technical Report.
- Chiesa, Paolo, Giovanni Lozza, and Luigi Mazzocchi. 2005. "Using Hydrogen as Gas Turbine Fuel." *Journal of Engineering for Gas Turbines and Power* 127, 1: 73-80. <https://doi.org/10.1115/1.1787513>.
- Colella, Whitney G, Brian D James, Jennie M Moton, Genevieve Saur, and Todd Ramsden. 2014. "Techno-Economic Analysis of PEM Electrolysis for Hydrogen Production." *Electrolytic Hydrogen Production Workshop. National Renewable Energy Laboratory*. February 27. https://www.energy.gov/sites/prod/files/2014/08/f18/fcto_2014_electrolytic_h2_wkshp_colella1.pdf.
- Cooley, G. 2019. "AGM Presentation — October 2019." *ITM Power*. October. https://itm-power-assets.s3.eu-west-2.amazonaws.com/AGM_Presentation_October_2019_web_44c461c369.pdf.
- Ditaranto, Mario, Tarjei Heggset, and David Berstad. 2020. "Concept of hydrogen fired gas turbine cycle with exhaust gas recirculation: Assessment of process performance." *Energy* 192, 1. <https://doi.org/10.1016/j.energy.2019.116646>.
- Engineering, Linde. n.d. "Pressurised storage tanks." *Linde Engineering. Powered by Hydrogen*. <https://www.linde-engineering.com/en/about-linde-engineering/success-stories/h2-mobility.html>.
- Erichsen, Gerrit, Christopher Ball, Alfons Kather, and Wilhelm Kuckshinrichs. 2019. "Data Documentation: VEREKON Cost Parameters for 2050 in its Energy System Model." October. https://tore.tuhh.de/bitstream/11420/4409/2/documentation_verekon_cost_parameters_for_2050_in_its_energy_system_model.pdf.
- Foh, S, M Novil, E Rockar, and P Randolph. 1979. "Underground hydrogen storage. Final report." *U.S. Department of Energy Office of Scientific and Technical Information*. <https://www.osti.gov/biblio/6536941>.
- Gençer, Emre, and Rakesh Agrawal. 2016. "A commentary on the US policies for efficient large scale renewable energy storage systems: Focus on carbon storage cycles." *Energy Policy* 88 (January): 477-484. <https://doi.org/10.1016/j.enpol.2015.11.003>.
- Gençer, Emre, Easa Al-musleh, Dharik S Mallapragada, and Rakesh Agrawal. 2014. "Uninterrupted renewable power through chemical storage cycles." *Current Opinion in Chemical Engineering* 5 (August): 29-36. <https://doi.org/10.1016/j.coche.2014.04.001>.
- Gielen, Dolf, Emanuele Taibi, and Raul Miranda. 2019. "Hydrogen: A Renewable Energy Perspective." *International Renewable Energy Agency*. https://www.irena.org/-/media/Files/IRENA/Agency/Publication/2019/Sep/IRENA_Hydrogen_2019.pdf.
- Goldmeer, Jeffrey. 2019. "Power to Gas: Hydrogen for Power Generation." *GE Power*. https://www.ge.com/content/dam/gepower/global/en_US/documents/fuel-flexibility/GEA33861%20Power%20to%20Gas%20-%20Hydrogen%20for%20Power%20Generation.pdf.
- Guerra, Omar J, Josh Eichman, Bri-Mathais Hodge, and Jennifer Kurtz. 2018. "Cost-Competitive Electrolysis-Based Hydrogen Under Current U.S. Electric Utility Rates." *National Renewable Energy Laboratory*. October 30. <https://www.nrel.gov/docs/fy19osti/72710.pdf>.
- Hernandez, Drake D., and Emre Gençer. 2021. "Techno-economic analysis of balancing California's power system on a seasonal basis: Hydrogen vs. lithium-ion batteries." *Applied Energy* 300, 117314. <https://doi.org/10.1016/j.apenergy.2021.117314>.
- Hydrogen and Fuel Cell Technologies Office. n.d. "Liquid Hydrogen Delivery." *U.S. Department of Energy*. <https://www.energy.gov/eere/fuelcells/liquid-hydrogen-delivery>.
- Hydrogenics. 2018. "Renewable Hydrogen Solutions."
- International Energy Agency. 2015. "Technology Roadmap — Hydrogen and Fuel Cells." *International Energy Agency*. <https://iea.blob.core.windows.net/assets/e669e0b6-148c-4d5c-816b-a7661301fa96/TechnologyRoadmapHydrogenandFuelCells.pdf>.
- . 2019. "The Future of Hydrogen: Seizing Today's Opportunities." *International Energy Agency*. <https://www.iea.org/reports/the-future-of-hydrogen>.

- . 2019. “Underground Natural Gas Storage Capacity.”
- International Renewable Energy Agency. 2020. “Green hydrogen cost reduction.” *International Renewable Energy Agency*. <https://www.irena.org/publications/2020/Dec/Green-hydrogen-cost-reduction>.
- ITM Power. 2020. “Interim Results Presentation.” *ITM Power*. https://itm-power-assets.s3.eu-west-2.amazonaws.com/Interim_Results_Feb_2020_b89786377.pdf.
- Keçebas, Ali, Muhammet Kayfeci, and Mutlucan Bayat. 2019. “Chapter 9 — Electrochemical hydrogen generation.” In *Solar Hydrogen Production: Processes, Systems and Technologies*. Academic Press.
- Linde Engineering. n.d. “Pressurised Storage Tanks.” *Powered by Hydrogen*. <https://www.linde-engineering.com/en/about-linde-engineering/success-stories/h2-mobility.html>.
- Lord, Anna S, Peter H Kobos, and David J Borns. 2014. “Geologic storage of hydrogen: Scaling up to meet city transportation demands.” *International Journal of Hydrogen Energy* 39 (28): 15570-15582. <https://doi.org/10.1016/j.ijhydene.2014.07.121>.
- Magnum Development. 2019. “World’s Largest Renewable Energy Storage Project Announced in Utah.” *Magnum Development*. May 30. <https://magnumdev.com/wp-content/uploads/2019/05/NEWS-RELEASE-MHPS-Magnum-Partnership-05-30-19-FINAL.pdf>.
- Malik, Naureen S. 2020. “Hydrogen Power Plants Are Coming to the U.S., Imperiling Gas’s Reign.” *Bloomberg Law*. September 2. <https://news.bloomberglaw.com/environment-and-energy/mitsubishi-plans-three-hydrogen-ready-power-plants-in-the-u-s>.
- Michalski, Jan, Ulrich Bünger, Fritz Crotogino, Sabine Donadei, Gregor-Sönke Schneider, Thomas Pregger, Karl-Kiên Cao, and Dominik Heide. 2017. “Hydrogen generation by electrolysis and storage in salt caverns: Potentials, economics and systems aspects with regard to the German energy transition.” *International Journal of Hydrogen Energy* 42 (19): 13427-13443. <https://doi.org/10.1016/j.ijhydene.2017.02.102>.
- Mitsubishi Hitachi Power Systems. 2020. “Intermountain Power Agency Orders MHPS JAC Gas Turbine Technology for Hydrogen Energy Hub.” *Mitsubishi Power*. March 10. <https://power.mhi.com/regions/amer/news/200310.html>.
- . 2019. “Powering the Next Generation with Renewable Hydrogen.” https://www.changeinpower.com/wp-content/uploads/2019/05/MHPS-Hydrogen-Turbine-Brochure_05-29-19.pdf.
- National Renewable Energy Laboratory. n.d. “H2A Model.”
- Parkinson, B, P Balcombe, J F Speirs, A D Hawkes, and K Hellgardt. 2019. “Levelized cost of CO₂ mitigation from hydrogen production routes.” *Energy and Environmental Science* 1. <https://doi.org/10.1039/C8EE02079E>.
- Penev, Michael, Neha Rustagi, Chad Hunter, and Josh Eichman. 2019. “Energy Storage: Days of Service Sensitivity Analysis.” *National Renewable Energy Laboratory*. May 19. <https://www.nrel.gov/docs/fy19osti/73520.pdf>.
- Preston, Carolyn. 2018. “The Carbon Capture Project at Air Products’ Port Arthur Hydrogen Production Facility.” IEA Greenhouse Gas R&D Programme.
- Ramsden, Todd, Ben Kroposki, and Johanna Levene. 2008. “Opportunities for Hydrogen-Based Energy Storage for Electric Utilities.” *U.S. Department of Energy Office of Scientific and Technical Information*. January 1. <https://www.osti.gov/biblio/1346937-opportunities-hydrogen-based-energy-storage-electric-utilities>.
- Ruth, Mark F, Paige Jadun, Nicholas Gilroy, Elizabeth Connelly, Richard Boardman, A J Simon, Amgad Elgowainy, and Jarett Zuboy. 2020. “The Technical and Economic Potential of the H2@Scale Hydrogen Concept within the United States.” *U.S. Department of Energy Office of Scientific and Technical Information*. October 1. <https://www.osti.gov/biblio/1677471-technical-economic-potential-h2-scale-hydrogen-concept-within-united-states>.
- Sargent and Lundy. 2010. “IPM model – revisions to cost and performance for APC technologies: SCR cost development methodology.” https://19january2017snapshot.epa.gov/sites/production/files/2015-07/documents/chapter_5_appendix_5-2a_scr.pdf.
- Saur, Genevieve, Jennifer Kurtz, Chris Ainscough, Sam Sprik, and Matt Post. 2016. “Stationary Fuel Cell Evaluation.” *National Renewable Energy Laboratory*. June 7. https://www.hydrogen.energy.gov/pdfs/review16/tv016_saur_2016_p.pdf.
- Schlögl, Robert. 2013. “1.1 The Solar Refinery.” In *Chemical Energy Storage*. De Gruyter.
- Schmidt, O, A Gambhir, A Staffell, A Hawkes, J Nelson, and S Few. 2017. “Future cost and performance of water electrolysis: An expert elicitation study.” *International Journal of Hydrogen Energy* 42 (52): 30470-30492. <https://doi.org/10.1016/j.ijhydene.2017.10.045>.
- Siemens Energy. 2020. “Power-to-X: The crucial business on the way to a carbon-free world.” *Siemens Energy*.

- U.S. Department of Energy. 2021. “Secretary Granholm Launches Hydrogen Energy Earthshot to Accelerate Breakthroughs Toward a Net-Zero Economy.” *U.S. Department of Energy*. June 7. <https://www.energy.gov/articles/secretary-granholm-launches-hydrogen-energy-earthshot-accelerate-breakthroughs-toward-net>.
- U.S. Energy Information Agency. 2021. “Table 5.6.A. Average Price of Electricity to Ultimate Customers by End-Use Sector.” *U.S. Energy Information Agency*. https://www.eia.gov/electricity/monthly/epm_table_grapher.php?t=epmt_5_6_a.
- Wei, Max. 2016. “Total Cost of Ownership Modeling for Stationary Fuel Cell Systems.” *Lawrence Berkeley National Lab*. December 13. https://www.energy.gov/sites/prod/files/2016/12/f34/fcto_webinarslides_total_cost_ownership_stationary_fc_121316.pdf.
- Weidner, E, R Ortiz Cebolla, and J Davies. 2019. “Global deployment of large capacity stationary fuel cells.” *European Commission Joint Research Center*.
- Wolf, Erik. 2015. “Chapter 9 — Large-Scale Hydrogen Energy Storage.” *Electrochemical Energy Storage for Renewable Sources and Grid Balancing* 129-142. <https://doi.org/10.1016/B978-0-444-62616-5.00009-7>.

Chapter 6 – Modeling storage in high VRE systems

6.1 Introduction

6.1.1 Chapter overview

As policy makers across the world design and implement policies to achieve long-term deep decarbonization of the power sector, the share of variable renewable energy (VRE) generation (i.e., wind and solar) is expected to grow substantially in the next few decades.¹ Unlike “dispatchable” generation that can be turned up and down by the system operator to balance supply and demand, VRE generation increases and decreases with exogenous variations in wind speed and direction and solar irradiation. The large-scale integration of wind and solar generation is contingent on designing flexible power systems that can balance variations in wind and solar output to continuously meet electricity demand, consistent with reliability criteria. Today, dispatchable generation (e.g., natural gas, nuclear, coal, and reservoir hydro-power) provides this kind of balancing service. But in low-carbon systems dominated by VRE generation, the availability of dispatchable resources will be severely limited.

In such systems, power system flexibility can be enhanced by deploying energy storage along with other enhancements to legacy electric power systems: (1) transmission network expansion to increase the geographic footprint of balancing areas and better exploit spatiotemporal variations in demand and weather-driven VRE resource availability, (2) demand flexibility

and demand response, and (3) deployment or retention of some dispatchable zero or low-carbon generation. Here, we use systems modeling approaches to examine the value of energy storage for achieving deep decarbonization of the electric sector and the implications for storage technology development and electricity market design under a wide range of technological and economic assumptions. The findings in this chapter focus on the role for grid-scale storage in developed country settings, such as the United States, with relatively high levels of grid reliability, universal access to electricity, well-developed wholesale electricity markets or regulated vertically integrated utilities, and increases in electricity demand driven by the electrification of segments of the transportation, buildings, and industrial sectors that currently use fossil fuels.

Specifically, we analyze power system evolution in three U.S. regions—the Northeast, Southeast, and Texas—as well as, with less detail, at a national level. All these regions, and the United States as a whole, experienced significant reductions in carbon dioxide (CO₂) emissions from electricity generation between 2005 and 2018—both in absolute terms (tons CO₂) and in terms of emissions intensity (grams CO₂ per kilowatt-hour or gCO₂/kWh). These reductions reflect the combined effects of stagnant electricity demand; a large reduction in coal-fired generation in favor of natural gas generation, largely for economic reasons; and significant

¹ For example, the International Energy Agency’s Roadmap to Net Zero by 2050 assumes that solar photovoltaics and wind will account for 70% of global electricity generation in 2050 (International Energy Agency 2021a). Strictly speaking, hydroelectric generation is also both variable and renewable. We do not model it here because it is not expected to expand significantly in coming decades in developed countries, and its primarily seasonal variability does not pose the sort of challenges associated with wind and solar generation, which are our focus.

increases in VRE generation, importantly (but not exclusively) driven by public policy. Notwithstanding these trends, electricity generation remains a major source of energy-related CO₂ emissions in the United States, accounting for roughly 31% of the nation's total energy-related CO₂ emissions in 2018 (Energy Information Administration 2021d).²

Given the central role for electrification in long-term U.S. decarbonization efforts, the model-based findings in this chapter primarily rely on electricity demand projections from a high-electrification scenario developed by the National Renewable Energy Laboratory (NREL) for its 2018 Electrification Futures (EFS) study. In NREL's high-electrification scenario, U.S. electricity consumption increases by a factor of 1.6 by 2050 relative to the 2018 level of roughly 4,000 terawatt-hours (TWh) (Mai, Jadun, et al. 2018). Subject to these demand assumptions, which in turn rest on assumptions regarding policy support for electrification of other sectors, we analyze power system evolution for different 2050 power system decarbonization targets, defined in terms of CO₂ emissions produced per kWh of electricity dispatched, for three different regions of the country in 2050. In our study, we focus on four emissions constraints: 0 gCO₂/kWh, 5 gCO₂/kWh, 10 gCO₂/kWh, and 50 gCO₂/kWh. We also consider an unconstrained ("No Limit") case that provides a consistent benchmark to compare the impact of imposing different emissions constraints. Additionally, we include some modeling runs with a 1 gCO₂/kWh constraint for Texas. Since

we do not consider technologies for removing CO₂ from the atmosphere (sometimes called "negative emissions technologies"³), the 0 gCO₂/kWh case represents a stricter constraint compared to the more common goal of achieving a "net-zero" power system, where a net-zero system could allow for the deployment of one or more negative emissions technologies.

When contemplating the common goal of "net-zero" carbon energy systems, where the term "net-zero" is understood to allow for the inclusion of negative emissions technologies, the 5 gCO₂/kWh or even the 10 gCO₂/kWh emissions constraint modeled here is likely more informative than the very strict 0 gCO₂/kWh constraint. At the 2018 level of electricity demand, reducing the average carbon intensity of generation for the U.S. electricity grid to 5 gCO₂/kWh or 10 gCO₂/kWh from the nation-wide average of 449 gCO₂/kWh in 2018 (Table 6.1) would result in total U.S. CO₂ emissions from electricity generation of 21 million metric tons (MMT) or 42 MMT respectively, delivering reductions of 99.2% or 98.3% respectively relative to 2005 electricity sector emissions of 2,544 MMT (Energy Information Administration 2021d).⁴ To meet a higher, 6,700-TWh level of demand (the load projected for 2050 in NREL's EFS high-electrification scenario), these same intensity targets would deliver reductions of 98.7% or 97.4% respectively, relative to emissions if average intensity remained at the 2005 level. While our analysis focuses on grid decarbonization by 2050, achieving zero or net-zero carbon emissions from electricity generation sooner than

² In addition to CO₂, there are also other greenhouse gases (GHG) that contribute to global warming, including methane (CH₄) (10% of U.S. GHG emissions in 2019); nitrous oxide (N₂O) (7%); and hydrofluorocarbons (HFCs), perfluorocarbons (PFCs), sulfur hexafluoride (SF₆), and nitrogen trifluoride (NF₃) (2.8%) (EPA 2021).

³ Examples of such technologies include biomass for energy production coupled with carbon capture and sequestration (CCS) or systems that capture CO₂ directly from the ambient air (sometimes called "direct air capture") (Daggash, Heuberger and Dowell 2019; Fajard et al. 2021).

⁴ The United States, Canada, Japan, Australia, and many other countries use 2005 as the baseline year for emission reduction commitments. Many European countries use 1990 as their baseline year.

**Table 6.1 Electricity generation and electricity-related emissions
(U.S. total and three regions modeled in this study)**

| | 2005 | 2018 | | |
|---|-------|-----------------------|-------|-----------------------|
| Electricity generation | TWh | % 2050 | TWh | % 2050 |
| U.S. total | 4,055 | 61% | 4,178 | 62% |
| Northeast | 283 | 62% | 238 | 52% |
| Southeast | 824 | 115% | 834 | 117% |
| Texas | 397 | 27% | 477 | 33% |
| Electricity-related CO ₂ emissions | MMT | gCO ₂ /kWh | MMT | gCO ₂ /kWh |
| U.S. total | 2,544 | 627 | 1,874 | 449 |
| Northeast | 118 | 416 | 55 | 232 |
| Southeast | 485 | 589 | 327 | 392 |
| Texas | 261 | 659 | 230 | 482 |

Regional figures are based on summing up emissions for the various states part of each region. Data source: “U.S. Electric Power Industry Estimated Emissions by State” (Energy Information Administration 2021c).

2050, say by 2035 (consistent with some decarbonization goals), would require more rapid shifts in the generation mix and possibly an expanded role for energy storage (for both short-duration and long-duration uses). It could involve much higher costs than those modeled here since our analysis incorporates significant reductions in the costs of VRE generation and storage by 2050. These cost reductions are unlikely to be realized by 2035. Accordingly, if 2035 is the target year for “net-zero” emissions it would likely have to be achieved with higher-cost technologies than those incorporated into our analyses for 2050.

6.1.2 Roles of storage in power systems

There is growing interest in deploying energy storage for a variety of applications on the electricity grid. For example, the U.S. Energy Information Administration (EIA) classifies battery projects based on 11 leading applications that overlap to some extent, including frequency regulation as well as other ancillary services (e.g., spinning reserves, voltage support), storage for excess wind and solar generation,

load management, system peak shaving, transmission and distribution network deferral, backup power, and energy arbitrage (where arbitrage involves effectively moving the electricity from one time period to another) (DNV GL 2017; Energy Information Administration 2020a). The latter enables time-shifting of energy supply and is functionally central to the other grid applications provided by energy storage. The model results presented in this chapter focus on the value of energy storage enabled by its arbitrage function in future electricity systems. Energy storage makes it possible to defer investments in generation and transmission, reduce VRE curtailment, reduce thermal generator startups, and reduce transmission losses.

While these use cases are likely to have the greatest long-term impact on grid evolution, there are other valuable use cases for energy storage that we do not consider. These include: (1) deployment of storage at the level of the distribution network for operational or investment deferral reasons, which can be valuable, but generally represent context-specific opportunities that cannot be easily generalized; and

(2) consumer adoption of storage to reduce consumption during peak demand hours, which can enable large users to manage demand charges that may constitute a significant part of their total bill and which can also increase the value of rooftop photovoltaics (PV) for all types of customers under alternative tariff structures (Neubauer and Simpson 2015; Darghouth et al. 2020). These use cases are strongly affected by available retail tariff structures as well as by the methods used to value rooftop PV injections back to the grid; thus, they cannot be generalized. A third use case we do not consider is storage to provide a variety of ancillary services that are required to meet reliability criteria at the bulk power system level. These reliability needs tend to be smaller than capacity requirements for electricity supply and thus are mainly important as short-term drivers for storage value and deployment. The distribution network and customer-level use cases for storage are partly addressed in the next chapter (Chapter 7) in the context of developing country settings.

6.2 Systems modeling approach

6.2.1 Capacity expansion modeling (GenX)

Our analysis uses an open-source capacity expansion model (CEM) called GenX (MIT Energy Initiative and Princeton University 2021). GenX takes the perspective of a cost-minimizing central planner to determine the optimal generation, storage, and transmission investments needed to meet a pre-defined time-path of system demand while adhering to various grid operational constraints, resource availability limits, and other imposed policy/

environmental constraints. Similar to other state-of-the-art CEMs (Brown, Hörsch and Schlachtberger 2018; Johnston et al. 2019; Kuepper, Teichgraeber and Brandt 2020), GenX incorporates a detailed temporal resolution of power sector operations, based on modeling either representative periods or one or more years at an hourly resolution, depending on the model configuration. As noted by recent inter-model comparison studies (Mai, Barrows, et al. 2015; Electric Power Research Institute and Resources for the Future 2017; Cole, Frew, et al. 2017; Mallapragada et al. 2018), increasing temporal resolution and preservation of chronology in CEMs allow for improved characterization of the temporal variability of demand or “load,” VRE generation, and the inter-temporal dynamics of various generators and energy storage technologies. GenX can also be used to model the available suite of demand- and supply-side resources and has the capability to represent non-electric energy demand and its impact on the power sector.

Several major grid operating constraints are activated in GenX for this study. The first is demand and supply balance for each hour at the zonal level, considering inter-zonal imports and exports as well as the option of shedding load in each zone at a value of lost load (VoLL) equal to \$50,000/MWh. A high VoLL was chosen to minimize instances of involuntary load shedding and incentivize investment in more capacity to meet demand within the energy-only market framework implemented in the model. Other operating constraints in the model include linearized unit commitment (start-up/shut-down) decisions,⁵ minimum

⁵ Many thermal generators have a non-zero minimum stable power output level below which the plant needs to be shut down. This discontinuity in power output is typically captured in power systems models using binary variables that are either 1 or 0 depending on the plant’s commitment status (1=committed, 0=not committed). Several operational constraints can be formulated using the commitment variable, but these constraints add significantly to computational complexity. Linearized unit commitment refers to implementations where the integrality of plant commitment variables is relaxed but the associated operational constraints are still enforced. Previous work has shown that this approximation provides a reasonable balance between computational tractability and accuracy in power systems planning models (Palmintier 2013; Poncelet, Delarue and D’haeseleer 2020).

up/down times, and hourly ramping limits for thermal generators; transmission capacity limits and linear line losses,⁶ where applicable; inter-temporal constraints governing storage state-of-charge and capacity constraints on maximum hourly charge/discharge and stored energy; and renewable resource (both VRE and hydropower) availability limits in each hour. To model system evolution to meet the decarbonization targets mentioned previously, we include constraints to enforce upper limits on annual average CO₂ emissions intensity that account for generation and storage discharge as well as storage losses. The long-run system-level optimization approach employed by GenX and other state-of-the-art CEMs (Brown, Hörsch and Schlachtberger 2018; Johnston et al. 2019; Kuepper, Teichgraeber and Brandt 2020) captures the declining marginal value of all resources, including energy storage, and their resulting least-cost equilibrium penetration levels. The shadow prices on the carbon emission limits imposed within the CEM can be thought of as carbon prices that are included in system prices when carbon-emitting generation is on the margin (Brown and Reichenberg 2021). This makes the model suitable for evaluating the impact of technology and system drivers on the role for energy storage in future power systems. Like most other CEMs, GenX models only bulk power supply and considers the costs of generation and storage, as well as additions to the transmission grid, where applicable. It seems likely that existing fossil fuel generating plants will have retired by 2050, so greenfield conditions are assumed for this study, with the exception of hydro (Northeast, Southeast) and some existing nuclear (Southeast), where available. We do not model distribution costs or compute estimates of retail rates.

Like any single-stage CEM, GenX outputs include cost-optimal installed capacities of generation, storage, and transmission assets, as well as their hourly utilization to meet the modeled load. Constant returns to scale are assumed—that is, investment costs for a facility are assumed to be proportional to its capacity. The objective function of the GenX model includes the sum of annualized investment cost and operating cost for all resources as well as the cost of non-served energy, if any. These outputs can be used to compute a metric called the system average cost of electricity (SCOE). SCOE is defined as the total annualized investment and operational cost of the modeled system (i.e., the objective function of the GenX model), divided by the total annual electricity demand served (Heuberger et al. 2017). SCOE is distinct from the levelized cost of energy (LCOE) or levelized cost of storage (LCOS), both of which are technology-specific cost metrics that are computed with a static view of the power system and require specifying a fixed dispatch profile for the resource in question, which often leads to misleading inter-technology cost comparisons. By contrast, the SCOE metric is computed as an output of the CEM—thus, changes in SCOE across different scenarios provide a view of the system impact of various technology and policy drivers under assumptions of perfect foresight, constant returns to scale, and optimal investment and operation. Further details on the formulation and implementation of the GenX model can be found elsewhere, including in prior publications that use GenX and in the open-source model itself (MIT Energy Initiative and Princeton University 2021).

The modeling results presented here should not be viewed as predictions or forecasts. We view

⁶ Generally, transmission losses scale as a quadratic function of power flows. To maintain model linearity, and thus, computational tractability, we approximate transmission losses to be a linear function of power flow across the line in each time interval (Brown et al. 2020).

GenX as a platform for performing a set of internally consistent experiments that in turn reflect alternative but realistic assumptions about the attributes of technologies, including their costs and availabilities, as well as the level and flexibility of demand and other factors. This allows us to examine how variations in these assumptions affect the optimal portfolios of technologies, their costs, and implicit bulk system electricity prices. Importantly, the modeling results shed light on which variations seem likely to be important and which do not.

6.2.2 Modeling energy storage in GenX

Energy storage technologies are differentiated in the GenX model based on their design as well as their assumed cost and performance characteristics. In terms of design, GenX includes two broad representations of storage technologies. The first category includes technologies that have equal charging and discharging power capacity (e.g., lithium-ion or other electrochemical flow batteries, pumped hydro); for these technologies, energy storage capacity and charging/discharging power capacity are the two independent design variables and feasible ranges for the ratio of energy capacity to power capacity can be specified.⁷ The second category includes technologies where both charging power and discharging power capacity, as well as energy storage capacity, are independent design variables (e.g., thermal or hydrogen storage). Depending on this classification, storage technologies are characterized by one, two, or three independent capital and fixed operations and maintenance (FOM) cost parameters (Table 6.2). For technologies where energy storage capacity is an independent design variable, we constrain the storage duration (ratio of energy to discharging power capacity)

to be less than 300 hours, but this constraint is never binding for the results reported here. Additionally, due to data limitations, we model pumped hydro storage with fixed storage duration (12 hours) and assume total capital costs scale with power capacity alone (Brown et al. 2020; U.S. Department of Energy 2018).

The inter-temporal operation of storage technologies is modeled using several parameters—highlighted in Table 6.3—including the hourly self-discharge rate and the variable O&M cost (VOM) for charging and discharging. We also model energy losses during charging and discharging, by parametrizing charging and discharging efficiency for each technology. As with other CEMs, to manage computational tractability, we do not model degradation of energy capacity with use, or dynamic charging or discharging efficiency as functions of the state of charge of storage. This approach, which is similar to the approach taken in other modeling studies, may overestimate the benefits of electrochemical storage technologies relative to other storage technologies that are less affected by these considerations (Jafari, Botterud and Sakti 2020; Sakti et al. 2017). In our analysis, the impact of this modeling simplification is partly mitigated by accounting for the periodic replacement of energy components in the FOM costs (Cole and Frazier 2020) for the electrochemical energy storage technologies considered here. This is akin to paying a fixed annual maintenance fee to guarantee a certain level of performance (further details are discussed in Chapter 2).

Our analysis focuses on modeling the supply–demand balance within the bulk power system enforced at an hourly resolution for each balancing area within the region considered. Storage contributes to the supply–demand

⁷ This classification includes the special case where the ratio of energy capacity to power capacity, or storage duration, is held constant, either due to lack of data or other factors, so there is only one independent design variable.

Table 6.2 Design variables for different types of storage technologies modeled in this study

| Type | Independent design variable | Dependent design variable | Classification of storage technologies modeled here |
|------|--|--|---|
| 1 | Discharge power capacity | Charge power capacity, energy capacity | Pumped hydro |
| 2 | Discharge power capacity, Energy capacity | Charge power capacity | Li-ion, Redox Flow batteries, Metal-air batteries |
| 3 | Discharge power capacity, Energy capacity, Charge power capacity | — | Thermal energy storage, H ₂ storage |

Table 6.3 Storage costs and operational assumptions

| Tech | | | Discharging capital cost (\$/kW) | Charging capital cost (\$/kW) | Storage capital cost (\$/kWh) | FOM (\$/kW-year) | FOM (\$/kWh-year) | VOM (\$/kWh) | Efficiency up (%) | Efficiency down (%) | RTE (%) |
|------|-----------|-----------|----------------------------------|-------------------------------|-------------------------------|------------------|-------------------|--------------|-------------------|---------------------|---------|
| [1] | PHS | Mid | 1,966 | — | 0.0 | 41.0 | 0.0 | 0.0 | 89% | 89% | 80% |
| [2] | Li-ion | Low | 32 | — | 70.9 | 0.3 | 1.4 | 0.0 | 92% | 92% | 85% |
| [3] | Li-ion | Mid | 110 | — | 125.8 | 0.8 | 2.2 | 0.0 | 92% | 92% | 85% |
| [4] | Li-ion | High | 154 | — | 177.0 | 1.4 | 3.2 | 0.0 | 92% | 92% | 85% |
| [5] | RFB | Low | 297 | — | 15.5 | 4.1 | 0.0 | 0.0 | 92% | 88% | 80% |
| [6] | RFB | Mid | 396 | — | 48.0 | 4.1 | 0.0 | 0.0 | 92% | 88% | 80% |
| [7] | RFB | High | 530 | — | 102.2 | 4.1 | 0.0 | 0.0 | 92% | 88% | 80% |
| [8] | Metal-air | Low | 595 | — | 0.1 | 14.9 | 0.0 | 0.0 | 70% | 59% | 41% |
| [9] | Metal-air | Mid | 643 | — | 2.4 | 16.1 | 0.1 | 0.0 | 73% | 63% | 46% |
| [10] | Metal-air | High | 950 | — | 3.6 | 23.7 | 0.1 | 0.0 | 72% | 60% | 43% |
| [11] | Hydrogen | Ultra-Low | 1,190 | 479.3 | 1.1 | 11.0 | 0.0 | 0.0 | 77% | 65% | 50% |
| [12] | Hydrogen | Low | 1,150 | 356.1 | 6.0 | 11.0 | 0.1 | 0.0 | 80% | 70% | 56% |
| [13] | Hydrogen | Mid | 1,190 | 479.3 | 7.0 | 11.0 | 0.1 | 0.0 | 77% | 65% | 50% |
| [14] | Hydrogen | High | 1,230 | 602.4 | 8.0 | 11.0 | 0.1 | 0.0 | 60% | 60% | 36% |
| [15] | Thermal | Low | 494 | 3.3 | 2.9 | 3.9 | 0.0 | 0.0 | 100% | 55% | 55% |
| [16] | Thermal | Mid | 736 | 3.3 | 5.4 | 3.9 | 0.0 | 0.0 | 100% | 50% | 50% |
| [17] | Thermal | High | 1,226 | 3.3 | 9.0 | 3.9 | 0.1 | 0.0 | 100% | 46% | 46% |

Values from the Future of Energy Storage technical teams; refer to previous chapters for detailed description of individual technologies: hydrogen (Chapter 5); thermal (Chapter 4); metal-air, RFB, and Li-ion (Chapter 2). PHS = Pumped Hydro Storage, RFB = Redox Flow Battery. Round-trip efficiency (RTE) is the fraction of energy used to charge a device that is available to be discharged; it is the product of efficiency up and efficiency down similarly expressed. Hourly self-discharge rates for storage technologies are also considered in the modeling but are very small at 0.002% for Li-ion and metal-air systems and 0.02% for thermal systems. Low-, mid-, and high- cost assumptions for hydrogen assume above-ground storage, while ultra-low-cost reflects cost assumptions for geological storage. PHS cost data sourced from the 2016 Hydropower Vision report (U.S. Department of Energy 2016).

balance as both a supply-side resource (via discharging) and as a demand-side resource (via charging). In addition, as previously noted, storage can contribute to the procurement and supply of grid ancillary services such as operating reserves. Since we do not model system operating reserve requirements, however, the benefit of providing these services is not captured in our valuation of energy storage technologies. Previous research using GenX that included operating reserve requirements has shown that the ability to satisfy reserve requirements does contribute significantly to the value of storage when storage is deployed at low levels. However, this incremental benefit is lost with increasing storage penetration (Mallapragada, Sepulveda and Jenkins 2020). This suggests that long-run valuations of alternative storage technologies may not be much affected by ignoring their participation in operating reserve markets.

6.2.3 Regional modeling

Selection of model regions

We focus on three U.S. regions in 2050: the Northeast, the Southeast, and Texas. We do not seek to develop detailed trajectories of the evolution of the resource mix in these regions, as this evolution will be affected by a range of factors, including the turnover of the existing generation fleet, market design, state incentives, permitting rules, etc. Instead, we focus on the effects of differences in VRE resource quality and the availability of long-lived, existing low-carbon hydro and nuclear generation assets, and pumped hydro storage assets, assuming cost-efficient investment and operation. The three selected regions differ across several key attributes that affect the potential

costs and benefits of achieving various decarbonization goals, including: (1) wind speeds and solar irradiation, land availability, and resulting installed costs of wind and solar generation; (2) hydroelectric and potential hydrogen (H_2) storage resources; and (3) industry structure and regulation and associated implications for nuclear power development. As noted above, we also assume that the existing stock of fossil fuel generating capacity retires by 2050, so that our analysis basically examines a greenfield system developed to meet 2050 demand, utilizing existing transmission assets and some other existing non-fossil assets, with some regional differences (as detailed below). New fossil generating capacity may be selected depending on its costs, utilization rates in an optimal system, and the stringency of the system-wide carbon constraint.

The **Northeast** region (New England and New York) is characterized by strong legislative and regulatory support for renewable generation, offset by siting difficulties that translate, in some cases, into increased infrastructure costs (Wiser and Bolinger 2018). Most states in this region have pledged to reduce their economy-wide greenhouse gas (GHG) emissions by at least 80% by 2050, with a few states committing to more ambitious targets.⁸ The region is largely restructured with competitive wholesale markets managed by two independent system operators (ISO-NE and NYISO) that govern system operations and partially govern investment in new generation and transmission capacity. The region has relatively low-quality solar, but high-quality onshore and offshore wind. However, siting difficulties have plagued onshore VRE and transmission developments, which may explain some of the recent,

⁸ For example, the Massachusetts' Global Warming Solutions Act of 2008 requires at least an 80% reduction in carbon emissions by 2050 (below a 1990 baseline level) (Massachusetts Executive Office of Energy and Environmental Affairs 2021). New York has a mandated goal to achieve zero-emissions electricity by 2040, including 70% renewable energy generation by 2030, and to reach economy-wide carbon neutrality by 2050 (New York State Energy Research and Development Authority 2021).

state-mandated procurements of relatively expensive offshore wind and supporting requirements for new transmission infrastructure investments. The region also imports non-trivial amounts of hydropower from Canada and has its own hydro resources that can help to support VRE integration. While the Northeast's electricity demand profile currently peaks in the summer, penetration of electric space heating anticipated to meet decarbonization commitments (and included in the NREL high electrification demand scenario), may transform the Northeast into a winter-peaking region (Mai, Jadun, et al. 2018; Sepulveda, Jenkins and Edington, et al. 2021). All the region's nuclear power plants are merchant plants that must cover their going-forward costs with wholesale market revenues to break even. Because many of these plants are financially challenged, and currently depend on state subsidies to continue operating, their licenses are unlikely to be renewed beyond their current license periods. Accordingly, we assume that all existing nuclear units retire by 2050 (in other words, that they do not renew their current operating licenses) and that new nuclear plants are not deployed by 2050 based on available information about the technology's cost and public acceptance challenges. We also assume that the existing stock of fossil generating capacity retires by 2050, but that existing hydro and pumped storage resources continue to be operational in 2050.

The **Southeast** region (Tennessee, Alabama, Georgia, North Carolina, South Carolina, and Florida) is characterized by the presence of regulated, vertically integrated utilities; the absence of organized wholesale markets; prevalence of winter-peaking demands for some states within the region; and an extensive nuclear generation fleet, which contributed

28% of the region's power generation in 2018.⁹ While nuclear plant economics have been adversely impacted in other parts of the United States that are currently served by wholesale electricity markets, the economics of nuclear generation remain more favorable in the regulated, vertically integrated utility environment of the U.S. Southeast (U.S. Department of Energy 2017; Szilard et al. 2017). Continued reliance on this regulatory structure in the U.S. Southeast, combined with greater public acceptance of nuclear energy, makes it more likely that nuclear plant operators will apply for, and be granted, second license renewals that extend the remaining life of the region's existing plants beyond 2050. Thus, our analysis includes existing nuclear plants in the region with an initial operating date of 1975 or later, which could operate to or beyond 2055 with a second license renewal (see Appendix C, Table C.1). We assume that 25 gigawatts (GW) of existing nuclear capacity will still be online through 2055 (assuming an 80-year lifetime for nuclear plants). Nuclear, as a dispatchable low-carbon resource, could partially mitigate the need for VRE resources and storage technologies and has the potential to lower the system costs of achieving deep decarbonization (Buongiorno et al. 2018; Sepulveda, Jenkins and de Sisternes, et al. 2018). The political environment in the Southeast is also more conducive to building new nuclear plants; indeed, the only two nuclear units currently under construction in the United States (Plant Vogtle) are in Georgia.¹⁰ The Southeast region is also endowed with relatively good-quality solar resources. While offshore wind may be a possibility in this region, we have not modeled its availability due to a lack of reliable data to characterize the resource. Thus, we model the Southeast as a mostly greenfield system in 2050, but for the continued operation of significant

⁹ Total electricity generation (866 TWh) and nuclear generation (241 TWh) from the U.S. Energy Information Administration (2021a).

¹⁰ We assume these units will be part of the 2050 existing nuclear fleet for the Southeast.

existing nuclear capacity and existing hydroelectric resources.

Texas is characterized by high-quality wind and solar resources, an organized wholesale market serving a restructured electricity sector, summer-peaking demand with a strong component of relatively inflexible air conditioning demand, significant penetration of weather-sensitive electric heating, proximity and access to CO₂ sequestration sites, and strong industrial energy demand. Notably, the petrochemical industry, which uses a majority of the hydrogen produced today for feedstock purposes, is concentrated in Texas and the other Gulf Coast states. As economy-wide decarbonization advances, there may be additional demand for hydrogen in energy applications. Supplying this incremental demand using electrolyzers¹¹ coupled with hydrogen storage could add demand flexibility to the grid. Texas also has underground salt caverns, which can serve as a cheaper medium than aboveground tanks for the long-duration storage of hydrogen. This allows us to use Texas to test our hydrogen storage cost sensitivities and hydrogen-as-a fuel sensitivities. We assume that the state's two existing merchant nuclear plants (four units) retire and are not replaced by 2050. As a simplification, we ignored the minimal existing hydroelectric resources in Texas.

As we will see in later sections, the availability of dispatchable low-carbon resources and the relative resource quality of solar and wind have significant implications for modeled system

costs and for the optimal amount of storage. Differences across the three modeled regions and obvious differences between these regions and other parts of the United States (i.e., exceptional-quality solar in the Southwest and extensive hydro in the Northwest) mean that there is no credible way to generalize or aggregate our regional results to produce national totals.

Regional commonalities in modeling

In GenX, each scenario is characterized by zonal hourly VRE capacity factors and demand, investment and operational parameters (e.g., costs, ramp rates, minimum generation levels) for each technology, and different carbon emission constraints (Table 6.4). Across all three regions, we use the latest mid-range EIA fuel-price projections for 2050 and NREL's Annual Technology Baseline 2020 (ATB) to characterize the capital cost of various generation technologies (Table 6.5), as well as lithium-ion (Li-ion) battery storage.¹²

Per our (mostly) greenfield modeling assumption, we restrict investment to the following technologies: utility-scale solar and onshore wind (as well as offshore wind and distributed solar in the Northeast); natural gas-fired plants (open cycle gas turbine (OCGT) and combined cycle gas turbine (CCGT)), with and without amine-based carbon capture and storage (CCS) technology; and hydro resources where they play a major role (Northeast, Southeast).¹³ We do not consider coal as a viable generating

¹¹ Electrolysis technologies considered here generally split water at or near ambient conditions and are capable of flexible operation over nearly the entire range of power loadings. Further description of electrolyzer technologies can be found in a 2019 IEA report, "The Future of Hydrogen" (IEA 2019).

¹² We assume 2045 technology costs from the 2020 NREL Annual Technology Baseline (ATB) database, reflecting the fact that the stock of resources in 2050 will likely have been built/financed a few years earlier.

¹³ Many of our capital cost assumptions were taken from the 2020 edition of the NREL annual technology baseline (ATB) report (National Renewable Energy Laboratory 2020). In the 2021 edition of the ATB, mid-cost projections for Li-ion battery power capital costs were higher than the values in the 2020 edition, while energy capital costs were lower. Using projections from the 2021 edition of the ATB would presumably increase the duration of Li-ion storage deployment across the scenarios evaluated in this study.

Table 6.4 Inputs and outputs of the GenX model

| Key Inputs | Key Outputs |
|--|--|
| <ul style="list-style-type: none"> Solar PV and wind hourly capacity factor 2050 hourly demand profile from NREL Electrification Futures Study Fixed (capital and O&M) and variable (O&M and fuel) costs for each resource technology Operational parameters for each technology Fuel parameters such as CO₂ emissions rate and cost | <ul style="list-style-type: none"> Optimal installed electricity generation capacity mix Total system cost Hourly operation of each resource technology System carbon emissions Energy contribution and capacity factor for each technology |

See Figure 6.2 and Appendix C.1 for further details.

Table 6.5 Mid-cost assumptions for VRE and natural gas generating resources

| | Tech | Capital cost (\$/kW) | FOM (\$/kW-year) | VOM (\$/MWh) | Modeled in regions |
|-----|---------------------|----------------------|------------------|--------------|--------------------|
| [1] | Onshore wind | 1,085 | 34.6 | 0.01 | NE, SE, TX |
| [2] | Offshore wind | 2,179 | 58.8 | 0.01 | NE |
| [3] | Utility-scale solar | 725 | 8.5 | 0.00 | NE, SE, TX |
| [4] | Distributed solar | 924 | 8.0 | 0.00 | NE |
| [5] | CCGT | 936 | 12.9 | 2.16 | NE, SE, TX |
| [6] | OCGT | 854 | 11.4 | 4.50 | NE, SE, TX |
| [7] | CCGT_CCS | 2,080 | 27.0 | 5.72 | NE, SE, TX |
| [8] | Allam | 1,929 | 48.0 | 2.07 | TX |
| [9] | Nuclear | 6,048 | 119.0 | 2.32 | SE |

The “Modeled in Regions” column indicates where the technologies are assumed to be available. Projected costs from National Renewable Energy Laboratory (2020). For onshore wind, we applied a 1.5x multiplier in the Northeast to reflect difficulties in siting and interconnection. “Allam” refers to the supercritical CO₂-based oxy-combustion power concept, also referred as the “Allam-Fetvedt” cycle (Weiland and White 2019).

technology in 2050 in the United States, given its declining cost-competitiveness and diminishing role in the U.S. power mix over the past few years, as well as its high carbon emissions. The exceptions to greenfield modeling are for existing hydro and pumped hydro storage in the Northeast and Southeast, existing nuclear in the Southeast that would still be operational in 2050 under an assumed 80-year lifetime (see Table C.1 in Appendix C), and existing transmission capacities in the Northeast and Southeast. As discussed below, we modeled Texas as a single transmission zone. In stand-alone regional case studies, we also assess the

impact of new nuclear and emerging natural gas-based power generation technologies with CCS (e.g., Allam-Fetvedt cycle (Weiland and White 2019)), and hydrogen for industrial uses.

The model characterizes hourly demand for each region using the 2050 demand profiles developed by NREL for its EFS study (specifically, NREL’s high-electrification-with-moderate-technology-advancement scenario) (Mai, Jadun, et al. 2018). These demand profiles correspond to 2012 weather year variations.¹⁴ They assume a high degree of electrification in residential and commercial buildings (e.g., 61%

¹⁴ Presumably, the NREL load projections do not account for the impacts of climate change on electricity demand, which, according to recent literature, could be important to consider in system planning, along with climate change impacts on generation (Fonseca et al. 2021; Steinberg et al. 2020).

of space heating, 52% of water heating, and 94% of cooking services) and transportation (e.g., plug-in electric vehicles account for 84% of light-duty vehicle stock in 2050), which collectively results in electricity providing 41% of final U.S. energy demand in 2050 as compared to 19% in 2016. We take as given that policies necessary to encourage these levels of electrification have been implemented and consider the incremental effects of limits on carbon emissions from the power sector. The projected demand profiles are also available with a breakdown of hourly demand among various end-use segments, which we use to explore the impact of demand flexibility for certain end uses, such as electric vehicle (EV) charging.

To represent PV and wind resources at a high level of spatial and temporal resolution, we follow the approach documented by Brown and Botterud (2021): (1) We develop supply curves of available land area for PV and wind development (excluding water bodies, national parks, urban areas, mountain ranges, and Native American territories), and (2) we quantify the cost of spur lines to connect new VRE generation to existing transmission infrastructure. For each site, the hourly capacity factor (CF) for PV is simulated assuming a horizontal one-axis-tracking PV system and using 2007–2013 satellite data from the National Solar Radiation Database (NSRDB). The hourly CF for wind is simulated using climate reanalysis data from the WIND Toolkit and manufacturer power curve data for the Gamesa G126/2500 turbine at 100-meter height. We develop different “quality bins” for VREs (based on the levelized cost of energy, considering generation and interconnection costs) by aggregating over these individual sites. Further details are provided in the Supplemental Information (Note S2) to Brown and Botterud (2021).

Regional differences in modeling

Since the sources of storage value we are trying to capture are highly sensitive to temporal resolution, we opted to model operational decisions on an hourly basis to capture the power system’s inter-temporal ramping and balancing needs with high VRE penetration and to estimate how these needs affect the value of different storage resources. Our emphasis on high temporal resolution leads to necessary trade-offs between the level of chronological and network detail we consider in the analysis to keep the model computationally tractable.

About 90% of electricity supply in Texas is managed by a single ISO, the Electric Reliability Council of Texas (ERCOT). Because ERCOT is almost completely electrically isolated from the rest of the country and because transmission capacity between wind-rich areas (designated as “Competitive Renewable Energy Zones”) in the northwestern and western portions of the state and demand centers in eastern and southern Texas have relatively recently been greatly expanded (Hulbert, Chernyakhovskiy and Cochran 2016), we decided to model all of Texas as a single zone. With this simplified spatial resolution, we were able to include the maximum temporal resolution of grid operations in the CEM, limited only by data availability: seven years at hourly resolution.

In contrast, the Northeast and Southeast regions of the United States are relatively large and geographically diverse, and they have well-documented intra-regional transmission constraints. This makes it important to consider intra-regional transmission expansion. For these two regions, we elected to use a spatially resolved network representation, which in turn meant that we had to use a lower temporal resolution to keep the model computationally tractable. We model annual grid operations in these two regions based on 35 representative periods of 10 days each

Table 6.6 EFS 2050 demand assumptions for the Northeast, Southeast, and Texas

| | System peak (GW) | | Annual demand (TWh) | |
|------------------|----------------------|---------------------------|----------------------|---------------------------|
| | High-electrification | Reference-electrification | High-electrification | Reference-electrification |
| Northeast | 94 | 57 | 454 | 298 |
| Texas | 151 | 111 | 715 | 543 |
| Southeast | 298 | 205 | 1,457 | 1,051 |

Hourly system peak (GW) and total annual demand (TWh) are shown for both the high and reference electrification scenarios.

(corresponding to 8,400 hours), which are sampled from the available time series data of seven years at an hourly resolution. Such a time-domain reduction approach is often employed in CEM studies to balance spatial/temporal resolution and level of operational detail (Heuberger et al. 2017; Kotzur et al. 2018; Mallapragada et al. 2018). The selection of 35 representative periods (350 days x 24 hours/day) follows an iterative clustering approach, as further described in Appendix C.2.

We also consider other regional differences with respect to resource quality and regulatory environment. Notably, we apply a 50% cost premium to onshore wind development in the Northeast to reflect well-documented siting challenges—this multiplier is consistent with regional multipliers for the Northeast used in other studies (Brown et al. 2020). To reflect difficulties in expanding transmission into and out of the New York City area (zone 4 in Figure 6.2), we apply a two-times (2X) expansion limit, based on existing transfer capacities. Finally, we include offshore wind as a viable technology with no limits on maximum deployable capacity in the Northeast, due to favorable water depths and supportive deployment policies at the state level.

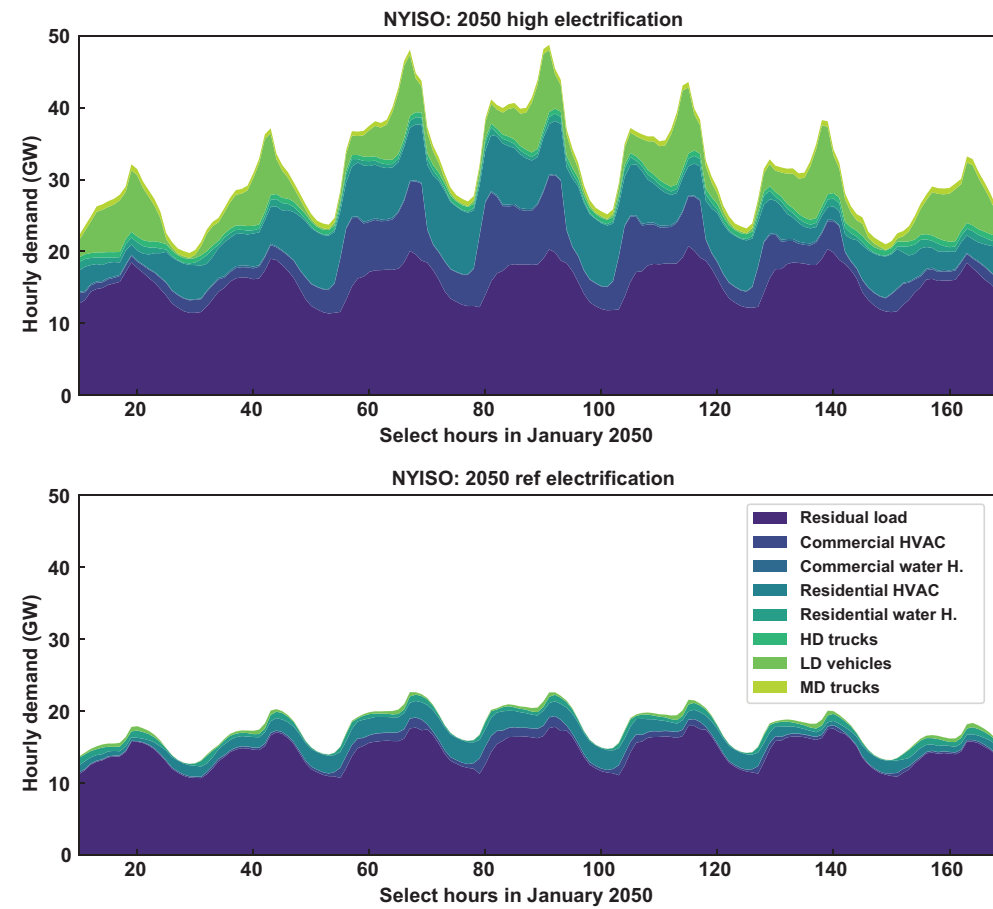
As described previously, we use the NREL EFS high-electrification load scenario in our base case (other assumptions in our base case are discussed in the next section), to reflect the levels of electrification needed to achieve deep

decarbonization on an economy-wide basis by 2050. The high-electrification load scenario assumes an increased role for electricity in meeting final energy demand compared to the reference scenario (41% vs. 23% in 2050). Regional differences arise due to local weather conditions and electrification potential. For example, in comparison to the NREL EFS reference load scenario case, the high-electrification load scenario has a 65% higher system peak and 52% higher annual demand in the Northeast region, and a 36% higher system peak and 32% higher annual demand in Texas. Under the high-electrification scenario, winter electricity consumption increases most substantially in the Northeast, due to a greater role for electrified space heating via cold-climate heat pumps. This partly explains the larger impact of electrification (high vs. reference scenario) on peak and annual electricity demand for the Northeast as compared to Texas (Table 6.6).

6.2.4 Model limitations

Before describing our results and key findings, we note some limitations of our modeling approach. Our use of historical weather to simulate multi-year VRE capacity factors provides range and variation for VRE availability; however, it does not capture correlations between the effects of extreme weather events on generation and their effects on demand. Thus, we can only partly capture events like the ERCOT outages experienced in Texas in

Figure 6.1 Example electricity demand in New York State in select hours in January 2050



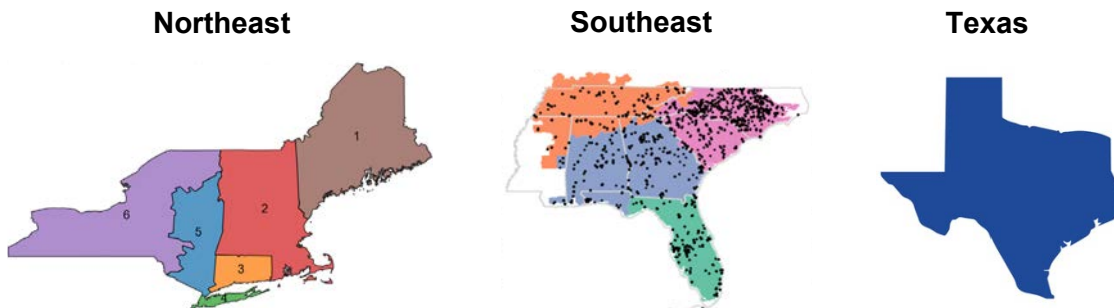
High electrification includes higher levels of electrified space heating (commercial and residential HVAC) and transportation (mainly light-duty electric vehicles). H Electrification = high electrification scenario; R Electrification = Reference electrification. HVAC = Heating, ventilation, and air conditioning. HD = Heavy-duty, LD = Light-duty; MD = Medium-duty. Data source: NREL Electrification Futures Study (Mai, Jadun, et al. 2018).

February 2021. As with most other CEMs, our hourly supply–demand balance assumes perfect foresight with respect to VRE availability and demand—in reality, forecasting is not perfect, and technologies that provide flexibility (e.g., storage) will be needed to manage short-term deviations from forecasts. The assumption of perfect foresight thus serves to produce a lower

bound on storage capacity requirements. A second limitation is that we model intra-regional transmission in a highly aggregated manner based on a “pipe-and-bubble” formulation (Mai, Barrows, et al. 2015).¹⁵ We also do not model sub-hourly VRE variability or planning reserve margins that mimic capacity markets in some jurisdictions. These

¹⁵ Pipe-and-bubble or transport models for transmission are often used in investment planning to simplify the modeling. In these formulations, the transmission of electricity is represented in the same manner as the transport of mass, instead of using the more complex physical laws (Kirchoff’s laws) that actually govern electricity flows.

Figure 6.2 Summary of regional modeling features and differences across the Northeast, Southeast, and Texas



| | Northeast | Southeast | Texas |
|----------------------------|--|--|--|
| Variable renewables | Wind: Onshore (50% cost premium) + offshore PV: Utility + distributed | Wind: Onshore PV: Utility | Wind: Onshore PV: Utility |
| Hydro | Yes (domestic + imports) | Yes (domestic) | No |
| Spatial resolution | 6 zones with existing intra-zonal transmission capacity | 4 zones with existing intra-zonal transmission capacity | Single zone |
| Temporal resolution | 35 representative periods of 10 days from 2007–2013 weather years, including “extreme” periods (8,400 hours) | 35 representative periods of 10 days from 2007–2013 weather years, including “extreme” periods (8,400 hours) | 2007–2013 weather years (61,314 hours) |

Assumptions & Sources

- After-tax WACC: 4.5%
- Load: NREL Electrification Futures Study (2012 weather year) – high electrification
- VRE resource: NREL WIND Toolkit, National Solar Radiation Database (PV) (2007-2013)
- Generation costs: NREL Annual Technology Baseline (ATB) 2020
- Storage costs: Technical teams + NREL ATB 2020 for Li-ion + other literature sources
- Gas price: EIA Annual Energy Outlook 2020 estimate for 2050—\$4.04/MMBtu (2019: \$2.88/MMBtu)
- Transmission capacity: EPA Integrated Planning Model’s existing capacity (Northeast, Southeast)
- Existing generation: Hydro & pumped hydro (Northeast, Southeast), distributed PV (Northeast), nuclear (Southeast)
- Hydropower: Oak Ridge National Laboratory database + EIA 923 + Canada energy board

Further details available in Appendix C.1.

simplifications have operational and cost implications and point to areas that should be considered in future work. Finally, it is important to keep in mind that this analysis relies on an optimization model that is designed to derive efficient solutions. The model does not account for real-world market imperfections, regulatory imperfections, or public policies that may favor one technology over another—all of which are likely to make it very difficult to achieve least-cost solutions in practice.

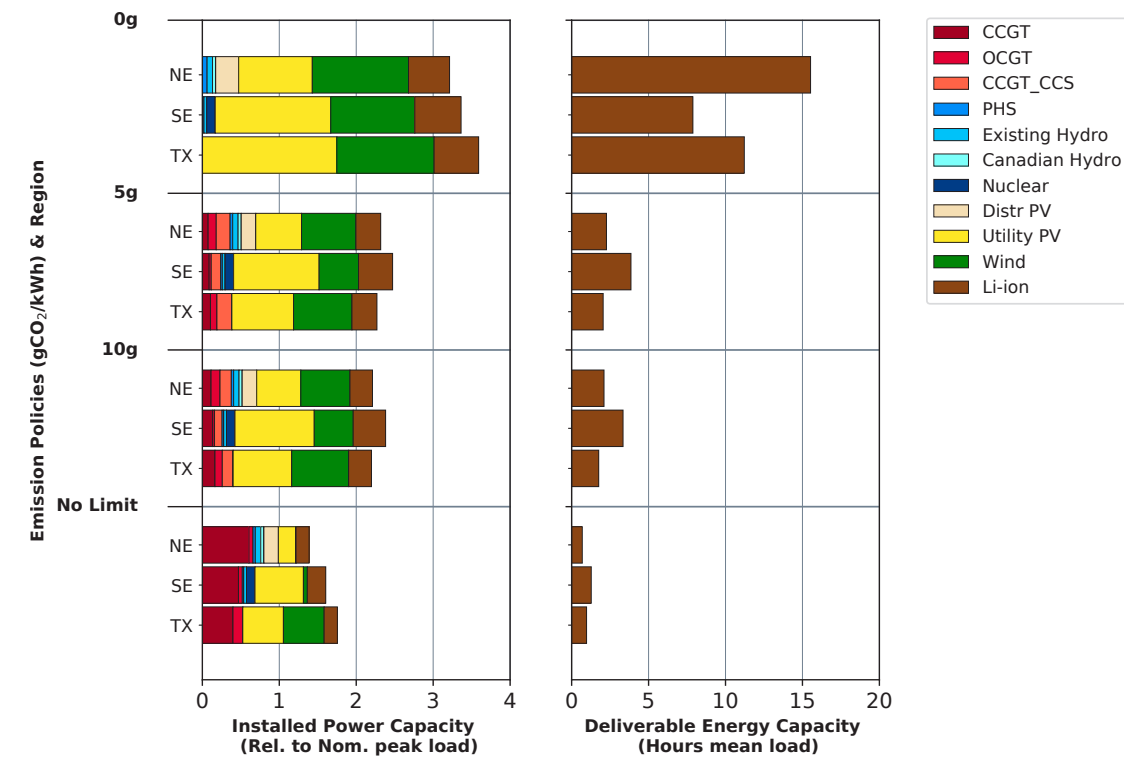
Nonetheless, our analysis provides a useful benchmark against which real-world results can be compared for policy evaluation.

6.3 Findings from the modeling analysis

6.3.1 Near-complete decarbonization with VRE, natural gas, and Li-ion battery storage

In our “base case” scenario, only today’s commercially available technologies, namely lithium-ion (Li-ion) battery storage and

Figure 6.3 Installed capacities in the Northeast (NE), Southeast (SE), and Texas (TX) under tightening CO₂ emissions constraints



Left side: installed power capacities (relative to the region's 2050 peak electricity demand); right side: deliverable storage energy capacity to the grid (i.e., product of energy capacity and discharge efficiency, relative to the region's annual electricity demand). Capacity factors of CCGTs can be found in Appendix C, Table C.10. For the Northeast, "wind" represents the sum of onshore and offshore capacity.

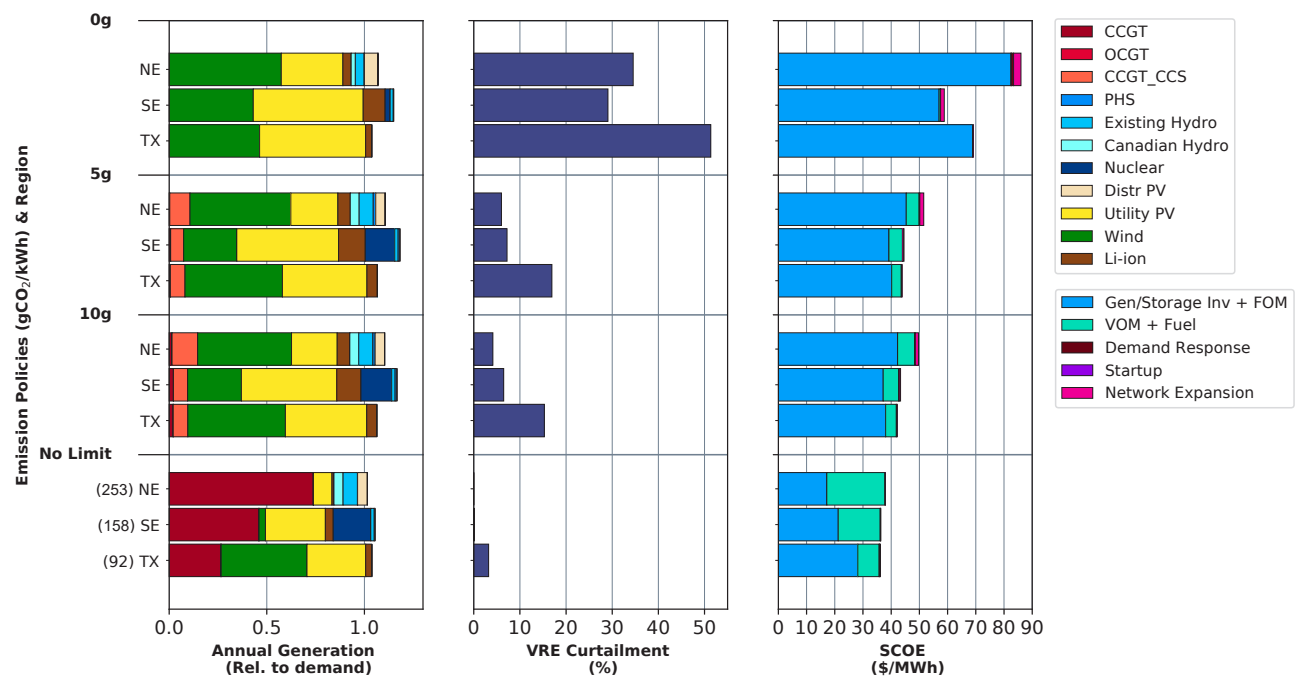
pumped hydro storage (within resource availability limits); wind and solar generating capacity; and natural gas, with and without CCS; can be deployed in 2050, all subject to 2050 mid-cost assumptions. Wind, solar, and Li-ion storage technologies, which have experienced significant cost reductions in recent years and are expected to become even less expensive in the future, play a greatly expanded role in this scenario even absent power system decarbonization goals—as reflected in our results for an emissions policy with no carbon limit.¹⁶ For the base case and “No Limit” emissions policy,

for example, wind and solar account for 73% of generation in Texas in 2050, compared to only 16.5% of generation in ERCOT in 2018.

Since we do not model negative emissions technologies, and since the incremental cost of driving emissions to zero in our models exceeds the likely per-ton cost of these technologies, we emphasize the findings for our 5 gCO₂/kWh case as being most representative of an extreme decarbonization scenario. Figure 6.3 and Figure 6.4 summarize the key modeled system outcomes for scenarios with tightening CO₂

¹⁶ As noted above, this case does assume that government policies outside the power sector have been implemented to support the substantial electrification assumed in the NREL demand scenario we employ.

Figure 6.4 Annual generation, VRE curtailment, and system average cost of electricity (SCOE) in the Northeast (NE), Southeast (SE), and Texas (TX) under tightening CO₂ emissions constraints



SCOE includes total annualized investment, fixed O&M, and operational costs of generation, storage, and transmission, as well as any non-served energy penalty. Emissions intensity under the No Limit policy case is noted in parentheses in the bottom panel. For the Northeast region, “wind” represents the sum of onshore and offshore wind generation.

limits across the three regions. System impacts can be observed in the trade-offs between technology-level installed capacities and system costs, and between storage capacities and VRE curtailment.

Base case summary system impacts

As CO₂ limits tighten across the three regions, natural gas generating capacity is incrementally replaced by larger buildouts of VRE and Li-ion battery storage, as well as by the deployment of gas capacity with CCS. Notably, the capacity factor of CCGTs (without CCS) declines from 36% in Texas, 54% in Southeast, and 66% in Northeast under the No Limit case to 2%–5% across the three regions in the 5 gCO₂/kWh case (see Table C.10 in Appendix C). Relative to the already very substantial VRE capacity

increases modeled in the No Limit policy scenario, VRE capacity increases by 48% (Texas), 139% (Southeast), and 257% (Northeast) in the 5 gCO₂/kWh case, and by 185% (Texas), 281% (Southeast), and 500% (Northeast) in the 0 gCO₂/kWh case.

Across the three regions, the variability of VRE generation is managed in the base case via three mechanisms: (1) flexible operation of natural gas generation to handle long periods of low VRE output, (2) deployment and utilization of energy storage for shorter periods of low VRE output, (3) optimization of the relative capacities of wind and solar generation, and (4) VRE deployment in excess of peak load. Use of the latter approach, often referred to as “overbuilding,” makes it cost-optimal to limit energy

storage capacity to 2–4 hours of mean system load¹⁷ in the 5 gCO₂/kWh case. In the regions where the model allows for intra-region transmission expansion, we also see 46 GW (Southeast) and 55 GW (Northeast) of added transmission capacity in the 5 gCO₂/kWh scenario to enable maximum utilization of high-quality VRE resource sites to serve high-demand areas. In the Southeast region, for example, transmission capacity expands to connect VRE sites in Florida to load in Georgia.

The optimal VRE curtailment level depends on the study region's resource mix and VRE quality (Figure 6.4); in the 5 gCO₂/kWh scenario, we observe 6%–7% VRE curtailment in the Southeast and Northeast regions, respectively, and 17% curtailment in Texas (where VRE generally accounts for a larger portion of generation because of higher-quality wind and solar resources). Curtailment involves “turning down” VRE generation using administrative or market mechanisms. The relatively high capacity cost of Li-ion energy storage under the mid-cost assumptions explains why the cost-optimal deployment of this technology has a storage duration (i.e., ratio of deliverable energy capacity to discharge power capacity) of less than five hours for the 5 gCO₂/kWh scenario.

Tightening the emissions constraint down to 5 gCO₂/kWh is accompanied by higher costs relative to having no CO₂ emissions limit (the “No Limit” policy case). In the base case, the percentage increase in SCOE to achieve an average grid carbon intensity of 5 gCO₂/kWh

(relative to the SCOE for the No Limit case) depends on resource availability and load variations and differs across the three regions, from 21% in Texas to 23% in the Southeast and 36% in the Northeast. This translates into an average CO₂ abatement cost¹⁸ relative to the “No Limit” policy case of \$54–\$88 per metric ton of CO₂ and marginal abatement costs of \$333–\$644 per metric ton of CO₂ (Table 6.7). These high marginal costs point to the value of reducing the cost of negative emissions technologies and/or long-term storage. They are also, effectively, measures of the carbon prices that would be required, absent other policies, to provide sufficient incentives for achieving these levels of decarbonization. Across all regions, an increase in investment costs for capital-intensive resources like VRE and storage is partly offset by a reduction in operating costs as the role of thermal generation resources declines.

Additionally, the model results show no major effect on non-served energy events (i.e., involuntary curtailments of demand) from decarbonizing the grid with VRE and Li-ion battery storage, at least when considering the demand and supply balance from an hourly perspective. With an assumed value of unserved load of \$50,000/MWh, non-served energy events for the modeled grid decarbonization scenarios were generally quite small (e.g., 0.0003% of annual demand for Texas, as shown in Table 6.8). As described earlier, these findings are based on modeling seven years of hourly VRE resource variability with perfect foresight of load (non-coincident with renewable resource variability) and generation, but they do not

¹⁷ Hours of mean system load is computed by taking the ratio of total storage deliverable energy capacity (i.e., the product of storage energy capacity multiplied by discharge efficiency) and mean annual system power demand. It is a measure of how long storage can serve mean system power demand when fully charged. In absolute terms, the deliverable storage capacity of installed Li-ion batteries corresponds to 167–639 GWh in the 5 gCO₂/kWh case.

¹⁸ Average CO₂ abatement cost to achieve an emissions target is computed by dividing the increase in SCOE (relative to the “No Limits” policy case) by the reduction in annual CO₂ emissions (relative to the “No Limits” policy case). Marginal CO₂ abatement costs are obtained as the shadow price of the carbon emissions constraint imposed in the capacity expansion model (which is a linear program).

Table 6.7 Marginal and average costs of carbon abatement for various emission policy constraints¹⁹

| | Marginal cost (\$/metric ton CO ₂) | | | Average cost (\$/metric ton CO ₂) | | |
|------------------|--|-----|-----|---|-----|----|
| | 50g | 10g | 5g | 50g | 10g | 5g |
| Northeast | 88 | 237 | 644 | 35 | 48 | 55 |
| Southeast | 67 | 181 | 333 | 23 | 48 | 54 |
| Texas | 48 | 246 | 516 | 19 | 73 | 88 |

Table 6.8 Base case reliability results in Texas

| CO ₂ constraint (gCO ₂ /kWh) | Number of NSE events | Max duration of a single event (hours) | Total NSE (GWh) | Max hourly demand loss (%) | Total NSE as fraction of nominal load |
|--|----------------------|--|-----------------|----------------------------|---------------------------------------|
| 0 | 0 | 0 | 0 | 0 | 0 |
| 5 | 0 | 0 | 0 | 0 | 0 |
| 10 | 0 | 0 | 0 | 0 | 0 |
| 50 | 1 | 2 | 4.2 | 3.9 | <10 ⁻⁶ |
| NL | 1 | 2 | 14.0 | 6.4 | <10 ⁻⁵ |

Non-served energy events are identified in the dispatch decisions optimized over the full 2007–2013 period. Appendix C.2 describes the reliability simulation approach used for the Northeast and Southeast regions, and associated reliability results.

account for the impact of extreme weather events (e.g., extreme heat waves and cold snaps) on correlated load and generation outages. Appendix C.2 describes the approach used in our modeling to ensure reliability (measured in terms of non-served energy events) in the Northeast and Southeast regions when using representative periods in the CEM.

In the 0 gCO₂/kWh scenario, deployment of Li-ion storage increases significantly, to 8–16 hours of mean system load across the three regions.²⁰ SCOE also increases (relative to the No Limit case), by 62% in the Southeast, 91% in Texas, and 127% in the Northeast. This cost increase corresponds to average CO₂ abatement costs of \$143–\$358 per metric ton CO₂ and substantially higher marginal abatement costs

compared to the 5 gCO₂/kWh emissions constraint. In the Northeast and Southeast, where pumped hydro storage (PHS) can be expanded, we also observe increases in installed PHS capacity (with a fixed duration of 12 hours) of 107% and 16% respectively in the 0 gCO₂/kWh case. However, as noted above, this scenario represents a strict definition of zero-carbon power systems that excludes any use of natural gas generation, even with existing CCS technologies (<100% capture rate), and any use of negative emissions technologies. Hence, we emphasize our findings for the 5 gCO₂/kWh scenario as more representative of a realistic strategy for the deep decarbonization of power systems. The results for our 0 gCO₂/kWh scenario highlight the value of natural gas or some other dispatchable generation capacity,

¹⁹ We ran experiments at 1 gCO₂/kWh in the Texas region and found that the marginal costs of carbon abatement at that level are eight times the marginal cost of abatement at the 5 gCO₂/kWh emissions limit.

²⁰ Based on modeled demand across the three regions, this corresponds to 797–1,307 GWh of deliverable Li-ion storage capacity.

used very sparingly, in moderating the cost of near-zero carbon electricity systems with Li-ion batteries as the sole form of energy storage. These results also illustrate the potential value of low-cost negative emissions technologies. Overall, the analysis for our base case indicates that the near-complete decarbonization of electricity systems will be feasible, from the perspective of balancing hourly energy supply and demand, with bulk power cost increases from 21% to 36% compared to the No Limit case, based on projected technology cost declines by 2050.

FINDING

Near-complete decarbonization of electricity systems appears feasible, from an hourly energy supply and demand balance perspective, using renewables, natural gas, and Li-ion battery storage alone, without creating significant reliability issues or very large increases in system average cost.

Base case regional differences

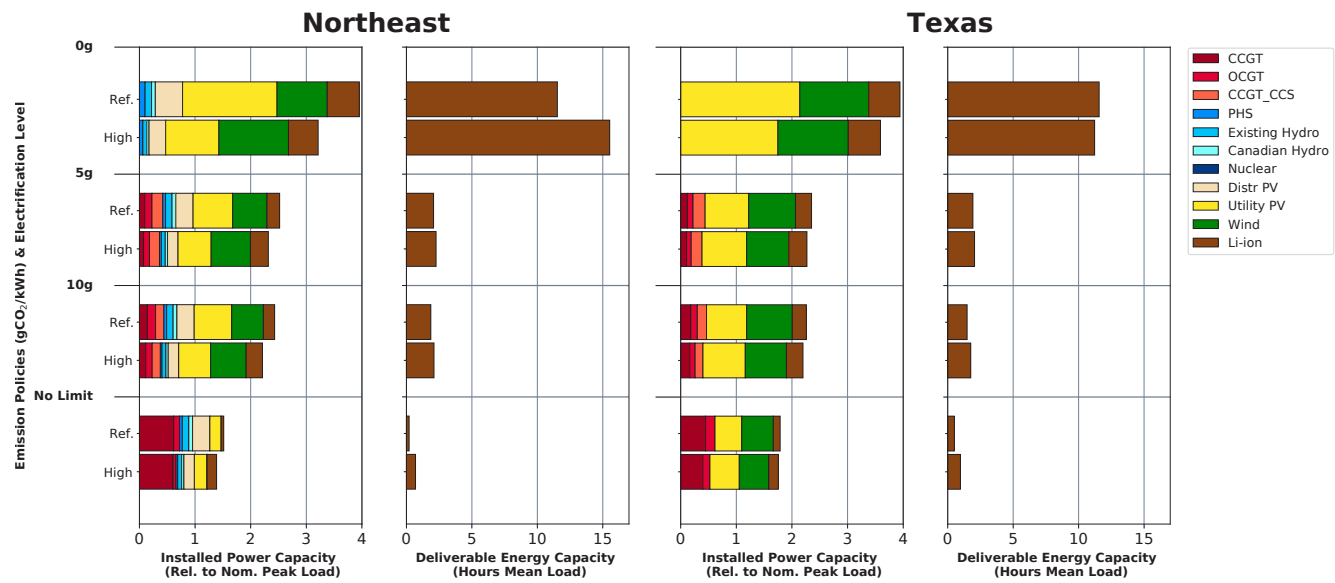
It is interesting to note that in the absence of any CO₂ emissions policy, the three U.S. regions studied here achieve very different CO₂ emission intensities, based on our 2050 technology cost assumptions and demand projections, which are based on NREL's high-electrification scenario (Mai, Jadun, et al. 2018) for end uses. The difference between actual emissions intensity in 2018 and modeled emissions intensity in 2050 in the No Limit case can be explained by three factors: (1) We are not modeling existing thermal generation assets that are assumed to retire by 2050; (2) even with no carbon constraint, deployment of new VRE and natural gas generation is economically favorable and is expected to largely replace existing assets; and (3) electricity demand in 2050 is projected to be much higher than demand in 2018 and is also expected to have a different

temporal profile owing to the electrification of additional end uses. The precise share of VRE generation in the No Limit policy case is driven both by the quality of wind and solar resources in each region and by changes in demand profiles and overall demand as a result of expanded electrification of end uses in sectors such as transportation and heating.

The level of electrification affects VRE penetration and subsequent needs for energy storage. Relative to NREL's reference-electrification scenario, the high-electrification scenario results in increased power and storage capacity requirements, but it has only minor impacts on VRE curtailment and average system cost (Figure 6.5). For instance, we observe only a 5% increase in SCOE for the 5 gCO₂/kWh policy case. The impact of electrification on emissions intensity is most notable when there are no emission constraints. In our No Limit case, average system-wide emissions in the Northeast under the high-electrification demand scenario are 253 gCO₂/kWh—11% higher than in the reference-electrification case (228 gCO₂/kWh). The change in demand profile due to increasing electrification of space heating and transportation reduces the value of VRE resources and increases the optimal level of dispatchable natural gas generation, which leads to higher system-average emissions intensity.

With high-electrification load assumptions, we observe the following regional emission intensities in our No Limit policy case: 92 gCO₂/kWh in Texas, 158 gCO₂/kWh in the Southeast, and 253 gCO₂/kWh in the Northeast. Based on these results, the amount of decarbonization predicted to occur by mid-century, even without any carbon constraints, is particularly striking in Texas, where modeled emissions intensity in 2050 is 81% lower than (actual) 2018 emissions intensity (Table 6.9). This is because, in Texas, low-cost VRE technologies combined with good-quality VRE resources drive the displacement of higher-capital-cost

Figure 6.5 System impacts of varying levels of electrification in the Northeast and Texas



Scenarios show the impacts of assuming the NREL EFS reference- vs. high-electrification load scenarios on installed power capacity and storage capacity across a range of CO₂ emission policies. Under the high-electrification load assumptions, both system peak and annual demand are higher (see Table 6.6 for details).

Table 6.9 Modeled emissions reduction results for different decarbonization targets summarized using alternative metrics commonly used in policy discourse

| | gCO ₂ /kWh | NL | 50 | 10 | 5 | 0 |
|------------------------------------|-----------------------|-----|-----|-----|-----|------|
| Relative to 2018 levels | | | | | | |
| Northeast | 249 | -2% | 80% | 96% | 98% | 100% |
| Southeast | 387 | 59% | 87% | 97% | 99% | 100% |
| Texas | 418 | 78% | 88% | 98% | 99% | 100% |
| Relative to No Limit levels | | | | | | |
| Northeast | 253 | 0% | 80% | 96% | 98% | 100% |
| Southeast | 158 | 0% | 68% | 94% | 97% | 100% |
| Texas | 92 | 0% | 46% | 89% | 95% | 100% |
| Carbon-free generation | | | | | | |
| Northeast | — | 26% | 85% | 86% | 90% | 100% |
| Southeast | — | 54% | 85% | 91% | 93% | 100% |
| Texas | — | 74% | 85% | 91% | 92% | 100% |

(1) Reductions relative to 2018 (current) emissions levels; (2) emission reductions relative to the No Limit policy case; and (3) carbon-free generation relative to modeled annual generation. For presentation purposes, carbon-free generation is defined in the table to include VRE, nuclear, and hydro resources, but does not include CCGT + CCS.²¹

²¹ If CCGT + CCS were to be included in the definition, the resulting emissions intensity will be lower at emission constraints more stringent than 10 gCO₂/kWh. At that level, the percentage of “carbon-free” generation is 98% across the three regions for 10 gCO₂/kWh (compared to 86%–91% without CCS).

thermal generators based on economics alone. In the Northeast, by contrast, modeled 2050 emissions intensity in the No Limit case is 2% higher than actual emissions intensity in 2018. This could partly be due to a substantial increase in annual demand, including a shift from summer peaking to winter peaking, the relatively small role for coal-based power generation in the region's power mix as of 2018,²² the presumed retirement of existing nuclear generation by 2050, and the lower quality and higher cost of VRE resources in the Northeast (based on historic patterns, we assume the region's onshore wind capital costs are 50% greater than in Texas and the Southeast).

Achieving an emissions intensity goal of 5 gCO₂/kWh requires a 98% reduction in power sector CO₂ emissions from 2018 levels and 90% carbon-free electricity in the Northeast by 2050, a 99% reduction in carbon emissions from 2018 levels and 93% carbon-free electricity in the Southeast by 2050, and a 99% reduction in carbon emissions from 2018 levels and 92% carbon-free electricity in Texas by 2050. Table 6.9 shows how these model results translate into other commonly used metrics of decarbonization (such as percentage emission reductions relative to historic emissions and carbon-free generation as a share of total generation).

The Southeast differs from other regions because of the possibility that significant nuclear capacity (25 GW) will be available for some years beyond 2050, assuming an 80-year lifetime for existing plants.²³ Figure 6.6 compares modeling results for scenarios where (1) most existing nuclear capacity is retained (as a zero-carbon dispatchable resource), and (2) all existing nuclear capacity is retired. We see that

in the former case, the availability of existing nuclear reduces system-wide cost in the Southeast by 6% in the No Limit scenario, 11% in the 5 gCO₂/kWh scenario, and 15% in the 0 gCO₂/kWh scenario, compared to a scenario where existing nuclear is retired. Benefits are derived from the displacement of new capital investments in VRE resources (mainly solar) that are not dispatchable. These results are consistent with prior research findings on the benefit of dispatchable low-carbon generation in terms of reducing the cost of power sector decarbonization (Buongiorno et al. 2018; Sepulveda, Jenkins and de Sisternes, et al. 2018).

FINDING

In the absence of any CO₂ constraint on the power sector, the three U.S. regions studied here (Texas, the Northeast, and the Southeast) achieve very different CO₂ emission intensities for the same set of 2050 technology cost assumptions. These differences primarily result from regional variations in renewable resource quality and load profiles.

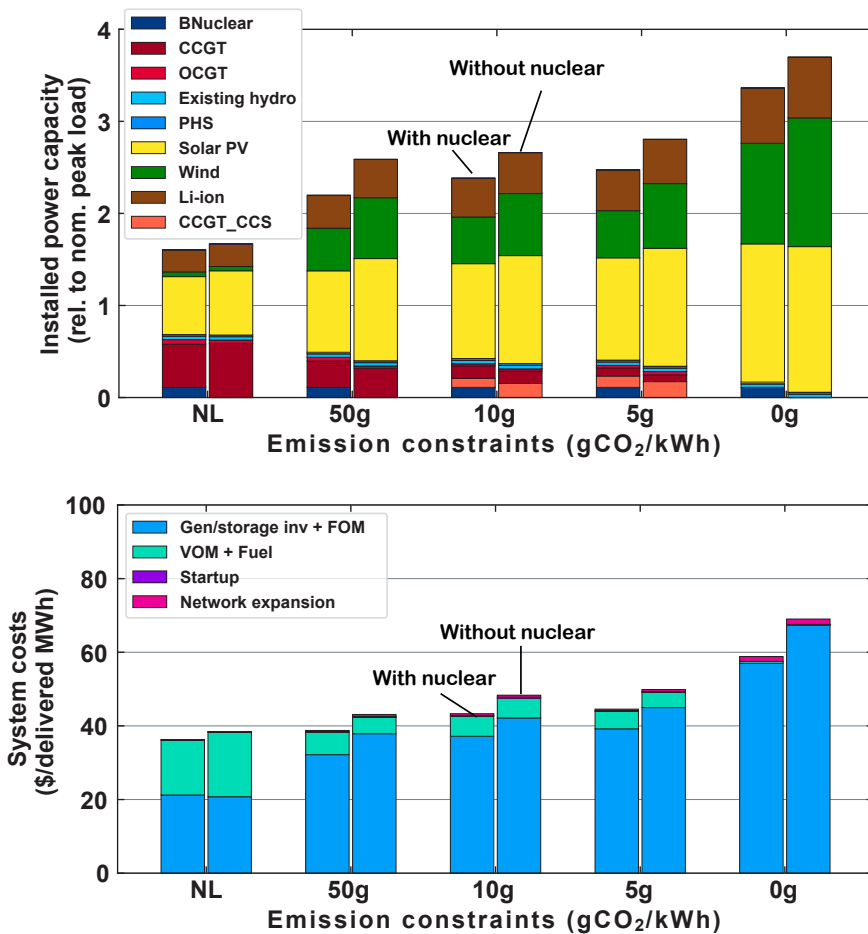
6.3.2 Impacts of adding long-duration energy storage (LDES)

As the penetration of VRE resources increases, needs for grid balancing on longer time scales (i.e., days and weeks) will grow. This could potentially create value for long-duration energy storage (LDES) technologies. Compared to Li-ion battery storage, the LDES technologies available in 2050 are projected to have lower energy capacity cost, higher power capacity cost, and lower overall round-trip efficiency (RTE) (Figure 6.7).

²² For instance, coal contributed 1% of total annual electricity supply in ISO-New England in 2018 (ISO New England 2020).

²³ Specifically, these are nuclear plants whose current licenses expire in 2055, assuming a second license extension (to 80 years of operating life).

Figure 6.6 System impacts of nuclear availability in the Southeast

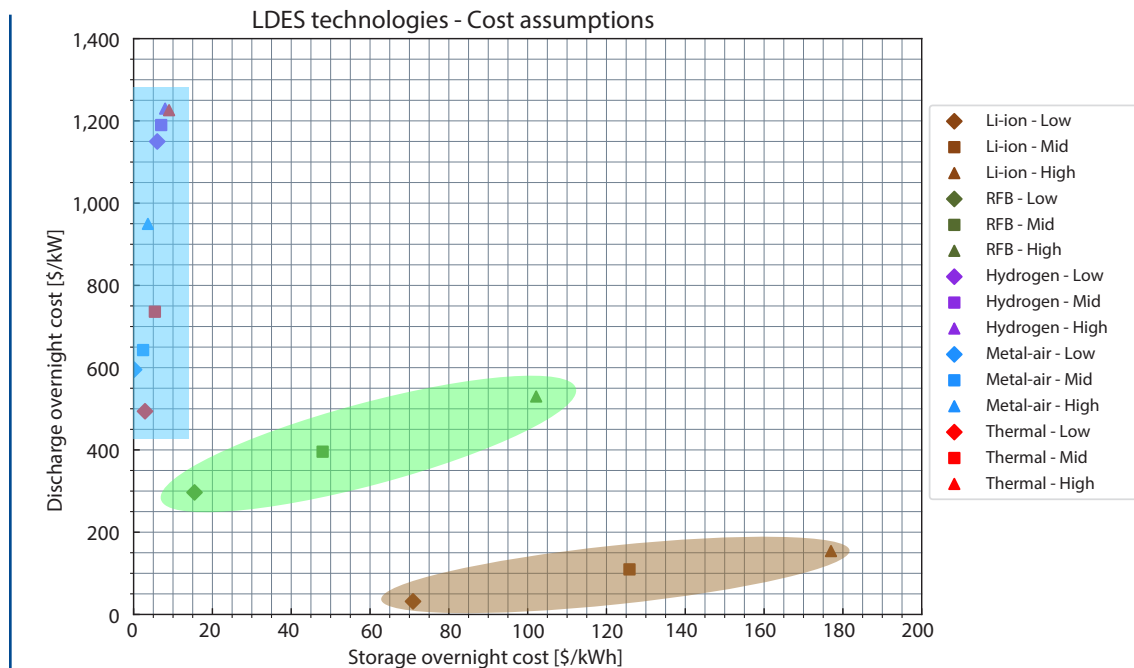


The two scenarios compare optimal generation capacity deployed and SCOE under two assumptions:
(1) existing nuclear plants remain part of the portfolio and can be dispatched to meet demand, and
(2) all existing nuclear plants retire by 2050, and no new nuclear is added.

Our analysis considers four distinct LDES technologies, as defined in the earlier, technology-focused chapters of this report: redox flow batteries (RFBs, Chapter 2), metal-air batteries (Chapter 2), hydrogen storage (Chapter 5), and thermal storage (Chapter 4). These technologies, which span a range of electrochemical, chemical, and thermal storage systems, are at varying levels of maturity; thus, our experimental design is aimed at understanding the relative merits of different classes of storage technology rather than identifying the most favorable technology within each class. Figure 6.7

highlights the classification of storage technologies based on two out of three key design attributes: Class 1 technologies have the lowest power capacity cost, relatively high energy capacity cost, and high RTE (e.g., Li-ion batteries); Class 2 technologies have mid-range power and energy capacity costs and RTE (e.g., current and future RFBs); and Class 3 technologies have high power capacity costs, low energy capacity costs, and low RTE (e.g., emerging LDES options including metal-air batteries, hydrogen, and thermal storage).

Figure 6.7 Classes of energy storage technologies, grouped by discharge power and storage overnight capital costs



We define the classes as: (1) technologies with the lowest power cost, relatively high energy capacity cost, high RTE; (2) technologies with mid-range power and energy capacity costs and RTE; and (3) technologies with high power costs, low energy capacity costs, and low RTE. Other salient design attributes can be seen in Table 6.3. Pumped hydro storage is modeled with a fixed duration of 12 hours for this study; since we do not have a breakdown of pumped hydro costs, we do not include this storage option on the chart.

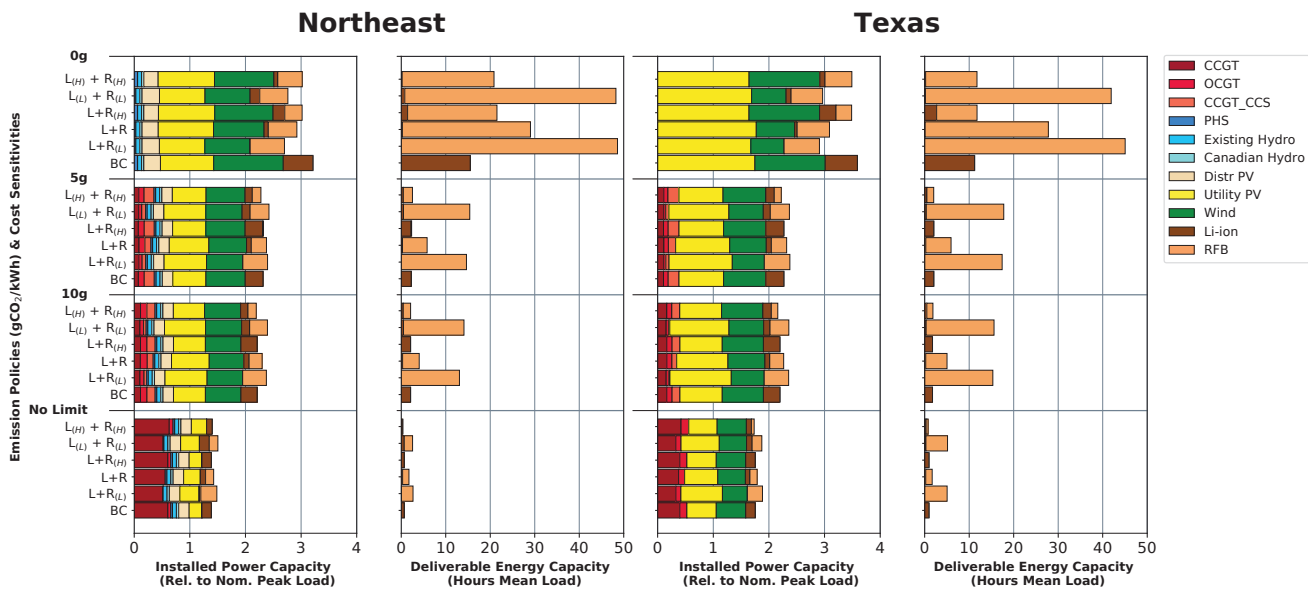
In addition to the attributes displayed in Figure 6.7, other cost and performance attributes (shown in Table 6.3) are also important when comparing storage technologies within and across each class. For example, recent studies have shown that in addition to energy capacity cost, discharge efficiency is another important technology design attribute that affects the value (i.e., cost reduction potential) of LDES in zero-carbon power systems (Sepulveda et al. 2021).

Impact of adding flow batteries (Class 1, 2)

We first explore the system impacts of adding RFB storage, using estimated cost and performance parameters discussed in Chapter 2. As we

note there, RFBs offer potentially lower energy capital costs compared to Li-ion batteries; they also have the potential added advantage of being able to recover energy capacity loss at a lower cost (either via rebalancing or via the replacement of chemicals that make up RFB systems). From a system perspective, this results in lower capital and FOM costs for RFB energy capacity compared to Li-ion technology, along with comparable RTE. The downside of RFBs compared to Li-ion batteries is their relatively high fixed cost for power capacity. This implies that RFBs could be favored over Li-ion batteries for applications involving more long-duration storage.

Figure 6.8 System impacts of adding RFB storage for the Northeast and Texas



Scenarios show the impacts of cost sensitivities around Li-ion and RFB technology in terms of installed power capacity and storage capacity, across a range of CO₂ emission policies. They are, in ascending order: (1) base case (i.e., mid-cost Li-ion only, BC), (2) mid-cost Li-ion + low-cost RFB (L+R_L), (3) mid-cost Li-ion + mid-cost RFB (L+R), (4) mid-cost Li-ion + high-cost RFB (L+R_H), (5) low-cost Li-ion + low-cost RFB (L_L+R_L), and (6) high-cost Li-ion + high-cost RFB (L_H+R_H). Low-, mid-, and high-cost assumptions for each storage technology are defined in Table 6.3.

Figure 6.8 compares capacity outcomes for the Northeast and Texas under plausible scenarios for future Li-ion and RFB costs.²⁴ When CO₂ constraints are binding, RFBs under mid-cost assumptions (third row from the bottom in each panel in Figure 6.8) largely (but not completely) displace Li-ion storage and increase deliverable energy storage capacity compared to the base case (shown in the bottom row in each panel in Figure 6.8). This shift from Li-ion to RFB storage has minor impacts on installed VRE capacity and VRE curtailment. Although it is difficult to see in the figure, RFBs displace substantial dispatchable fossil fuel capacity. For the 5 gCO₂/kWh case, the availability of mid-cost RFB technology (defined in Table 6.3) results in a 9% decline in natural gas generation capacity in the Southeast, and a 16% decline in both the

Northeast and Texas, compared to the base case. This effect increases with more stringent CO₂ constraints.

Exploring the sensitivity of these findings to plausible low-, medium-, and high-cost assumptions for Li-ion and RFB storage (defined in Table 6.3), several points emerge: (1) Across all the scenarios we analyzed with RFB technology, RFB storage duration was between 7 and 27 hours compared to Li-ion storage duration of 1–5 hours. (2) When available, both technologies are deployed in all scenarios, indicating that neither technology is dominant from a power system perspective. (3) RFB availability enables more buildouts of VRE to substitute for gas capacity, reflecting the value of LDES with low energy capital costs. For example, mid-cost and low-cost RFB (and

²⁴ Results for the Southeast are discussed in Appendix C.

mid-cost Li-ion) reduces natural gas capacity in Texas by 9–27 GW and increases VRE capacity by 10–23 GW relative to the base case (compared to a system peak load of 151 GW). (4) The addition of RFB storage reduces system costs compared to the base case, with the largest cost reductions observed in the 5 gCO₂/kWh case that includes low-cost assumptions for both battery technologies (12% in the Northeast, 14% in Texas, and 16% in the Southeast).

Impact of adding emerging LDES technologies (Class 1, 2, 3)

Class 3 LDES²⁵ technologies (represented by the blue box in Figure 6.7) have lower energy capital costs than RFBs, but their power capacity costs are generally higher. Though they generally also have much lower round-trip efficiency than either Li-ion or RFB technology, they are potentially appealing for much longer-duration energy storage and near-complete displacement of dispatchable generation capacity. Given the relative immaturity of this class of LDES technologies, we evaluate their potential system impacts one technology at a time, with the assumption that any or all of these technologies could be commercially scalable by 2050. Across the mid-range LDES cost and performance scenarios we evaluated, we find that LDES substitutes for natural gas and VRE capacity, leads to reduced curtailment of wind and solar generation, and modestly reduces SCOE compared to scenarios without LDES. Figure 6.9 and Figure 6.10 summarize key model outputs for different levels of LDES availability across the three regions.

LDES technologies with lower energy capacity costs and lower discharge efficiency compared to Li-ion batteries have the greatest impacts on electricity system decarbonization when natural gas generation without CCS is not an

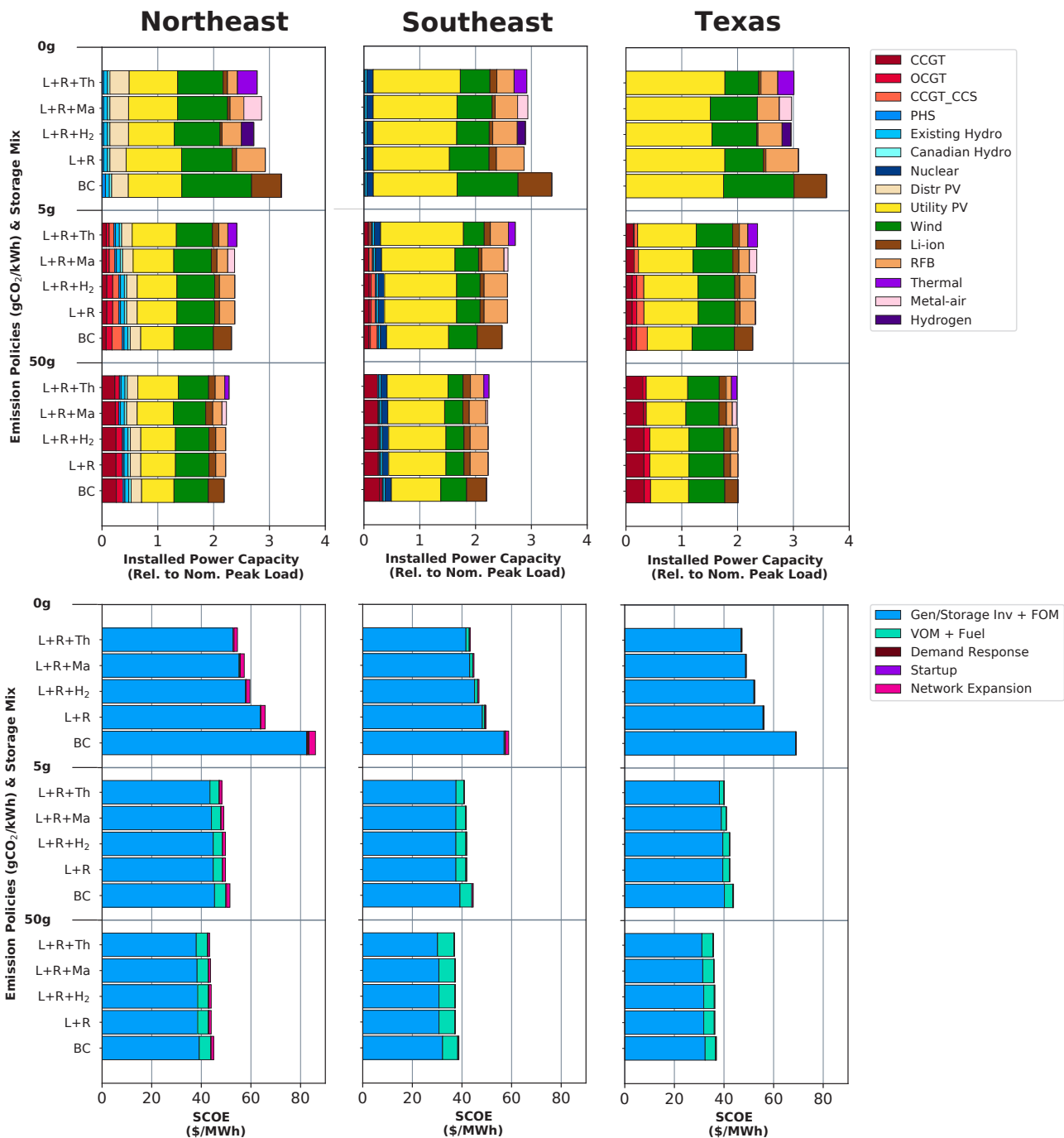
option (as in the highly restrictive 0 gCO₂/kWh scenario). This is because LDES directly competes with natural gas generation in providing supply during long periods of low VRE output. How important this is depends on the region's relative VRE resource quality. In the 5 gCO₂/kWh case, optimal deployment of LDES (Class 3) resources reduces the need for thermal generating capacity (i.e., gas with and without CCS, and nuclear) by 9%–45% (Figure 6.9) relative to the base case. Thermal capacity is replaced by VRE capacity, which increases by 6%–9% in the Northeast, 5%–14% in the Southeast, and 4%–9% in Texas, relative to the base case. In effect, the availability of LDES makes VRE capacity more nearly dispatchable and thus increases its value to the power system. Under mid-cost assumptions, the incremental availability of low energy capital cost LDES technologies contributes to SCOE reductions of between 3% and 9% across the three regions for the 5 gCO₂/kWh scenarios shown in Figure 6.9.

Our analysis also reveals that there is a clear trade-off between installed storage capacity and VRE curtailment in the modeled regions. When it is optimal to employ LDES in the 5 gCO₂/kWh case, it is generally optimal to have storage durations much greater than those associated with Li-ion or RFB storage (Figure 6.10). Across the scenarios analyzed, the storage duration for LDES resources ranges between 39 and 59 hours, as compared to Li-ion storage duration of 1–2 hours and RFB storage duration of 6–11 hours.²⁶ These storage durations translate to total deliverable storage energy capacity (across the various technologies) of 6–18 hours of mean system load (across the LDES options and regions modeled). In the 5gCO₂/kWh case, optimal VRE curtailment in the Northeast and Southeast is reduced from 5%–6% without LDES deployment to 2%–6%

²⁵ For this section, we use “LDES” to refer specifically to storage technologies with the potential for still lower energy capital costs compared to RFBs.

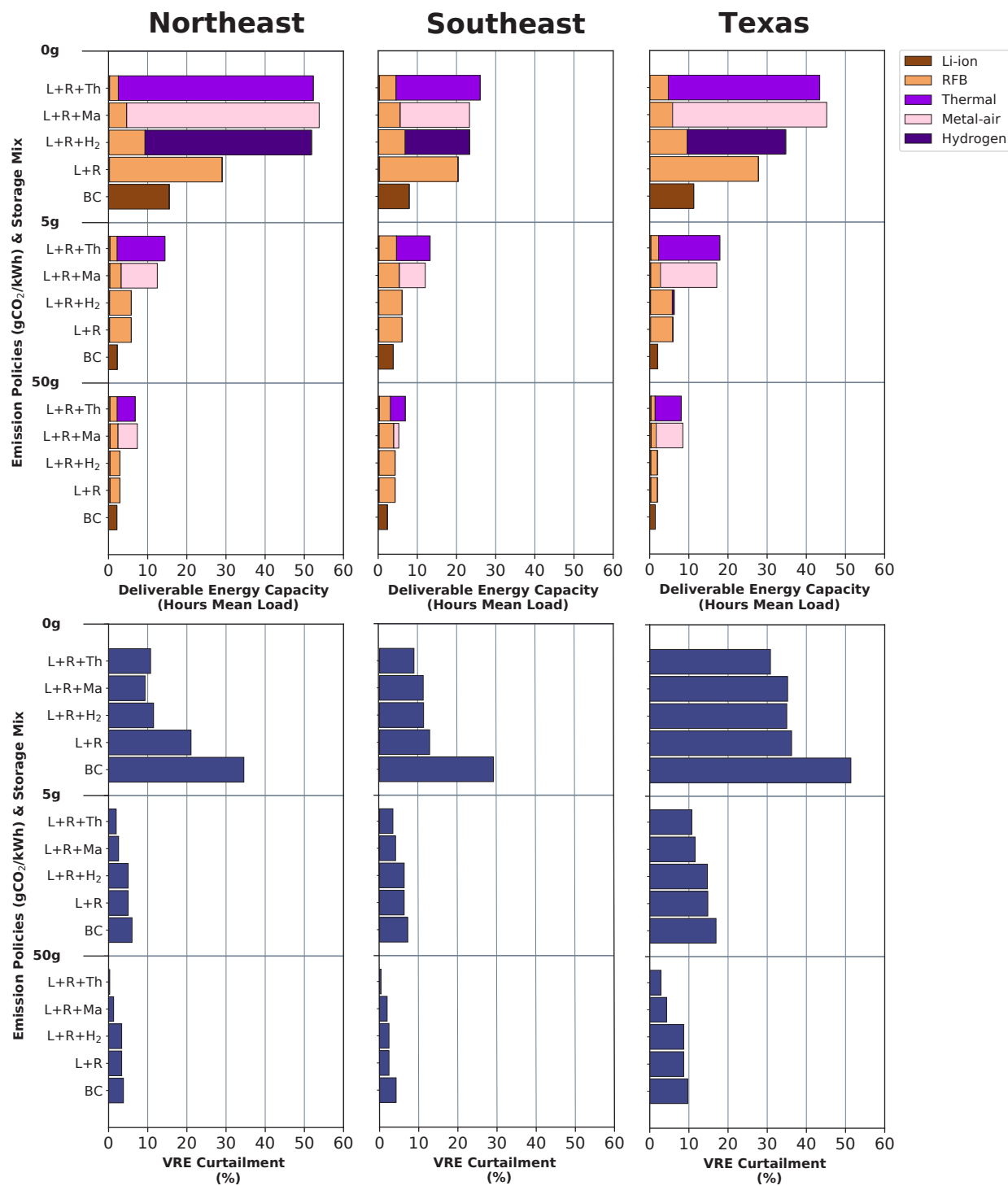
²⁶ In absolute terms, results for the deliverable storage capacity of Li-ion batteries, RFB, and LDES in Figure 6.10, correspond to 15–41 GWh, 93–983 GWh, and 38–1,422 GWh, respectively.

Figure 6.9 Impacts of adding RFB + LDES on installed power capacity and SCOE, across a range of CO₂ constraints for the Northeast, Southeast, and Texas regions



They are, in ascending order: (1) base case (i.e., Li-ion only, BC); (2) Li-ion + RFB (L+R); and (3-5) Li-ion + RFB + incrementally adding an LDES option in the form of hydrogen (+H₂), metal-air batteries (+MA), or thermal storage (+Th)—all at mid-cost assumptions. As discussed previously, we evaluate the Class 3 LDES technologies one at a time, with the assumption that any or all of these technologies could be commercially scalable by 2050. Mid-cost assumptions for each storage technology are defined in Table 6.3.

Figure 6.10 Impacts of adding RFB + LDES on installed storage capacity and VRE curtailment, across a range of CO₂ emission constraints



They are, in ascending order: (1) base case (i.e., Li-ion only, BC); (2) Li-ion + RFB (L+R); and (3-5) Li-ion + RFB + incrementally adding an LDES option in the form of hydrogen (+H₂), metal-air batteries (+MA), and thermal storage (+Th)—all at mid-cost assumptions (as defined in Table 6.3).

with LDES deployment (Figure 6.10). Optimal VRE curtailment in Texas is reduced from 19% without LDES to 13%–17% with LDES with a 5 gCO₂/kWh emissions intensity constraint. Relatively higher VRE curtailment in Texas, even with LDES, reflects the region's higher VRE resource quality, which reduces the cost penalty of “overbuilding” VRE capacity and, consequently, the marginal value of incremental storage additions.

In scenarios where all three classes of storage technology (i.e., Li-ion, RFB, and one Class 3 LDES technology) are available, we observe partial substitution of Li-ion batteries by RFB and LDES. This substitution is more prominent for energy capacity. For example, in the 5 g CO₂/kWh case, the deliverable energy capacity of Li-ion storage in the Northeast decreases by 97%–98% when both RFB and an LDES technology are considered. This indicates that it is more economically efficient to build LDES facilities mainly for longer-duration storage cycles. The availability of LDES has less impact on Li-ion discharge power capacity since it remains more efficient to deploy Li-ion battery storage for short-duration cycles. Substitution is even stronger between Li-ion and RFB because these technologies are more similar to each other in terms of power/energy capacity costs and RTE.

Given the significant cost and operational variations associated with different classes of LDES technology (Table 6.3), we also explore how low- and high-cost assumptions for LDES resources affect system outcomes. These experiments lead to the following observations: (1) They underscore the finding that LDES has the greatest impacts on electricity system decarbonization when natural gas generation without CCS is not an option (e.g., in the case of the 0 gCO₂/kWh scenario modeled here); (2) the availability of LDES resources even in

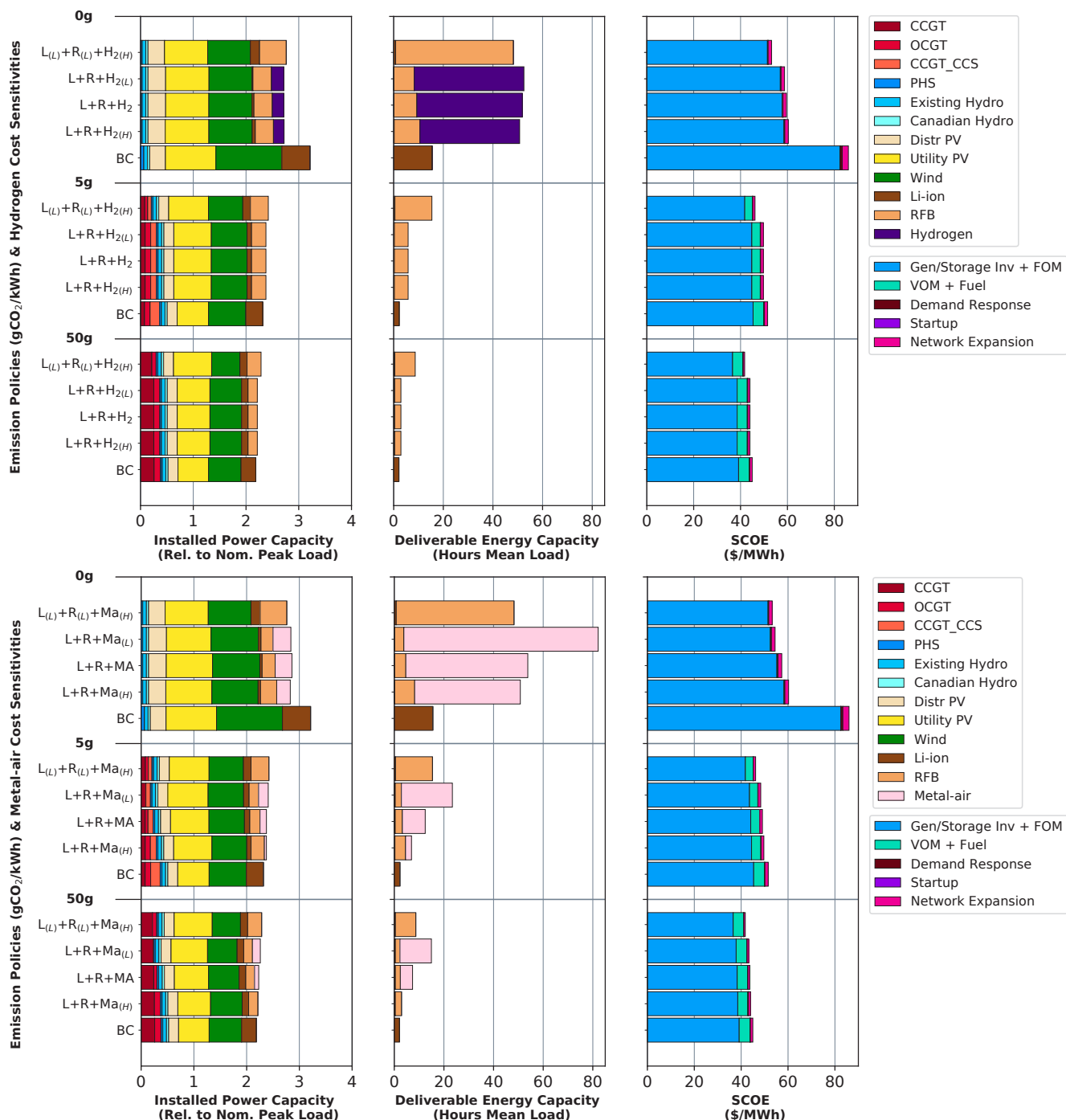
our high-cost case enables increased VRE deployment and displaces natural gas capacity, relative to the base case; and (3) cost variations between Li-ion and RFB technologies have greater total system impacts than cost variations between the specific LDES technologies we modeled.

We show the 0 gCO₂/kWh case here because, in the Northeast, hydrogen is only deployed in this extreme case (Figure 6.11). As discussed earlier, this is a stricter definition of a zero-carbon power system than the “net-zero” carbon goal being contemplated by policy makers. Still, the 0 gCO₂/kWh case is helpful for making comparisons across LDES technologies and across the modeled regions. In particular, differences in the deployment of hydrogen vs. metal-air batteries at this very stringent level of carbon constraint show that technologies with higher discharge efficiency are likely to be more valuable for grid-scale energy storage applications (Sepulveda, Jenkins and Edington, et al. 2021). In Texas, hydrogen is deployed at lower (less stringent) levels of decarbonization—for example, at 5 gCO₂/kWh (Figure 6.12). At this emissions constraint, the availability of low-cost hydrogen changes the relative mix of wind and solar in Texas, but it does not produce a net change in optimal VRE capacity relative to the mid-cost hydrogen case. The availability of low-cost hydrogen does, however, reduce natural gas capacity by 9% while increasing total deliverable energy capacity by more than ten times (again assuming a 5 gCO₂/kWh carbon constraint).

Figure 6.11 shows that optimal VRE capacity mix and system costs for the Northeast region do not change appreciably in response to the LDES cost variations evaluated here (see results for the Texas and Southeast regions in Appendix C.4).²⁷ For the 5 gCO₂/kWh case, low-cost metal-air battery storage reduces

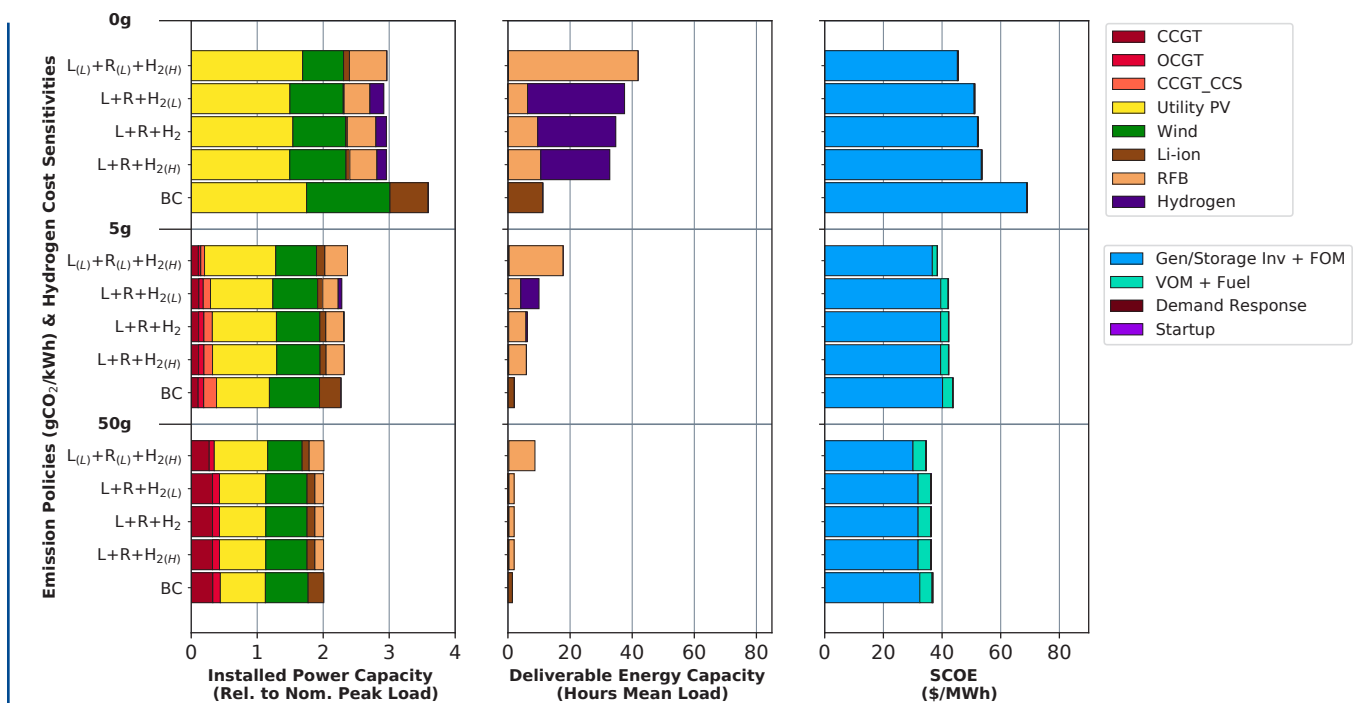
²⁷ Results for the Southeast and Texas are discussed in Appendix C, specifically Figure C.8 and Figure C.9.

Figure 6.11 Impact of low-, mid-, and high-cost hydrogen (top row) and metal-air battery (bottom row) storage on installed power capacity, storage capacity, and SCOE, across a range of CO₂ constraints for the Northeast region



They are, in ascending order: (1) base case (i.e., mid-cost Li-ion only, BC); (2-4) mid-cost Li-ion and RFB + incremental additions of high-cost hydrogen or metal-air (L+R+H₂/MA_H), mid-cost hydrogen or metal-air (L+R+H₂/MA), and low-cost hydrogen or metal-air (L+R+H₂/MA_L); and (5) low-cost Li-ion and RFB + high-cost hydrogen or metal-air (L_L+R_L+H₂/MA_H). Low-, mid-, and high-cost assumptions for each storage technology are defined in Table 6.3.

Figure 6.12 Impacts of low-, mid-, and high-cost hydrogen on installed power capacity, storage capacity, and SCOE, across a range of CO₂ constraints for the Texas region



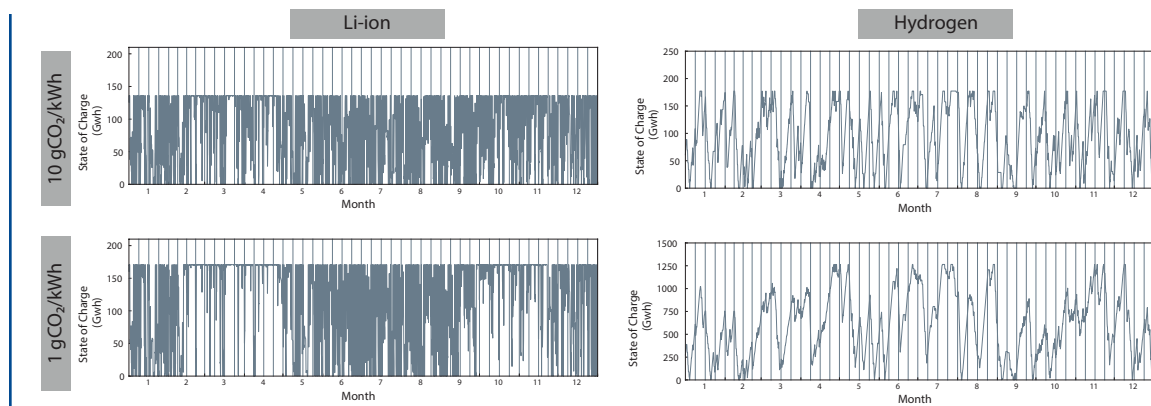
They are, in ascending order: (1) base case (i.e., mid-cost Li-ion only, BC); (2-4) mid-cost Li-ion and RFB + incremental additions of high-cost hydrogen ($L+R+H_{2H}$), mid-cost hydrogen ($L+R+H_2$), and low-cost hydrogen($L+R+H_{2L}$); and (5) low-cost Li-ion and RFB + high-cost hydrogen ($L_{(L)}+R_{(L)}+H_{2H}$). Low-, mid-, and high-cost assumptions for each storage technology are defined in Table 6.3.

SCOE by 1%, and high-cost metal-air battery storage increases SCOE by 1%, relative to mid-cost metal-air. Impacts on storage energy capacity and gas substitution are more pronounced than impacts on VRE capacity: With low-cost metal-air, optimal storage deliverable energy capacity is 123% higher relative to a scenario that assumes mid-cost metal-air (optimal storage capacity is 303% higher in the Southeast). This increase in storage capacity has the effect of displacing 23% of natural gas capacity (CCGT with and without CCS), relative to the scenario that assumes mid-cost metal-air. In terms of storage duration, low-cost metal-air makes 61 hours of storage optimal, compared to 34–41 hours in the high- and mid-cost scenarios. This translates to deliverable energy capacity equivalent to 21 hours of mean load in the low-cost case,

9 hours in the mid-cost case, and less than 3 hours in the high-cost case.

Cost variations for Li-ion and RFB storage affect system costs more strongly than cost variations across LDES technologies. In all regions and across all the LDES cost ranges we considered, the availability of low-cost Li-ion and RFB technology displaces all need for LDES capacity (top row in Figure 6.11 and Figure 6.12). This indicates that system reliability requirements can be met economically by shorter-duration storage technologies alone if the costs of those technologies are sufficiently low. We should note that the alternative cost assumptions for hydrogen considered here and defined in Table 6.3, still reflect costs for aboveground storage as a compressed gas. Lower storage costs are possible with geological

Figure 6.13 Example state of charge (SoC) of Li-ion battery and hydrogen storage systems in Texas



Scenarios show the hourly state of charge (SoC) for Li-ion and hydrogen storage for the scenario with mid-cost Li-ion, RFB (not shown), and hydrogen storage technologies available across two emissions constraints. Here, we show 12 months of operation. Results correspond to mid-cost assumptions for each storage technology as defined in Table 6.3.

hydrogen storage in some locations (see Chapter 5 for further discussion). As discussed later, the availability of geological hydrogen storage increases the value of hydrogen storage for grid decarbonization. Of course, the large-scale use of hydrogen outside the power sector would also increase the value of hydrogen storage.

FINDING

With lower energy capacity costs and lower round-trip efficiency compared to Li-ion battery technology, LDES has the greatest impact on electricity system decarbonization when natural gas generation without CCS is not an option (corresponding to our 0 gCO₂/kWh policy case), under the assumptions used in this analysis. Generally, LDES, when optimally deployed, substitutes for natural gas capacity, increases the value of VRE generation, and produces moderate reductions in system average electricity cost.

Operational behavior of short- vs. long-duration storage technologies

Our modeling highlights the differing operating patterns of various classes of storage technologies, as influenced by the attributes of individual technologies and by system conditions (such as the stringency of the CO₂ constraint). Figure 6.13 shows how frequently storage resources are cycled (deep discharge and charge cycle) in our model of the deeply decarbonized Texas system with Li-ion batteries and hydrogen as the available storage technologies. As expected, Li-ion batteries, with their relatively low power capacity cost, relatively high energy capacity cost, and high RTE are used primarily for short-cycle operations, while hydrogen storage, with higher power costs but much lower energy capacity costs and RTE than Li-ion, is mostly used for longer-cycle operations. These operational modes are not exclusive to each storage technology, however, and we see that Li-ion batteries sometimes perform relatively long charge/discharge cycles, while hydrogen systems are sometimes cycled rapidly. Moreover, the optimal operating pattern for

Table 6.10 Relative root mean square (RMS) contribution of different frequency bands to the optimal storage state of charge temporal profile

| Frequency band | Mode of operation | 10 gCO ₂ /kWh | | 1 gCO ₂ /kWh | |
|-----------------------|-------------------|--------------------------|----------------|-------------------------|----------------|
| | | Li-ion | H ₂ | Li-ion | H ₂ |
| Above 365 cycles/year | Daily | 39% | 1% | 23% | 0% |
| 52 to 365 cycles/year | Weekly | 34% | 15% | 29% | 4% |
| 12 to 52 cycles/year | Monthly | 12% | 59% | 12% | 32% |
| 0 to 12 cycles/year | Seasonal | 16% | 25% | 35% | 64% |

storage technologies is also influenced by the CO₂ constraint: Tighter constraints lead to longer cycles, as can be seen by comparing the top and bottom portions of Figure 6.13.

As discussed in Junge, Mallapragada, and Schmalensee (2022), storage technologies do not follow simple cycling patterns. Optimal operation is more complex than the marginal cost dispatch rule for generation technologies. In effect, the marginal cost of using storage energy depends on the (shadow) value of stored energy, which changes from one period to the next.

Frequency analysis²⁸ applied to the time series of the state of charge of storage technologies is a useful way to unpack complexity and quantify operating behavior, since this type of analysis can be used to quantify the relative importance of different frequencies (or cycling patterns) in the optimal storage state of charge temporal

profile. The results of the frequency analysis, applied to the model outputs related to storage state-of-charge variables shown in Figure 6.13, are listed in Table 6.10. The table shows that for the 10 gCO₂/kWh case, hydrogen storage behaves mostly in cycles that occur within a month (intra-month charge and cycle); for the 1 gCO₂/kWh case,²⁹ the cycles decrease in frequency and become mostly seasonal (64%). Conversely, Li-ion battery storage shows a tendency towards daily and weekly cycles. In the 10 gCO₂/kWh case, daily and weekly charge and discharge cycles account for 73% of the operational patterns; they account for only 52% of operational patterns in the 1 gCO₂/kWh case. It is worth highlighting the observation that Li-ion storage in the 1 gCO₂/kWh case also displays a significant proportion of seasonal cycling (35%), reflecting the fact that this technology is used less frequently during some periods of the year than during others.

²⁸ Frequency analysis is performed by applying a fast Fourier transform (FFT) to the time-dependent variable corresponding to the hourly storage state of charge. Next, the root mean square (RMS) contribution of selected frequency bands is computed. The frequency bands of interest are listed in Table 6.10.

²⁹ For the Texas case study, we also examined scenarios with the 1gCO₂/kWh emissions intensity constraint for certain technology and system assumptions. However, because we did not evaluate this emissions intensity constraint for other regions, we primarily rely on results from the 5g CO₂/kWh scenario when describing trends in system outcomes under deep decarbonization.

FINDING

When it is cost-optimal to deploy multiple storage technologies, the technologies with the lowest capital cost of energy storage capacity are generally best suited to provide long-term storage. However optimal storage operation, unlike optimal generation dispatch, is complicated by the changing shadow value of stored energy. As a result, all storage technologies deployed will operate with charge/discharge cycles of various durations. Simplified assessments of storage economics based on stylized charge/discharge profiles overlook such dynamics and may provide inaccurate assessments of storage value.

6.3.3 Storage substitutes for grid resources

Energy market arbitrage involves buying when prices and net demand (the difference between demand and VRE output) are low and selling when prices (and net demand) are high. In performing arbitrage, energy storage can substitute for other grid resources (and vice versa). Candidate substitutes for grid resources include VRE “overbuilding” (i.e., deploying VRE capacity in excess of system peak load), demand flexibility, dispatchable generation, and increased network capacity (transmission and distribution). The degree to which storage can substitute for these resources depends not only on the cost and performance of storage technologies relative to competing resources, but also on system conditions, such as the stringency of the carbon constraint, the amount of storage deployed already, the availability of demand flexibility resources, and the ability to expand transmission. This section quantifies the cost-optimal substitution between various types of resources and storage under scenarios for deep grid decarbonization. We evaluate four potential substitutions: (1) storage vs. VRE

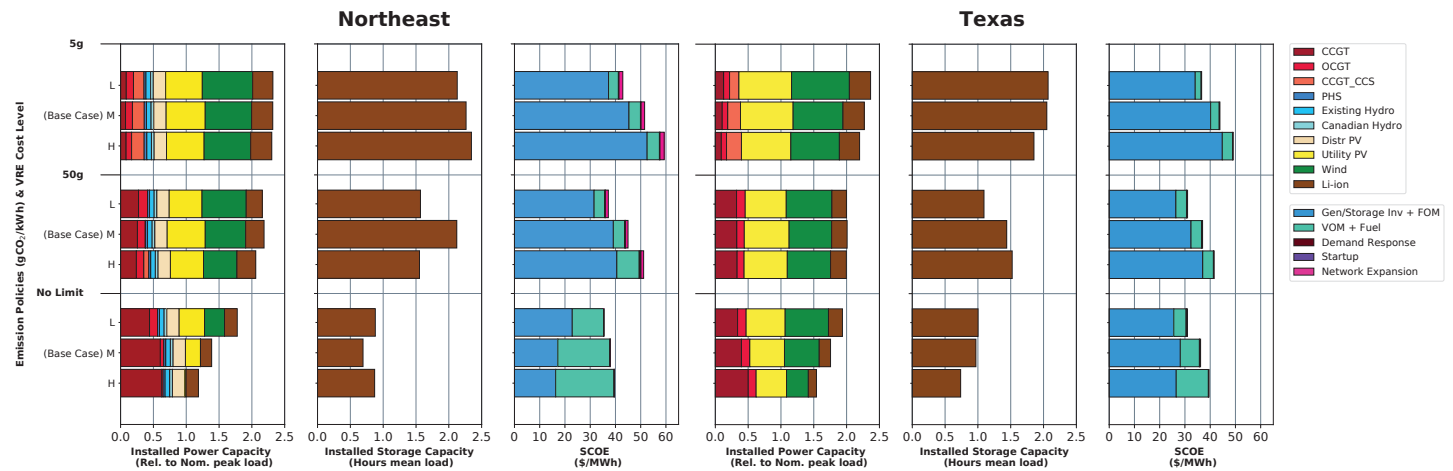
generation capacity, (2) storage vs. demand-side resources, (3) storage vs. dispatchable low-carbon generation, and (4) storage vs. transmission. The systems modeling framework we employ to study the substitutability of storage with other resources (and vice versa) implicitly accounts for the fact that the marginal value of all resources, including storage, declines with increasing penetration.

Impact of VRE cost on storage deployment

As discussed above, low-cost storage options can reduce the need to overbuild VRE capacity by more effectively balancing VRE intermittency and by, in effect, shifting generation to hours of high net demand. The degree to which storage substitutes for VRE capacity in our modeling depends on the cost and performance of storage technologies and on VRE resource availability and costs. Figure 6.14 explores the sensitivity of storage deployment across a range of VRE capital cost scenarios. We find, first, that storage deployment is relatively robust to VRE costs, as the deployment of VRE resources is driven more by the carbon emissions constraint than by cost considerations. Second, we find that the impact of VRE costs is most pronounced in the No-Limit policy scenario. This is particularly true in regions with lower-quality VRE resources, such as the Northeast, relative to regions with higher-quality VRE resources, such as Texas.

When only Li-ion batteries are available as a storage technology and we apply a 5 gCO₂/kWh carbon constraint, low-cost VRE (where “low-cost” is defined as a 23% cost reduction for utility-scale solar and a 33% cost reduction for onshore wind compared to our mid-cost assumptions) increases optimal VRE capacity by 2%–10% across the three regions (favoring wind over solar). This increased VRE deployment leads to 0%, 6%, and 16% lower delivered energy storage capacity compared to the mid-cost VRE scenario in Texas, the Northeast,

Figure 6.14 Impacts of low-, mid-, and high-cost VRE on installed power capacity, storage capacity, and SCOE across a range of CO₂ constraints for the Northeast and Texas regions



They are, in ascending order: (1) high-cost VRE (H), (2) mid-cost VRE (M), and (3) low-cost VRE (L). Low-, mid-, and high-cost assumptions for VRE are defined in Appendix C.1.

and the Southeast, respectively (5 gCO₂/kWh policy case in Figure 6.14 and Figure C.10). The regional differences in the impact of low-cost VRE on storage capacity can be explained by differences in the availability of dispatchable generation (e.g., nuclear) and the quality of VRE output.³¹ As expected, over-building resulting from low-cost VRE increases VRE curtailment—for example, from 17% to 22% in Texas in the 5 gCO₂/kWh case. Most noticeably, VRE costs have significant impacts on system cost. At the 5 gCO₂/kWh emissions limit, assuming optimal deployment, SCOE is 14%–17% lower across the modeled regions in the low-cost VRE scenario compared to the mid-cost VRE scenario. Conversely, for the same emission policy constraint, SCOE is 12%–15% higher with optimal deployment in the high-cost VRE scenario (where “high-cost” is defined as a 29% cost increase for solar and a 16% increase for wind compared to mid-cost assumptions).

Across all scenarios we considered, system outcomes are most sensitive to VRE technology costs in the No Limit policy case, since this is where VRE deployment is most sensitive to capital costs (as opposed to binding carbon constraints). The substitution effect between VRE resources and natural gas is most pronounced in regions with lower-quality VRE resources (the Northeast) compared to regions with higher-quality VRE (Texas). For example, in the No Limit case, low VRE costs increase VRE capacity by 111% in the Northeast, compared to 19% in Texas. As with optimal storage deployment at higher levels of decarbonization, low costs for VRE have a greater impact in terms of natural gas capacity reductions in Texas (6%) than they do in the Northeast (1%). These results are robust to the addition of storage technologies with lower energy capital costs.

³¹ Low-cost VRE favors “overbuilding” VRE over deploying storage capacity. However, low-cost VRE also improves the competitiveness of VRE + storage to displace dispatchable low-carbon generation (CCGT with CCS). Collectively, these two factors explain why storage capacity remains unchanged for Texas when modifying VRE costs from mid to low for the 5 gCO₂/kWh emissions case. With low-cost VRE, gas capacity declines by 6% compared to the mid-cost VRE scenario (Figure 6.14).

Table 6.11 Demand flexibility assumptions for Texas under 2050 load conditions

| Demand subsector | Hours delay | Hours advance | Share of end use that is flexible | Maximum hourly demand flexibility [GW] |
|---------------------------|-------------|---------------|-----------------------------------|--|
| Commercial HVAC | 1 | 1 | 25% | 8.6 |
| Residential HVAC | 1 | 1 | 35% | 7 |
| Commercial water heating | 2 | 2 | 25% | 0.2 |
| Residential water heating | 2 | 2 | 25% | 1 |
| Light duty vehicles | 5 | 0 | 90% | 33 |
| Medium duty trucks | 5 | 0 | 90% | 3 |
| Heavy-duty trucks | 3 | 0 | 90% | 5 |

HVAC = heating, ventilation, and air conditioning. Data sourced from NREL Electrification Futures Study (Mai, Jadun, et al. 2018).

Impact of intra-day demand flexibility

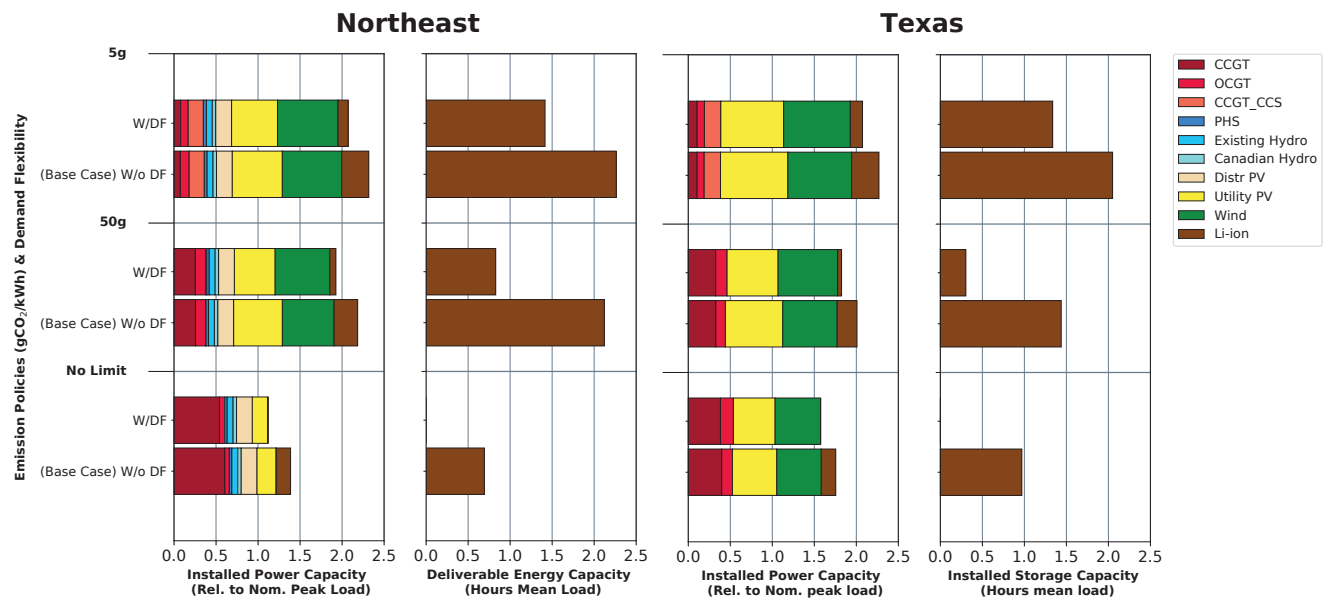
The potential value of flexibility in electricity consumption for various end uses increases with greater deployment of smart meters and related technologies and expanded electrification in sectors such as transportation. Here, we explore how enabling intra-day demand flexibility affects the cost-optimal grid configuration and, in particular, how it changes the role for energy storage under various CO₂ constraints and different assumptions regarding storage technology. For these experiments, we consider a very optimistic version of demand flexibility: the ability to shift electricity consumption from specific demand subsectors, highlighted in Table 6.11, over constrained (feasible) time windows at zero cost and with zero energy efficiency losses.

Our assumptions about demand flexibility are based on the NREL EFS enhanced flexibility scenario, which provides potential hours of delay and advance for specific demand subsectors, along with the share of the load that can be shifted (Mai, Jadun, et al. 2018). Since the load from each subsector changes over time, potential demand flexibility also varies from hour to hour. For this reason, Table 6.11 notes

the maximum load that could be shifted for each subsector at any point in time for the Texas region in 2050 under the high-electrification load scenario. (Data for the Northeast and the Southeast are shown in Table C.6 in Appendix C.1.) It is important to notice that these subsector peaks do not occur at the same time; the actual maximum potential demand flexibility in any single hour is 47 GW, which corresponds to 31% of total demand in that hour (Mai, Jadun, et al. 2018).

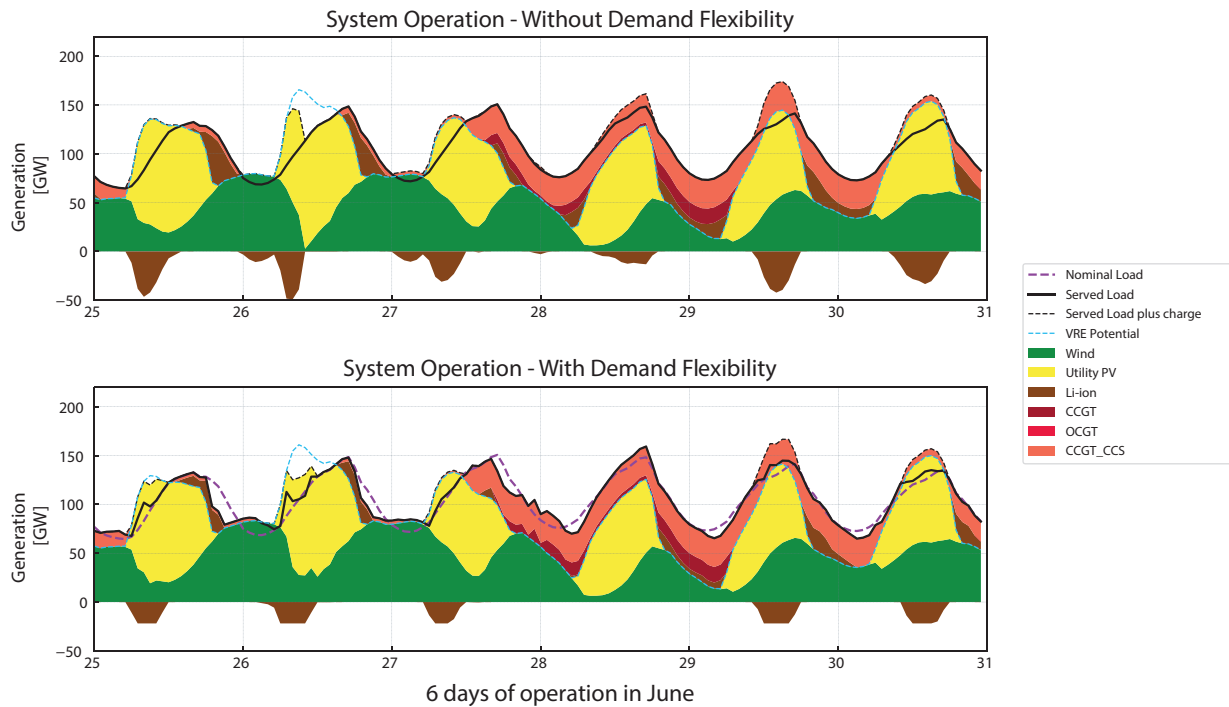
Since the assumed temporal flexibility of demand-side resources spans hours rather than days, we focus on how demand flexibility affects the cost-optimal substitution of short-duration (Li-ion battery) storage rather than how it affects LDES resources. Together Figure 6.15 and Figure C.11 in Appendix C.4 show the impact of short-term demand flexibility across the three regions under various carbon constraints. In all three modeled regions, the impact of demand flexibility on optimal deployment of Li-ion storage declines with more stringent emission policies. For example, in all regions, demand flexibility substitutes for almost 100% of short-duration storage in the No Limit case, while in the 5 gCO₂/kWh case, it substitutes for just 19% of Li-ion storage on an

Figure 6.15 Impacts of demand flexibility in terms of installed power capacity, storage capacity, and SCOE, across a range of CO₂ constraints for the Northeast and Texas regions



Demand flexibility (DF) assumptions are summarized in Table 6.11.

Figure 6.16 Impact of demand flexibility on system operations in Texas



The figure shows six days of stacked dispatch in winter under a CO₂ emissions constraint of 5 gCO₂/kWh. The upper plot shows the operation of the system without demand flexibility; the lower plot shows how the system operates with assumed levels of demand flexibility. Demand flexibility assumptions are summarized in Table 6.11.

energy basis in the Southeast, 35% in Texas, and 37% in the Northeast. Differences in the impacts of demand flexibility across the three regions are partly explained by underlying differences in the temporal profiles of demand and zero-carbon resource availability (including the hydro available in the Northeast and Southeast, and nuclear in the Southeast).

Figure 6.16 illustrates how the system operates with and without demand flexibility under a carbon constraint of 5 gCO₂/kWh for the Texas region. The figure shows that charge and discharge cycles for Li-ion storage are less frequent when demand flexibility is implemented. For this case, the daily component of the frequency analysis, introduced in Table 6.10, decreases by 20%. The bottom panel in Figure 6.16 shows how the availability of short-duration demand flexibility shifts load toward hours with more VRE generation.

Lower requirements for short-term storage with flexible demand translate into reductions in SCOE, with cost reductions in line with how much Li-ion storage is displaced. In all three regions, cost reductions are modest, ranging from 5%–6% in the No Limit case to 3% in the 5 gCO₂/kWh case (shown for the Southeast case in Figure C.11).

Hydrogen use in industry

Whereas prior sections concerned with LDES technologies have focused exclusively on power system drivers that affect the value of these technologies, the value of long-duration storage options that involve hydrogen could also be affected by the co-existence of non-power-sector uses for hydrogen. This creates the opportunity to share hydrogen production technology and associated costs across sectors. Here, we explore the impact of hydrogen demand outside the power sector on the cost-effectiveness of hydrogen storage that could be deployed by the power sector, using

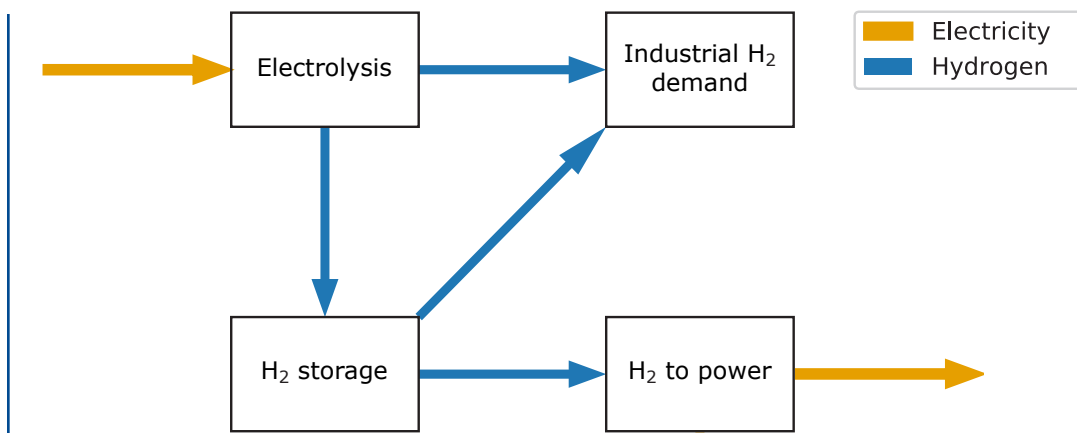
industrial decarbonization as an example.

Figure 6.17 highlights the potential opportunity to share hydrogen technology components to serve both the power sector and external hydrogen demand simultaneously. This is a special case of demand flexibility, whereby the use of electricity to produce hydrogen via water-splitting (or electrolysis) can be flexibly scheduled because hydrogen can be stored at relatively low energy capital cost (see Table 6.3) even though external hydrogen demand is modeled to be constant and inflexible across all hours of the year.

We evaluate the impact of varying levels of hydrogen demand on power system outcomes under different CO₂ intensity constraints, with a focus on Texas because it is one of the largest energy consuming states in the country and one in which more than half of overall energy consumption comes from industrial activity (Energy Information Administration 2021b). Our industrial hydrogen demand scenarios are developed by assuming that this sector adopts hydrogen to substitute for natural gas used in process heating. We consider a range of scenarios based on different levels of hydrogen substitution for natural gas as a heat source in industrial applications: 0%, 25%, 50%, 75%, and 100%. Here 100% substitution corresponds to 19.7 GWt (thermal) of hydrogen demand and the 0% case corresponds to no hydrogen demand. For comparison purposes, a constant 19.7 GWt load is equivalent to average power demand of 25.6 GWe assuming mid-range charging (electrolyzer) efficiency as per Table 6.3. (Note that 25.6 GWe is equal to approximately 17% of projected 2050 peak demand in Texas.) Details of our approach to modeling hydrogen demand are provided in Appendix C.

Different levels of hydrogen demand were simulated under a range of power sector CO₂ intensity constraints, including 1, 5, 10, and 50 gCO₂/kWh and a No Limit case.³² Our initial

Figure 6.17 Representation of how industrial hydrogen demand is modeled within GenX



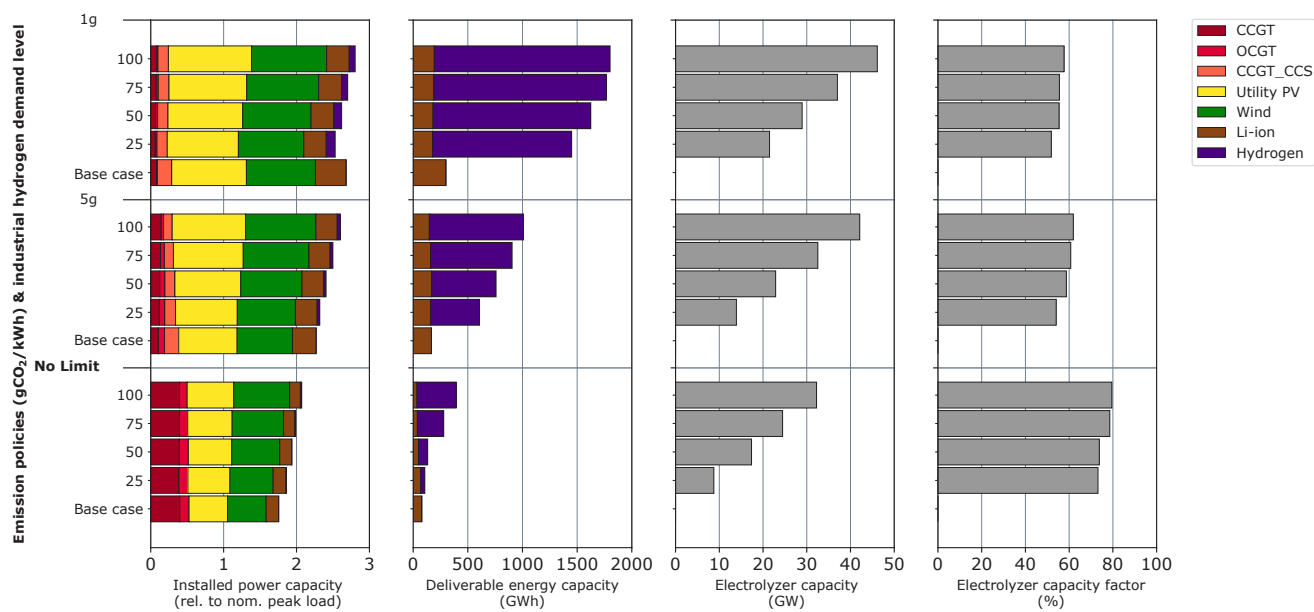
We assume that a portion (0%–100%) of industrial hydrogen demand is met by electricity; this hydrogen can be produced either directly through electricity from the grid (electrolysis to H₂ demand) or through electricity from storage (electrolysis to storage to H₂ demand). Storage in this framework can provide hydrogen either for industry (storage to H₂ demand) or to serve electric load (storage to H₂ to power).

results assume aboveground storage of hydrogen in tanks, with mid-level costs from Table 6.3. From the installed capacity perspective, our findings show that for a given CO₂ constraint, increased industrial hydrogen demand with incremental hydrogen production using flexible electrolysis favors the deployment of VRE generation and displaces gas generation (both with and without CCS) and Li-ion power capacity (Figure 6.18). For example, in the 5 gCO₂/kWh scenario, Li-ion and gas power capacities with 100% industrial hydrogen demand are 10% and 23% lower, respectively, than in the case without any industrial hydrogen demand (the 0% case).

Including industrial hydrogen demand reduces the percentage increase in power capacity optimally built to achieve increasingly stringent CO₂ constraints. Whereas installed power capacity increases 53% from the No Limit case to the 1 gCO₂/kWh case without hydrogen demand, the increase falls to 35% for the case of 100% hydrogen substitution. A second, related effect of increased hydrogen demand is a reduction in VRE curtailment. Across the range of carbon constraints we considered, VRE curtailment is 30% lower on average with 100% hydrogen substitution than with zero industrial hydrogen demand. (It is 46% lower in the 1 gCO₂/kWh case.)

³² It should be noted that scenarios with industrial hydrogen demand are associated with greater annual electricity consumption than scenarios without hydrogen demand. For example, including constant external hydrogen demand at the level of 25.6 GWe translates into incremental electricity consumption of 224.25 TWh or a 31% increase in total annual electricity consumption. Consequently, for the same CO₂ intensity constraint on dispatched generation, power sector CO₂ emissions in the case with industrial hydrogen demand will be greater than in the case without hydrogen demand. However, overall energy sector CO₂ emissions will be lower due to the substitution for natural gas by electrolytic hydrogen in the industrial sector.

Figure 6.18 Impacts of serving 0%–100% of baseline industrial hydrogen demand (19.7 GW_t) with electricity in terms of installed power capacity, storage capacity, electrolyzer capacity, and electrolyzer capacity factor, across a range of annual CO₂ emission constraints for the Texas region

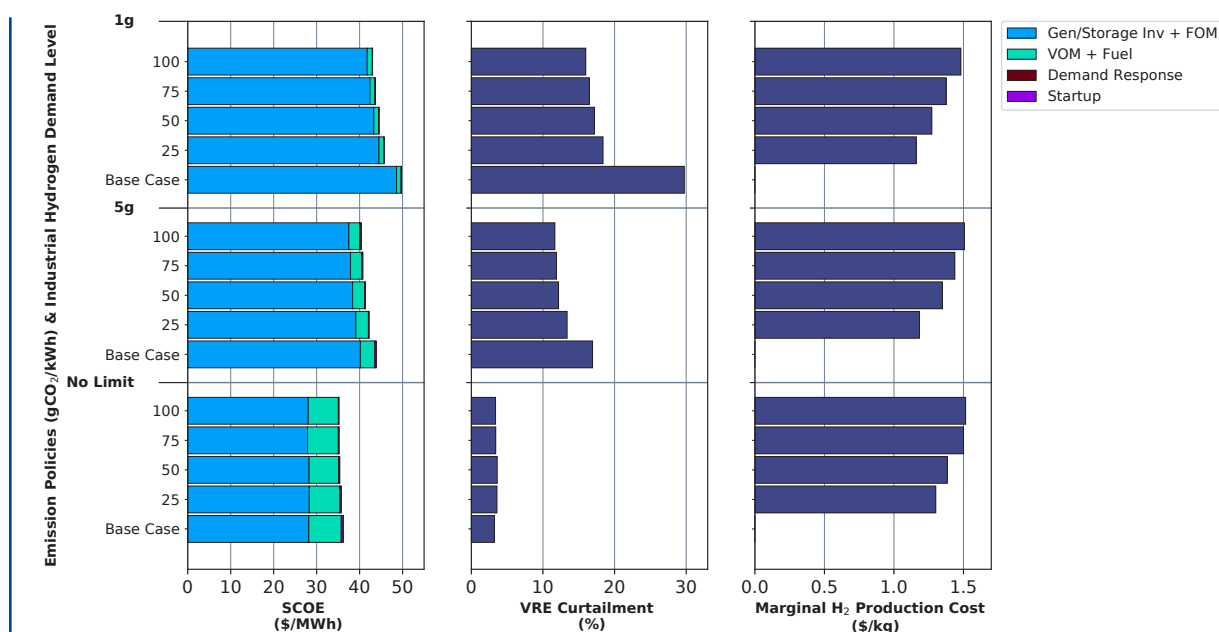


Hydrogen technology assumptions reflect mid-range costs as reported in Table 6.3.

Higher industrial hydrogen demand enables improved utilization of both electrolyzer and VRE assets, which leads to a lower SCOE to achieve the same CO₂ intensity target (Figure 6.19). The magnitude of the maximum SCOE reduction depends on the stringency of the CO₂ constraint; in our modeling results it ranges from a 3% reduction (in the No Limit case) to a 14% reduction (in the 1 gCO₂/kWh case). Stated another way: As compared to the No Limit case, achieving a grid emissions intensity of 1 gCO₂/kWh increases SCOE by 37% without industrial hydrogen demand and by 22% with 100% hydrogen substitution (Figure 6.19). For context, the modeled increase in SCOE as a result of going from the No Limit case to the 1 gCO₂/kWh case with LDES but without industrial hydrogen demand is 31%.

The diminishing marginal benefits of increasing industrial hydrogen demand are reflected in increasing marginal hydrogen production costs, shown in Figure 6.19. This suggests that strategies that are purely based on electrolytic production of hydrogen to meet non-power hydrogen demand may be limited in the quantity of hydrogen that can be cost-effectively supplied. As our analysis does not account for other means of hydrogen production or for hydrogen imports, and because we model industrial hydrogen demand as constant and inflexible, increasing industrial hydrogen demand under a given CO₂ intensity constraint results in increased marginal hydrogen production cost. This effect is explained by the fact that extra electricity generating capacity (mostly VRE) and hydrogen storage are needed to satisfy increased industrial demand.

Figure 6.19 Cost and VRE curtailment impacts of alternative industrial hydrogen demand levels for Texas



Scenarios show the impacts of serving 0%–100% of baseline industrial hydrogen demand (19.7 GW_t) with electricity in terms of SCOE,³³ VRE curtailment, and marginal hydrogen production, across a range of CO₂ constraints for the Texas region. Hydrogen technology assumptions reflect mid-range costs as reported in Table 6.3.

To explore the broader potential of a system in which hydrogen is partly used to meet industrial demand for process heat as well as for storage in the electric power system, we consider the effects of the availability of underground geological storage as a potential technology that can be deployed by the model. The main difference between geological and tank storage of hydrogen is the investment needed per unit of stored energy (assumed to be 84% less for geologic storage compared to the mid-level cost projections for aboveground hydrogen storage; see “ultra-low” value reported in Table 6.3 and Chapter 5 for further discussion). Our findings (Figure 6.20) show that geological hydrogen storage has a positive effect across the different metrics we consider.

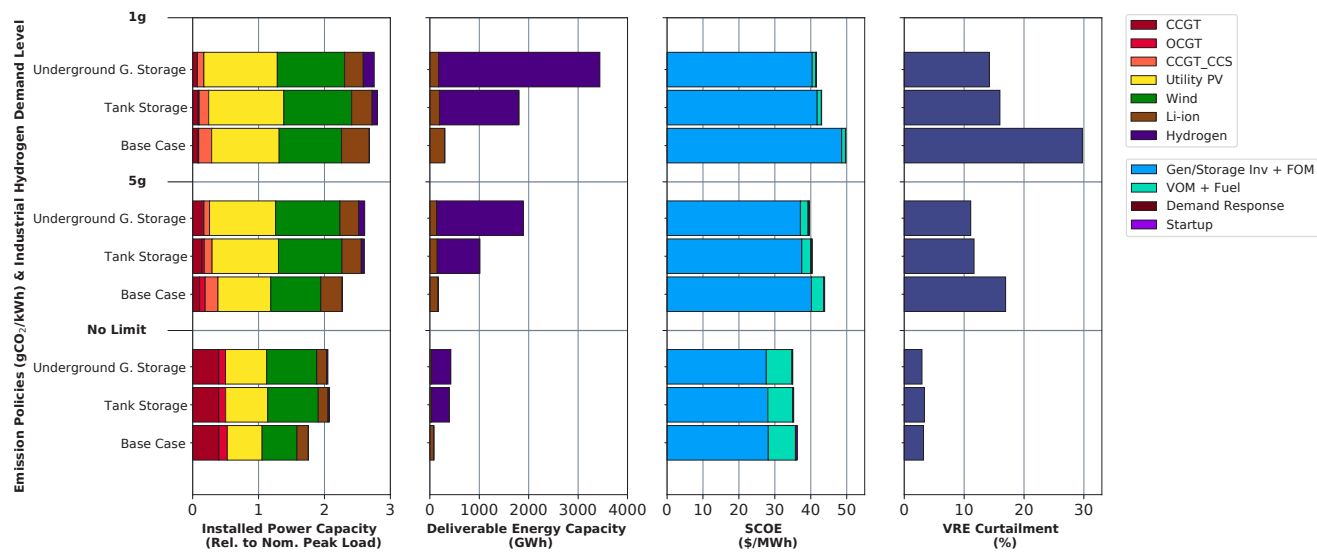
In the 1 gCO₂/kWh case with 100% hydrogen substitution, relative to tank storage the availability of underground geological storage results in a 91% increase in optimal storage capacity, a 3.5% reduction in SCOE, a 30% reduction in natural gas capacity, an 11% decrease in VRE curtailments, and an 11% reduction in VRE capacity.

Competition with low-carbon dispatchable resources

Storage makes it possible to shift VRE generation over time, thus increasing the value of VRE resources. This can place storage resources in direct competition with dispatchable low- or zero-carbon resources. We examine this

³³ In the context of producing hydrogen for industrial heat, the system cost of electricity (SCOE) is computed as the ratio of total system cost to total served demand, where the latter includes both the electric demand in the power system and the equivalent electrical energy used to produce hydrogen for industry.

Figure 6.20 System impacts of the availability of underground geological hydrogen storage



The base case assumes 0% industrial hydrogen demand; the other scenarios involve 100% hydrogen substitution (19.7 GW_t). The figure shows impacts on power capacity mix, storage capacity, SCOE, and VRE curtailment across a range of CO₂ emissions constraints. Hydrogen technology assumptions reflect mid-range (tank storage) and ultra-low (underground storage) costs as reported in Table 6.3.

competition by comparing storage penetration and utilization with the deployment of two dispatchable low-carbon resources: (1) an advanced natural gas power plant with close-to-100% CO₂ capture (also known as “Allam” or “Allam-Fetvedt” cycle) (Weiland and White 2019) and (2) new nuclear capacity. In our modeling, the advanced natural gas technology with CCS is made available in Texas, where CO₂ sequestration appears most viable (see cost assumptions in Table 6.5); substituting LDES with new nuclear capacity is an option in the Southeast region.

If the Allam cycle becomes commercially available,³⁴ our modeling predicts that it will dominate CCGT+CCS deployment in Texas. Compared to a scenario in which this technology is not available, the option to deploy the

Allam cycle increases total gas capacity by 13% and reduces VRE capacity by 7% in the 5 gCO₂/kWh case, for mid-cost hydrogen in Texas (Table 6.12). The Allam cycle can serve as a partial substitute for storage, as evidenced by a reduction in modeled deliverable storage capacity of 28% with LDES in the form of hydrogen storage, 20% with LDES in the form of metal-air battery storage, and 3% with LDES in the form of thermal storage.³⁵ Table 6.12 documents the (relatively small) incremental SCOE reductions obtained by adding the Allam cycle to a system with hydrogen storage under different cost assumptions. Table C.11 in Appendix C.4 presents the similar results obtained by adding the Allam cycle to a system with metal-air storage. Collectively, the availability of the Allam cycle along with LDES enables SCOE reductions of 5%–13% relative

³⁴ As per recent announcements, prototype near-zero-emission natural gas power plants are being developed and have reached various stages of technology readiness. For an example, see McMahon (2021).

³⁵ The results for metal-air systems can be found in Appendix C, Table C.11.

Table 6.12 System impacts of a dispatchable low-carbon generating technology in Texas

| | Low-cost hydrogen | | | Mid-cost hydrogen | | | High-cost hydrogen | | |
|--|---------------------------|------------------------|--------|---------------------------|------------------------|--------|---------------------------|------------------------|--------|
| | Without allam cycle | With allam cycle | % Diff | Without allam cycle | With allam cycle | % Diff | Without allam cycle | With allam cycle | % Diff |
| Firm dispatchable installed capacity (GW) | | | | | | | | | |
| CCGT | 17.6 | 19.4 | 10% | 17.0 | 19.3 | 14% | 17.0 | 19.3 | 14% |
| OCGT | 10.1 | 12.2 | 21% | 12.1 | 13.1 | 8% | 12.2 | 13.1 | 7% |
| CCGT CCS | 16.6 | 0.0 | -100% | 19.4 | 0.0 | -100% | 19.6 | 0.0 | -100% |
| Allam | 0.0 | 20.1 | — | 0.0 | 22.3 | — | 0.0 | 22.3 | — |
| Total | 44.2 | 51.7 | 17% | 48.5 | 54.7 | 13% | 48.8 | 54.7 | 12% |
| VRE installed capacity (GW) | | | | | | | | | |
| Wind | 102.6 | 94.7 | -8% | 99.4 | 93.8 | -6% | 99.2 | 93.8 | -5% |
| Utility PV | 142.7 | 137.2 | -4% | 146.7 | 135.9 | -7% | 147.0 | 135.9 | -8% |
| Total | 245.3 | 231.9 | -5% | 246.1 | 229.6 | -7% | 246.2 | 229.6 | -7% |
| Energy storage (Li-ion + RFB + LDES) | | | | | | | | | |
| Power (GW) | 55.3 | 48.8 | -12% | 55.4 | 46.0 | -17% | 55.3 | 46.0 | -17% |
| Energy (GWh) | 817 | 542 | -34% | 510 | 369 | -28% | 484 | 369 | -24% |
| System cost of electricity | | | | | | | | | |
| Average \$/MWh | 42.2 | 41.7 | -1% | 42.4 | 41.7 | -2% | 42.4 | 41.7 | -2% |

Scenarios show the impact of low-, mid-, and high-cost hydrogen with and without the Allam cycle in terms of installed power capacity, storage capacity, and SCOE, across 5 gCO₂/kWh emissions scenarios. Low-, mid-, and high-cost assumptions for hydrogen storage are given in Table 6.3. Cost assumptions for the Allam cycle are given in Appendix C.1.

to the base case across low-, mid-, and high-cost assumptions for all three LDES technologies under the 5 gCO₂/kWh emissions policy case.

We also tested the impact of allowing for new nuclear builds in the Southeast region. At an assumed completion cost of \$6,048/kW (National Renewable Energy Laboratory 2020), the model does not choose to deploy new nuclear capacity under the 5 gCO₂/kWh emission constraint. This result differs from findings in the 2018 MIT study, *The Future of Nuclear in a Carbon-Constrained World*, for two main reasons. First, following NREL, we assume higher costs for new nuclear generation (\$6,048/kW vs. \$5,500/kW in the *Future of Nuclear* study). Second, this study assumes

lower costs for solar (\$725/kW vs. \$917/kW) and wind (\$1,085/kW vs. \$1,550/kW) based on NREL's 2020 mid-cost projections for 2050. Together, these cost assumptions combine to make new nuclear builds less attractive. However, we also looked at the effect of applying low-cost assumptions for new nuclear capital costs from the 2018 MIT study.³⁶ At \$4,202/kW (the “low” cost for new nuclear from the 2018 study) and \$2,818/kW (the “ultra-low” cost from the 2018 study), the model deploys 21 GW and 78 GW, respectively, of new nuclear in the Southeast under the 5 gCO₂/kWh policy constraint. This new nuclear displaces mainly VRE capacity (15% and 49% in the low- and ultra-low nuclear cost scenarios, respectively) as well as some gas peaking capacity.

³⁶ Cost numbers are from Buongiorno et al. (2018), plus a 2.49% inflation rate to bring them to 2018 dollars.

Role of regional and inter-regional transmission

The modeling results presented thus far assume the co-optimization of generation and transmission investments and operations. For transmission planning, this means that regional transmission systems have been sized to deliver the highest-value service at lowest total cost. In the Northeast and Southeast regions this means investments have been made to meet intra-regional demand by relieving transfer congestion (for example, in capacity-constrained areas such as New York City), enabling the integration of lower-cost VRE resources in other zones in the region, increasing system flexibility, and reducing overall balancing costs. However, current planning processes do not consider the full, stacked benefits of transmission upgrades, instead relying only on traditional metrics to assure reliability and meet local needs (Pfeifenberger 2021). Permitting and siting challenges create further barriers to transmission expansion. In this sensitivity analysis, we assume no transmission expansion—meaning that regional transmission systems are limited to existing capacities—and assess the impact on VRE and storage deployment.³⁷

In the model, increased regional transmission capacity provides two main benefits: (1) It allows for increased VRE deployment in regions with higher-quality VRE resources (lower cost of energy), which in turn reduces overall system costs; and (2) it improves VRE integration, by balancing resource intermittency across connected regions and smoothing the effects of geographical differences. Thus, limiting the optimal deployment of transmission capacity to the levels that currently exist in these regions focuses VRE deployment into the same zone as the demand being served, rather than allowing deployment at sites with the highest-quality

resources. For example, Table 6.13 shows that for the Northeast, in the 5 gCO₂/kWh case with intra-regional transmission expansion allowed, the model optimizes by adding 55 GW of new transfer capacity within the region to connect better-quality VRE resources from other zones. Restricting intra-region transmission expansion, on the other hand, increases average SCOE by \$3/MWh (or 5%) in the 5 gCO₂/kWh case, because it forces greater reliance on lower-quality VRE capacity that is located closer to demand (e.g., distributed and utility PV over wind). Limited regional supply–demand balancing increases the role for energy storage, particularly under very tight carbon constraints. For example, a scenario with no transmission expansion increases energy storage requirements in the Northeast by 36%, in the 5 gCO₂/kWh policy case. By contrast, enabling transmission expansion in the Southeast has little impact on VRE integration, because VRE resource quality is similar across all four modeled zones in that region. In the Southeast, restricting transmission expansion has the effect of increasing reliance on gas generation with CCS, which can be located closer to demand, in place of VRE and storage capacity (Table C.12 in Appendix C.4).

Brown and Botterud (2021) extend this analysis to the entire continental United States. While our analysis applies different cost assumptions and modeling approaches, the trends in the Brown and Botterud (2021) results are important to note because of the continental scope of their analysis and its implications for the impacts of expanding inter-regional transmission on zero-carbon power systems using today’s VRE and storage technologies. Incrementally increasing the level of regional coordination (even without adding new transmission capacity) yields system cost savings and reduces the need for generation

³⁷ For more expansive studies of the benefits of inter-regional transmission, see Brown and Botterud (2021) and Brinkman et al. (2020).

Table 6.13 System impacts of enabling intra-regional transmission expansion in the U.S. Northeast

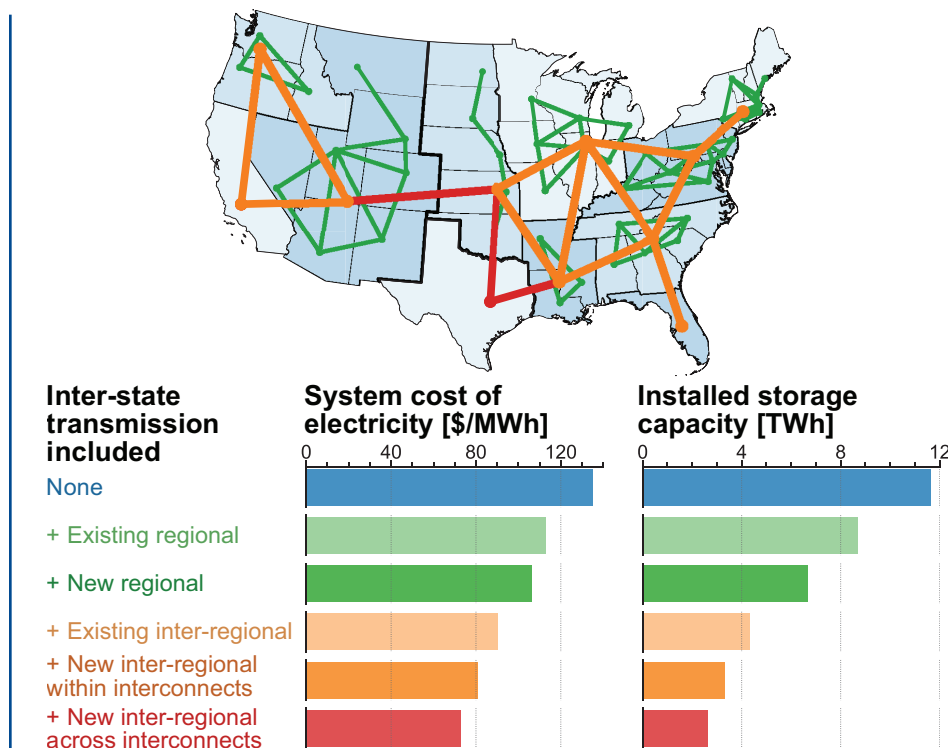
| | 0 gCO ₂ /kWh | | | 5 gCO ₂ /kWh | | | No Limit policy | | |
|--|-------------------------|-------------------|--------|-------------------------|-------------------|--------|-----------------|-------------------|--------|
| | With trans exp | Without trans exp | % Diff | With trans exp | Without trans exp | % Diff | With trans exp | Without trans exp | % Diff |
| Firm dispatchable installed capacity (GW) | | | | | | | | | |
| CCGT | 0.0 | 0.0 | — | 7.1 | 9.2 | 29% | 57.0 | 57.0 | 0% |
| OCGT | 0.0 | 0.0 | — | 9.9 | 5.1 | -49% | 5.0 | 5.0 | 0% |
| CCGT CCS | 0.0 | 0.0 | — | 17.0 | 18.9 | 12% | 0.0 | 0.0 | — |
| Total | 0.0 | 0.0 | — | 34.0 | 33.2 | -2% | 62.0 | 62.0 | 0% |
| VRE installed capacity (GW) | | | | | | | | | |
| Wind | 117.7 | 93.2 | -21% | 66.5 | 59.2 | -11% | 0.1 | 0.1 | 0% |
| Utility PV | 90.1 | 113.3 | 26% | 56.0 | 62.0 | 11% | 21.5 | 21.5 | 0% |
| Distr PV | 28.1 | 63.0 | 124% | 17.7 | 24.9 | 41% | 17.7 | 17.7 | 0% |
| Total | 235.9 | 269.4 | 14% | 140.3 | 146.1 | 4% | 39.3 | 39.3 | 0% |
| Energy storage (Li-ion only) | | | | | | | | | |
| Power (GW) | 50.2 | 69.3 | 38% | 30.3 | 33.7 | 11% | 16.0 | 16.0 | 0% |
| Energy (GWh) | 797 | 1,258 | 58% | 116 | 158 | 36% | 36 | 36 | 0% |
| Transmission expansion | | | | | | | | | |
| Total (GW) | 98.4 | — | — | 55.4 | — | — | 0.0 | — | — |
| System cost of electricity | | | | | | | | | |
| Average \$/MWh | 86.0 | 105.9 | 23% | 51.5 | 54.1 | 5% | 37.9 | 37.9 | 0% |

Scenarios show the impacts of allowing transfer capacities to expand vs. restricting transfer capacities to existing levels, on installed power capacity, storage capacity, and SCOE, across a range of CO₂ constraints. Cost assumptions for transmission expansion are defined in Appendix C.1.

and storage capacities: SCOE decreases by \$22/MWh between Brown and Botterud's "isolated states" and "existing regional" transmission scenarios, and by \$16/MWh between their "new regional" and "existing inter-regional" transmission scenarios (Figure 6.21). Brown and Botterud's "new regional" transmission scenario corresponds to the assumptions made in the regional studies discussed above in the base case. Allowing new, inter-regional AC transmission within the three U.S. interconnects (Eastern, Western, and Texas) reduces SCOE by \$10/MWh compared to the "existing inter-regional" transmission scenario; allowing new DC transmission between interconnects reduces SCOE by a further \$8/MWh (Figure 6.21).

Since expanded transmission capacity partly substitutes for storage deployment, it follows that increased transmission and greater regional coordination (transmission expansion effectively increases the geographic extent of economic dispatch areas) leads to a decline in optimal storage deployment. The most connected scenario ("new inter-regional transmission across interconnects") deploys 40% of the energy storage used in the "new regional" transmission scenario and 23% of the energy storage used in the "isolated states" scenario (Figure 6.21).

Figure 6.21 System impacts of incrementally expanding regional coordination and transmission capacity in a U.S.-wide context



Scenarios show the impacts on SCOE and optimal storage deployment if the country is modeled as isolated states (blue bars), isolated zones without and with new regional transmission (green bars), and a fully interconnected system with different levels of inter-regional transmission (orange and red bars) (Brown and Botterud 2021). The transmission assumptions in the regional case study discussed above are most similar to the “new regional” transmission scenario shown here.

FINDING

In performing energy market arbitrage—that is, buying when prices (and net demand) are low and selling when prices (and net demand) are high—energy storage can substitute for other grid resources, both on the demand side and on the supply side.

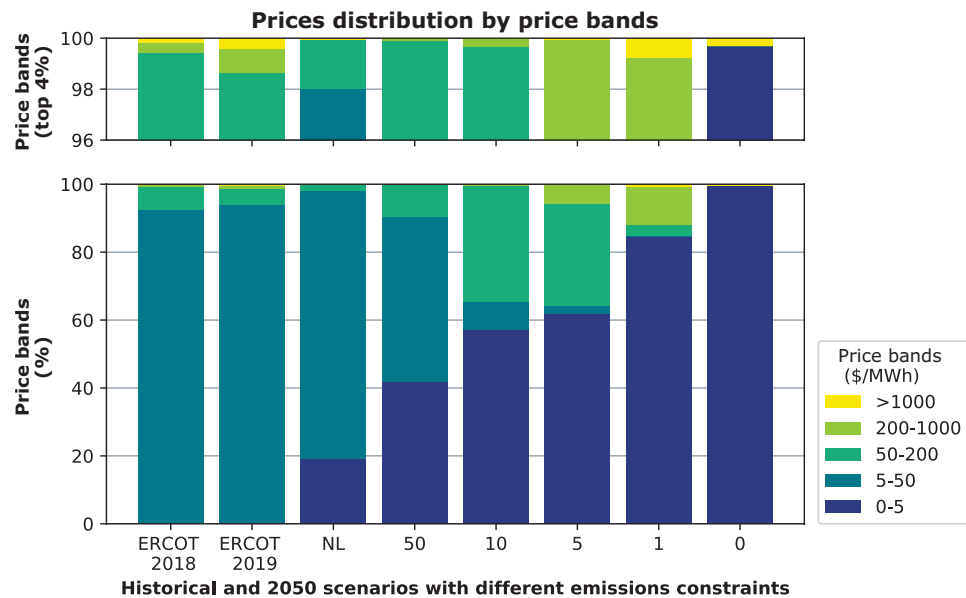
6.3.4 Future marginal values of electrical energy

Wholesale energy price variability

The modeled system’s time-dependent marginal value of energy³⁸ serves as a proxy for the spot price or locational marginal price in wholesale U.S. power markets organized by regional

³⁸ The modeled marginal value of energy in each time period is computed as the dual variable of the hourly supply–demand balance constraint in the capacity expansion model and represents the increase in (minimized) objective function value to serve the next unit of demand. Because the model includes the option of adding new generation, storage, or transmission capacity, the computed marginal value of energy represents the long-run marginal value of electricity rather than the short-run value in which capacity decisions are fixed. Finally, the marginal value of energy computed here does not reflect the impact of short- and long-term capacity requirements that are often included in organized markets to ensure resource adequacy (Levin and Botterud 2015).

Figure 6.22 Marginal value of energy under base case assumptions (Li-ion battery storage only) for Texas



The price bands are based on the known marginal cost of various generation technologies; we zoom in on the top 4% to show the price distributions at that extreme. Results for the Northeast and Southeast are presented in Appendix C.4. ERCOT historical prices are from ERCOT (2021).

transmission organizations (RTOs) or independent system operators (ISOs). We study the impact of CO₂ constraints and energy storage capacity on the frequency distribution of the marginal value of energy by examining the distribution of the marginal value using the bands shown in Figure 6.22. These bands include the following marginal values:

(1) \$0–\$5/MWh, characterized mostly by periods of high VRE generation; (2) \$5–\$50/MWh when natural gas capacity is the marginal generator;³⁹ (3) \$50–\$200/MWh when natural gas capacity needs to be started up and associated start-up costs must be recovered; and (4) >\$200/MWh, which corresponds to scarcity events, including times when storage facilities operate (either charging to dispatch in higher-price periods or

discharging based on having charged in lower-price periods) and load-shedding events, if any. Because the marginal cost of generation from storage is based on opportunity cost rather than being physically defined, it varies from period to period—consequently, storage charging and discharging can occur in all of the price bands.

Consistent with prior research (Levin and Botterud 2015), we find that increasing VRE penetration leads to many hours of very low prices interspersed with a few periods when prices are very high (approaching the value of lost load, which is assumed to be \$50,000/MWh in our modeling) owing to scarcity events (e.g., high load and low VRE output).

³⁹ When carbon emissions from natural gas generation are penalized, the penalty (the shadow price of carbon emissions) is reflected in the marginal prices when natural gas generators are on the margin. Under stringent CO₂ emissions constraints, natural gas marginal costs, therefore, could be much higher than \$50/MWh and might be responsible for high prices (i.e., \$200/MWh or greater).

Counter-intuitively, the volatility in the price distribution, as measured by the coefficient of variation (CoV), declines with increasing stringency of CO₂ emissions constraints (Table 6.14), since the limited number of high-priced hours increase the unweighted average value. Thus, the level, range, and variation in wholesale spot prices is likely to be drastically different from that seen in RTO/ISO-managed wholesale markets today, as illustrated for Texas in Figure 6.22.⁴⁰

Our findings show a consistent increase in the number of hours at less than \$5/MWh and a consistent decrease in the price band of \$5–\$50/MWh as the CO₂ constraint tightens. These trends reflect an increase in the share of VRE generation and a decline in natural gas generation. Figure 6.22 shows that the \$0–\$5/MWh price band includes up to 62% of hours in the 5 gCO₂/kWh case. As discussed earlier, the 0 gCO₂/kWh case modeled here reflects a strict definition of a net-zero carbon power system—one that relies solely on VRE and storage resources and leads to large increases in both ends of the distribution for the marginal value of generation. Thus, although decarbonization increases the number of hours with near-zero prices, it also increases the number of hours with high prices. This leads to a consistent increase in the mean price as the carbon constraint is tightened.

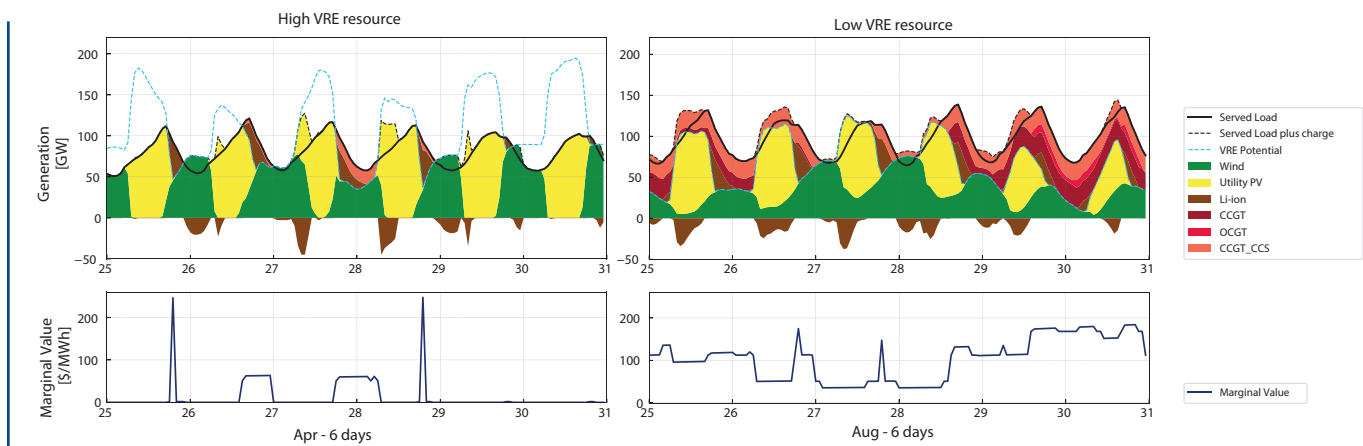
Our model findings are based on what is effectively a representation of a pure, energy-only electricity market structure, in which all wholesale (and, implicitly, all retail) transactions occur at the spot market price of electricity. While not directly comparable, we pull the most recent available (2019) spot prices from

ERCOT and summarize their distribution below. It is clear from Figure 6.22 that the wholesale energy price distribution would change rather dramatically as the Texas system decarbonizes. Our model results imply many more very low-price hours and many more high-price hours compared to ERCOT in 2019. We note, however, that we are not trying to model ERCOT in any detail. ERCOT employs market intervention and capacity remuneration mechanisms that may affect price signals. Moreover, the ERCOT energy-only wholesale market model has not been adopted by other RTOs/ISOs in the United States or by grid operators in the European Union. Most U.S. systems also have capacity markets and relatively low price caps on energy markets, which will shift some spot price variation (and revenue variation, as we discuss presently) to capacity prices. Since any system must satisfy break-even constraints, however, total revenues and revenues earned by each technology should, in theory, be unaffected, though the addition of capacity markets may affect the break-even capacity mix.

To illustrate how the marginal value of energy relates to system operation and VRE resource availability, we compare two timeframes in Figure 6.23. The time interval on the left side has high VRE resource availability, which leads to frequent periods of VRE curtailment (shown as the area between VRE potential and served load)—consequently marginal values of energy are near \$0/MWh. Prices of about \$60/MWh are realized when natural gas generation with CCS needs to operate for specific intervals, and peaks of around \$250/MWh are also observed when storage is discharging to meet load. In contrast, the right side of the figure shows a

⁴⁰ The precise implementation of short- and long-term resource adequacy requirements will impact the volatility of wholesale electricity prices in each region, but the trend of increasing hours of near-zero marginal value of electricity interspersed with high prices, is a robust conclusion supported by other modeling in the literature as well. See for example, Levin and Botterud (2015), Levin, Kwon and Botterud (2019), and Ela et al. (2014).

Figure 6.23 System operation and marginal value of energy under base case assumptions (Li-ion battery storage only) for Texas at 10 gCO₂/kWh



The figure shows two periods of time with high (left side) and low (right side) VRE resource availability.

period of low VRE availability, in which gas generation is often needed to meet load requirements that exceed VRE output. When CCGT with CCS is on the margin, price levels are about \$60/MWh. If CCGT without CCS is also needed, prices climb to \$100–\$130/MWh and when OCGT without CCS operates (days 29–30) prices are in the range of \$150–\$180/MWh.

Figure 6.24 shows that the cost-optimal deployment of LDES (redox flow batteries plus metal-air batteries, thermal storage, or hydrogen) primarily serves to reduce the frequency of periods when the marginal value of energy is high, i.e., above \$200/MWh, and increases instances of marginal value near or below \$50/MWh. The latter effect is consistent with the reduced VRE curtailment seen with LDES deployment (Figure 6.10). Table 6.14 shows that LDES tends to reduce the unweighted average value of energy while also reducing the volatility of the marginal value of energy, as measured by the CoV, relative to the base case (TM0 in Table 6.14). Across the different CO₂ constraints modeled, volatility decreases by 33% on average compared to the base case

when LDES resources are present in the system. While the dispatch of LDES can help to smooth out some fluctuations in the marginal value of energy, the presence of LDES alone does not alter the broader trend of increasing hours with near-zero marginal value of energy and increasing peak prices under tightening CO₂ constraints.

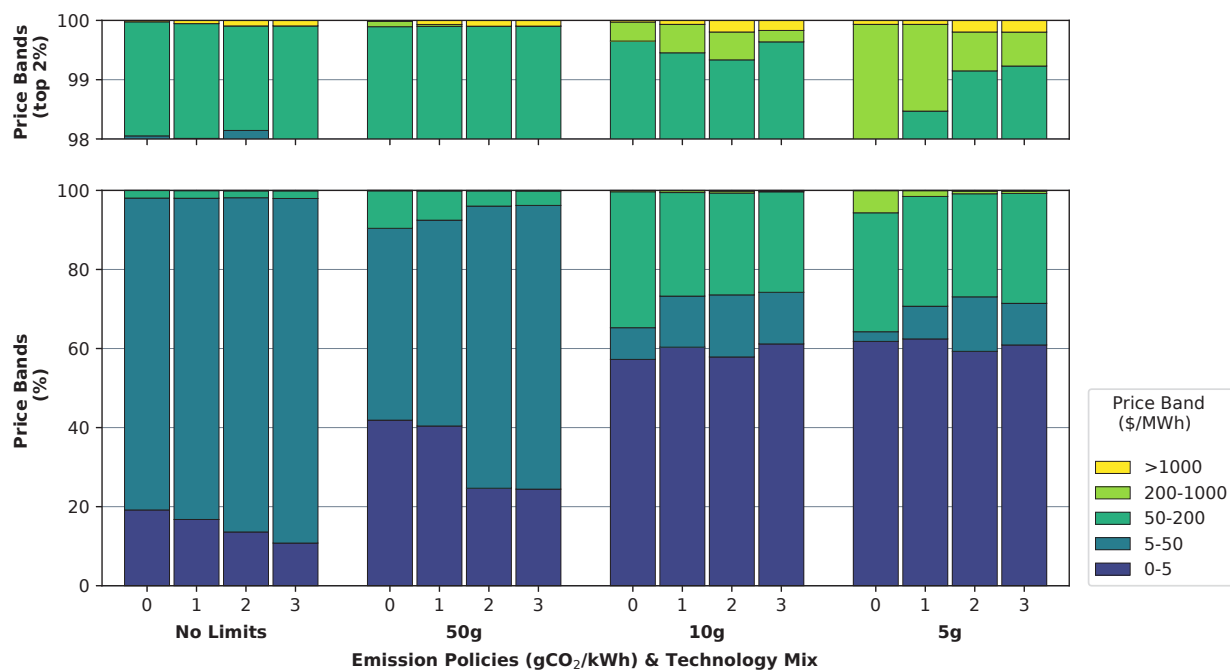
FINDING

The level, range, and variation in the marginal value of energy in future low-carbon electricity systems will be drastically different than values seen in ISO/RTO-managed wholesale markets today.

Revenue analysis

In the CEM modeling used here, which involves least-cost linear optimization with perfect foresight and constant returns to scale, all resources just break even, meaning that total revenues over the modeled period equal total investment and operational costs (Junge, Mallapragada and Schmalensee 2022).

Figure 6.24 Marginal value of energy across different storage mixes in Texas



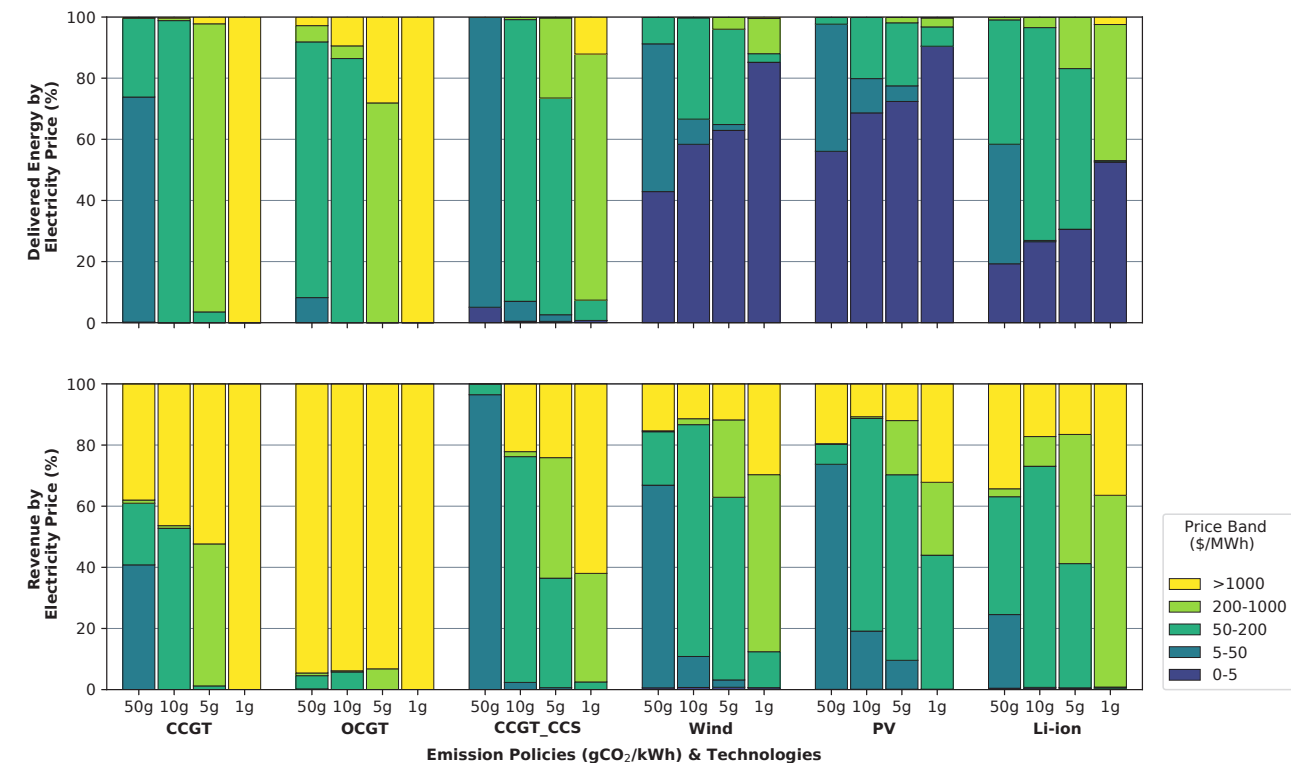
Scenarios shown are, from left to right: (0) base case (i.e., Li-ion battery storage only), (1) Li-ion + RFB + H₂, (2) Li-ion + RFB + metal-air, and (3) Li-ion + RFB + thermal. The price bands reflect the costs of the marginal technology; we zoom in on the top 2% to show the price distributions at that extreme.

Table 6.14 Comparison of the average marginal value of energy (simple average of prices over time) and volatility, as measured by the coefficient of variation (standard deviation divided by mean) for modeled 2050 prices in Texas

| Emission policy (gCO ₂ /kWh) | Unweighted average value of energy | | | | Price volatility (CoV) | | | |
|--|------------------------------------|------|------|------|------------------------|------|------|------|
| | Base case | TM1 | TM2 | TM3 | Base case | TM1 | TM2 | TM3 |
| 5 | 42.1 | 39.6 | 38.0 | 37.3 | 9.8 | 7.4 | 6.9 | 7.7 |
| 10 | 40.5 | 38.8 | 37.5 | 36.8 | 10.9 | 7.5 | 7.0 | 7.9 |
| 50 | 34.1 | 34.9 | 33.4 | 33.0 | 17.6 | 8.8 | 10.2 | 11.6 |
| NL | 31.0 | 31.4 | 31.4 | 31.3 | 18.3 | 12.5 | 12.3 | 12.7 |

For comparison, actual figures for ERCOT in 2019 were \$37.6/MWh for the average value of energy and 4.4 for price volatility (CoV). The technology mixes in the table correspond to (TM 0) base case (i.e., Li-ion battery storage only), (TM 1) Li-ion + RFB + H₂, (TM 2) Li-ion + RFB + Metal-air, and (TM 3) Li-ion + RFB + Thermal.

Figure 6.25 Technology operation by price band in Texas – base case



The upper panel shows the distribution of delivered energy by price band for different technologies and emission constraints. The lower panel shows the revenue distribution by price band.

Analyzing system operation and revenue distribution by price bands, we find that different technologies operate at different price bands and earn revenue in different ways, based on the likelihood that a given technology is the marginal resource (Figure 6.25). With more stringent CO₂ constraints, VRE technologies operate more at lower prices and begin to rely on fewer hours of higher prices to earn the revenue required to break even. For example, for wind generation in the 10 and 5 g CO₂/kWh cases, 90% and 96% of revenues come from the 33% and 35% of energy delivered by wind during periods when prices are high (above \$50/MWh), respectively. We find similar results for solar photovoltaics, Li-ion battery storage, and gas generation (OCGT, CCGT, CCGT_CCS), meaning that these resources would need to earn most of their revenue in a handful of

hours under an energy-only wholesale power market design. Moreover, optimization ensures full cost recovery in the model because the model assumes perfect foresight of load and VRE availability. In reality, it could be difficult to finance investments in generation and storage assets that have to rely for most of their revenues on a handful of operating hours in any given year.

6.4 Conclusion and key takeaways

This chapter, detailing the results of our modeling analysis, explores the drivers for adopting energy storage in the transition to low-carbon power systems by 2050. We consider the interplay between storage technology cost and performance attributes and other factors, including the costs of alternative

generation technologies, demand growth, demand flexibility, and VRE resource quality, among others. We also examine how varying the stringency of the carbon constraint affects these interactions.

We find that the near-complete decarbonization of power systems (i.e., average emissions intensity of 5 gCO₂/kWh) can be achieved with VRE deployment, in conjunction with available (Li-ion) battery energy storage, along with infrequent use of dispatchable natural gas generation, with bulk power cost increases of 21% (Texas) to 36% (Northeast) compared to a scenario with no emission limits, without creating reliability issues for hourly grid operations. At the same time, we find that full decarbonization based on deploying VRE and Li-ion storage technologies while ruling out any use of natural gas generation (in other words, targeting “zero” CO₂ emissions rather than “net-zero” emissions) is significantly more expensive at the margin. Put another way, the incremental cost of increasing the share of carbon-free electricity generation⁴¹ from around 90%–93% (as seen in the 5 gCO₂/kWh emission case in Table 6.9) to 100%, via a combination of VRE and Li-ion storage, is quite high. This observation is consistent with findings from other studies modeling zero-carbon power systems based on VRE and Li-ion storage (Cole et al. 2021; Brown and Botterud 2021; Sepulveda, Jenkins and de Sisternes, et al. 2018). It provides a compelling reason to focus public and private RD&D resources on further improving the cost and performance attributes of a range of technologies, including emerging

long-duration energy storage (LDES) technologies, alternative low- or no-carbon generation technologies that are dispatchable, and negative emissions technologies that can remove CO₂ from the atmosphere.

While these broad observations apply across all regions studied here, our modeling reveals significant regional variation in system costs, optimal storage capacity deployment, and optimal generation mix under different emission constraints. The differences primarily reflect differences in the quality of wind and solar resources and thus in the cost of zero-carbon generating technologies in the three regions we examine. Notably, among these regions, the Northeast has the lowest-quality VRE resources and the highest CO₂ emissions under a No Limits policy scenario. Relative to other regions, the Northeast also generally sees the highest system average electricity cost to achieve a given CO₂ emissions goal for the same technological assumptions. That is, without policies that significantly constrain CO₂ emissions, the Northeast would not “naturally” reduce its emissions per unit of electricity generated.⁴² By contrast, Texas, due to its excellent wind and solar resources, sees a significant “natural” reduction in CO₂ per kWh in our modeling without any additional policy interventions, though policy interventions are necessary to get to complete decarbonization of the electricity sector in that state also. The Southeast falls between the Northeast and Texas on these dimensions. In short, the challenges of “getting to zero” vary across regions based on their resource endowments.

⁴¹ As noted in the caption of Table 6.9, carbon-free electricity generation is defined to include VRE, nuclear, and hydro resources, but it excludes generation from CCGT with CCS. Such a definition decreases the perceived level of decarbonization achieved in each case since it does account for the substantially reduced carbon intensity of the remaining generation. See footnote 21 for further discussion.

⁴² As noted earlier (in footnote 8), many northeastern states have passed legislation that mandates reductions in economy-wide greenhouse gas (GHG) emissions of at least 80% by 2050, with a few states committing to more ambitious targets. In this context, our No Limits policy scenario for the Northeast is mainly a consistent internal benchmark to systematically quantify the impact of other technology or demand drivers that encourage electrification outside the power sector.

Our modeling highlights the multiple impacts of LDES availability on decarbonized power systems, which includes reducing the need for dispatchable generation, lowering the system average cost of electricity, reducing VRE curtailment, and reducing variability in wholesale electricity prices. The strength of these effects depends on LDES cost and performance attributes but also on system factors and on the attributes of other technologies (for example, VRE capital cost and availability). The most important LDES performance parameters (in terms of value to the system) are energy storage capacity cost followed by discharge efficiency—this finding is supported by our modeling as well as by a recent paper that uses the same analytical approach (Sepulveda et al. 2021). This paper also notes that charge and discharge power capacity costs and charge efficiency are of secondary importance. Similarly, our findings suggest that when LDES is deployed, the cost-optimal storage duration ranges over days rather than weeks or months. Among LDES technology options, we find that hydrogen (and other forms of derived chemical energy storage) offers a unique value proposition if it is produced with electricity and used as a fuel to decarbonize other end uses, thereby creating a large flexible load that supports VRE integration in the power sector.

The fact that the cost-optimal dispatch of storage, unlike the cost-optimal dispatch of generation resources, cannot be reduced to simplistic merit-order or time-invariant economic principles highlights the increased complexity of actual power system dispatch with significant storage deployment. Whereas our modeling results assume perfect foresight with respect to load and VRE availability in future periods, uncertainty in real-world power

system operations (regarding both load and VRE availability) will make optimal storage dispatch more challenging. Thus, there is a need to improve the software tools used for power system dispatch to support cost-efficient utilization of resources like storage as well as demand flexibility and VRE in future low-carbon power systems. In this context, knowledge sharing forums between industry and academia, such as the annual technical conference on improved software organized by the Federal Energy Regulatory Commission (FERC) are noteworthy.⁴³ From the U.S. perspective, our first recommendation on p. 226 can be implemented by (1) increasing funding for demonstration activities to be undertaken by the Energy Delivery Grid Operations Technology program proposed by DOE's Office of Electricity in its FY22 budget request, and (2) expanding the grid resilience, reliability, and flexibility programs proposed by the Advanced Research Projects Agency–Energy (ARPA–E) to support research and commercialization of software for reliable grid operations.

Our modeling of least-cost power systems and alternative storage technology deployments considered inter-annual and intra-annual variations in VRE availability as well as increased demand from expanded electrification in other sectors of the economy, assuming perfect foresight with respect to future costs and operational conditions. While this approach represents an improvement over previous studies that have explored power and energy system decarbonization pathways (Larson et al. 2020; Phadke et al. 2020; Cochran et al. 2021), it still does not fully address all the factors that will impact the evolution of future low-carbon power systems and the role of energy storage.

⁴³ FERC convenes this technical conference annually to discuss opportunities to enhance operational efficiency through improved software (Federal Energy Regulatory Commission 2021).

First, due to data limitations, we did not model the demand-side impacts of very extreme weather events. Such events, which can affect both electricity demand and supply, are likely to become more important in the future owing to climate change. Thus, further work to characterize weather-driven demand and supply uncertainty would be very useful. Second, for reasons of computational tractability, we had to resort to approximating annual grid operations using representative weeks for two of the study regions (Southeast and Northeast) using multi-zonal grid representation. Collectively, these factors, coupled with our assumption of perfect foresight, mean that our results likely *underestimate* the value of storage and the magnitude of storage deployment that would be cost-effective in low-carbon power systems. Clear opportunities exist to advance understanding of these issues through further data collection, data analysis, and optimal system modeling.

At the same time, other assumptions in our modeling may contribute to results that overestimate the value of storage. First, as is common practice in state-of-the-art power system planning studies, we ignore use-based degradation of electrochemical storage (instead we account for degradation as a fixed O&M cost related to battery cell replacement). If degradation were included, it might limit the value of these storage resources. Second, our modeling does not consider the availability of bioenergy-based power generation with or without carbon capture or other dispatchable renewable generation sources such as geothermal. If, when, and where such sources become available, their deployment could help minimize the cost impacts of going from near-complete decarbonization to full decarbonization and could significantly reduce the value of LDES. If bioenergy systems with CCS or direct air capture were feasible at reasonable cost, for

example, the negative CO₂ emissions that they could produce could make it possible to reach a “net-zero” carbon power system while still allowing for some use of natural-gas-based generation. A few recent studies have shown that access to negative emissions, generated either within or outside the power sector, reduces the value of energy storage technologies in the power sector (Daggash, Heuberger and Dowell 2019; Larson et al. 2020; Williams et al. 2021). Finally, our analysis is based on least-cost investment planning for a future year (2050) with corresponding technology cost projections for that year. In reality, VRE and other resource investments will be added incrementally over time, likely leading to higher investment costs than were assumed here. Higher system costs would almost certainly be incurred if the target date for power sector decarbonization is brought forward, say between 2035 and 2050, owing to the cost associated with potentially stranding some existing thermal generation and the reduced opportunity for learning-induced cost reductions in emerging storage technologies. We have not attempted to quantify the cost and system implications of these factors in our analysis.

The discussion in this chapter illustrates the complexity of long-term investment planning aimed at efficiently achieving deeply decarbonized and reliable power systems. It also highlights the importance of fundamental research to advance the state-of-the-art in models used for investment planning, as well as the need for system operators to continuously review and update their planning approaches to incorporate best-available methodologies. Existing practices for power system planning and reliability assessment in various jurisdictions increasingly recognize the importance of incorporating increased temporal resolution of grid operations as well as inter-annual variability (California Public Utilities

Commission 2019; Federal Energy Regulatory Commission 2021; National Academies of Sciences, Engineering, and Medicine 2021), but these are only two of several factors to be addressed. As the grid outages that occurred in Texas in February 2021 highlighted, system planning needs to account more effectively for variability in demand and supply, especially under extreme weather events, and for correlations between the supplies from individual generators in the portfolio and between total generator output and demand. This variability is likely to increase with climate change, and recent studies have highlighted its impacts on grid operations and planning (Fonseca et al. 2021; Steinberg et al. 2020). Demand response and demand flexibility, as well as distributed energy resources, also can play an important role and deserve much more attention than we were able to give them in this analysis. Similar to other CEM studies (Mai, Jadun, et al. 2018), our modeling assumes inelastic demand that is either very responsive to economic signals, such as when modeling demand flexibility from certain end uses (e.g., electric vehicle charging), or completely inflexible. This representation overlooks the potential for differentiated consumer responses (elasticity as well as flexibility) to economic signals noted in empirical research; it also does not consider potential behavioral changes caused by the adoption of new technologies. While our modeling shows that increased demand flexibility generally tends to reduce storage needs and costs, understanding the impact of demand flexibility on storage needs and grid operations in practice requires further analysis and efforts to model the realistic responses of different customer classes. Another aspect of electricity demand that is not considered here concerns the relative merits of electrification vs. other approaches for decarbonizing end-use sectors that currently rely on fossil fuels (e.g., industry). As shown by our case study of industrial hydrogen

demand in Texas, technological approaches to decarbonizing these end uses can directly affect cost-effective decarbonization pathways for the electricity sector. This suggests that integrated energy systems analysis—not just electricity systems analysis—would be essential to understand the costs and benefits of technology choices in the electricity sector from the perspective of economy-wide decarbonization. Finally, electricity and energy system models can also be expanded to shed light on the non-GHG environmental impacts of investment portfolios aligned with deep decarbonization as well as the resulting distribution of the economic and environmental impacts across various regions and segments of the population. Understanding these outcomes may be as important to building public acceptance as the cost and reliability metrics that are typically the focus of existing modeling efforts.

Finally, our modeling points to increased variability in the marginal value of energy, used here as a proxy for wholesale energy prices in an energy-only wholesale market, in future low-carbon electricity systems. This creates challenges for financing investments since, although assets recover costs under assumptions of perfect foresight for purposes of the modeling analysis, in reality, the risk of negative returns is high when many assets generate the dominant portion of their overall revenues from just a handful of operating hours in an average year. As discussed in Chapter 8, this potential for increased price variability also points to the value of retail rate reform that can encourage electrification by enabling flexible consumers to increase demand in the many hours in which the social marginal cost of electricity is at or close to zero. This issue impacts all resources, including energy storage, and points to the need for electricity market reforms, which are the focus of Chapter 8.

Key takeaways based on the findings from our modeling analysis and from the discussion in this chapter are summarized below (recommendations for future work in this area appear in italics):

- Near-complete decarbonization of electricity systems appears feasible from an hourly energy supply and demand balance perspective, using renewables, natural gas, and lithium-ion battery storage alone, without creating significant reliability issues or very large increases in system average cost.
- In the absence of any CO₂ constraint on the power sector, the three U.S. regions studied here (Texas, the Northeast, and the Southeast) achieve very different CO₂ emission intensities for the same 2050 technology cost assumptions. These differences primarily result from regional variations in renewable resource quality and load profiles.
- With lower energy capacity costs and lower round-trip efficiency compared to lithium-ion battery technology, long-duration energy storage has the greatest impacts on electricity system decarbonization when natural gas generation without carbon capture and sequestration is not an option. Generally, LDES, when optimally deployed, substitutes for natural gas capacity, increases the value of variable renewable generation, and produces moderate reductions in system average electricity cost.
- When it is cost-optimal to deploy multiple storage technologies, the technologies with the lowest capital cost of energy storage capacity are generally best suited to provide long-term storage. However, while optimal generation dispatch is determined by roughly constant marginal costs, optimal storage operation is driven by the changing and unobservable shadow values of stored energy.
- As a result, all storage technologies deployed will operate with charge/discharge cycles of various durations. Simplified assessments of storage economics based on stylized charge/discharge profiles overlook such dynamics and may provide inaccurate assessments of storage value.
- In performing energy market arbitrage—that is, buying when prices (and net demand) are low and selling when prices (and net demand) are high—energy storage can substitute for other grid resources, both on the demand side and on the supply side.
- The level, range, and variation in the marginal value of energy in future low-carbon electricity systems will be drastically different than values seen in ISO/RTO-managed wholesale markets today.
- Our results highlight the multi-dimensional value of long-duration energy storage to decarbonized power systems. However, the presence of significant storage capacity also greatly increases the complexity of cost-optimal power system dispatch, especially under real-world conditions of imperfect information about load and VRE availability in future time periods.
- Improved modeling and software tools are needed to accurately represent the inter-temporal complexity introduced by extensive deployment of storage as well as demand-side resources in future high-VRE electricity systems. *The U.S Department of Energy, in cooperation with ISO/RTOs, state regulators, and other institutions, should support fundamental research and demonstration projects to accelerate the development and deployment of advanced software tools for enabling cost-efficient grid operations.*

- Scalable methodologies are also needed to model the least-cost planning and dispatch of future low-carbon electricity systems while considering imperfect information about future costs, resource availability, wholesale market prices, and demand. *The U.S Department of Energy, in cooperation with ISO/RTOs, state regulators, and other institutions, should support research to develop such methodologies.*
- Our findings with respect to increased price variability in decarbonized electricity systems—specifically, the potential for many hours of very low or zero marginal energy value but a small number of hours with very high value—also point to increased challenges for financing future investments in grid assets, including storage. This issue impacts all resources and underscores the need for thoughtful electricity market reforms and retail rate design to encourage efficient economy-wide decarbonization.

References

- Black, Jon. 2021. "Final 2021 PV Forecast."
- Brinkman, Gregory, Joshua Novacheck, Aaron Bloom, and James McCalley. 2020. *Interconnection Seams Study*. Glden, CO: National Renewable Energy Laboratory.
- Brown, Maxwell, Wesley Cole, Kelly Eurek, Jon Becker, David Bielen, Ilya Chernyakhovskiy, Stuart Cohen, et al. 2020. *Regional Energy Deployment System (ReEDS) Model Documentation Version 2019*. Golden, CO: National Renewable Energy Laboratory.
- Brown, Patrick R, and Audun Botterud. 2021. "The value of inter-regional coordination and transmission in decarbonizing the US electricity system." *Joule* 115–134. <https://doi.org/10.1016/j.joule.2020.11.013>.
- Brown, T., and L. Reichenberg. 2021. "Decreasing market value of variable renewables can be avoided by policy action." *Energy Economics*.
- Brown, T., J. Hörsch and D. Schlachtberger. 2018. PyPSA: Python for Power System Analysis. *Journal of Open Research Software*, 6(1), p.4. DOI: <http://doi.org/10.5334/jors.188>
- Buongiorno, J, M Corradini, J Parsons, and D Petti. 2018. "The future of nuclear energy in a carbon-constrained world: An interdisciplinary MIT Study."
- California Public Utilities Commission. 2019. *Unified Resource Adequacy and Integrated Resource Plan Inputs and Assumptions: Guidance for Production Cost Modeling and Network Reliability Studies*.
- Cochran, Jaquelin, Paul Denholm, Meghan Mooney, Daniel Steinberg, Elaine Hale, Garvin Heath, Bryan Palmintier, et al. 2021. *Los Angeles 100% Renewable Energy Study (LA100)*. Golden, CO: National Renewable Energy Laboratory.
- Cole, Wesley J. et al. "Quantifying the challenge of reaching a 100% renewable energy power system for the United States." *Joule* 5.7 (2021): 1732–1748.
- Cole, Wesley, and A. Will Frazier. 2020. *Cost Projections for Utility-Scale Battery Storage: 2020 Update*. Golden, CO: National Renewable Energy Laboratory.
- Cole, Wesley, Bethany Frew, Trieu Mai, and Yinong Sun. 2017. *Variable Renewable Energy in Long-Term Planning Models: A Multi-Model Perspective*. NREL.
- Daggash, H. A., C. F. Heuberger, and N. Mac Dowell. 2019. "The role and value of negative emissions technologies in decarbonising the UK energy system." *International Journal of Greenhouse Gas Control* 181–198.
- Darghouth, N. R., G. Barbose, J. Zuboy, P. J. Gagnon, A. D. Mills, & L. Bird (2020). Demand charge savings from solar PV and energy storage. *Energy Policy*, 146, 111766.
- DNV GL. 2017. "Safety, operation and performance of gridconnected energy storage systems."
- Draxl, C., A. Clifton, B. M. Hodge, & J. McCaa (2015). The wind integration national dataset (wind) toolkit. *Applied Energy*, 151, 355–366.
- Energy Information Administration. 2020. "Battery Storage in the United States: An Update on Market Trends."
- . 2021a. *Form EIA-923 detailed data with previous form data (EIA-906/920)*. June 11. <https://www.eia.gov/electricity/data/eia923>.
- . 2021b. *Open Data*. Accessed 6 2021. <https://www.eia.gov/opendata>.
- . 2021c. "U.S. Electric Power Industry Estimated Emissions by State." *Electricity Data*. March 26. <https://www.eia.gov/electricity/data/state>.
- . 2021d. *What are U.S. energy-related carbon dioxide emissions by source and sector?* May 14. Accessed June 3, 2021. <https://www.eia.gov/tools/faqs/faq.php?id=75&t=11>.
- Ela, E, M Milligan, A Bloom, A Botterud, A Townsend, and T Levin. 2014. *Evolution of Wholesale Electricity Market Design with Increasing Levels of Renewable Generation*. Golden, CO: National Renewable Energy Laboratory.
- Electric Power Research Institute and Resources for the Future. 2017. *Systems Analysis in Electric Power Sector Modeling: Evaluating Model Complexity for Long-Range Planning*. Palo Alto: Electric Power Research Institute and Resources for the Future.
- Electric Reliability Council of Texas. 2021. *Historical RTM Load Zone and Hub Prices*. Accessed May 2021. <http://mis.ercot.com/misapp/GetReports.do?reportTypeId=13061&reportTitle=Historical%20RTM%20Load%20Zone%20and%20Hub%20Prices&showHTMLView=&mimicKey>.
- Environmental Protection Agency. 2018. *Documentation for EPA's Power Sector Modeling Platform v6 Using the Integrated Planning Model*. Washington DC: U.S. Environmental Protection Agency.

- . 2021. *Inventory of U.S. Greenhouse Gas Emissions and Sinks: 1990-2019*. Environmental Protection Agency.
- Environmental Protection Agency Clean Air Markets Division. 2018. *Documentation for EPA's Power Sector Modeling Platform v6 Using the Integrated Planning Model*. Washington DC: U.S. Environmental Protection Agency.
- Fajard, Mathilde, Jennifer Morris, Angelo Gurgel, Howard Herzog, Niall Mac Dowell, and Sergey Paltsev. 2021. "The economics of bioenergy with carbon capture and storage (BECCS) deployment in a 1.5 °C or 2 °C world." *Global Environmental Change* 102262.
- Federal Energy Regulatory Commission. 2021. *Increasing Efficiency through Improved Software*. Accessed June 2021. <https://www.ferc.gov/industries-data/electric/power-sales-and-markets/increasing-efficiency-through-improved-software>.
- Fonseca, Francisco Ralston, Michael Craig, Paulina Jaramillo, Mario Bergés, Edson Severini, Aviva Loew, Haibo Zhai, et al. 2021. "Effects of Climate Change on Capacity Expansion Decisions of an Electricity Generation Fleet in the Southeast U.S." *Environmental Science & Technology* 2522-2531.
- Gamesa. 2017. *G126-2.5 MW*. <https://docplayer.net/24040007-Gamesa-g-mw-greater-energy-produced-from-low-wind-sites-minimum-power-density-improved-coe-maximum-profitability.html>.
- He, Guannan, Dharik S. Mallapragada, Abhishek Bose, Clara F. Heuberger, and Emre Gençer. 2021. "Sector coupling via hydrogen to lower the cost of energy system decarbonization." *Energy & Environmental Science* 14: 4635-4646. <https://pubs.rsc.org/en/content/articlelanding/2021/ee/d1ee00627d>.
- Heuberger, Clara F. Iain Staffell, Nilay Shah, and Niall Mac Dowell. 2017. "A systems approach to quantifying the value of power generation and energy storage technologies in future electricity networks." *Computers & Chemical Engineering* 247-256.
- Holmgren, William F., Clifford W. Hansen, and Mark A. Mikofski. 2018. *pvlb python: a python package for modeling solar energy systems*. <http://joss.theoj.org/papers/10.21105/joss.00884>.
- Hulbert, David, Ilya Chernyakhovskiy, and Jacqueline Cochran. 2016. *Renewable Energy Zones: Delivering Clean Power to Meet Demand*. Golden, CO: National Renewable Energy Laboratory. <https://www.nrel.gov/docs/fy16osti/65988.pdf>.
- International Energy Agency. 2021a. "Net Zero by 2050: A Roadmap for the Global Energy Sector."
- . 2021b. *Global Energy Review 2021: CO₂ Emissions*. Accessed June 2021. <https://www.iea.org/reports/global-energy-review-2021/CO2-emissions>.
- . 2019. "The Future of Hydrogen: Seizing Today's Opportunities."
- ISO New England. 2020. *2018 ISO New England Electric Generator Air Emissions Report*. Holyoke, MA: ISO New England, Inc.
- Jafari, Mehdi, Audun Botterud, and Apurba Sakti. 2020. "Estimating revenues from offshore wind-storage systems: The importance of advanced battery models." *Applied Energy* 115417.
- Jenkins, J.D., R. Ponciroli, R. Vilim, F. Ganda, F. Sisternes, and A. Botterud. 2018. "The benefits of nuclear flexibility in power system operations with renewable energy." *Applied Energy* 872-884.
- Jenkins, Jesse, and Nestor Sepulveda. 2017. "Enhanced Decision Support for a Changing Electricity Landscape: The GenX Configurable Electricity Resource Capacity Expansion Model." *MIT Energy Initiative Working Paper*.
- Johnston, Josiah, Rodrigo Henriquez-Auba, Benjamín Maluenda, and Matthias Fripp. 2019. "Switch 2.0: A modern platform for planning high-renewable power systems." *SoftwareX* (SoftwareX 10) 100251.
- Junge, Cristian, Dharik Mallapragada, and Richard Schmalensee. 2022. "Energy Storage Investment and Operation in Efficient Electric Power Systems." <https://www.iaee.org/en/publications/ejarticle.aspx?id=3900>.
- Kotzur, Leander, Peter Markewitz, Martin Robinius, and Detlef Stolten. 2018. "Time series aggregation for energy system design: Modeling seasonal storage." *Applied Energy* (Applied Energy) 213: 123-135. <https://www.sciencedirect.com/science/article/abs/pii/S0306261918300242>.
- Kuepper, Lucas Elias, Holger Teichgraeber, and Adam R. Brandt. 2020. "Capacity Expansion: A capacity expansion modeling framework in Julia." *Journal of Open Source Software* 2034.
- Larson, Eric, Chris Greig, Jesse Jenkins, Erin Mayfield, Andrew Pascale, Chuan Zhang, Joshua Grossman, Robert Williams, Steve Pacala, and Robert Socolow. 2020. *Net-Zero America: Potential Pathways, Infrastructure, and Impacts (Interim Report)*. Princeton, NJ: Princeton University.
- Levin, Todd, and Audun Botterud. 2015. "Electricity market design for generator revenue sufficiency with increased variable generation." *Energy Policy* 392-406.

- Levin, Todd, Jonghwan Kwon, and Audun Botterud. 2019. "The long-term impacts of carbon and variable renewable energy policies on electricity markets." *Energy Policy* 53-71.
- Mai, Trieu, Clayton Barrows, Anthony Lopez, Elaine Hale, Mark Dyson, and Kelly Eurek. 2015. *Implications of Model Structure and Detail for Utility Planning: Scenario Case Studies Using the Resource Planning Model*. Golden, CO: National Renewable Energy Laboratory. <https://www.nrel.gov/docs/fy15osti/63972.pdf>.
- Mai, Trieu, Paige Jadun, Jeffrey Logan, Colin McMillan, Matteo Muratori, Daniel Steinberg, Laura Vimmerstedt, Ryan Jones, Benjamin Haley, and Brent Nelson. 2018. *Electrification Futures Study: Scenarios of Electric Technology Adoption and Power Consumption for the United States*. Golden, CO: National Renewable Energy Laboratory.
- Mallapragada, Dharik S., Dimitri J. Papageorgiou, Aranya Venkatesh, Cristiana L. Lara, and Ignacio E. Grossmann. 2018. "Impact of model resolution on scenario outcomes for electricity sector system expansion." *Energy* 1231-1244.
- Mallapragada, Dharik S., Nestor A. Sepulveda, and Jesse D. Jenkins. 2020. "Long-run system value of battery energy storage in future grids with increasing wind and solar generation." *Applied Energy* 115390.
- Massachusetts Executive Office of Energy and Environmental Affairs. 2021. *GWSA Implementation Progress*. Accessed June 2021. <https://www.mass.gov/service-details/gwsa-implementation-progress>.
- McMahon, Jeff. 2021. *NET Power CEO Announces Four New Zero-Emission Gas Plants Underway*. January 8. Accessed 2021. <https://www.forbes.com/sites/jeffmcmahon/2021/01/08/net-power-ceo-announces-four-new-zero-emission-gas-plants-underway/?sh=3b4e9e86175b>.
- McMillan, Colin. 2019. *2018 Industrial Energy Data Book*. November 14. Accessed March 21, 2021. <https://data.nrel.gov/submissions/122>.
- MIT Energy Initiative and Princeton University. 2021. *GitHub: GenX Project*. Accessed June 2021. <https://github.com/GenXProject/GenX>.
- National Academies of Sciences, Engineering, and Medicine. 2021. *The Future of Electric Power in the United States*. Washington, DC: The National Academies Press.
- National Renewable Energy Laboratory. 2020. *Electricity Annual Technology Baseline (ATB) Data Download*. <https://atb-archive.nrel.gov/electricity/2020/data.php>.
- . 2021. NSRDB Data Viewer. <https://maps.nrel.gov/nsrdb-viewer/>.
- . 2019. *Regional CAPEX Parameter Variations and Adjustments*. Accessed June 2021. <https://atb-archive.nrel.gov/electricity/2019/regional-capex.html>.
- Neubauer, J., and M Simpson. 2015. *Deployment of Behind-The-Meter Energy Storage for Demand Charge Reduction*. Golden, CO: National Renewable Energy Laboratory.
- New York ISO. 2020. *2020 Load & Capacity Data*. Rensselaer, NY: NYISO.
- New York State Energy Research and Development Authority. 2021. *Governor Cuomo Announces More Than \$17 Million to Help Communities Drive High Impact Clean Energy Actions and Combat Climate Change*. January 26. Accessed June 2021. <https://www.nyserda.ny.gov/About/Newsroom/2021-Announcements/2021-01-26-Governor-Cuomo-Announces-More-Than-17-Million-to-Help-Communities-Drive-High-Impact-Clean-Energy-Actions-and-Combat-Climate-Change>.
- Oak Ridge National Laboratory. 2020. *Existing Hydropower Assets Plant Dataset, 2020*. Accessed 2020. <https://hydrosource.ornl.gov/dataset/existing-hydropower-assets-plant-dataset-2020>.
- Palmintier, Bryan S. 2013. "Incorporating operational flexibility into electric generation planning: Impacts and methods for system design and policy analysis." *MIT Thesis*.
- Pfeifenberger, Johannes. 2021. *Transmission Planning and Benefit-Cost Analyses*. Boston, MA: The Brattle Group.
- Phadke, Amol, Umed Paliwal, Nikit Abhyankar, Taylor McNair, Ben Paulos, David Wooley, and Ric O'Connell. 2020. *The 2035 Report*. Berkeley, CA: Goldman School fo Public Policy, UC Berkeley.
- Poncelet, Kris, Erik Delarue, and William D'haeseleer. 2020. "Unit commitment constraints in long-term planning models: Relevance, pitfalls and the role of assumptions on flexibility." *Applied Energy*.
- Sakti, Apurba, Kevin G. Gallagher, Nestor Sepulveda, Canan Uckun, Claudio Vergara, Fernando J. de Sisternes, Dennis W. Dees, and Audun Botterud. 2017. "Enhanced representations of lithium-ion batteries in power systems models and their effect on the valuation of energy arbitrage applications." *Journal of Power Sources* 279-291.
- Sepulveda, Nestor A., Jesse D. Jenkins, Aurora Edington, Dharik S. Mallapragada, and Richard K. Lester. 2021. "The design space for long-duration energy storage in decarbonized power systems." *Nature Energy* 1-11.

Sepulveda, Nestor A., Jesse D. Jenkins, Fernando J. de Sisternes, and Richard K. Lester. 2018. "The role of firm low-carbon electricity resources in deep decarbonization of power generation." *Joule* 2403-2420.

Steinberg, Daniel C., Bryan K. Mignone, Jordan Macknick, Yinong Sun, Kelly Eurek, Andrew Badger, Ben Livneh, and Kristen Averyt. 2020. "Decomposing supply-side and demand-side impacts of climate change on the US electricity system through 2050." *Climatic Change* 125-139.

Sunny, Nixon, Niall Mac Dowell, and Nilay Shah. 2020. "What is needed to deliver carbon-neutral heat using hydrogen and CCS?" *Energy & Environmental Science* 13: 4204-4224.

Szilard, R., P. Sharpe, E. Kee, E. Davis, and E. Grecheck. 2017. "Economic and Market Challenges Facing the U.S. Nuclear Commercial Fleet - cost and revenue study."

U.S. Department of Energy. 2018. *Hydropower Vision*. Oak Ridge, TN: Office of Scientific and Technical Information.

—. 2016. *Hydropower Vision: A new chapter for America's 1st Renewable Electricity Source*. Washington, DC: U.S. Department of Energy.

—. 2017. "Staff Report to the Secretary on Electricity Markets and Reliability."

U.S. Department of Energy Office of Energy Efficiency and Renewable Energy, Office of Energy Efficiency & Renewable Energy. 2019. "2018 Industrial Energy Data Book."

Weiland, Nathan, and Charles White. 2019. *Performance and Cost Assessment of a Natural Gas-Fueled Direct sCO₂ Power Plant*. Pittsburgh, PA: National Energy Technology Laboratory. <https://www.netl.doe.gov/projects/files/Performance%20and%20Cost%20of%20a%20NG-Fueled%20Direct%20sCO2%20Plant.pdf>.

Williams, James H., Ryan A. Jones, Ben Haley, Gabe Kwok, Jeremy Hargreaves, Jamil Farbes, and Margaret S. Torn. 2021. "Carbon-neutral pathways for the United States." *AGU Advances (AGU Advances 2)*.

Wiser, Ryan, and Mark Bolinger. 2018. *2018 Wind Technologies Market Report*. Oak Ridge, TN: Office of Scientific and Technical Information.



Chapter 7 – Considerations for emerging markets and developing economies

7.1 Context

Trends in electricity generation, conversion, and end use in emerging market and developing economy (EMDE) countries, such as Brazil, India, Indonesia, Nigeria, and South Africa over the next few decades will significantly impact the success of global climate mitigation efforts (Rao, Min and Mastrucci 2019). Resulting demand growth for electricity will place burdens on the electricity infrastructure in these countries when that infrastructure is, in many cases, not entirely reliable and operated by utilities with significant financial constraints. This scenario could lead to use cases for energy storage that are different from the use cases discussed for developed countries in Chapter 6, where deep decarbonization coupled with expanded electrification of transportation and other non-traditional electricity end uses is the primary driver for grid transformation. In situations where grid supply is limited, either by available generation capacity and/or by issues of network extent and access, stand-alone minigrids and solar home systems that incorporate energy storage may serve as alternative modes of electrification, and thus support efforts to rapidly expand energy access.

In fact, *supply-constrained* conditions are prevalent in sub-Saharan Africa, as well as in some parts of rural India, where off-grid electrification systems have already attracted considerable interest from private developers as well as from development finance institutions such as the World Bank (Tenenbaum et al. 2014). In other situations, where bulk generation supply is adequate and most customers are grid-connected, and where a combination of increased electricity demand, driven by economic growth and rapid expansion of

variable renewable energy (VRE) generation create network congestion, novel opportunities to deploy energy storage are emerging to support efficient and reliable grid operations. These conditions are common, for example, in India and Southeast Asia (Debnath and Mourshed 2018; McNeil et al. 2013; Nhalur and Josey 2012). In such *demand-driven* contexts, electricity load, driven by the adoption of energy-intensive electric appliances, air conditioning (AC), and the increasing electrification of transportation, is expected to grow at a much faster rate than total energy demand (International Energy Agency 2020). By one estimate, growth-driven energy consumption could result in India's final energy use being 81% greater in 2040 than it was in 2019 (International Energy Agency 2020), with demand for electricity growing even faster in this scenario—by 161% over the same period—than demand for other forms of energy (International Energy Agency 2020). While decadal electricity demand growth projections for developed countries are driven primarily by transportation (Mai et al. 2018), in India and many EMDE countries with hot climates, the buildings sector is projected to dominate electricity demand growth, primarily due to AC adoption (International Energy Agency 2018). Compared to other new sources of demand (such as electric vehicles), relatively high and inflexible demand for space cooling throughout the day means that buildings will contribute to an increase in aggregate demand and a significant increase in peak consumption.

The above use cases for energy storage in EMDEs are further differentiated by other factors that motivate the analysis described in this chapter. These factors include:

- (1) a relatively high cost of financing for grid

Table 7.1 Summary of storage deployment scenarios for demand- and generation-driven electricity system development in the EMDE countries investigated in this chapter

| | Demand-driven | Supply-constrained |
|--------------------------|--|--|
| Example countries | India, Indonesia, Egypt, Brazil | Nigeria, South Africa |
| Use cases | Storage at the distribution level for non-wires alternative network upgrades and at the transmission level for VRE penetration. | Storage for minigrid solutions at the distribution level. |
| Analysis approach | 1) Accounts for electricity demand growth projections and storage investments at the distribution level through a flexible valuation framework. 2) Investigates interplay of demand, technology, and policy drivers on bulk power system design and storage deployment. | Optimizes grid-connected minigrid solutions that complement grid supply to maintain overall quality of supply. Solar with storage and diesel generation are investigated as options within grid-connected minigrids. |

investments (relative to financing costs in developed economies) and limited financial resources of electric utility companies; (2) predominance of coal for primary energy supply, with natural gas (NG) use often limited by availability or infrastructure constraints, which puts increased emphasis on VRE (and storage) deployment for power sector decarbonization; and (3) differentiated technology costs compared to developed economies. For example, in demand-driven EMDEs such as India, VRE capital costs are 50%–70% lower than in the United States due to several regional factors, including cheaper labor. In contrast, VREs are frequently more expensive in sub-Saharan Africa because of its smaller markets and dearth of sophisticated manufacturing.

Our analysis considers storage in the context of two types of EMDE countries (Table 7.1): (1) demand-driven countries (e.g., India), where understanding demand growth and patterns in future electricity use is crucial to understanding storage use cases, and (2) supply-constrained countries (e.g., Nigeria), where uncertainty regarding the duration and timing of grid availability to meet demand are key drivers for storage deployment. To analyze storage use cases in demand-driven EMDEs, we undertake demand-side modeling to explore how AC use could impact the long-term evolution of

the electricity demand profile in the Indian context. We then use our demand-side findings to explore the possible value of storage in India's distribution and transmission systems (Sections 7.2.2 and 7.2.3, respectively) across a range of technology and policy scenarios. The findings from our analysis in the Indian context can be broadly generalized to other regions that exhibit similar conditions, notably throughout Southeast Asia. To evaluate the role of storage in supply-constrained regions, by contrast, we investigate the value proposition for deploying storage as part of the buildup of grid-connected solar photovoltaic (PV) microgrids for commercial and industrial (C&I) consumers in Nigeria (Section 7.3).

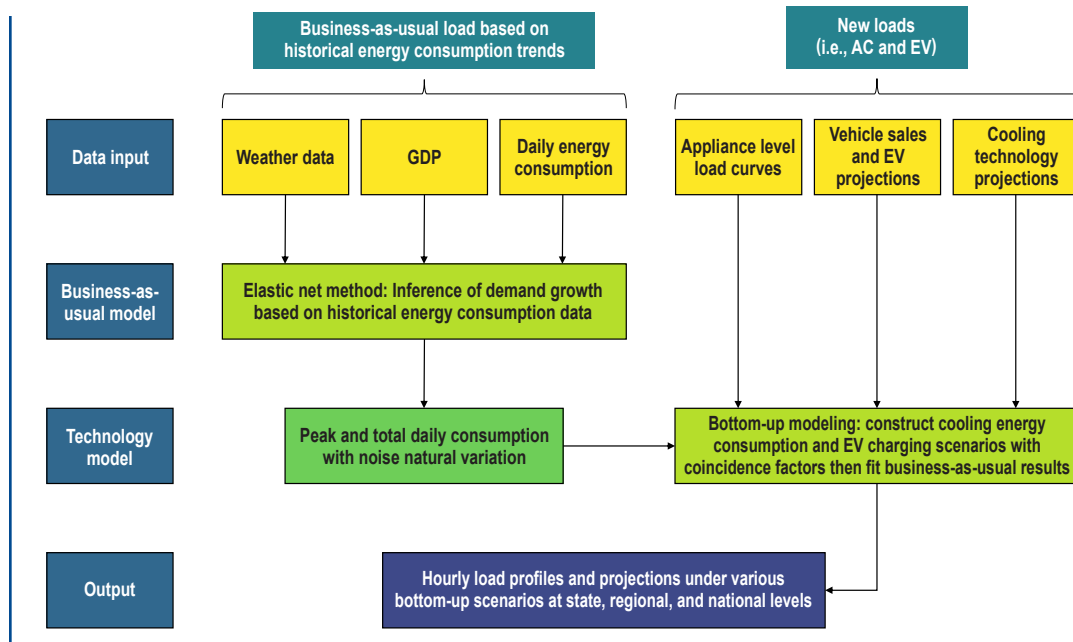
7.2 Assessing the role of storage in demand-driven emerging economy contexts

7.2.1 Approach

Demand-side modeling

We treat India as a case study of a fast-growing EMDE where demand is a key driver for the evolution of the electricity system. Our analysis uses a detailed model to quantify plausible alternative electricity demand scenarios, distinguishing between established electricity end uses and emerging end uses, such as AC units

Figure 7.1 Simplified schematic of methods used for demand-side modeling in the Indian context



See Barbar, Mallapragada, and Alsup, et al. (2021) for further details.

Table 7.2 Demand projections for India assuming AC and EV demand growth

| | | 2020 | 2030 | 2040 | 2050 |
|---------------------------------------|----------------------------|-------|-------|-------|-------|
| Evening peak demand (GW) | | 197 | 334 | 607 | 890 |
| Total demand (TWh) | | 1,421 | 2,282 | 3,523 | 4,773 |
| AC contribution to peak demand | Baseline efficiency | 17% | 19% | 32% | 49% |
| | High efficiency | 15% | 16% | 19% | 23% |
| EV contribution to peak demand | Evening charging | 0.9% | 2.9% | 4.5% | 6% |
| | Morning charging | 1% | 3% | 5% | 8.5% |

Source: Barbar, Mallapragada, and Alsup, et al. (2021)

and electric vehicles (EVs), and employing separate approaches to project future demand from each type of end use, as shown in Figure 7.1 (Barbar, Mallapragada and Alsup, et al. 2021). In contrast to available demand projections for India in the literature, our bottom-up analysis produces spatio-temporally resolved demand profiles that capture the impact of factors such as end-use appliance efficiency (Table 7.2) on annual and peak electricity

consumption at various spatial scales—e.g., state, regional, and national (Figures 7.2 and 7.5). The results are comparable to other published electricity demand projections for 2040 (Figure 7.4), but also provide a more granular picture of intra-annual variations and spatial distribution of demand that is useful for bulk power system and distribution system planning, as well as for storage valuation (discussed in later sections of this chapter).

Figure 7.2 Regional electricity demand in India in 2040

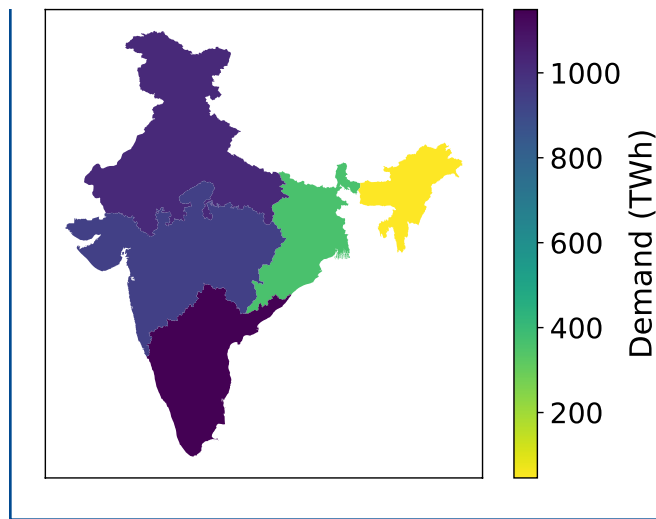
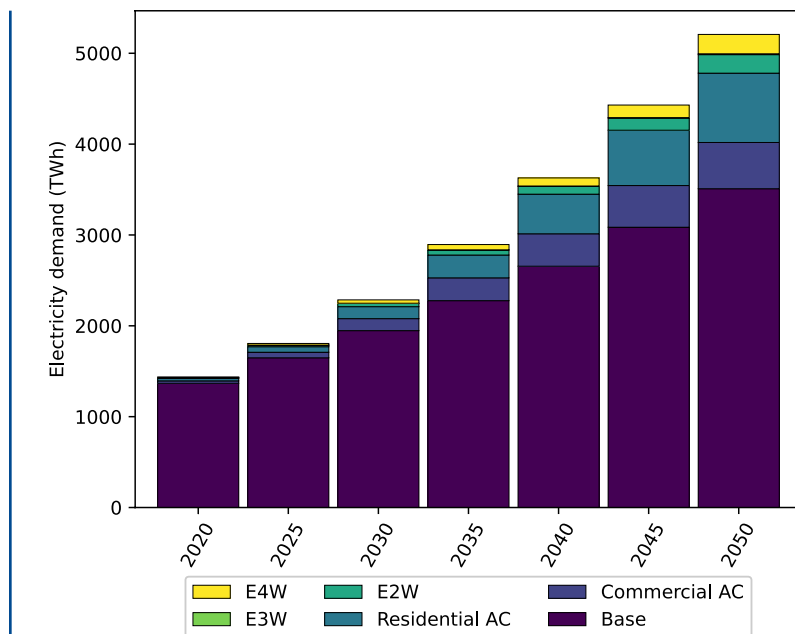
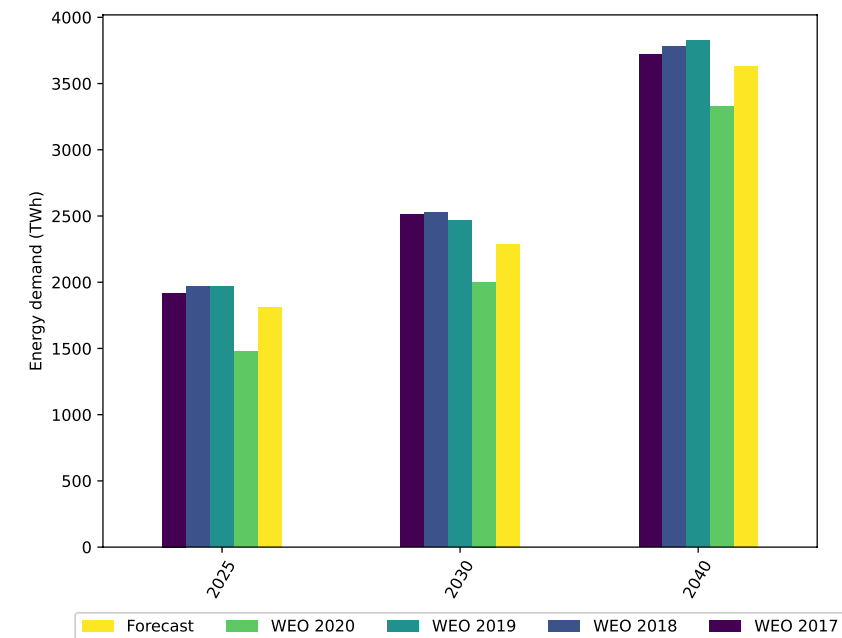


Figure 7.3 Electricity demand projections for India at the national level assuming stable GDP growth, baseline cooling, and home electric vehicle (EV) charging



Source: Barbar, Mallapragada, and Alsup, et al. (2021). E4W = electric 4-wheeled vehicle, E2W = electric 2-wheeled vehicle, E3W = electric 3-wheeled vehicle.

Figure 7.4 Comparison of forecasts



Comparison of forecasts from a demand estimation model (Barbar, Mallapragada and Alsup, et al. 2021) and forecasts from the stated policy scenario developed by the International Energy Agency for the World Energy Outlook (International Energy Agency 2020; International Energy Agency 2019; International Energy Agency 2018).

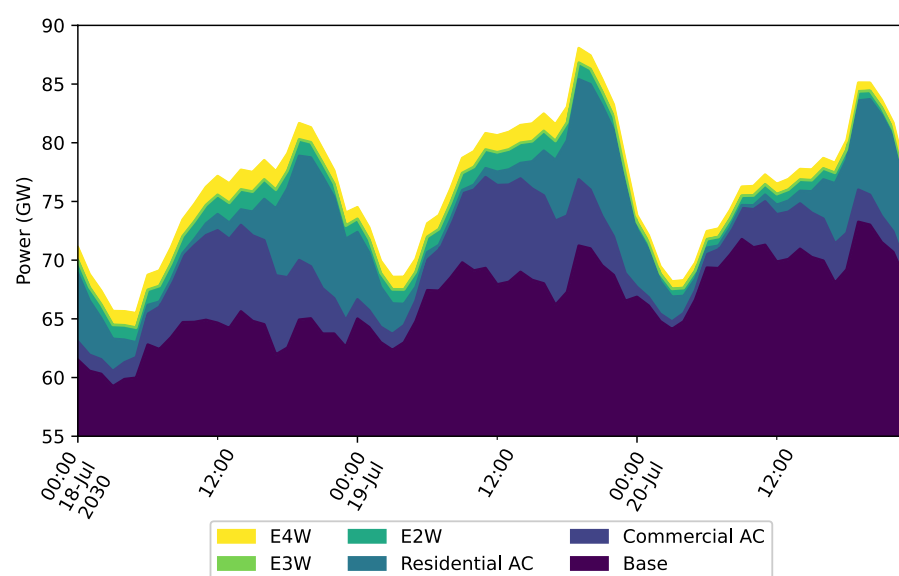
The demand-side analysis proceeds in two stages. First, electricity demand from existing end uses is estimated for future periods using a regression model that is trained on historical regional electricity demand over the period 2012–2019 at a daily resolution, combined with hourly demand for 2015 (Rudnick 2019). The model uses seasonal and long-term growth trends estimated using daily weather data and monthly state-level GDP forecasts.

Second, the technology model shown in Figure 7.1 is used to estimate bottom-up demand from new loads, which in this study include residential and commercial AC, as well as EV charging (Barbar, Mallapragada and Alsup, et al. 2021).

The model makes use of AC sales projections by unit type based on size. Two AC scenarios were considered: a baseline scenario with electricity sales projections based on currently available AC units and a high-efficiency scenario that assumes preferential adoption of efficient AC units as defined by a recent study (International Energy Agency 2018) that assumes the global average Seasonal Energy Efficiency Ratio (SEER) rating of AC units reaches 8.5 by 2050. As of 2018, by comparison, the sales-weighted average SEER for AC units in India was 3 and the global average was 4 (International Energy Agency 2018).¹ AC efficiency, as reflected in SEER ratings, often differs greatly between the United States and India due to the types of AC

¹ SEER ratings for AC units exhibit significant regional variation within and across countries due to differences in type of equipment, size of cooling systems, consumer sensitivity to upfront equipment cost vs. operating cost, as well as differences in the stringency and enforcement of policies around minimum energy performance standards (International Energy Agency 2018).

Figure 7.5 Load profile in 2030 for the southern region of India across three days in summer



Scenario: stable GDP growth, baseline cooling, home EV charging.

units installed. While central air conditioning systems using efficiency measures such as variable refrigeration are common in the U.S. context, cheaper but less efficient split units are significantly preferred in India (International Energy Agency 2018). Residential and commercial AC demand growth was estimated at the state level and then aggregated to the regional level (Barbar, Mallapragada and Alsup, et al. 2021) as an input to the supply-side analysis for India, described below.

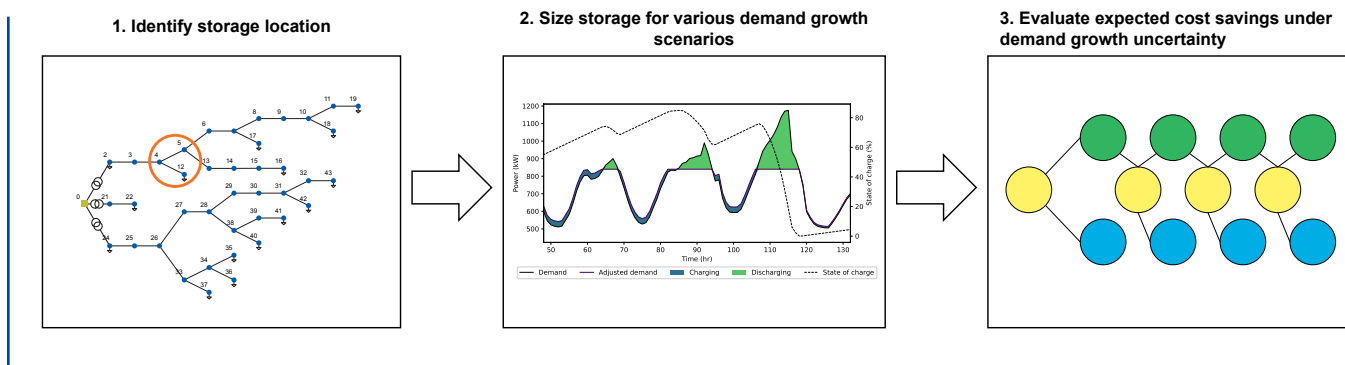
For EVs, our model uses vehicle sales data and government targets for EV sales in future years (NITI Aayog 2018) to estimate EV charging demand. Hourly projections were derived from 2020 to 2050 using survey data related to typical charging patterns (Barbar, Mallapragada and Alsup, et al. 2021). Compared to AC demand, we project electricity demand from EV charging to be relatively modest, both in terms of annual consumption and in terms of contribution to peak demand. This finding is consistent with other studies for

India (International Energy Agency 2020). It contrasts with projections for other regions such as the United States and Europe, where most of the growth in electricity demand is expected to come from EV charging, with consequences for long-term grid evolution (see Chapter 6). Among EVs, Figure 7.3 shows that two and three-wheeled EVs are likely to dominate four-wheeled EVs in India, assuming that the distribution of vehicles in the Indian market remains the same (Society of India Automobile Manufacturers 2020).

Distribution-level storage modeling

There is widespread interest in deploying battery storage as a non-wires alternative (NWA) to offset line upgrades and serve rapidly growing peak demand within electricity distribution networks (Barbar, Mallapragada and Alsup, et al. 2021). This use case is particularly relevant for loaded urban distribution systems in megacities in fast-growing EMDE countries (e.g., Cairo, Delhi, Jakarta), where space cooling comprises a growing share of evening peak

Figure 7.6 Flowchart showing steps in the flexible valuation framework

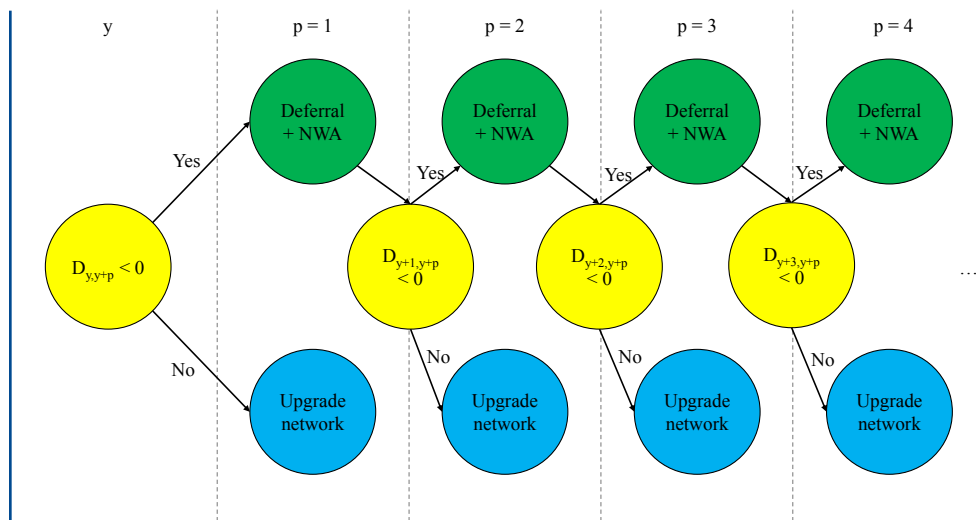


electricity demand. We quantify the role for distribution-level storage (DLS) as an NWA for urban distribution feeders in EMDE settings by studying nine representative urban feeders for four megacities in India (Bengaluru, Delhi, Kolkata, and Mumbai). We employ a flexible valuation framework that uses a multi-year real options analysis via the Markov chain Monte Carlo (MCMC) method to identify the time evolution of the least-cost investment strategy between battery storage and network upgrades under uncertain demand growth.

Figure 7.6 summarizes the three steps of our approach (Barbar, Mallapragada and Alsup, et al. 2021). First, we identify the optimal storage location to relieve the distribution network from overloading. Congestion occurs primarily during peak hours because of high simultaneity in demand for electricity, implying that various components of the network overload simultaneously. The optimal storage location is identified based on providing the maximum demand relief on the feeder from a minimum number of locations. Second, we evaluate the cost-optimal sizing of the battery storage system at the identified location for a given demand scenario, depending on the hourly load profile and the thermal limits of the network components. A time-series linear program is used to size the system for various demand growth scenarios. These optimizations identify the capacity of battery storage to be

deployed, from which we infer the capital and operating cost of DLS. We repeat this second step for three demand growth scenarios: slow, stable, and rapid. In the final part of the flexible valuation framework, we use a MCMC simulation of all demand growth scenarios and their respective posterior probabilities to identify the expected cost-saving option value of DLS and network deferrals under demand uncertainty (Barbar, Mallapragada and Stoner, et al. 2021). For DLS, we compute the annualized fixed cost based on the storage sizing (Figure 7.6, step 2). The real option value of flexibility consists of the difference between the investments required for traditional network upgrades and the investments required for a storage system with postponed upgrades; this is the value of network upgrade deferral. We use annualized investment cost for all calculations, so that multiple deferrals can be considered sequentially, and we account for the salvage value of the battery storage when the real option value of flexibility is no longer favorable. In Figure 7.7, D refers to the deferral value, which is calculated by computing the expected cost, defined as the sum of the product of the MCMC probabilities and their object cost (i.e., storage, network upgrades as defined in Appendix D, Table D.1). If $D < 0$, then the expected cost of storage with deferred network upgrades is *lower* than the expected cost of traditional network upgrades, and therefore storage has a non-negative NWA value. The

Figure 7.7 Real options decision tree



NWA=non-wires alternative, y =first decision year, p =deferral period, D =deferral value.

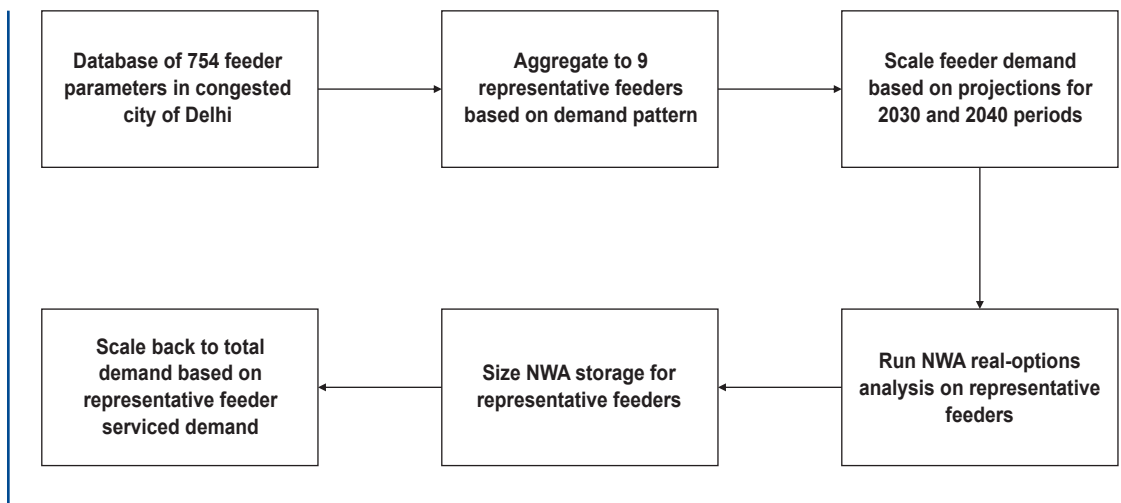
process is repeated at every decision point p with corresponding costs, projections, and probabilities (Figure 7.7).

We apply the flexible valuation framework to estimate the potential of DLS across select megacities in India (Bengaluru, Delhi, Kolkata, Mumbai) using the approach outlined in Figure 7.8. First, nine representative feeders were identified for DLS analysis based on applying clustering techniques to a library of urban feeders (and their respective hourly demand profiles) for the city of Delhi using data provided by Tata Power Delhi Distribution Limited (TPDDL) (Tata Power Delhi Distribution Limited 2018). Each representative feeder is characterized by: (1) a loading percentage that varies from 40% to 80% based on the collected data (Tata Power Delhi Distribution Limited 2018); (2) represented demand, defined as the hourly load profile modeled on the feeder, which will vary by megacity according to available survey data (Nhalur and Josey 2012); (3) serviced demand, which is the total annual demand (in mega-watt-hours or MWh) that the distribution network feeders service with the same loading

percentage; and (4) serviced circuit kilometers, which corresponds to the total circuit kilometers (km) that are at the corresponding loading percentage. The feeder data from Delhi show that 28% of feeders were loaded at 60% or more on an ampere capacity basis; we assume a similar distribution in feeder loading for the other megacities.

In addition, we estimate the circuit kilometers that each of the nine feeders represents in other megacities based on the respective serviced demand and the ratio of serviced demand to circuit kilometers available for these feeders in Delhi. The flexible valuation framework is applied on each representative feeder for each megacity by using the appropriate growth rates from the demand-side modeling for various demand projections in 2030 and 2040 (Barbar, Mallapragada and Alsup, et al. 2021). Network investment costs are calculated based on the circuit kilometer length of each representative feeder in each megacity. The resulting DLS capacity for the representative feeders is scaled using the ratio of each feeder's serviced demand to represented demand (Barbar, Mallapragada and Stoner, et al. 2022).

Figure 7.8 Approach for computing megacity-level DLS potential in the Indian context



Supply-side modeling

We use a multi-period version of GenX, the same power system capacity expansion model (CEM) used for the U.S.-based modeling analysis in Chapter 6, to evaluate the least-cost investment and operation of the Indian bulk power system under alternate technology, demand, and policy scenarios. The multi-period system framework allows us to model the existing power generation fleet and its long-term evolution, which is less relevant in countries such as the United States that have relatively older generation fleets. For the analysis presented in this chapter, GenX is configured as a multi-period investment planning model with four investment periods (2020, 2030, 2040, 2050) and an hourly representation of grid operations. For each investment period, the model includes several grid operation constraints: (1) flexibility limits for thermal power plant operations via linearized unit commitment constraints (Palmintier 2013; Poncelet, Delarue and D'haeseler 2020); (2) supply–demand balance at each hourly time step and each zone, with power flow associated with linear losses and transfer capacity limits between zones; (3) hydropower plant operation consistent with available information on

inflows and reservoir capacity (Rudnick 2019); and (4) for other storage resources, inter-temporal storage balance constraints as well as capacity constraints on the maximum rate of charging and discharging.

These operational constraints are modeled over 20 representative weeks of grid operation selected from a single year of load data based on 2015 weather patterns, with VRE and hydro resource profiles developed via clustering techniques (Mallapragada, Sepulveda and Jenkins 2020; Mallapragada, Papageorgiou, et al. 2018). We represent the Indian grid using five separate balancing regions (North, West, South, East, and Northeast) defined by the grid operator (Central Electricity Authority 2017), with region-specific load profiles developed for each investment period based on the above-described demand-forecasting model (Barbar, Mallapragada and Alsup, et al. 2021). Power flows between these regions are modeled based on a simplified network representation that enforces power exchange limits between the regions. For 2020, these power limits are derived from the system operator (Rudnick 2019; Central Electricity Authority 2017); in future periods, these limits may be expanded with additional transmission investment.

We note some of the key limitations of the supply-side model used here. With respect to technology, we did not consider the deployment of certain low-carbon resources such as hydro, nuclear, or fossil fuel plants with carbon capture and storage (CCS). These resources either have a small role or are not considered part of the long-term expansion plans developed by India's Central Electricity Authority (CEA) (Central Electricity Authority 2018). While India currently has hydro generation, the expected increase in capacity for this resource is just 12 gigawatts (GW) which is very modest compared to projected peak demand. We also restrict our analysis of short-duration battery storage technology to lithium-ion (Li-ion) batteries, whose declining cost is driving widespread adoption. With respect to VRE resource characterization, we use resource availability maps using satellite capacity factor data which includes 14% system losses, assuming 1.5% losses corresponding to light-induced degradation (National Renewable Energy Laboratory 2020). We do not attempt to account for possible losses due to poor air quality, which can affect PV performance. Nor did we account for administrative transmission losses due to theft and other exogenous events when modeling a simplified regional transmission network for India. Consequently, our results may overestimate the value of PV to some extent. Finally, it is important to note that modeling grid operations based on least-cost economic dispatch in real time, which is the norm in many high-income countries such as the United States, does not reflect the realities of bulk power system operations in India today, where long- and short-term contracts dominate power supply (Central Electricity Regulatory Commission 2018). However, regulatory developments suggest that the long-term aim is to have economic dispatch drive grid operations (Central Electricity Regulatory Commission 2018); thus, our least-cost approach represents a reasonable assumption.

7.2.2 Distribution-level storage for network investment deferral

Investments in electrical transmission and distribution networks tend to be “lumpy” (Pérez-Arriaga 2016), because they require large capital commitments initially and involve significant economies of scale, and because the resulting assets have long lifetimes (20–40 years). Consequently, network planning is often employed to identify the investments needed to meet future demand reliably and cost-effectively while maximizing asset utilization. For reliable grid operations, network capacity must meet peak electricity demand while adhering to equipment operating constraints (e.g., line thermal limits). At the transmission level, substantial economies of scale and voltage step-up encourage investment in high-capacity lines and very long-term planning, but this is not always the case at the distribution level in EMDE countries, where distribution companies are usually financially constrained and networks are more congested (World Energy Council 2009; Pargal and Banerjee 2014; United Nations Economic and Social Council 2021; Barbar 2019). Here, we analyze the optimal sizing and placement of storage and its economic value as an NWA at the primary feeder level in urban electricity distribution networks. Although our analysis is based on available feeder conditions in Delhi, this approach offers general insights about the conditions under which it is economically valuable to defer network investment by deploying battery storage. These insights apply in a wide range of situations (Barbar, Mallapragada and Stoner, et al. 2022).

Delhi is a city-state where 55% of electricity use is residential—this is more than double the national average (24%) (Barbar, Mallapragada and Alsup, et al. 2021). Distribution companies in Delhi are witnessing growth in residential cooling demand that is capable of overloading

Table 7.3 Projected peak demand (GW) under the baseline and high-AC-efficiency scenarios, assuming stable GDP growth for the city state of Delhi

| | High AC efficiency | Baseline |
|------|--------------------|----------|
| 2020 | 6.7 | 6.7 |
| 2030 | 12.7 | 15.2 |
| 2040 | 25 | 36.7 |
| 2050 | 34 | 63.8 |

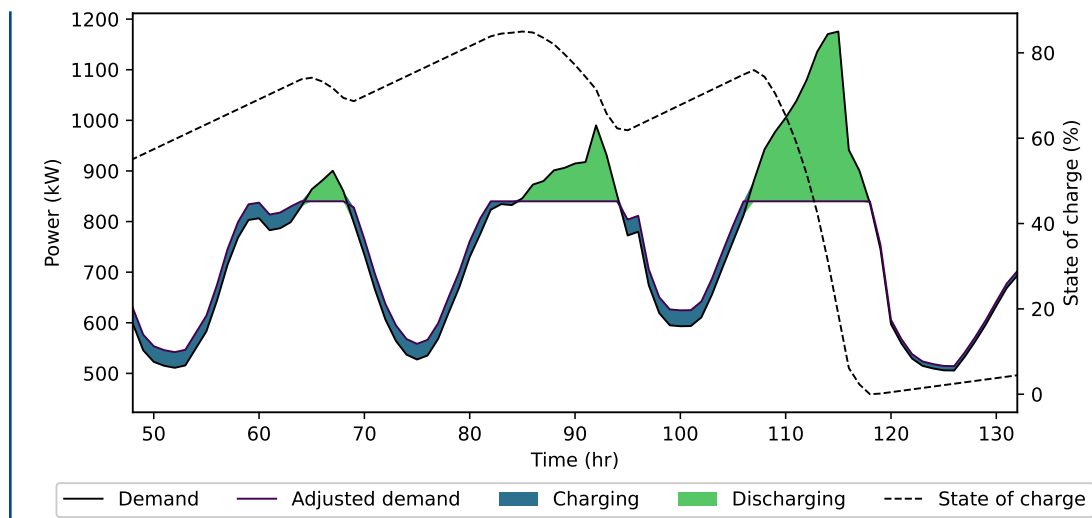
Further details in Barbar, Mallapragada, and Stoner, et al. (2022) and Barbar, Mallapragada, and Alsup, et al. (2021).

network equipment. Megacities such as Delhi are highly congested, which makes carrying out the regular activities of wire reconductoring or large equipment installation operationally challenging. In many cases, these activities are not even feasible due to space and geographical constraints. This situation is not unique to Delhi: Major cities worldwide are experiencing a rise in electricity demand (McNeil et al. 2013; Rao, Min and Mastrucci 2019; Olaniyan et al. 2018). As of 2020, Delhi's peak demand was 6.7 GW (Central Electricity Authority 2018); according to the demand-side modeling analysis undertaken here, the difference in projected peak demand for the city between the baseline and high-AC-efficiency demand scenarios is at least 20% (Table 7.3) (Barbar, Mallapragada and Alsup, et al. 2021). This creates significant uncertainty for investment planning in the distribution network. While the difference in the projected demand is (not surprisingly) widest in 2050, we focus on the deferral value that DLS can provide in the nearer-term model periods of 2030 and 2040.

Historically, distribution companies have not considered forecasting uncertainty in their long-term network planning, but have instead resorted to deterministic net-present-value methodologies (Evans 2020). Nevertheless, forecasting may be useful in comparing plan outcomes under several possible policy, technology, and efficiency scenarios. Given the

magnitude of the gaps between peak demand forecasts under different scenarios and assumptions for a city like Delhi (Table 7.3), it is appropriate to use probabilistic forecasting and flexible planning. This is particularly important when distribution companies contemplate using distributed energy resources (DERs) as an alternative to grid expansion. DER deployment is driven by the modularity of DER technologies and the speed with which they can be installed. Until recently, the most widely deployed DER technology in EMDE countries has been diesel generators, which are usually installed near large C&I loads (International Finance Council Corporation 2019). However, declining costs for Li-ion battery storage make it a more attractive option. Moreover, battery storage provides the added advantage of not creating local air pollution, a major environmental externality in most megacities. Furthermore, depending on the energy source used for battery recharging, the carbon footprint of energy discharged from battery storage is smaller than the carbon footprint from diesel generation commonly used in EMDE countries to meet peak demand (Jakhiani et al. 2012). We apply the flexible valuation framework of Figure 7.6 (Barbar, Mallapragada and Stoner, et al. 2022) to evaluate the role of Li-ion battery storage for short-term peak shaving and network congestion relief as indicated by the optimal dispatch presented in Figure 7.9.

Figure 7.9 Hourly dispatch of NWA battery storage for one summer week load profile from Delhi



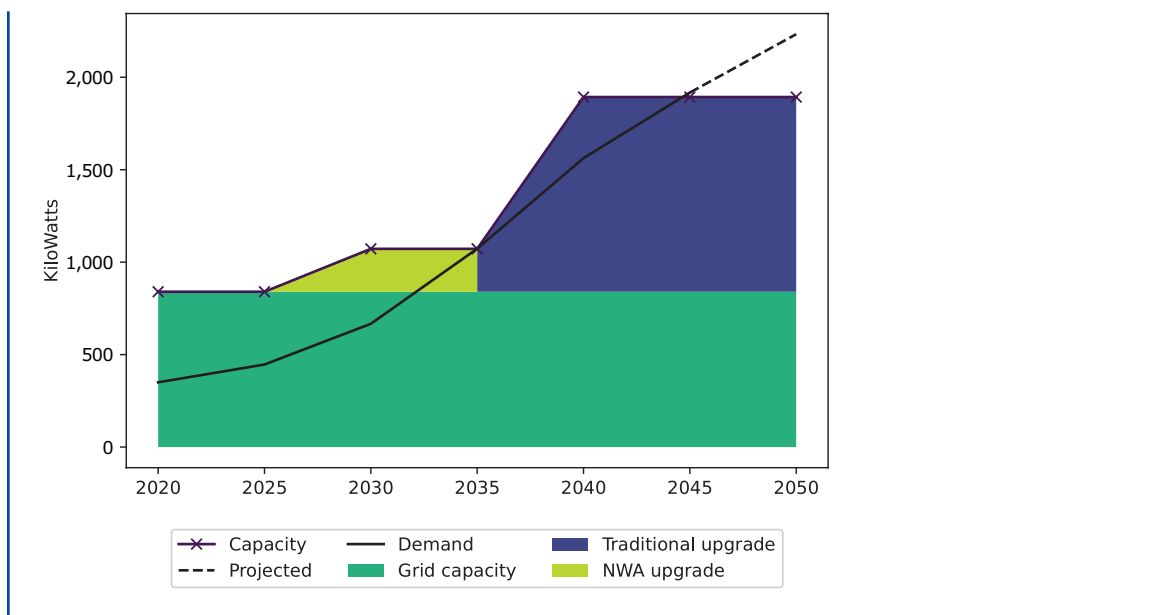
The outcomes generated by our flexible valuation framework depend on technology cost assumptions (e.g., network upgrade costs, battery storage capital costs) and demand growth projections. The timeframe over which battery storage can function to defer other investments may be well short of its useful operating life. It is therefore necessary to assess the flexible framework over multiple investment periods, as described in Figure 7.7. Figure 7.10 illustrates the time-domain evolution of network investment where the initial installment of DLS allows for a period when demand growth can be observed before committing to longer-term network investments. Our analysis indicates that when projected growth is highly uncertain, a flexible valuation framework favors DLS deployment when peak demand growth is slower than anticipated. DLS deployment allows the utility to adopt a *wait and see* strategy without compromising the quality of supply. Finally, since Delhi and other cities in India mostly contract for power, we do not consider the potential value of arbitrage that DLS offers to those utilities that are served by markets. Note that in the analysis, DLS is only

valued based on the peak shifting ability of storage without including the potential added value from ancillary services.

As of 2018, India had installed over 10 million kilometers of electric distribution lines (Central Electricity Authority 2018) with 8% of these lines covering dense urban areas (World Energy Council 2009). Growing urban demand adds to the physical stress on distribution networks and to financial stress on the already strained utilities that operate them (Pargal and Banerjee 2014). An increase in peak demand during the evening hours due to residential space-cooling can overload feeders.

To meet growing peak demand while preserving reliability of service, the system operator must either shed load or invest in network upgrades. Shedding load is increasingly penalized and distribution network upgrades are very costly, especially when they include reconductoring (i.e., replacing or refurbishing conductors in existing lines) in densely populated areas (Horowitz 2019). We identify four megacities in India that accounted

Figure 7.10 Real options framework time series simulation



for 52 terawatt-hours (TWh) of annual electricity consumption in 2019; together, the dense urban areas in these cities are served by an estimated 72,763 circuit kilometers of distribution wires operated by their respective utilities (Central Electricity Authority 2018; Tata Power Delhi Distribution Limited 2016). Without any distribution network expansion and with stable projected demand and AC efficiency, we estimate that 20,373 km of these networks will be overloaded by 2030, meaning that they will be operating at more than 80% of maximum current or ampacity. An additional 23,640 km will be overloaded by 2040 in these megacities, according to our estimates (Barbar, Mallapragada and Stoner, et al. 2022).

Applying our flexible valuation framework to representative feeders and then scaling back the total demand they represent, we estimate that it is cost-effective to install a total of 29 gigawatt-hours (GWh) of short-duration storage (i.e., less than 5–6 hours) by 2030 and 140 GWh by 2040. This would defer 15,914 km of network upgrades for 2030 and an additional 18,127

km for 2040 (Table 7.4). These results assume DLS costs for 2030 to be the same as projected capital costs for transmission-level storage in the annual technology baseline report published by the U.S. National Renewable Energy Laboratory (National Renewable Energy Laboratory 2020; Government of India Ministry of Commerce 2019). From an investment standpoint, deploying DLS before traditional network upgrades are needed produces 16% capital cost savings in 2030 and 15% cost savings in 2040 (Barbar, Mallapragada and Stoner, et al. 2022). More DLS is deployed per unit kilometer in 2040 than in 2030 due to the increasing concentration of load during peak times in projections of future demand (Barbar, Mallapragada and Stoner, et al. 2022). DLS is assumed to remain on the system as long as it is dispatchable, since the longer DLS remains on the feeder, the more value it provides in deferred network investments. The flexible valuation framework yields a useful life range between 5 and 10 years for DLS systems, given the ability to deploy the battery over multiple modeling periods.

Table 7.4 Storage cost impact on outputs of the flexible valuation framework applied to the four Indian megacities for year 2030

| | Low | Mid | High | Breakeven |
|-------------------------------------|--------|--------|--------|-----------|
| Storage energy cost (\$/kWh) | 116 | 168 | 236 | 261 |
| Storage power cost (\$/kW) | 101 | 146 | 205 | 227 |
| DLS energy capacity (GWh) | 29 | 29 | 18 | 0 |
| Deferred upgrades (km) | 15,914 | 15,914 | 11,752 | 0 |

Low-, mid-, and high-cost assumptions for storage technology are sourced from the National Renewable Energy Laboratory (2020).

Table 7.5 Estimated megacity-level DLS potential as a “non-wires alternative” under mid-range cost projections

| | 2019 Demand (TWh) | 2030 | | 2040 | |
|------------------|-------------------|--------------------------|---------------------|--------------------------|---------------------|
| | | Overloaded circuits (km) | DLS potential (GWh) | Overloaded circuits (km) | DLS potential (GWh) |
| Bengaluru | 10 | 1,265 | 3 | 1,467 | 15 |
| Delhi | 23 | 6,093 | 14 | 7,070 | 50 |
| Kolkata | 4 | 792 | 1 | 919 | 35 |
| Mumbai | 15 | 12,224 | 11 | 14,184 | 40 |

Source: Barbar, Mallapragada, and Stoner, et al. (2022).

The determination of optimum DLS capacity is constrained by the cost of storage and by how often it is dispatched. In both the low- and mid-cost storage scenarios (Table 7.4), the flexible valuation framework yields the same results for optimum DLS capacity, which indicates that the only binding constraint is dispatch—i.e., the availability of off-peak network capacity on the feeder to charge DLS for use during peak hours. This result also suggests that DLS may not be viable for heavily loaded feeders that always have high average loading percentages and therefore require traditional network upgrades. Under high storage costs (National Renewable Energy Laboratory 2020), we estimate that cost-effective DLS deployment would defer 11,752 km and 13,717 km of network upgrades in 2030 and 2040, respectively, and would produce corresponding capital cost savings of 12% and 10%—implying, not surprisingly, that at higher costs of storage, less DLS is economic (Barbar,

Mallapragada and Stoner, et al. 2022). Based on extensive sensitivity analysis, we find that the deferral value of DLS is positive in the Indian context assuming storage costs (for a 4-hour battery duration) of less than \$262 per kWh. Table 7.4 summarizes our results applying the flexible valuation framework to the same demand projections under low-, mid-, and high-cost assumptions for storage in 2030.

DLS adoption is driven by potential capital cost savings to distribution utilities who would otherwise have to upgrade their networks. Here, we compare DLS and network upgrade costs, setting aside the question of DLS ownership—that is, who makes the investment. DLS is modeled as a network upgrade strategy to minimize distribution-level capital expenditures. Because DLS systems would be discharged during peak hours and recharged during off-peak hours, deploying storage at the distribution level also provides costless peak

shifting at the transmission level. We estimate greater DLS deployment in Delhi and Mumbai than in Bengaluru and Kolkata in 2030 because Delhi and Mumbai are expected to see higher growth rates for average and peak electricity demand, which leads to more congested urban feeders.

This issue is addressed in the next section, where we use outcomes from our DLS analysis for the four megacities to study how DLS deployment impacts cost-optimal transmission-level resource planning, including investment in generation, transmission, and grid-scale storage. Specifically, the DLS analysis is used to compute a modified regional demand profile, as seen by the transmission system. This modified profile, termed the “DLS demand scenario,” captures the off-peak charging and peak discharging of DLS assets in urban distribution feeders.

Distribution-level storage for network deferral: Comparing the United States and India

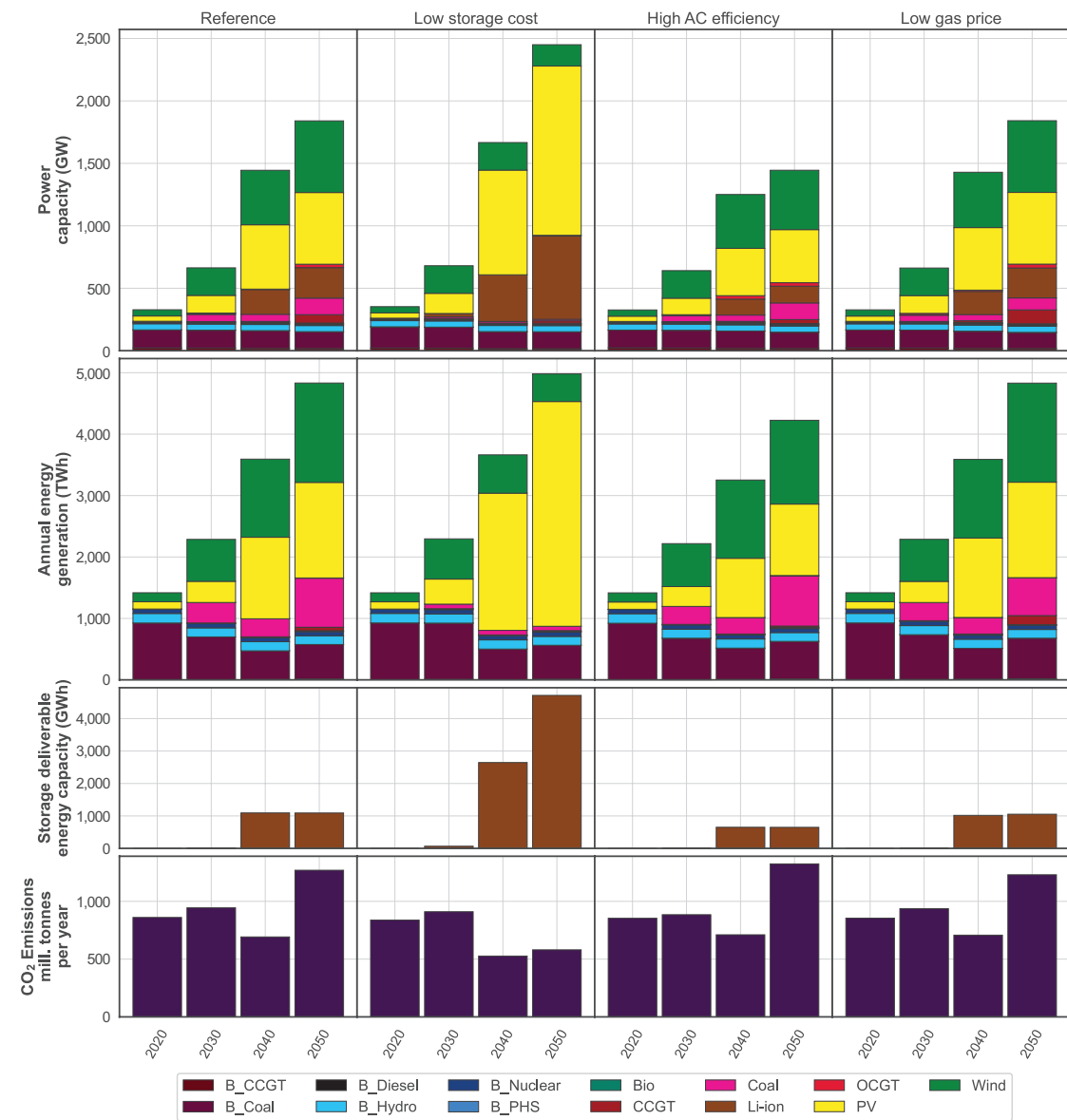
The choice between DLS investments and network upgrades in India is influenced to a far higher degree than in the United States and Europe by the limited availability of low-cost, long-term capital, and by the relative ease with which DLS technologies can be accommodated physically within the urban environment (Stanfield et al. 2017). In addition, expected peak electricity demand is not expected to grow as strongly in the United States as in countries where electricity is not reliably accessible everywhere and space cooling is currently minimal (4% of total Indian electricity consumption in 2018) (International Energy Agency 2018). While U.S. electricity consumption is expected to grow because of electrification in other sectors, notably transportation (e.g., through the proliferation of electric vehicles), this growth relates to distribution network hosting capacity (Electric Power Research Institute 2017). Moreover, demand for EV charging is expected to be more flexible throughout

the day than demand for space cooling, therefore cooling demand is expected to play a greater role in network congestion problems. Storage may serve as an ancillary service in improving resiliency and quality of supply and in expanding the hosting capacity of rooftop PV through arbitrage in settings such as the U.S. market. The use case for storage at the distribution level points to a more essential role in infrastructure planning and capital allocation in EMDE countries than in the developed world. In these countries, the threshold storage cost below which storage deployment in distribution network settings makes sense will likely be lower than the cost threshold for developed regions, including the United States, where lower costs for financing will favor traditional network upgrades at the margin.

7.2.3 Drivers of storage adoption in the bulk power system: Insights from the Indian grid

As noted in Chapter 6, the level of VRE generation is a key driver for cost-optimal storage deployment in the bulk power system. While this relationship likely holds everywhere to some degree, it is notable that socioeconomic factors also have an important influence on cost-optimal storage deployment in EMDE countries. First, rapid growth in electricity demand for air conditioning and, to a lesser extent, for EV charging, is likely to modify temporal patterns of electricity use in EMDE countries. For example, a recent study estimates that space cooling could contribute as much as 45% of peak electricity demand in India by 2050 compared to 10% in 2016 (International Energy Agency 2018). Second, in India and other EMDEs (including Cambodia, Indonesia, and Vietnam), the preponderance of coal over natural gas generation makes VRE deployment (with storage) especially valuable as a means of reducing CO₂ emissions. In these contexts, using renewables to displace a given kWh of coal generation rather than natural gas generation leads to greater CO₂ reductions for

Figure 7.11 Installed capacity (1st row), annual energy generation (2nd row), storage energy capacity (3rd row), and annual CO₂ emissions (4th row) for reference case (1st column), as well as cases with alternative assumptions for battery storage capital cost (2nd column), high AC efficiency (3rd column), and gas prices (4th column)



Detailed assumptions for each case are provided in Appendix D, Table D.4. Resources labeled with a “B_” prefix in the legend refer to existing capacity at the beginning of model horizon in 2020.

the same cost and, consequently, increases the potential value of storage in supporting grid decarbonization (by enabling VRE integration). Third, the relatively higher cost of financing VRE investments in EMDEs favors new fossil generation, although this effect is mitigated somewhat by lower labor costs that make VRE deployment cheaper. This section assesses the interplay between these supply- and demand-side factors in terms of the long-term, least-cost evolution of the bulk power system in India and the role for storage under various technology and policy scenarios. We address supply–demand interactions by using the outputs of the demand-side analysis (Section 7.2.1) as inputs to a high-temporal-resolution CEM with a detailed spatial resolution of VRE resource availability and costs (Jenkins and Sepulveda 2017) (Section 2.1.3). Using this framework, we explore the following questions:

- How do demand-side factors (e.g., AC load growth, DLS deployment) impact investments in energy storage at the transmission level?
- How does the cost and availability of storage and competing technologies (such as natural gas generation) affect long-term prospects for grid decarbonization if there is no carbon constraint or only moderate carbon constraints?

Here we consider only AC demand. The effect of EV demand, which is far smaller, is described in the appendix to this chapter (Appendix D, Figure D.1).

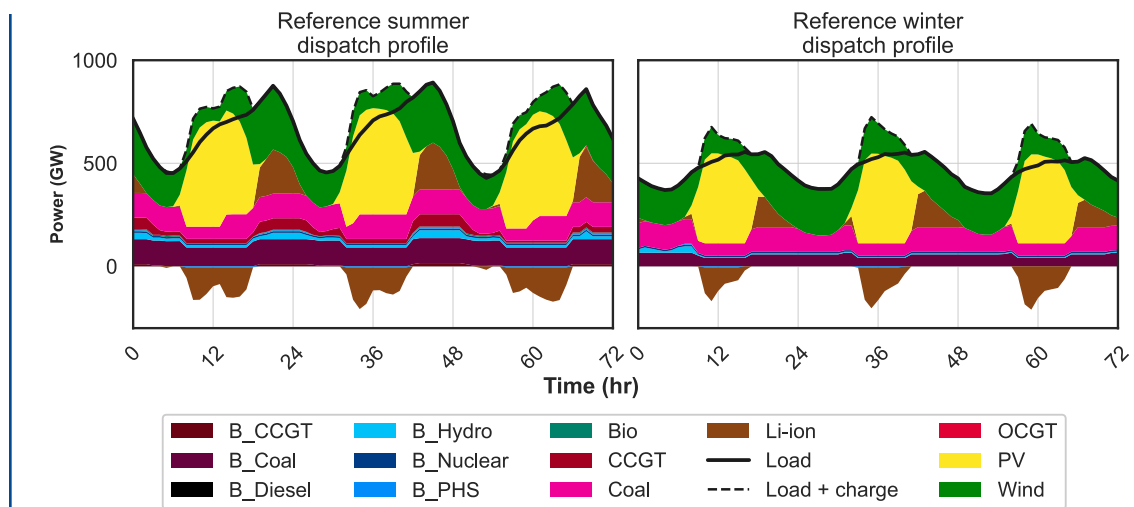
System outcomes under the reference scenario

With business-as-usual demand growth and baseline AC efficiency, and without any carbon policy (defined as the reference scenario in

Table 7.6), we estimate that VRE generation in India could contribute between 46% and 67% of total generation in 2030 depending on the VRE installation limits per investment period enforced in the model to reflect supply chain limitations. These constraints are derived based on fitting the growth curve to trends in VRE capacity deployment seen in China (Barbar, Mallapragada and Stoner 2022). It is important to note that the rates of VRE installation we model are far more aggressive than current trends: For example, in 2019, 3 GW of wind and 10 GW of solar PV were installed in India. Applying our reference assumption about VRE installation limits, the total VRE generation deployed by 2030 contributes to a 56% reduction in CO₂ emissions intensity, compared to 2020. However, absolute CO₂ emissions increase by 47% over the same period because of load growth.² Modeled emissions in 2050 under the reference scenario likewise remain higher than in 2020, even though CO₂ intensity is 52% lower and installed VRE capacity is 3.2 times greater than in 2030: 362 GW and 1,148 GW in 2030 and 2050, respectively (Figure 7.11). Grid-average emissions intensity actually increases again over this period (2030–2050) in the reference scenario because of the addition of new coal capacity in later investment periods to meet continued demand growth. At the same time, VRE growth plateaus due to declining value with increasing penetration. Due to disparities in VRE resource quality and land availability, much of the VRE capacity is concentrated in the southern and western regions of India. This requires a near doubling of transmission capacity between 2020 and 2050 (Figure 7.13). Li-ion battery storage is not cost-competitive until 2040, but by 2050 about 244 GW of Li-ion storage capacity is installed and 1,091 GWh of stored energy is supplied to balance load and minimize VRE curtailment.

² Doubling the VRE installation limits in our model reduces modeled CO₂ emissions by 29%; conversely, capping VRE installation at 50% of the limit assumed in our reference case results in modeled CO₂ emissions that are 34% higher in 2030 than in 2020.

Figure 7.12 Hourly generation dispatch and load profile for three days during summer (left) and winter (right) periods for 2050



Model outcomes are based on the reference case as defined in Table 7.6. Storage charging is shown in the “Load + charge” curve as well as by the negative generation shown for storage. Resources labeled with a “B_” prefix in the legend refer to existing capacity at the beginning of the model horizon in 2020.

As illustrated in Figure 7.12, Li-ion battery storage is dispatched to shift solar generation to meet evening peak demand, with an average storage duration of less than five hours in 2050 (where average storage duration is defined as the ratio of deliverable energy capacity to discharge power capacity per modeling period, multiplied by the discharge efficiency). In the reference case, AC use in the residential and commercial sectors introduces daytime and nighttime peaks in the bulk electricity demand profile and accounts for 15% and 12% of peak and annual demand in 2030, respectively, and 42% and 40% of peak and annual demand in 2050, respectively (Figure 7.14). The importance of AC demand in terms of peak consumption and consequent storage needs is illustrated by the relative difference in storage discharging during the winter and summer peaks shown in Figure 7.12.

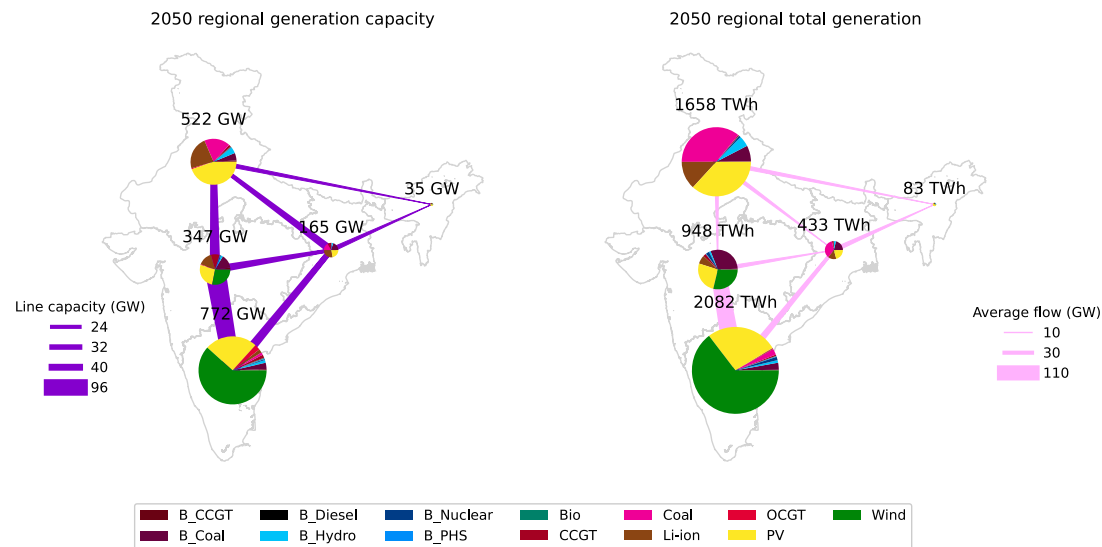
Impact of AC demand

As described earlier, we use a bottom-up demand forecasting model (Barbar, Mallapragada and Alsup, et al. 2021) to evaluate electricity demand under a high-AC-efficiency scenario that assumes India will reduce its AC efficiency gap to align with the global weighted average.³ Figure 7.14 highlights the impact of reduced space cooling needs on peak demand under the high-AC-efficiency scenario compared to the reference scenario.

Our supply–demand modeling approach shows that adoption of higher AC efficiency standards, commensurate with best-in-class global standards (International Energy Agency 2018), could lead to reductions of 22% and 13% in installed capacity and generation respectively, but a 4% increase in annual CO₂ emissions by

³ The assumed SEER rating for our high-AC-efficiency scenario for India is based on the IEA’s Future of Cooling study (International Energy Agency 2018), which considers regional variations in consumer sensitivity to upfront costs vs. operating costs for AC units.

Figure 7.13 Regional capacity and utilization trends for generation and transmission in 2050



Technology names and abbreviations are listed in Appendix D, Table D.3. Resources labeled with a “B_” prefix in the legend refer to existing capacity at the beginning of the model horizon in 2020.

2050 (Figure 7.11, 3rd column). AC demand contributes more than 40% of the evening demand peak (between 8 PM and 12 AM) during the summer season under our reference case assumptions. It contributes less than 20% in the high-AC-efficiency case. Reducing demand reduces capacity and generation requirements. Peak demand reductions also result in a flatter demand profile that reduces the need for peaking generation provided by natural gas plants and battery storage. However, a flatter demand profile also reinforces investment in and utilization of “baseload” generation, which generally involves technologies with high capital costs and low operational costs. Absent a carbon policy, coal (both existing and new) remains a cost-effective baseload generation resource in the Indian context. This explains why grid CO₂ intensity is higher in 2050 in the high-AC-efficiency case than in the reference case (316 vs. 267 gCO₂/MWh).

Moreover, our modeling results point to a relationship between grid-scale storage deployment and AC demand: Under baseline AC demand conditions, 1,091 GWh of storage energy capacity is installed in 2050 (Figure 7.11, 1st column) as opposed to 649 GWh (Figure 7.11, 3rd column) under the high-AC-efficiency demand scenario. This 40% drop in energy storage capacity can be directly attributed to a 55% reduction in the space cooling contribution to peak demand. As seen in Figure 7.12, grid-scale storage is primarily charged by solar power and dispatched in the evening to meet peak demand. It should be noted that India still deploys a relatively large amount of Li-ion battery storage, accounting for 38% of a recent estimate of global grid-scale energy storage capacity in 2040 (BloombergNEF 2019). Finally, tightening AC efficiency standards also avoids energy storage investments in the distribution system that would otherwise be needed to defer network upgrades in the near term (2030).

Table 7.6 Baseline parameters and sensitivity cases

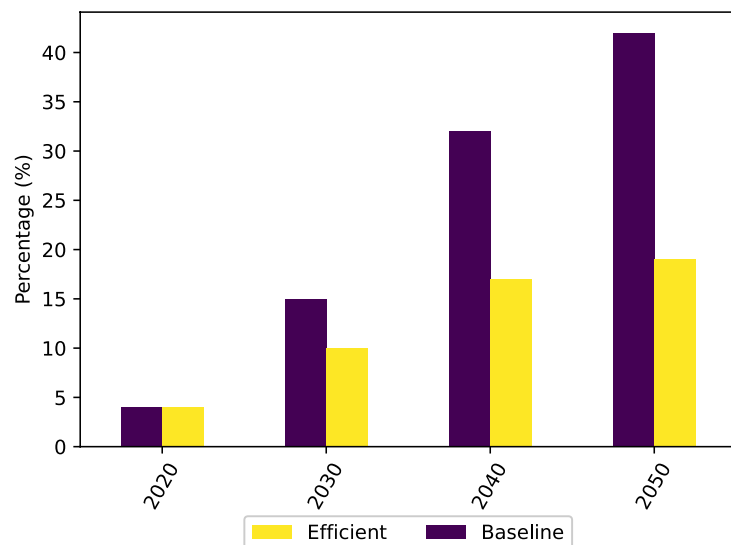
| Parameter | Reference value | Sensitivity cases considered |
|--|---|--|
| Demand projections | Stable GDP growth, baseline AC, evening EV charging | High AC efficiency |
| Gas prices | \$11/MMBtu | \$8/MMBtu |
| Storage costs | Reference as per Appendix D, Table D.4 | Low cost as per Appendix D, Table D.4 |
| Decadal VRE installation limit | Baseline | Half of baseline, no decadal installation limit |
| Li-ion storage capital cost | Reference as per Appendix D, Table D.4 | Low cost as defined in Appendix D, Table D.4 |
| Distribution-level storage deployment | None | Modified load based on distribution-level storage dispatch (section 2.2) |
| CO₂ policy | None | 2030: \$20/tonne, 2040: \$33/tonne and 2050: \$53/tonne |

Impact of supply-side drivers: Cost of storage and natural gas prices

In the low-cost Li-ion storage case (Table 7.4), storage power and energy capacity increase by 424 GW and 3,625 GWh, respectively, which enables 33% more solar and wind generation in 2050 compared to the reference case. This results in 54% lower annual CO₂ emissions compared to the reference case in 2050, the highest reduction among the sensitivity cases we considered (by contrast, Figure 7.11 shows that 2050 emissions are only 3% lower in the low-gas-price case and 4% higher in the high-AC-efficiency case, compared to the reference case). Low-cost storage has the largest impact on emissions primarily because it makes VRE (especially solar) more competitive, which in turn reduces new coal installations 91% by 2050. With low-cost storage reinforcing VRE deployment, VRE supplies 65% of annual generation in 2050. Expanded VRE generation is accompanied by transmission-level storage of average duration under seven hours. The resulting average system cost of electricity in 2040 and 2050 is 22% and 39% lower than in the reference case (see Appendix D, Figure D.7) and required additions of transmission capacity

by 2050 are 92% less than in the reference case (see Appendix D, Figure D.5). At the same time, the low-cost Li-ion storage scenario and the other non-storage-related technology scenarios considered here (i.e., low-cost natural gas and high AC efficiency) affect only the deployment of new coal capacity—they do not impact the phase-out of existing coal generation by 2050 in India. We also evaluated model outcomes using more optimistic Li-ion cost projections than the low-cost storage scenario defined in Table 7.4, to account for the possibility that Li-ion storage follows trends seen for VRE, where costs are lower in India than in the United States. Not surprisingly, model results for these scenarios point to increased VRE generation and reduced coal generation in 2050, compared to the low-cost storage scenario. However, we observe diminishing returns in terms of the incremental VRE generation and CO₂ reductions achievable in 2050 with lower Li-ion storage costs, owing to increasing marginal storage duration requirements to displace coal generation. Finally, due to its large size, India is likely to be a major market for Li-ion energy storage in grid applications by mid-century. Across our scenarios for Li-ion storage costs, gas prices, and AC efficiency, modeled grid-scale storage

Figure 7.14 Cooling demand contribution to peak demand given space cooling demand growth, AC unit sales of various types, and average SEER projections for AC units sold in India



Source: Barbar, Mallapragada, and Alsup, et al. (2021).

energy and power capacity deployments in India by 2040 are between 132 and 668 GW and 649 and 4,716 GWh, respectively.

The role of natural gas in India's electricity system is limited by the relatively high cost of imported fuel (\$11/MMBtu under the reference case) (International Energy Agency 2021) and competition from both coal generation and VRE generation. Peak electricity demand driven by AC demand growth creates the need for peaking generation capacity. Combined cycle gas turbines (CCGT) and open cycle gas turbines (OCGT) are best suited to meet this need, owing to their greater operational flexibility compared to coal power plants and lower capital costs (see Appendix D, Tables D.6 and D.7). Moreover, given the relatively high cost of natural gas vs. coal, natural gas generating capacity is deployed but utilized sparingly, with annual capacity utilization for CCGT and OCGT units at 5% and 3%, respectively, in 2040 (see Appendix D, Figure D.6). Because

of this peak-use pattern, the deployment of new natural gas generating capacity is closely tied to AC demand growth, with the high-AC-efficiency scenario virtually eliminating the need for new gas capacity in 2050 (this can be seen by comparing columns 3 and 4 in Figure 7.11). At the same time, lower gas prices improve the economic viability of natural gas generation, leading to higher CCGT deployment and utilization in 2050 compared to the reference case (see Appendix D, Figure D.6). As a result, the deployment of new coal capacity is reduced by 28%. Low gas prices impact coal and Li-ion storage deployment without significantly changing VRE deployment, resulting in 3% lower (annual) CO₂ emissions in 2050 than in the reference case. With reduced gas prices, Li-ion storage power and energy capacity are, respectively, 2% and 4% lower in 2050, indicating that natural gas generation competes with storage to meet peak demand needs and provide operational flexibility in support of VRE generation.

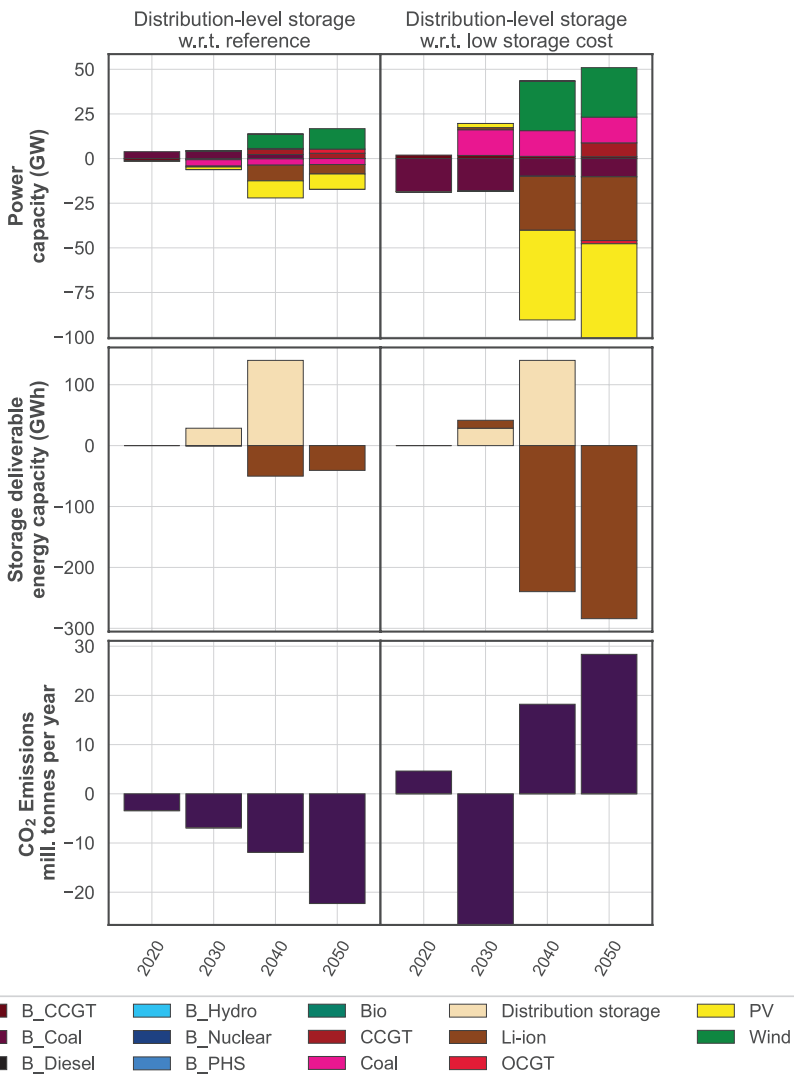
Impact of distribution-level storage (DLS)

The deployment of Li-ion storage to help meet peak demand at the distribution level modifies the demand profile seen by the transmission system owing to the timing and duration of battery charging and discharging. As discussed earlier (Section 7.2.2), we compute such “transmission level” demand for two cases with DLS deployment: (1) the reference demand case (demand driver) and (2) the low storage cost case (technology driver). Because DLS is deployed only when network deferrals are economic (Barbar, Mallapragada and Stoner 2022)—in other words, the present value of investment in battery storage is less than the present value of the network upgrades that can be avoided by implementing battery storage—DLS can be treated as a zero-cost load shifting mechanism for the transmission system. The impact of DLS on the transmission system is captured via the modified demand case that results when DLS is implemented (demand + storage charging - storage discharging; see Appendix D, Figure D.2) without representing DLS capital or operating costs. Across the regions of India we model, cost-optimal DLS sizing points to storage durations of two to four hours, consistent with the duration of periods of peak demand overload and available off-peak charging hours subject to network capacity constraints. For 2030, our modeling shows a total of 93 peak hours shaved with a storage capacity of 29 GWh deployed across the four megacities in the reference case. Figure 7.15 highlights the incremental bulk power system impacts of deploying DLS in the reference and low-cost storage cases (with reference demand assumptions). DLS is charged during off-peak hours, which may not necessarily coincide with periods of peak solar generation because, as modeled, DLS operation aims to minimize peak demand and network upgrade costs rather than maximizing charging with low-marginal cost generation. This results in

DLS charging being spread out throughout the day (Barbar, Mallapragada and Stoner, 2022) such that the incremental demand is met by the cheapest available generation resource, as shown in Figure 7.15 (note that changes in Figure 7.15 are an order of magnitude smaller than the absolute values seen in Figure 7.11).

Consequently, Figure 7.15 shows that DLS deployment tends to shift the installed capacity mix from solar with battery storage to wind, which typically has higher capacity factors at night and in the early morning, as well as coal generation. By 2050, demand growth has reached the point where DLS is no longer cost-effective as an alternative to network upgrades; consequently, DLS capacity is retired. The correlation between storage and peak demand is most pronounced under the low-cost-storage case (Figure 7.15, 2nd column), where DLS-enabled peak shifting has knock-on effects on generation design: With less storage discharging needed during peak hours, less solar capacity is installed to charge up the storage. Since demand is met by either alternative VRE with less intra-day variability (i.e., wind) or coal, DLS reduces the role for solar with storage at scale, even in the low-cost-storage case. Because DLS flattens the demand profile, more than 55 GW of additional capacity is installed by 2050 in the DLS case compared to the low-cost-storage case (Figure 7.15, 2nd column). Much of this additional capacity consists of wind, but it also includes more coal. Overall, factors such as DLS deployment and AC efficiency improvement shift or reduce the demand-side peak. Depending on the cost of storage, these peak effects can indirectly reduce CO₂ emissions (relative to the reference case) or increase emissions (relative to the low-cost-storage case) in 2050. It is worth reiterating that DLS has a modest impact on emissions relative to the differences in overall CO₂ emissions estimated for 2050 across our modeling scenarios (Figure 7.11).

Figure 7.15 Distribution-level storage deployment



Impact on dispatched generation (1st row), installed energy storage capacity (2nd row), and annual CO₂ emissions (3rd row) in the reference case (1st column) and the low-cost-storage case (2nd column) (Barbar, Mallapragada and Stoner 2022). Resources labeled with a “B_” prefix in the legend refer to existing capacity at the beginning of the model horizon in 2020.

At the distribution level, DLS or high AC efficiency are clearly cost saving and can help distribution companies minimize capital investment. However, when aggregating the impacts of DLS at the transmission level or for national planning purposes, the overall system cost of electricity (SCOE) does not improve compared to the reference case (see Appendix D, Table D.2). On a simple SCOE basis, the

flexible option of deferring distribution network investments results in an SCOE of 0.28 \$/MWh in 2030 and 0.36 \$/MWh in 2040. The traditional network investment option yields an SCOE of 0.46 and 0.42 \$/MWh in 2030 and 2040, respectively. Thus, from a distribution system perspective, DLS deployment can deliver a 27% annualized capital investment savings. However, when aggregating DLS effects

at the transmission level for bulk power system planning purposes, the impact on overall system cost may not be strictly positive (Barbar, Mallapragada and Stoner, 2022). Depending on the generation resource(s) used to charge DLS, system costs could increase, particularly in India and in other markets that are heavily dependent on coal generation.

Technology vs. policy drivers

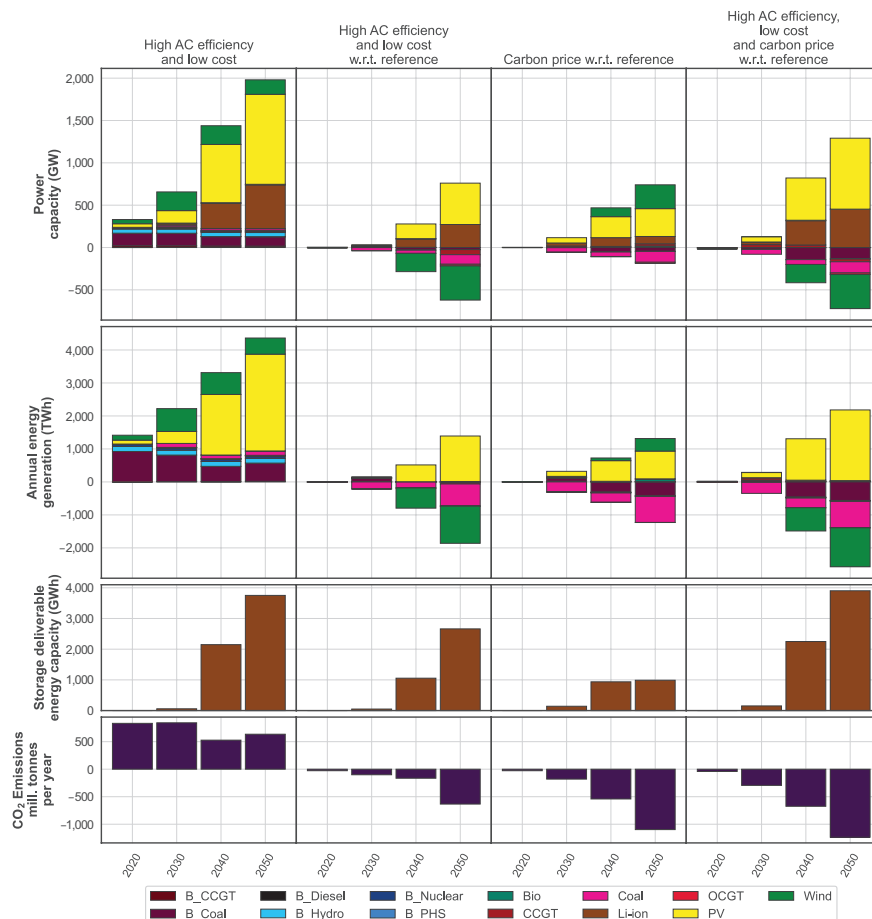
Although faster-than-historical VRE deployment over the next decade can reduce India's annual power sector CO₂ emissions in 2030 compared to 2020, the rapid rise in electricity demand anticipated in later decades and the declining value of VRE with increasing penetration mean that our reference scenario projects an overall increase in coal capacity and 48% higher CO₂ emissions in 2050 compared to 2020. Outcomes for alternative scenarios that explore the impact of individual demand and technology drivers highlight the potential for one or more drivers to minimize investments in new coal capacity that might otherwise be stranded under international climate mitigation commitments. This raises the question whether a combination of policy and technology scenarios will be most beneficial in terms of reducing the potential for stranded coal assets. Figure 7.16 (see also Appendix D, Figure D.8) shows the collective impact of low storage capital costs, low gas prices, and high AC efficiency (we call this combination of assumptions the "high-AC-efficiency/low-cost" case) on the evolution of the power system and highlights the interaction between these supply- and demand-side drivers. As discussed, low gas prices and high AC efficiency favor fossil generation (gas and coal, respectively) over battery storage for meeting peak demand (based on comparing these scenarios to

the reference case), while low storage costs increase the deployment of VRE and storage. Combined, these factors lead to a 112% increase in energy storage power by 2050 in the high-AC-efficiency/low-cost case compared to the reference case (Figure 7.16, column 2), and a 244% increase energy storage capacity (see Appendix D, Figure D.4). This is because a flatter demand profile (on account of high AC efficiency) and lower energy storage costs make it more cost-effective to store energy for longer periods of time (see Appendix D, Table D.5).

Overall, the high-AC-efficiency/low-cost case—of all the individual technology cases we consider—leads to the lowest investments in new coal capacity over the modeled time horizon. As shown in Figure 7.16, it also leads to an 18% reduction in annual CO₂ emissions compared to the reference case in 2050. Yet, even in the high-AC-efficiency/low-cost case, existing coal capacity still accounts for 17% of total generation as late as 2050. This suggests that demand- and supply-side mechanisms are insufficient to achieve deep grid decarbonization and that additional policy measures may be needed. As one potential policy measure, Figure 7.16 shows the impact of a CO₂ price that starts at \$20 per metric ton (tonne) in 2030 and increases by 5% annually, approaching \$50/tonne by 2050.⁴ Compared to the reference case (Figure 7.16), the expectation of a rising CO₂ price leads to reduced utilization and early retirement of existing coal and the near-complete displacement of new coal, as well as increasing investments in low-carbon generation, mainly VRE, and storage. This reduces CO₂ emissions in 2050 by 86% compared to the reference case. The relatively large impact of a \$50/tonne carbon price on SCOE in 2050 (see Appendix D, Figure D.7) can be mitigated somewhat by the adoption of more efficient

⁴ There is precedent for carbon pricing in India. Since 2010, India has imposed a cess (or tax) on coal production, which has increased steeply from INR 50 (\$0.70)/tonne coal in 2010 to INR 400 (\$5.61)/tonne coal since 2016 (INR=Indian rupee). This policy is included in India's "nationally determined contribution" or NDC under the Paris Agreement (International Institute for Sustainable Development 2018).

Figure 7.16 Model outcomes for the high-AC-efficiency/low-cost case (defined by low battery storage capital cost, high AC efficiency, and low gas prices) (1st column) and for the impact of a carbon price with and without scenario assumptions



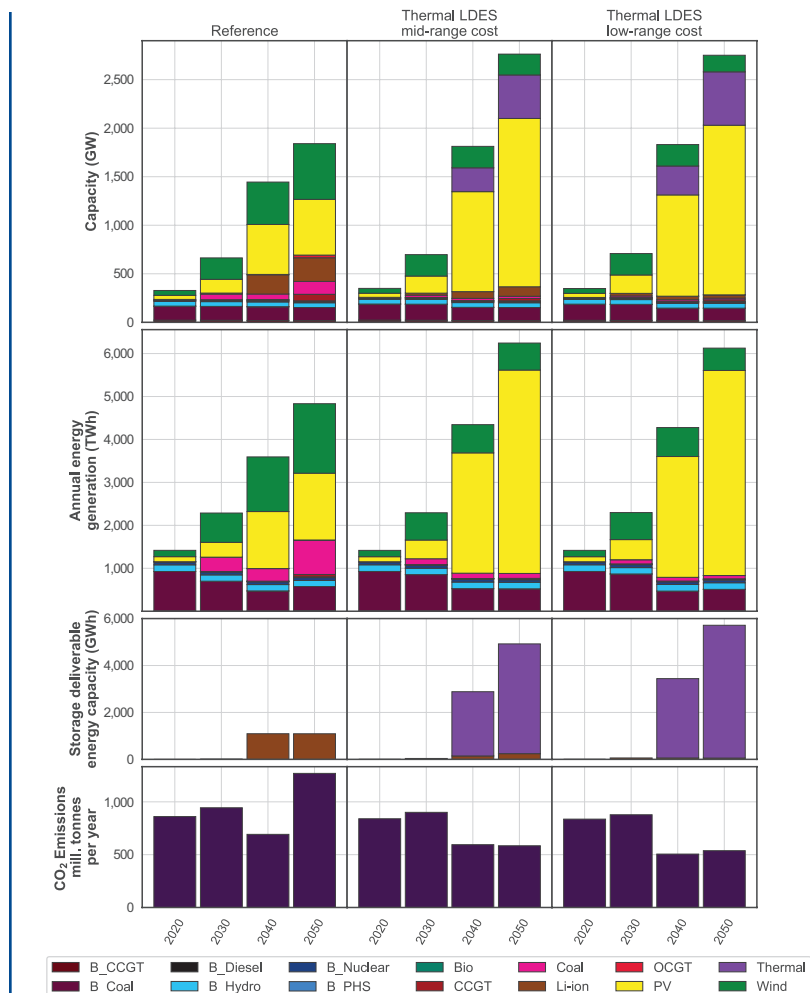
Model outcomes include installed capacity (1st row), generation (2nd row), energy storage capacity (3rd row), and annual CO₂ emissions (4th row). Columns 2–4 highlight outcomes with regard to (w.r.t.) the reference case for the following cases: high-AC-efficiency/low-cost case (2nd column); carbon price case, where CO₂ price starts at \$20/tonne in 2030 and grows by 5% each year (3rd column); and high-AC-efficiency/low-cost + carbon price case (4th column). Resources labeled with a “B_” prefix in the legend refer to existing capacity at the beginning of the model horizon in 2020.

AC technology, whether motivated by favorable cost considerations or policy. Assuming universal adoption of efficient AC, a carbon price of \$50/tonne, and the retirement of all existing coal generation produces an estimate of 2050 CO₂ emissions that is 97% lower than the reference case estimate, with system average emissions at 8 gCO₂/kWh (Figure 7.16, column 4).

Impact of long-duration storage availability

The model results presented in Chapter 6 for several U.S. regions, together with the low-cost Li-ion storage scenario discussed as part of our assessment of DLS impacts in Section 7.2.3 of this chapter, emphasize the importance of access to low-cost capital for both VRE and storage deployment, and consequently for grid decarbonization. The expected downward

Figure 7.17 Model outcomes for the reference case (1st column) and mid- and low-cost LDES cases (2nd and 3rd columns respectively)



Model outcomes include installed capacity (1st row), generation (2nd row), energy storage capacity (3rd row), and annual CO₂ emissions (4th row). Resources labeled with a “B_” prefix in the legend refer to existing capacity at the beginning of the model horizon in 2020.

trend in technology costs (also discussed in previous chapters), including particularly costs for long-duration energy storage (LDES), will also be important. Here, we explore how the availability of LDES technology, starting in 2040, is likely to affect the evolution of the bulk power system in India. For our analysis, we use thermal storage as the representative LDES technology and examine its role under different carbon policy scenarios, including a reference case that assumes no carbon policy and a scenario in which the carbon price increases

linearly from \$20/tonne in 2030 to near \$50/tonne by 2050. We also consider the role of LDES technology under alternative cost and performance assumptions (namely low- and mid-range cost assumptions, held constant for 2040 and 2050, as described in Table 6.3 of Chapter 6).

Figure 7.17 shows that LDES with thermal storage attributes is deployed in India in our reference case, and that it reduces VRE curtailment by 76% and increases VRE capacity by

70% in 2050 (assuming mid-range LDES costs). Because the charge energy and discharge power capacities⁵ of LDES technologies such as flow batteries can be independently sized, these technologies can be optimized to maximize capacity utilization and thereby minimize cost. Comparing our mid- and low-cost LDES (thermal) cases to the reference case (which shows a 48% increase in CO₂ emissions between 2020 and 2050), LDES availability contributes to reducing coal generation by 53%–58%, CO₂ emissions by 54%–58%, and total system costs by 56%–59% in 2050. Our results also show partial substitution of Li-ion storage with LDES deployment where lower energy capital costs for LDES favor greater substitution of Li-ion energy capacity over power capacity. Without LDES, installed energy storage capacity in 2050 can meet two hours of mean system load.⁶ With LDES, by contrast, installed energy storage capacity increases to 8.6 and 10.4 hours of mean system load for the mid- and low-cost scenarios, respectively.

Despite these favorable outcomes, LDES technology deployments alone are insufficient to completely displace new coal generation and have a relatively minor impact on the existing coal fleet. In contrast, Figure 7.18 shows that under a carbon price, the availability of LDES could make it cost-optimal to fully displace new coal generation and eliminate existing coal by 2050. This results in the virtual elimination of coal use by 2050 and a 97%–98% reduction in annual CO₂ emissions relative to 2020 for the low- and mid-cost LDES (thermal) scenarios, respectively. LDES availability in these scenarios also reduces total discounted system costs by 56%–62% compared to a carbon policy scenario without LDES deployment (see Appendix D, Figure D.9). This highlights the

pivotal role that access to LDES technologies like thermal storage can play in decarbonizing grids in EMDE countries that currently rely on coal generation.

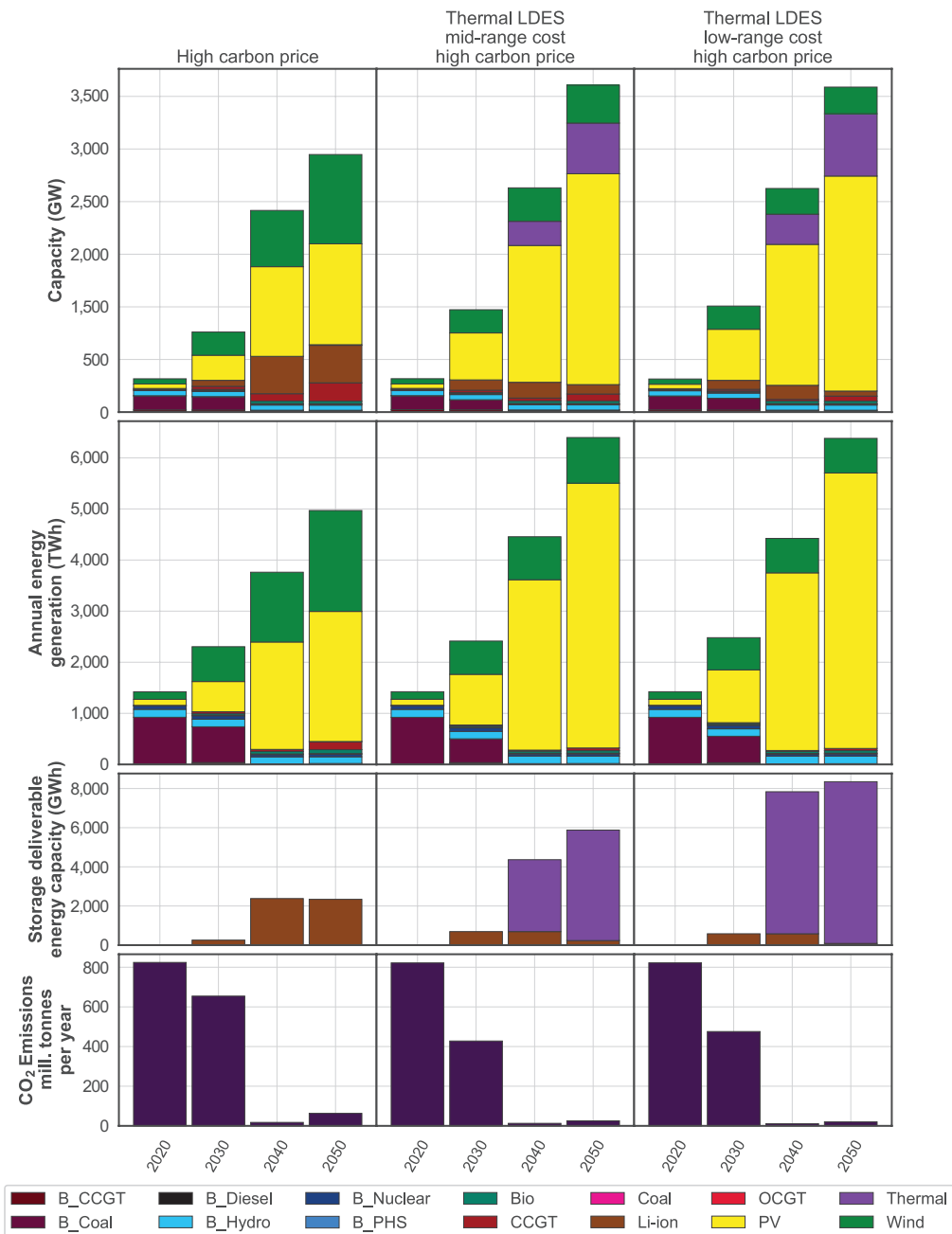
7.3 Assessing the role of energy storage in supply-constrained development contexts

In EMDE countries where generation is often insufficient to meet load, rolling blackouts are commonplace. Nigeria, where electricity generation capacity is just 26% of peak demand, is an example (Olatunji et al. 2018). Commercial and industrial (C&I) customers who require reliable power typically have to install large backup generators (usually diesel) or contract with minigrid developers. Electricity from minigrids, which is commonly provided by a combination of solar PV with batteries or diesel generation, whether contracted or owned by the user, is typically significantly more expensive than grid-supplied electricity. The Nigerian distribution utility, Abuja Electric Distribution Company (AEDC), recently introduced a program called “Distributed Energy Solutions and Strategy for AEDC” (DESSA) in an effort to provide reliable, lower-cost service to willing customers by efficiently combining local backup power, provided by a third party, and grid service, when available. Under the DESSA program, the regulator permits the distributor to contract with a third party to supply power to its customers within a portion of its service territory for an agreed portion of the day at a tariff negotiated separately between those customers and the third-party supplier, subject to regulatory approval. At other times of the day, the distributor (in this case, AEDC) is obligated to supply the same customers at the regulated tariff and must pay a penalty to the third party if grid supply is unavailable.

⁵ This description is also applicable to hydrogen storage, but not to electrochemical storage systems like Li-ion or metal-air batteries where charge and discharge capacity are constrained to be the same.

⁶ To compute hours of mean system load, we take the ratio of total storage deliverable energy capacity (i.e., product of storage energy capacity times discharge efficiency) to mean annual system power demand. This ratio provides a measure of how long storage can serve mean system power demand.

Figure 7.18 Model outcomes for the high carbon price case (1st column) and the mid- and low-cost LDES with high carbon price cases (2nd and 3rd columns respectively)



Model outcomes include Installed capacity (1st row), generation (2nd row), energy storage capacity (3rd row), and annual CO₂ emissions (4th row).

At such times, the third-party provider is obligated to supply the customer. Depending on the predictability and duration of outages, and the temporal character of the load, the third-party supplier generally seeks to design a hybrid generator that minimizes the sum of the supplier's fixed and operating costs. This generally involves a combination of PV with battery backup, plus a diesel generator (Perez-Arriaga and Stoner 2020). Under present conditions, the third-party supplier is charged a distributed use of system (DUoS) fee when the supplier distributes power through the grid network infrastructure. AEDC does not currently have a program to buy excess generation from third-party suppliers.

Our analysis is solely concerned with the design and cost of the generation system. Here, we investigate hybrid generation designs under various grid outage simulations to assess the role of storage in a supply-constrained environment such as Nigeria, where failure to meet load at the distribution level is generally due to under-supply at the bulk power level and not, as in urban India, due to network congestion. We do not discuss storage at the transmission level because storage cannot usefully alleviate the overall supply deficit—instead, storage can only be used to move supply shortfalls from one place, or one period, to another. The customers served by a third-party hybrid generation system are assumed to be connected to an existing local network, which in turn is connected to the grid via a suitable transformer. We refer to this as a “minigrid.”

7.3.1 Approach

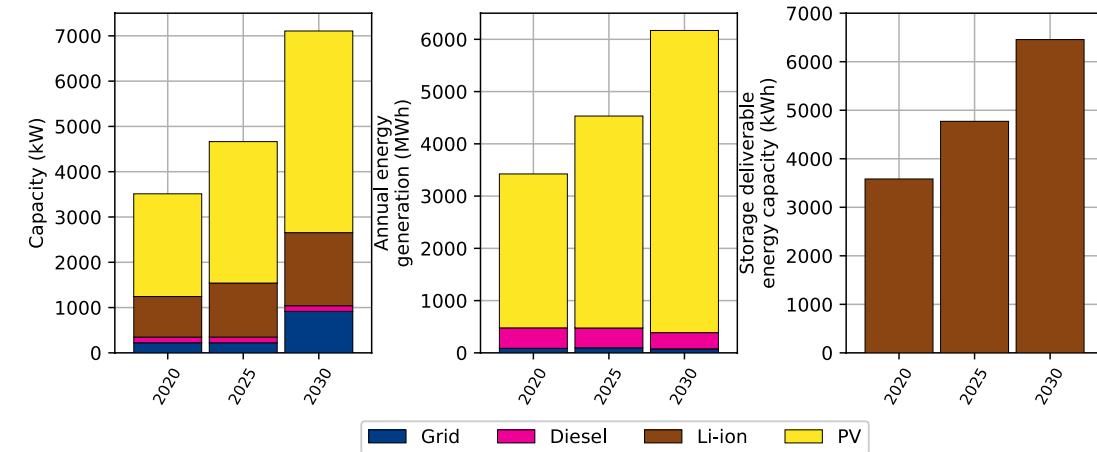
We use an hourly, operations-based design optimization model to size the least-cost minigrid system under different grid availability scenarios. The resources considered are solar generation, battery storage, diesel backup generation, and grid supply. The model's objective function includes annualized investment

and operational costs for the above-mentioned resources. These costs are minimized subject to operational constraints related to (1) hourly solar and grid-supply resource availability throughout the year and (2) short-duration battery storage operation, accounting for inter-temporal storage balance and constraints with respect to maximum rate of charging, discharging, and battery degradation. We include the following charges in the model: (1) DUoS charge, referring to the per-kWh fee the developer pays the utility for using the distribution network, and (2) a developer tariff, which refers to the per-kWh price at which the developer buys power from the utility to either supply consumers or charge the battery storage system. Grid availability is constructed as an hourly time series by including outages, of randomly simulated frequency and duration, in each modeled period (see Appendix D, Table D.10). For each investment period, the resulting linear program generates a deterministic solution given the grid availability specified. To explore the evolution of minigrid design and resource mix over time, we carry out a multi-period myopic optimization over three investment periods: 2020, 2025, and 2030. In this optimization, the design from one period is used as the initial condition for the next period (e.g., the design for 2020 sets the initial condition for 2025), with the ability to add or retire capacity as required to meet the load specified for that period. To study the impact of uncertain grid outages, we perform a Monte Carlo simulation using the ensemble of grid availability profiles described in Appendix D, Table D.10. We report the most frequently occurring system design for the ensemble.

7.3.2 The role of storage in grid-connected minigrids: Insights from Nigeria

For our case study we use the load profile of Wuse Market in Abuja, Nigeria. Wuse Market is an open-air merchandise and food market; it hosts more than 2,155 small businesses

Figure 7.19 Minigrid design results without any simulated grid outages



The reference case assumes mid-range costs for solar generation and Li-ion battery storage (National Renewable Energy Laboratory 2020) (see Appendix D, Tables D.8, D.9, and D.10).

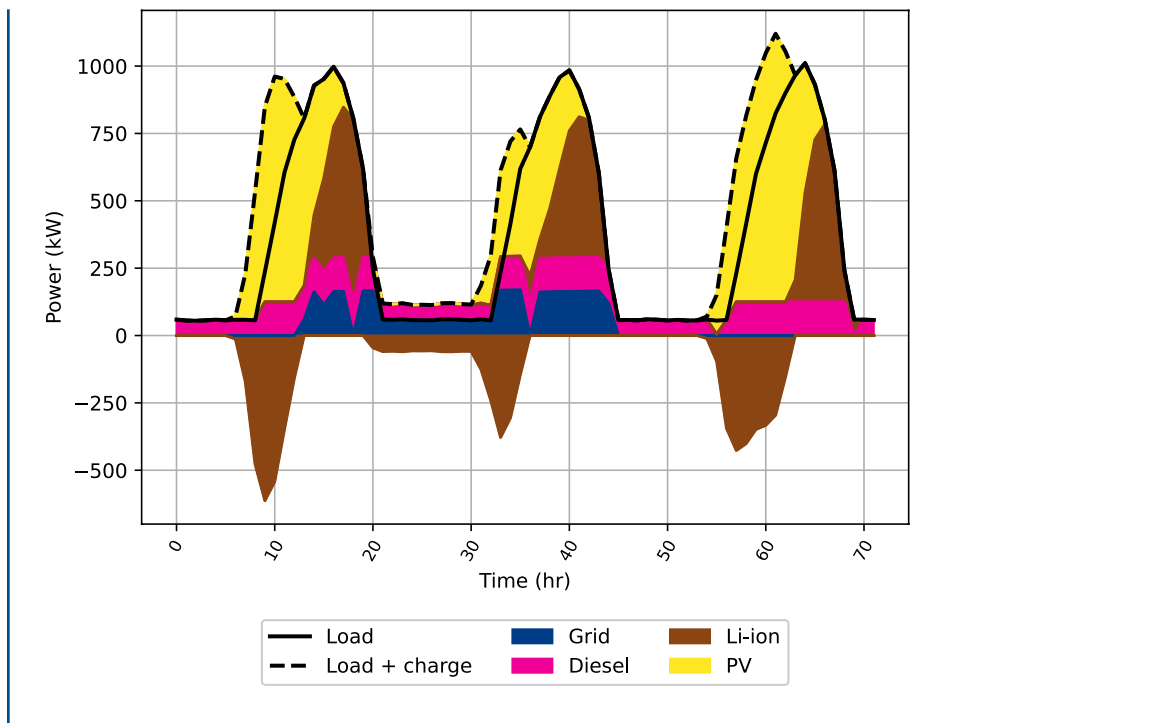
and generated peak demand of 993 kW in 2019. This peak occurs between the hours of 1 pm and 4 pm. At night, when the market is closed, load—mostly from a shared cold storage room—is modest. Annual grid generation supplied to Wuse Market was 10% of total annual grid demand in 2018. Using the approach described above, we model the cost-optimal design of the generation system under specified PV and Li-ion battery costs (National Renewable Energy Laboratory 2020), taking into account known negotiated tariffs for the third-party generator and regulated tariffs available to the utility (Abuja Electric Distribution Company 2019), local diesel fuel costs (\$2.20 per gallon) (National Bureau of Statistics, Nigeria 2021), local diesel generator costs (Ciller et al. 2019) (see Appendix D, Tables D.8 and D.9), and projected demand growth for Wuse Market through 2030 (Abuja Electric Distribution Company 2019). We find that the cost-optimal generation mix under these assumptions is primarily from solar with battery storage to extend service into the

late afternoon. Figure 7.19 presents our reference case results with grid supply availability corresponding to AEDC’s forecast of scheduled grid outages in the 2020 and 2025 periods (see Appendix D, Table D.10). No outages are forecasted for the 2030 period.

Under economic dispatch, the minigrid developer may opt to not dispatch available grid supply to meet demand if another resource is available at a lower cost, and instead use grid supply to charge the battery storage system, as seen in Figure 7.20. Diesel generation primarily serves nighttime demand and is available as a generation source during scheduled grid outages. The economically dispatched minigrid has a system cost of electricity generation and operation of \$0.30/kWh in 2020, while the leveled cost of diesel generators ranges between \$0.30 and \$0.60 per kWh for capacity factors of 36% and 16%, respectively.⁷ The lower upfront cost of diesel generators makes them attractive to minigrid developers for meeting nighttime demand and to provide

⁷ Over the lifetime of the minigrid, the leveled cost of electricity supply (including capital investment and operation) ranges between \$0.20 and \$0.60 per kWh in Nigeria (Roche, Ude and Donald-Ofoegbu 2017).

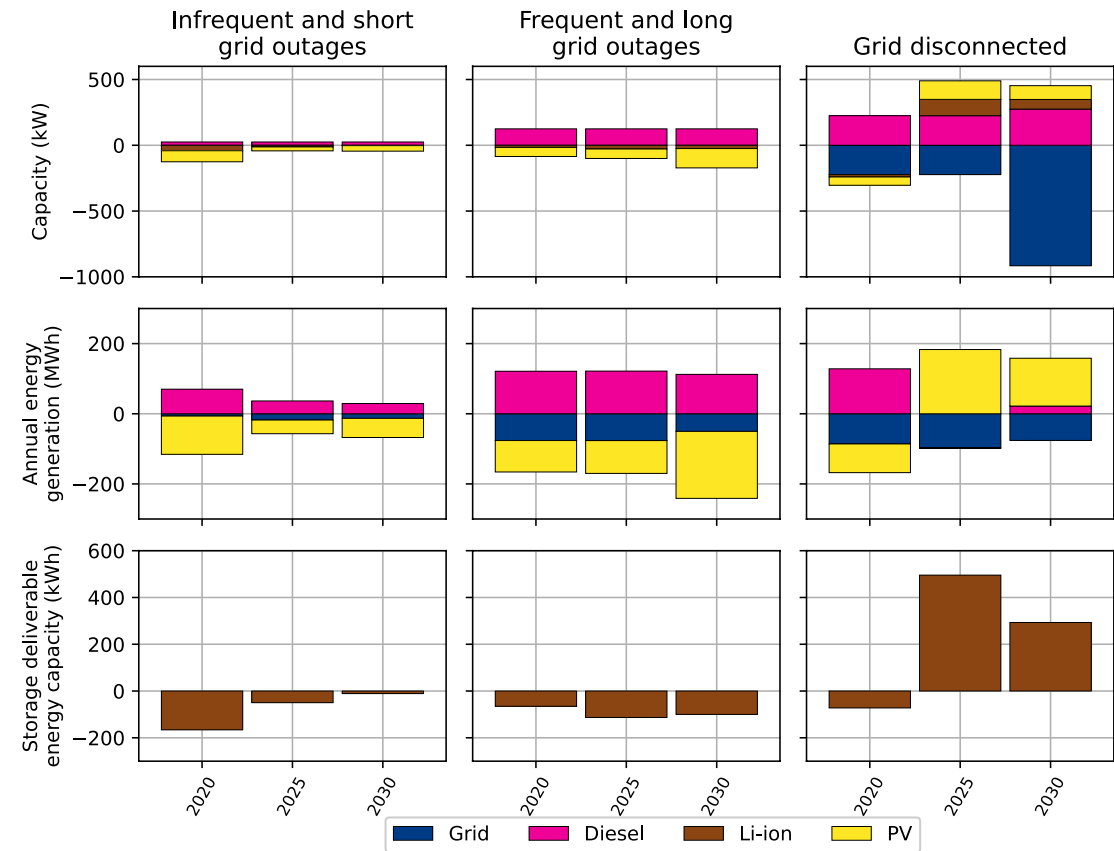
Figure 7.20 Minigrid hourly dispatch without any simulated grid outages (reference case)



backup generation during grid outages. Therefore, even under low storage cost assumptions (see values in Appendix D, Table D.4), we find that diesel generation is included, albeit at 68% less capacity than in the reference case (Appendix D, Figure D.10). Low-cost storage leads to expanded PV installation but reduces the need for grid supply. Under prevailing tariff rates (Abuja Electric Distribution Company 2019), grid supply becomes less competitive with off-grid generation (via storage discharge) during certain hours of the day due to the fixed operation and maintenance costs of the seldom-used distribution network, which is extended to Wuse Market. Note that grid supply profits from economies of scale under normal operating conditions and therefore is more economically viable than a minigrid system. Nevertheless, due to upstream generation shortages, tariffs negotiated with AEDC are necessarily higher to recover fixed operation and maintenance costs.

To understand how grid outages affect the role and value of storage, we investigate optimum system operation and sizing under conditions of uncertain grid supply—in other words, when generation outages are random rather than scheduled. Figure 7.21 highlights the results of three simulations when compared to the reference case: (1) infrequent grid outages, (2) frequent grid outages, and (3) grid disconnection (i.e., no grid availability). Grid outages are simulated at a decreasing rate per modeled period (Appendix D, Table D.10). Figure 7.21 shows that unscheduled grid outages tend to favor diesel generation since it is dispatchable and has low capital costs. Furthermore, the installation of storage energy capacity decreases compared to the reference case under the different grid outage schemes modeled. Focusing on the first period (2020)—when the initial investment in the minigrid takes place under the highest frequency and length of outages per modeling period—we note that

Figure 7.21 Cost-optimum minigrid design (compared to reference case) under conditions of infrequent outages (1st column), frequent outages (2nd column), and no grid connection (3rd column)



Outages are randomly simulated by frequency and duration. Infrequent outages occur less than once a week for less than 6 hours. Frequent grid outages occur more than once a week (less than seven times) and last up to 12 hours. Grid outage duration and frequency are simulated to decline over the modeled periods as per Table D.10 in Appendix D.

more frequent grid outages result in more diesel generation and less storage capacity installed on the system (Figure 7.21). When the grid is disconnected, storage complements PV installation. The grid–diesel–storage relationship described above and illustrated in Figure 7.21 remains the same under low storage cost assumptions (see Appendix D, Figure D.11). We conclude that battery storage plays a limited role in the short term in providing backup for C&I minigrid customers, given grid supply uncertainty. Moreover, with the expectation

that grid supply will improve over time, storage is not an economically viable solution since the return on investments in storage as a backup solution for outages would decline as more grid supply becomes available at lower cost. The role of storage in a supply-constrained environment is limited to complementing VRE deployment. Note that the situation for AEDC may be similar to that of the distribution utility in Delhi with energy storage functioning as a non-wires alternative for deferring network upgrades *once the grid is adequately supplied*.

7.4 Conclusion and key takeaways

This chapter considers storage in the context of three distinct use cases that are typical of countries with emerging markets and developing economies (EMDE):

1. Distribution system storage applications in demand-driven countries (e.g., India), where storage can serve as a non-wires alternative to defer expensive distribution system upgrades that would otherwise be required to address rapidly growing peak load, primarily driven by growth in air conditioning (AC) loads.
2. Generation and transmission system storage applications in demand-driven countries where the overall growth in electricity demand and a shift toward increased reliance on VRE generation drive storage adoption (this use case has some commonalities with the situation in developed countries that are facing similar changes in their generation mix).
3. Applications in supply-constrained countries (e.g., Nigeria), where uncertainty regarding the duration and timing of grid availability to meet demand is a key driver for storage use as an alternative to on-site self-generation using petroleum fuels.

Key takeaways from our analysis of distribution system storage applications in India:

- India, like many other EMDE countries, is experiencing sustained, rapid electricity demand growth. The need to serve peak loads on residential distribution systems where peak demand is growing even faster than overall demand provides an important use case for storage.

- Compared to developed countries, the electrification of transport plays a much smaller role in driving projected peak demand growth. This primarily reflects the much larger role of two- and three-wheeled vehicles in India.
- Based on an analysis of four major cities in India, cost-effective applications of battery storage to defer distribution upgrades that would otherwise be necessary to accommodate rapidly rising peak residential loads are economically attractive. Our analysis shows that distribution system applications in India's four major megacities could absorb up to 140 GWh of short-duration (Li-ion battery) storage by 2040. Several factors explain the relatively large role for storage in distribution system applications in India compared to the situation in the United States and other developed countries:
 - In general, urban distribution systems are significantly more congested in India than in developed countries. In Delhi, for example, available feeder data indicate that 28% of feeders are loaded, on average, at 60% or more of their capacity. By contrast, feeders in National Grid's service territory in the U.S. state of Massachusetts have average loadings of 34% of capacity.
 - High financing costs in India increase the relative value of storage to defer wire upgrades in distribution networks.
 - Air conditioning rather than electric vehicle charging is the primary driver of projected demand growth in India's major cities. Moreover, the characteristics of AC use in developing countries such as India (e.g., reliance on split AC units rather than centralized AC units) make AC use less flexible than in developed countries and contribute to higher and more concentrated peaks in electricity demand.

Key takeaways from our analysis of grid storage applications in India:

- Additional demand through 2050 can be largely met with a combination of VRE generation and short-duration (Li-ion battery) storage, while substantially reducing reliance on coal and/or gas generation relative to current levels. This will require a rate of VRE deployment that far exceeds historical trends. New and existing coal continues to be used as a major generation source through 2050 unless constrained by policy. The same is not true for natural gas because of its high cost.
- Short-duration (Li-ion battery) storage at the transmission level can cost-effectively accommodate the substantial VRE generation likely to be installed by 2050 in India. Short-duration storage requirements are closely tied to electricity demand for space cooling; these requirements decline with high AC efficiency.
- Due to its large size, India is likely to be a major market for grid applications of Li-ion energy storage by mid-century. For example, across the different scenarios for Li-ion storage cost, natural gas prices, and AC efficiency evaluated in this study, grid-scale Li-ion storage power and energy capacity deployments in India by 2040 could be as high as 668 GW and 4,716 GWh, respectively.
- If long-duration energy storage (LDES) technologies with independently sized charge and discharge rates, higher energy capacity, and lower capital cost than Li-ion batteries become available, LDES can substantially displace new coal generation and reduce grid CO₂ emissions in 2050, even absent policies to constrain emissions. A moderate carbon price, starting at \$20/tonne in 2030

and approaching \$50/tonne in 2050, is sufficient to virtually displace all new coal and substantially reduce existing coal generation by 2050. Coupling such a carbon policy with other favorable technology scenarios, such as low-cost Li-ion storage plus high AC efficiency plus low gas prices (\$8/MMBtu) or access to LDES technologies with the above-mentioned characteristics, could virtually eliminate coal use and achieve near-complete grid decarbonization by 2050, while also partly mitigating system cost increases due to carbon constraints.

Key takeaways from our analysis of the role of storage in supply-constrained electricity systems:

- Battery storage within the transmission or distribution systems of countries that are undersupplied with generation offers a potentially important means of improving service reliability for short-duration outages, reducing diesel consumption by residential and commercial consumers, and reducing these consumers' overall electricity costs (including for diesel backup).
- In some residential and commercial settings, grid-interactive PV with storage backup systems and grid-interactive minigrids may be sized to be competitive with diesel backup when grid outages are predictably frequent and of short duration (i.e., several hours). If, however, outages are unpredictable and potentially long, creating the need for long-term backup that is rarely used, then the economics favor diesel backup, even absent the fuel subsidies that are common among EMDE countries.

References

- Abuja Electric Distribution Company. 2019. *Wuse market energy audit report*. Technical report, Abuja Electric Distribution Company.
- Ali, Sahil. 2018. "The future of Indian electricity demand: How much, by whom and under what conditions?" Technical report, The Brookings Institute. <https://www.brookings.edu/wp-content/uploads/2018/10/The-future-of-Indian-electricity-demand.pdf>.
- Barbar, Marc. 2019. "Resiliency and reliability planning of the electric grid in natural disaster affected areas." Master's thesis, Massachusetts Institute of Technology. <https://dspace.mit.edu/handle/1721.1/122752>.
- Barbar, Marc, Dharik S. Mallapragada, and Robert Stoner. 2022. "Impact of demand growth on decarbonizing India's electricity sector and the role for energy storage."
- Barbar, Marc, Dharik S. Mallapragada, Meia Alsup, and Robert Stoner. 2021. "Scenarios of future Indian electricity demand accounting for space cooling and electric vehicle adoption." *Nature Scientific Data*.
- Barbar Marc, Dharik S. Mallapragada, Robert Stoner, 2022, "Decision making under uncertainty for deploying battery storage as a non-wire alternative in distribution networks."
- Batra, Rakesh, Somesh Kumar, Shuvendu Bose, Regan Grant, Kany Garg, Shikhar Gupta, Randall J. Miller, et al. 2018. *Standing up India's EV ecosystem— who will drive the charge?* Ernest and Young.
- BloombergNEF. 2019. "New Energy Outlook 2019." BNEF.
- Brown, Patrick R., and Audun Botterud. 2020. "The Value of Inter-Regional Coordination and Transmission in Decarbonizing the US Electricity System." *Joule* (Cell Press). doi:10.1016/j.joule.2020.11.013.
- Brown, Richard E. 2017. *Electric power distribution reliability*. CRC Press.
- Burger, Scott P., Jesse D. Jenkins, Carlos Battie, and Ignacio J. Perez-Arriaga. 2019. "Restructuring Revisited Part 2: Coordination in Electricity Distribution Systems." *The Energy Journal* (International Association for Energy Economics (IAEE)) 40. doi:10.5547/01956574.40.3.jen.
- Central Electricity Authority. 2018. "Growth of Electricity Sector in India from 1947-2019." Central Electricity Authority.
- . 2018. "Guidelines for distribution utilities for development of distribution infrastructure." *Guidelines for distribution utilities for development of distribution infrastructure*. Central Electricity Authority, Government of India, Ministry of Power.
- . 2018. *National Electricity Plan Volume 1: Generation*. Delhi, India: Ministry of Power, Government of India. https://cea.nic.in/wp-content/uploads/2020/04/nep_jan_2018.pdf.
- . 2017. *Revised Draft National Electricity Plan Volume II: Transmission*. Technical report, Ministry of Power, Government of India, Delhi, India: Central Electricity Authority. <https://powermin.nic.in/sites/default/files/uploads/NEP-Trans.pdf>.
- Central Electricity Regulatory Commission. 2018. "Discussion Paper on re-designing Real Time Electricity Markets in India." *Discussion Paper on re-designing Real Time Electricity Markets in India*. CERC.
- Ciller, Pedro and Ellman, Douglas and Vergara, Claudio and González-García, Andrés and Lee, Stephen J. and Drouin, Cailinn and Brusnahan, Matthew and Borofsky, Yael and Mateo, Carlos and Amatya, Reja and Palacios, Rafael and Stoner, Robert and de Cuadra, Fernando and Pérez-Arriaga, Ignacio. "Optimal Electrification Planning Incorporating On- and Off-Grid Technologies: The Reference Electrification Model (REM)". *Proceedings of the IEEE*, vol. 107, no. 9, pp. 1872-1905, Sept. 2019, doi: 10.1109/JPROC.2019.2922543.
- Colelli, Francesco Pietro, and Enrica De Cian. 2020. "Cooling demand in integrated assessment models: a methodological review." *Environmental Research Letters* (IOP Publishing) 15: 113005. doi:10.1088/1748-9326/abb90a.
- Debnath, Kumar Biswajit, and Monjur Mourshed. 2018. "Challenges and gaps for energy planning models in the developing-world context." *Nature Energy* 3: 172-184. doi:10.1038/s41560-018-0095-2.
- Deshmukh, Ranjit, Amol Phadke, and Duncan S. Callaway. 2021. "Least-cost targets and avoided fossil fuel capacity in India's pursuit of renewable energy." *Proceedings of the National Academy of Sciences* (National Academy of Sciences) 118. doi:10.1073/pnas.2008128118.
- Deshmukh, Ranjit, Grace C. Wu, Duncan S. Callaway, and Amol Phadke. 2019. "Geospatial and techno-economic analysis of wind and solar resources in India." *Renewable Energy* 134: 947-960. doi:<https://doi.org/10.1016/j.renene.2018.11.073>.
- Electric Power Research Institute. 2017. "Distribution Resource Integration and Value Estimation (DRIVE)." Technical report.

- Evans, Anna. 2020. "The value of flexibility: Application of real options analysis to electricity network investments." Master's thesis, Massachusetts Institute of Technology. <http://dspace.mit.edu/handle/1721.1/7582>.
- Gamesa. 2017. "G126-2.5 MW." *G126-2.5 MW*. <http://docplayer.net/24040007-Gamesa-gmw-greater-energy-produced-from-low-wind-sites-minimum-power-density-improved-coemaximum-profitability.html>.
- Garg, Amit, Jyoti Maheshwari, and Jigeesha Upadhyay. 2010. "Load Research for Residential and Commercial Establishments in Gujarat." Technical report, Indian Institute of Management Ahmedabad.
- Government of India Ministry of Commerce. 2019. "Index Files For WPI Series."
- Government of India National Institution for Transforming India. 2018. "Zero emission vehicles: towards a policy framework."
- Horowitz, Kelsey. 2019. "2019 Distribution System Upgrade Unit Cost Database Current Version." *2019 Distribution System Upgrade Unit Cost Database Current Version*. National Renewable Energy Laboratory.
- Indian Energy Exchange Limited. 2021. "Area Prices: Northern Region (N2 – Delhi)." *Area Prices: Northern Region (N2 – Delhi)*.
- International Energy Agency. 2020. "IEA Atlas of Energy – India." *IEA Atlas of Energy – India*. <http://energyatlas.iea.org/#!/profile/WORLD/IND>.
- . 2021. *India Energy Outlook 2021*. IEA. <https://www.iea.org/reports/india-energy-outlook-2021>.
- . 2018. *The Future of Cooling*. International Energy Agency. doi:<https://doi.org/https://doi.org/10.1787/9789264301993-en>.
- . 2018. *World Energy Outlook 2018*. International Energy Agency.
- . 2019. *World Energy Outlook 2019*. International Energy Agency.
- . 2020. *World Energy Outlook 2020*. International Energy Agency. doi:<https://doi.org/https://doi.org/10.1787/557a761b-en>.
- International Finance Council Corporation. 2019. "The Dirty Footprint of the Broken Grid: The Impacts of Fossil Fuel Back-up Generators in Developing Countries." Technical report, World Bank Group.
- International Institute for Sustainable Development. 2018. "The evolution of the clean energy cess on coal production in India." IISD.
- Jakhrani, Abdul Qayoom, Andrew Ragai Henry Rigit, Al-Khalid Othman, Saleem Raza Samo, and Shakeel Ahmed Kamboh. 2012. "Estimation of carbon footprints from diesel generator emissions." *2012 International Conference on Green and Ubiquitous Technology*. 78–81. doi:10.1109/GUT.2012.6344193.
- Jenkins, Jesse, and Nestor Sepulveda. 2017. "Enhanced Decision Support for a Changing Electricity Landscape: the GenX Configurable Electricity Resource Capacity Expansion Model." Technical report, MIT Energy Initiative, 1–40. <https://energy.mit.edu/wp-content/uploads/2017/10/Enhanced-Decison-Support-for-a-Changing-Electricity-Landscape.pdf>.
- Lara, Cristiana L., Dharik S. Mallapragada, Dimitri J. Papageorgiou, Aranya Venkatesh, and Ignacio E. Grossmann. 2018. "Deterministic electric power infrastructure planning: Mixed-integer programming model and nested decomposition algorithm." *European Journal of Operational Research* (North-Holland) 271: 1037–1054. doi:10.1016/J.EJOR.2018.05.039.
- Lu, Tianguang, Peter Sherman, Xinyu Chen, Shi Chen, Xi Lu, and Michael McElroy. 2020. "India's potential for integrating solar and on- and offshore wind power into its energy system." *Nature Communications* (Nature Research) 11: 1–10. doi:10.1038/s41467-020-18318-7.
- MacLaurin, Galen J., Nicholas W. Grue, Anthony J. Lopez, and Donna M. Heimiller. 2019. "The Renewable Energy Potential (reV) Model: A Geospatial Platform for Technical Potential and Supply Curve Modeling." Technical report, National Renewable Energy Laboratory. doi:10.2172/1563140.
- Mai, Trieu, Paige Jadun, Jeffrey Logan, Colin McMillan, Matteo Muratori, Daniel Steinberg, and Laura Vimmerstedt. 2018. "Electrification Futures Study: Scenarios of Electric Technology Adoption and Power Consumption for the United States." Technical report, National Renewable Energy Laboratory, Golden, CO. <https://www.nrel.gov/docs/fy18osti/71500.pdf>.
- Malik, Aman, Christoph Bertram, Jacques Despres, Johannes Emmerling, Shinichiro Fujimori, Amit Garg, Elmar Kriegler, et al. 2020. "Reducing stranded assets through early action in the Indian power sector." *Environmental Research Letters* (IOP Publishing Ltd) 15: 094091. doi:10.1088/1748-9326/ab8033.

- Mallapragada, Dharik S., Dimitri J. Papageorgiou, Aranya Venkatesh, Chrtiana L. Lara, and Ignacio E. Grossmann. 2018. "Impact of model resolution on scenario outcomes for electricity sector system expansion." *Energy* (Pergamon) 163: 1231–1244. doi:10.1016/j.energy.2018.08.015.
- Mallapragada, Dharik S., Indraneel Naik, Karthik Ganeshan, Rangan Banerjee, and Ian J. Laurenzi. 2018. "Life Cycle Greenhouse Gas Impacts of Coal and Imported Gas-Based Power Generation in the Indian Context." *Environmental Science & Technology* (American Chemical Society) 53: 539–549. doi:10.1021/acs.est.8b04539.
- Mallapragada, Dharik S., Nestor A. Sepulveda, and Jesse D. Jenkins. 2020. "Long-run system value of battery energy storage in future grids with increasing wind and solar generation." *Applied Energy* (Elsevier Ltd) 275: 115390. doi:10.1016/j.apenergy.2020.115390.
- McNeil, Michael A., Virginie E. Letschert, Stephane de la Rue du Can, and Jing Ke. 2013. "Bottom-Up Energy Analysis System (BUENAS)—an international appliance efficiency policy tool." *Energy Efficiency* 6: 191–217. doi:10.1007/s12053-012-9182-6.
- Muratori, Matteo. 2018. "Impact of uncoordinated plug-in electric vehicle charging on residential power demand." *Nature Energy* 3: 193–201. doi:10.1038/s41560-017-0074-z.
- National Bureau of Statistics, Nigeria. 2021. "Diesel Price Watch." *Diesel Price Watch*.
- National Renewable Energy Laboratory. 2020. "Annual Technology Baseline: Electricity." *Annual Technology Baseline: Electricity*. <https://atb.nrel.gov/electricity/2020/data.php>.
- . 2020. "System Advisor Model Version 2020.11.29 (SAM 2020.11.29)." National Renewable Energy Laboratory.
- Nhalur, Sreekumar, and Ann Josey. 2012. "Electricity in Megacities." Technical report, Prayas Energy Group.
- NITI Aayog. 2018. "Zero Emission Vehicles (ZEVs): Towards a Policy Framework." *Zero Emission Vehicles (ZEVs): Towards a Policy Framework*. Government of India National Institution for Transforming India.
- Olaniyan, Kayode, Benjamin C. McLellan, Seiichi Ogata, and Tetsuo Tezuka. 2018. "Estimating Residential Electricity Consumption in Nigeria to Support Energy Transitions." *Sustainability* 10. doi:10.3390/su10051440.
- Olatunji, Obafemi, Stephen Akinlabi, Ajayi Oluseyi, Abiodun Abioye, Felix Ishola, Mashinini Peter, and Nkosinathi Madushele. 2018. "Electric Power Crisis in Nigeria: A Strategic Call for Change of Focus to Renewable Sources." *IOP Conference Series: Materials Science and Engineering* (IOP Publishing) 413: 012053. doi:10.1088/1757-899x/413/1/012053.
- OpenStreetMap contributors. 2020. "India Power Substations." *India Power Substations*.
- Palchak, David, Ilya Chernyakhovskiy, Thomas Bowen, and Vinayak Narwade. 2019. "India 2030 Wind and Solar Integration Study: Interim Report." Technical report, National Renewable Energy Laboratory, Golden, CO. <https://www.nrel.gov/docs/fy19osti/73854.pdf>.
- Palmintier, Bryan S. 2013. *Incorporating operational flexibility into electric generation planning: impacts and methods for system design and policy analysis*. Ph.D. dissertation, Massachusetts Institute of Technology. <https://dspace.mit.edu/handle/1721.1/79147>.
- Pargal, Sheoli, and Sudeshna Ghosh Banerjee. 2014. *More Power to India: The Challenge of Electricity Distribution*. Washington, DC: World Bank. doi:10.1596/978-1-4648-0233-1.
- Pérez-Arriaga, Ignacio. 2016. "Utility of the future: An MIT Energy Initiative response to an industry in transition." Technical report, Massachusetts Institute of Technology. <https://energy.mit.edu/wp-content/uploads/2016/12/Utility-of-the-Future-Full-Report.pdf>.
- Perez-Arriaga, Ignacio, and Robert Stoner. 2020. *Abuja Electric's proposed franchising model: DESSA*. Technical report, Global commission to end energy poverty.
- Poncelet, Kris, Erik Delarue, and William D'haeseleer. 2020. "Unit commitment constraints in long-term planning models: Relevance, pitfalls and the role of assumptions on flexibility." *Applied Energy* (Elsevier Ltd) 258: 113843. doi:10.1016/j.apenergy.2019.113843.
- Rao, Narasimha D., Jihoon Min, and Alessio Mastrucci. 2019. "Energy requirements for decent living in India, Brazil and South Africa." *Nature Energy* 4: 1025–1032. doi:10.1038/s41560-019-0497-9.
- Roche, Maria Yetano, Nnanna Ude, and Ikenna Donald-Ofoegbu. 2017. *Comparison of Cost of Electricity Generation in Nigeria*. Technical report, Nigerian Economic Summit Group.

- Rose, Amy, Ilya Chernyakhovskiy, David Palchak, Sam Koebrich, and Mohit Joshi. 2020. "Least-Cost Pathways for India's Electric Power Sector." Technical report, National Renewable Energy Laboratory, Golden, CO. <https://www.nrel.gov/docs/fy20osti/76153.pdf>.
- Rossol, Michael, Grant Buster, and Mike Bannister. 2021. "NREL/reV: lat_lon_cols cleanup." *NREL/reV: lat_lon_cols cleanup*. Zenodo, 2. doi:10.5281/zenodo.4501717.
- Roy, P.S., P. Meiyappan, P.K. Joshi, M.P. Kale, V.K. Srivastav, S.K. Srivastava, M.D. Behera, et al. 2016. "Decadal Land Use and Land Cover Classifications across India, 1985, 1995, 2005." *Decadal Land Use and Land Cover Classifications across India, 1985, 1995, 2005*. ORNL Distributed Active Archive Center. doi:10.3334/ORNLDAAAC/1336.
- Rudion, K., A. Orths, Z. A. Styczynski, and K. Strunz. 2006. "Design of benchmark of medium voltage distribution network for investigation of DG integration." *2006 IEEE Power Engineering Society General Meeting*. 6 pp.-. doi:10.1109/PES.2006.1709447.
- Rudnick, Ivan. 2019. "Decarbonizing the Indian Power Sector by 2037: Evaluating Different Pathways that Meet Long-Term Emissions Targets." Master's thesis, Massachusetts Institute of Technology. <http://dspace.mit.edu/handle/1721.1/127737?show=full>.
- Sepulveda, Nestor A., Jesse D. Jenkins, Aurora Edington, S. Mallapragada, and Richard K. Lester. 2021. "The Design Space for Long-duration Energy Storage in Decarbonized Power Systems." *Nature Energy* Accepted.
- Sepulveda, Nestor A., Jesse D. Jenkins, Fernando J. de Sisternes, and Richard K. Lester. 2018. "The Role of Firm Low-Carbon Electricity Resources in Deep Decarbonization of Power Generation." *Joule* (Cell Press) 2: 2403–2420. doi:10.1016/J.JOULE.2018.08.006.
- Society of India Automobile Manufacturers. 2020. "Automobile domestic sales trends 2015-2020." SIAM.
- Spencer, Thomas, and Aayushi Awasthy. 2019. *Analysing and projecting Indian electricity demand to 2030*. The Energy and Resources Institute.
- Spencer, Thomas, Neshwin Rodrigues, Raghav Pachouri, Shubham Thakre, and G. Renjith. 2020. "Renewable Power Pathways: Modelling the Integration of Wind and Solar in India by 2030." Technical report, The Energy and Resources Institute, Delhi, India. <https://www.teriin.org/sites/default/files/2020-07/Renewable-Power-Pathways-Report.pdf>.
- Stanfield, Sky, Stephanie Safdi, L. L. P. Shute Mihaly Weinberger, and Attorneys for the Interstate Renewable Energy Council. 2017. "Optimizing the grid. A Regulator's Guide to Hosting Capacity Analyses for Distributed Energy Resources." Technical report, Interstate Renewable Energy Council.
- Tata Power Delhi Distribution Limited. 2016. "Excellence journey progress report." *Excellence journey progress report*. Tata Power Delhi Distribution Limited.
- . 2018. "Technical specification cover sheets: 33KV and 11 KV Grid."
- Tenenbaum, Bernard, Chris Greacen, Tilak Siyambalapitiya, and James Knuckle. 2014. "From the Bottom Up: How Small Power Producers and Mini-Grids Can Deliver Electrification and Renewable Energy in Africa. Directions in Development, Energy and Mining." Technical report, World Bank Group.
- United Nations Economic and Social Council. 2021. "Short-Term Financing, Creation of Repo Market Crucial to Assist Poor Countries Facing Escalating Debt, Economic Contraction, Speakers Tell Financing for Development Forum." Vol. ECOSOC/7037. United Nations.
- von Meier, Alexandra. 2018. "EV infrastructure planning and grid impact assessment: a case for Mexico." Unpublished.
- Waite, Michael, Elliot Cohen, Henri Torbey, Michael Piccirilli, Yu Tian, and Vijay Modi. 2017. "Global trends in urban electricity demands for cooling and heating." *Energy* (Elsevier Ltd) 127: 786–802. doi:10.1016/j.energy.2017.03.095.
- Winsor, Charles P. 1932. "The Gompertz Curve as a Growth Curve." *Proceedings of the National Academy of Sciences of the United States of America* (National Academy of Sciences) 18: 1–8. <http://www.jstor.org/stable/86156>.
- World Bank Group. 2020. "Electric power consumption (kWh per capita)." *Electric power consumption (kWh per capita)*.
- World Bank. 2020. "Terrain Elevation Above Sea Level ELE GIS Data."
- World Energy Council. 2009. "Transmission and Distribution in India." *Transmission and Distribution in India*. World Energy Council.
- Zhou, Nan, Nina Khanna, Wei Feng, Jing Ke, and Mark Levine. 2018. "Scenarios of energy efficiency and CO₂ emissions reduction potential in the buildings sector in China to year 2050." *Nature Energy* 3: 978–984. doi:10.1038/s41560-018-0253-6.

Chapter 8 – Governance of decarbonized power systems with storage

8.1 Introduction

The overall goal of this study is to address the roles of energy storage in reducing the total cost of future deeply decarbonized electric power systems.¹ This chapter considers how alternative regulatory rules and policy regimes will affect the ability of storage to contribute to cost-effective and equitable power system and economy-wide decarbonization. We focus primarily on the United States, though the general issues we discuss are relevant in other developed regions. Our basic conclusion is that future decarbonized power systems will differ from current systems in important ways that will render today's governance arrangements increasingly inadequate. We recommend a number of steps that should be taken now by regulators and others to deal with this challenge. Because effective governance of future decarbonized power systems will require development and deployment of new tools as well as reform of rules and regulations, research has an important role to play.

In future decarbonized power systems, wind and solar generation will be much more important than today. For example, in a recent study of global decarbonization pathways, the International Energy Agency (IEA) projects that wind and solar generation will account for almost 70% of global electricity generation by 2050, up from 9% in 2020 (International Energy Agency 2021, Table 3.2). Wind and solar generators, often collectively labeled VRE (variable renewable energy), are intermittent: Their output is both variable and imperfectly

predictable because it is primarily determined by variations in wind and solar resource availability rather than by system operators' decisions to balance supply and demand by moving up and down a reasonably stable bid-based or marginal cost-based economic dispatch curve as demand varies (the way system operators now manage output from mostly fossil fuel generation resources) (See Figure 8.1). In contrast, in a system with high VRE penetration, supply will vary widely and possibly quite suddenly over time due to exogenous changes in wind conditions and solar irradiation. As a consequence, future systems will need to cope with unprecedented supply fluctuations to balance supply and demand reliably. Existing systems are used to coping with weather-induced demand fluctuations; in the future, weather-induced fluctuations will affect both supply and demand; those effects will generally be correlated; and these correlations will also vary with weather conditions. For example, very hot days may be associated with both increased demand for air conditioning and reduced output from wind generators. On days when there is heavy cloud cover over a large region, the output from all solar generators on the system will be reduced, creating a high correlation between all solar generators on the system—a correlation between generators that is largely absent in conventional thermal systems. Energy storage will play an important role in balancing supply and demand reliably in systems with high VRE penetration by filling the gaps between exogenous variations in VRE supply and demand.

¹ Total cost includes investment and operating cost, as well as the cost of any involuntary blackouts or load shedding, conditional on satisfying carbon emissions constraints.

Economy-wide electrification of various end uses—a core element of most economy-wide decarbonization scenarios—may worsen this problem. Some uses of electricity, for example to charge electric vehicles (EVs) or produce hydrogen via electrolysis, could potentially help balance supply and demand by reducing operations in response to decreases in electricity supply. Others, such as increased electrification of space heating, could result in new peak loads that may be correlated with weather variations that reduce VRE generation at the same time,² making it more difficult to balance supply and demand.

Because of the key role storage can play in balancing supply and demand and thus maintaining reliability in systems with high VRE penetration, and because of substantial projected declines in the costs of storage technologies, storage should be much more important in future decarbonized power systems and play a larger variety of roles than it does today. The methods used by today's system operators and the associated regulatory rules and policy regimes that constrain them were developed for power systems that relied primarily on dispatchable generators and in which storage was of negligible importance. As we discuss in this chapter, investing in and operating storage so that it effectively plays appropriate roles in future decarbonized power systems will pose novel operational and financing challenges. It will also pose challenges in terms of regulation and market design—the focus of this chapter.

In today's competitive electricity markets, wholesale prices reflect generators' marginal costs of producing electricity at each potential level of demand. When demand is low, the system's marginal cost is relatively low,

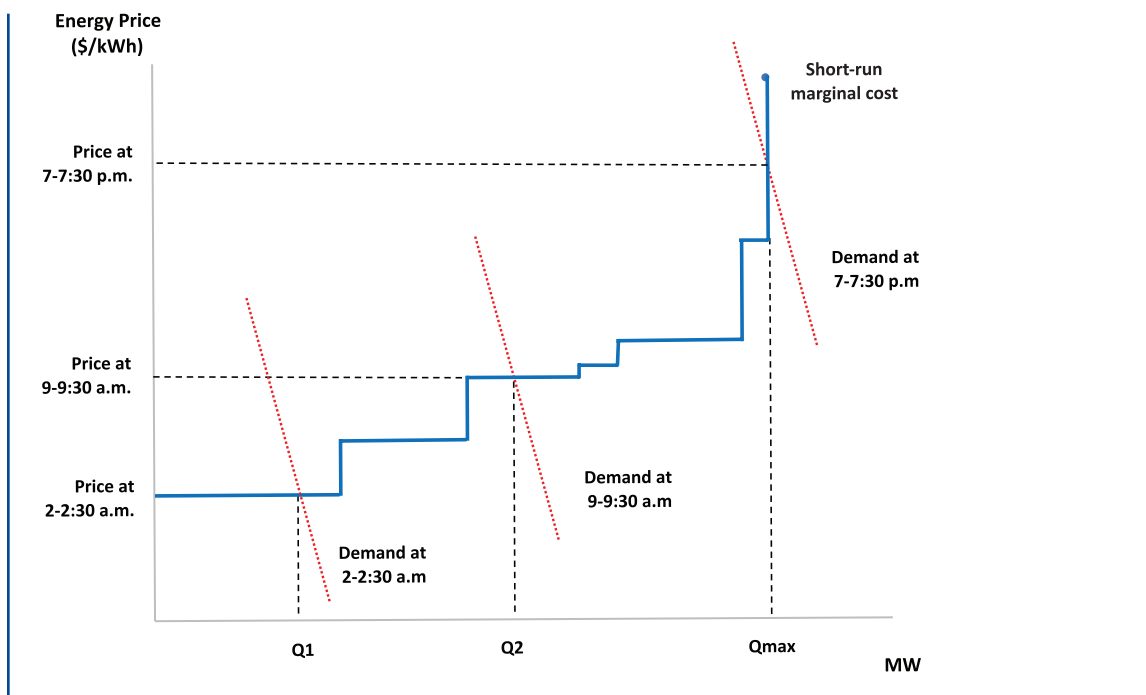
reflecting the marginal cost of the lowest-cost generator. When demand is very high, the marginal cost of the highest-cost generation needed to balance supply and demand can be very high. In short, the economic dispatch curve is upward sloping and reasonably stable, as illustrated in Figure 8.1. The challenge for the system operator is to adjust dispatchable generator output along the economic dispatch curve as demand varies from hour to hour, day to day, season to season, etc. There is no storage in the classical economic dispatch model for systems with dispatchable thermal generators.

In contrast to the system depicted in Figure 8.1, which is built upon dispatchable generators with stable marginal costs (reflecting different thermal efficiencies and fuel costs), the supply of VRE generation varies up and down based on sometimes wide and rapid exogenous changes in wind and solar conditions. Thus, there is no simple equivalent of the economic dispatch curve depicted in Figure 8.1. Moreover, the short-run marginal costs of wind and solar generation are always close to zero. Markets dominated by such generators present market design challenges: how to deliver wholesale and retail price signals that reflect the marginal cost of production while still yielding expected revenues that cover both investment and operating costs.³ Moreover, as discussed in Chapters 1 and 6, many storage technologies also have near-zero marginal operating costs and lose relatively little energy in charge/discharge cycles. These technologies thus raise similar market design issues. In addition, the operating characteristics of electricity systems that are dominated by VRE and storage technologies raise significant equity and risk-tolerance issues that must be addressed in devising future retail pricing regimes.

² The Texas power crisis of February 2021 dramatically illustrated this possibility (Weber 2021).

³ Systems with high VRE penetration face other challenges as well. For example, how to manage a system reliably where supply can fluctuate widely and rapidly in response to exogenous changes in weather? Responding to these challenges will likely require additional market design changes, especially in ancillary service products. However, we do not discuss this type of operational challenge in this study.

Figure 8.1 A contemporary electricity market in the short run



This chapter is organized as follows. The next section, Section 8.2, discusses requirements for overall power system efficiency, both in general and in light of the modeling results presented in Chapter 6. Section 8.3 provides a brief overview of the wide variety of organizational structures and regulatory frameworks within the U.S. electric power sector and of their evolution. In the two subsequent sections, we consider two polar opposite structures described in Section 8.3 at the bulk power (wholesale) level. Section 8.4 considers barriers to least-cost production in the first of these: the traditional structure of a regulated investor-owned firm that provides generation, transmission, and distribution and has a monopoly within its state-designated service area. Section 8.5 then considers the polar opposite case in which generation, transmission, and distribution

functions have been separated, and generation has been horizontally disaggregated to support competitive wholesale markets. In systems of this general sort, organized wholesale markets play key roles in guiding resource allocation in both the short run and the long run—consequently, market design challenges are present that do not arise in vertically integrated structures, which lack organized markets.

Finally, Section 8.6 considers the challenge of designing equitable retail rate regimes in either structure that guide efficient investment and consumption decisions without imposing excessive risks on households and small firms. In most of the country, a single regulated entity sets retail rates, but about nineteen U.S. states have allowed competition in marketing electricity to some or all retail customers.⁴

⁴ Retail competition has been a political issue at the state level, and the number of states that allow it has changed from time to time (American Coalition of Competitive Energy Suppliers).

8.2 Efficiency in high-VRE power systems

There are two general requirements for overall power system efficiency in a decarbonizing economy.⁵ First, and most obvious, electricity should be produced and delivered at the lowest possible total cost, including the cost of any involuntary blackouts or load shedding, compatible with satisfying applicable carbon constraints and given the available technologies and their costs. This requirement, which is often termed *productive efficiency*, means production and delivery costs must reflect the efficient uses of available technologies given their costs and production attributes. It is the focus of Sections 8.4 and 8.5. Two novel challenges to productive efficiency deserve emphasis.

First, productive efficiency requires achieving carbon constraints through policies that support efficient investment and operating decisions at all levels in the system. As economists have argued for decades, a central element of an efficient approach to reducing carbon emissions is to place an appropriate price on carbon emissions, either in the form of an economy-wide tax on carbon emissions or a comparable cap-and-trade regime with the same economy-wide scope (Hafstead 2019).⁶ In what follows, we assume that carbon pricing policies are in place, as they are in our modeling exercises in Chapter 6, since it is simply not possible to deal with the consequences of the host of politically more popular but less efficient policy alternatives that can be—and, indeed, have been—widely deployed. Use of any of these alternatives—which include renewable

portfolio standards, clean energy standards, investment tax credits and production tax credits, feed-in tariffs, and net metering policies applied to generation and storage facilities on customers' premises—instead of carbon pricing raises the cost of electricity unnecessarily and thus works against reaching economy-wide decarbonization goals via electrification. That said, the recommendations developed in this chapter are generally desirable even in the face of inefficient policies for achieving decarbonization, though their benefits, in the context of inefficient carbon policies, will be reduced. Since we focus on 2050 in our modeling work, we hope that public policy will evolve by that time to rely primarily on more efficient mechanisms to provide incentives for decarbonization.

A second novel and complex challenge to achieving the least-cost production and delivery of electricity is that, as noted above, existing markets and institutional arrangements were not designed to make efficient use of energy storage. While the modeling analysis described in Chapter 6 concentrates on the potential to use storage to perform intertemporal energy arbitrage—effectively moving VRE generation from one time period to another—storage can also, as we discuss in Chapter 1, perform a variety of other functions in power systems. Least-cost production and delivery of electricity requires that investment and operations decisions involving storage reflect the value of all those functions. In addition, some battery storage technologies (notably lithium-ion batteries) can be deployed relatively efficiently at small scale. Batteries in homes, commercial

⁵ Throughout this chapter, we assume, consistent with public policy in the United States and elsewhere, that retail electricity rates must produce revenues sufficient to cover all investment and operating costs for the system as a whole.

⁶ A recent World Bank report finds that 64 carbon pricing initiatives had been implemented as of late July 2021, covering just over 21% of global carbon emissions (World Bank 2021). Sadly, even though both major political parties' presidential candidates endorsed carbon pricing in 2008, prospects for carbon pricing at the national level in the United States have dimmed considerably since then.

buildings, or industrial facilities can also efficiently deliver a variety of services at the wholesale level, but existing utility regulations, wholesale power markets, and retail pricing regimes are not designed to facilitate their efficient participation at the wholesale level.

The second requirement for overall power system efficiency is related: “Retail prices”—that is, prices faced by end-use electricity consumers and service contracts that may be made available to them and that might provide incentives for third-party control of some appliances, vehicle charging, or other electric loads—should support short-run and long-run decisions on energy use that reflect marginal cost or, more generally, the marginal value of energy.⁷ This requirement for *allocative efficiency* means that energy use should be discouraged in the short run when electricity is expensive on the margin, but it should be encouraged when electricity is cheap—for instance, when available VRE generation exceeds demand. The marginal value of energy should guide decisions on investment in and operation of small-scale generation and storage assets located on customer premises, as well as investment to enable demand to respond to short-run price changes. Retail rates that support allocative efficiency, the focus of Section 8.6, are critical to support least-cost economy-wide electrification as a key component of economy-wide decarbonization.

Despite its limitations, the optimization analysis in Chapter 6 has important implications for the features of high-VRE power systems that produce and deliver bulk power efficiently.⁸ Our optimizations seek to minimize total system cost subject to a constraint on carbon emissions.⁹ All decisions are optimally driven by a single variable: the marginal value of electric energy, a shadow value that reflects the cost of incremental supply from generation and/or storage in each time interval. In theory, one can translate the results of these optimization analyses into market equilibria under perfect competition in a system with only energy markets by treating the marginal value of energy as the actual spot price. In an optimized system, the marginal value is used as a market price would be used under conditions of perfect competition: to guide dispatch and other operating decisions, as well as all investment decisions.

Two features of the efficient systems modeled in Chapter 6 have particularly important implications for the design of markets and governance institutions. First, the modeled distribution of (shadow) spot wholesale prices for energy is very different from current distributions of spot prices. Even when storage is optimally deployed to “buy low and sell high”—thus moving electric energy from periods of abundance to periods of scarcity—there are many more hours of very low prices than at present,

⁷ This distinction reflects the fact that the cost of supplying electricity from storage is mainly an opportunity cost—the value of the foregone opportunity of supplying it later—rather than an out-of-pocket cost like the fuel used in thermal generation.

⁸ Importantly, that analysis assumes perfect foresight with respect to both demand and supply of renewable generation and we do not model so-called ancillary services (such as frequency regulation) or load-uncertainty-related resource adequacy challenges. Both enormously simplify the analysis. The assumption of perfect foresight removes the need for reserve margins and, along with the assumption of constant returns to scale, ensures that all technologies optimally deployed earn zero economic profits.

⁹ The limit on carbon emissions is specified as a constraint on carbon emissions per megawatt-hour (MWh) of output, and the shadow price on that constraint gives the carbon price that would need to be imposed under competition to ensure satisfaction of the emissions constraint.

along with more hours of very high prices.¹⁰ This reflects the variability of VRE supply with near-zero short-run marginal cost, the excess supply of VRE generation at some times in the optimal solution, and demand-side variability.

Translating the solutions of our optimization exercises into market equilibria in a system with only an energy market implies that generators and storage facilities would earn a disproportionate share of the revenues needed to recover investment costs during only a few hours every year (or every few years) when prices are very high. In the world of the model, end users who actually have to pay marginal system costs for all the electricity they demand at each point in time would, in theory, face correct incentives for efficient consumption and investment. In practice, however, the price risks to end users in this scenario would be enormous and, for households and small businesses, likely intolerable. These risks were made visible in the February 2021 energy crisis in Texas (Blumsack 2021). Luckily, as we discuss in Section 8.6, a complete pass-through of wholesale prices into retail rates is not necessary to induce efficient behavior by producers and consumers.

The second feature of high-VRE systems that has significant governance implications is that storage, both grid-scale and at customer premises, is a potential substitute for, or complement to, essentially all other elements of a power system. Efficient governance must enable least-cost choices among all these elements. As shown in Chapter 6, optimal storage deployment in high-VRE systems complements VRE generation, increasing its

value by reducing the need for curtailments and mitigating the consequences of intermittency.¹¹ Tighter constraints on carbon emissions reduce the possible use of natural gas generation, which substitutes for long-term storage, and thus increases the value of storage. The ability to reduce load in times of supply scarcity through demand response reduces the optimal amount of storage deployed.

A stronger regional and inter-regional transmission network permits access to better wind and solar resource sites and enables broader geographic diversification, which reduces average variability and allows, for example, solar generators in the west to help meet evening loads farther east.¹² Increased transmission capacity also reduces the optimal amount of storage deployed. Finally, Chapter 7 reveals that for systems experiencing rapid growth, storage can reduce costs by delaying the need to expand transmission or distribution systems.

8.3 Market and institutional structures

As noted above, U.S. bulk power systems exhibit a wide range of market and institutional structures (Cleary and Palmer 2020). Traditionally, most electricity was generated by vertically integrated, investor-owned utilities, which mainly sold to ultimate customers pursuant to retail tariffs regulated by state regulatory commissions. In a vertically integrated (VI) system, a single organization (“the VI utility”) owns and controls the generation, transmission, and distribution facilities to serve retail consumers within the organization’s geographic footprint. In addition, some sales were made

¹⁰ As we discuss below, many of today’s wholesale energy markets have low price caps that limit the variability of spot energy prices. The comparison in Chapter 6 between the price distributions produced by our model of Texas in 2050 and the distribution of 2018 and 2019 wholesale prices in ERCOT (the Electric Reliability Council of Texas), which operates a wholesale market covering most of the state of Texas with a very high price cap, provides strong support for this statement.

¹¹ We do not discuss the properties of alternative curtailment mechanisms here: We simply assume that when curtailments are necessary to balance supply and demand, they are implemented efficiently.

¹² This is discussed in Chapter 6 and several references cited there.

by vertically integrated utilities to cooperatives and municipal utilities that, in turn, sold to ultimate customers under wholesale contracts or tariffs regulated by the Federal Energy Regulatory Commission (FERC).¹³

In the Southeast, Southwest, and much of the West, the traditional VI-utility model still dominates (Federal Energy Regulatory Commission 2021). Accordingly, the next section (Section 8.4) considers the efficient governance of a regulated, vertically integrated, investor-owned utility that owns or contracts for all generation, transmission, bulk storage, and distribution assets.¹⁴ This utility does not own generation or storage assets on customer premises. It is regulated at the state and federal levels, with state regulation being more important. There is no competition in the provision of electricity to final customers, and retail customers pay for the electricity they consume according to the utility's regulated retail tariffs. In this polar case structure, there are no transparent wholesale market prices. Absent transparent wholesale prices, efficiency requires that the short-run marginal cost of supplying electricity should drive decisions, even though, traditionally, time-invariant retail rates were set to cover utilities' average costs. When the system's supply is constrained, and

supply–demand balance must come from the demand side, the relevant marginal cost and spot price is the value of unserved load—referred to as the value of “lost” load (VoLL)—or, if there is an active, price-sensitive demand side, the relevant price is the price that clears the market without implementing involuntary load curtailments (Joskow and Tirole 2007).

Beginning in the 1990s, the electric power sector in much of the United States (and in many other nations) was restructured to increase reliance on competitive wholesale markets to supply energy and so-called ancillary services such as reserve capacity and frequency regulation. The basic idea was that the actual spot price of electricity in these markets would guide all bulk power operation and investment decisions, as the shadow value of electricity does in our optimization model. Seven regional entities, called independent system operators (ISOs) or regional transmission organizations (RTOs), now operate those markets and regional transmission systems and engage in some regional planning.¹⁵ (For simplicity, we refer to all of them as ISOs in the discussion that follows.) ISOs manage about 60% of U.S. electricity supply (U.S. Energy Information Administration 2011).

¹³ In some regions, federally owned utilities, notably the Tennessee Valley Authority in the Southeast and the Western Area Power Administration and Bonneville Power Authority in the West, had significant shares of generation and regional transmission capacity. These federal utilities by law sold almost exclusively to cooperatives and utilities owned by state and local governments. Cooperatives and municipal utilities have remained important in some regions. In 2019, 856 cooperatives and 2,003 government-owned utilities served 28% of all U.S. customers, supplied approximately 15% of all the electricity delivered to U.S. end users from generating plants they own, and produced approximately 10% of all the electricity generated in the United States (American Public Power Association 2021).

¹⁴ We recognize that even vertically integrated utilities may engage in some short-term bilateral wholesale transactions with interconnected utilities, may participate in more organized short-term energy markets (as in the Western Energy Imbalance Market), or may be integrated into organized wholesale markets. However, it is useful to consider this pure case since, even in these other contexts, state regulation typically plays the central role in resource planning, resource adequacy determinations, revenue determinations, and retail rate design.

¹⁵ All of the ISOs except ERCOT, which has a service territory entirely within Texas and no substantial connections with other states, are regulated by FERC. For a discussion and a map of service territories, see Federal Energy Regulatory Commission (2021).

In some U.S. regions, though not all, electric sector restructuring was accompanied by the vertical separation of generation, transmission, and distribution, as well as by additional, horizontal disaggregation of generation. These changes and the entry of merchant generators led to a far greater role for non-utility generators, which accounted for about 47% of U.S. electricity supply in 2020 (Edison Electric Institute 2021). In addition, fourteen states have allowed retail competition for all retail customers (American Coalition of Competitive Energy Suppliers). In these states, the physical distribution of electricity remains a regulated monopoly, but competitive retail providers can purchase electricity in the wholesale market and resell it to retail customers. A few additional states allow some but not all retail customers access to competitive suppliers.

Developing competitive wholesale power markets for energy and ancillary services was more complicated than many had anticipated, but in today's systems that primarily rely on dispatchable fossil fuel generation resources, these markets now have good operational performance under most conditions. Energy prices have been capped at levels well below reasonable estimates of VoLL, however, and bulk power system reliability standards have been set that are often excessive from an economic perspective.¹⁶ ISOs sometimes engage in "out of market" actions to respond to situations in which the system's supply–demand balance is stressed and to manage associated reliability concerns. As a result, revenues from energy and ancillary service markets have generally not provided adequate

incentives for generation investments at the level needed to meet applicable reliability standards. This gives rise to what is often called the "missing money" problem (Milligan 2015). Similarly, because they constrain price variability, energy and ancillary service markets with low price caps would likely lead to sub-optimal investment in energy storage.

In response to the "missing money" problem and the reliability concerns raised by potential underinvestment in generating capacity, most restructured regions in the United States have added markets for capacity or related "resource adequacy" mechanisms to supplement energy and ancillary service market revenues in order to ensure that capacity is adequate to meet reliability standards.¹⁷ More recently, climate and clean energy policies, including mandates for VRE generation and storage, have led to additional regulatory interventions in investment decisions within restructured regions. This has resulted in so-called *hybrid* systems in which wholesale markets guide operations, but investment decisions are heavily affected by resource adequacy policies, government decarbonization commitments, government mandated VRE and storage procurements, and associated regulatory decisions (Roques 2021). The rules commonly applied to energy, ancillary service, and capacity markets in these systems were not designed with storage in mind, however, and the owners of existing assets are not eager to encourage competitive storage. As discussed below, efforts to reform those rules are underway at the federal level and in several states. These efforts are important and should be encouraged.

¹⁶ That is, the value of lost load implied by these reliability standards is typically implausibly high. For example, Astrape Consulting (2013) estimates that the common 1-event-in-10-year standard corresponds to an implied VoLL of \$300,000/MWh—one or two orders of magnitude higher than typical estimates of VoLL.

¹⁷ ERCOT, which serves most of Texas, is a notable exception, but it does have a mechanism embedded in the energy market that provides supplemental payments for energy supplies in the real-time market when operating reserves fall below specified levels (Electricity Reliability Council of Texas n.d.).

Section 8.5 considers the polar case of a fully restructured bulk power system with merchant suppliers of generation and grid-level storage. In this structure, transmission and distribution remain regulated and an ISO develops rules for, and operates, wholesale markets for energy and ancillary services, subject to federal (FERC) oversight. As in the contrasting polar case of a vertically integrated utility with no wholesale markets, customers make investment and operating decisions for distributed generation and storage facilities on their premises. Both state and federal regulation are important in this structure. ERCOT, which serves most of Texas, probably comes closest to exemplifying this model, but electricity systems in the northeastern United States (specifically, the PJM, NYISO, and ISO-NE systems) have also been largely restructured, using similar wholesale energy market designs but with added capacity markets (Federal Energy Regulatory Commission 2021).

8.4 Regulated, vertically integrated bulk power systems

In principle, regulated, vertically integrated systems can minimize total system costs at the bulk power level, thus attaining productive efficiency, with system marginal costs and the value of unserved load (VoLL) standing in for a wholesale market spot price. In practice, however, even if productive efficiency is one of the integrated utility's objectives, achieving it is difficult, for several reasons. The cost-containment discipline provided by competitive markets is mostly absent, regulatory oversight is imperfect and subject to interest group politics, and VRE generation and storage at scale pose new problems for operations and investment decision-making.

As noted in Chapter 6, neither vertically integrated utilities (nor ISOs that manage wholesale markets and transmission in

restructured systems) have much experience operating high-VRE systems in which storage plays multiple, significant roles. Similarly, most utilities and system operators have historically had separate planning processes for generation (including purchased power), transmission, and distribution, and have little experience with including grid-level storage in planning. Because high-VRE systems with storage will pose new operational and planning challenges, Chapter 6 recommends that utilities and system operators, with the support of state and federal regulators, engage in cooperative research with universities, national labs, and other institutions to develop the tools needed to operate high-VRE systems with storage and to better integrate generation, transmission, storage, and distribution options in their long-term planning processes.

High-VRE systems with storage will also pose significant new challenges for state and federal regulators. Since utilities respond to the incentives created by regulation, it is important that regulatory agencies have the expert staff and resources necessary to devise and implement efficiency-enhancing incentives appropriate to a rapidly changing environment. At present, most agencies lack sufficient technical and economic expertise to respond effectively to these challenges. To decarbonize the power system and the wider economy without incurring excessive costs, these deficiencies must be remedied.

RECOMMENDATION 8.1

Staff with technical and economic expertise and budgets for state and federal regulatory agencies should be substantially increased to enhance these agencies' capabilities to design and implement regulatory mechanisms that can guide the transition to least-cost high-VRE systems with storage.

Because FERC regulates transmission and wholesale energy and capacity markets in the United States, whereas states regulate retail rates and everything else, regulated, vertically integrated utilities may have incentives to exploit differences between state and federal regulation (this practice is sometimes called regulatory arbitrage) in ways that lead to inefficient investment decisions. On the other hand, there may be value in having FERC and states experiment with a variety of organizational and regulatory approaches. Greater communication among regulatory agencies may have considerable value as all stakeholders in the electric power sector head into uncharted waters.

In many cases, storage assets located “behind the meter” on customer premises can provide grid-level and generation-related services cost-effectively, particularly if they are operated by aggregators.¹⁸ Regulated utilities, however, will prefer to employ storage assets that they own. State regulators should attempt to ensure that this preference does not lead to uncompetitive, excessively costly outcomes.¹⁹ On the other hand, restrictions on the ownership of storage (and other state interventions to influence the amount and type of storage installed) may increase overall costs by preventing storage options from capturing all wholesale, wires, and customer-related value streams.

RECOMMENDATION 8.2

State regulators should develop rules that allow owners of storage (and generation) assets installed on customer premises to sell services to vertically integrated utilities under appropriate terms and conditions that facilitate efficient investment in and use of “behind-the-meter” generation and storage.

Ensuring “appropriate terms” for storage services provided by devices installed on customer premises will likely require enabling purchases and sales of energy from these devices at system marginal cost (or at VoLL when there is unserved load).

Rather than owning and operating facilities that are subject to traditional rate-of-return regulation, it will often be efficient for a regulated, vertically integrated utility to use competitive bidding to procure generation, storage, and transmission capacity, or, preferably, to use technology-neutral bidding for services that could be provided by different types of assets (without specifying the asset types to be employed) through long-term contracts with third-party VRE and storage suppliers. These contracts should involve fixed payments if performance criteria (e.g., availability) are met, since the system-wide marginal cost of producing more or less electricity from the facilities involved will frequently be close to zero. Contracts that tie payment directly to the quantity of energy supplied by VRE generation

¹⁸ See, for example, Green Mountain Power’s Home Battery program (Spector 2020) under which the utility now controls several thousand Tesla Powerwall batteries sited in customers’ homes. For a general discussion of programs of this sort, with a focus on New England, see “Comments of the Energy Storage Association to the Public Utility Commission of New Hampshire,” January 11, 2021 (Howland 2021).

¹⁹ The California Public Utilities Commission and the California Independent System Operator have been engaged on this issue for some time (California Public Utilities Commission 2018; California Independent System Operator 2019).

or storage at prices above the facility's marginal cost (e.g., \$70/MWh supplied when the marginal cost is close to zero) will raise system costs by distorting dispatch decisions and should therefore be avoided.

8.5 Restructured and hybrid bulk power systems

Competitive markets generally provide stronger cost-minimization incentives than cost-of-service/rate-of-return regulation, and the possibility of merchant entry into various functions can be a powerful force for static and dynamic efficiency. Existing rules in organized regional wholesale power markets were not designed for high-VRE systems in which storage is important, however. In addition, incumbents (including owners of thermal generators) are not eager for the entry of new competitors in the form of storage providers. FERC Order 841 (Federal Energy Regulatory Commission 2018), which required ISOs to enable the participation of storage providers in regional markets, was an important first step. FERC took another important step with Order 2222 (Federal Energy Regulatory Commission 2020), which required ISOs to remove barriers to the participation, through aggregators, of distributed energy resources (including behind-the-meter storage) in regional markets.

These orders need to be translated into workable market rules and aligned with state regulations, particularly with respect to integrating wholesale markets and the distribution and customer-side values of storage. In California, the public utility commission (CPUC) and the ISO (CAISO) have already done much work on this kind of integration, perhaps helped by the fact that CAISO is a single-state ISO with an integrated, single-state regulatory framework and climate-policy regime to guide its actions. This sort of integration may be more challenging for multi-state ISOs.

Devising state and federal rules that are aligned and provide incentives for efficiency will not be simple, but it will be essential for the high-VRE systems of the future, in which avoiding unnecessary costs will require that storage play an important role. At a minimum, storage providers must be able to buy and sell energy at the wholesale spot market price. When charging, storage facilities should be treated as negative supply, not as another form of ultimate customer load. This means storage providers should not be burdened with the recovery of fixed costs for transmission or distribution or for out-of-market payments unless there is a clear rationale, based on cost-causality considerations, for doing so—for example, if the addition of a storage facility to the system creates transmission interconnection costs. Storage providers should also be permitted to participate in markets for capacity and ancillary services, recognizing, as discussed below, that the capacity value of specific storage facilities will vary with the maximum duration of the energy these facilities are capable of storing (see Chapter 1).

RECOMMENDATION 8.3

The Federal Energy Regulatory Commission (FERC), state regulators, and ISOs should reform and align market rules to enable efficient participation—in wholesale energy and ancillary service markets, as well as in capacity markets—by providers of both grid-based storage and distribution-level generation and storage (including from facilities located on customer premises). These rule reforms should accommodate the participation of aggregators in wholesale markets.

Because of the disaggregated industry structures that exist in many parts of the United States, allowing customer-based and distribution-level resources to participate in wholesale markets raises complex market design issues. Nonetheless, the growing importance of such distributed assets and the potential system-level benefits they can provide make this an important issue to address. Minimizing total system costs will require that providers of customer-premises and distribution-level generation and storage be allowed to buy and sell at the wholesale energy price, adjusted for transmission and distribution losses (and be allowed to participate in ancillary services and capacity markets, as discussed below)—at least through aggregators, as FERC Order 2222 requires. Efficient operations may also require that system operators be able to track the capacities, resource status (e.g., state-of-charge for storage facilities), and operations of behind-the-meter generation and storage facilities.

As noted above, various designs for capacity markets and other capacity compensation mechanisms have been deployed to encourage investments in generation by supplementing revenues earned from energy and ancillary service markets. These efforts have had mixed results and have necessitated frequent market design changes. Existing capacity market mechanisms were originally designed for systems with fully dispatchable, utility-scale generation. In such systems, installed capacity (sometimes derated by a few percentage points to reflect typical forced outage rates) is a good measure of the ability to provide power in times of system stress—typically during demand peaks on hot summer afternoons or, less commonly, on very cold winter days.

Computing the expected ability of VRE generators and storage resources to provide both capacity and energy in times of system stress is more complicated.²⁰ Essentially, it requires an examination of (1) the full probability distribution of supply, both at the bulk power level and from behind-the-meter providers, and (2) the full probability distribution of demand. Analyzing the latter requires properly accounting for correlations between expected production from different types of VRE generators (e.g., output from wind generators in the same area will be much more highly correlated than output from dispatchable generators today) and for correlations between VRE supply and energy demand, both of which will be much more sensitive to variations in weather conditions. A high-VRE system could be stressed in the late evening of a hot day, for example, when demand is below the system peak but there is no solar generation and (potentially) very little wind generation. Widespread electrification of space heating as part of an economy-wide decarbonization strategy is also likely to increase the relative importance of winter demand peaks for capacity planning. In addition, the expected capacity contribution of a VRE generator of any particular type will depend on the structure of the generation fleet. The higher the share of solar generation, for instance, the more likely it is that system stress occurs in the late afternoon or early evening (after system demand peaks), when solar output is declining or zero. In California, for example, the involuntary load shedding that occurred in August 2020 took place after the peak demand hour but at a time of “net peak demand” later in the evening, as the sun went down (California Independent System Operator 2021).²¹

²⁰ The problems discussed in this paragraph and the next also arise as planning problems for vertically integrated systems, but, in the absence of markets, they do not raise market design issues.

²¹ “Net peak demand” is defined as the total demand on a bulk power system less the supplies from intermittent wind and solar generators.

Although existing capacity mechanisms are being adapted to account for the “effective load carrying capability” (ELCC) of VRE generation, fully adapting these mechanisms for systems that include significant storage resources will pose new market design challenges. Unlike VRE generators, the power that a fully or partially charged storage facility can supply is not likely to vary much over time. However, the length of time over which a storage facility can supply this power (and thus “carry load”) is limited both by the facility’s design duration and, in the short run, by its state of charge. And state of charge at any given instant in time will be determined by prior operating decisions. Since periods of system stress are typically characterized by high energy prices, storage operators will have incentives to have their facilities fully charged just before such periods. System stress, however, cannot be forecast perfectly, and there is essentially no experience with the operating decisions that owners of storage facilities are likely to make when participating in systems with significant VRE and storage resources. Moreover, as more storage resources with a particular design duration (e.g., four hours) are added to the system, their ELCC will start to decline. Market rules will need to be developed to address these challenges and to correctly determine the capacity value that storage resources can provide to meet reliability standards.

RECOMMENDATION 8.4

ISOs should either (1) redesign existing capacity mechanisms as they apply to VRE generation and storage, taking into account the stochastic properties of VRE generation and demand and the fact that storage is energy-limited, or (2) replace those capacity mechanisms with an increased reliance on integrated resource planning that properly accounts for these factors.

Power system planners and operators face a fundamental problem: It is not clear how resource adequacy standards should be set for systems with high levels of VRE and storage. There would seem to be a complex trade-off between energy-limited and non-energy-limited capacity, depending on the nature and duration of expected stress events. We believe this issue has not yet received adequate study.

Rather than hoping that well-intentioned modifications to current market designs will produce acceptable results, it may be better in the short run to implement well-structured integrated resource planning processes, similar to the planning processes that could be (but are not always) employed by vertically integrated utilities to set targets for various levels of VRE and storage capacities. Even recognizing that integrated resource planning has not always worked well in the past, in part because of a tendency among planners to minimize uncertainty, some vertically integrated utilities in the United States may have already made the most progress on this front. These utilities could have a structural advantage in managing the transition to a decarbonized system by virtue of their ability to capture all related value streams internally. In contrast, mandates and requirements by individual states, which have become increasingly common, will lead to inefficient outcomes and higher costs if they are uncoupled from rigorous integrated resource planning.

Finally, as discussed in Chapter 7, the ability of storage to delay or displace investments in transmission and distribution can be quite valuable in systems with rapidly growing demand. The efficient use of storage requires that providers of storage resources be compensated for such benefits. Accordingly, storage must be (1) fully integrated into ISO-managed transmission planning processes; (2) allowed to compete with traditional transmission and

distribution expansion options; and (3) compensated for providing reliability, market efficiency, and/or public policy services as wires-based options would be, pursuant to FERC Order 1000 (Federal Energy Regulatory Commission 2011). Efficiently integrating storage resources also requires that storage assets that provide wires-related services be allowed to participate in wholesale power markets (at least where that is possible while still providing the wires-related services). Making this happen will require significant regulatory efforts at both the state and federal levels.

RECOMMENDATION 8.5

FERC should move to integrate storage into transmission planning processes, while state regulators should require the integration of storage in distribution system planning—and storage devices should be allowed to provide wholesale power market services where physically possible.

This recommendation, which also applies to market structures that rely on vertically integrated utilities, focuses on developing regulatory frameworks and market designs that recognize the full set of value streams that storage assets can provide (with respect to wholesale power, transmission, distribution, and customer-side services) without overstating their combined value. In this context, simplifications that do not allow storage to capture all available value streams—such as the concept of “storage as a transmission-only asset”—should be avoided.²²

8.6 Retail rates and economy-wide decarbonization

Currently, retail electricity rates for most residential and small commercial and industrial customers in the United States do not vary over time or in response to system conditions at the bulk power level as reflected in spot wholesale prices. These rates, which are dominated by volumetric (per-kWh) charges, do not encourage or even enable demand response to changes in the marginal value of electricity, and they do not encourage efficient patterns of electricity consumption or efficient investments in energy storage and generation capabilities on customer premises. They are thus inconsistent with allocative efficiency. The benefits of introducing more efficient rate designs will rise sharply as VRE generation and storage play a greater role and as the spot price of electricity (or, in the case of vertically integrated utilities, the system marginal cost) at the bulk power level becomes more variable.

In addition, large commercial and industrial customers frequently pay significant charges based on their demand during the system’s peak demand hours (“coincident peak charges”) that incentivize them to invest in on-site energy storage that can be used to reduce their coincident peak (CP) demand and thus reduce their electricity bills. Often, these investments constitute a form of “uneconomic bypass,” as they reduce storage investors’ bills without providing commensurate benefits system-wide, thereby shifting the burden of cost recovery to other customers. In high-VRE systems, the effect may be to shift demand to periods of “net peak demand” rather than away from these periods and thus to further stress the system.

²² FERC has recently allowed the Midcontinent ISO to employ this concept (Mid-Continent Independent System Operator 2021).

Near-term reform of CP demand charges for large customers seems both feasible and increasingly important. As the cost of storage continues to fall, profitable opportunities for large customers to avoid CP-based demand charges will grow. Failure to address this issue would enable large customers to greatly reduce the revenues collected via demand charges, substantially shifting the burden of covering utility costs to other customer classes. This would have adverse impacts in terms of both total system costs and equity. Avoiding these impacts will require a redesign of retail rates to recover system fixed costs through charges that are less easily gamed—such as customer charges or different types of demand charges.

RECOMMENDATION 8.6

State regulators should replace coincident peak (CP) demand charges for large customers with measures of impact on system supply costs that are less easily gamed.

The best approach to ideal, efficient, and equitable retail rate design is not obvious at this point, and significant additional research efforts are called for. While rate design issues are being explored in many forums (National Association of Regulatory Utility Commissioners 2016; Alliance to Save Energy 2018; Lo et al. 2019; Lazar and Gonzalez 2015; Sergeci 2018; Hledik and Zahniser-Word 2018; Faruqui and Bourbonnais 2020), efforts to continue current research are critical—including efforts to analyze retail rate mechanisms that closely link the marginal component of retail prices to

variations in wholesale prices, as well as voluntary contracting options that allow retail suppliers (in either competitive or monopoly structures) to adjust customers' electricity demand in response to wholesale prices in return for discounts of one sort or another. Programs for cycling air conditioning and water heating loads, which fit this mold, have been around for many years and are popular with consumers. These options likely need to be extended to include other sources of load, such as for EV charging and customer-owned energy storage. In addition, insurance-like designs that limit the impacts of high wholesale prices on residential and small commercial and industrial customers in return for fixed payments deserve further study.

RECOMMENDATION 8.7

The U.S. Department of Energy (DOE), in cooperation with state regulators, should increase support for independent research, including support for well-designed randomized controlled experiments, aimed at (1) devising efficient and equitable retail rate designs for high-VRE systems with storage and (2) encouraging their widespread adoption.²³

Arguably, responsibility for all the research recommendations in this chapter and Chapter 6 should be given to the DOE, along with levels of funding that fully reflect the high importance and complexity of the topics involved.

²³ The U.S. government provided support at the federal level for a number of innovative retail rate experiments in the 1970s (Kohler and Mitchell 1984). It would be worthwhile to draw on that experience to structure more advanced randomized controlled trials of alternative rate structures.

Two important but competing principles should guide continued research on retail rate design. First, efficient electrification and efficient investment in customer-based generation and storage require that *marginal* retail rates be allowed to vary with wholesale spot prices that include the cost of carbon constraints. As we show in Chapter 6, decarbonization will increase average power costs compared to a policy with no carbon constraint. In this context, achieving efficient and rapid electrification means that small customers must be able to adjust their demand to avoid high-cost periods (or have a supplier make such adjustments for them) and to take advantage of the significant periods when spot prices (and thus marginal system costs) are low—particularly to charge electric vehicles. On the other hand, as some customers in Texas recently learned (Blumsack 2021), tying the entire generation component of retail rates directly to wholesale spot prices for electricity would expose small customers to potentially enormous financial risks. It is possible, however, to mitigate that risk while maintaining efficient marginal rates through various types of forward contracting with insurance features and/or “load control” arrangements (e.g., contracts to manage air conditioning or water heating cycles²⁴) between utilities or competitive retail suppliers and customers. Such contracts or arrangements can take advantage of smart metering, communications, and behind-the-meter “smart” appliance control technologies to mitigate consumers’ risks while linking a portion of retail rates to wholesale prices. Potential retail rate designs

will need to be explored in more detail to evaluate both the allocative efficiency properties of alternative pricing and contracting mechanisms and their income distribution properties.²⁵

A second competing principle follows from the fact that most of the costs in a high-VRE system with energy storage will be fixed in the short run, and overall efficiency requires that such fixed costs be recovered through charges that are also fixed in the short run (as with mobile phone subscriptions). Moreover, given the extreme spot price volatility to be expected in future energy-only systems based on the modeling in Chapter 6, and the near ubiquity of capacity mechanisms (and price caps well below VOLL) in the less volatile systems of today, it seems inevitable that price caps and capacity mechanisms will become even more important in high-VRE systems. Revenues from these capacity mechanisms will also need to cover much of the costs of VRE generators and, likely, storage facilities. Recovering those costs through volumetric (per-kWh) retail charges will discourage electrification at the margin. At the same time, high, uniform fixed charges levied on all customers are plainly inequitable. Thus, further research is required to identify alternative regimes that provide efficient price signals to retail consumers and in which an appreciable fraction of consumers’ bills is independent of current consumption. Potentially useful rate designs must also generally be perceived as fair by the public and by policy makers.²⁶

²⁴ See for example, Comed and The Town of Concord Massachusetts.

²⁵ Many “first-generation” decarbonization policies, such as net metering for rooftop solar generation and subsidies for electric vehicles, have favored wealthier consumers. Devising decarbonization policies that are both equitable and efficient is well beyond the scope of this study, but is profoundly important.

²⁶ For some interesting preliminary explorations of this issue, see Burger (2019). In Spain and elsewhere, retail customers can enter medium-term contracts for maximum kW levels of power consumption. Since maximum power consumption is generally correlated with income, one might think this would be a reasonably equitable way to structure fixed charges. We were told, however, that in Southern California, many low-income people live in hot areas away from the coast to reduce their housing costs. As a consequence, they use more electricity for air conditioning than wealthier households that can afford to live nearer the ocean.

Even if there is consensus in the research community about the best retail rate designs, it will be largely up to state regulators to implement the necessary retail pricing reforms. Not all state regulators are likely to embrace those reforms with great enthusiasm, of course, and even where they do, cooperative and municipal utilities often are not subject to state retail rate regulation, and competitive retailers must have some freedom to design their own rate structures. Some customers will benefit from retail rate design changes while others will see higher costs. These distributional effects will lead to controversies in the regulatory process and potentially undermine efficient changes to retail rate designs. Efficient mechanisms to reduce any adverse distributional impacts should be given more consideration.

Large industrial customers are already more likely to face retail prices that vary with actual or expected system conditions, in part because they are generally considered more able to manage price risk than small customers. In states with retail competition, large customers typically negotiate the terms and conditions of their individual contracts with competing retail suppliers. In states without retail competition, state regulators are already likelier to allow utilities to offer alternative pricing options to large customers that are more closely tied to movements in wholesale prices.

8.7 Conclusion and key takeaways

This chapter considers how alternative organizational, regulatory, and policy arrangements can enable energy storage to contribute to the broader goal of decarbonizing the entire economy at the lowest possible total cost. The decarbonized electricity systems of the future, because of their far greater dependence on variable renewable energy (VRE) generation and energy storage, will pose novel operational and financing challenges, as well as complex

challenges in regulation and market design. The recommendations included in this chapter, and in the summary of key takeaways that follows, are designed to address these challenges.

- With high shares of zero-carbon, intermittent renewable energy generating technologies, electricity systems circa 2050 will need to cope with unprecedented supply fluctuations. Energy storage will play a much larger role in these systems, which will also have to contend with the mixed supply and demand impacts of a large number of newly electrified end uses.
- Two features of the efficient, decarbonized systems modeled in Chapter 6 have particularly important implications for the design of markets and governance institutions. The first is a very different distribution of wholesale spot prices with many hours of very low prices, along with a few hours of very high prices. The second is that storage, both grid-scale and at customer premises, is a potential substitute for, or complement to, essentially all other elements of the power system.
- State and federal regulatory agencies need increased expert staffing and budgets to enhance their capabilities to design and implement regulatory mechanisms that can guide the transition to efficient high-VRE systems with storage.
- State regulators should develop rules that allow owners of storage (and generation) assets installed on customer premises to sell services to the vertically integrated utilities within whose geographic footprint they are located under appropriate terms and conditions that facilitate efficient investment in and use of “behind-the-meter” generation and storage.

- Devising state and federal rules that are both efficient and aligned will not be simple, but it will be essential for the high-VRE systems of the future. The Federal Energy Regulatory Commission (FERC), state regulators, and ISOs should reform and align market rules to enable efficient participation—in wholesale energy and ancillary service markets, as well as in capacity markets—by providers of both grid-based storage and distribution-level generation and storage (including from facilities located on customer premises). These reformed rules should accommodate the participation of aggregators in wholesale markets.
- Market rules will need to be developed to adapt capacity mechanisms for the “effective load carrying capability” of VRE generation and to correctly determine the capacity value that storage resources can provide to meet reliability standards. ISOs should either (1) redesign existing capacity mechanisms as they apply to VRE generation and storage, taking into account the joint stochastic properties of VRE generation and demand and the fact that storage is energy-limited, or (2) replace those capacity mechanisms with an increased reliance on integrated resource planning that properly accounts for these factors.
- Storage can provide benefits for transmission and distribution systems that can be particularly important in rapidly growing systems, such as those discussed in Chapter 7. To efficiently realize these benefits, federal regulators should integrate storage into transmission planning processes, while state regulators should require the integration of storage in distribution system planning. In addition, storage devices should be allowed to provide wholesale power market services where physically possible.
- The best approach to ideal, efficient, and equitable retail rate design is not obvious at this point, though it is clear that overall reliance on uniform volumetric (per-kWh) charges must be reduced, and it is likely that a larger fraction of revenues must be raised by charges that do not vary with current consumption. Significant additional research is called for. The U.S. Department of Energy, in cooperation with state regulators, should increase support for independent work aimed at (1) devising efficient and equitable retail rate designs for high-VRE systems with storage and (2) encouraging their widespread adoption.
- Even if there is consensus in the research community about the best retail rate designs, it will be largely up to state regulators to implement the necessary reforms. Some customers will benefit from retail rate design changes while others will see higher costs. Retail competition in some states adds a further layer of regulatory complexity. Efficient mechanisms to reduce any adverse distributional impacts should be given more consideration.

References

- Alliance to Save Energy. 2018. "Forging a Path to the Modern Grid." February. <https://www.ase.org/sites/ase.org/files/forging-a-path-to-the-modern-grid.pdf>.
- American Coalition of Competitive Energy Suppliers. n.d. "State-by-State Information." Accessed February 20, 2022. <https://competitiveenergy.org/consumer-tools/state-by-state-links>.
- American Public Power Association. 2021. "2021 Statistical Report." Accessed July 28, 2021. <https://www.publicpower.org/system/files/documents/2021-Public-power-Statistical-Report.pdf>.
- . 2021. *Electricity Generation Fact Sheet*. Accessed July 28, 2021. <https://www.publicpower.org/policy/electricity-generation>.
- Astrapé Consulting. 2013. "The Economic Ramifications of Resource Adequacy." Accessed February 21, 2022. <https://pubs.naruc.org/pub.cfm?id=536DBE4A-2354-D714-5153-70FEAB9E1A87>.
- Blumsack, Seth. 2021. *What's Behind \$15,000 Electricity Bills in Texas?* February 2021. Accessed July 27, 2021. <https://theconversation.com/whats-behind-15-000-electricity-bills-in-texas-155822>.
- Burger, Scott. 2019. "Rate Design for the 21st Century: Improving Economic Efficiency and Distributional Equity in Electricity Rates." Unpublished dissertation. *MIT Institute for Data, Systems, and Society*. <https://dspace.mit.edu/handle/1721.1/123564>.
- California Independent System Operator. 2019. "Energy Storage: Perspectives from California and Europe." October. Accessed July 27, 2021. <http://www.caiso.com/Documents/EnergyStorage-PerspectivesFromCalifornia-Europe.pdf>.
- . 2021. "Final Root Cause Analysis: Mid-August 2020 Extreme Heat Wave." January 13. Accessed February 21, 2022. <http://www.caiso.com/Documents/Final-Root-Cause-Analysis-Mid-August-2020-Extreme-Heat-Wave.pdf>.
- California Public Utilities Commission. 2018. "Decision on Multiple-Use Application Issues." January 11. Accessed July 27, 2021. <https://docs.cpuc.ca.gov/PublishedDocs/Published/G000/M206/K462/206462341.PDF>.
- Cleary, Katherine, and Karen Palmer. 2020. "Electricity Markets 101." *Resources for the Future*. March 3. Accessed February 20, 2022. <https://www.rff.org/publications/explainers/us-electricity-markets-101>.
- Comed. n.d. "Central AC Cycling." <https://www.comed.com/WaysToSave/ForYourHome/Pages/CentralACCycling.aspx>.
- Edison Electric Institute. 2021. "Sources of Electric Generation." Accessed July 28, 2021. <https://www.eei.org/-/media/Project/EEI/Documents/Resources-and-Media/Sources%20of%20Electric%20Generation.pdf>.
- Electricity Reliability Council of Texas. n.d. "Operating Reserve Demand Curve - WBT." <https://www.ercot.com/services/training/courses/details?name=Operating%20Reserve%20Demand%20Curve%20-%20WBT#overview>.
- Faruqui, Ahmad, and Cecile Bourbonnais. 2020. "The Tariffs of Tomorrow: Innovations in Rate Designs." *IEEE* Vol. 18, no. 3, 18-25. <https://ieeexplore.ieee.org/document/9069846/authors#authors>.
- Federal Energy Regulatory Commission. 2021. "Electric Power Markets." July 21. <https://www.ferc.gov/electric-power-markets>.
- . 2011. "Order 1000: Transmission Planning and Cost Allocation by Transmission Owning and Operating Public Utilities." July 21. Accessed February 21, 2022. <https://www.ferc.gov/sites/default/files/2020-06/Order-1000.pdf>.
- . 2020. "Order 2222: Participation of Distributed Energy Resource Aggregations in Markets Operated by Regional Transmission Organizations and Independent System Operators." September 17. Accessed July 28, 2021. https://www.ferc.gov/sites/default/files/2020-09/E-1_0.pdf.
- . 2018. "Order 841: Electric Storage Participation in Markets Operated by Regional Transmission Organizations and Independent System Operators." February 15. Accessed July 28, 2021. <https://www.ferc.gov/media/order-no-841>.
- Hafstead, Marc. 2019. "Carbon Pricing 101." *Resources for the Future*. Accessed July 27, 2021. <https://www.rff.org/publications/explainers/carbon-pricing-101>.
- Hledik, Ryan, and Jake Zahniser-Word. 2018. "Storage-Oriented Rate Design: Stacked Benefits or the Next Death Spiral?" *The Electricity Journal*. October 31. <https://www.brattle.com/insights-events/publications/storage-oriented-rate-design-stacked-benefits-or-the-next-death-spiral>.
- Howland, Debra A. 2021. "Comments of the Energy Storage Association to the Public Utility Commission of New Hampshire." *Energy Storage Association*. January 11. https://www.puc.nh.gov/Regulatory/Docketbk/2020/20-166/LETTERS-MEMOS-TARIFFS/20-166_2021-01-11_ESA_COMMENTS.PDF.

- International Energy Agency. 2021. “Net Zero by 2050: A Roadmap for the Global Energy Sector.” <https://www.iea.org/reports/net-zero-by-2050>.
- Joskow, Paul, and Jean Tirole. 2007. “Reliability and Competitive Electricity Markets.” *Rand Journal of Economics* 38(1): 60-84.
- Kohler, David F., and Bridger M. Mitchell. 1984. “Response to Residential Time-of-Use Electricity Rates: How Transferable are the Findings?” *Journal of Econometrics* 26: 1-2, 141-177.
- Lazar, Jim, and Wilson Gonzalez. 2015. “Smart Rate Design for a Smart Future.” *Regulatory Assistance Project*. July 15. <https://www.raponline.org/knowledge-center/smart-rate-design-for-a-smart-future>.
- Lo, Helen, Seth Blumsack, Paul Hines, and Sean Meyn. 2019. “Electricity Rates for the Zero Marginal Cost Grid.” *The Electricity Journal* 32: 39-43.
- Mid-Continent Independent System Operator. 2021. “Storage as Transmission-Only Asset (SATOA) PAC004.” June 30. Accessed July 28, 2021. <https://web.archive.org/web/20210805121733/https://www.misoenergy.org/stakeholder-engagement/issue-tracking/storage-as-transmission-only-asset>.
- Milligan, Michael. 2015. “Missing Money — Will the Current Electricity Market Structure Support (~50%) Wind/Solar?” *AWEA WindPower Conference*. Accessed July 29, 2021. <https://www.nrel.gov/docs/fy15osti/64324.pdf>.
- National Association of Regulatory Utility Commissioners. 2016. “NARUC Manual on Distributed Energy Resources Rate Design and Compensation.” <https://pubs.naruc.org/pub/19FDF48B-AA57-5160-DBA1-BE2E9C2F7EA0>.
- National Renewable Energy Laboratory. 2016. “Competitive Electricity Market Regulation in the United States: A Primer.” *Technical Report NREL/TP-6A20-67106*. December. Accessed July 28, 2021. <https://www.nrel.gov/docs/fy17osti/67106.pdf>.
- Roques, Fabien. 2021. “Hybrid Electricity Markets: Key Principles and Possible Approaches (presentation).” June 21. Accessed July 27, 2021. http://www.ceem-dauphine.org/assets/dropbox/17h45_2-2_Fabien.pdf.
- Sergeci, Sanem. 2018. “Rate Design in a High DER Environment.” https://www.brattle.com/wp-content/uploads/2021/05/14504_sergici_slides_for_sepa_workshop_on_alternative_rate_design_20180920_sent.pdf.
- Spector, Julian. 2020. “From Pilot to Permanent: Green Mountain Power’s Home Battery Network is Here to Stay.” *Greentech Media*. October 16. <https://www.greentechmedia.com/articles/read/from-pilot-to-permanent-green-mountain-powers-home-battery-network-is-sticking-around>.
- The Town of Concord Massachusetts. n.d. “Controlled Water Heating.” <https://concordma.gov/494/Controlled-Water-Heating>.
- U.S. Energy Information Administration. 2011. “About 60% of the U.S. Electric Power Supply is Managed by RTOs.” April 4. Accessed February 21, 2022. <https://www.eia.gov/todayinenergy/detail.php?id=790>.
- Weber, Michael E. 2021. “The Texas Power Crisis Didn’t Have to Happen.” *American Society of Mechanical Engineers*. June 15. Accessed July 27, 2021. <https://www.asme.org/topics-resources/content/the-texas-power-crisis-didn-t-have-to-happen>.
- World Bank. 2021. “Carbon Pricing Dashboard.” Accessed July 27, 2021. <https://carbonpricingdashboard.worldbank.org>.

Chapter 9 – Innovation and the future of energy storage

9.1 Introduction

This chapter examines the role of technology innovation in ensuring that energy storage can play a significant role in future electric power systems. For purposes of this discussion, we use the term “innovation” to refer to the transition of new products or business practices from idea creation to commercial deployment. The process of innovation for energy technologies and all other technologies passes through five stages:

idea creation → R&D → engineering at pilot scale → technology demonstration → deployment

Innovation does not proceed in a smooth or predictable way. Many feedbacks can call for modifying, accelerating, or slowing an innovation plan. For example, fundamental research normally plays its decisive role in early-stage idea creation. But occasions will arise when limitations that appear only in deployment will be overcome by targeted fundamental research. Similarly, experience with deployed technologies often suggests new ideas that deserve to be explored.

In a market economy, successful innovation requires the integration of technical, economic, and often regulatory considerations at each stage. The early stages of the process typically rely on a “technology push” in the form of public or private investments in idea creation and R&D; in the later stages, “market pull” plays a growing role. Early-stage projects primarily require financial support to cover development costs in advance of deployment. Later-stage projects must attract a mix of private equity and debt by investors who are

willing to take a financial risk in expectation of returns that are based on a credible projection of project revenues and cost. The goal in such projects is to convince equity and debt investors of a new technology’s commercial viability by demonstrating performance and cost. Thus, different financial instruments or regulatory mandates are needed to encourage progress in the early and later stages of the innovation process.

The primary risks for commercializing a new technology go beyond unanticipated technical difficulties or overoptimistic cost estimates to external factors such as market uncertainties, changing regulatory standards, shifts in government policy, public objections, and planning based on faulty assumptions about the future. For energy technologies, the involvement of an integrated project development team composed of individuals with technical, economic, regulatory, and public outreach expertise can help anticipate and respond to challenges that likely will not be recognized if only technical experts are involved.

America’s innovation infrastructure is the envy of the world. With research funding largely from the federal government, an open university system that works closely with U.S. industry has created a cornucopia of fundamental research. This research, developed under the protection of an effective intellectual property system, has prompted substantial flows of private capital to finance an enormous number of startup ventures in a wide range of fields. America’s comparative advantage in innovation is in early-stage idea creation and R&D. Outside of biomedicine, the United States is not as strong in manufacturing and supply-chain management as many Asian countries and some countries

in the European Union. An iconic example among energy innovations is photovoltaic (PV) technology. In the 1970s and 1980s, the U.S. Department of Energy (DOE) provided generous support for R&D on materials and instrumentation to produce low-defect silicon wafer PV cells. But it was companies in China and other Asian countries (South Korea, Malaysia, and Japan) that learned to manufacture quality PV modules on a large scale and at lower cost, enabling them to gain competitive advantage in U.S. and E.U. markets.

The DOE's strengths in innovation, built on the accomplishments of the department's predecessor agencies, continue to support idea creation and early-stage energy R&D. The DOE's large, capable, and well-funded Office of Science is the largest supporter of physical science in the United States. The largest of the DOE national laboratories receive about \$10 billion in funding each year for national security and energy-related R&D. Despite their excellent work and efforts to encourage technology transfer to the private sector, the national laboratories have not been as productive as universities and private companies in creating commercial products from R&D. This is, in part, because the focus of innovation in the DOE national laboratories is on achieving high technical performance; as a result, there is little emphasis on cost, design for serial manufacturing, and meeting customer preferences.

Perhaps the most important recent development with respect to federal support for energy innovation was the creation of a new agency within the DOE, the Advanced Research Projects Agency-Energy (ARPA-E). Modeled on DARPA (the well-regarded Defense Advanced Research Projects Agency), ARPA-E has introduced entirely new methods for soliciting, evaluating, and rapidly funding new ventures, while also overseeing project progress, with the aim of more effectively supporting the development of disruptive clean energy

technologies. The Biden administration has proposed creating a new agency: ARPA-Climate (The White House 2021a). The purpose and scope of a new ARPA-C and its relationship to ARPA-E are not clear.

The DOE's record in downstream innovation is decidedly mixed. Its management of several large-scale energy technology demonstration projects, primarily through contracts that were directly negotiated between private companies and the federal government, led to expensive failures; prominent examples include the 1972 Clinch River Breeder Reactor, the 2003 FutureGen carbon capture and sequestration project, and the 1981 Barstow Solar Power Tower in California. Downstream ventures have typically involved a private-sector partner who is seeking government assistance to help either (1) defer the initial cost of a first-of-kind plant or (2) demonstrate the cost and performance of a new technology that advances a policy objective such as reducing greenhouse gas emissions. Indirect financial incentives, such as feed-in tariffs, production payments, and state-sponsored competitive procurements by regulated utilities, are more efficient assistance mechanisms in the later stages of innovation because they allow projects to proceed on as much of a commercial basis as possible.

Most observers believe these incentives can be made more effective. A first recommendation is to extend the annual cycle of congressional appropriations for multi-year demonstration projects since the annual cycle creates uncertainty and often introduces schedule disruptions; a further concern is that members of Congress understandably favor local constituencies. A second recommendation is for the DOE to focus on recruiting individuals with the experience and skills required to craft and oversee large technology demonstration projects. In addition, such demonstration projects should not be required to comply with the Federal Acquisition Regulation (FAR), which distorts

commercial practices. Among energy experts, there is widespread skepticism that the DOE, or the federal government more broadly (as presently organized), has the capability to effectively support innovation at the pace and scale needed to transition the United States to a carbon-free economy.

9.2 The current context for energy storage innovation

This study focuses on “the future of energy storage” in the context of the electricity sector’s transition away from fossil fuels (coal and natural gas) to variable renewable energy (VRE) resources, principally wind and solar.

That transition implies an enormous change in the configuration of the electricity system, including generation, transmission, and storage. Achieving an electricity system with net-zero carbon emissions will require new policies and regulations (discussed in Chapters 4, 5, and 8), as well as additional net investment that McKinsey & Co. estimates could be as high as \$2.5 trillion out to 2035 (McKinsey and Company 2021). In addition, planning for this transition also entails assumptions about future electricity demand that will be influenced by economic growth and decarbonization in sectors outside electricity, such as buildings, industry, and transportation. While carbon-free electricity by 2035 is possible, in principle, there are at least four reasons to doubt that this goal can be achieved in practice.

First, it is important to stress that the absence of a serious, comprehensive, and stable national climate policy will amplify the uncertainties that bear on all elements of the clean energy transition including, perhaps especially, energy

storage. The authors of this study believe that an economy-wide mechanism for pricing carbon emissions that provides significant incentives to reduce emissions (with mechanisms for compensating economically disadvantaged communities and individuals), together with federal authority over siting decisions for transmission and other key components of the electricity system are necessary for an economically efficient transition.¹

Adopting a comprehensive carbon pricing policy is widely viewed as politically impractical. The Biden administration instead announced its intention to pursue a national clean electricity standard, although the design and implementation of such a standard is far from clear. Political opposition to the Biden administration’s clean electricity standard led to its being dropped from legislation currently pending in Congress. By contrast, the patchwork of state and regional plans and subsidy programs that exists today to reduce carbon emissions does not encourage economically efficient mitigation strategies and low-carbon innovations (Commonwealth of Massachusetts 2020). Moreover, many states have declined to make rapid decarbonization a policy goal, and it is not technically or economically feasible for the policies in the states that have credibly pursued deep decarbonization policies to carry the water for the entire country.

Second, the scale of investment required to achieve net-zero electric sector carbon emissions by 2035 is massive. If undertaken, investments of the required magnitude could create unanticipated perturbations in the U.S. economy and lead to unwelcome market dislocations in some sectors and regions.

¹ The Infrastructure Investment and Jobs Act (IIJA; P.L. 117-58) includes several provisions related to transmission modernization and expansion, with the general goals of improving electric grid reliability and resilience (Congressional Research Service 2021).

Third, 2035 as a near-term target for a carbon-free electricity system, whether this target is intended to be practical or aspirational, shifts federal and state direct support (subsidies) and mandatory regulations to favor near-term, “shovel ready” projects that may produce measurable results by 2030, but that may also invite hurried investments in projects that are less economically efficient in terms of achieving longer-term climate mitigation goals. Some of the financial support will likely end up going to projects that would have occurred anyway. Regardless of the scope and timing of emissions targets, a successful innovation project or program requires a disciplined approach that incorporates ongoing evaluation of progress toward meeting technical milestones, cost goals, regulatory requirements, and schedule demands. Successful innovation must be driven by meeting technical milestones, not by meeting an arbitrary set of temporal goals.

Fourth, as this study has demonstrated, the outlook for energy storage technologies is complicated because storage is linked to other elements of the electricity system: demand-side management, expansion of the geographic extent of wholesale market or dispatch areas, and enhanced transmission capacity. Most importantly, the objective of carbon-free electricity has implications for expanding competition between technologies. For example, small amounts of natural gas generation with tailored carbon capture and storage (CCS) can enable and reduce the costs of an electricity system that is largely based on VRE resources to meet demand with near-zero carbon emissions.

Finally, innovations that are introduced to reduce greenhouse gas emissions should be *sustainable*—in other words, these innovations should avoid or minimize new environmental burdens. If electric vehicle (EV) deployment grows at an average annual rate of 31%–36%

through the remainder of this decade (to 2030), as the International Energy Agency (IEA) expects, and if the lifetime of early lithium-ion batteries is 10 years or less at anticipated levels of use, then a large inventory of end-of-life EV batteries will build up sometime during the 2030s. Opportunities will emerge to find useful second-life applications for these batteries, perhaps in grid storage applications where depth-of-discharge specifications are less important. Alternatively, batteries may be recycled to retrieve component materials that will have increasing value. The federal government should consider establishing policies today to clarify whether battery manufacturers or purchasers are responsible for end-of-life disposal. A major purpose of such policies would be to give battery manufacturers an incentive to design batteries that have potential for end-of-life reuse or recycling rather than ending up in a landfill (Morse 2021).

9.3 Implications for federal support of energy storage innovation

The considerations discussed above have implications for how the DOE and the private sector should approach innovation in energy storage technologies. Support for early-stage idea creation and fundamental research, which historically has been the DOE’s strength, should continue. This report makes several recommendations concerning promising storage technologies that can be ready for market introduction in the near term—i.e., before 2030—and over the longer term. Table 9.1 summarizes our findings with respect to the innovation status of different storage technologies. Additional technologies are likely to play a role in the longer term—several are mentioned in the report—but there is greater uncertainty about the pace and character of innovation for these technologies.

**Table 9.1 Summary of MITEI's Future of Energy Storage study findings
on the current innovation status of selected technologies**

| Technology | Current Innovation Status | | | | | Chapter |
|---|---------------------------|---|---|---|---|---------|
| | ① | ② | ③ | ④ | ⑤ | |
| Electrochemical storage | | | | | | 2 |
| Li-ion | | X | | X | X | 2 |
| Flow batteries (aqueous inorganic) | | X | | X | X | 2 |
| Flow batteries (aqueous organic) | X | X | X | | | 2 |
| NaS batteries | | | | X | X | 2 |
| Metal-air batteries | | X | X | | | 2 |
| Critical materials supply (metals and rare earths) | X | X | X | | | 2 |
| Battery re-cycling | X | X | X | X | | 2 |
| Battery second use | X | X | | | | 2 |
| Advanced power electronics | | X | X | X | | |
| Pumped hydro storage | | | | X | X | 3 |
| Thermal storage | | X | X | X | | 4 |
| Hydrogen | | | | | | 5 |
| Production, transport, storage | X | X | | X | | 5 |
| H ₂ generation – photoelectric, very high T HTGR, advanced electrolysis | | X | | | | 5 |

① Idea creation, study, and analysis—both public and private sponsors
 ② R&D—university, national laboratory, and private sector performers
 ③ Pilot-scale engineering
 ④ Demonstration & testing
 ⑤ Deployment—depends on progress and market conditions

Further discussion is found in the chapters listed.

In general, there is no great need for federal R&D support directed to near-term technology options. The rapid growth of the EV market has led to ongoing cost reductions in lithium-ion battery technology that can be applied to batteries configured for grid storage. The private sector has responded by providing significant venture capital for storage technologies generally. In contrast to other times and other categories of energy technology, insufficient funding for R&D is not the primary constraint on innovation with respect to energy storage technologies.

As is frequently stressed in the relevant literature, successful innovation requires integration of economic, regulatory, and technical considerations. There is a stronger case for federal support for storage technologies that may not be developed or deployed until after 2030; several opportunities are mentioned in the technology chapters of this study. Timing is important: For example, long-duration storage technologies may be important only in a future low-carbon electricity system that is powered almost entirely by wind and solar generation.

Such technologies, which may be on the horizon but for which market demand is just developing, should be considered for federal RD&D support today.

Uncertainty and risk will of course influence the actions that federal and state governments and private-sector firms and investors will take to implement the many recommendations advanced in this report. Three categories of implementing actions must be considered: (1) support for the development and demonstration of various storage technologies; (2) direct federal and state support (subsidies), mandatory regulations, and procurement obligations by utilities to accelerate the deployment of grid-level storage technologies; and (3) private-sector investment. Near-term actions should be designed to produce measurable results between 2021 and 2030 while results for longer-term actions would be expected after 2030.

A zero-carbon goal by 2035 for the electric sector will push public and private efforts to the downstream stages of technology innovation—specifically, to near-term technology demonstration and deployment and much greater private-sector investment. Accordingly, the DOE's storage innovation efforts should move in three directions. First, the DOE should sponsor more joint technology demonstration projects with industry. These projects should be unfettered by FAR and other rules that constrain technology development and demonstration on commercial terms. A particularly interesting example put forward in this study is to explore the possibility of low-capacity integrated natural gas generation tailored to work with small CCS facilities to close the gap between high- and 100%-available VRE generation. Another potentially interesting target for technology demonstration is the use of EV batteries in grid storage applications.

In the past, the DOE has insisted that private sector partners share project costs as a way to “stretch” federal dollars. Because private partners are typically granted intellectual property rights in return, this practice compromises the basic objective of publicly supported technology demonstration projects, which is to spread information among all industry participants, thereby creating the conditions for efficient competition. Federal demonstration projects should include explicit requirements for information sharing with other U.S. entities that have not been partners, even if this requires a greater federal contribution.

Second, while the recently passed Integration and Investment Jobs Act (IIJA) includes several incentives for hydrogen development, notably the creation of “at least” four hydrogen hubs, much remains to be done to develop hydrogen’s potential to play a major role in a net-zero energy economy. Hydrogen is an energy carrier with many potential applications. Chapter 5 of this study focuses on hydrogen as a potential chemical storage medium for VRE-generated electricity. But hydrogen can also be used in industrial chemical applications and for transportation and heating—and, as Chapter 6 illustrates, use of hydrogen in such applications can enhance its value in the electric power system. The ability of existing natural gas pipelines to carry hydrogen without suffering embrittlement either at reduced pressures or after blending with natural gas remains an open technical question that deserves further study with support from the DOE and the Department of Transportation. Different hydrogen applications require different kinds of system integration that go beyond technology development. However, all applications require lower-cost methods for producing hydrogen (absent very high CO₂ emission charges), which justifies significant DOE support for R&D to lower the cost of hydrogen production using electrolyzers or methane pyrolyzers.

Third, federal efforts to accelerate the downstream deployment of any commercial technology should rely on “indirect” incentives such as production payments or feed-in tariffs that do not interfere in the management of related demonstration projects. Demand-side incentives are generally more efficient (less costly) than production-side subsidies if the aim is to encourage deployment, as demonstrated by experience in Europe (Germany and Spain) compared to the United States. Loan guarantees are popular with Congress because they give the illusion of being “off budget.” Such guarantees should be avoided because they are administered by the Department of the Treasury which, understandably, does not favor this mechanism and adds burdensome restrictions. More importantly, the DOE loan guarantees protect the private-sector partner from failure rather than rewarding success. Policy makers should instead favor production payments for generating assets because these payments are based on kilowatt-hours of actual production, at benchmarked cost. Production payments for non-generating energy technologies such as storage must be based on preset development requirements and operational testing measures. Some failures are to be expected in any reasonably ambitious innovation effort. However, when a federal project fails, the entire program often becomes the target of political controversy, threatening the continuation of the innovation effort.

Two additional areas of innovation that are not a focus of this study deserve mention: manufacturing and supply-chain management for energy storage devices, especially electrochemical batteries. A related concern is the international competitiveness of U.S. storage products compared to those of foreign manufacturers, notably from manufacturers in China and other Asian countries such as South Korea, Taiwan, and Japan.

The DOE’s energy storage program was announced on January 8, 2020 (U.S. Department of Energy 2020) with a corresponding appropriations request of \$158 million for FY2020. This modest request included efforts to support manufacturing and supply chain management. However, the DOE has had little success in manufacturing assistance programs, manufacturing technology centers, and public/private partnerships for reasons that include a lack of commercial expertise, onerous requirements under the FAR, congressional interference, and frequent failure to emphasize the value of competition between technologies. Outside its nuclear weapons program, the DOE and its national laboratories have little experience in manufacturing and supply-chain management in commercial markets. Developing this expertise will require close cooperation with private-sector participants and commercial market activities.

An additional complicating factor is widespread, bipartisan concern among members of Congress about unfair and illicit trade practices by China. President Biden’s February 2021 *Executive Order #14017 on America’s Supply Chain* directs the Secretary of Energy to submit a report within 100 days identifying “risks in the supply chain for high-capacity batteries, including electric vehicle batteries.”

On June 21, 2021, the White House released a 250-page report, *Building Resilient Supply Chains, Revitalizing American Manufacturing, and Fostering Broad-Based Growth* (The White House 2021b), that included a 60-page DOE submission addressing large-format batteries. The DOE section addresses many subjects covered in this study. Other sections of the June 2021 report address semiconductors (Department of Commerce), critical materials (Department of Defense), and pharmaceuticals (National Institutes of Health).

The White House report deserves serious attention; at a minimum, it signals that attention to foreign competition, especially from China,² and America's lagging position in manufacturing and supply-chain management will remain prominently on the agenda in Congress, the administration, and the business community. The White House report also makes many far reaching and costly recommendations, unfortunately without setting priorities or indicating how the many new initiatives it proposes will be managed, monitored, and coordinated. Taken as a whole, the report signals a new and aggressive U.S. industrial policy. Its emphasis on preferentially building U.S. capability and on trade practices and subsidies that favor domestic producers will likely raise many issues at the World Trade Organization.

One recommendation of this Future of Energy Storage study that is not mentioned in the White House report, but that may prove to have the greatest benefit in terms of achieving a net-zero electricity system in this country, is the recommendation to develop new, open-access modeling, simulation, and analysis tools under the direction of the DOE's Office of Electricity (see Chapter 6 for a discussion). Such tools would permit stakeholders engaged in evaluating new electricity system designs to explore alternative pathways to achieving key goals. Their analyses can then provide a basis for objective discussion of alternatives and, hopefully, more rapid decision-making.

A new set of modeling and analysis tools would also be of considerable benefit to developing countries. The United States could make an important contribution by providing technical assistance to these countries on how to collect data and use state-of-the-art tools for energy and climate planning.

9.4 Key takeaways

- The process of technology innovation is typically described in terms of five distinct stages: idea creation, R&D, engineering at pilot scale, technology demonstration, and deployment.
- The United States has historically been very strong in the early stages of innovation (idea creation and R&D), while Asian countries and some European countries have excelled at manufacturing and supply-chain management.
- Among energy experts, there is widespread skepticism that the DOE, or the federal government more broadly, is organized to effectively support innovation at the pace and scale needed to transition the United States to a carbon-free economy.
- In general, there is no great need for federal R&D support directed to near-term energy storage options; the case for federal support is stronger for storage technologies that may not be developed or deployed until after 2030.
- To achieve a zero-carbon electricity system by 2035, it will be necessary to accelerate innovation, which, to be successful, requires integration of economic, regulatory, and technical considerations.
- The DOE should sponsor more joint technology demonstration projects with industry.

² "Across all four reports, China stands out for its aggressive use of measures—many of which are well outside globally accepted fair trading practices—to stimulate domestic production and capture global market share in critical supply chains," (The White House 2021b, page 11, reference 6).

- Federal efforts to accelerate the downstream deployment of any commercial technology should rely on “indirect” incentives such as production payments or feed-in tariffs that do not interfere in the management of related demonstration projects.
- In the context of U.S. government support for innovation, two additional areas deserve greater attention: manufacturing and supply-chain management for energy storage devices, especially electrochemical batteries.
- The DOE Office of Electricity should direct efforts to develop new, open-access modeling, simulation, and analysis tools.

References

- Commonwealth of Massachusetts. 2020. “Press Release: Baker-Polito Administration Releases Roadmap to Achieve Net Zero Emissions by 2050.” *Commonwealth of Massachusetts*. December 30. <https://www.mass.gov/news/baker-polito-administration-releases-roadmap-to-achieve-net-zero-emissions-by-2050>.
- Congressional Research Service. 2021. “IIJA: Efforts to Address Electric Transmission for Reliability, Resilience, and Renewables.” *Congressional Research Service*. December 9. <https://crsreports.congress.gov/product/pdf/IN/IN11821>.
- McKinsey and Company. 2021. “Net zero by 2035: A pathway to rapidly decarbonize the US power system.” *McKinsey and Company*. October 14. [https://www.mckinsey.com/industries/electric-power-and-natural-gas/our-insights/netzero-by-2035-a-pathway-to-rapidly-decarbonize-the-us-power-system](https://www.mckinsey.com/industries/electric-power-and-natural-gas/our-insights/net-zero-by-2035-a-pathway-to-rapidly-decarbonize-the-us-power-system).
- Morse, Ian. 2021. “A dead battery dilemma.” *Science*. May 21. <https://www.science.org/doi/abs/10.1126/science.372.6544.780>.
- The White House. 2021a. “Biden-Harris Administration Launches American Innovation Effort to Create Jobs and Tackle the Climate Crisis.” *The White House*. February 11. <https://www.whitehouse.gov/briefing-room/statements-releases/2021/02/11/biden-harris-administration-launches-american-innovation-effort-to-create-jobs-and-tackle-the-climate-crisis>.
- . 2021b. “Building Resilient Supply Chains, Revitalizing American Manufacturing, and Fostering Broad-Based Growth.” June. <https://www.whitehouse.gov/wp-content/uploads/2021/06/100-day-supply-chain-review-report.pdf>.
- U.S. Department of Energy. 2020. “U.S. Department of Energy Launches Energy Storage Grand Challenge.” *U.S. Department of Energy*. January 8. <https://www.energy.gov/articles/us-department-energy-launches-energy-storage-grand-challenge>.

Appendix A – Cost and performance calculations for electrochemical energy storage technologies

This appendix provides details about the cost and performance calculations used to compare electrochemical energy storage (i.e., battery) technologies in Chapter 2 of the main report.

A.1 Chemical cost of stored energy for battery chemistries

Table A.1 lists the chemical cost of storage (CCS) for battery chemistries plotted in Figure 2.2 in the main report. To calculate CCS for each battery type, we follow the methodology reported by Li et al. (2017) as discussed below. Unit prices for chemicals are tabulated in Table A.2, with sources given in the references. While we sought to obtain reliable supplier pricing information from multiple sources, including materials vendors and

industry experts, materials prices do fluctuate and evolve, and it is possible that the numbers presented here may not accurately represent values at the time of reading. These cost numbers are intended to facilitate comparisons among the different battery types discussed in this study, and care should be taken if using them for other purposes.

A.1.1 Cost calculations for redox flow batteries (RFBs)

All RFBs we considered are aqueous systems for which the solvent cost is negligible. The costs of all dissolved species, including redox-active components and supporting species, are included in the CCS. Assuming a redox flow battery with unit capacity (1 Ah) operated at infinitely low current, the CCS is:

$$CCS \left(\frac{\text{US\$}}{\text{kWh}} \right) = \frac{Cost \text{ of } negative \text{ electrolyte } (\text{US\$}) + Cost \text{ of } positive \text{ electrolyte } (\text{US\$})}{Voltage \text{ (V)} \cdot 1(\text{Ah}) \cdot 0.001 \left(\frac{\text{kWh}}{\text{Wh}} \right)}$$

where voltage (V) is the average open circuit voltage (OCV) across the state-of-charge range corresponding to the utilized capacity.

The costs of the negative and positive electrolyte (US\$) are calculated as follows:

$$\text{Cost of negative electrolyte (US\$)} = \left\{ P_a \left(\frac{\text{US\$}}{\text{mol}} \right) \cdot c_a \left(\frac{\text{mol}}{\text{L}} \right) + \sum \left[P_{a,s} \left(\frac{\text{US\$}}{\text{mol}} \right) \cdot c_{a,s} \left(\frac{\text{mol}}{\text{L}} \right) \right] \right\} \cdot \frac{1 \text{ (Ah)}}{Cap_c \left(\frac{\text{Ah}}{\text{L}} \right)}$$

$$\text{Cost of positive electrolyte (US\$)} = \left\{ P_c \left(\frac{\text{US\$}}{\text{mol}} \right) \cdot c_c \left(\frac{\text{mol}}{\text{L}} \right) + \sum \left[P_{c,s} \left(\frac{\text{US\$}}{\text{mol}} \right) \cdot c_{c,s} \left(\frac{\text{mol}}{\text{L}} \right) \right] \right\} \cdot \frac{1 \text{ (Ah)}}{Cap_c \left(\frac{\text{Ah}}{\text{L}} \right)}$$

Where P_a (US\$/mol) and P_c (US\$/mol) are the respective costs of active species in the negative and positive electrolyte, c_a (mol/L) and c_c (mol/L) are the respective concentrations of active species in the negative and positive electrolyte, $P_{a,s}$ (US\$/mol) and $P_{c,s}$ (US\$/mol) are the respective costs of supporting species in the negative and positive electrolyte, and $c_{a,s}$ (mol/L) and $c_{c,s}$ (mol/L) are the respective concentrations of supporting species in the negative and positive electrolyte. Costs are summed over all species used. Cap_a (Ah/L) and Cap_c (Ah/L) are the respective volume-specific capacities of the negative and positive electrolyte.

A.1.2 Cost calculations for all other listed battery types

We assume a cell of unit capacity (1 Ah) based on its practical specific capacity. The CCS is calculated as follows:

$$CCS \text{ (US$/kWh)} = \frac{m_a \text{ (kg)} \cdot P_a \text{ (US$/kg)} + m_c \text{ (kg)} \cdot P_c \text{ (US$/kg)} + m_e \text{ (kg)} \cdot P_e \text{ (US$/kg)}}{\text{Voltage (V)} \cdot 1(\text{Ah}) \cdot 0.001(\text{kWh}/\text{Wh})}$$

In the above equation, the mass of the negative electrode, positive electrode, and electrolyte are given, respectively, by

$$m_a \text{ (kg)} = (1(\text{Ah})) / (C_a \text{ (Ah/kg)}),$$

$$m_c \text{ (kg)} = (1(\text{Ah})) / (C_c \text{ (Ah/kg)}), \text{ and}$$

$m_e \text{ (kg)} \cdot C_a \text{ (Ah/kg)}$ and $C_c \text{ (Ah/kg)}$ are the practical specific capacity of the negative and positive electrode, respectively. Voltage (V) is the average voltage or projected average voltage over the practical specific capacity. P_a (US\$/kg), P_c (US\$/kg), and P_e (US\$/kg) are unit costs for the negative electrode active

material, positive electrode active material, and electrolyte (salt + solvent), respectively. Where available, we use market prices for these materials traded in large volume.

The positive electrode and negative electrode are assumed to have equal capacity, except for electrochemical couples that use a metal electrode (Li, Na, Mg, Zn). In those cases, we assume 100% excess of the metal electrode. The relative amount of electrolyte to active material differs between battery types, as discussed below. For high-temperature batteries (Na/S, Na/NiCl₂, and molten metal batteries), a solid or molten electrolyte layer is typically used as the separator between the positive electrode and the negative electrode. The cost of this separator/electrolyte is not included in the CCS, since the cost of separator is not included in the CCS for the other battery types we analyze.

A.1.3 Electrolyte-to-active-material ratio for all battery types

Different cell constructions require different amounts of electrolyte relative to the amount of positive electrode and negative electrode. We distinguish between four basic types of batteries:

The first type (Type I) has two porous electrodes. Batteries utilizing powder-based active materials, such as typical lithium-ion batteries, typically have porous negative and positive electrodes,

as well as separators, all of which are infused with electrolyte. There is also some excess electrolyte within the cell beyond that necessary to completely infiltrate the pore space.

We assume that the volume ratio of electrolyte to active material is 35%/65%. The mass of electrolyte, m_e , is then calculated as:

$$m_e = d_{\text{electrolyte}} \cdot (V_{\text{positive electrode}} + V_{\text{negative electrode}}) \cdot \frac{35}{65}$$

We calculate the volume of positive electrode and negative electrode by assuming that the active materials account for 80% of the electrode mass, and that the mass density of the electrodes is 2 kg/L. Using these assumptions,

$$V_{\text{electrode}} = \frac{m_{\text{active material}}}{0.8} \cdot \frac{1}{2\text{kg/L}}$$

The second type of battery (Type II) has a solid plate electrode and a porous electrode. Batteries of this type include lithium-, sodium-, and magnesium-metal batteries. We assume the porosity of the porous electrode to be 35%. The mass of electrolyte needed to completely fill this porosity, m_e , is then calculated as:

$$m_e = d_{\text{electrolyte}} \cdot V_{\text{positive electrode}} \cdot \frac{35}{65}$$

The metal electrode is assumed to have twice the capacity of the porous electrode. The volume of the porous electrodes is calculated as for batteries of Type I.

The third type of battery we consider (Type III) is the plate electrode battery. The lead-acid battery is the exemplar of this type. We assume the mass of electrolyte, m_e , is 20% of the combined mass of electrolyte, electrode, and packaging.

$$\frac{m_e}{m_{\text{electrodes}}} = \frac{20}{70}$$

A fourth type of battery (Type IV) is the metal-air battery. For Li-air batteries, the liquid electrolyte, lithium metal negative electrode, and porous positive electrode (particulate carbon) are typically present in mass ratios of 70:5:5, with the balance of the mass being taken up by packaging and supporting materials.

We assume these mass ratios to calculate the amount of electrolyte relative to lithium metal or positive electrode. The same mass ratio of electrolyte to positive electrode is assumed for all other metal-air batteries (Zn, Fe, Al). We also assume the same metal electrode *capacity* for all metal-air batteries. Thus, the mass of the negative electrode is normalized by applying the ratio of the specific capacity of the corresponding metal (Zn, Fe, Al) to that of Li metal.

Table A.1 Rechargeable battery types, year of introduction, and chemical cost as plotted in Figure 2.2 in the main report

| Couple | Type | Introduction Year | Cost (\$/kWh) |
|--|-------------------------------|-------------------|---------------|
| C ₆ /LMO | Li-ion (C ₆ anode) | 1984 | 38.8 |
| C ₆ /LCO | Li-ion (C ₆ anode) | 1991 | 92.0 |
| C ₆ /LFP | Li-ion (C ₆ anode) | 1997 | 37.5 |
| C ₆ /LNMO | Li-ion (C ₆ anode) | 1997 | 46.0 |
| LTO/LMO | Li-ion (C ₆ anode) | 1998 | 76.9 |
| C ₆ /NCM(1:1:1) | Li-ion (C ₆ anode) | 2001 | 41.6 |
| C ₆ /NCA | Li-ion (C ₆ anode) | 2002 | 58.6 |
| C ₆ /NCM(8:1:1) | Li-ion (C ₆ anode) | 2017 | 48.5 |
| C ₆ /NCM(6:2:2) | Li-ion (C ₆ anode) | 2016 | 43.8 |
| Si/NCM(6:2:2) | Li-ion (Si anode) | 2016 | 46.0 |
| Si/NCM(8:1:1) | Li-ion (Si anode) | 2018 | 50.9 |
| SiO-C/NCM(8:1:1) | Li-ion (SiO/C anode) | 2019 | 54.7 |
| Li/S | Lithium metal | 1958 | 14.8 |
| Li/TiS ₂ | Lithium metal | 1976 | 187.1 |
| Li/MoS ₂ | Lithium metal | 1979 | 34.4 |
| Li/LCO | Lithium metal | 1980 | 85.8 |
| Na/S | High temperature | 1966 | 1.6 |
| Na/NiCl ₂ | High temperature | 1978 | 6.6 |
| Li/Pb ₂ Sb | High temperature | 2014 | 62.3 |
| Ca/Sb | High temperature | 2014 | 20.4 |
| Na/P2-MN | Na ion (nonaqueous) | 2001 | 32.2 |
| NTP/NMO | Na ion (aqueous) | 2013 | 212.2 |
| Li/O ₂ | Metal-air | 1996 | 1.1 |
| Zn/O ₂ | Metal-air | 1878 | 2.9 |
| Fe/O ₂ | Metal-air | 1968 | 0.3 |
| Al/O ₂ | Metal-air | 1962 | 0.7 |
| Zn/MnO ₂ | Other | 1959 | 6.4 |
| Cd(OH) ₂ /Ni(OH) ₂ | Other | 1899 | 66.1 |
| Pb/PbO ₂ | Other | 1859 | 18.3 |
| LaNi ₅ /Ni(OH) ₂ | Other | 1978 | 82.9 |
| Zn/NiOOH | Other | 1899 | 42.0 |
| Fe/Cr | Redox flow | 1976 | 28.3 |
| Fe/Fe | Redox flow | 1981 | 15.5 |
| S/Br | Redox flow | 1984 | 7.4 |
| VRFB | Redox flow | 1985 | 124.4 |
| Cu/Cu | Redox flow | 2014 | 53.0 |
| AQDS/Br | Redox flow | 2014 | 57.9 |
| Aq-S/air (Na, H ⁺) | Redox flow | 2017 | 1.7 |
| Aq-S/air (Na, OH ⁻) | Redox flow | 2017 | 4.0 |
| Zn/Fe | Redox flow | 2015 | 9.3 |
| Zn/Br ₂ | Redox flow | 1972 | 8.0 |

Table A.2 Price of chemicals

| Chemical | Price (\$/kg) | Source |
|---|---------------|--------|
| Al | 2.50 | [1] |
| AQDS | 4.74 | [2] |
| Ca | 3.00 | [3] |
| CaCl ₂ | 0.10 | [3] |
| Carbonate electrolyte | 8.00 | [4] |
| Cd(OH) ₂ | 3.40 | [3] |
| CrCl ₃ 6H ₂ O | 2.00 | [3] |
| CuCl | 4.50 | [3] |
| Fe | 0.21 | [1] |
| FeCl ₂ | 2.50 | [3] |
| Graphite | 6.00 | [4] |
| H ₂ SO ₄ | 0.20 | [3] |
| HBr | 1.60 | [3] |
| HCl | 0.20 | [3] |
| KOH | 0.74 | [3] |
| LaNi ₅ | 10.00 | [3] |
| LCO | 45.00 | [4] |
| LFP | 7.50 | [3] |
| Li | 100.00 | [1] |
| Li ₂ S | 11.00 | [5] |
| LMO | 5.00 | [3] |
| LNMO | 20.00 | [4] |
| LTO | 12.00 | [4] |
| MnO ₂ | 1.50 | [3] |
| MoS ₂ | 30.00 | [3] |
| Chemical | Price (\$/kg) | Source |
| Na | 3.00 | [3] |
| Na ₂ S | 0.43 | [3] |
| Na ₂ SO ₄ | 0.07 | [3] |
| NaBr | 1.50 | [3] |
| NaOH | 0.34 | [3] |
| NCA | 34.00 | [4] |
| NCM111 | 20.00 | [4] |
| NCM622 | 22.00 | [4] |
| NCM811 | 30.00 | [4] |
| NH ₄ Cl | 0.14 | [3] |
| Ni(OH) ₂ | 20.00 | [3] |
| NiOOH | 20.00 | [3] |
| NiCl ₂ 6H ₂ O | 5.00 | [3] |
| NMO | 5.00 | [6] |
| NTP | 10.00 | [7] |
| P2-Na ₂ Mn ₂ NiO ₆ | 15.00 | [4] |
| Pb | 2.27 | [1] |
| Pb ₂ Sb | 3.60 | [8] |
| S | 0.25 | [3] |
| Sb | 8.00 | [3] |
| Si | 50.00 | [4] |
| SiO/C | 30.00 | [4] |
| TiS ₂ | 80.00 | [9] |
| VOSO ₄ xH ₂ O | 10.00 | [3] |
| Zn | 3.00 | [1] |

This table contains the price of chemicals (US\$/kg) used as active materials or electrolytes for the battery chemistries shown in Figure 2.2. The values in the table were obtained in November 2021. The sources are as follows:

- [1]. Metalary
- [2]. Huskinson et al. 2014
- [3]. Alibaba n.d.
- [4]. Based on quotes from multiple commercial vendors
- [5]. Yuan et al. (2020)
- [6]. NMO = estimate assuming Na₂CO₃ cost of \$0.2/kg and MnCO₃ cost of \$0.65/kg
- [7]. NTP = estimate based on costs of chemicals for compounds with a similar synthesis process, such as LiFePO₄
- [8]. Pb₂Sb = estimate for reaction synthesis 2Pb + Sb = Pb₂Sb, assuming Sb price of \$8/kg
- [9]. TiS₂ = estimate based on titanium powder price of \$30/kg and processing with oxygen and moisture sensitivity in mind.

A.2 Estimated and projected capital costs, operating costs, efficiency, and self-discharge rates for different battery chemistries (as shown in Table 2.1 of the main report)

As part of this study, we estimate figures of merit for performance and cost for Li-ion batteries, redox flow batteries (RFBs), and metal-air batteries for the present day (2020) and the future (2050), which are used in the grid modeling analyses discussed in Chapter 6 of the main report. The following sections detail the methodology we used for cost estimation. Our estimates of future cost include a low, medium, and high value. Note that for the less-developed technologies (i.e., RFBs and metal-air batteries), any techno-economic assessment is challenged by uncertainty with respect to manufacturing methods and their costs, poorly established supply chains for some materials, and limited information regarding various model inputs. Results presented here are based on surveys of the published literature and input from industry experts, where available. While our estimates of cost for RFBs and metal-air batteries are in general agreement with those in other published reports at the time of writing, they should be considered early-stage estimates and should be further refined as the field expands and specific technologies develop.

A.2.1 Li-ion batteries

Numerous studies have examined historic, current, and projected future costs for Li-ion batteries. We use numbers from the National Renewable Energy Laboratory (NREL) Annual Technology Baseline (ATB) of 2020, a widely cited source that is in good agreement with

many other published reports. For current (2020) costs, the NREL ATB uses a bottom-up cost model that contains detailed cost information for components of the battery storage system (Feldman et al. 2021), including Li-ion battery pack, inverter, and the balance of system needed for installation. For future (2050) Li-ion battery costs, the NREL ATB makes projections based on a literature review of 19 sources published in 2018 or 2019 (Cole and Frazier 2020). We use the lower-bound, median, and higher-bound projections from this literature review as the low-, mid-, and high-cost assumptions in our modeling analysis, respectively.

A.2.2 Redox flow batteries

Here, we develop current (2020) and projected future (2050) estimates for RFB energy cost (C_{energy}), power cost (C_{power}), and round-trip energy efficiency ($\epsilon_{\text{E,RT}}$). The present-day RFB is assumed to be a vanadium redox flow battery (VRFB). The chemistry for a representative RFB in 2050 is currently unknown, but we assume it has the following qualities: symmetric chemistry (same elemental species in the positive and negative electrode), based on low-cost and high-abundance elements or compounds, and dissolved in aqueous solution. Our estimates of total capital cost for RFBs in 2020 (Table A.4) are in good agreement with other techno-economic analyses of RFB chemistries in the literature (Lazard 2018; Kear, Shah and Walsh 2011; Zhang et al. 2012; Vionx Energy 2018; Minke and Turek 2018; Crawford et al. 2015; Darling et al. 2014; Zheng et al. 2018). To develop cost estimates for 2050, we changed values (relative to 2020) for only those parameters that have the biggest impact on resulting costs.

Table A.3 Estimated and projected capital costs, operating costs, efficiencies, and self-discharge rates

| Tech | | Discharging capital cost (\$/kW) | Storage capital cost (\$/kWh) | FOM (\$/kW-year) | FOM (\$/kWh-year) | Efficiency-charge (%) | Efficiency-discharge (%) | Self-discharge rate (%/month) |
|-----------|-----------|----------------------------------|-------------------------------|------------------|-------------------|-----------------------|--------------------------|-------------------------------|
| Li-ion | 2020 | 257 | 277 | 1.4 | 6.8 | 92% | 92% | 1.5 |
| | 2050 Low | 32 | 70.9 | 0.3 | 1.4 | 92% | 92% | 1.5 |
| | 2050 Mid | 110 | 125.8 | 0.8 | 2.2 | 92% | 92% | 1.5 |
| | 2050 High | 154 | 177.0 | 1.4 | 3.2 | 92% | 92% | 1.5 |
| RFB | 2020 | 583–650 | 171 | 4.1 | 0.0 | 92% | 88% | 0.0 |
| | 2050 Low | 297 | 15.5 | 4.1 | 0.0 | 92% | 88% | 0.0 |
| | 2050 Mid | 396 | 48.0 | 4.1 | 0.0 | 92% | 88% | 0.0 |
| | 2050 High | 530 | 102.2 | 4.1 | 0.0 | 92% | 88% | 0.0 |
| Metal-air | 2020 | 1,068–1,135 | 3.7 | 26.7–28.4 | 0.1 | 72% | 60% | 7.3 |
| | 2050 Low | 595 | 0.1 | 14.9 | 0.0 | 70% | 59% | 1.5 |
| | 2050 Mid | 643 | 2.4 | 16.1 | 0.1 | 73% | 63% | 1.5 |
| | 2050 High | 950 | 3.6 | 23.7 | 0.1 | 72% | 60% | 1.5 |

Table A.4 Input parameters for the cost model

| | 2020 | 2050 low | 2050 mid | 2050 high |
|--|-----------|----------|----------|-----------|
| C_{power} for greenfield [\$/kW] | 583 – 650 | 297 | 396 | 530 |
| C_{power} for brownfield [\$/kW] | 501 | 259 | 319 | 380 |
| C_{energy} [\$/kWh] | 171 | 15 | 48 | 102 |
| Resulting greenfield C_{capital} at $d = 4h$ [\$/kWh] | 317 – 334 | 89.63 | 147 | 235 |
| Charging efficiency | 0.917 | 0.917 | 0.917 | 0.917 |
| Discharging efficiency | 0.875 | 0.875 | 0.875 | 0.875 |
| FOM (\$/kW-year) | | 4.08 | | |
| VOM (\$/kWh) | | 0.00085 | | |

A.2.2.1 Cost calculations via modified bottom-up models (Darling et al. 2014; Dmello et al. 2016)

$$C_{\text{capital}} \left(\frac{\$}{\text{kWh}} \right) = \left(\frac{C_{\text{reactor}} + C_{\text{BOP system}}}{d} + C_{\text{electrolyte}} + C_{\text{tank}} \right) * (1 + f_{\text{install}}) + \frac{C_{\text{BOP grid}}^{\wedge}}{d} + \frac{C_{\text{add}}}{d}$$

or

$$C_{\text{capital}} \left(\frac{\$}{\text{kWh}} \right) = \frac{C_{\text{power}} \left(\frac{\$}{\text{kWh}} \right)}{d(h)} + C_{\text{energy}} \left(\frac{\$}{\text{kWh}} \right)$$

where

$$C_{\text{power}} \left(\frac{\$}{\text{kW}} \right) = (C_{\text{reactor}} + C_{\text{BOP system}}) * (1 + f_{\text{install}}) + C_{\text{BOP grid}}^{\wedge} + C_{\text{add}}$$

$$C_{\text{energy}} \left(\frac{\$}{\text{kWh}} \right) = (C_{\text{electrolyte}} + C_{\text{tank}}) * (1 + f_{\text{install}})$$

\wedge Indicates costs that are not included in brownfield cases.

Power cost

$$C_{\text{power}} \left(\frac{\$}{\text{kW}} \right) = (C_{\text{reactor}} + C_{\text{BOP system}}) * (1 + f_{\text{install}}) + C_{\text{BOP grid}}^{\wedge} + C_{\text{add}}$$

where C_{reactor} is calculated using a bottom-up model from Darling et al. (2014):

$$C_{\text{reactor}} \left(\frac{\$}{\text{kW}} \right) = C_a * \frac{ASR}{\varepsilon_{\text{sys,d}} * \varepsilon_{\text{v,d}} * (1 - \varepsilon_{\text{v,d}}) * U^2}$$

In the above equation, reactor areal cost can be broken down by individual components, adapted from Mellentine (2011) and Zheng et al (2019):

$$c_a \left(\frac{\$}{\text{m}^2 \text{ of geometric active area}} \right) = c_{\text{electrodes}}^{\text{tot}} + c_{\text{membranes}}^{\text{tot}} + c_{\text{FF}}^{\text{tot}} + c_{\text{EP}}^{\text{tot}} + c_{\text{CP}}^{\text{tot}} + c_{\text{BP}}^{\text{tot}} + c_{\text{gaskets}}^{\text{tot}} + c_{\text{bolts}}^{\text{tot}}$$

where

$$c_{\text{electrodes}}^{\text{tot}} = 2 \left(\frac{\text{m}^2 \text{ electrode}}{\text{m}^2 \text{ cell}} \right) * c_{\text{electrode}} \left(\frac{\$}{\text{m}^2} \right)$$

$$c_{\text{membranes}}^{\text{tot}} = c_{\text{membrane}} \left(\frac{\$}{\text{m}^2} \right)$$

$$c_{\text{FF}}^{\text{tot}} = 2 \left(\frac{\text{m}^2 \text{ flow field}}{\text{m}^2 \text{ cell}} \right) * c_{\text{FF}} \left(\frac{\$}{\text{m}^2} \right)$$

$$c_{\text{gaskets}}^{\text{tot}} = 2 \left(\frac{\text{m}^2 \text{ gasket}}{\text{m}^2 \text{ cell}} \right) * c_{\text{gasket}} \left(\frac{\$}{\text{m}^2} \right)$$

$$c_{\text{EP}}^{\text{tot}} = 2 \left(\frac{\text{plates}}{\text{stack}} \right) * c_{\text{EP}} \left(\frac{\$}{\text{plate}} \right) * \left(cps \left(\frac{\text{cells}}{\text{stack}} \right) \right)^{-1} \left(A_{\text{cell}} \left(\frac{\text{m}^2}{\text{cell}} \right) \right)^{-1}$$

$$c_{\text{CP}}^{\text{tot}} = 2 \left(\frac{\text{plates}}{\text{stack}} \right) * c_{\text{CP}} \left(\frac{\$}{\text{plate}} \right) * \left(cps \left(\frac{\text{cells}}{\text{stack}} \right) \right)^{-1} \left(A_{\text{cell}} \left(\frac{\text{m}^2}{\text{cell}} \right) \right)^{-1}$$

$$c_{\text{BP}}^{\text{tot}} = \left(cps \left(\frac{\text{cells}}{\text{stack}} \right) - 1 \right) \left(\frac{\text{plates}}{\text{stack}} \right) * c_{\text{BP}} \left(\frac{\$}{\text{plate}} \right) * \left(cps \left(\frac{\text{cells}}{\text{stack}} \right) \right)^{-1} \left(A_{\text{cell}} \left(\frac{\text{m}^2}{\text{cell}} \right) \right)^{-1}$$

$$c_{\text{bolts}}^{\text{tot}} = 4 \left(\frac{\text{bolts}}{\text{end plate}} \right) * 2 \left(\frac{\text{end plates}}{\text{stack}} \right) * \left(cps \left(\frac{\text{cells}}{\text{stack}} \right) \right)^{-1} \left(A_{\text{cell}} \left(\frac{\text{m}^2}{\text{cell}} \right) \right)^{-1} * c_{\text{bolt}} \left(\frac{\$}{\text{bolt}} \right)$$

We note that the number and costs of some components, such as bolts and gaskets, may not scale linearly with stack area as is assumed here.

Table A.5 Parameters for power cost calculation

| Parameter | 2020 value | 2050 value (low, high) | Sources/notes |
|---|-------------------------------|--|---|
| C_{BOP} system * – balance-of-plant costs for RFB system | 166 [\$/kW] | 136 [\$/kW], 141 [\$/kW] | Includes pumps, a heat exchanger, a central inverter, and controls for the management of battery state-of-charge (see A.2.2.4 in the following pages). |
| C_{BOP} grid * – balance-of- plant costs for RFB grid connection | 82-149 [\$/kW] | 38 [\$/kW], 150 [\$/kW] | Includes grid interconnection and integration hardware/software (see A.2.2.4 in the following pages). Note: these costs are not included in our brownfield scenario calculations. |
| C_{add} – additional costs | 125 [\$/kW] | 50 [\$/kW], 125 [\$/kW] | Darling et al. (2014), include labor for assembly, depreciation of manufacturing equipment, variable costs, general costs, sales, administration costs, and profit. |
| $f_{install}$ – installation factor | 0.18 | — | From discussions with industry (Li et al. 2017). Assumes 15% for EPC (engineer-procure- construct) and 3% for transportation. |
| Reactor cost parameters | | | |
| A_{cell} – area per cell | 0.3 [m ² per cell] | — | Mellentine (2011), Zheng et al. (2019), Ha and Gallgher (2015). We note that the cell area will be determined by the current collection and/or pressure drop losses. |
| cps – # cells per stack | 75 [cells per stack] | — | Mellentine (2011), Zheng et al. (2019), Ha and Gallgher (2015). We note that the number of cells per stack will vary based on the voltage rating of the output stack (and thus the standard voltage that can be received by the power electronics). |
| $c_{electrode}$ – cost of electrode material | 27 [\$/m ²] | 10 [\$/m ²], 27 [\$/m ²] | Zheng et al. (2019), Darling et al. (2014). |
| $c_{membrane}$ – cost of membrane material | 300 [\$/m ²] | 10 [\$/m ²], 75 [\$/m ²] | Present day (Nafion): Ha and Gallagher (2015), Skyllas-Kazacos (2019), Noack et al. (2016). 2050 (Nafion or low- cost separator): Ha and Gallagher (2015), Petek (2015). |
| c_{FF} – cost of flow field material | 30 [\$/m ²] | — | Zheng et al. (2019), Darling et al. (2014). |
| c_{gasket} – cost of gasket material | 2.6 [\$/m ²] | — | Zheng et al. (2019), Darling et al. (2014). |
| c_{CP} – cost per collector plate | 15 [\$ per plate] | — | Simplifying assumption of 50 \$/m ² for all plate materials (Darling et al. 2014; James, Kalinoski and Baum 2010). |
| c_{EP} – cost per end plate | 15 [\$ per plate] | — | — |
| c_{BP} – cost per bipolar plate | 15 [\$ per plate] | — | — |
| c_{bolt} – cost per bolt | 1 [\$ per bolt] | — | Estimate from online vendors. |
| c_a – a real reactor cost (resulting calculation from above parameters) | 442.27 [\$/m ²] | 118.27 [\$/m ²], 217.27 [\$/m ²] | — |
| ASR – area-specific resistance | 0.5 [Ω·cm ²] | — | Darling et al. (2014). |
| U – cell open circuit voltage | 1.4 [V] | — | VRFB OCV and an appropriate assumption for a generic aqueous chemistry. |
| $\epsilon_{sys,d}$ – discharge system efficiency | 0.96 | — | Modified from Darling et al. (2014) (see A.2.2.2). |
| $\epsilon_{v,d}$ – discharge voltaic efficiency | 0.916 | — | Darling et al. (2014). |

Note that unit conversion may be required for use in the equations above. “Mid” values for 2050 in Table A.4 are the mean of the 2050 “low” and “high” values.

* The balance-of-plant cost is assumed to scale linearly with nominal system power. This may not be strictly true for all components; for example, the cost of a thermal management system may scale with tank volume or configuration rather than with system power rating.

Energy cost

$$C_{\text{energy}} \left(\frac{\$}{\text{kWh}} \right) = (C_{\text{electrolyte}} + C_{\text{tank}}) * (1 + f_{\text{install}})$$

where $C_{\text{electrolyte}}$ is calculated from a bottom-up model from Darling et al. (2014) and Dmello et al. (2016):

$$C_{\text{electrolyte}} \left(\frac{\$}{\text{kWh}} \right) = \frac{OF}{F * U * \epsilon_{\text{sys,d}} * \epsilon_{\text{v,d}} * \epsilon_{\text{c,RT}}} * (C_{\text{e-transfer}}^+ + C_{\text{e-transfer}}^-)$$

where the cost per electron transfer of the positive and negative electrolytes ($C_{\text{e-transfer}}^+$ and $C_{\text{e-transfer}}^-$, respectively) is defined as:

$$C_{\text{e-transfer}}^{+/-} \left(\frac{\$}{\text{mol e-}} \right) = \frac{MW_{\text{active}}^{+/-}}{X^{+/-} * n_e^{+/-}} * \left(c_{\text{active}}^{+/-} + \frac{c_{\text{solvent}}^{+/-}}{S^{+/-}} \right)$$

Here, we assume symmetric chemistries, and thus the costs per electron transfer of the positive and negative electrolytes are equal. The cost of the tank, C_{tank} , is calculated as:

$$C_{\text{tank}} \left(\frac{\$}{\text{kWh}} \right) = C_{\text{tank}} * (NRG_{\text{dens}})^{-1} * 2 \frac{\text{tanks}}{\text{system}}$$

where the volumetric energy density (NRG_{dens}) is defined as:

$$NRG_{\text{dens}} \left(\frac{\text{kWh}}{\text{L}} \right) = \frac{1}{OF} * conc_{\text{active}} * F * n_e * U * \epsilon_{\text{sys,d}} * \epsilon_{\text{v,d}} * \epsilon_{\text{c,RT}}$$

Note that tank cost, in reality, is not linear with volume but exhibits a minimum for medium-sized tanks. Here we assume a constant cost per volume for a mid-sized tank.

Table A.6 Parameters for energy cost calculation

| Parameter | 2020 value | 2050 value (low, high) | Sources/Notes |
|---|-----------------------|--------------------------|---|
| f_{install} – install factor | 0.18 | — | From discussions with industry (Li et al. 2017). Assumes 15% for EPC (engineer-procure-construct) and 3% for transportation. |
| U – cell open circuit voltage | 1.4 [V] | — | VRFB OCV and an appropriate assumption for a generic aqueous chemistry. |
| $\epsilon_{\text{sys,d}}$ – discharge system efficiency | 0.96 | — | Modified from Darling et al. (2014) (see A.2.2.2). |
| $\epsilon_{\text{v,d}}$ – discharge voltaic efficiency | 0.916 | — | Darling et al. (2014). |
| $\epsilon_{\text{c,RT}}$ – roundtrip coulombic efficiency | 0.99 | — | Modified from Darling et al. (2014) (see A.2.2.2). |
| F – Faraday's constant | 96,485 [C/mol e-] | — | — |
| OF – oversizing factor | 1.2 | — | Rodby et al. (2020). |
| MW_{active} – active species molecular weight | 51 [g/mol] | 50 [g/mol], 150 [g/mol] | MW of vanadium, and a range to encompass future chemistries (inorganic active materials with or without ligands, organics, etc.). |
| $\chi^{+/-}$ – depth of discharge | 0.8 | — | Darling et al. (2014). |
| n_e – number of electron transfers | 1 [mol e-/mol active] | — | Darling et al. (2014). |
| C_{active} – active species cost | 29 [\$/kg] | 1 [\$/kg], 5 [\$/kg] | 2030: Rodby et al. (2020), Vanadium Price (2020). 2050: Li et al. (2017), Darling et al. (2014). |
| C_{solvent} – solvent cost | 0.1 [\$/kg] | — | Darling et al. (2014). |
| S – solubility of active species per unit mass of electrolyte | 0.1 [kg/kg] | — | Darling et al. (2014). |
| C_{tank} – tank cost | 0.08 [\$/L] | — | Zheng et al. (2019). |
| $conc_{\text{active}}$ – concentration of active species | 1.5 [M] | — | Common concentration generally just below the solubility limit for aqueous systems. |
| $C_{\text{electrolyte}}$ – electrolyte cost (resulting calculation from above parameters) | 141 [\$/kWh] | 28 [\$/kWh], 83 [\$/kWh] | — |
| C_{tank} – tank cost (resulting calculation from above parameters) | 4 [\$/kWh] | — | — |

Unit conversion may be required for use in the equations above. “Mid” values for 2050 in Table A.4 are the average of the “low” and “high” 2050 values.

A.2.2.2 Energy efficiency calculations

If we define energy efficiency as the product of the round-trip efficiencies of the system, voltage, and coulombic efficiencies, and define round-trip efficiency as the product of the charge and discharge efficiencies, we can determine the round-trip energy efficiency ($\epsilon_{E,RT}$), charging efficiency ($\epsilon_{E,C}$), and discharging efficiency ($\epsilon_{E,D}$) using parameters defined in Darling et al. (2014):

$$\epsilon_{E,RT} = \epsilon_{sys,d} * \epsilon_{sys,c} * \epsilon_{v,d} * \epsilon_{v,c} * \epsilon_{C,RT}$$

$$\epsilon_{E,C} = \epsilon_{sys,c} * \epsilon_{v,c} * \sqrt{\epsilon_{C,RT}}$$

$$\epsilon_{E,D} = \epsilon_{sys,d} * \epsilon_{v,d} * \sqrt{\epsilon_{C,RT}}$$

where the values of these parameters are as listed in Tables A.5 and A.6, except for the charging system efficiency ($\epsilon_{sys,c}$), which we assume is the same as the discharging system efficiency, and the charging voltaic efficiency ($\epsilon_{v,c}$), which we set to 0.96 (per Darling et al. (2014)). We assume the system efficiency accounts for electrical losses only through the DC current collection and power electronics, and increase both charging and discharging system efficiencies to 0.96 (from 0.94 in Darling et al. (2014)) and the round-trip coulombic to 0.99 (from 0.97 in Darling et al. (2014)). This results in a calculated round-trip energy efficiency of 0.80, which is consistent with present-day achievable efficiencies per discussions with industry experts. Charging and discharging energy efficiencies are calculated as 91.7% and 87.5%, respectively. We assume no change in energy efficiency for 2050, given that new chemistries may present their own unique limitations to voltaic or coulombic efficiency.

A.2.2.3 O&M cost calculations

Economical RFB systems, which will likely use a symmetric chemistry, have minimal operating and maintenance costs, as we show here. A symmetric chemistry allows for continuous rebalancing to remediate capacity losses from crossover. The only cost to this process is the energy to recharge the battery because of the self-discharge that may occur, which is conservatively estimated to be 0.35% per cycle (Rodby et al. 2020). Additional operating losses for aqueous systems may result from side reactions, which can sometimes be remediated through the use of a secondary electrochemical cell to maintain the average oxidation state. The O&M cost of this remediation method is the cost of the energy needed to drive this cell (the cell capital cost is assumed to be small and is not considered in the calculations in A.2.2.1). The rate of side reaction losses is chemistry dependent; we conservatively assume 0.5% per cycle (Rodby et al. 2020). Thus, for every 1 kWh of energy output, 0.0085 kWh is needed to remediate capacity losses. At an electricity cost of 10 cents per kWh, this produces a negligible 0.00085 \$/kWh variable O&M cost.

We assume that the electrodes and membrane are replaced every 10 years and use the average of low and high values for the cost of these components in 2050 as the average cost. At 18.50 \$/kW for the electrodes and 42.50 \$/kW for the membrane, the total replacement cost is 61 \$/kW. We assume a labor cost to execute the maintenance of 4 \$/kW (Viswanathan et al. 2014). To translate this to a yearly O&M cost, we use MATLAB's present value function (pvvar), assuming a discount rate of 10%, and solve for the annual fee "x" that gives the same present value as paying 65 \$/kW at year 10. This gives a yearly maintenance cost of 4.08 \$/(kW-year).

A.2.2.4 Balance-of-plant (BOP) cost calculations

Balance-of-plant (BOP) components were divided into two categories, electrical BOP and non-electrical BOP. Electrical BOP consists of equipment/components needed to connect the energy storage system to the grid; non-electrical BOP consists of other essential equipment to

ensure proper operation of the energy storage system. Costs for electrical BOP may be expected to be similar among electrochemical energy storage technologies, while the cost of non-electrical BOP depends on the technology. For “brownfield” projects that leverage existing facilities and connections, the costs for grid integration hardware, software, and interconnection costs are not included.

Table A.7 Costs for electrical BOP components

| Component | Cost [\$/kW] | Notes |
|-------------------------------------|--|---|
| Central inverter | 55 (present) 25,27,30 (future low, medium, high) | These are the costs assumed for a utility-scale inverter. For present-day cost, value as obtained from i. 50 \$/kW, 2020, report from energy consulting firm ii. 60 \$/kW, 2017, (Fu, Feldman and Margolis 2018) For future cost, a value was obtained from a learning curve provided by Fraunhofer Institute, for 10 TW PV deployment (Fraunhofer ISE 2015). |
| Grid integration hardware | 25 (present) 20, 25, 30 (future low, medium, high) | Cost obtained from industrial collaborator. |
| Grid integration software | 40 (present) 8, 21, 40 (future low, medium, high) | Cost includes energy storage management software, SCADA, controller. Cost obtained from industrial collaborator. |
| Interconnection | 17–84 (present) 10, 30, 80 (future low, medium, high) | Cost obtained from industrial collaborator. |
| State-of-charge management controls | 20 (present and future) | Cost obtained from industrial collaborator. |

Table A.8 Costs for non-electrical BOP components

| Component | Present-day value [\$/kW] | Notes |
|----------------|---------------------------|--|
| Heat exchanger | 41 | Cost obtained from PNNL (Viswanathan et al. 2014). |
| Pump | 50 | Cost obtained from PNNL (Viswanathan et al. 2014). Cost estimated for flow through type flow-field. Cost may vary with type of flow field, viscosity, and mass transfer properties of the electrolyte. |

A.2.3 Metal-air batteries

To estimate costs for metal-air batteries, we used a model similar to the Darling et al. (2014) model for RFBs as described in section A.2.2. Since the metal electrode serves to store charge in a metal-air battery (in contrast to its

role as a current collector in an RFB), costs for the metal electrode are included in the energy cost rather than the power cost, as in Darling et al. (2014). FOM is assumed to be a yearly 2.5% of capital costs, based on discussions with industry experts. The cost parameters in Tables A.10 and A.11 include shipping and installation.

Table A.9 Input parameters for the cost model

| | 2020 | 2050 high | 2050 mid | 2050 low |
|---|-------------------|-----------|----------|----------|
| Greenfield C_{power} [\$/kW] | 1,067.75–1,134.75 | 949.56 | 642.77 | 595.21 |
| Brownfield C_{power} [\$/kW] | 985.75 | 799.56 | 565.77 | 557.21 |
| C_{energy} [\$/kWh] | 3.70 | 3.63 | 2.41 | 0.13 |
| Charging efficiency | 72.02 | 72.02 | 72.73 | 70.2 |
| Discharging efficiency | 60.09 | 60.09 | 62.99 | 58.9 |
| Greenfield FOM_{power} [\$/kW-y] | 26.69–28.37 | 23.74 | 16.07 | 14.88 |
| Brownfield FOM_{power} [\$/kW-y] | 24.64 | 19.99 | 14.14 | 13.93 |
| FOM_{energy} [\$/kWh-y] | 0.09 | 0.09 | 0.06 | 0.003 |
| VOM (\$/kWh) | 0 | 0 | 0 | 0 |

Table A.10 Power cost parameters for 20-hour discharge

| Parameter | 2020 | 2050 (low, high) | Notes |
|-------------------------------|---|---|--|
| Balance of plant cost [\$/kW] | Greenfield: 433.64–512.70 Brownfield: 336.88 | Greenfield: 123.90, 483.20 Brownfield: 64.90, 307.38 | AC and DC electrical numbers (inverter, grid integration hardware and software, interconnection) same as in RFB writeup. This number also includes costs of electrolyte management and HVAC based off discussions with industry. Natural air-breathing design assumed for 2050 low and mid. |
| Cathode(s) cost [\$/kW] | 397.43 | 215.81, 255.49 | Numbers based off a real cost of electrode material and cell performance—bifunctional single cathode design assumed for 2050 low value, otherwise we assume dual cathode design (Record 14014: Fuel Cell System Cost – 2014 (U.S. DOE), historical commodity prices for metals such as nickel with an added cost factor for processing, wholesale suppliers on Alibaba, discussions with industry for future low cathode materials). |
| Electrolyte cost [\$/kW] | 51.57 | 23.26, 36.81 | Numbers include volume of electrolyte, cost of alkaline electrolyte, and cost of additives—this is solely the power contribution of the electrolyte cost. From wholesale suppliers on Alibaba and cost estimate for generalized additives. |
| Cell components cost [\$/kW] | 199.87 | 253.24, 199.87 | Numbers based off generic cell design, number of cells, cell performance, and costs of separator, gaskets, end plates, current collectors, and assembly components (Darling et al. 2014; Li et al. 2017). |
| Equilibrium cell voltage [V] | 1.636 | 1.317, 1.636 | 2050 low value assumes a generalized metal anode with ~20% lower equilibrium cell voltage. |
| Discharge voltage [V] | 1.04 | 0.820, 1.04 | Overpotentials for charge and discharge based on cell design and ASR, expected performance changes in cathode. |
| Charge voltage [V] | 2.06 | 1.704, 2.06 | |
| Installation factor [%] | 15 | 15 | Added on top of base costs, based on discussions with industry. |
| Shipping factor [%] | 3 | 3 | Added on top of base costs, based on discussions with industry. |

Table A.11 Energy cost parameters for 20-hour discharge

| Parameter | 2020 | 2050 (low, high) | Notes |
|---------------------------|------|------------------|--|
| Metal anode cost [\$/kWh] | 3.47 | 0.09, 3.47 | Number based off generic cell design, cell performance, utilization, processing costs, and cost of metal. Cost of metal based on historical commodity prices, added cost factor to account for processing, design. |
| Metal utilization [%] | 50 | 90, 50 | Estimated utilization for existing systems and for improvements to the metal anode such as high area electrodes. |
| Electrolyte cost [\$/kWh] | 0.22 | 0.04, 0.16 | Numbers include volume of electrolyte, cost of alkaline electrolyte, and cost of additives—this is solely the energy contribution of electrolyte cost. From wholesale sellers such as high transaction level suppliers on Alibaba. |
| Installation factor [%] | 15 | 15 | Added on top of base costs, based on discussions with industry. |
| Shipping factor [%] | 3 | 3 | Added on top of base costs, based on discussions with industry. |

References

- Alibaba. n.d. *Prices for materials from Alibaba "Gold Suppliers" i.e., those with high transaction level.* www.alibaba.com.
- Cole, W, and A W Frazier. 2020. "Cost Projections for Utility-Scale Battery Storage: 2020 Update." *Renewable Energy* 21.
- Crawford, Alasdair, Vilayanur Viswanathan, David Stephenson, Wei Wang, Edwin Thomsen, David Reed, Bin Li, Patrick Balducci, Michael Kinter-Meyer, and Vincent Sprenkle. 2015. "Comparative analysis for various redox flow batteries chemistries using a cost performance model." *Journal of Power Sources* 293 (2015) 388–399. <https://doi.org/10.1016/j.jpowsour.2015.05.066>.
- Darling, Robert M., Kevin G. Gallagher, Jeffrey A. Kowalski, Seungbum Ha, and Fikile R. Brushett. 2014. "Pathways to low-cost electrochemical energy storage: a comparison of aqueous and nonaqueous flow batteries." *Energy and Environmental Science* 7 (2014) 3459–3477. <https://doi.org/10.1039/C4EE02158D>.
- Dmello, Rylan, Jarrod D. Milshtein, Fikile R. Brushett, and Kyle C. Smith. 2016. "Cost-driven materials selection criteria for redox flow battery electrolytes." *Journal of Power Sources* 330 (2016) 261–272. <https://doi.org/10.1016/j.jpowsour.2016.08.129>.
- Feldman, D, V Ramasamy, R Fu, A Ramdas, J Desai, and R Margolis. 2021. "U.S. Solar Photovoltaic System and Energy Cost Benchmark: Q1 2020." *Renewable Energy* 120.
- Fraunhofer ISE. 2015. *Current and Future Cost of Photovoltaics: Long-term Scenarios for Market Development, System Prices and LCOE of Utility-Scale PV Systems.* Agora Energiewende.
- Fu, Ran, David Feldman, and Robert Margolis. 2018. *U.S. Solar Photovoltaic System Cost Benchmark: Q1 2018.* NREL/TP-6A20-72399, Golden, CO: National Renewable Energy Laboratory (NREL).
- Ha, Seungbum, and Kevin G. Gallagher. 2015. "Estimating the system price of redox flow batteries for grid storage." *Journal of Power Sources* 296 (2015) 122–132. <https://doi.org/10.1016/j.jpowsour.2015.07.004>.
- Huskinson, Brian, Michael P. Marshak, Changwon Suh, Süleyman Er, Michael R. Gerhardt, Cooper J. Galvin, Xudong Chen, Alán Aspuru-Guzik, Roy G. Gordon, and Michael J. Aziz. 2014. "A metal-free organic-inorganic aqueous flow battery." *Nature* 505.7482: 195–198. <https://doi.org/10.1038/nature12909>.
- James, Brian D., Jeffrey A. Kalinoski, and Kevin N. Baum. 2010. "Mass Production Cost Estimation for Direct H₂ PEM Fuel Cell Systems for Automotive Applications: 2009 Update." *U.S. Department of Energy* 62.
- Kear, Gareth, Akeel A. Shah, and Frank C. Walsh. 2011. "Development of the all-vanadium redox flow battery for energy storage: a review of technological, financial and policy aspects." *International Journal of Energy Research* 36 (2012) 1105–1120. <https://doi.org/10.1002/er.1863>.
- Lazard. 2018. "Lazard's Levelized Cost of Storage Analysis - Version 4.0."
- Li, Zheng, Menghsuan Sam Pan, Liang Su, Kai Xiang, and Fikile R. Brushett. 2017. "Air-Breathing Aqueous Sulfur Flow Battery for Ultralow-Cost Long-Duration Electrical Storage." *Joule* 1(2): 206–327. <https://doi.org/10.1016/j.joule.2017.08.007>.
- Mellentine, James A. 2011. "Performance Characterization and Cost Assessment of an Iron Hybrid Flow Battery." *The University of Iceland* (University of Iceland) 136. https://skemman.is/bitstream/1946/7698/1/RES_Mellentine_Thesis%20Paper_FINAL.pdf.
- Metalary. n.d. Metalary. www.metalary.com.
- Minke, Christine, and Thomas Turek. 2018. "Materials, system designs and modelling approaches in techno-economic assessment of all-vanadium redox flow batteries – A review." *Journal of Power Sources* 376 (2018) 66–81. <https://doi.org/10.1016/j.jpowsour.2017.11.058>.
- Noack, Jens, Lars Wietschel, Nataliya Roznyatovskaya, Karsten Pinkwart, and Jens Tübke. 2016. "Techno-Economic Modeling and Analysis of Redox Flow Battery Systems." *Energies* 9(8), 627. <https://doi.org/10.3390/en9080627>.
- Petek, Tyler J. 2015. "Enhancing The Capacity of All-Iron Flow Batteries: Understanding Crossover and Slurry Electrodes." *Case Western Reserve University*.
- Rodby, Kara E., Thomas J. Carney, Yasser Ashraf Gandomi, John L. Barton, Robert M. Darling, and Fikile R. Brushett. 2020. "Assessing the levelized cost of vanadium redox flow batteries with capacity fade and rebalancing." *Journal of Power Sources* 460 (2020) 227958. <https://doi.org/10.1016/j.jpowsour.2020.227958>.
- Skyllas-Kazacos, Maria. 2019. "Performance Improvements and Cost Considerations of the Vanadium Redox Flow Battery." *ECS Transactions* 89 (2019) 29–45. <https://doi.org/10.1149/08901.0029ecst>.

- Vanadium Price. 2020. *Vanadium Price*. Accessed August 1, 2020. <https://www.vanadiumprice.com>.
- Vionx Energy. 2018. "Vanadium Redox Flow Battery: A Better Solution." *Vionx Energy*. Accessed March 31, 2019. <https://www.vionxenergy.com/products>.
- Viswanathan, Vilayanur, Alasdair Crawford, David Stephenson, Soowhan Kim, Wei Wang, Bin Li, Greg Coffey, et al. 2014. "Cost and performance model for redox flow batteries." *Journal of Power Sources* 247: 1040–1051. <https://doi.org/10.1016/j.jpowsour.2012.12.023>.
- Yuan, Kai, Jie Chen, Jingwei Xiang, Yawi Liao, Zhen Li, and Yunhui Huang. 2020. "Methods and Cost Estimation for the Synthesis of Nanosized Lithium Sulfide." *Small Structures* 2.3: 2000059.
- Zhang, Mengqi, Mark Moore, J. S. Watson, Thomas A. Zawodzinski, and Robert M. Counce. 2012. "Capital Cost Sensitivity Analysis of an All-Vanadium Redox-Flow Battery." *Journal of Electrochemical Society* 159 (2012) A1183–A1188. <https://doi.org/10.1149/2.041208jes>.
- Zheng, Menglian, Jie Sun, Christoph J. Meinrenken, and Tao Wang. 2019. "Pathways Toward Enhanced Techno-Economic Performance of Flow Battery Systems in Energy System Applications." *Journal of Electrochemical Energy Conversion and Storage* 16 (2019) 021001-1-021001-11. <https://doi.org/10.1115/1.4040921>.

Appendix B – Cost and performance calculations for thermal energy storage technologies

This appendix provides details about the cost and performance calculations used to compare thermal energy storage (TES) technologies in Chapter 4 of the main report. The key parameters discussed here include coefficient of performance, discharge efficiency, and cost.

B.1 Coefficient of performance

As discussed in Chapter 4, the coefficient of performance (COP) is the figure of merit for converting electricity to heat. In Figure 4.2, resistive heaters are shown with a COP between 90% and 99.5%. To calculate COP for heat pumps, we applied the following equations and assumptions:

$$COP_{Q_h + Q_c} = \eta * \frac{\tau * \Theta - 1}{\tau * \Theta - \eta^2} * \frac{\tau + 1}{\tau - 1} \quad (1)$$

$$COP_{Q_h} = \eta * \frac{\tau * \Theta - 1}{\tau * \Theta - \eta^2} * \frac{\tau}{\tau - 1} \quad (2)$$

$$\tau = \frac{T_2}{T_1} \quad \Theta = \frac{T_1}{T_3}$$

$$\eta = 0.85 \quad T_1 = T_3 = 298K$$

The points labeled in Figure B.1 correspond to the subscripts in the variables for temperature T. Equation 1 is given by Olympios et al. (2021) and Equation 2 is derived from the same. For another thermodynamic analysis of pumped heat TES, see Laughlin (2017). Temperature is expressed in Kelvin. The exact values for η , T_1 , and T_3 depend on system configuration. For the Carnot case, $\eta = 1$.

Figure B.1 Thermodynamic cycle for a heat pump

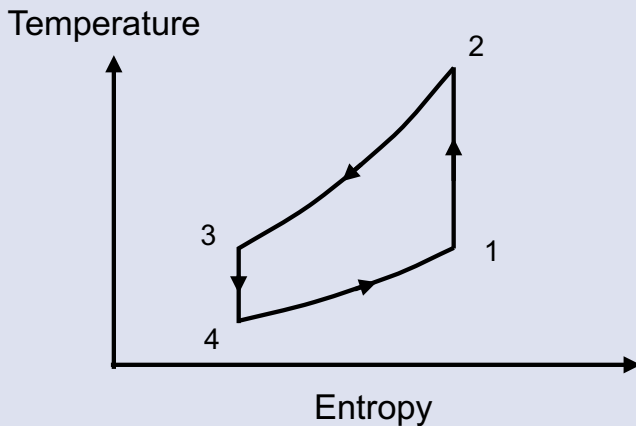


Table B.1 Data used in Figure 4.4

| Material | Type | T _{melt} | Density | Enthalpy | Enthalpy (volumetric) |
|--------------------|-----------|-------------------|-------------------|----------|-----------------------------------|
| — | — | °C | kg/m ³ | kJ/kg | kWh _{th} /m ³ |
| Silicon | Metalloid | 1,414 | 2,330 | 1,787 | 1,157 |
| Iron | Metal | 1,668 | 7,850 | 247.3 | 539 |
| Nickel | Metal | 1,455 | 8,902 | 293 | 725 |
| Manganese | Metal | 1,246 | 7,260 | 240 | 484 |
| Copper | Metal | 1,085 | 8,940 | 208.7 | 518 |
| Aluminum | Metal | 660 | 2,712 | 396.9 | 299 |
| Zinc | Metal | 420 | 7,135 | 112 | 222 |
| Potassium fluoride | Salt | 858 | 2,480 | 468 | 323 |
| Sodium chloride | Salt | 801 | 2,160 | 482 | 289 |
| Magnesium chloride | Salt | 714 | 2,320 | 452 | 291 |
| Sodium nitrate | Salt | 307 | 2,260 | 172 | 108 |

Table B.2 Cost data for thermal energy storage materials used in Figure 4.5

| Material | Type | Cost _{low} | Cost _{high} | T _{h,low} | T _{h,high} | T _c | c _p | h _{sf} |
|---|----------|---------------------|----------------------|--------------------|---------------------|----------------|----------------|-----------------|
| — | — | \$/kg | \$/kg | °C | °C | °C | J/(kg*K) | kJ/kg |
| Graphite | Sensible | 0.70 | | 2,150 | 2,400 | 1,900 | 2,000 | |
| Mixture of sodium and potassium nitrate | Sensible | 1.23 | | 500 | 565 | 293 | 1,386 | |
| Rock | Sensible | 0.10 | | 700 | 1,000 | 100 | 1,100 | |
| Silica | Sensible | 0.35 | | 700 | 1,650 | 100 | 1,128 | |
| Aluminum | Latent | 1.40 | 2.50 | | 660 | | | 396 |
| Magnesium chloride | Latent | 0.11 | 0.18 | | 714 | | | 453 |
| Sodium chloride | Latent | 0.06 | 0.12 | | 801 | | | 482 |
| Silicon | Latent | 1.60 | 3.00 | | 1,414 | | | 1,800 |

Sources for material costs are as follows: graphite (Kelsall, Buznitsky and Henry 2021; Statista 2019), mixture of sodium and potassium nitrate (Glatzmaier 2011), rock (Alibaba 2021c), silica (Ma, Davenport and Zhang 2020), aluminum (Robinson 2018; Trading Economics 2021), magnesium chloride (Alibaba 2021b; Gibson 2011; Balakrishnan 2015), sodium chloride (Gibson 2011; Alibaba 2021a; U.S. Geological Survey 2021), silicon (Amy et al. 2018; U.S. Geological Survey 2021).

Table B.3 Assumptions used to estimate costs for TES systems

| | | |
|--------------------------------------|----------|---|
| Sales tax | 7.5% | |
| EPC (engineer-procure-construct) fee | 20% | |
| Project contingency | 10% | |
| Overhead (multiplier) | 1.4 | (1 + EPC fee + Sales tax) * (1 + Contingency) |
| Interconnection | 30 \$/kW | |

B.2 Discharge efficiency

Two equations were used to calculate nominal discharge efficiencies for heat-to-electricity conversion technologies in Figure 4.6. The first equation is the formula for Carnot cycle efficiency. The Carnot cycle takes place between low- and high-temperature thermal reservoirs at T_C and T_H in units of Kelvin. The second equation is a formula for thermal efficiency of a cycle using a compressible fluid heated from T_C to T_H in units of Kelvin (Henry and Prasher 2014). The second formula is descriptive of Rankine and Brayton cycles.

$$\eta = 1 - \frac{T_C}{T_H}$$

$$\eta = 1 - \frac{T_C}{T_H - T_C} \ln \left(\frac{T_H}{T_C} \right)$$

B.3 Cost estimation

Table B.3 summarizes the values used to estimate all-in cost for TES systems. The values are based on numbers from Sargent & Lundy (2020) and the other technology chapters.

B.3.1 Charge power cost

Both the crushed rock and liquid silicon TES systems we considered use resistive heaters. The charge power cost for the crushed rock and sCO₂ (supercritical carbon dioxide) system is sourced from Stack, Curtis, and Forsberg (2019) and is held constant across the three cost scenarios. Stack et al. (2019) use an installation factor (of 1.5x), so overhead costs were not applied. Our

calculations do not account for inflation of 1.2% between 2019 and 2020, but this omission has a negligible impact on the modeling results. Charging costs for a liquid silicon system are also held constant across the three scenarios; for these costs we use the value from Amy et al. (2018) adjusted for inflation and the overhead costs described in the table above.

B.3.2 Discharge power cost

The methods used to estimate discharge power capacity cost for the two TES systems are similar to the ones in Schmidt et al. (2017). From a high level, a logistic curve models annual production rates of power components (GW/yr). The formula for the logistic curve is

$$f(x) = \frac{L}{1 + e^{-k(x - x_0)}}$$

where L is the maximum value, k is the growth rate, x is the number of years from 2020, and x_0 is the midpoint.

Annual production rates are summed to calculate cumulative production. A single-factor power law relates cumulative production to cost per power (\$/W) using a constant factor and an exponent based on learning rates. The formula for the power law is

$$g(y) = C_0 * y^{-b}$$

$$b = -\log_2 (1 - LR)$$

where C_0 is a constant term, y is the cumulative capacity, and the exponent b is calculated from the learning rate, LR .

The logistic curve is modeled with a maximum value of 58 GW/yr. This results from an estimated 7,000 GW of global power capacity installed for TES, with power systems having a lifetime of 30 years for both technologies and the two technologies each having a 25% share of the 7,000 GW total ($7,000 \text{ GW}/30 \text{ years} * 25\% = 58 \text{ GW}/\text{yr}$). The value of 7,000 GW is estimated from early modeling results for both Texas and New England. The power capacity necessary for the United States was estimated by scaling values for each region by the ratio of overall net U.S. generation to the region's net generation (U.S. Energy Information Agency 2015). Using the ratio of net generation as a proxy for storage power capacity, we apply a factor of 10, which is an order-of-magnitude estimate used in this report to estimate the need for global energy storage capacity relative to U.S. capacity in 2050. In 2020, global electricity generation was 6.3 times greater than the United States and on an increasing trend (BP 2021). Capacity built for non-storage applications of TPV (thermophotovoltaics) and sCO₂ cycles was not included in the global capacity estimate but would be beneficial for reducing costs.

The inflection point of the logistic curve is set at 2045. The assumption that it will take 25 years (from 2020, when costs were modeled) to reach the inflection point is an aggressive but plausible timeframe given that there has been progress on both technologies already (Gross et al. 2018). The logistic growth rate is calculated by assuming the production rate in 2020 is 1 MW/yr.

For the “liquid silicon and multi-junction TPV” system, our mid- and low-cost estimates are based on Amy et al. (2018). Values from this paper are adjusted for overhead and interconnection costs as well as inflation. For our high-cost estimate, we use values from the

literature to calculate the constant factor in the power law formula. Essig et al. (2017) estimate \$0.84/W (2020\$, Supplementary Figure 3) as the cost for a multi-junction cell in a long-term scenario for a plant with a production volume of 1 GW/yr. The cell efficiency in Essig et al. (2017) is lower than in Table 5.3. We assume that more efficient cells can be produced from similar equipment and processes; accordingly, we adjust the cost per watt to reflect higher efficiency, which results in a lower cost (2017). Assuming that a company with a single, large manufacturing plant has a maximum market share of 10% (Statista 2017), the constant in the power law is calculated using the corresponding cumulative capacity when global annual production is 10 GW/yr (such that 10 GW/yr multiplied by a 10% market share results in a 1 GW/yr plant). The learning rate is set at 15%, less than the historical rate for crystalline silicon PV cells (Kavlak, McNerney and Trancik 2018). Non-cell costs are applied from Amy et al. along with overhead costs from Table B.3 (2018).

We use a similar approach for the “crushed rock and sCO₂” system. First, we calculate the average of three cost estimates for the main components of a sCO₂ cycle in Carlson, Middleton, and Ho (2017), adjust for inflation, and assume these costs will be achievable in 2025. From this, the constant factor in the power law is calculated for learning rates of 5%, 10%, and 15%; these learning rates correspond to our high-, mid-, and low-cost estimates. Values for civil, electrical, and indirect costs from case 6 of Sargent & Lundy (2020) are added onto the cost of system components, for a subtotal of 221 \$/kW in 2020. These additional costs decline at the percentage rate given in NREL’s Annual Technology Baseline with 2020 as the baseline, which results in a 14% cost reduction by 2050. Following this, we apply overhead costs.

Table B.4 High-, medium-, and low-cost estimates for the “crushed rock and sCO₂” and “liquid silicon and multi-junction TPV” TES systems

| Technology | | Crushed rock & sCO ₂ | | | Liquid silicon & multi-junction TPV | | |
|--------------------------|-----------|---------------------------------|------|------|-------------------------------------|------|------|
| Cost scenario | | High | Mid | Low | High | Mid | Low |
| Charging capital cost | \$/kW | 3.3 | 3.3 | 3.3 | 24 | 24 | 24 |
| Discharging capital cost | \$/kW | 1,226 | 736 | 494 | 880 | 498 | 362 |
| Energy capital cost | \$/kWh | 9 | 5.4 | 2.9 | 26 | 16 | 6.4 |
| Efficiency up | – | 99.5 | 99.5 | 99.5 | 99.5 | 99.5 | 99.5 |
| Efficiency down | – | 46 | 50 | 55 | 50 | 54 | 57 |
| Capital recovery period | yr | 30 | 30 | 30 | 30 | 30 | 30 |
| FOM discharge | \$/kW-yr | 3.9 | 3.9 | 3.9 | 3.6 | 2.1 | 1.5 |
| FOM charge | \$/kW-yr | 0.08 | 0.08 | 0.08 | 0.58 | 0.58 | 0.58 |
| FOM storage | \$/kWh-yr | 0.05 | 0.03 | 0.02 | 0.15 | 0.09 | 0.04 |
| VOM | \$/kWh | 0 | 0 | 0 | 0 | 0 | 0 |
| Self-discharge | % per hr | 0.04 | 0.02 | 0.02 | 0.04 | 0.02 | 0.02 |

B.3.3 Energy cost

Energy costs for the “liquid silicon and multi-junction TPV” system are based on Amy et al. (2018). Our high- and low-cost scenarios use the high and low estimates from this paper adjusted for discharge efficiency and overhead costs. The mid-cost scenario is the average of the high- and low- cost scenarios.

To estimate energy cost for the “crushed rock and sCO₂” system, we used a bottom-up model of a rectangular trench filled with basalt (Forsberg and Aljefri 2020). Basalt was assumed to cost \$73 per ton (Alibaba 2021c; Strefler et al. 2018); insulation and containment were assumed to cost approximately \$4,200 per m² (Black and Veatch 2010); and the cost for excavation was set at \$130 per m³ (Specialty Grading 2020).

Early capacity expansion model runs suggested roughly 100 hours of duration would be optimal for a system with similar values as the mid-cost case. Therefore, with a nominal power capacity of 1 GW_e and discharge efficiency of 50%, we estimated energy cost for a capacity of 200 GWh_{th}. The high-, mid-, and low-cost values

were calculated by varying the depth of the trench between 20 and 30 meters and the temperature difference between roughly 200°C and 500°C. For a sense of scale, a trench with an energy capacity of 200 GWh_{th} would be about 20 m deep, 60 m wide, and 550 m in length, although exact values depend on the assumptions used.

At smaller scales, the surface-area-to-volume ratio increases, so the energy capacity cost increases as well (as described in Section 4.3.2). But this increase is generally less than 10% even for a system with an energy capacity of 20 GWh_{th}.

The low temperature difference reflects a scenario where molten salt is used as the heat transfer fluid that comes into direct contact with the rock. At higher temperature differences (and correspondingly higher temperatures), molten salts may not be a viable heat transfer fluid, but other fluids could be used with indirect heat transfer. Other storage concepts may also be able to provide heat at the same temperatures with similarly low cost (Ma, Davenport and Zhang 2020).

References

- Alibaba. 2021a. "99.5% NaCl Pool Salt Refined Industrial Salt." Alibaba. https://web.archive.org/web/20210827145841/https://sgdinghao.en.alibaba.com/product/1600056895051-821750555/99_5_NaCl_Pool_Salt_Refined_Industrial_Salt.html.
- . 2021b. "MgCl₂ Price per Ton." Alibaba. <https://web.archive.org/web/20210827144939/https://www.alibaba.com/showroom/mgcl2-price-per-ton.html>.
- . 2021c. "Natural Black Basalt Price Ton Stones For Construction." <https://web.archive.org/web/20210827143705/https://www.alibaba.com/showroom/basalt-price-ton.html>.
- Amy, Caleb, Hamid Reza Seyf, Myles A. Steiner, Daniel J Friedman, and Asegun Henry. 2018. "Thermal Energy Grid Storage Using Multi-Junction Photovoltaics." *Energy and Environmental Science* 12 (1): 334–343. <https://doi.org/10.1039/C8EE02341G>.
- Balakrishnan, Anita. 2015. "Road Salt: Winter's \$2.3 Billion Game Changer." *NBC News*. February 18. <https://www.nbcnews.com/business/economy/road-salt-winters-2-3-billion-game-changer-n308416>.
- Black and Veatch. 2010. "Solar Thermocline Storage Systems: Preliminary Design Study." *EPRI*.
- BP. 2021. "BP's Statistical Review of World Energy 2021." <https://www.bp.com/en/global/corporate-energy-economics/statistical-review-of-world-energy.html>.
- Carlson, Matthew D., Bobby M. Middleton, and Clifford K. Ho. 2017. "Techno-Economic Comparison of Solar-Driven SCO₂ Brayton Cycles Using Component Cost Models Baseline With Vendor Data and Estimates." *ASME 2017 11th International Conference on Energy Sustainability, V001T05A009*. Charlotte, North Carolina, USA: American Society of Mechanical Engineers. <https://doi.org/10.1115/ES2017-3590>.
- Essig, Stephanie, Christophe Alleb  , Timothy Remo, John F. Geisz, Myles A. Steiner, Kelsey Horowitz, and Loris Barraud. 2017. "Raising the One-Sun Conversion Efficiency of III–V/Si Solar Cells to 32.8% for Two Junctions and 35.9% for Three Junctions." *Nature Energy* 2 (9): 1–9. <https://doi.org/10.1038/nenergy.2017.144>.
- Forsberg, Charles, and Ali S. Aljefri. 2020. "100-Gigawatt-Hour Crushed-Rock Heat Storage for CSP and Nuclear." 8.
- Gibson, David. 2011. "Common Road Salt is Toxic." *The Adirondack Almanack*. January 12. <https://www.adirondackalmanack.com/2011/01/dave-gibson-common-road-salt-is-toxic-to-the-adirondacks.html>.
- Glatzmaier, Greg. 2011. "Developing a Cost Model and Methodology to Estimate Capital Costs for Thermal Energy Storage." *National Renewable Energy Laboratory NREL/TP-5500-53066*, 1031953. <https://doi.org/10.2172/1031953>.
- Gross, Robert, Richard Hanna, Ajay Gambhir, Philip Heptonstall, and Jamie Speirs. 2018. "How Long Does Innovation and Commercialisation in the Energy Sectors Take? Historical Case Studies of the Timescale from Invention to Widespread Commercialisation in Energy Supply and End Use Technology." *Energy Policy* 123 (December): 682–99. <https://doi.org/10.1016/j.enpol.2018.08.061>.
- Henry, Asegun, and Ravi Prasher. 2014. "The Prospect of High Temperature Solid State Energy Conversion to Reduce the Cost of Concentrated Solar Power." *Energy and Environmental Science* 7 (6): 1819–28. <https://doi.org/10.1039/C4EE00288A>.
- Kavlak, Goksin, James McNerney, and Jessika E. Trancik. 2018. "Evaluating the Causes of Cost Reduction in Photovoltaic Modules." *Energy Policy* 123 (December): 700–710. <https://doi.org/10.1016/j.enpol.2018.08.015>.
- Kelsall, Colin C., Kyle Buznitsky, and Asegun Henry. 2021. "Technoeconomic Analysis of Thermal Energy Grid Storage Using Graphite and Tin." *ArXiv:2106.07624 [Physics]* <http://arxiv.org/abs/2106.07624>.
- Laughlin, Robert B. 2017. "Pumped Thermal Grid Storage with Heat Exchange." *Journal of Renewable and Sustainable Energy* 9 (4): 044103. <https://doi.org/10.1063/1.4994054>.
- Ma, Zhiwen, Patrick Davenport, and Ruichong Zhang. 2020. "Design Analysis of a Particle-Based Thermal Energy Storage System for Concentrating Solar Power or Grid Energy Storage." *Journal of Energy Storage* 29 (June): 101382. <https://doi.org/10.1016/j.est.2020.101382>.
- Olympios, Andreas V., Joshua D. McTigue, Paul Sapin, and Christos N. Markides. 2021. "Pumped-Thermal Electricity Storage Based on Brayton Cycles." In *Reference Module in Earth Systems and Environmental Sciences*, <https://doi.org/10.1016/B978-0-12-819723-3.00086-X>. Elsevier.

Robinson, Adam. 2018. "Ultra-High Temperature Thermal Energy Storage. Part 2: Engineering and Operation." *Journal of Energy Storage* 18 (August): 333–39. <https://doi.org/10.1016/j.est.2018.03.013>.

Sargent and Lundy. 2020. "Capital Costs and Performance Characteristics for Utility Scale Power Generating Technologies." *Energy Information Agency*.

Schmidt, O., A. Hawkes, A. Gambhir, and I. Staffel. 2017. "The Future Cost of Electrical Energy Storage Based on Experience Rates." *Nature Energy* 2 (8): 1–8. <https://doi.org/10.1038/nenergy.2017.110>.

Specialty Grading. 2020. "Rock Excavation Cost in Prescott, AZ (2020 Prices)." July 16. <https://www.specialtygrading.com/rock-excavation-cost/>.

Stack, Daniel C., Daniel Curtis, and Charles Forsberg. 2019. "Performance of Firebrick Resistance-Heated Energy Storage for Industrial Heat Applications and Round-Trip Electricity Storage." *Applied Energy* 242 (May): 782–96. <https://doi.org/10.1016/j.apenergy.2019.03.100>.

Statista. 2019. "Global Graphite Price 2018–2019." Statista June. <https://www.statista.com/statistics/1075217/graphite-price-worldwide>.

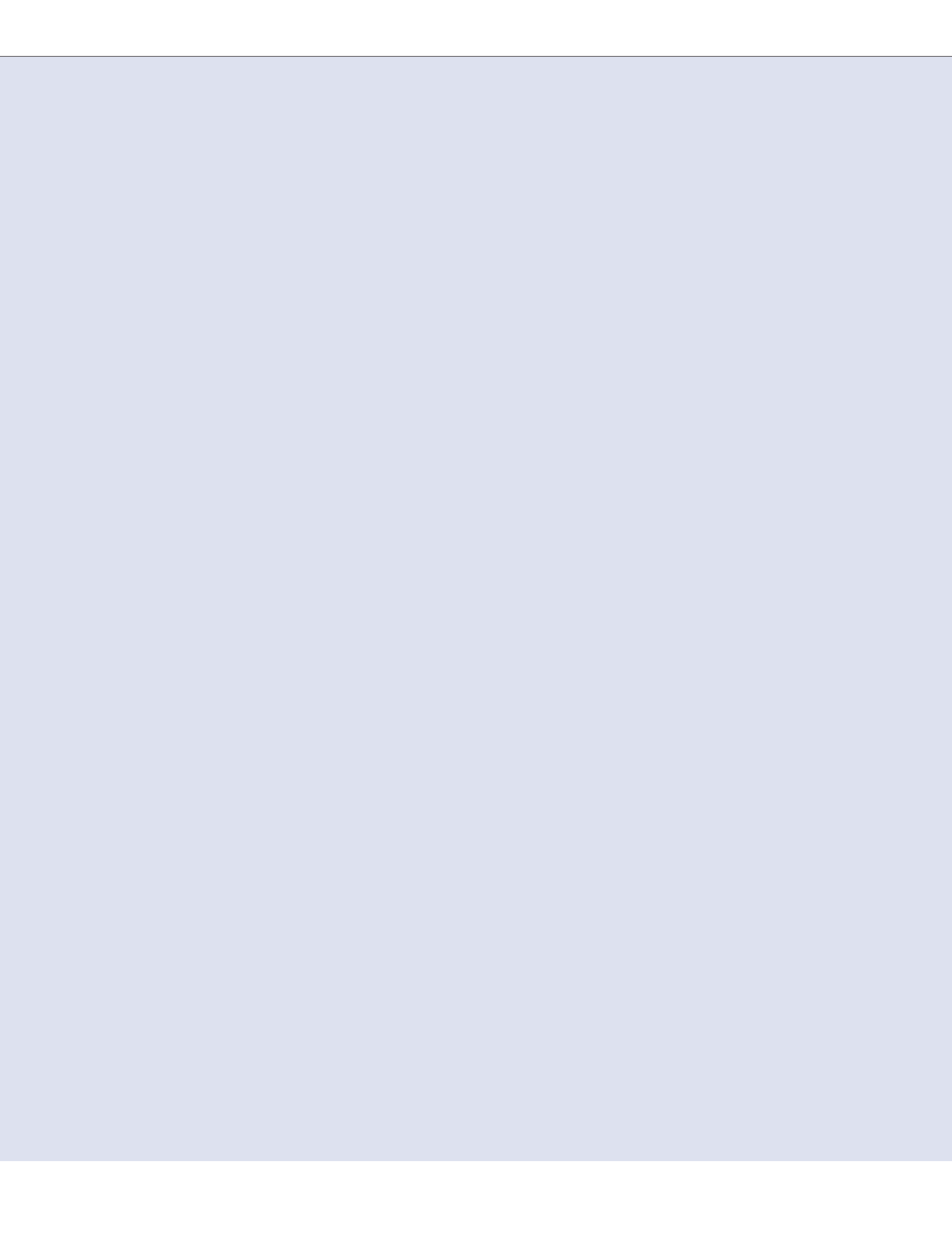
Statista. 2017. "Market Distribution of Photovoltaic Module Manufacturers 2017." *Statista* www.statista.com/statistics/269812/global-market-share-of-solar-pv-module-manufacturers/.

Strefler, Jessica, Thorben Amann, Nico Bauer, Elmar Kriegler, and Jens Hartmann. 2018. "Potential and Costs of Carbon Dioxide Removal by Enhanced Weathering of Rocks." *Environmental Research Letters* 13 (3): 034010. <https://doi.org/10.1088/1748-9326/aaa9c4>.

Trading Economics. 2021. "Aluminum | 1989–2021 Data | 2022–2023 Forecast | Price | Quote | Chart | Historical." *Trading Economics*. <https://tradingeconomics.com/commodity/aluminum>.

U.S. Energy Information Agency. 2015. "State Electricity Profiles: Data for 2013." <https://www.eia.gov/electricity/state/archive/2013/> 2015.

U.S. Geological Survey. 2021. "Mineral Commodity Summaries 2021." <https://doi.org/10.3133/mcs2021>.



Appendix C – Details of the modeling analysis for high-VRE systems with energy storage in three U.S. regions

This appendix provides additional information concerning the methodology and assumptions used to develop the modeling analysis presented in Chapter 6 of the main report.

C.1 Cost and operational assumptions

Transmission: Existing inter-zonal transfer capacity is approximated from the EPA Integrated Planning Model (IPM) model (EPA 2018). The IPM model uses a selection of 64 regions based on North American Electric Reliability Corporation (NERC) regions, which represent fractions of states. We follow these zonal definitions to get the aggregate transfer capacities between zones within each region. Existing transmission capacity is assumed to be available at no cost in our modeling. When transmission expansion is enabled, new capacity can be added along existing network paths. Transmission upgrades on 345 kV lines (U.S. Northeast and Texas) are assumed to cost \$1,670/MW-km; upgrades on 500 kV lines for the Southeast are assumed to cost \$960/MW-km (Brown et al. 2019).¹

Brownfield capacity: We assume mainly greenfield capacity additions in our modeling of the U.S. Northeast, Southeast, and Texas, apart from existing hydropower in all regions and nuclear capacity in the Southeast. For existing hydropower generators, we classify

individual plants into run-of-river (ROR) or reservoir generators using the Oak Ridge National Lab HydroSource database (Oak Ridge National Laboratory 2020). ROR generators are modeled as must-run or non-dispatchable resources that do not have the ability to spill water (i.e., they do not respond to economic dispatch). Hydro reservoir generators are modeled as storage devices that receive exogenous inflows to their storage reservoirs, but cannot charge from the grid. We get hydro-power generators' installed capacities from Form EIA-860 (EIA 2020), and historical monthly generation from Form EIA-923 (EIA 2021a), then aggregate up to the zonal level.

In the Southeast, we assume that a portion of the existing fleet of nuclear generators will remain operational in 2050. That is, based on each generator's start date, we assume plants can run to 2055 or beyond with a second life extension license (80 years from the plant's start date). Our modeling includes the Vogtle 3 and 4 units (with a combined capacity of 2,500 MW), which are still under construction in Georgia (see Table C.1).

In the Northeast, we enforce a minimum build for distributed solar PV to reflect existing policies.² The minimum build is based on a projection of new capacity installed through

¹ Distances between zones are measured as the shortest distance between the urban areas of the respective zones.

² As discussed in Chapter 6, distributed PV is always more expensive than utility-scale PV; therefore, the model would not choose to optimally build distributed PV endogenously, unless there are transmission constraints that prevent other forms of intra-zonal generation.

Table C.1 Brownfield nuclear capacity in the Southeast

| EIA plant-generator | EIA nameplate capacity (MW) | EIA start date | Date entering extended operations |
|---------------------------|-----------------------------|----------------|-----------------------------------|
| Browns Ferry_3 | 1,190 | 3/1/1977 | 7/2/2016 |
| Brunswick Nuclear_1 | 1,002 | 3/1/1977 | 9/8/2016 |
| Catawba_1 | 1,205 | 6/1/1985 | 12/5/2023 |
| Catawba_2 | 1,205 | 8/1/1986 | 12/5/2023 |
| Edwin I Hatch_2 | 865 | 9/1/1979 | 6/13/2018 |
| Grand Gulf_1 | 1,440 | 7/1/1985 | 11/2/2024 |
| Harris_1 | 951 | 5/1/1987 | 10/24/2026 |
| Joseph M Farley_1 | 888 | 12/1/1977 | 6/25/2017 |
| Joseph M Farley_2 | 888 | 7/1/1981 | 3/31/2021 |
| McGuire_1 | 1,220 | 9/1/1981 | 6/12/2021 |
| McGuire_2 | 1,220 | 3/1/1984 | 3/3/2023 |
| Sequoyah_1 | 1,221 | 7/1/1981 | 9/17/2020 |
| Sequoyah_2 | 1,221 | 6/1/1982 | 9/15/2021 |
| St Lucie_1 | 1,080 | 5/1/1976 | 3/1/2016 |
| St Lucie_2 | 1,080 | 6/1/1983 | 4/6/2023 |
| V C Summer_1 | 1,030 | 1/1/1984 | 8/6/2022 |
| Vogtle_1 | 1,160 | 5/1/1987 | 1/16/2027 |
| Vogtle_2 | 1,160 | 5/1/1989 | 2/9/2029 |
| Vogtle_3 | 1,250 | 1/1/2021 | — |
| Vogtle_4 | 1,250 | 1/1/2022 | — |
| Watts Bar Nuclear Plant_1 | 1,270 | 5/1/1996 | — |
| Watts Bar Nuclear Plant_2 | 1,270 | 6/1/2016 | — |

List of nuclear generators that could run to 2055 or beyond with a second life extension license (80 years from start date). Plant-level detail from Form EIA-860 (EIA 2020).

2050 (i.e., not including existing capacity, see Table C.2). For states in ISO-NE, the projections are extrapolated to 2050 using the implied EIA Annual Energy Outlook 2030–2050 growth factor of 110%. For zones in the New York ISO, our projections are directly taken and aggregated from the 2020 Gold Book (New York ISO 2020).

Load: Electricity demand is from the NREL Electrification Futures Study (Mai et al. 2018). These demand data include assumptions around electrification and its impacts on the load profile; they are available on an hourly

basis (8,760 hours per year) as well as on a state-by-state basis. The “2050 High-Moderate” profiles are used for the bulk of the study, except for the Reference Electrification scenario, which is based on the “2050 Reference_Moderate” profiles. These profiles reflect different levels of electrification (“High” vs. “Reference” and a “moderate” pace of energy-efficiency improvements). To align these state-based demand data to our IPM-based zonal definitions, we use 2018 utility state-level sales data (Form EIA-861) to allocate fractions of state demand to our defined zones.

Table C.2 Rooftop PV minimum build in New York and New England

| | Existing capacity (MWdc) | Cumulative installations through 2050 (MWdc) | Existing capacity (MWac) | Cumulative installations through 2030 (MWac) | Cumulative installations through 2050 (MWac) | New installations through 2050 (MWac) |
|---------------------------|--------------------------|--|--------------------------|--|--|---------------------------------------|
| ISO-NE projections | | | | | | |
| [1] CT | — | — | 682.3 | 1,242.8 | 2,607.1 | 1,924.8 |
| [2] MA | — | — | 2,502.3 | 2,738.2 | 5,744.1 | 3,241.8 |
| [3] ME | — | — | 68.8 | 320.6 | 672.5 | 603.7 |
| [4] NH | — | — | 125.3 | 259.5 | 544.4 | 419.1 |
| [5] RI | — | — | 223.8 | 196.7 | 412.6 | 188.8 |
| [6] VT | — | — | 393.5 | 607.2 | 1,273.8 | 880.3 |
| NYISO projections | | | | | | |
| [7] A | 125.0 | 1,276.0 | 108.7 | — | 1,109.6 | 1,000.9 |
| [8] B | 63.0 | 371.0 | 54.8 | — | 322.6 | 267.8 |
| [9] C | 169.0 | 977.0 | 147.0 | — | 849.6 | 702.6 |
| [10] D | 5.0 | 101.0 | 4.3 | — | 87.8 | 83.5 |
| [11] E | 123.0 | 974.0 | 107.0 | — | 847.0 | 740.0 |
| [12] F | 299.0 | 1,168.0 | 260.0 | — | 1,015.7 | 755.7 |
| [13] G | 251.0 | 705.0 | 218.3 | — | 613.0 | 394.8 |
| [14] H | 34.0 | 70.0 | 29.6 | — | 60.9 | 31.3 |
| [15] I | 46.0 | 109.0 | 40.0 | — | 94.8 | 54.8 |
| [16] J | 210.0 | 791.0 | 182.6 | — | 687.8 | 505.2 |
| [17] K | 537.0 | 880.0 | 467.0 | — | 765.2 | 298.3 |

Assumes a DC-AC ratio of 1.15. Capacities from the ISO-NE Final 2021 PV Forecast (Black 2021), pp. 23–28, extrapolated to 2050 using the EIA AEO implied 2030–2050 growth rate of 110%. Source: NYISO 2020 Gold Book (New York ISO 2020), Table I-9a.

VRE supply curves: We developed zonal VRE supply curves based on the methodology described in Brown and Botterud (2021). Hourly PV capacity factors are simulated using 2007–2013 weather data from the NREL National Solar Radiation Database (National Renewable Energy Laboratory 2021) through the PVLIB model framework (Holmgren, Hansen and Mikofski 2018), at a 4 km by 4 km spatial resolution. Hourly wind capacity factors are simulated using the same temporal and spatial resolution using the NREL Wind Integration National Dataset Toolkit (Draxl et al. 2015) and power curve data for the commercially available Gamesa:G126/2500 wind turbine (Gamesa 2017) at 100-meter height. To reduce the spatial resolution of the

VRE capacity factor data, we aggregate sites within a zone on the basis of average LCOE (including the cost of interconnecting to the nearest substation). Thus, for each resource and zone, we get a supply curve, with each bin representing increasing resource quality with an associated maximum availability (based on land area), interconnection cost, and hourly capacity factor profile.

Generator and storage costs: Fossil-powered generation and VRE capital and operational costs are shown in Table 6.5 in Chapter 6 of the main report. Costs for gas, nuclear, VRE, and Li-ion energy storage are taken from the 2020 NREL Annual Technology Baseline 2045 “Mid” cost projections (National Renewable Energy

Table C.3 Load allocation from states to IPM zones

| GWh | TVA | Carolinas | SOCO | Florida |
|-----------------------|--------|-----------|--------|---------|
| Tennessee | 100.81 | 0.01 | 0.00 | 102.91 |
| Alabama | 23.66 | 0.00 | 66.62 | 90.28 |
| North Carolina | 0.79 | 131.74 | 0.00 | 138.29 |
| South Carolina | 0.00 | 81.64 | 0.00 | 81.64 |
| Georgia | 3.40 | 0.00 | 136.12 | 139.87 |
| Florida | 0.00 | 0.00 | 13.25 | 238.57 |
| Mississippi | 16.29 | 0.00 | 11.73 | 50.39 |

| % Total | TVA | Carolinas | SOCO | Florida |
|-----------------------|-------|-----------|-------|---------|
| Tennessee | 98.0% | 0.0% | 0.0% | 0.0% |
| Alabama | 26.2% | 0.0% | 73.8% | 0.0% |
| North Carolina | 0.6% | 95.3% | 0.0% | 0.0% |
| South Carolina | 0.0% | 100.0% | 0.0% | 0.0% |
| Georgia | 2.4% | 0.0% | 97.3% | 0.2% |
| Florida | 0.0% | 0.0% | 5.6% | 94.4% |
| Mississippi | 32.3% | 0.0% | 23.3% | 0.0% |

Utility bundled retail sales by state from Form EIA-861 (EIA 2020). Utility-to-IPM zonal mapping from EPA IPM model documentation (EIA 2018). SOCO refers to the territory serviced by the Southern Company. TVA refers to the territory serviced by the Tennessee Valley Authority.

Laboratory 2020). “Low” VRE and Li-ion costs are also taken from the NREL ATB for the sensitivity analysis.³ Additionally, we apply a small, non-zero VOM for wind, hydropower, and storage to distinguish their dispatch as part of the economic dispatch modeled within GenX—this addition does not meaningfully affect resulting system costs.

For storage, system costs are separated as energy-only components (e.g., battery packs for Li-ion, tanks for long-duration energy storage) or power-only components (e.g., inverter, interconnection and permitting fees, land acquisition costs). Power-only components can further be parsed into charging or discharging power costs, depending on the type of storage technology (see Table 6.2 in Chapter 6). This

separation of function-based costs enables the model to independently vary the energy, discharging power, and charging power capacities of energy storage systems for optimal sizing. Low-, mid-, and high-cost Li-ion estimates are taken from the NREL ATB 2050 cost projections (National Renewable Energy Laboratory 2020); cost projections for other storage technologies are from the analysis described in the technology-focused chapters of this report (see Table 6.3).

Operations and fuel assumptions: Operational assumptions for gas- and nuclear-powered generators are summarized in Table C.4. Fuel price assumptions are taken from the EIA AEO 2020 Reference (EIA 2021b) 2050 case (see Table C.5).

³ The mid-cost and low-cost Li-ion cost assumptions for 2050 from NREL are broadly consistent with estimates reported in Chapter 2. We chose to use the NREL estimates since they are widely used by other power system modeling studies. See further discussion on Li-ion cost in Chapter 2.

Table C.4 Thermal generator operational characteristics

| Tech | Capacity size (MW) | Start cost (\$) | Start cost (\$/MW/start) | Start fuel (MMBTU/start) | Start fuel (MMBTU/MW/start) | Heat rate (MMBTU/MWh) |
|----------------------|--------------------|-----------------|--------------------------|--------------------------|-----------------------------|-----------------------|
| [1] OCGT | 237 | 33,147 | 140 | 45 | 0.19 | 9.51 |
| [2] CCGT | 573 | 34,982 | 61 | 115 | 0.20 | 6.40 |
| [3] CCGT + CCS | 377 | 36,419 | 97 | 75 | 0.20 | 7.12 |
| [4] Existing Nuclear | 1,000 | 1,000,000 | 1,000 | 0 | 0.00 | 10.46 |
| [5] New Nuclear | 1,000 | 1,000,000 | 1,000 | 0 | 0.00 | 10.46 |

| Tech | Min stable output (%) | Ramp up (%) | Ramp down (%) | Up time (Hours) | Down time (Hours) |
|----------------------|-----------------------|-------------|---------------|-----------------|-------------------|
| [1] OCGT | 25 | 100 | 100 | 0 | 0 |
| [2] CCGT | 30 | 100 | 100 | 4 | 4 |
| [3] CCGT + CCS | 50 | 100 | 100 | 4 | 4 |
| [4] Existing Nuclear | 50 | 25 | 25 | 36 | 36 |
| [5] New Nuclear | 20 | 100 | 100 | 36 | 36 |

Compiled from multiple sources: Buongiorno et al. (2018), Sepulveda et al. (2018), National Renewable Energy Laboratory (2020), GE (2017), Jenkins et al. (2018).

Table C.5 Technology-specific fuel prices

| Fuel | \$/MMBtu |
|------------------|----------|
| Uranium | 0.72 |
| Natural Gas (NG) | 4.04 |
| NG + CCS | 5.00 |

Fuel prices from EIA AEO 2020 Reference (EIA 2021b) 2050 case. The fuel cost for conventional NGCC with CCS plant also includes a \$20 per metric tonne CO₂ transportation and sequestration cost. This cost is applied based on 90% CO₂ capture in the power plant flue gas.

Demand flexibility: As described in Chapter 6, modeling assumptions for simulated demand flexibility are based on the NREL Electrification Futures Study (EFS) enhanced flexibility scenario, which proposes hours of delay and advance for specific demand subsectors, along with the share of load that can be shifted (Mai et al. 2018). Table 6.11 in the main report shows assumptions for how many hours of demand in each demand subsector can be advanced or

delayed, as well as the maximum hourly demand that can be flexible in Texas. Table C.6 shows the maximum hourly demand flexibility for all three regions. Coincident maximum potential demand flexibility is 37 GW (39% of hourly demand) for the Northeast and 113 GW (37% of hourly demand) for the Southeast; both figures are proportionately higher than the maximum demand flexibility potential (47 GW or 31% of hourly demand) in Texas.

Table C.6 Non-coincident maximum hourly demand flexibility in GW across the three modeled regions under 2050 load conditions

| Demand subsector | Northeast | Southeast | Texas |
|----------------------------------|-----------|-----------|-------|
| Commercial HVAC | 1.5 | 3.0 | 8.6 |
| Residential HVAC | 2.0 | 6.2 | 7.0 |
| Commercial water heating | 0.0 | 0.1 | 0.2 |
| Residential water heating | 0.2 | 0.7 | 1.0 |
| Light-duty vehicles | 27.6 | 79.4 | 33 |
| Medium-duty trucks | 1.6 | 4.6 | 3.0 |
| Heavy-duty trucks | 1.2 | 6.0 | 5.0 |

HVAC = heating, ventilation, and air conditioning. Data sourced from NREL Electrification Futures Study (Mai et al. 2018).

C.2 Time domain reduction approach

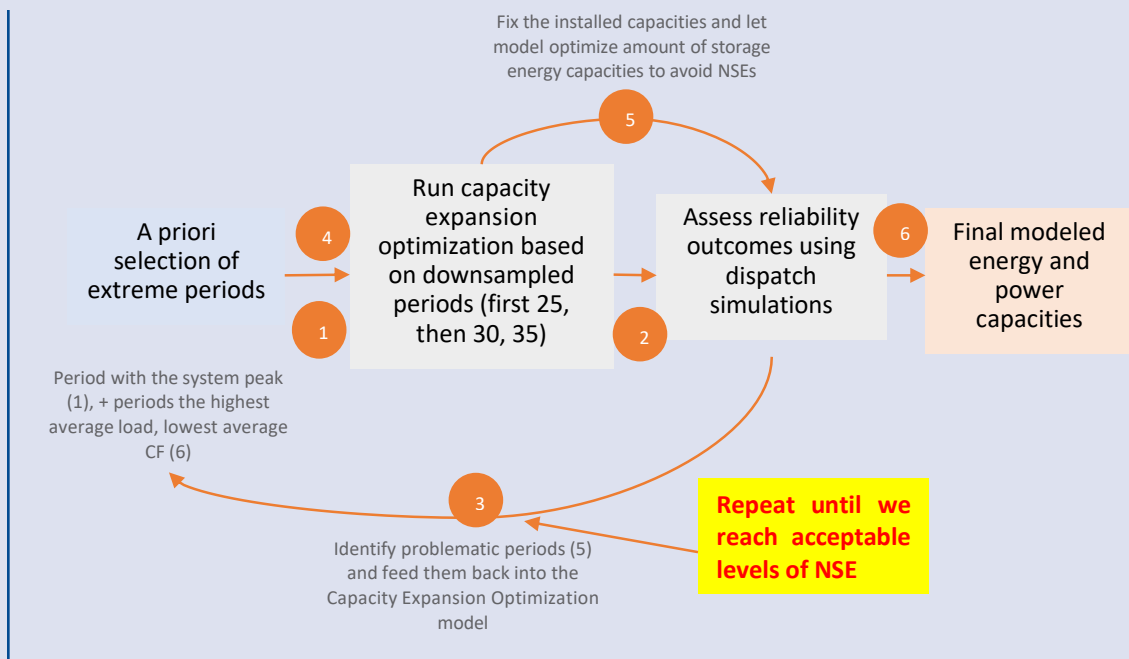
Capacity expansion models (CEMs) rely on a compact temporal, spatial, and network representation of the power system to maintain computational tractability. Traditional CEMs have relied on a “time slice” approach (e.g., 12 representative days across the year) that is usually based on disaggregating the load duration curve based on seasonal and time-of-day blocks. The intuition of this approach is to represent conditions of system peak, based on the idea that if there is sufficient generating capacity to cover the peak, then reliability can be ensured at all other times too. However, recent studies show that systems with high penetrations of VRE will require increased temporal resolution and operational detail to adequately capture the temporal and spatial dynamics of a highly decarbonized electricity grid. Specifically, with increasing VRE penetration, the system peak “net load” (i.e., the residual load after accounting for VRE generation) is likely to be more important than the system peak load for resource planning purposes.

In this study, we model hourly grid operations to capture intra- and inter-annual variability in load and VRE generation. For the Northeast

and Southeast case studies, which involve multi-zonal representations of these regions, we approximate annual outcomes for grid operations by modeling hourly operations over a set of representative periods that are selected through a hybrid clustering scheme (described below). The use of representative periods via clustering represents an improvement over time-slice approaches since it is based on prevailing variability in all of the input time series, not just load, and since it also allows for preserving chronology in operations as well as inter-period energy transfers in the case of energy storage.

The hybrid clustering employed here to select representative periods is adapted to provide both sufficient temporal resolution and extreme weather coverage. While the clustering procedure seeks to closely approximate the underlying temporal distributions of historical load and VRE capacity factor profiles, the extreme periods selection procedure seeks to incorporate sufficient “reliability” events corresponding to extended periods of low VRE output and high demand (e.g., heat waves, cold snaps). We outline our iterative approach to selecting the periods used in the CEM below (Figure C.1).

Figure C.1 Hybrid clustering approach used to select representative periods for CEM in the case of the Northeast and Southeast regions



Step 1: We slice the zonal load and VRE capacity factor data into 10-day periods. For each period, we calculate average load, solar capacity factor (CF), and wind CF, and identify some “a priori extreme periods,” defined as those periods that have the highest system peak, highest average load, and lowest PV and onshore wind output, at a zonal level. We then stitch together the time series of all resources (solar, onshore wind, hydro) for each period, to create a single concatenated time series for each 10-day period; thus, each vector is of length: 24 hours/day x 10 day/period x 4 time series (load, solar, onshore wind, hydro) x number of modeled zones. Due to overlap between the extreme periods that meet the above criteria, we identify six extreme periods for the Northeast through this process and eight for the Southeast.

Step 2: We employ the k-means clustering technique to group the remaining periods (non-extreme periods, total (255) minus the number of extreme periods chosen) into 25 clusters. For each cluster, we select the historical

period closest to the centroid of the cluster as the most representative period. This is because the centroid of the cluster may not reflect actual conditions that exist on the system; thus, we ensure that the most representative periods are based on actual data. We then weigh each representative period based on cluster size, to achieve a total weight of 8,760 hours to approximate annual grid operations. To preserve the system peak, we did not scale the weighted time series to match the annual load in the original data; this results in a 2%–3% increase in annual load relative to the NREL EFS data.

Step 3: The iterative process starts by inputting CEM outputs into a simplified production cost model to simulate overall reliability under the proposed portfolios. This process is more effective at identifying periods of great importance for reliability that were not already flagged as “a priori extreme” or “representative” periods. We call the periods that cause the most reliability issues (i.e., frequent and long-lasting non-served energy events), “reliability periods.”

We repeat this last step one or two times to ensure that we're optimizing for system reliability at each hour (i.e., no significant load shedding due to capacity shortages). The threshold we are applying is the often-used reliability standard of 1-in-10 years, which we interpret as one day in ten years of involuntary load shedding.

Steps 4–6: After we reach an acceptable level of reliability, we can finalize the selection of representative and extreme periods and interpret the model results (shown in the main report). Step 5 is optional; it can allow the CEM to re-optimize for storage power and energy capacities over the full seven years of weather data once the capacities for the other technologies and transmission have been fixed. We did not end up needing this step.

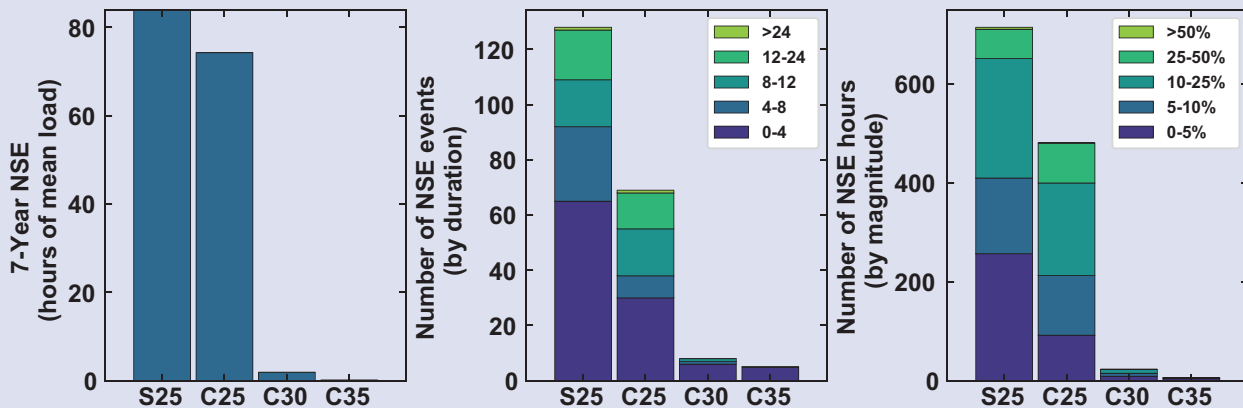
To test this approach, we assessed reliability outcomes, which we define as the frequency, duration, and magnitude of resulting non-served energy (NSE) events, across multiple model configurations. We start with a simple chronology-based approach that selects 25 periods across one single year of weather data (2012) to resolve the optimal capacity mix (S25-CEM). Then, we consider a suite of CEMs, while incrementally increasing the number of selected periods (therefore, the number of hours the model “sees” to make its investments and dispatch decisions). This corresponds to the C25, C30, and C35 scenarios annotated in Figure C.1 and shows the breakdown of all NSE events. As expected, a CEM based on one year of weather data (S25-CEM) yields a lower level of reliability than one based on multiple years of weather data (C25-CEM), particularly around extended periods of low VRE output (especially with respect to wind, since solar follows a fairly consistent diurnal pattern). We can also see how individual events break down in terms of their duration (e.g., consecutive hours of NSE) and magnitude (e.g., as a

proportion of total system load during each hour). We see that for the Southeast (Figure C.2), moving from the S25-CEM to the C25-CEM configuration decreases total NSE by 12% (or 1,535 GWh) and the total duration of such events by 33% (or 234 hours), across the seven weather years considered. The decrease in frequency of NSE events that last for more than four hours (shown in different shades of green), as well as the frequency of NSE hours with more than 10% of total system load, is particularly noteworthy.

Reliability outcomes for the Northeast (Figure C.3) are a bit different in that the frequency of outage events actually seems to increase between S25-CEM and C25-CEM, and between C30-CEM and C35-CEM. Upon closer inspection, however, we can see that the number of severe events (i.e., events of a duration longer than 12 hours, or that shed more than 25% of hourly load) actually decreases, which is what we would expect. In general, because the Northeast does not have other forms of firm capacity (e.g., existing nuclear) and has poorer VRE resource quality, we'd expect to see more instances of NSE events relative to the Southeast.

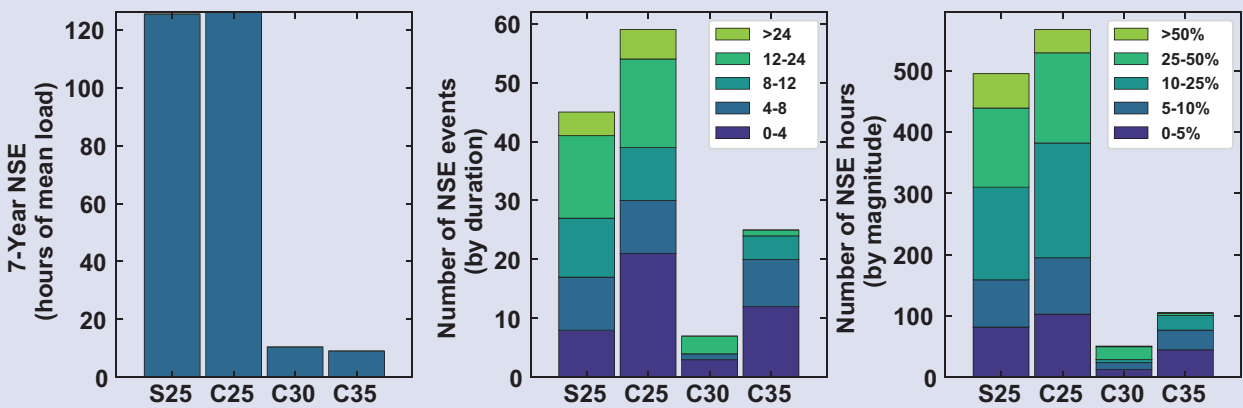
Most striking in both regions is the large improvement in reliability that comes with the exogenous addition of extreme periods into the initial capacity expansion optimization problem, which allows the model to “see” these extended periods of low VRE output that are particularly prone to reliability issues. Moving from S25-CEM to C35-CEM decreases total NSE by almost 100% in the Southeast and by 93% in the Northeast. It also decreases the total duration of such events by 99% in the Southeast and by 78% in the Northeast. Thus, these results show that using our proposed methodology dramatically reduces the frequency, duration, and magnitude of expected NSE events.

Figure C.2 Reliability outcomes in the Southeast across different model configurations



From left to right: (1) Total magnitude of NSE events across the seven test years, standardized to the system mean load (157.6 GW). (2) Number of NSE events by duration buckets. (3) Number of NSE hours by magnitude (as a percentage of hourly load) buckets.

Figure C.3 Reliability outcomes in the Northeast across different model configurations



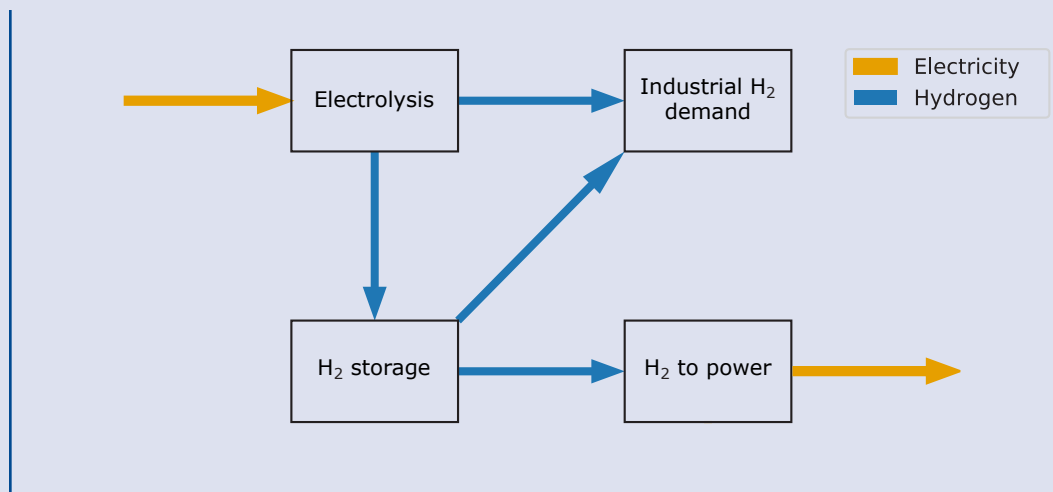
From left to right: (1) Total magnitude of NSE events across the seven test years, standardized to the system mean load (49.9 GW). (2) Number of NSE events by duration buckets. (3) Number of NSE hours by magnitude (as a percentage of hourly load) buckets.

C.3 Modeling hydrogen demand in industry and its impact on power sector evolution

The configuration of Figure C.4 is included in the GenX model, where, along with specifying cost and performance assumptions for the elements noted previously (e.g., electrolyzer, storage tank, and gas turbines for hydrogen

storage), we add a constraint that requires the specified hydrogen (H_2) demand from industry to be met either by the electrolyzer or by discharging stored H_2 . With this single constraint the design of a traditional power-to- H_2 -to-power storage system can also be optimized, in terms of component sizes and utilization, to meet H_2 demand in the industrial sector.

Figure C.4 Representation of the power-to-H₂-to-power system in GenX with use of the system to also meet industrial hydrogen demand



Since we are primarily interested in understanding impacts on the power system from external H₂ demand, we make the following approximations to simplify the representation of the H₂ supply chain: (1) We ignore potential sources of H₂ supply, such as H₂ produced from natural gas with and without carbon capture to meet external demand. Instead, we vary the H₂ demand from industry that is to be met by electrolyzer-driven H₂ supply and thereby account for the possibility of other sources of H₂ supply. (2) We do not consider any spatial distribution in H₂ production and industrial demand and thus ignore H₂ transportation. (3) We are not including source-dependent delivery costs for H₂ supply that could be associated with adjusting the state of delivered H₂ from different sources to meet industrial customer requirements. Other studies have included these factors in the hydrogen supply chain while also contemplating their impacts on the evolution of the power system (He et al. 2021; Sunny, Mac Dowell and Shah 2020).

Hydrogen demand is modeled as exogenous and uniform throughout the year. Hydrogen demand was estimated using NREL's 2018 Industrial Data Book as a reference (McMillan 2019). This publication contains a dataset detailing the annual energy consumed by large energy-using facilities⁴ in 2016. Here, we focus on hydrogen demand from substituting hydrogen for natural gas used for heating purposes in Industry.

Natural gas consumption by large energy users in Texas totaled 0.93 quadrillion BTU (QBTU) in 2016, which represents about 44% of the 2.1 QBTU of industrial natural gas consumption in Texas, as reported by EIA (Figure C.5). From that 0.93 QBTU, we considered for the analysis process heaters, furnaces, boilers, and other combustion sources as potential units that use natural gas for heating purposes. Moreover, we excluded units whose unit name suggests natural gas is being used as feedstock. This results in 0.59 QBTU of natural gas used for heating. We further assume that demand for heat from natural gas is flat at 0.59 QBTU/year, which is equivalent to 19.7 GW_t of hydrogen.

⁴ Defined as those facilities that are required to report greenhouse gas emissions under EPA's Greenhouse Gas Reporting Program.

Figure C.5 Natural gas consumption by large energy users in Texas

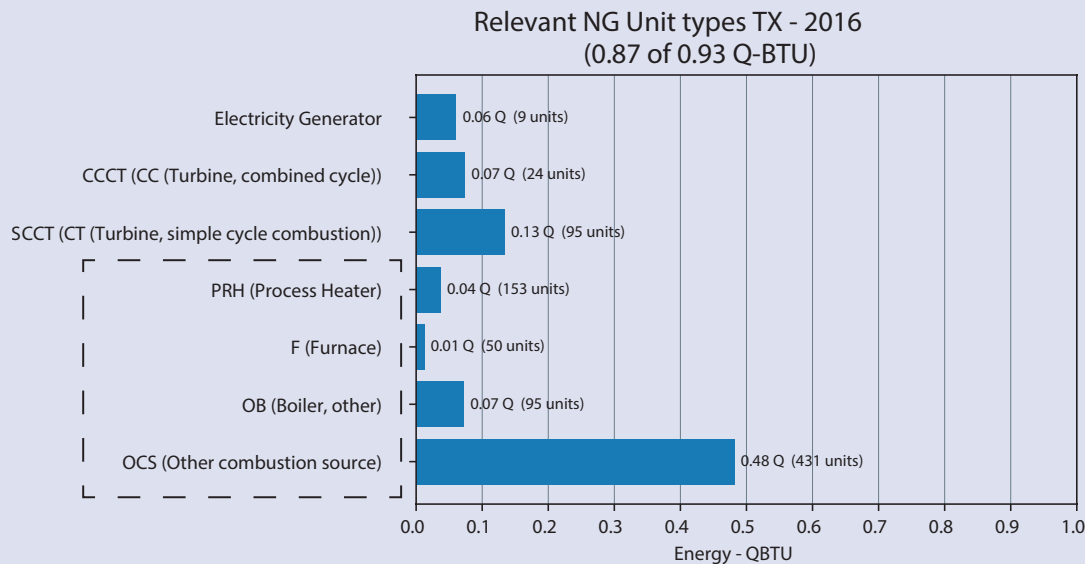


Table C.7 Installed power capacity (relative to peak load)

| Emission policy (gCO ₂ /kWh) | Hydrogen demand as % of baseline hydrogen demand (19.7 GW _t) | | | | | |
|--|--|------|------|------|------|------|
| | 0% | 25% | 50% | 75% | 100% | 125% |
| 1 | 2.68 | 2.50 | 2.60 | 2.70 | 2.80 | 2.90 |
| 5 | 2.27 | 2.39 | 2.49 | 2.60 | 2.72 | 2.83 |
| 10 | 2.20 | 2.38 | 2.47 | 2.58 | 2.69 | 2.80 |
| 50 | 2.01 | 2.03 | 2.13 | 2.24 | 2.35 | 2.45 |
| NL | 1.76 | 1.90 | 1.99 | 2.11 | 2.20 | 2.32 |

Increasing hydrogen demand and imposing a more stringent CO₂ constraint increases the total installed power capacity.

Table C.8 VRE curtailment level (% of available generation based on capacity)

| Emission policy (gCO ₂ /kWh) | Hydrogen demand | | | | | |
|--|-----------------|------|------|------|------|------|
| | 0% | 25% | 50% | 75% | 100% | 125% |
| 1 | 29.7 | 12.0 | 11.7 | 11.4 | 10.8 | 10.2 |
| 5 | 16.9 | 10.0 | 9.5 | 9.5 | 9.4 | 9.3 |
| 10 | 15.3 | 10.1 | 9.7 | 9.0 | 8.6 | 8.3 |
| 50 | 9.7 | 2.9 | 2.7 | 2.5 | 2.4 | 2.3 |
| NL | 3.2 | 1.4 | 1.0 | 1.0 | 0.7 | 0.8 |

Increasing the stringency of the CO₂ constraint increases VRE curtailment levels, but increasing industrial hydrogen demand decreases it.

Table C.9 Average system cost of energy, SCOE (\$/MWh)

| Emission policy (gCO ₂ /kWh) | Hydrogen demand | | | | | |
|--|-----------------|------|------|------|------|------|
| | 0% | 25% | 50% | 75% | 100% | 125% |
| 1 | 49.8 | 40.6 | 39.2 | 38.1 | 37.2 | 36.4 |
| 5 | 43.9 | 39.0 | 37.7 | 36.6 | 35.7 | 35.0 |
| 10 | 42.2 | 37.9 | 36.6 | 35.6 | 34.7 | 34.1 |
| 50 | 37.0 | 34.8 | 33.8 | 33.0 | 32.4 | 31.9 |
| NL | 36.2 | 34.6 | 33.6 | 32.8 | 32.2 | 31.7 |

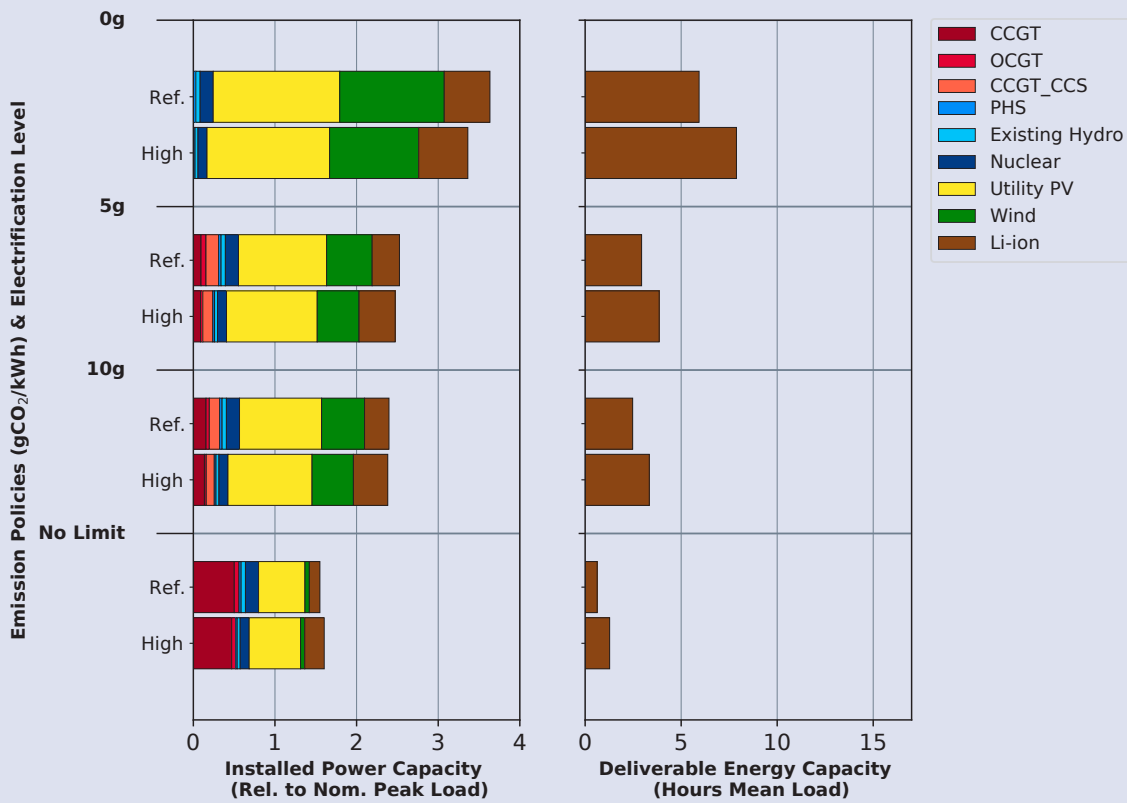
Increasing the stringency of the CO₂ constraint increases SCOE, but increasing industrial hydrogen demand decreases it.

C.4 Additional modeling results

Table C.10 Capacity factors for CCGTs without CCS in the base case for various emission policy constraints (gCO₂/kWh)

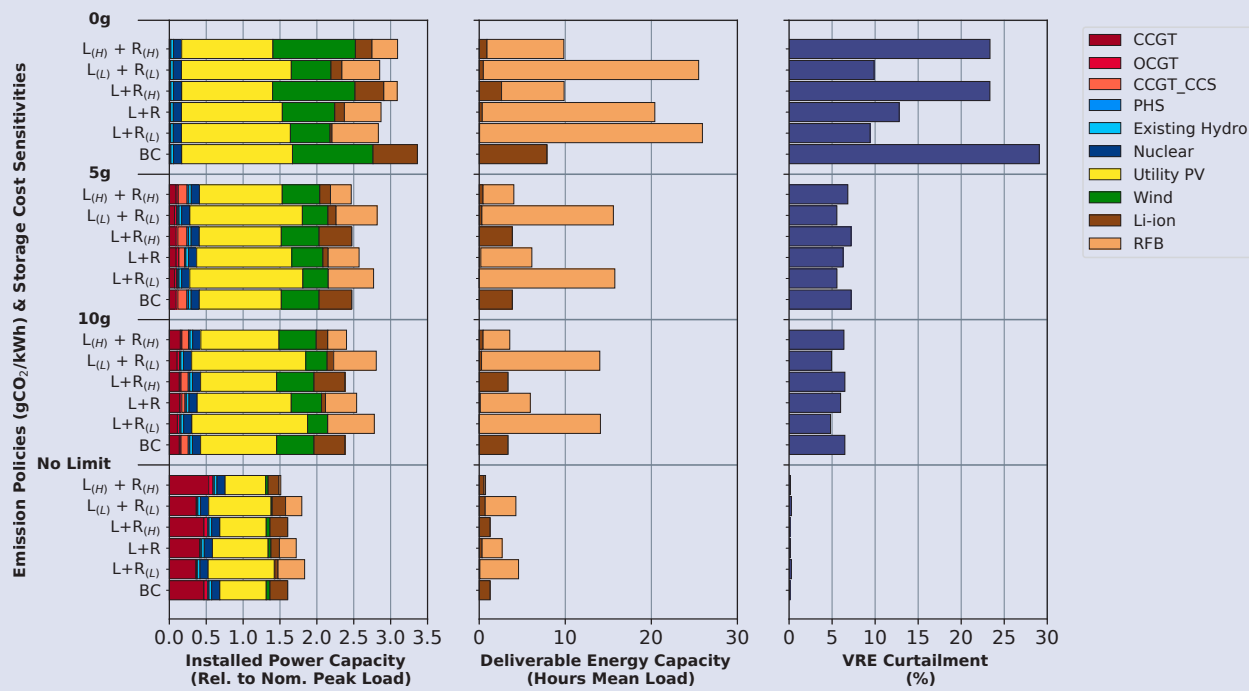
| | 5g | 10g | 50g | NL |
|-----------|----|-----|-----|-----|
| Northeast | 2% | 7% | 31% | 66% |
| Southeast | 5% | 9% | 29% | 54% |
| Texas | 3% | 7% | 24% | 36% |

Figure C.6 Impacts of assuming the NREL EFS Reference vs. High Electrification load scenarios in the Southeast in terms of installed power capacity and storage capacity across a range of CO₂ policies



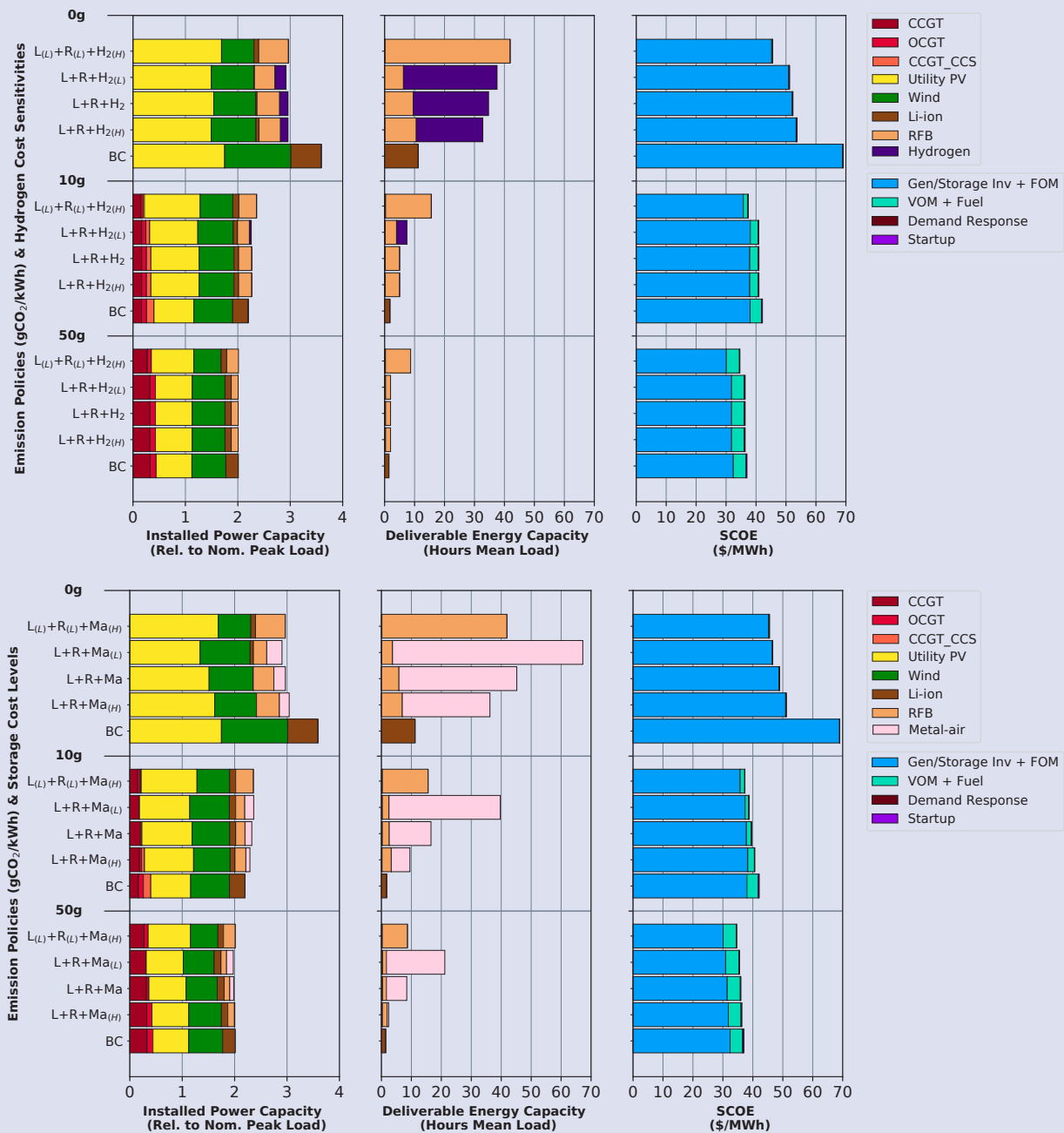
Under the High Electrification scenario, both system peak and annual demand are higher, see Table 6.6 for details. See discussion of the impacts of electrification around Figure 6.5 in the main report.

Figure C.7 Scenarios showing the impacts of cost sensitivities around Li-ion and RFB technology in the Southeast in terms of installed power capacity, storage capacity, and VRE curtailment, across a range of CO₂ policies



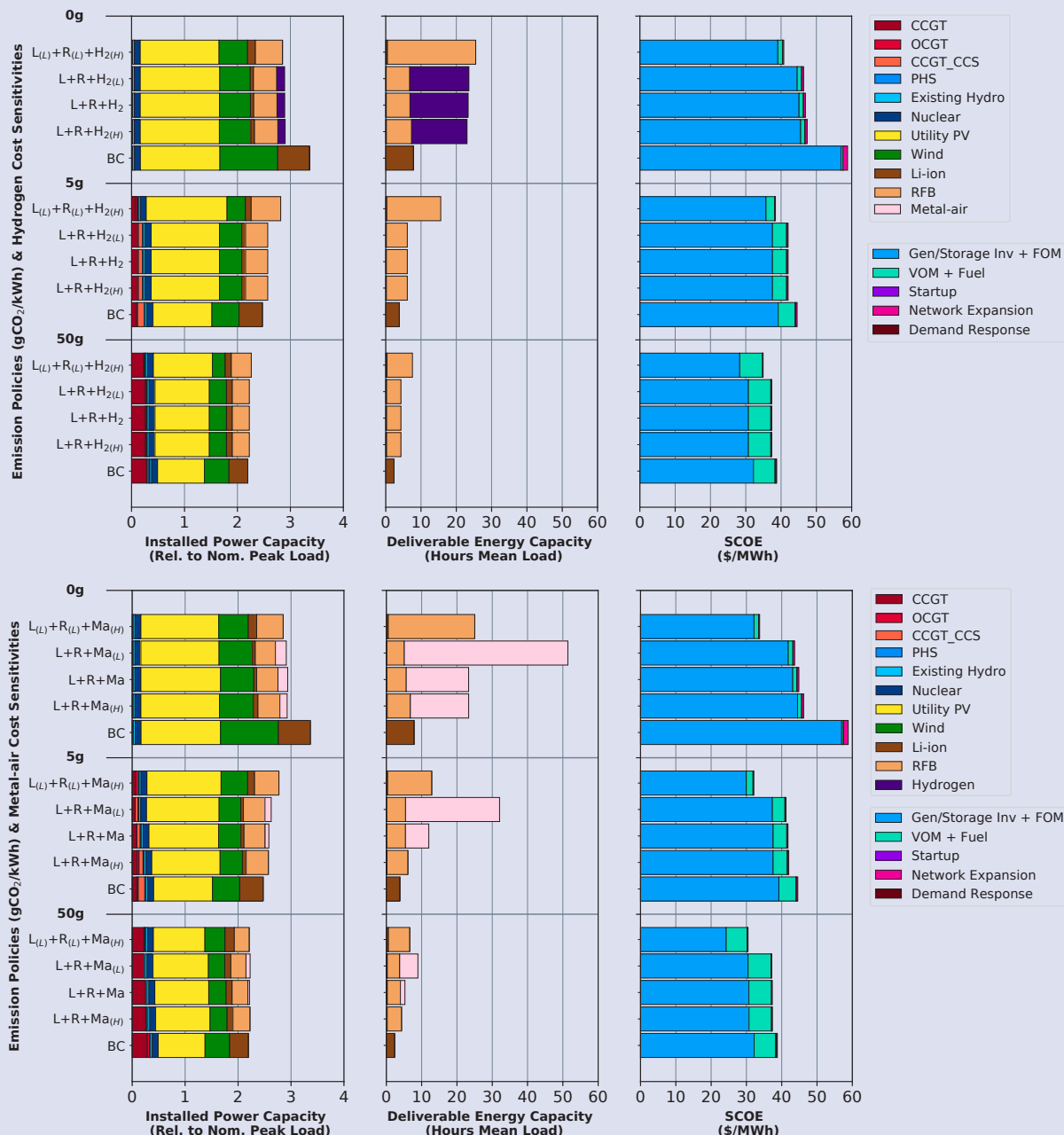
The scenarios shown are, in ascending order: (1) base case (i.e., mid-cost Li-ion only, BC), (2) mid-cost Li-ion + low-cost RFB (L+R_L), (3) mid-cost Li-ion + mid-cost RFB (L+R), (4) low-cost Li-ion + low-cost RFB (L_L+R_L), and (5) high-cost Li-ion + high-cost RFB (L_H+R_H). Low-, mid-, and high-cost assumptions for each storage technology are defined in Table 6.3. See discussion of the impacts of Li-ion and RFB costs around Figure 6.8 in the main report.

Figure C.8 System impacts of LDES availability at different assumed cost levels in Texas



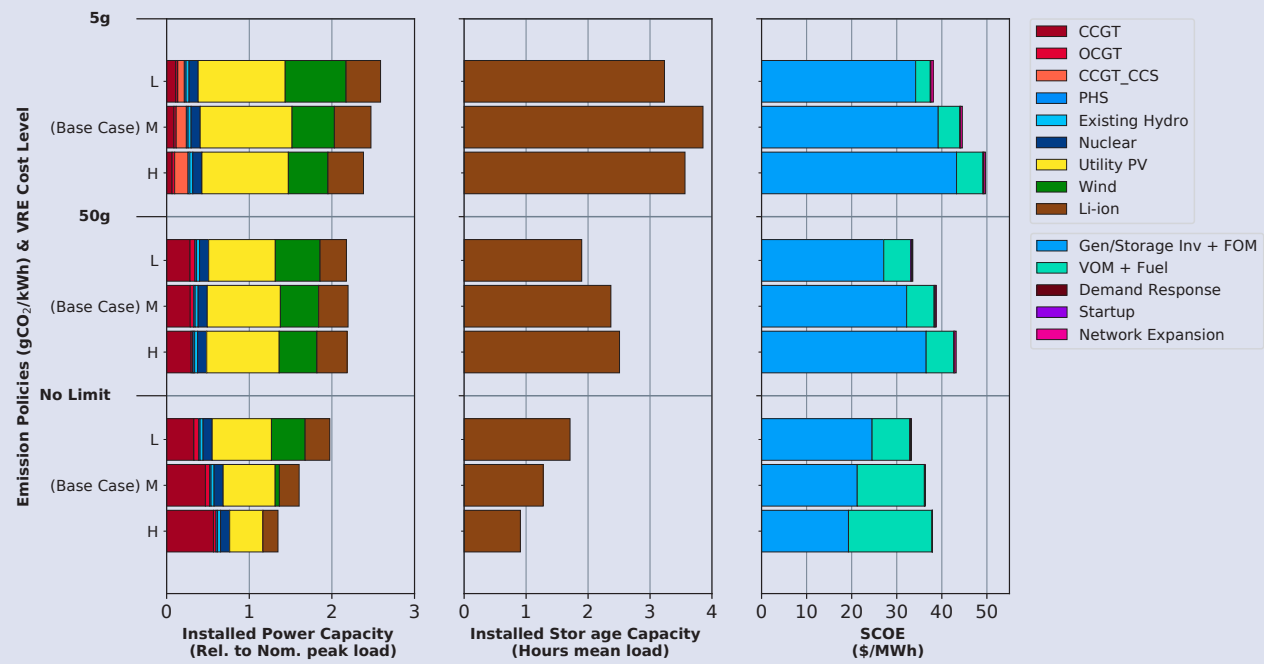
Scenarios show the impacts of low-, mid-, and high-cost hydrogen and metal-air batteries on installed power capacity, storage capacity, and SCOE, across a range of CO₂ policies. They are, in ascending order: (1) base case (i.e., mid-cost Li-ion only, BC); (2–4) mid-cost Li-ion and RFB + incrementally adding high-cost hydrogen or metal-air batteries (L+R+H₂/MA_H), mid-cost hydrogen or metal-air (L+R+H₂/MA), and low-cost hydrogen or metal-air (L+R+H₂/MA_L); and (5) low-cost Li-ion and RFB + high-cost hydrogen or metal-air (L_L+R_L+H₂/MA_H). Low-, mid-, and high-cost assumptions for each storage technology are defined in Table 6.3. See discussion of the impacts of LDES costs around Figures 6.11 and 6.12 in the main report.

Figure C.9 System impacts of LDES availability at different assumed cost levels in the Southeast



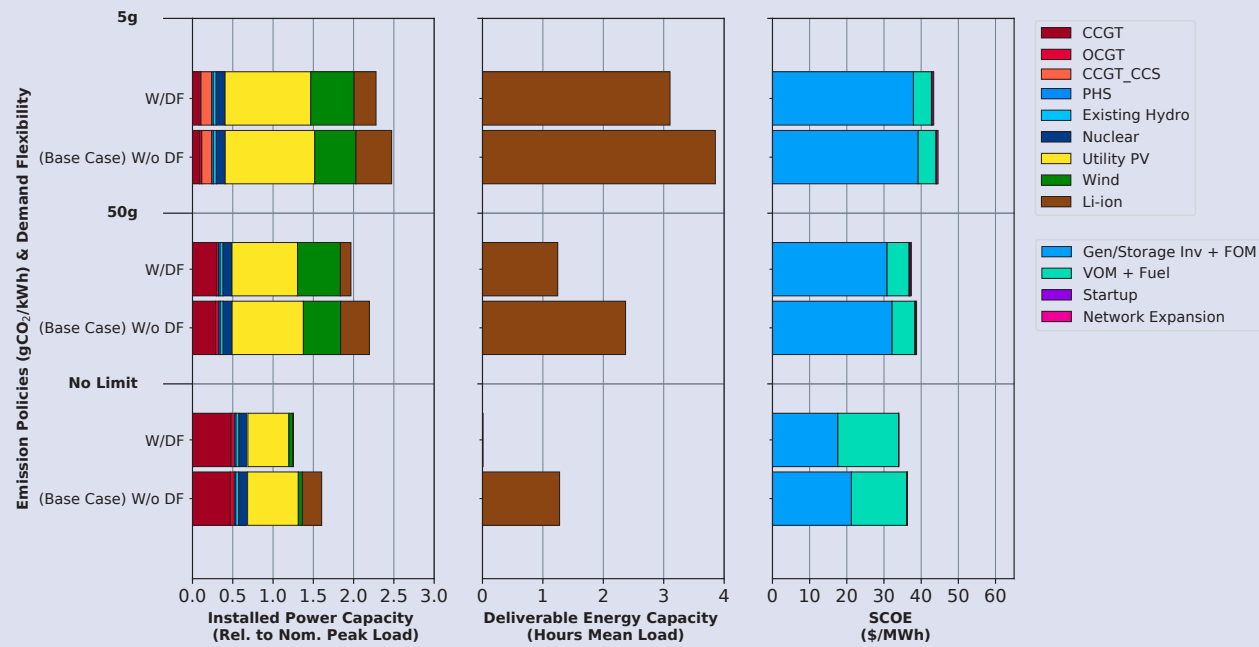
Scenarios show the impacts of low-, mid-, and high-cost hydrogen and metal-air batteries on installed power capacity, storage capacity, and SCOE, across a range of CO₂ policies. They are, in ascending order: (1) base case (i.e., mid-cost Li-ion only, BC); (2–4) mid-cost Li-ion and RFB + incrementally adding high-cost hydrogen or metal-air (L+R+H₂/MA_H), mid-cost hydrogen or metal-air (L+R+H₂/MA), and low-cost hydrogen or metal-air (L+R+H₂/MA_L); and (5) low-cost Li-ion and RFB + high-cost hydrogen or metal-air (L_L+R_L+H₂/MA_H). Low-, mid-, and high-cost assumptions for each storage technology are defined in Table 6.3. See discussion of the impacts of LDES costs around Figures 6.11 and 6.12 in the main report.

Figure C.10 System impacts of VRE at varying cost levels in the Southeast



Scenarios show the impacts of low-, mid-, and high-cost VRE on installed power capacity, storage capacity, and SCOE, across a range of CO₂ policies. They are, in ascending order: (1) high-cost VRE (H), (2) mid-cost VRE (M), and (3) low-cost VRE (L). Low-, mid-, and high-cost assumptions for VRE are defined in Appendix C.1. See discussion of the impacts of VRE costs around Figure 6.14 in the main report.

Figure C.11 System impacts of demand flexibility in the Southeast



Scenarios show impacts with and without demand flexibility in terms of installed power capacity, storage capacity, and SCOE, across a range of CO₂ policies. Demand flexibility assumptions are reported in Table 6.11. See discussion of the impacts of demand flexibility around Figure 6.15 in the main report.

Table C.11 System impacts of a dispatchable low-carbon generating technology in Texas

| | Low-cost metal-air | | | Mid-cost metal-air | | | High-cost metal-air | | |
|--|---------------------|------------------|--------|---------------------|------------------|--------|---------------------|------------------|--------|
| | Without Allam cycle | With Allam cycle | % diff | Without Allam cycle | With Allam cycle | % diff | Without Allam cycle | With Allam cycle | % diff |
| Firm dispatchable installed capacity (GW) | | | | | | | | | |
| CCGT | 19.5 | 20.2 | 4% | 22.6 | 23.0 | 2% | 19.0 | 20.1 | 6% |
| OCGT | 0.0 | 0.0 | — | 0.1 | 2.1 | 2,294% | 6.2 | 9.2 | 47% |
| CCGT_CCS | 7.7 | 0.0 | -100% | 11.2 | 0.0 | -100% | 15.4 | 0.0 | — |
| Allam | 0.0 | 9.8 | — | 0.0 | 13.9 | — | 0.0 | 18.7 | — |
| Total | 27.2 | 30.0 | 10% | 33.9 | 25.1 | 15% | 40.6 | 29.3 | 18% |
| VRE installed capacity (GW) | | | | | | | | | |
| Wind | 113.2 | 108.6 | -4% | 107.6 | 102.3 | -5% | 104.4 | 97.3 | -7% |
| Utility PV | 147.5 | 142.8 | -3% | 148.0 | 140.6 | -5% | 145.4 | 137.0 | -6% |
| Total | 260.7 | 251.4 | -4% | 255.6 | 243.0 | -5% | 249.8 | 234.3 | -6% |
| Energy storage (Li-ion + RFB + LDES) | | | | | | | | | |
| Power (GW) | 70.7 | 68.6 | -3% | 64.6 | 60.4 | -6% | 58.7 | 52.3 | -11% |
| Energy (GWh) | 3,168 | 3,121 | -2% | 1,399 | 1,114 | -20% | 840 | 626 | -25% |
| System cost of electricity | | | | | | | | | |
| Average \$/MWh | 40.1 | 39.9 | -1% | 41.0 | 40.7 | -1% | 42.0 | 41.6 | -1% |

Scenarios show the impact of low-, mid-, and high-cost metal-air batteries with and without the Allam cycle in terms of installed power capacity, storage capacity, and SCOE, for a 5 gCO₂/kWh scenario. Low-, mid-, and high-cost assumptions for each storage technology are defined in Table 6.3. Cost assumptions for the Allam cycle are presented in Table 6.5 in the main report.

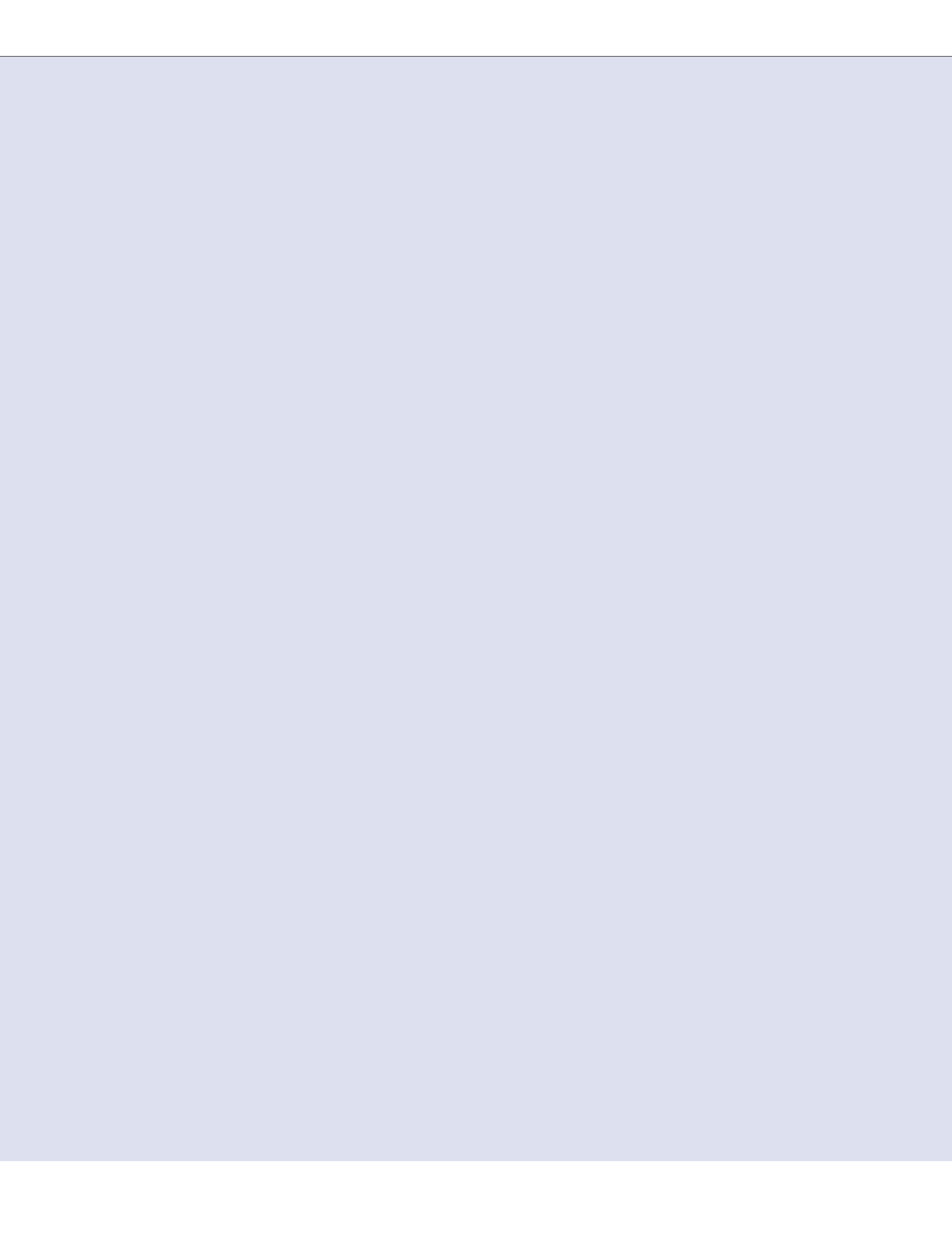
Table C.12 System impacts of expanding inter-zonal transfer capacity in the Southeast

| | 0 gCO ₂ /kWh | | | 5 gCO ₂ /kWh | | | No limit policy | | |
|--|-------------------------|----------------|--------|-------------------------|----------------|--------|-------------------|----------------|--------|
| | Without trans exp | With trans exp | % diff | Without trans exp | With trans exp | % diff | Without trans exp | With trans exp | % diff |
| Firm dispatchable installed capacity (GW) | | | | | | | | | |
| CCGT | 0.0 | 0.0 | — | 26.4 | 21.7 | -18% | 139.9 | 144.9 | 4% |
| OCGT | 0.0 | 0.0 | — | 8.1 | 18.1 | 124% | 14.9 | 15.7 | 5% |
| CCGT_CCS | 0.0 | 0.0 | — | 36.7 | 43.9 | 20% | 0.0 | 0.0 | — |
| Nuclear | 32.9 | 32.9 | — | 32.9 | 32.9 | 0% | 32.9 | 32.9 | — |
| Total | 32.9 | 32.9 | — | 104.1 | 116.6 | 12% | 187.7 | 193.4 | 3% |
| VRE installed capacity (GW) | | | | | | | | | |
| Wind | 325.6 | 297.2 | -9% | 152.7 | 145.4 | -5% | 15.3 | 14.0 | -8% |
| Utility PV | 447.7 | 470.8 | 5% | 331.3 | 326.2 | -2% | 187.6 | 181.3 | -3% |
| Total | 773.3 | 768.0 | -1% | 484.1 | 471.6 | -3% | 202.9 | 195.3 | -4% |
| Energy storage (Li-ion only) | | | | | | | | | |
| Power (GW) | 179.4 | 195.1 | 9% | 132.0 | 130.1 | -1% | 71.3 | 66.3 | -7% |
| Energy (GWh) | 1,307 | 1,873 | 43% | 639 | 612 | -4% | 212 | 189 | -11% |
| Transmission expansion | | | | | | | | | |
| Total (GW) | 145.3 | — | — | 45.5 | — | — | 2.0 | — | — |
| System cost of electricity | | | | | | | | | |
| Average \$/MWh | 58.8 | 64.9 | 10% | 44.6 | 44.9 | 1% | 36.3 | 36.3 | 0% |

Scenarios show the impacts of allowing transfer capacities to expand vs. restricting transfer capacities to existing levels in terms of installed power capacity, storage capacity, and SCOE, across a range of CO₂ policies. Cost assumptions for transmission expansion are discussed in Section C.1.

References

- Black 2021, Jon. 2021. "Final 2021 PV Forecast." https://www.iso-ne.com/static-assets/documents/2021/03/final_2021_pv_forecast.pdf.
- Brown, Maxwell, Wesley Cole, Kelly Eurek, Jon Becker, David Bielen, Ilya Chernyakhovskiy, and Stuart Cohen. 2019. *Regional Energy Deployment System (ReEDS) Model Documentation Version 2019*. Golden, CO: National Renewable Energy Laboratory.
- Brown, Patrick R, and Audun Botterud. 2021. "The value of inter-regional coordination and transmission in decarbonizing the US electricity system." *Joule* 5(1): 115-134. <https://doi.org/10.1016/j.joule.2020.11.013>.
- Buongiorno, Jacopo, J M Corradini, John Parsons, and D Petti. 2018. "The future of nuclear energy in a carbon-constrained world: An interdisciplinary MIT Study." *MIT Energy Initiative*.
- Draxl, Caroline, Andrew Clifton, Bri-Mathias Hodge, and Jim McCaa. 2015. *The Wind Integration National Dataset (WIND) Toolkit*. 8. <https://linkinghub.elsevier.com/retrieve/pii/S0306261915004237>.
- . 2020. *Form EIA-860 detailed data with previous form data (EIA-860A/860B)*. June 3. <https://www.eia.gov/electricity/data/eia860/>.
- EIA 2021a. *Form EIA-923 detailed data with previous form data (EIA-906/920)*. June 11. <https://www.eia.gov/electricity/data/eia923/>.
- EIA 2021b. "EIA Annual Energy Outlook 2020 Reference." *EIA*.
- EPA. 2018. *Documentation for EPA's Power Sector Modeling Platform v6 Using the Integrated Planning Model*. Washington DC: U.S. Environmental Protection Agency.
- Gamesa. 2017. G126-2.5 MW. <https://docplayer.net/24040007-Gamesa-g-mw-greater-energy-produced-from-low-wind-sites-minimum-power-density-improved-coe-maximum-profitability.html>.
- He, Guannan, Dharik S. Mallapragada, Abhishek Bose, Clara F. Heuberger, and Emre Gençer. 2021. "Sector coupling via hydrogen to lower the cost of energy system decarbonization." *Energy & Environmental Science* 14: 4635-4646. <https://pubs.rsc.org/en/content/articlelanding/2021/ee/d1ee00627d>.
- Holmgren, William F., Clifford W. Hansen, and Mark A. Mikofski. 2018. *pvlib python: a python package for modeling solar energy systems*. <http://joss.theoj.org/papers/10.21105/joss.00884>.
- Jenkins, J D, R Ponciroli, R Vilim, F Ganda, F de Sisternes, and A Botterud. 2018. "The benefits of nuclear flexibility in power system operations with renewable energy." *Applied Energy* 222: 872-884. <https://doi.org/10.1016/j.apenergy.2018.03.002>.
- Mai, Trieu, Paige Jadun, Jeffrey Logan, Colin McMillan, Matteo Muratori, Daniel Steinberg, Laura Vimmerstedt, Ryan Jones, Benjamin Haley, and Brent Nelson. 2018. *Electrification Futures Study: Scenarios of Electric Technology Adoption and Power Consumption for the United States*. Golden, CO: National Renewable Energy Laboratory.
- McMillan, Colin. 2019. *2018 Industrial Energy Data Book*. November 14. Accessed March 21, 2021. <https://data.nrel.gov/submissions/122>.
- National Renewable Energy Laboratory. 2020. "Electricity Annual Technology Baseline (ATB) Data Download." <https://atb-archive.nrel.gov/electricity/2020/data.php>.
- National Renewable Energy Laboratory. 2021. "NSRDB Data Viewer." <https://maps.nrel.gov/nsrdb-viewer>.
- New York ISO. 2020. *2020 Load & Capacity Data*. Rensselaer, NY: NYISO.
- Oak Ridge National Laboratory. 2020. *Existing Hydropower Assets Plant Dataset, 2020*. Accessed 2020. <https://hydrosource.ornl.gov/dataset/existing-hydropower-assets-plant-dataset-2020>.
- Sepulveda, Nestor A, Jesse D Jenkins, Fernando J de Sisternes, and Richard K Lester. 2018. "The role of firm low-carbon electricity resources in deep decarbonization of power generation." *Joule* 2(11): 2403-2420. <https://doi.org/10.1016/j.joule.2018.08.006>.
- Sunny, Nixon, Niall Mac Dowell, and Nilay Shah. 2020. "What is needed to deliver carbon-neutral heat using hydrogen and CCS?" *Energy & Environmental Science* 13: 4204-4224.



Appendix D – Details of the modeling analysis for developing country markets

This appendix provides additional results and detail about input assumptions for the modeling analysis presented in Chapter 7 of the main report.

D.1 Impact of EV charging demand on bulk power system evolution in the Indian context

In India, electric vehicle (EV) charging is projected to have only a modest impact—compared to air conditioning (AC) demand—on the need for energy storage at the transmission and distribution levels to manage peak demand. This contrasts with the situation in developed-country settings like the United States and Europe, where most of the growth in electricity demand is expected to come from EVs, which will have different impacts on long-term grid evolution. Two-wheelers, being the dominant vehicle type in terms of annual sales in India (Society of India Automobile Manufacturers 2020), are expected to be electrified first, followed by three-wheelers and regular cars (Batra et al. 2018). The Indian government has set a goal of converting 100% of two-wheeler sales and 30% of all vehicle sales to electric by 2030 (Government of India National Institution for Transforming India 2018). Unlike AC use, EV charging also has the potential to offer flexibility to the system in terms of when it is scheduled (Mai et al. 2018). Different EV charging schemes are expected to have different impacts on peak demand, as seen in Figure D.1, and thus different impacts on the

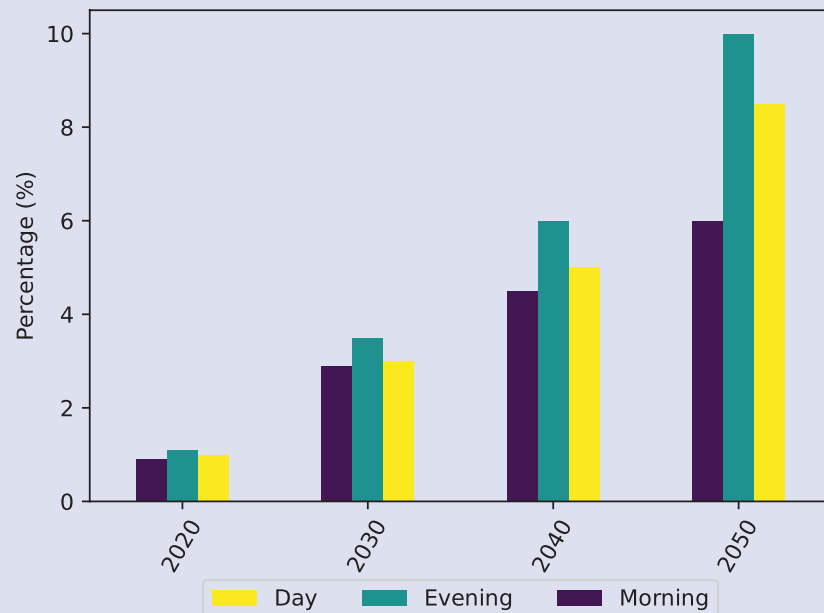
need for grid-scale battery storage. Evening EV charging has been the most adopted charging scheme (von Meier 2018) and is therefore considered in the reference case. EV charging demand during the evening hours can be met via short-duration battery storage charged during daytime hours when solar generation is prevalent. However, Figure D.1 shows that if EV charging demand were to occur in the early morning hours (i.e., 5 AM to 10 AM), deployment of overnight energy storage to discharge in the morning is not cost-effective—instead, coal deployment is favored. The net impact is that morning EV charging schemes favor coal deployment over VRE and storage and result in a 2% higher system average cost of electricity in the three investment periods as well as 3% higher annual CO₂ emissions in 2050. As one might expect, aligning EV charging with periods of high solar irradiation gives rise to more solar with little or no storage and no new coal generation. In this case, the installed capacity of coal is reduced by 2% while solar and wind capacity increases by 2%, resulting in a less than 2% reduction in annual CO₂ emissions.

D.2 Modeling results for India

This section provides additional figures and tables detailing the results of our modeling analysis for India. Where referenced, the CO₂ price is \$20/tonne in 2030, increasing by 5% per year.

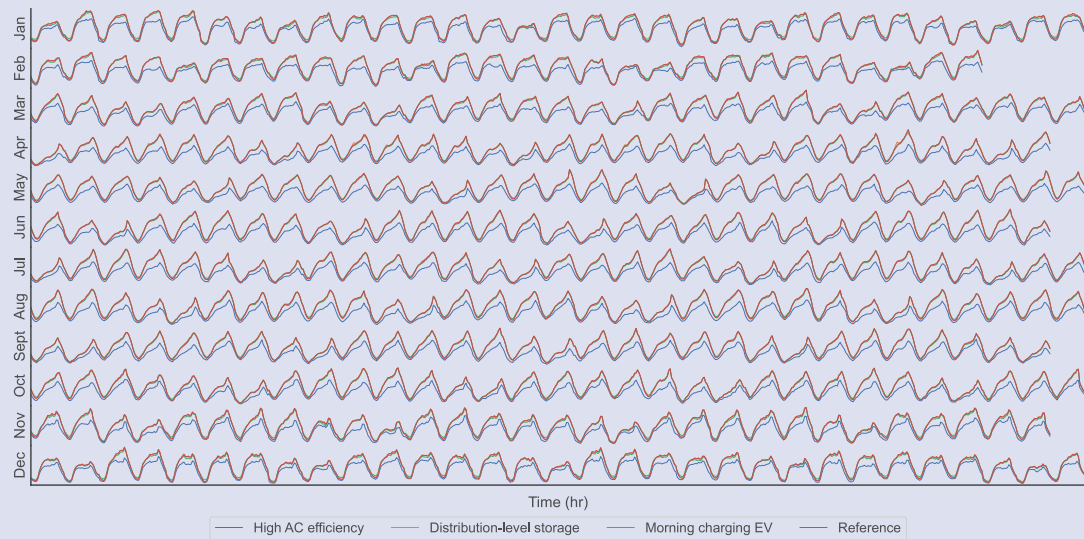
D.2.1 Demand modeling for India

Figure D.1 Electric vehicle charging demand contribution to peak demand



Electric vehicle charging demand contribution to peak demand for the modeled years.
Peak demand hours are between 8 PM and 12 AM.

Figure D.2 Hourly load profile by month in 2040



Hourly load profile by month for the reference case and for cases described in the text of high AC efficiency, distribution-level storage, and morning charging EV. Note that the distribution-level storage impact is almost unobservable in the figure.

D.2.2 Distribution-level storage analysis for Indian megacities

Table D.1 Distribution-level storage cost assumptions and wires upgrade cost for new line and reconductoring of existing lines

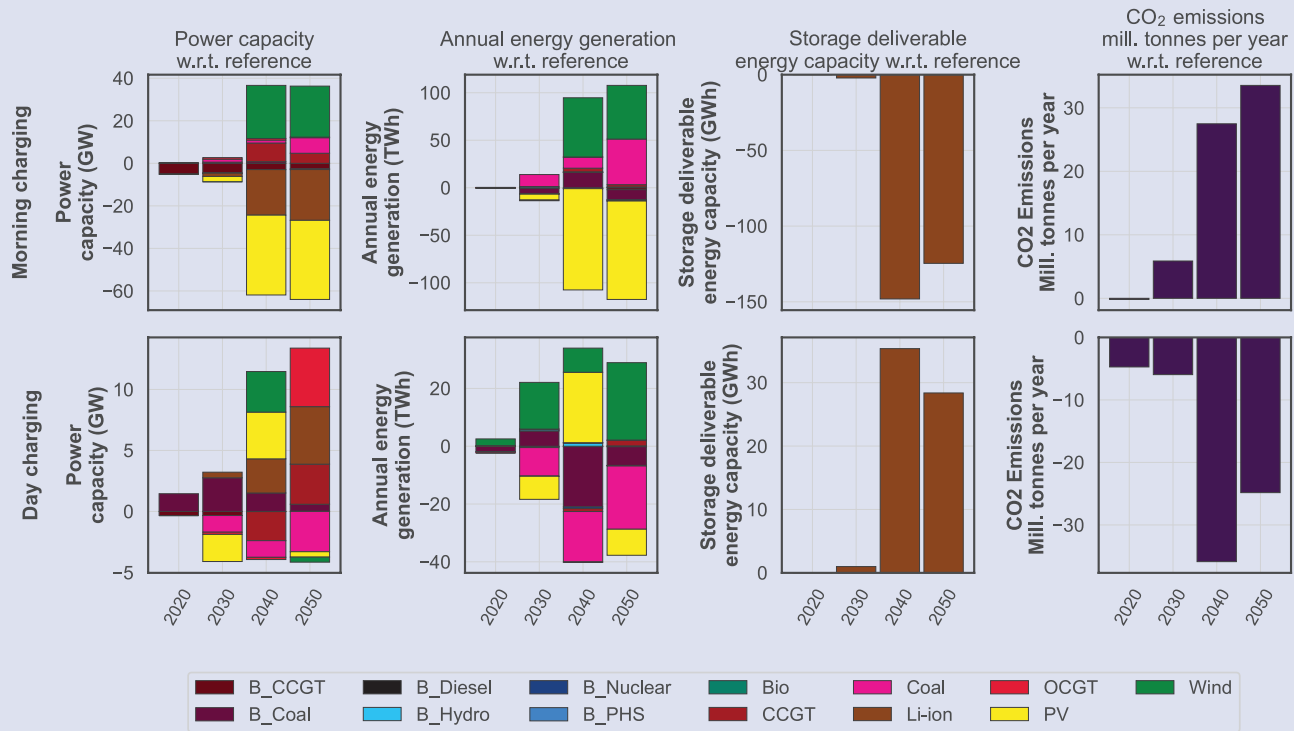
| | 2030 | 2040 |
|-------------------------------|---------|---------|
| Energy cost (\$/kWh) | 168 | 147 |
| Power cost (\$/kW) | 146 | 128 |
| Battery O&M cost (\$/kW-year) | 20 | 18 |
| Charge cost (\$/MWh) | 55 | 55 |
| New line (\$/km) | 350,000 | 350,000 |
| Reconductoring (\$/km) | 650,000 | 650,000 |

Table D.2 Distribution-level storage system cost of electricity comparison at transmission level using system cost of electricity calculation

| | Reference case | | Reference SCOE |
|------|-----------------------|---------|--------------------------|
| | DLS SCOE | DLS COE | |
| 2030 | 26.7 | 0.4 | 26.8 |
| 2040 | 21.1 | 0.5 | 20.9 |
| | Low-cost storage case | | Low-cost storage SCOE |
| | DLS SCOE | DLS COE | |
| 2030 | 26.5 | 0.4 | 26.4 |
| 2040 | 17.7 | 0.5 | 18 |

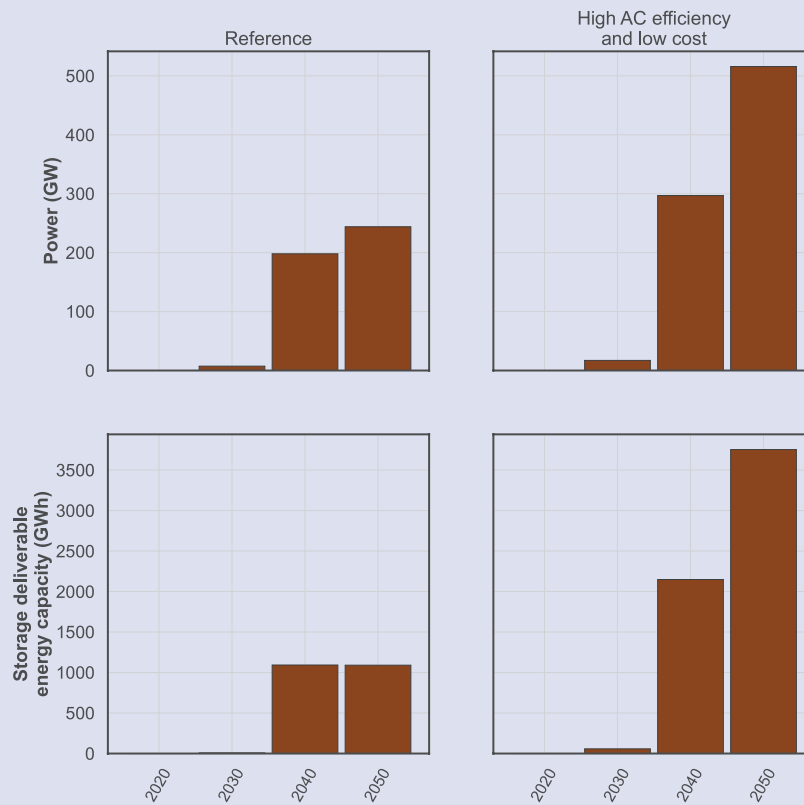
D.2.3 Bulk power system analysis for India

Figure D.3 Charging schemes comparison



Morning (top) and day (bottom) charging schemes compared to evening charging scheme reference scenario. Morning charging occurs in the early hours of the morning, day charging is aligned with peak solar capacity factor hours. Evening charging (i.e., most charging occurs in the evening hours of the day) is used in the reference case.

Figure D.4 Storage power and energy capacity



Storage power and energy capacity in the reference and high-AC-efficiency/low-cost cases.

Figure D.5 Technology impact on emissions intensity and transmission expansion

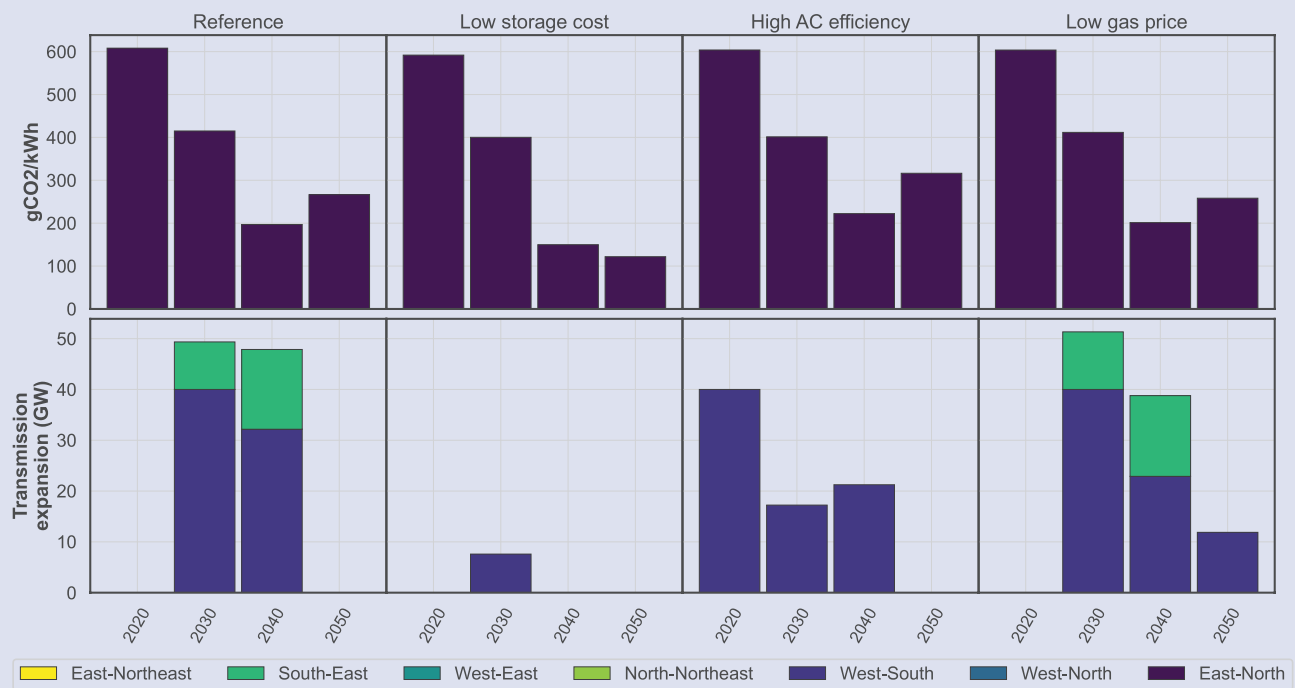


Figure D.6 Technology capacity factors across scenarios over modeling periods

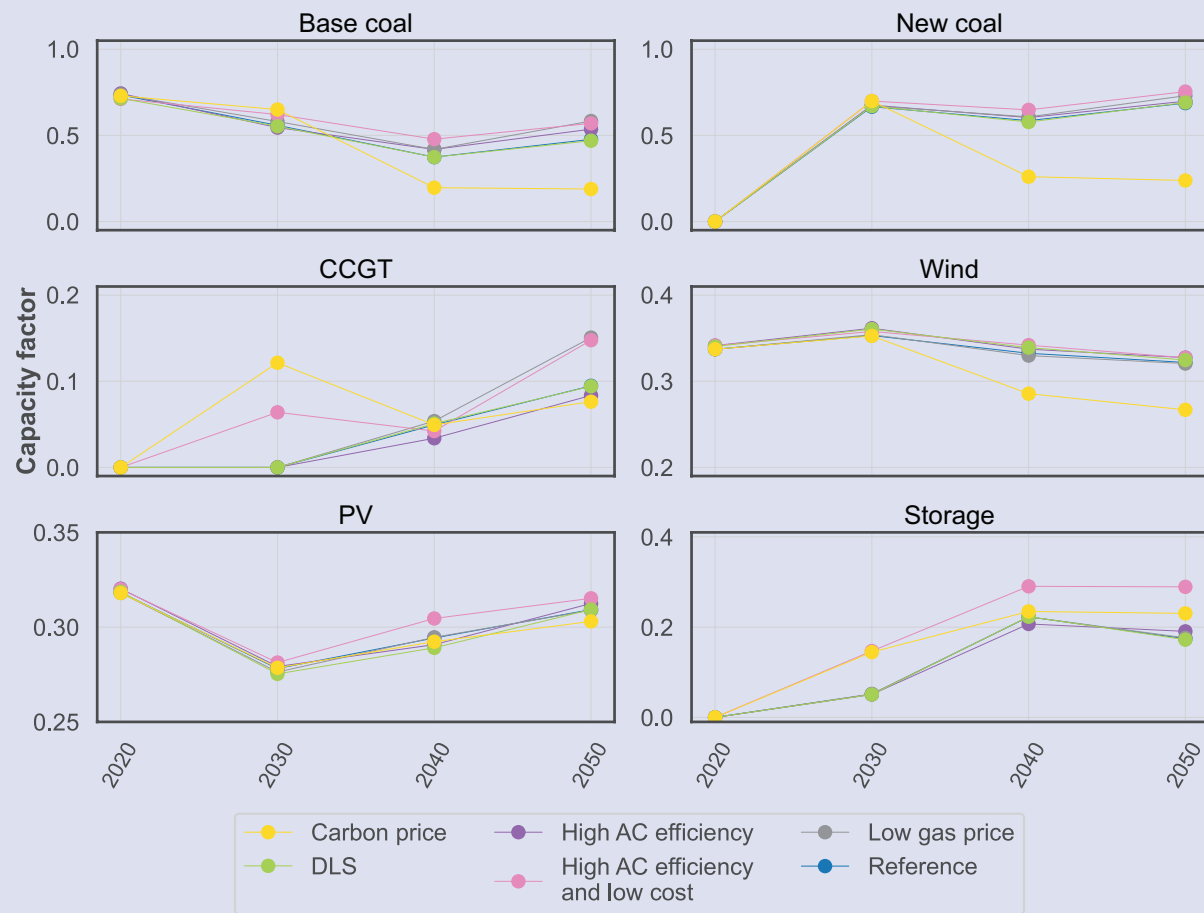
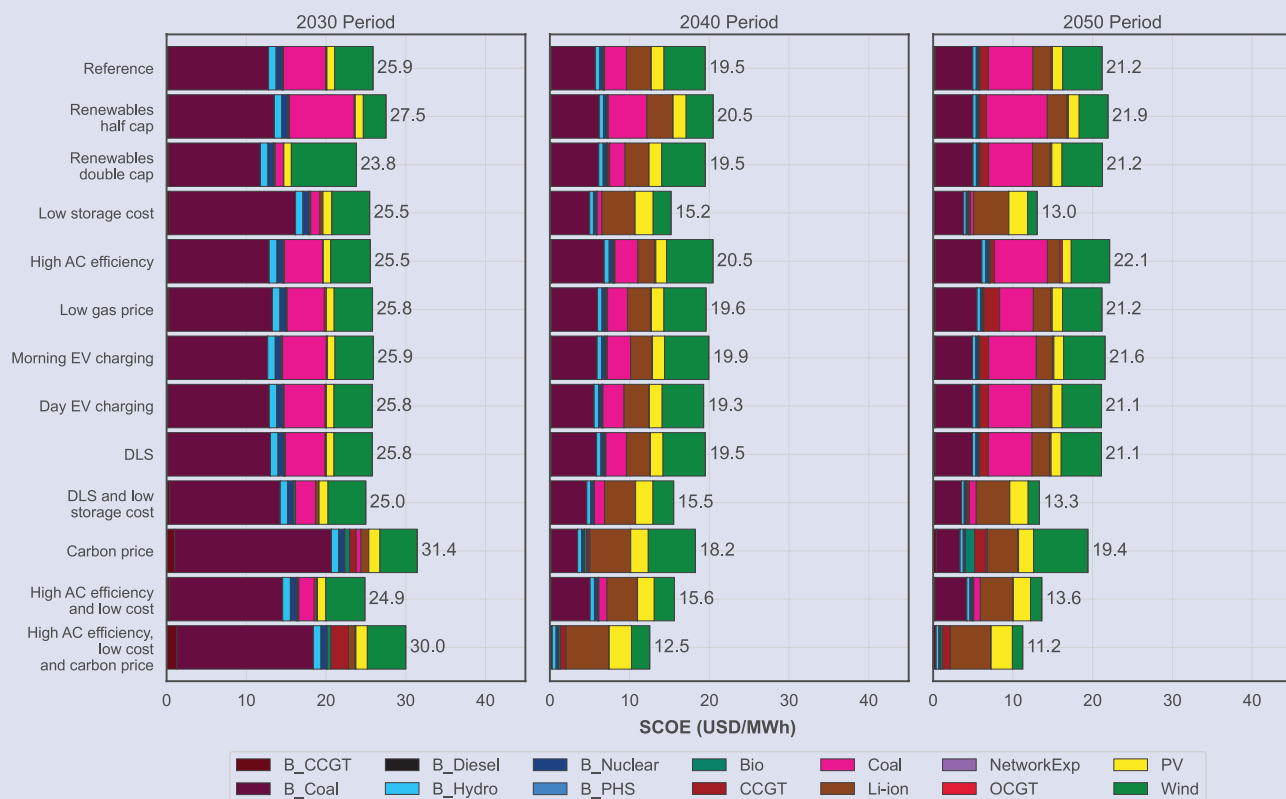
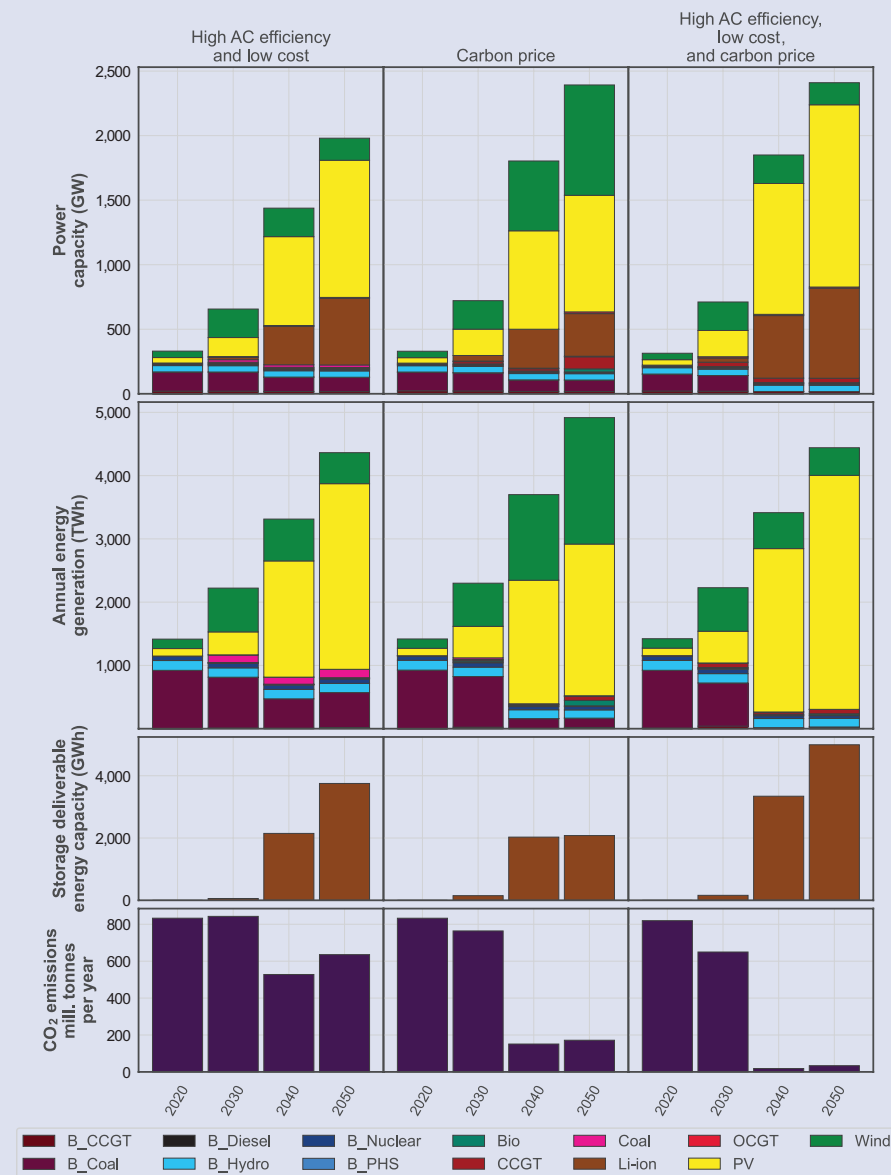


Figure D.7 System average cost of electricity (SCOE)



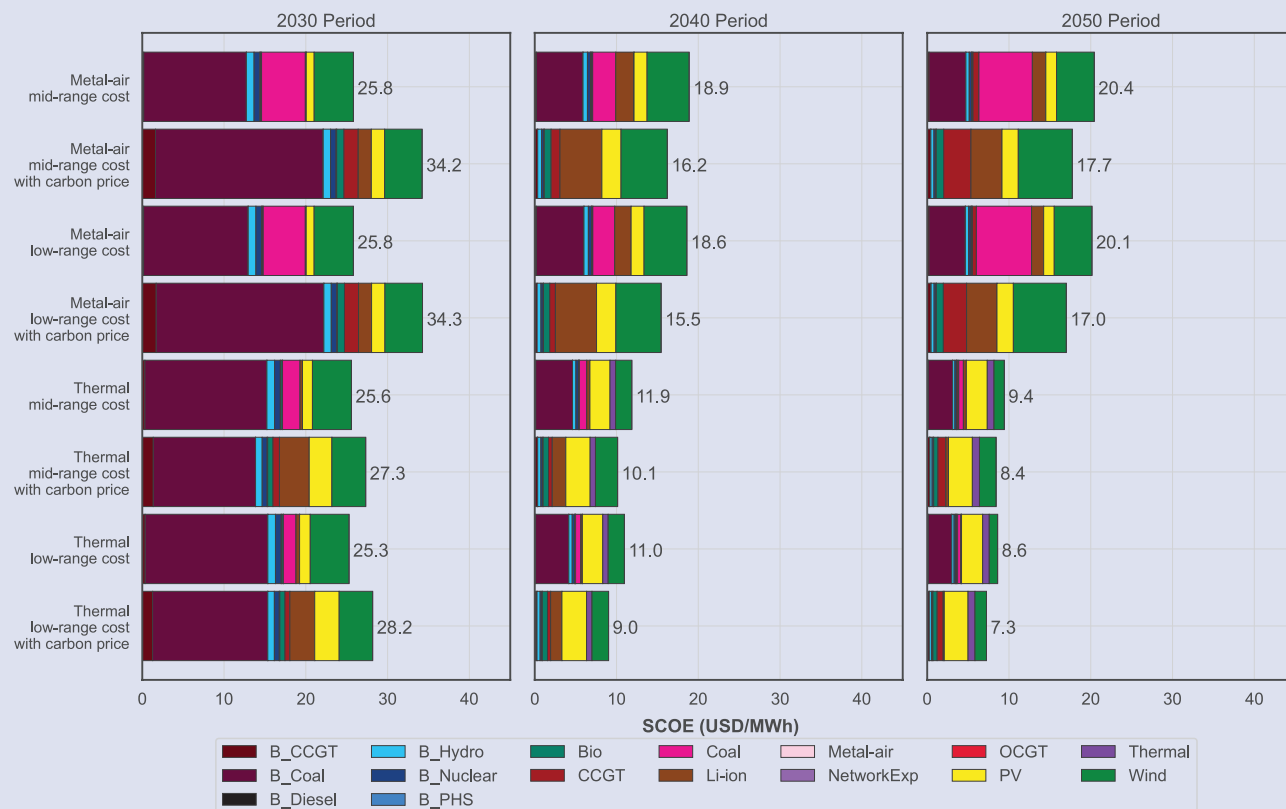
System average cost of electricity (SCOE) per modeling period for a range of cases evaluated in the study (Barbar, Mallapragada and Stoner 2021).

Figure D.8 Model outcomes for high-AC-efficiency/low-cost case



Model outcomes for high-AC-efficiency/low-cost case, defined by low battery storage capital cost, high AC efficiency, and low gas price (1st column), as well as impact of carbon price with and without scenario assumptions. Model outcomes include installed capacity (1st row), generation (2nd row), energy storage capacity (3rd row), and annual CO₂ emissions (4th row). Columns 2–4 highlight outcomes for the following cases: (a) high-AC-efficiency/low-cost case (2nd column); (b) carbon price case, where CO₂ price starts at \$20 per metric ton in 2030 and increases by 5% each year (3rd column); and (c) high-AC-efficiency/low-cost + carbon price scenario (4th column). Resource labels in legend where “B” prefix refers to existing capacity at the beginning of the model horizon in 2020.

Figure D.9 System average cost of electricity (SCOE) for long-duration energy storage (LDES) cases



System average cost of electricity (SCOE) by modeling period for LDES cases evaluated in the study (Barbar, Mallapragada and Stoner 2021).

Table D.3 List of technology names and corresponding abbreviations

| Technology | Abbreviation |
|--|--------------|
| Existing combined cycle gas turbine generation | B_CCGT |
| Existing coal generation | B_Coal |
| Existing diesel generation | B_Diesel |
| Existing hydro generation | B_Hydro |
| Existing nuclear generation | B_Nuclear |
| Existing pumped hydro storage generation | B_PHS |
| New biomass generation | Bio |
| New combined cycle gas turbine generation | CCGT |
| New coal generation | Coal |
| New lithium-ion battery storage power | Li-ion |
| New open cycle gas turbine generation | OCGT |
| New solar generation | PV |
| New wind generation | Wind |
| Network expansion | NetworkExp |

Table D.4 Capital cost assumptions for various resources

| Resource & units | Scenario | Capital costs for each model year | | |
|--|-----------|-----------------------------------|------|------|
| | | 2030 | 2040 | 2050 |
| PV (\$/kW AC) | Reference | 558 | 407 | 369 |
| Wind (\$/kW AC) | Reference | 995 | 843 | 754 |
| Li-ion storage - energy (\$/kWh) | Reference | 168 | 147 | 126 |
| | Low cost | 116 | 94 | 71 |
| Li-ion storage - power (\$/kW AC) | Reference | 146 | 128 | 110 |
| | Low cost | 101 | 82 | 62 |
| CCGT (\$/kW) | Reference | 706 | 675 | 655 |
| OCGT (\$/kW) | Reference | 647 | 616 | 598 |
| Nuclear (\$/kW) | Reference | 2,800 | | |
| Coal (\$/kW) | Reference | 1,200 | | |
| Biomass (\$/kW) | Reference | 864 | | |
| Inter-regional transmission (\$/MW-km) | Reference | 312 | | |

All costs in 2018 dollars, unless otherwise noted. Solar costs assume direct current (DC) to alternating current (AC) ratio of 1.34 (Rose et al. 2020).

Table D.5 Storage duration comparison

| | Reference | Low storage cost | High AC efficiency | Low gas price | High AC efficiency-low cost |
|------|-----------|------------------|--------------------|---------------|-----------------------------|
| 2040 | 4.5 | 5.4 | 4.4 | 4.6 | 6.8 |
| 2050 | 3.7 | 5.5 | 3.7 | 3.6 | 6.2 |

Comparison of storage duration (where storage duration is storage deliverable energy capacity divided by storage power) across scenarios and modeled periods.

Table D.6 Thermal generation power capacity in India

| Resource | 2020 capacity (MW) | Minimum retirement (MW) | | | VOM (\$/MWh) | FOM (\$/kW/y) | Heat rate (MMBtu/MWh) | Max cap MW |
|----------------|--------------------|-------------------------|--------|--------|--------------|---------------|-----------------------|------------|
| | | 2030 | 2040 | 2050 | | | | |
| Coal | | | | | | | | |
| North | 41,220 | 3,919 | 11,755 | 13,588 | 1.0 | 55.1 | 10.0 | |
| West | 87,431 | 5,812 | 28,890 | 37,398 | 0.9 | 55.1 | 9.1 | |
| South | 40,965 | 5,150 | 10,868 | 16,368 | 1.1 | 55.1 | 10.6 | |
| East | 39,080 | 4,010 | 5,295 | 5,895 | 0.9 | 55.0 | 10.5 | |
| CCGT | | | | | | | | |
| Northeast | 750 | 0 | 0 | 250 | 1.0 | 55.0 | 9.8 | |
| North | 5,752 | 179 | 685 | 910 | 1.2 | 9.4 | 7.8 | |
| West | 10,239 | 870 | 2,686 | 3,022 | 1.5 | 12.0 | 6.9 | |
| South | 6,505 | 1,147 | 1,948 | 2,115 | 1.4 | 11.0 | 6.2 | |
| Nuclear | | | | | | | | |
| Northeast | 1,306 | 19 | 351 | 390 | 1.9 | 10.8 | 7.7 | |
| North | 1,720 | | | | | | | |
| West | 3,240 | | | | | | | |
| South | 3,820 | | | | | | | |
| North | 2,431 | | | | | | | 9,721 |
| West | 678.75 | | | | | | | 6,835 |
| South | 2,934 | | | | | | | 5,336 |
| East | 463 | | | | | | | 1,906 |
| Biomass | | | | | | | | |
| Northeast | 0 | | | | | | | 274 |

Thermal generation (coal, gas, nuclear, biomass) power capacity for different regions of India with projected minimum retirement for the modeled periods, variable and fixed operational costs, heat rate (if applicable), and maximum capacity (if applicable).

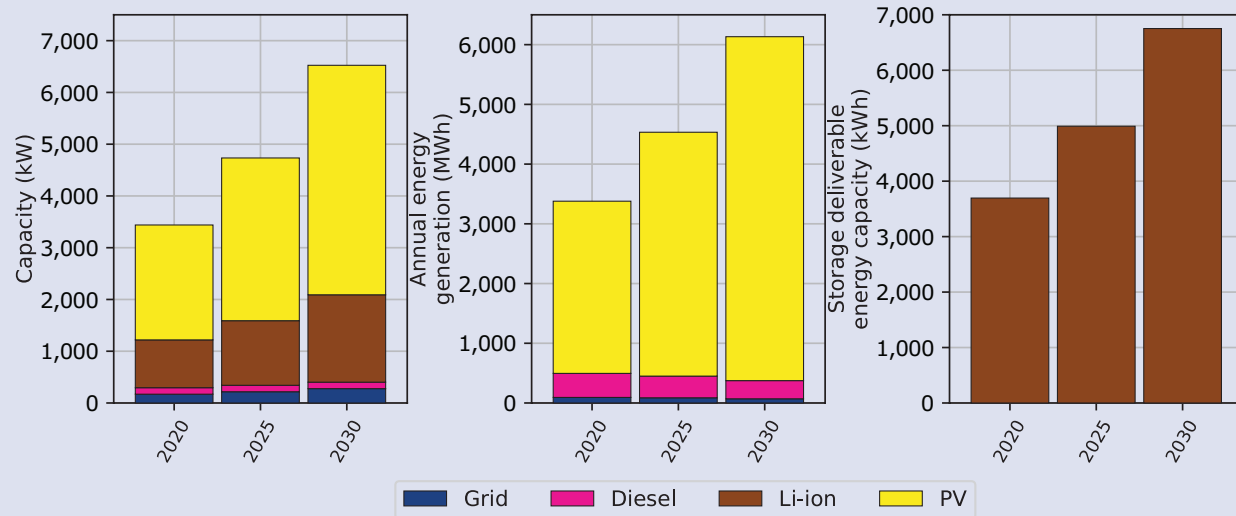
Table D.7 Input parameters for thermal generation for existing and new assets

| Resource | Fuel | VOM (\$/MWh) | FOM (\$/kW/y) | Start cost (\$/MW) | Start fuel (MMBtu per MW) | Heat rate (MMBtu per MWh) | Min. up time (hours) | Min. down time (hours) | Flexibility (% nameplate capacity) | | Min. stable power | Max. power output | Avg plant size (cap size, MW) | Lifetime |
|----------|-------------|-----------------|------------------|-----------------------|------------------------------|------------------------------|-------------------------------|---------------------------------|--|--------------|-------------------------|-------------------------|--|----------|
| | | | | | | | | | Ramp up | Ramp down | | | | |
| Coal | Coal | | | 236.8 | 0.0 | | 24 | 24 | 60% | 60% | 55% | 90% | | 30 |
| CCGT | Natural gas | | | 106.5 | 0.0 | | 8 | 8 | 100% | 100% | 50% | 90% | | 30 |
| Nuclear | Uranium | 0.6 | 75 | 1,000.0 | | 10.1 | 36 | 36 | 0 | 0 | 90% | 90% | 1,000 | 40 |
| Biomass | Biomass | 0.0 | 37.879 | | | 16.7 | 24 | 24 | 60% | 60% | 55% | 90% | 1.00 | 20 |
| New Coal | Coal | 0.9 | 30 | 214 | 0 | 9.5 | 24 | 24 | 60% | 60% | 45% | 90% | 620 | 30 |
| New CCGT | Natural gas | 1.5 | 10 | 107 | 0 | 6.6 | 8 | 8 | 100% | 100% | 33% | 90% | 573.00 | 30 |
| New OCGT | Natural gas | 7 | 11 | 96 | | 9.1 | 2 | 2 | 100% | 100% | 26% | 90% | 384 | 30 |
| Backup | Diesel | | 0 | 0 | 0 | 10.90047 | 0 | 0 | 100% | 100% | 0 | 90% | | |

Input parameters for thermal generation (coal, gas, nuclear, biomass) for existing and new assets. Relevant optimization parameters (cost, technical) are listed in column headers.

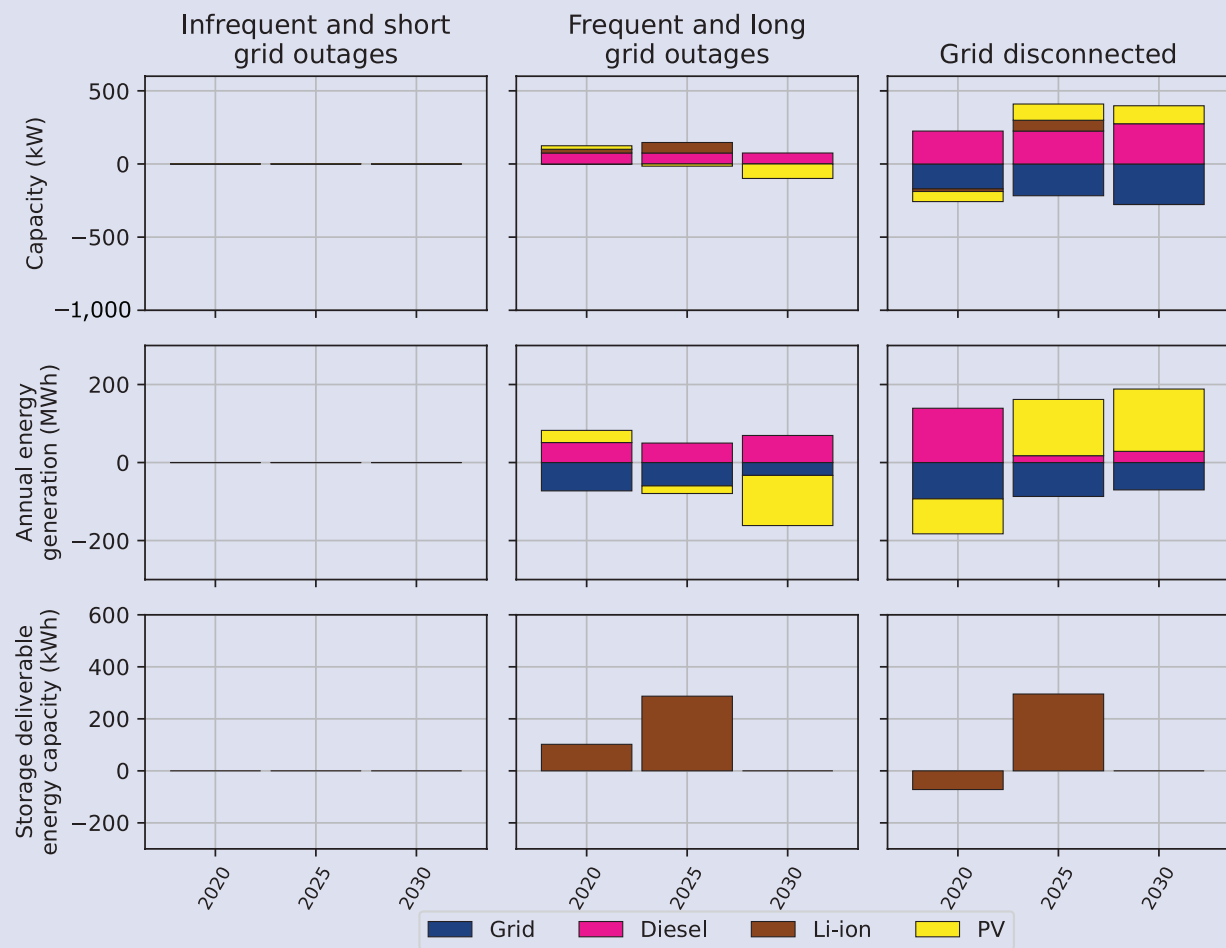
D.3 Analysis of supply-constrained minigrids in Abuja, Nigeria

Figure D.10 Results for 2020 minigrid design



Results for 2020 minigrid design without any simulated grid outages with low-range solar and storage cost assumptions (National Renewable Energy Laboratory 2020) and with full grid connection (see Tables D.8 and D.9).

Figure D.11 Low storage cost minigrid design compared to reference case



Low storage cost minigrid design compared to reference case under infrequent outages (1st column), frequent outages (2nd column), and no grid connection (3rd column). See Tables D.8, D.9, and D.10 for input assumptions.

Table D.8 Capital cost assumptions for various resources

| Resource & units | Scenario | Capital costs for each model year | | |
|-----------------------------------|-----------|-----------------------------------|-------|------|
| | | 2020 | 2025 | 2030 |
| PV (\$/kW AC) | Reference | 1,354 | 1,095 | 836 |
| Li-ion storage – energy (\$/kWh) | Reference | 299 | 206 | 168 |
| | Low cost | 247 | 160 | 116 |
| Li-ion storage – power (\$/kW AC) | Reference | 260 | 179 | 146 |
| | Low cost | 215 | 139 | 101 |
| Diesel generator (\$/kW) | Reference | 400 | 400 | 400 |
| Grid connection (\$/kW) | Reference | — | — | — |

Capital cost assumptions for various resources. All costs in 2018 dollars, unless otherwise noted. Solar costs assume DC to AC ratio of 1.34 (Rose et al. 2020; Ciller et al. 2019).

Table D.9 Operation and maintenance cost assumptions for various resources

| Resource & units | Scenario | Operation and maintenance costs for each model year | | |
|--|-----------|---|-------|-------|
| | | 2020 | 2025 | 2030 |
| PV (\$/kW-year AC) | Reference | 16 | 13 | 10 |
| Li-ion storage – energy (\$/kWh-year) | Reference | 36 | 25 | 20 |
| | Low cost | 30 | 20 | 14 |
| Diesel generator (\$/kW-year) | Reference | 100 | 100 | 100 |
| Diesel fuel cost (\$/gal) ¹ | Reference | 2.2 | 2.2 | 2.2 |
| Grid end-use tariff (\$/kWh) | Reference | 0.031 | 0.033 | 0.038 |
| Grid distribution tariff (\$/kWh) | Reference | 0.15 | 0.2 | 0.27 |

Operation and maintenance cost assumptions for various resources. All costs in 2018 dollars, unless otherwise noted. Solar costs assume DC to AC ratio of 1.34 (Rose et al. 2020; Ciller et al. 2019; Abuja Electric Distribution Company 2019).

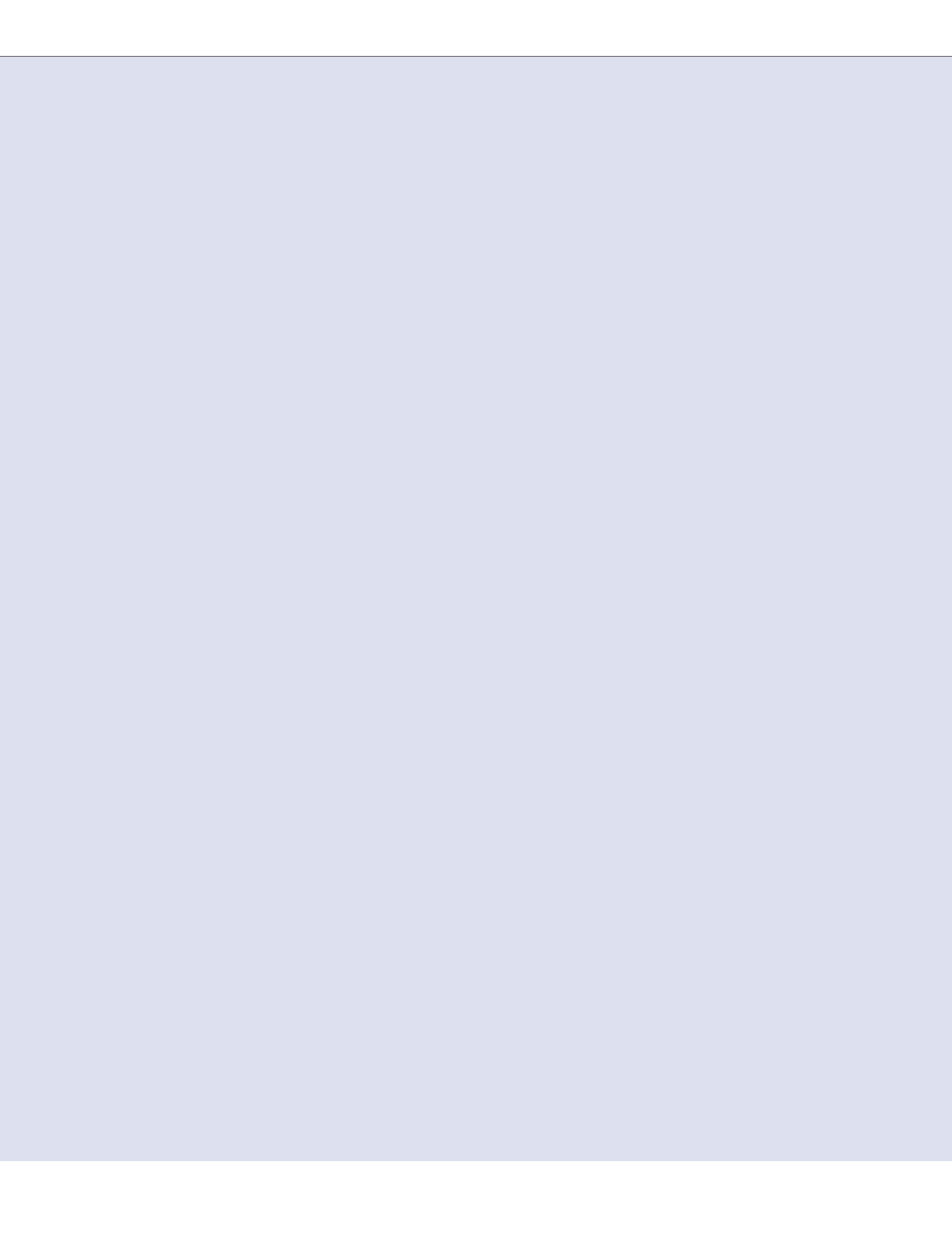
¹ Diesel generator heat rate is fixed to 0.85 gallons per hour per kW.

Table D.10 Assumed ranges for the frequency and duration of outages for simulated cases based on discussion with Abuja Electric Distribution Company

| | | 2020 | 2025 | 2030 |
|---------------------------|----------------------|---------|--------|------|
| Frequent, long outages | Frequency (per year) | 100–200 | 50–100 | 0 |
| | Duration (hours) | 24–12 | 12–6 | 0 |
| Infrequent, short outages | Frequency (per year) | 50–100 | 0–50 | 0 |
| | Duration (hours) | 6–3 | 3–0 | 0 |

References

- Abuja Electric Distribution Company. 2019. *Wuse market energy audit report*. Tech. rep., Abuja Electric Distribution Company.
- Barbar, Marc, Dharik S. Mallapragada, and Robert Stoner. 2022. “Impact of demand growth on decarbonizing India’s electricity sector and the role for energy storage.”
- Batra, Rakesh, Somesh Kumar, Shuvendu Bose, Regan Grant, Kany Garg, Shikhar Gupta, Randall J. Miller, et al. 2018. *Standing up India’s EV ecosystem – who will drive the charge?* Ernest and Young.
- Ciller, Pedro and Ellman, Douglas and Vergara, Claudio and González-García, Andrés and Lee, Stephen J. and Drouin, Cailinn and Brusnahan, Matthew and Borofsky, Yael and Mateo, Carlos and Amatya, Reja and Palacios, Rafael and Stoner, Robert and de Cuadra, Fernando and Pérez-Arriaga, Ignacio. “Optimal Electrification Planning Incorporating On- and Off-Grid Technologies: The Reference Electrification Model (REM)”. Proceedings of the IEEE, vol. 107, no. 9, pp. 1872-1905, Sept. 2019, doi: 10.1109/JPROC.2019.2922543.
- Government of India National Institution for Transforming India. 2018. “Zero emission vehicles: towards a policy framework.”
- Mai, Trieu, Paige Jadun, Jeffrey Logan, Colin McMillan, Matteo Muratori, Daniel Steinberg, and Laura Vimmerstedt. 2018. “Electrification Futures Study: Scenarios of Electric Technology Adoption and Power Consumption for the United States.” Tech. rep., National Renewable Energy Laboratory, Golden, CO. <https://www.nrel.gov/docs/fy18osti/71500.pdf>.
- National Renewable Energy Laboratory. 2020. “Annual Technology Baseline: Electricity.” *Annual Technology Baseline: Electricity*. <https://atb.nrel.gov/electricity/2020/data.php>.
- Rose, Amy, Ilya Chernyakhovskiy, David Palchak, Sam Koebrich, and Mohit Joshi. 2020. “Least-Cost Pathways for India’s Electric Power Sector.” Tech. rep., National Renewable Energy Laboratory, Golden, CO. <https://www.nrel.gov/docs/fy20osti/76153.pdf>.
- Society of India Automobile Manufacturers. 2020. “Automobile domestic sales trends 2015-2020.” SIAM.
- von Meier, Alexandra. 2018. “EV infrastructure planning and grid impact assessment: a case for Mexico.” unpublished.



Acronyms and abbreviations

| | | | |
|--------|---|-------------------|--|
| A-CAES | adiabatic compressed air energy storage | EHS | environmental, health, and safety |
| AC | air conditioning | EIA | U.S. Energy Information Administration |
| ACES | Advanced Clean Energy Storage Project | ELCC | effective load carrying capability |
| AEDC | Abuja Electric Distribution Company (Nigeria) | EMDE | emerging market and developing economy |
| AQDS | 9,10-anthraquinone-2,7-disulfonic acid | ERCOT | Electric Reliability Council of Texas |
| ARES | advanced rail energy storage | ESG | environment, social, and governance |
| ATB | Annual Technology Baseline (NREL) | EV | electric vehicle |
| BMS | battery management system | Fe-Cr | iron-chromium |
| BTM | behind-the-meter | FERC | Federal Energy Regulatory Commission |
| C&I | commercial and industrial | FOM | fixed operation and maintenance costs |
| CAES | compressed air energy storage | GES | gravitational energy storage |
| CAGR | compound annual growth rate | GHG | greenhouse gas |
| CAISO | California Independent System Operator | GPS | geomechanical pumped storage |
| CapEx | capital expenditures | GWh | gigawatt-hours |
| CCGTs | combined cycle gas turbines | GW | gigawatts |
| CCS | carbon capture and sequestration | INPO | Institute of Nuclear Operations |
| CEA | Central Electricity Authority (India) | ISO | independent system operator |
| CEM | capacity expansion model | ISO-NE | Independent System Operator, New England |
| CEM | cation-ion exchange membrane (chapter 2) | kW | kilowatts |
| CF | capacity factor | kWh | kilowatt-hours |
| COP | coefficient of performance | kWh _e | kilowatt-hours electric |
| CP | coincident peak | kWh _{th} | kilowatt-hours thermal |
| CPUC | California Public Utility Commission | LAES | liquid air energy storage |
| CSP | Concentrated solar power | LCO | lithium cobalt oxide |
| D-CAES | diabatic compressed air energy storage | LCOE | levelized cost of energy |
| DER | distributed energy resource | LCOS | levelized cost of storage |
| DESSA | Distributed Energy Solutions and Strategy for AEDC | LDES | long-duration energy storage |
| DLS | distribution-level storage | LFP | lithium iron phosphate |
| DOE | Department of Energy | Li-ion | lithium-ion |
| DUoS | distributed use of system | LMO | lithium manganese oxide |
| EFS | enhanced flexibility scenario | LNMO | lithium nickel manganese oxide |
| eGRID | Emissions & Generation Resource Integrated Database | LOHCs | liquid organic hydrogen carriers |
| | | LTO | lithium titanium oxide |
| | | MCMC | Markov chain Monte Carlo (method) |
| | | MISO | Midcontinent Independent System Operator |

| | | | |
|-------|---|-------|--|
| MMBtu | metric million British thermal unit | PCM | phase-change material |
| MMT | million metric tons | PEM | proton exchange membrane |
| MW | megawatts | PFSA | perfluorosulfonic acid |
| MWh | megawatt-hours | PHS | pumped hydro storage |
| NCA | lithium nickel cobalt aluminum oxide | PJM | Pennsylvania-New Jersey-Maryland Interconnection |
| NCM | lithium nickel cobalt manganese oxide | PSH | pumped storage hydropower |
| NDRC | National Development and Reform Commission | PV | photovoltaic |
| NG | natural gas | R&D | research and development |
| NiCd | nickel-cadmium | RFB | redox flow battery |
| NiMH | nickel metal hydride | RTE | round-trip efficiency |
| NiOOH | nickel oxide hydroxide | RTO | regional transmission organization |
| NMC | nickel, manganese, and cobalt (composition for lithium-ion batteries) | SCOE | system average cost of electricity |
| NMO | nickel manganese oxide | SEER | seasonal energy efficiency ratio |
| NOx | nitrogen oxides | SGCC | State Grid Corporation of China |
| NREL | National Renewable Energy Laboratory | SMR | steam methane reforming |
| NSRDB | National Solar Radiation Database | SMUD | Sacramento Municipal Utilities District |
| NTP | sodium titanium phosphate | SPP | Southwest Power Pool |
| NWA | non-wires alternative | TES | thermal energy storage |
| NYISO | New York Independent System Operator | TPV | thermophotovoltaic |
| O&M | operations and maintenance | TRL | technology readiness level |
| OCGT | open cycle gas turbine | TW | terawatts |
| OEMs | original equipment manufacturers | TWh | terawatt-hours |
| P2-MN | P2-type sodium manganese nickel oxide | VOM | variable operation and maintenance costs |
| | | VRE | variable renewable energy |
| | | VRFB | vanadium redox flow batteries |
| | | VoLL | value of lost load |
| | | Zn-Br | zinc-bromine |

List of figures

| | |
|---|-------|
| Figure ES.1 Three groups of storage technologies based on power- and energy-capacity costs | xii |
| Figure ES.2 Illustration of cross-sector (power-industry) coupling of hydrogen | xvi |
| Figure ES.3 Annual generation relative to demand | xviii |
| Figure ES.4 Hourly marginal wholesale price of energy for Texas | xix |
| Figure ES.5 Impact of Li-ion storage cost projections on cost-optimal bulk power system evolution in India | xx |
| Figure 1.1 U.S. and global installed capacity of (a) solar and (b) wind generation | 2 |
| Figure 1.2 Installed cost of solar and wind generation in the United States as a function of time | 3 |
| Figure 1.3 Global Li-ion battery prices for 2010–2021 | 4 |
| Figure 1.4 Global deployment of Li-ion batteries over the period 2011–2021 for electric vehicles and energy storage in the electricity sector | 5 |
| Figure 1.5 Daily variability of wind and solar resources in Texas | 7 |
| Figure 1.6 Three groups of storage technologies based on power- and energy-capacity costs | 10 |
| Figure 2.1 Categories of electrochemical storage technologies | 16 |
| Figure 2.2 The chemical cost of stored energy for battery electrochemistries | 17 |
| Figure 2.3 Schematic of a Li-ion battery cell | 20 |
| Figure 2.4 Cost breakdown | 22 |
| Figure 2.5 Historical increases and decreases | 24 |
| Figure 2.6 Projected growth in Li-ion battery manufacturing capacity and demand worldwide from 2020 to 2030 | 26 |
| Figure 2.7 Schematic diagram of an RFB | 28 |
| Figure 2.8 History of metal-air battery development and schematic design of a typical metal-air battery cell | 35 |
| Figure 2.9 Static metrics of resource use | 46 |
| Figure 2.10 Lithium CAGR for Li-NMC deployment through 2050 | 49 |
| Figure 2.11 Cobalt CAGR for Li-NMC deployment through 2050 | 50 |
| Figure 2.12 Nickel CAGR for Li-NMC deployment through 2050 | 51 |
| Figure 2.13 Vanadium CAGR for VFB deployment through 2050 | 52 |
| Figure 3.1 Growth of pumped storage capacity by region | 71 |
| Figure 3.2 Capital cost per kW | 77 |
| Figure 3.3 Capital cost per kWh | 78 |
| Figure 3.4 A model of the Energy Vault technology | 86 |
| Figure 3.5 Flowsheet of a conventional diabatic CAES system with two combustors | 89 |
| Figure 3.6 Flowsheet of a diabatic CAES system with a recuperator | 89 |
| Figure 3.7 Flowsheet of a conventional adiabatic CAES system with two compression and two expansion stages | 92 |
| Figure 3.8 Mechanical and thermal exergy of compressed air | 93 |
| Figure 3.9 Typical ranges of energy density | 95 |
| Figure 3.10 Illustrations of underground formations to store compressed air | 96 |
| Figure 3.11 Regions of the United States favorable for CAES | 97 |
| Figure 3.12 Surface reservoir provides pressure to enable air extraction at constant pressure | 99 |
| Figure 4.1 Energy losses in a thermal energy storage system | 114 |
| Figure 4.2 Charging coefficient of performance (COP) | 116 |

| | | |
|-------------|--|-----|
| Figure 4.3 | Classification of thermal storage materials | 118 |
| Figure 4.4 | Latent heat materials | 121 |
| Figure 4.5 | Material temperature vs. storage cost | 122 |
| Figure 4.6 | Approximate efficiencies of heat-to-electricity technologies plotted against Carnot efficiency | 123 |
| Figure 4.7 | Images of heat-to-power technologies | 128 |
| Figure 4.8 | Schematic for steam turbine retrofit with TES | 130 |
| Figure 4.9 | Age distribution of U.S. steam turbine capacity | 131 |
| Figure 4.10 | Geographic distribution of steam turbine capacity in the United States | 131 |
| Figure 4.11 | Steam turbine capacity for plants that will be 50 years old or less in 2050 for top-ten countries and the rest of the world (RoW) | 132 |
| Figure 4.12 | Diagram of recuperated, closed Brayton power cycle | 134 |
| Figure 4.13 | A sample of high-temperature TES systems with different designs | 135 |
| Figure 5.1 | Representation of alkaline electrolyzer reaction | 149 |
| Figure 5.2 | Representation of PEM electrolyzer | 150 |
| Figure 5.3 | A pressurized hydrogen storage tank | 151 |
| Figure 5.4 | Salt deposits in the United States | 152 |
| Figure 5.5 | Stylized representation of underground salt cavern | 152 |
| Figure 5.6 | Rendition of a PEM fuel cell | 154 |
| Figure 5.7 | Stylized chemical energy storage system | 154 |
| Figure 5.8 | Forecast capital costs for alkaline and PEM electrolyzers | 156 |
| Figure 5.9 | Modeled cost of hydrogen produced via electrolysis in 2021 | 157 |
| Figure 5.10 | Cost breakdown by variable | 158 |
| Figure 5.11 | Forecast 2050 hydrogen production costs | 159 |
| Figure 5.12 | Modeled 2020 cost of power produced from hydrogen-fueled power generator vs. capacity factor of plant | 164 |
| Figure 5.13 | 2020 modeled cost of power produced from hydrogen-fueled generator vs. hydrogen price at plant's gate | 164 |
| Figure 5.14 | 2050 forecast cost of power produced by technology vs. capacity factor | 165 |
| Figure 5.15 | Forecast cost of power produced by technology vs. price of hydrogen at plant gate | 165 |
| Figure 5.16 | Histogram of 2019 day-ahead hourly electricity prices in the Los Angeles area | 166 |
| Figure 6.1 | Example electricity demand in New York State in select hours in January 2050 | 184 |
| Figure 6.2 | Summary of regional modeling features and differences across the Northeast, Southeast, and Texas | 185 |
| Figure 6.3 | Installed capacities in the Northeast (NE), Southeast (SE), and Texas (TX) under tightening CO ₂ emissions constraints | 186 |
| Figure 6.4 | Annual generation, VRE curtailment, and system average cost of electricity (SCOE) in the Northeast (NE), Southeast (SE), and Texas (TX) under tightening CO ₂ emissions constraints | 187 |
| Figure 6.5 | System impacts of varying levels of electrification in the Northeast and Texas | 191 |
| Figure 6.6 | System impacts of nuclear availability in the Southeast | 193 |
| Figure 6.7 | Classes of energy storage technologies, grouped by discharge power and storage overnight capital costs | 194 |
| Figure 6.8 | System impacts of adding RFB storage for the Northeast and Texas | 195 |
| Figure 6.9 | Impacts of adding RFB + LDES on installed power capacity and SCOE, across a range of CO ₂ constraints for the Northeast, Southeast, and Texas regions | 197 |

| | | |
|-------------|--|-----|
| Figure 6.10 | Impacts of adding RFB + LDES on installed storage capacity and VRE curtailment, across a range of CO ₂ emission constraints..... | 198 |
| Figure 6.11 | Impact of low-, mid-, and high-cost hydrogen (top row) and metal-air battery (bottom row) storage on installed power capacity, storage capacity, and SCOE, across a range of CO ₂ constraints for the Northeast region | 200 |
| Figure 6.12 | Impacts of low-, mid-, and high-cost hydrogen on installed power capacity, storage capacity, and SCOE, across a range of CO ₂ constraints for the Texas region | 201 |
| Figure 6.13 | Example state of charge (SoC) of Li-ion battery and hydrogen storage systems in Texas..... | 202 |
| Figure 6.14 | Impacts of low-, mid-, and high-cost VRE on installed power capacity, storage capacity, and SCOE across a range of CO ₂ constraints for the Northeast and Texas regions | 205 |
| Figure 6.15 | Impacts of demand flexibility in terms of installed power capacity, storage capacity, and SCOE, across a range of CO ₂ constraints for the Northeast and Texas regions | 207 |
| Figure 6.16 | Impact of demand flexibility on system operations in Texas | 207 |
| Figure 6.17 | Representation of how industrial hydrogen demand is modeled within GenX | 209 |
| Figure 6.18 | Impacts of serving 0%–100% of baseline industrial hydrogen demand (19.7 GW _t) with electricity in terms of installed power capacity, storage capacity, electrolyzer capacity, and electrolyzer capacity factor, across a range of annual CO ₂ emission constraints for the Texas region | 210 |
| Figure 6.19 | Cost and VRE curtailment impacts of alternative industrial hydrogen demand levels for Texas | 211 |
| Figure 6.20 | System impacts of the availability of underground geological hydrogen storage..... | 212 |
| Figure 6.21 | System impacts of incrementally expanding regional coordination and transmission capacity in a U.S.-wide context..... | 216 |
| Figure 6.22 | Marginal value of energy under base case assumptions (Li-ion battery storage only) for Texas | 217 |
| Figure 6.23 | System operation and marginal value of energy under base case assumptions (Li-ion battery storage only) for Texas at 10 gCO ₂ /kWh | 219 |
| Figure 6.24 | Marginal value of energy across different storage mixes in Texas | 220 |
| Figure 6.25 | Technology operation by price band in Texas – base case | 221 |
| Figure 7.1 | Simplified schematic of methods used for demand-side modeling in the Indian context | 235 |
| Figure 7.2 | Regional electricity demand in India in 2040 | 236 |
| Figure 7.3 | Electricity demand projections for India at the national level assuming stable GDP growth, baseline cooling, and home electric vehicle (EV) charging | 236 |
| Figure 7.4 | Comparison of forecasts | 237 |
| Figure 7.5 | Load profile in 2030 for the southern region of India across three days in summer | 238 |
| Figure 7.6 | Flowchart showing steps in the flexible valuation framework | 239 |
| Figure 7.7 | Real options decision tree | 240 |
| Figure 7.8 | Approach for computing megacity-level DLS potential in the Indian context | 241 |
| Figure 7.9 | Hourly dispatch of NWA battery storage for one summer week load profile from Delhi..... | 244 |
| Figure 7.10 | Real options framework time series simulation | 245 |
| Figure 7.11 | Installed capacity (1st row), annual energy generation (2nd row), storage energy capacity (3rd row), and annual CO ₂ emissions (4th row) for reference case (1st column), as well as cases with alternative assumptions for battery storage capital cost (2nd column), high AC efficiency (3rd column), and gas prices (4th column) | 248 |
| Figure 7.12 | Hourly generation dispatch and load profile for three days during summer (left) and winter (right) periods for 2050 | 250 |
| Figure 7.13 | Regional capacity and utilization trends for generation and transmission in 2050 | 251 |

| | | |
|-------------|--|-----|
| Figure 7.14 | Cooling demand contribution to peak demand given space cooling demand growth, AC unit sales of various types, and average SEER projections for AC units sold in India..... | 253 |
| Figure 7.15 | Distribution-level storage deployment..... | 255 |
| Figure 7.16 | Model outcomes for the high-AC-efficiency/low-cost case (defined by low battery storage capital cost, high AC efficiency, and low gas prices) (1st column) and for the impact of a carbon price with and without scenario assumptions..... | 257 |
| Figure 7.17 | Model outcomes for the reference case (1st column) and mid- and low-cost LDES cases (2nd and 3rd columns respectively) | 258 |
| Figure 7.18 | Model outcomes for the high carbon price case (1st column) and the mid- and low-cost LDES with high carbon price cases (2nd and 3rd columns respectively) | 260 |
| Figure 7.19 | Minigrid design results without any simulated grid outages | 262 |
| Figure 7.20 | Minigrid hourly dispatch without any simulated grid outages (reference case) | 263 |
| Figure 7.21 | Cost-optimum minigrid design (compared to reference case) under conditions of infrequent outages (1st column), frequent outages (2nd column), and no grid connection (3rd column). | 264 |
| Figure 8.1 | A contemporary electricity market in the short run..... | 273 |
| Figure B.1 | Thermodynamic cycle for a heat pump | 319 |
| Figure C.1 | Hybrid clustering approach used to select representative periods for CEM in the case of the Northeast and Southeast regions | 333 |
| Figure C.2 | Reliability outcomes in the Southeast across different model configurations | 335 |
| Figure C.3 | Reliability outcomes in the Northeast across different model configurations | 335 |
| Figure C.4 | Representation of the power-to-H ₂ -to-power system in GenX with use of the system to also meet industrial hydrogen demand | 336 |
| Figure C.5 | Natural gas consumption by large energy users in Texas | 337 |
| Figure C.6 | Impacts of assuming the NREL EFS Reference vs. High Electrification load scenarios in the Southeast in terms of installed power capacity and storage capacity across a range of CO ₂ policies | 339 |
| Figure C.7 | Scenarios showing the impacts of cost sensitivities around Li-ion and RFB technology in the Southeast in terms of installed power capacity, storage capacity, and VRE curtailment, across a range of CO ₂ policies | 340 |
| Figure C.8 | System impacts of LDES availability at different assumed cost levels in Texas..... | 341 |
| Figure C.9 | System impacts of LDES availability at different assumed cost levels in the Southeast..... | 342 |
| Figure C.10 | System impacts of VRE at varying cost levels in the Southeast | 343 |
| Figure C.11 | System impacts of demand flexibility in the Southeast..... | 344 |
| Figure D.1 | Electric vehicle charging demand contribution to peak demand | 350 |
| Figure D.2 | Hourly load profile by month in 2040 | 350 |
| Figure D.3 | Charging schemes comparison | 352 |
| Figure D.4 | Storage power and energy capacity..... | 353 |
| Figure D.5 | Technology impact on emissions intensity and transmission expansion | 354 |
| Figure D.6 | Technology capacity factors across scenarios over modeling periods | 355 |
| Figure D.7 | System average cost of electricity (SCOE) | 356 |
| Figure D.8 | Model outcomes for high-AC-efficiency/low-cost case | 357 |
| Figure D.9 | System average cost of electricity (SCOE) for long-duration energy storage (LDES) cases | 358 |
| Figure D.10 | Results for 2020 minigrid design | 362 |
| Figure D.11 | Low storage cost minigrid design compared to reference case..... | 363 |

List of tables

| | | |
|------------|---|-----|
| Table ES.1 | Summary of findings on the current innovation status of selected energy storage technologies | xiv |
| Table 2.1 | Estimated and projected capital costs, operating costs, efficiencies, and self-discharge rates | 19 |
| Table 2.2 | Classes of positive electrode materials | 22 |
| Table 2.3 | World annual production, world reserves, and resources of lithium, cobalt, nickel, and vanadium in 2020 | 47 |
| Table 2.4 | Material intensities | 48 |
| Table 2.5 | Years of current production for 100 TWh of Li-ion batteries | 48 |
| Table 3.1 | PSH projects licensed in the United States since 1990 | 80 |
| Table 3.2 | Siting time for recently licensed PSH projects in the United States | 80 |
| Table 3.3 | Developer/owner of new PSH projects 2000–2019 | 84 |
| Table 3.4 | Cost assumptions for A-CAES in 2020 and 2050 | 102 |
| Table 4.1 | Comparison of heat-to-electricity conversion methods | 124 |
| Table 4.2 | Three near- and long-term strategies for TES | 129 |
| Table 4.3 | System cost estimate | 137 |
| Table 5.1 | Assumptions for hydrogen production cost modeling | 155 |
| Table 5.2 | Operating variables for electrolyzer technologies | 157 |
| Table 5.3 | Cost and operational assumptions by production technology (2020 and 2050) | 159 |
| Table 5.4 | Techno-economic estimates for hydrogen storage technologies (2020 and 2050) | 161 |
| Table 5.5 | Global assumptions used in downstream model | 163 |
| Table 5.6 | Techno-economic inputs for different generation technologies (2020 and 2050) | 163 |
| Table 6.1 | Electricity generation and electricity-related emissions (U.S. total and three regions modeled in this study) | 173 |
| Table 6.2 | Design variables for different types of storage technologies modeled in this study | 177 |
| Table 6.3 | Storage costs and operational assumptions | 177 |
| Table 6.4 | Inputs and outputs of the GenX model | 181 |
| Table 6.5 | Mid-cost assumptions for VRE and natural gas generating resources | 181 |
| Table 6.6 | EFS 2050 demand assumptions for the Northeast, Southeast, and Texas | 183 |
| Table 6.7 | Marginal and average costs of carbon abatement for various emission policy constraints | 189 |
| Table 6.8 | Base case reliability results in Texas | 189 |
| Table 6.9 | Modeled emissions reduction results for different decarbonization targets summarized using alternative metrics commonly used in policy discourse | 191 |
| Table 6.10 | Relative root mean square (RMS) contribution of different frequency bands to the optimal storage state of charge temporal profile | 203 |
| Table 6.11 | Demand flexibility assumptions for Texas under 2050 load conditions | 206 |
| Table 6.12 | System impacts of a dispatchable low-carbon generating technology in Texas | 213 |
| Table 6.13 | System impacts of enabling intra-regional transmission expansion in the U.S. Northeast | 215 |
| Table 6.14 | Comparison of the average marginal value of energy (simple average of prices over time) and volatility, as measured by the coefficient of variation (standard deviation divided by mean) for modeled 2050 prices in Texas | 220 |
| Table 7.1 | Summary of storage deployment scenarios for demand- and generation-driven electricity system development in the EMDE countries investigated in this chapter | 234 |

| | | |
|------------|---|-----|
| Table 7.2 | Demand projections for India assuming AC and EV demand growth | 235 |
| Table 7.3 | Projected peak demand (GW) under the baseline and high-AC-efficiency scenarios, assuming stable GDP growth for the city state of Delhi | 243 |
| Table 7.4 | Storage cost impact on outputs of the flexible valuation framework applied to the four Indian megacities for year 2030 | 246 |
| Table 7.5 | Estimated megacity-level DLS potential as a “non-wires alternative” under mid-range cost projections | 246 |
| Table 7.6 | Baseline parameters and sensitivity cases | 252 |
| Table 9.1 | Summary of MITEI’s Future of Energy Storage study findings on the current innovation status of selected technologies | 295 |
| Table A.1 | Rechargeable battery types, year of introduction, and chemical cost as plotted in Figure 2.2 in the main report | 304 |
| Table A.2 | Price of chemicals | 305 |
| Table A.3 | Estimated and projected capital costs, operating costs, efficiencies, and self-discharge rates | 307 |
| Table A.4 | Input parameters for the cost model | 307 |
| Table A.5 | Parameters for power cost calculation | 309 |
| Table A.6 | Parameters for energy cost calculation | 311 |
| Table A.7 | Costs for electrical BOP components | 313 |
| Table A.8 | Costs for non-electrical BOP components | 313 |
| Table A.9 | Input parameters for the cost model | 314 |
| Table A.10 | Power cost parameters for 20-hour discharge | 315 |
| Table A.11 | Energy cost parameters for 20-hour discharge | 316 |
| Table B.1 | Data used in Figure 4.4 | 320 |
| Table B.2 | Cost data for thermal energy storage materials used in Figure 4.5 | 320 |
| Table B.3 | Assumptions used to estimate costs for TES systems | 321 |
| Table B.4 | High-, medium-, and low-cost estimates for the “crushed rock and sCO ₂ ” and “liquid silicon and multi-junction TPV” TES systems | 323 |
| Table C.1 | Brownfield nuclear capacity in the Southeast | 328 |
| Table C.2 | Rooftop PV minimum build in New York and New England | 329 |
| Table C.3 | Load allocation from states to IPM zones | 330 |
| Table C.4 | Thermal generator operational characteristics | 331 |
| Table C.5 | Technology-specific fuel prices | 331 |
| Table C.6 | Non-coincident maximum hourly demand flexibility in GW across the three modeled regions under 2050 load conditions | 332 |
| Table C.7 | Installed power capacity (relative to peak load) | 337 |
| Table C.8 | VRE curtailment level (% of available generation based on capacity) | 337 |
| Table C.9 | Average system cost of energy, SCOE (\$/MWh) | 338 |
| Table C.10 | Capacity factors for CCGTs without CCS in the base case for various emission policy constraints (gCO ₂ /kWh) | 338 |
| Table C.11 | System impacts of a dispatchable low-carbon generating technology in Texas | 345 |
| Table C.12 | System impacts of expanding inter-zonal transfer capacity in the Southeast | 346 |
| Table D.1 | Distribution-level storage cost assumptions and wires upgrade cost for new line and reconductoring of existing lines | 351 |

| | | |
|------------|---|-----|
| Table D.2 | Distribution-level storage system cost of electricity comparison at transmission level using system cost of electricity calculation | 351 |
| Table D.3 | List of technology names and corresponding abbreviations | 359 |
| Table D.4 | Capital cost assumptions for various resources..... | 359 |
| Table D.5 | Storage duration comparison | 360 |
| Table D.6 | Thermal generation power capacity in India..... | 360 |
| Table D.7 | Input parameters for thermal generation for existing and new assets..... | 361 |
| Table D.8 | Capital cost assumptions for various resources..... | 364 |
| Table D.9 | Operation and maintenance cost assumptions for various resources..... | 364 |
| Table D.10 | Assumed ranges for the frequency and duration of outages for simulated cases based on discussion with Abuja Electric Distribution Company | 364 |

Glossary

| | |
|------------------------------|---|
| Adiabatic | Occurring without loss or gain of heat. |
| Behind-the-meter storage | Customer-sited stationary storage systems that are connected to the distribution system on the customer's side of the utility's service meter. |
| Black start resource | An electricity system resource that can start or remain energized without support from the grid. A black start resource can be used to energize one or more transmission buses and provide power capability, frequency control, and voltage control needed to implement a transmission system restoration plan. |
| Brownfield storage project | A storage project located at a current electricity infrastructure site that uses the existing grid interconnection and possibly other available equipment (for example, inverters, turbines, or dams) to lower cost and/or accelerate the project timeline. |
| Bulk power system | A large interconnected electrical system made up of generation and transmission facilities and their control systems. Storage facilities may also be included. |
| Carnot efficiency | The maximum thermal efficiency achievable by a theoretically ideal heat engine. |
| Charge-storage species | A material that stores an electric charge within a battery. |
| Coincident peak | A facility's (electricity) demand during the time when electricity demand system-wide is the highest. |
| Diabatic | Involving the transfer of heat. |
| Electrolyzer | A system that uses electricity to split water into hydrogen and oxygen. This process is called electrolysis. |
| Energy arbitrage | Shifting electrical energy from low-value times or locations to high-value ones. |
| Fischer–Tropsch process | A collection of chemical reactions that converts a mixture of carbon monoxide and hydrogen (syngas, or synthesis gas) into a multiphase mixture of hydrocarbons, oxygenates, and water, that can be separated and further processed into a variety of useful fuels and other compounds. |
| Frequency regulation | The rapid and often automatic adjustment of inputs or withdrawals of electrical energy by a balancing authority to maintain the oscillation frequency of the alternating current in an electric power system within a specified tolerance of the scheduled value (60 cycles/second in the United States). |
| Geomechanical pumped storage | The storage of energy using fluids that are pressurized by the weight of overlying rock. |
| Greenfield storage project | A newly-built storage project that does not rely on existing grid interconnections or other existing equipment at current sites with electricity infrastructure. |
| Hydrostatic pressure | The pressure exerted by a fluid at equilibrium due to the force of gravity. |
| Induction heating | The process of heating electrically conductive materials like metals by electromagnetic induction—heat transfer passing through an induction coil that creates an electromagnetic field. An important feature of the induction heating process is that the heat is generated inside the object itself, instead of by an external heat source via heat conduction. |
| Intercalation | The reversible inclusion or insertion of a molecule (or ion) into compounds with layered structures—a process that occurs during the charging and discharging of batteries. For example, when a lithium-ion battery is discharging, a lithium ion moves from the negative electrode (usually graphite) and enters the positive electrode (usually lithium oxide) through the electrolyte solution. During charging, the opposite process occurs, which is why intercalation is known as a <i>reversible process</i> . |

| | |
|------------------------------|---|
| Isobaric | Compressed air storage that uses a fluid to maintain the compressed air at a constant pressure. |
| Isochoric | Compressed air storage in which the volume of compressed air stays constant while the pressure changes. |
| Least-cost planning | A process (also known as integrated resource planning) by which electric utilities evaluate the costs, benefits, and risks of different resources for meeting electric power demand (including power generation and energy efficiency) in an effort to arrive at the mix of resources that will meet future demand at the lowest cost while providing reliable electric service. |
| Lithium-ion (Li-ion) battery | A rechargeable battery that uses solid compounds at both the negative and positive electrodes as hosts for reversible lithium-ion storage. During discharge, lithium ions migrate internally from the negative electrode to intercalate into the positive electrode through an electrolyte, while electrons simultaneously move in the same direction through an external circuit, powering the device to which the battery is connected. During charge, the process is reversed, with lithium ions migrating from the positive to the negative electrode under voltage supplied by an external power source. |
| Load following | An increase or decrease in the level of dispatchable generation and/or the net withdrawal from dispatchable energy storage to match changes in electricity demand. |
| Load shedding | The deliberate shutdown of electric power in a part or parts of an electricity distribution system, generally to prevent the failure of the entire system when the demand strains the capacity of the system. |
| Metal-air battery | A battery in which metal serves as the negative electrode (the anode, during discharge) and is paired with a positive electrode (the “air cathode,” during discharge), which does not store any electrical charge itself, but which takes oxygen from the air and produces hydroxyl ions in the electrolyte during discharge—an electrochemical reduction process. |
| Minigrid | A set of small-scale electricity generators, and possibly energy storage systems, interconnected to a distribution network that supplies electricity to a small, localized group of customers. |
| Net-zero emissions | Achievement of a balance between greenhouse gases emitted to the atmosphere and those removed from the atmosphere. |
| Photovoltaic | In common usage, the direct conversion of light into electrical energy. More generally, the generation of a voltage when radiant energy falls on the boundary between dissimilar substances, typically two different semiconductors of a solar panel. |
| Pidgeon process | A method of magnesium metal production in which calcined dolomite is thermally reduced to metallic magnesium using ferrosilicon as a reducing agent in vacuum (silico-thermic reduction). |
| Power system dispatch | Decisions by system operators to schedule generation, storage, and demand response assets under their control to meet electricity demand in a manner that is both reliable and cost-effective. |
| Pyroelectric | Related to pyroelectricity, a state of electrical charge produced (as in a crystal) by a change of temperature. |
| Rankine cycle | An idealized thermodynamic cycle describing the process by which certain heat engines, such as steam turbines or reciprocating steam engines, allow mechanical work to be extracted from a fluid as it moves between a heat source and a heat sink. |

| | |
|---|---|
| Redox flow battery | A rechargeable electrochemical device in which charge-storage materials are dissolved in liquid electrolytes, stored in inexpensive tanks, and circulated through a power-converting reactor where they are oxidized and reduced to alternately charge and discharge the battery. |
| Reserves (electricity system) | Resources available to supply extra power to the grid (historically from extra generating capacity) over a variety of time horizons. Spinning reserves are synchronized to the grid, with a response time of less than 10 minutes (and sometimes meeting other requirements) that can be used to maintain system frequency stability during unforeseen load swings or emergency conditions. |
| Resistive heating | A process by which the passage of an electric current through a conductor produces heat. |
| Specific energy (or gravimetric energy density) | A mass-based measure of energy density, often expressed in watt-hours per kilogram. |
| Thermocline tank | The storage of hot and cold liquid in the same tank with a means to reduce internal heat transfer losses. |
| Turbomachinery | Machinery consisting of, incorporating, or constituting a turbine. |
| Variable renewable energy | Electricity generation technologies whose primary energy source varies over time and cannot easily be stored. Sources include solar, wind, ocean, and some hydropower. |
| Vertically integrated utility | A utility that owns and controls generation, transmission, and distribution components. |
| Voltage support | The maintenance of voltage levels in the transmission and distribution system. |
| Volumetric energy density | A volume-based measure of energy density, often expressed in watt-hours per liter. |
| Wholesale electricity market | The buying and selling of power between generators and resellers. Resellers include electricity utility companies, competitive power providers, and electricity marketers. |



Massachusetts
Institute of
Technology